MYCOSPHERE 16(1): 2002–2258(2025) www.mycosphere.org ISSN 2077 7019
Doi 10.5943/mycosphere/16/1/12

ARTICLE

Microfungi associated with walnut trees in southwestern China

Wang FH[1,2], Xu XL[1,3], Zeng Q[1,2], Liu LJ[1,2], Liu F[1,2], Deng Y[1,2], Sun QR[1,2], Yan YQ[1,2], Li XY[1,2], Xiang SS[1,2], Shuai Q[1,2], Liu YG[1,2], Li SJ[1,2], Yang H[1,2], Han S[1,2], Liu L[1,2], Yang CL[1,2*]

[1] College of Forestry, Sichuan Agriculture University, Chengdu 611130, Sichuan, China
[2] National Forestry and Grassland Administration Key Laboratory of Forest Resources Conservation and Ecological Safety on the Upper Reaches of the Yangtze River & Forestry Ecological Engineering in the Upper Reaches of the Yangtze River Key Laboratory of Sichuan Province, Chengdu 611130, Sichuan, China
[3] Forestry Research Institute, Chengdu Academy of Agriculture and Forestry Sciences, Chengdu 611130, Sichuan, China

Citation – Wang FH, Xu XL, Zeng Q, Liu LJ, Liu F, Deng Y, Sun QR, Yan YQ, Li XY, Xiang SS, Shuai Q, Liu YG, Li SJ, Yang H, Han S, Liu L, Yang CL 2025 – Microfungi associated with walnut trees in southwestern China. Mycosphere 16(1): 2002–2258, Doi 10.5943/mycosphere/16/1/12

Abstract

The plant family, *Juglandaceae* comprises economically important tree species that are extensively cultivated worldwide, with the *Juglans* and *Carya* genera representing the largest areas of cultivation. Fungi associated with *Juglandaceae* plants are diverse and widespread, with about 200 walnut-related species identified in China based on around 120 fragmented references. To date, there have been few systematic studies conducted on walnut fungi in China. In this study, diseased branches, leaves, fruits, and litter showing symptoms of infection were collected to conduct an in-depth investigation of *Ascomycota* fungi associated with walnuts in Sichuan, southwestern China. The fungi were identified through morphological analysis and multi-gene phylogenetic methods, revealing one phylum, four classes, 14 orders, 26 families, 42 genera, and 90 species among our newly collected specimens. This paper describes one new genus, *Neomelanconis* (*Gnomoniaceae*, *Diaporthales*), and 25 new species, including *Alternaria ganziense*, *Aurantiascoma juglandis*, *Botryosphaeria gaoxianense*, *B. neijiangense*, *B. yibinense*, *Colletotrichum beichuanense*, *Co. shehongense*, *Cladosporium rugae*, *Dothiorella pugeense*, *Diaporthe mianyangense*, *Juglanconis magnatum*, *J. mucosporium*, *Kirschsteiniothelia yantingense*, *Lasiodiplodia chongzhouense, L. juglans*, *Nectria fusiformispora*, *Neomelanconis juglandis*, *Neofusicoccum juglans*, *Neof. wenchuanense*, *Ophiognomonia pseudopterocaryae*, *Paraeutypella neijiangense*, *Periconia yantingense*, *Scopulariopsis pseudobrevicaulis*, *Sphaerulina curvecylindrospora*, and *Trichothecium downum*. In addition, 37 new host records and 35 new geographical records were documented. Morphologically similar species and phylogenetically related taxa are compared and discussed, with detailed descriptions and illustrations provided for each species. This study did not perform pathogenicity tests on all species, and potential pathogens were identified mainly based on field symptoms and existing literature on their pathogenicity, with future experiments planned to systematically assess these species in accordance with Koch's postulates. This study further highlights the fungal diversity associated with walnut plants, uncovering numerous previously unknown species.

Keywords – 25 new taxa – *Juglans* – *Carya* – morphology – phylogeny – *Ascomycota*

TABLE OF CONTENTS

Submitted: 02 January 2025; **Accepted:** 12 June 2025; **Published:** 10 July 2025
***Corresponding Author:** Chun-Lin Yang – e-mail – yangcl0121@163.com
Accepted by: Asha J. Dissanayake

The new fungal collections in this study are organized according to the classification framework of *Ascomycota* (Wijayawardene et al. 2022), with updates incorporated from recent relevant publications.

Ascomycota Caval. -Sm.
Dothideomycetes sensu O.E. Erikss. & Winka
Botryosphaeriales C.L. Schoch, Crous & Shoemaker
Botryosphaeriaceae Theiss. & P. Syd.

Botryosphaeria Ces. & De Not.
1. ***Botryosphaeria dothidea*** (Moug.) Ces. & De, **recollected in China**
2. ***Botryosphaeria gaoxianense*** F.H. Wang & C.L. Yang, **sp. nov.**
3. ***Botryosphaeria neijiangense*** F.H. Wang & C.L. Yang, **sp. nov.**
4. ***Botryosphaeria wangensis*** G.Q. Li & S.F. Chen, **new host and geographical record**
5. ***Botryosphaeria yibinense*** F.H. Wang & C.L. Yang, **sp. nov.**

Dothiorella Sacc.
6. ***Dothiorella pugeense*** F.H. Wang & C.L. Yang, **sp. nov.**
Lasiodiplodia Ellis & Everh.
7. ***Lasiodiplodia chongzhouense*** F.H. Wang & C.L. Yang, **sp. nov.**
8. ***Lasiodiplodia juglans*** F.H. Wang & C.L. Yang, **sp. nov.**
9. ***Lasiodiplodia pseudotheobromae*** A.J.L. Phillips, A. Alves & Crous, **recollected in China**
10. ***Lasiodiplodia theobromae*** (Pat.) Grif. & Maubl. **recollected in China**

Neofusicoccum Crous, Slippers & A.J.L. Phillips
11. ***Neofusicoccum juglans*** F.H. Wang & C.L. Yang, **sp. nov.**
12. ***Neofusicoccum parvum*** (Pennycook & Samuels) Crous, Slippers & A.J.L. Phillips. **recollected in China**
13. ***Neofusicoccum sichuanense*** X.L. Xu & C.L. Yang, **recollected in China**
14. ***Neofusicoccum wenchuanense*** F.H. Wang & C.L. Yang, **sp. nov.**

Cladosporiales **Abdollahz. & Crous**.
Cladosporiaceae Chalm. & R.G. Archibald
Cladosporium Link
15. ***Cladosporium cladosporioides*** (Fresen.) G.A. de Vries, **recollected in China**
16. ***Cladosporium rugae*** F.H. Wang & C.L. Yang, **sp. nov.**

Hysteriales Lindau
Hysteriaceae Chevall.
Rhytidhysteron Speg.
17. ***Rhytidhysteron rufulum*** (Spreng.) Speg., **new host record.**
18. ***Rhytidhysteron sichuanense*** X.L. Xu & C.L. Yang, **new host record**
19. ***Rhytidhysteron subrufulum*** X.L. Xu & C.L. Yang, **new host record**

Kirschsteiniotheliales Hern. -Restr., R.F. Castañeda, Gené & Crous
Kirschsteiniotheliaceae Boonmee & K.D. Hyde
Kirschsteiniothelia D. Hawksw
20. ***Kirschsteiniothelia yantingense*** F.H. Wang & C.L. Yang, **sp. nov.**

Mycosphaerellales (Nannf.) P.F. Cannon
Mycosphaerellaceae Lindau
Cercospora Fresen. ex Fuckel

21. ***Cercospora nicotianae*** Ellis & Everh, **new host record**

Ragnhildiana Solheim

22. ***Ragnhildiana diffusa*** (Heald & F.A. Wolf) Videira & Crous, **recollected in China**

Sphaerulina Sacc

23. ***Sphaerulina curvecylindrospora*** F.H. Wang & C.L. Yang, **sp. nov.**

24. ***Sphaerulina juglandina*** X.L. Xu & C.L. Yang, **recollected in China**

Pleosporales Luttr. ex M.E. Barr

Bambusicolaceae D.Q. Dai & K.D. Hyde

Palmiascoma Phook. & K.D. Hyde

25. ***Palmiascoma qujingense*** Monkai & Phookamsak, **recollected in China**

Macrodiplodiopsidaceae Voglmayr, Jaklitsch & Crous

Pseudochaetosphaeronema Punith

26. ***Pseudochaetosphaeronema kunmingense*** D.P. Wei, Wanas. & K.D. Hyde, **new host and geographical record**

Massarinaceae Munk

Helminthosporium Link

27. ***Helminthosporium juglandinum*** Voglmayr & Jaklitsch, **new geographical record**

28. ***Helminthosporium velutinum*** Link, **recollected in China**

Periconiaceae Nann.

Periconia Tode

29. ***Periconia byssoides*** Pers, **recollected in China**

30. ***Periconia pseudobyssoides*** Markovsk. & A. Kačergius, **new host record**

31. ***Periconia thailandica*** N.G. Liu, K.D. Hyde & Hongsanan, **new host and geographical record**

32. ***Periconia yantingense*** F.H. Wang & C.L. Yang, **sp. nov.**

Phaeosphaeriaceae M.E. Barr

Paraphoma Morgan-Jones & J.F. White

33. ***Paraphoma dioscoreae*** Quaedvl., H.D. Shin, Verkley & Crous, **new host and geographical record**

Pleosporaceae Nitschke

Alternaria Nees

34. ***Alternaria alternata*** (Fr.) Keissl., **recollected in China**

35. ***Alternaria doliconidium*** J.F. Li, Camporesi & K.D. Hyde, **new host and geographical record**

36. ***Alternaria ganziense*** F.H. Wang & C.L. Yang, **sp. nov.**

37. ***Alternaria italica*** J.F. LI, Camporesi & K.D. Hyde, **new host and geographical record**

38. ***Alternaria longipes*** (Ellis & Everh.) E.W. Mason, **new host and geographical record**

Teichosporaceae M.E. Barr

Aurantiascoma Thambugala & K.D. Hyde

39. ***Aurantiascoma juglandis*** F.H. Wang & C.L. Yang, **sp. nov.**

Valsariales Jaklitsch, K.D. Hyde & Voglmayr

Valsariaceae Jaklitsch, K.D. Hyde & Voglmayr

Myrmaecium Nitschke ex Fuckel

40. ***Myrmaecium fulvopruinatum*** (Berk.) Jaklitsch & Voglmayr, **recollected in China**

Eurotiomycetes O.E. Erikss. & Winka

Eurotiales G.W. Martin ex Benny & Kimbr.
Aspergillaceae Link
Penicillium Link
41. ***Penicillium citrinum*** Thom, **new host and geographical record**

Leotiomycetes O.E. Erikss. & Winka
Helotiales Nannf.
Sclerotiniaceae Whetzel
Botrytis P. Micheli ex Pers
42. ***Botrytis cinerea*** Pers, **new host and geographical record**

Sordariomycetes O.E. Erikss. & Winka
Amphisphaeriales D. Hawksw. & O.E. Erikss.
Sporocadaceae Corda

Neopestalotiopsis Maharachch., K.D. Hyde & Crous
43. ***Neopestalotiopsis chiangmaiensis*** Tibpromma & K.D. Hyde, **new host and geographical record**

Pestalotiopsis Steyaert
44. ***Pestalotiopsis kenyana*** Maharachch., K.D. Hyde & Crous, **new host and geographical record**
45. ***Pestalotiopsis vismiae*** (Petr.) J. Xiang Zhang & T. Xu, **new host record**

Diaporthales Nannf.
Diaporthaceae Höhn. ex Wehm.

Diaporthe Nitschke
46. ***Diaporthe citri*** (H.S. Fawc.) F.A. Wolf, **new host record**
47. ***Diaporthe eres*** Nitschke, **recollected in China**
48. ***Diaporthe mianyangense*** F.H. Wang & C.L. Yang, **sp. nov.**
49. ***Diaporthe novem*** J.M. Santos, Vrandečić & A.J.L. Phillips, **new host and geographical record**
50. ***Diaporthe pseudomangiferae*** R.R. Gomes, Glienke & Crous, **new host and geographical record**
51. ***Diaporthe ravennica*** Thambug., Camporesi & K.D. Hyde, **new host record**
52. ***Diaporthe tectonae*** Doilom, Dissan. & K.D. Hyde, **new host record**
53. ***Diaporthe tulliensis*** R.G. Shivas, Vawdrey & Y.P. Tan, **new host and geographical record**
54. ***Diaporthe vawdreyi*** Y.P. Tan & R.G. Shivas, **new host and geographical record**

Gnomoniaceae G. Winter
Neomelanconis F.H. Wang & C.L. Yang, **gen. nov.**
55. ***Neomelanconis juglandis*** F.H. Wang & C.L. Yang, **sp. nov.**
Ophiognomonia (Sacc.) Speg.
56. ***Ophiognomonia leptostyla*** (Fr.) Sogonov, **recollected in China**
57. ***Ophiognomonia pseudopterocaryae*** F.H. Wang & C.L. Yang, **sp. nov.**
58. ***Ophiognomonia pterocaryae*** D.M. Walker, in Walker, **new host and geographical record**

Juglanconidaceae Voglmayr & Jaklitsch
Juglanconis Voglmayr & Jaklitsch
59. ***Juglanconis appendiculata*** Voglmayr & Jaklitsch, in Voglmayr, **recollected in China**
60. ***Juglanconis magnatum*** F.H. Wang & C.L. Yang, **sp. nov.**

61. ***Juglanconis mucosporium*** F.H. Wang & C.L. Yang, **sp. nov.**
62. ***Juglanconis juglandina*** (Kunze) Voglmayr & Jaklitsch, **new geographical record**

Glomerellales Chadef. ex Réblová, W. Gams & Seifert
Glomerellaceae Locq. ex Seifert & W. Gams
Colletotrichum Corda
63. ***Colletotrichum beichuanense*** F.H. Wang & C.L. Yang, **sp. nov.**
64. ***Colletotrichum fioriniae*** (Marcelino & Gouli) Pennycook, **new geographical record**
65. ***Colletotrichum fructicola*** Prihast., L. Cai & K.D. Hyde, **new geographical record**
66. ***Colletotrichum gloeosporioides*** (Penz.) Penz. & Sacc, **new geographical record**
67. ***Colletotrichum godetiae*** Neerg, **new geographical record**
68. ***Colletotrichum scovillei*** Damm, P.F. Cannon & Crous, **new host and geographical record**
69. ***Colletotrichum shehongense*** F.H. Wang & C.L. Yang, **sp. nov.**
70. ***Colletotrichum siamense*** Prihast., L. Cai & K.D. Hyde, **new geographical record**

Hypocreales Lindau
Bionectriaceae Samuels & Rossman
Acremonium Link
71. ***Acremonium hennebertii*** W. Gams, **new host record**
Clonostachys Corda
72. ***Clonostachys rosea*** (Link) Schroers, Samuels, Seifert & W. Gams, **new host and geographical record**

Cordycipitaceae Kreisel ex G.H. Sung, J.M. Sung, Hywel-Jones & Spatafora
Lecanicillium W. Gams & Zare
73. ***Lecanicillium dimorphum*** (J.D. Chen) Zare & W. Gams, **new host and geographical record**

Nectriaceae Tul. & C. Tul.
Albonectria Rossman & Samuels
74. ***Albonectria rigidiuscula*** (Berk. & Broome) Rossman & Samuels, **new host and geographical record**
Fusarium Link
75. ***Fusarium coffeatum*** L. Lombard & Crous, **new host and geographical record**
76. ***Fusarium graminearum*** Schwabe, **new geographical record**
77. ***Fusarium incarnatum*** (Desm.) Sacc, **new geographical record**
78. ***Fusarium lateritium*** Nees, **new geographical record**
Microcera Desm.
79. ***Microcera chrysomphali*** Feng Liu & C.L. Yang, **recollected in China**
Nectria (Fr.) Fr.
80. ***Nectria fusiformispora*** F.H. Wang & C.L. Yang, **sp. nov.**
81. ***Nectria pseudotrichia*** Berk. & M.A. Curtis, **new host record**
Neocosmospora E.F. Sm.
82. ***Neocosmospora solani*** (Mart.) L. Lombard & Crous, **recollected in China**
Trichothecium Link
83. ***Trichothecium downum*** F.H. Wang & C.L. Yang, **sp. nov.**

Microascales Luttr.
Microascaceae Luttr. ex Malloch
Scopulariopsis Bainier
84. ***Scopulariopsis pseudobrevicaulis*** F.H. Wang & C.L. Yang, **sp. nov.**

Xylariales Nannf.

Diatrypaceae Nitschke

Diatrypella (Ces. & De Not.) De Not.

85. ***Diatrypella vulgaris*** Trouillas, W.M. Pitt & Gubler, **new host and geographical record**

Eutypella (Nitschke) Sacc.

86. ***Eutypella microtheca*** Trouillas, W.M. Pitt & Gubler, **new host and geographical record**

Paraeutypella L.S. Dissan., J.C. Kang, Wijayaw. & K.D. Hyde

87. ***Paraeutypella citricola*** (Speg.) L.S. Dissan., Wijayaw., J.C. Kang & K.D. Hyde, **new host and geographical record**

88. ***Paraeutypella neijiangense*** F.H. Wang & C.L. Yang, **sp. nov.**

Peroneutypa Berl.

89. ***Peroneutypa rubiformis*** Q.J. Shang, Phukhamsak & K.D. Hyde, **new host and geographical record**

Hypoxylaceae DC.

Hypoxylon Bull.

90. ***Hypoxylon perforatum*** (Schwein.) Fr, **new host record**

INTRODUCTION

Walnut, a member of the *Juglandaceae* family, broadly encompasses all *Carya* and *Juglans* plants, there are at least 53 species, varieties, or hybrids worldwide (retrieved from http://www.theplantlist.org on 7 June 2024). Walnut species thrive in various climates and are distributed across six continents, excluding Antarctica, with significant populations in northern Asia, Australia, Europe, North South America, and New Zealand, but relatively few species in Africa (Luo et al. 2022). As a model species for environmental protection, walnuts provide unique advantages over other trees (Orlandi et al. 2022). Their extensive root systems aid in soil and water conservation, while broad leaves enhance photosynthesis and carbon sequestration. Additionally, their fruits and dense branches offer food and habitat for rodents and birds (Vande & Wall 2010, Chang & Zhang 2014).

Walnut occupies an irreplaceable position in the nut market and is also widely used in edible oil, healthcare products, snacks, flavored treats, and so forth (Adrián et al. 2018). With the development of food technology, more innovative and creative walnut processing methods have been discovered, leading to continuous improvements in walnut products (Robyn 2018). In Europe, walnut wood is also a popular material in wood processing, with even synthetic boards being manufactured from waste of walnut wood processing (Pędzik et al. 2022). In the United States, *Carya cathayensis*, *Juglans nigra*, and *Prunus serotina* are recognized as three premium species of hardwood timber trees. In China, walnut fruit is edible, and wood can be produced and processed, or used as ornamental trees, all of which play an important role in reducing carbon emissions, greening the environment, and alleviating poverty (Yang et al. 2015, Pantera et al. 2018). Furthermore, walnut green shell extract possesses certain medical value (Fang et al. 2022). Activated carbon derived from walnut green peel has been used as an electrode material for high-performance supercapacitors (Tian et al. 2022). More importantly, people play with walnut fruit as a form of art (Zhang et al. 2024b).

Fungal species associated with walnuts have been documented since the late 18th century, with ascomycetes being reported more frequently. Studies on the taxonomy and phylogeny of *Ascomycota* fungi associated with *Juglandaceae* (*Juglans* and *Carya*) can be of economic significance. A review of the literature and records from the United States National Fungus Collections (Farr & Rossman 2024) pertaining to fungi associated with *Juglandaceae* reveals that, to date, nearly 282 species belonging to 143 genera of ascomycetes have been described or recorded worldwide. Related research is primarily concentrated in Europe, Asia, and North America. Some fungi are pathogens that cause spots or malformations on walnut leaves and stems (Chen et al. 2000, Liu et al. 2018). Additionally, some fungi can cause diseases in flowers and fruits (Wang et al. 2017, Varjas et al. 2019). Fungal diseases of walnuts can reduce their production and, in severe cases, lead to the death of the trees, causing significant economic losses (Tisserat et al. 2009). The spores of *Ascomycota* are

indeed easily disseminated by wind, water, soil, or insects. They are well-adapted to saprobic, parasitic, or mutualistic life modes (Hyde et al. 2019a, Naranjo-Ortiz & Gabaldón 2019). Despite all research indicating the extremely rich diversity of fungi associated with walnuts, there are only a few documents that systematically study the diversity of fungi on walnuts (Xu et al. 2022a).

China is the world's leading producer of walnuts, followed by the United States, India, Iran, Romania, Turkey, Ukraine, and France (Martínez et al. 2010, Fan et al. 2018a). Sichuan, the second-largest walnut-growing province in China, offers extensive walnut cultivation and a rich ecological environment that provides abundant habitats for fungi (Wu et al. 2018). At present, a comprehensive catalog for fungi associated with walnuts is lacking, with most previous research focusing on individual pathogens (Li et al. 2016a). As an economically important species, walnut research has primarily focused on the impact of fungal diseases on production, neglecting fungal diversity, while the absence of molecular data in earlier studies has led to unclear species boundaries and difficulty in distinguishing between and within species (Wang & Liu 2007, Yu et al. 2015). Our research revealed that walnut plants host a diverse range of fungi, including pathogenic, saprobic, and endophytic species, with new species still being discovered (Xu et al. 2022a). Spanning from 2020 to 2023, this study aimed to enhance our understanding of fungal diversity on walnut trees by identifying new species, new records, and novel sexual-asexual connections, with fungal specimens collected from various tissues across 22 counties and regions in 11 cities of Sichuan Province. Samples were primarily collected from widely distributed walnut tree species in Sichuan, including *Carya illinoinensis*, *Juglans regia*, and *J. sigillata*, mainly focusing on leaves, branches, and fruits. A multigene phylogenetic analysis, integrated with morphological assessments, was conducted to accurately classify the newly collected specimens.

MATERIALS AND METHODS

Sample Collection

From September 2020 to June 2023, specimens were collected from walnut plant in commercial plantations of walnut located in the Sichuan (Fig. 1), and collect the necrotic tissues of walnuts. Samples were collected from 11 cities (Dazhou, Bazhong, Guangyuan, Mianyang, Suining, Neijiang, Luzhou, Yibin, Chengdu, Ya'an, and Panzhihua) and three autonomous states (Aba Tibetan and Qiang Autonomous Prefecture, Garze Tibetan Autonomous Prefecture, and Liangshan Yi Autonomous Prefecture), encompassing 36 villages across 22 counties. Fresh samples were collected from the diseased branches, stems, leaves, fruits, and roots, with some samples being obtained from the host's dead and withered tissues. Each sample was individually placed in a plastic bag, and relevant information such as (latitude and longitude, altitude, host) was recorded before being sent back to the laboratory for observation and isolation. The spore-producing structures were observed and photographed using a dissecting microscope (NVT-GG, Shanghai Advanced Photoelectric Technology Co., Ltd., Shanghai, China) equipped with a VS-800C micro-digital camera (Shenzhen Weishen Times Technology Co., Ltd., Shenzhen, China). Vertical sections of fruiting bodies were made using a razor blade and mounted in double-distilled water for microscopy. The dimensions of both asexual and sexual structures in the collected samples were measured, encompassing ascomata, peridia, asci, ascospores, conidiophores, conidiogenous cells, paraphyses, conidiomata walls, conidia, the number of septa, and so forth. These structures were photographed using an Olympus BX43 compound microscope (Olympus Industrial Co., Ltd., Japan) equipped with an Olympus DP22 digital camera in conjunction with ACDSee (v3.1) software, as well as an Olympus BX53 compound microscope (Olympus Industrial Co., Ltd., China) fitted with an SD1600AC digital camera and Cap Studio (3.8.10.0) software (Image Technology Company, Suzhou, China). Single ascospore or conidium isolations were carried out following the method described by Senanayake et al. (2020). Germinating spores were transferred to PDA, incubated at 25℃ with a 12-h photoperiod. After incubation for 7 days to 2 months depending on growth, colonies were examined for their diam., shape, and appearance. The iodine reaction of the ascus wall was tested in Melzer's reagent (MLZ). Type specimens were deposited at the Herbarium of Sichuan Agriculture University, Chengdu, China

(SICAU). Ex-type cultures were deposited at the Culture Collection in Sichuan Agriculture University (SICAUCC). Faces of fungi numbers (Jayasiri et al. 2015) and Index Fungorum numbers (http://www.indexfungorum.org) are provided.

DNA Extraction, Amplification, and Sequencing

Genomic DNA was extracted directly from the spore mass, fruiting bodies or 30 d pure cultures using a Plant Genomic DNA Extraction Kit (Tiangen, China). Polymerase chain reaction (PCR) was performed in a 25 μL reaction mixture containing 22 μL Master Mix (Beijing TsingKe Biotech Co., Ltd., Beijing, China), 1 μL DNA template, and 1 μL of each primer (10 μM). Primers used for amplification of different gene regions are listed in Table 1. The PCR thermal cycling procedure of each gene region follows the procedure in Table 2. Amplicon size and concentration were assessed by gel electrophoresis with 1.2% agarose stained with ethidium bromide. PCR products were purified and sequenced at TsingKe Biological Technology Co., Ltd. (Chengdu, China). The newly generated sequences were deposited in GenBank.

Table 1 PCR reaction primers (forward and reverse) for amplification of gene loci of each fungal genus.

Genera	Primers	Forward	Reverse	References
Botryosphaeria	ITS	ITS5	ITS4	White et al. (1990)
	*rpb*2	Frpb2-5F	Frpb2-7Cr	Liu et al. (1999)
	*tef*1-α	EF1-728F	986F	Carbone & Kohn (1999)
	*tub*2	Bt2a	Bt2b	Glass & Donaldson (1995)
Dothiorella	ITS	ITS5	ITS4	White et al. (1990)
	*tef*1-α	EF1-728F	986F	Carbone & Kohn (1999)
	*tub*2	Bt2a	Bt2b	Glass & Donaldson (1995)
Lasiodiplodia	ITS	ITS5	ITS4	White et al. (1990)
	*tef*1-α	EF1-728F	986F	Carbone & Kohn (1999)
	*tub*2	Bt2a	Bt2b	Glass & Donaldson (1995)
Neofusicoccum	ITS	ITS5	ITS4	White et al. (1990)
	*rpb*2	Frpb2-5F	Frpb2-7Cr	Liu et al. (1999)
	*tef*1-α	EF1-728F	986F	Carbone & Kohn (1999)
	*tub*2	Bt2a	Bt2b	Glass & Donaldson (1995)
Cladosporium	ITS	ITS5	ITS4	White et al. (1990)
	*tef*1-α	EF1-728F	986F	Carbone & Kohn (1999)
	act	ACT-512F	ACT-783R	Carbone & Kohn (1999)
Rhytidhysteron	ITS	ITS5	ITS4	White et al. (1990)
	LSU	LR0R	LR5	Vilgalys & Sun (1994)
	SSU	NS1	NS4	White et al. (1990)
	*tef*1-α	ef1-983F	ef1-2218R	Rehner & Buckley (2005)
Kirschsteiniothelia	ITS	ITS5	ITS4	White et al. (1990)
	LSU	LR0R	LR5	Vilgalys & Sun (1994)
	SSU	NS1	NS4	White et al. (1990)
Cercospora	ITS	ITS5	ITS4	White et al. (1990)
	cal	CAL228F	CAL737R	Carbone & Kohn (1999)
Ragnhildiana	ITS	ITS5	ITS4	White et al. (1990)
	LSU	LR0R	LR5	Vilgalys & Sun (1994)
	*rpb*2	Frpb2-5F	Frpb2-7Cr	Liu et al. (1999)
Sphaerulina	ITS	ITS5	ITS4	White et al. (1990)
	LSU	LSU1Fd	LR5	Vilgalys & Sun (1994); Crous et al. (2009)
	*tef*1-α	ef1-983F	ef1-2218R	Rehner & Buckley (2005)
	*tub*2	T1	β-S&y-R	Glass & Donaldson (1995); Stukenbrock et al. (2012)
	*rpb*2	Frpb2-5F	Frpb2-7Cr	Liu et al. (1999)
Palmiascoma	ITS	ITS5	ITS4	White et al. (1990)
	LSU	LR0R	LR5	Vilgalys & Sun (1994)

Table 1 Continued.

Genera	Primers	Forward	Reverse	References
	SSU	NS1	NS4	White et al. (1990)
	*rpb*2	Frpb2-5F	Frpb2-7Cr	Liu et al. (1999)
Pseudochaetosphaeronema	ITS	ITS5	ITS4	White et al. (1990)
	LSU	LR0R	LR5	Vilgalys & Sun (1994)
	SSU	NS1	NS4	White et al. (1990)
	*tef*1-α	ef1-983F	ef1-2218R	Rehner & Buckley (2005)
Helminthosporium	ITS	ITS5	ITS4	White et al. (1990)
	LSU	LR0R	LR5	Vilgalys & Sun (1994)
	SSU	NS1	NS4	White et al. (1990)
	*tef*1-α	ef1-983F	ef1-2218R	Rehner & Buckley (2005)
	*rpb*2	fRPB2-5F	fRPB2-7cR	Liu et al. (1999)
Periconia	ITS	ITS5	ITS4	White et al. (1990)
	LSU	LR0R	LR5	Vilgalys & Sun (1994)
	SSU	NS1	NS4	White et al. (1990)
	*tef*1-α	ef1-983F	ef1-2218R	Rehner & Buckley (2005)
Paraphoma	ITS	ITS5	ITS4	White et al. (1990)
	*tef*1-α	ef1-983F	ef1-2218R	Rehner & Buckley (2005)
	*tub*2	T1	Bt2b	Glass & Donaldson (1995); O'Donnell & Cigelnik (1997)
Alternaria	ITS	ITS5	ITS4	White et al. (1990)
	LSU	LR0R	LR5	Vilgalys & Sun (1994)
	*tef*1-α	ef1-983F	ef1-2218R	Rehner & Buckley (2005)
	*rpb*2	fRPB2-5F	fRPB2-7cR	Liu et al. (1999)
	gapdh	GDF1	GDR1	Berbee et al. (1999)
Aurantiascoma	ITS	ITS5	ITS4	White et al. (1990)
	LSU	LR0R	LR5	Vilgalys & Sun (1994)
	SSU	NS1	NS4	White et al. (1990)
	*tef*1-α	ef1-983F	ef1-2218R	Rehner & Buckley (2005)
	*rpb*2	fRPB2-5F	fRPB2-7cR	Liu et al. (1999)
Myrmaecium	ITS	ITS5	ITS4	White et al. (1990)
	LSU	LR0R	LR5	Vilgalys & Sun (1994)
	*tef*1-α	ef1-983F	ef1-2218R	Rehner & Buckley (2005)
	*rpb*2	fRPB2-5F	fRPB2-7cR	Liu et al. (1999)
Penicillium	ITS	ITS5	ITS4	White et al. (1990)
	*tub*2	T1	Bt2b	Glass & Donaldson (1995); O'Donnell & Cigelnik (1997)
	CaM	CF1	CF4	Peterson et al. (2005)
Botrytis	*gapdh*	GDF1	GDR1	Berbee et al. (1999)
	*hsp*60	HSP60for	HSP60rev	Staats et al. (2005)
	*rpb*2	fRPB2-5F	fRPB2-7cR	Liu et al. (1999)
Neopestalotiopsis	ITS	ITS5	ITS4	White et al. (1990)
	*tef*1-α	ef1-983F	ef1-2218R	Rehner & Buckley (2005)
	*tub*2	T1	Bt2b	Glass & Donaldson (1995); O'Donnell & Cigelnik (1997)
Pestalotiopsis	ITS	ITS5	ITS4	White et al. (1990)
	*tef*1-α	ef1-983F	ef1-2218R	Rehner & Buckley (2005)
	*tub*2	T1	Bt2b	Glass & Donaldson (1995); O'Donnell & Cigelnik (1997)
Diaporthe	ITS	ITS5	ITS4	White et al. (1990)
	*tef*1-α	ef1-983F	ef1-2218R	Rehner & Buckley (2005)
	*tub*2	T1	Bt2b	Glass & Donaldson (1995); O'Donnell & Cigelnik (1997)
	cal	CAL228F	CAL737R	Carbone & Kohn (1999)
	his	CYLH4F	CYLH3-1b	Crous et al. (2006b); Glass & Donaldson (1995)
Neomelanconis	ITS	ITS5	ITS4	White et al. (1990)
	LSU	LR0R	LR5	Vilgalys & Sun (1994)

Table 1 Continued.

Genera	Primers	Forward	Reverse	References
	*tef*1-α	ef1-983F	ef1-2218R	Rehner & Buckley (2005)
	*rpb*2	fRPB2-5F	fRPB2-7cR	Liu et al. (1999)
Ophiognomonia	ITS	ITS5	ITS4	White et al. (1990)
	*tef*1-α	ef1-983F	ef1-2218R	Rehner & Buckley (2005)
	*ms*204	MSE1F1n1	MS-E5R2n	Walker et al. (2012b)
Juglanconis	ITS	V9G	LR5	De Hoog & Gerrits van den Ende 1998; Vilgalys & Hester 1990
	LSU	LR0R	LR5	Vilgalys & Sun (1994)
	*tub*2	T1	BtHV2r	Glass & Donaldson (1995); Voglmayr et al. (2017b)
Colletotrichum	ITS	ITS5	ITS4	White et al. (1990)
	*tub*2	T1	Bt2b	Glass & Donaldson (1995); O'Donnell & Cigelnik (1997)
	act	ACT-512F	ACT-783R	Carbone & Kohn (1999)
	chs-1	CHS-79F	CHS-354R	Carbone & Kohn (1999)
Acremonium	ITS	ITS5	ITS4	White et al. (1990)
	LSU	LR0R	LR5	Vilgalys & Sun (1994)
	*tef*1-α	ef1-983F	ef1-2218R	Rehner & Buckley (2005)
	*tub*2	T1	Bt2b	Glass & Donaldson (1995); O'Donnell & Cigelnik (1997)
	*rpb*2	fRPB2-5F	fRPB2-7cR	Liu et al. (1999)
Clonostachys	ITS	ITS5	ITS4	White et al. (1990)
	LSU	LR0R	LR5	Vilgalys & Sun (1994)
	*tef*1-α	ef1-688F	ef1-1251R	Alves et al. (2008)
	*tub*2	T1	Bt2b	Glass & Donaldson (1995); O'Donnell & Cigelnik (1997)
Lecanicillium	ITS	ITS5	ITS4	White et al. (1990)
	LSU	LR0R	LR5	Vilgalys & Sun (1994)
	*rpb*2	fRPB2-5F	fRPB2-7cR	Liu et al. (1999)
	*tef*1-α	ef1-983F	ef1-2218R	Rehner & Buckley (2005)
Fusarium	*rpb*2	fRPB2-5F	fRPB2-7cR	Liu et al. (1999)
Albonectria	*tef*1-α	EF-1	EF-2	O'Donnell et al. (1998)
Neocosmospora	*tub*2	T1	Bt2b	Glass & Donaldson (1995); O'Donnell & Cigelnik (1997)
Microcera	ITS	ITS5	ITS4	White et al. (1990)
	LSU	LR0R	LR5	Vilgalys & Sun (1994)
	*tef*1-α	ef1-728F	EF-2	Carbone & Kohn (1999); O'Donnell et al. (1998)
Nectria	ITS	ITS5	ITS4	White et al. (1990)
	LSU	LR0R	LR5	Vilgalys & Sun (1994)
	*tef*1-α	ef1-728F	ef1-986R	Carbone & Kohn (1999)
	*rpb*2	fRPB2-5F	fRPB2-7cR	Liu et al. (1999)
	act	ACT-512F	ACT1Rd	Carbone & Kohn (1999)
Trichothecium	LSU	LR0R	LR5	Vilgalys & Sun (1994)
	SSU	NS1	NS4	White et al. (1990)
Scopulariopsis	LSU	LR0R	LR5	Vilgalys & Sun (1994)
	*tef*1-α	ef1-983F	ef1-2218R	Rehner & Buckley (2005)
	*tub*2	Bt2a	Bt2b	Glass & Donaldson (1995)
Diatrypella	ITS	ITS5	ITS4	White et al. (1990)
	*tub*2	T1	Bt2b	Glass & Donaldson (1995); O'Donnell & Cigelnik (1997)
Eutypella	ITS	ITS5	ITS4	White et al. (1990)
	*tub*2	T1	Bt2b	Glass & Donaldson (1995); O'Donnell & Cigelnik (1997)
Paraeutypella	ITS	ITS5	ITS4	White et al. (1990)
	*tub*2	T1	Bt2b	Glass & Donaldson (1995); O'Donnell & Cigelnik (1997)

Table 1 Continued.

Genera	Primers	Forward	Reverse	References
Peroneutypa	ITS	ITS5	ITS4	White et al. (1990)
	*tub*2	T1	Bt2b	Glass & Donaldson (1995); O'Donnell & Cigelnik (1997)
Hypoxylon	ITS	ITS5	ITS4	White et al. (1990)
	LSU	LR0R	LR5	Vilgalys & Sun (1994)
	*rpb*2	fRPB2-5F	fRPB2-7cR	Liu et al. (1999)
	*tub*2	T1	Bt2b	Glass & Donaldson (1995); O'Donnell & Cigelnik (1997)

Note – ITS, the rRNA internal transcribed spacer region; SSU, the nuclear rRNA small subunit gen e (18S); LSU, the nuclear rRNA large subunit gene (28S); *tef*1-α, the translation elongation factor1-α gene region; *rpb*2, the RNA polymerase II second largest subunit gene; *tub*2, the β-tubulin gene; *ms*204, the guanine nucleotide-binding protein subunit beta (MS204) gene; *CaM*, calmodulin gene; *hsp*60, the *hsp*60 gene; *his*, the histone gene; *act*, the actin gene; *chs*-1, the chitin synthase I gene; *g apdh*, the glyceraldehyde-3-phosphate dehydrogenase gene.

Table 2 PCR primer amplification program.

Cycles	Temperature (℃)	Duration
ITS, LSU, SSU, *tef*1-α, *hsp*60		
1	94 denature	3 min
35	94 denature	30 s
	55 anneal	50 s
	72 extensions	1 min
1	72 extensions	10 min
*rpb*2		
1	95 denature	5 min
35	95 denature	1 min
	52 anneal	2 min
	72 extensions	90 s
1	72 extensions	10 min
*ms*204		
1	94 denature	5 min
30	94 denature	30 s
	55 anneal	30 s
	72 extensions	1 min
1	72 extensions	10 min
cal, *gapdh*, *chs*-1		
1	95 denature	4 min
35	95 denature	30 s
	58 anneal	30 s
	72 extensions	45 s
1	72 extensions	45 s
act		
1	94 denature	3 min
35	94 denature	30 s
	60 anneal	50 s
	72 extensions	1 min
1	72 extensions	10 min

Table 2 Continued.

Cycles	Temperature (℃)	Duration
his		
1	96 denature	5 min
30	96 denature	30 s
	52 anneal	30 s
	72 extensions	1 min
1	72 extensions	5 min
*tub*2		
1	96 denature	5 min
30	96 denature	30 s
	52 anneal	30 s
	72 extensions	1 min
1	72 extensions	5 min
CaM		
1	94 denature	4 min
30	94 denature	1 min
	55 anneal	50 s
	72 extensions	2 min
1	72 extensions	10 min

Sequence Alignment and Phylogenetic Analyses

The sequences of closely related strains were identified through a BLAST search in GenBank, and all molecular data for this study were confirmed and obtained in accordance with recent publications. The sequences were downloaded from GenBank (http://www.ncbi.nlm.nih.gov/). To compare all sequences of single genes and multigene (*act*, *cal*, *chs*-1, *gapdh*, *his*, *hsp*60, ITS, LSU, *ms*204, *rpb*2, SSU, *tef*1-α, and *tub*2), MAFFT v.7 (available at https://mafft.cbrc.jp/alignment/server/, Katoh et al., 2019) was used. If necessary, manual adjustments were made using BioEdit v.7.0.5.2 software (Hall 1999). The consistency of the single gene sequence data was evaluated, allowing for the determination of the overall topological structure. The multigene sequences were concatenated using Mesquite version 3.11 (build 766) (Maddison & Maddison, 2019). Phylogenetic analysis of the multigene sequences was conducted by integrating Bayesian inference (BI) and maximum likelihood (ML) methods. The best nucleotide substitution model was determined using MrModeltest v. 2.2 based on the Akaike Information Criterion (AIC) (Nylander 2004). Clustal X version 1.81 was used to convert the alignment into a NEXUS file (.nxs) (Thompson et al. 1997), after which Bayesian inference (BI) analysis was performed (Ronquist & Huelsenbeck 2003). Six Markov chains were run simultaneously for a total of 5,000 generations, with tree sampling occurring every 100th generation. The aging frequency was set to 0.25, and the system automatically stopped running when the average standard deviation of split frequencies dropped below 0.01 (Maharachchikumbura et al. 2015). Maximum likelihood analysis was performed using the CIPRES Science Gateway network server (Miller et al. 2017), selecting RAxML-HPC2 on XSEDE (version 8.2.10) (Stamatakis, 2014) with the GTRGAMMA substitution model for 1,000 bootstrap iterations. The phylogenetic tree was visualized using FigTree v. 1.4.3 (Rambaut 2014), and Adobe Illustrator CS6 v. 16.0.0 was employed for layout and enhancement. The maximum likelihood bootstrap values (MLBS), which are equal to or greater than 60%, and the Bayesian posterior probability values (BYPP), which exceed 0.90, are indicated in these phylogenetic trees. All sequences used and generated in this paper are submitted to GenBank and listed in Appendix Table 1.

Genealogical concordance phylogenetic species recognition analysis

Genealogical concordance phylogenetic species recognition analysis is a model test that can effectively detect significant recombination events (Taylor et al. 2000). In this study, SplitsTree V4 software was used, and data were analyzed using the pairwise homoplasy index (PHI) test to determine the recombination level among closely related species (Bruen et al. 2006, Quaedvlieg et al. 2014). If the pairwise homoplasy index is below the 0.05 threshold ($\Phi w < 0.05$), it indicates that significant recombination is present in the dataset. A multi-locus concatenated dataset comprising closely related species was used for the analysis. Split graphs were constructed from the concatenated dataset using the LogDet transformation and splits decomposition options to visualize the relationships among closely related taxa.

RESULTS AND DISCUSSION

Symptom Identification and Overall Species Summary

In this study, a total of 245 fungal strains were isolated from various parts of walnut plants, including their branches, leaves, fruits, and litter. The fungi were identified through morphological characteristics and multigene phylogenetic approaches, resulting in the classification of one phylum, four classes, 14 orders, 26 families, 42 genera, and 90 species from our newly collected specimens. Among them, *Fusarium*, *Colletotrichum*, and *Diaporthe* are the most commonly isolated genera, with higher isolation frequencies compared to other fungal genera (Table 3). This study only introduces species of *Ascomycota*, and the sequence analysis of all species is fully consistent with the latest taxonomic outline of the *Ascomycota* or recently published papers (Wijayawardene et al. 2024). The classes, orders, families, genera and species are arranged in alphabetical order.

Samples with obvious disease characteristics were also collected at the site. In the wild, disease manifestations are primarily observed on leaves, branches, and fruits (see Fig. 1). Among them, leaf diseases are the most evident, but their impact on the plants is relatively weak. However, branch diseases have the highest diversity of pathogenic fungi and have the most severe impact on the plants, potentially causing death in severe cases. Fruit diseases have the deepest economic impact on walnuts, with massive fruit drop leading to complete crop failure.

Taxonomy

Dothideomycetes sensu O.E. Erikss. & Winka.
Dothideomycetes O.E. Erikss. & Winka, Myconet 1(1): 5 (1997).

Dothideomycetes is the foremost classes within *Ascomycota* with an estimated 19,000 species (Kirk et al. 2008, Schoch et al. 2009a). Rossman et al. (2015) provided recommended names for pleomorphic genera in *Dothideomycetes*. We follow the latest treatments and updated accounts of *Dothideomycetes* in Hyde et al. (2024).

Botryosphaeriales C.L. Schoch, et al., Mycologia 98(6): 1050 (2007)

Botryosphaeriales was introduced to accommodate a single family *Botryosphaeriaceae,* by Schoch et al. (2006). Schoch et al. (2009a) accepted its position in the *Pleosporomycetidae*. Later, *Planistromellaceae* was recognised as a distinct family within *Botryosphaeriales* (Minnis et al. 2012). Liu et al. (2012) provided a phylogenetic analysis of *Botryosphaeriales* and included the families *Botryosphaeriaceae* and *Phyllostictaceae*. Wikee et al. (2013) redefined the *Phyllosticta*, and shows that it clusters sister to the *Botryosphaeriaceae* (*Botryosphaeriales*, *Dothideomycetes*), for which the older family name *Phyllostictaceae* is resurrected. Subsequently, six families, *Aplosporellaceae*, *Saccharataceae*, *Melanopsaceae*, *Septorioideaceae*, *Endomelanconiopsidaceae* and *Pseudofusicoccaceae*, were introduced (Slippers et al. 2013, Wyka & Broders 2016, Yang et al. 2017). Phillips et al. (2019) re-assessed the families of *Botryosphaeriales* in terms of morphology, phylogeny and evolution analysis, and synonymized three families, *Endomelanconiopsidaceae* with *Botryosphaeriaceae*, *Pseudofusicoccaceae* with *Phyllostictaceae*, and *Septorioideaceae* with

Saccharataceae. Currently, through divergence time estimation and phylogenetic analysis, a total of six families have been identified within the *Botryosphaeriales*, namely, *Aplosporellaceae*, *Botryosphaeriaceae*, *Melanopsaceae*, *Phyllostictaceae*, *Planistromellaceae*, and *Saccharataceae*, which are accepted as familial classifications within this order (Hongsanan et al. 2020a, Rathnayaka et al. 2023).

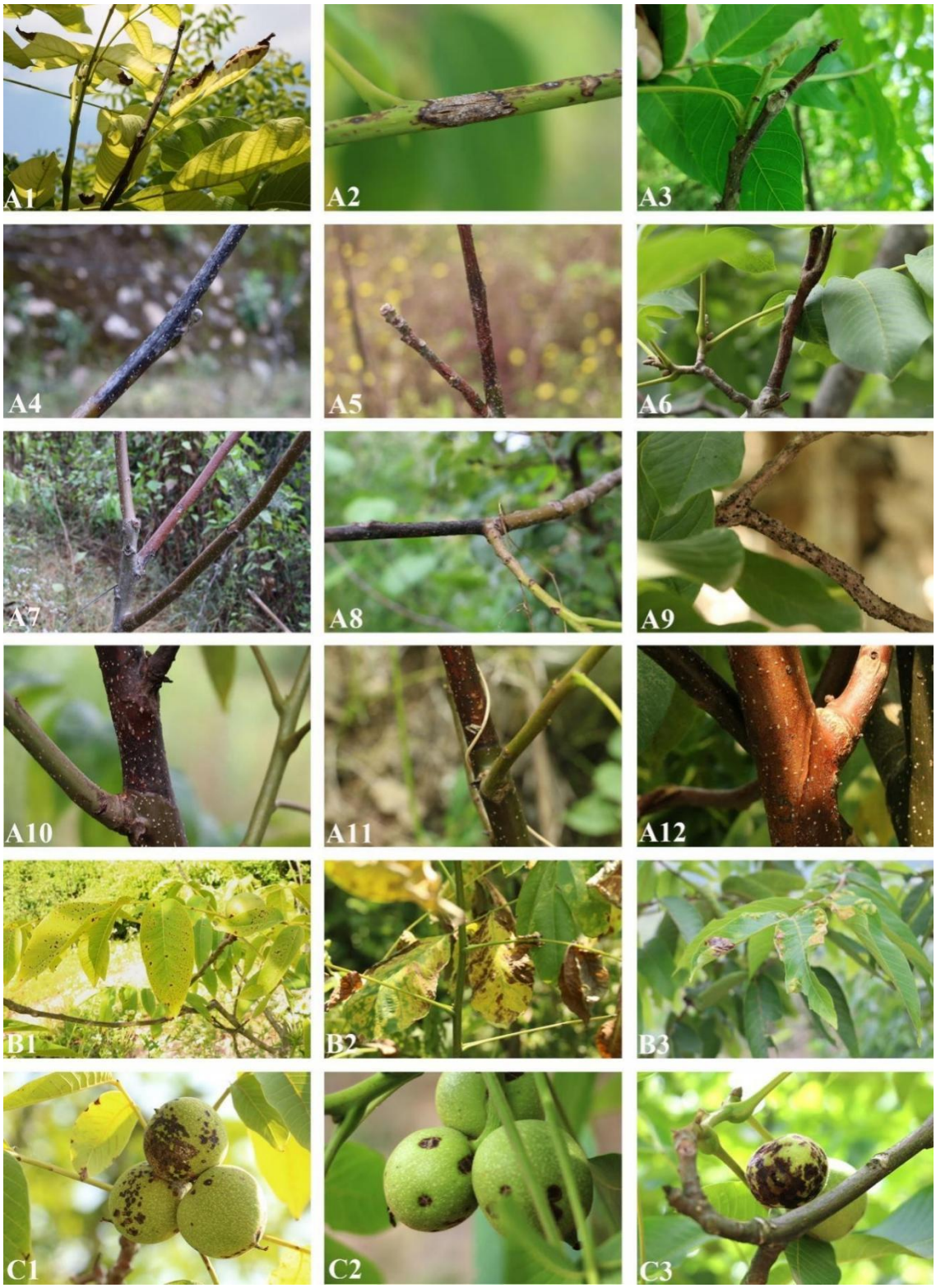


Figure 1 – Representative symptoms of disease in walnut orchards. A1–A12: Symptoms of disease on branches and trunks; B1–B3: Symptoms of disease on leaves; C1–C3: Symptoms of disease on fruits.

Table 3 List of fungal species identified in this study.

Species	Host	Tissue	Geographical distribution
Acremonium hennebertii	*Juglans regia*	Branch	Neijiang
Albonectria rigidiuscula	*J. regia*	Leaf	Chongzhou
Alternaria alternata	*J. regia*	Leaf	Shehong
A. doliconidium	*J. regia*	Leaf	Bazhong
A. ganziense	*J. regia*	Leaf	Ganzi
A. italica	*J. regia*	Leaf	Wenchuan, Huili
A longipes	*J. regia*	Leaf	Luding
Aurantiascoma juglandis	*J. sigillata*	Branch	Huili
Botrytis cinerea	*J. regia*	Fuit	Wanyuan
Botryosphaeria dothidea	*J. regia*	Branch	Chongzhou
B. gaoxianense	*J. regia*	Branch	Yibin
B. neijiangense	*J. regia*	Twig	Neijiang, Huili
B. wangensis	*J. regia*	Twig	Shehong
B. yibinense	*J. regia*	Twig	Yibin
Cercospora nicotianae	*J. regia*	Leaf	Bazhong
Cladosporium cladosporioides	*J. regia*	Leaf	Bazhong
C. rugae	*J. regia*	Leaf	Lixian
Clonostachys rosea	*J. regia*	Branch	Chongzhou
Colletotrichum beichuanense	*J. regia*	Leaf	Beichuan
C. fioriniae	*J. regia*	Leaf	Guangyuan
C. fructicola	*J. regia*	Leaf	Shehong
C. gloeosporioides	*J. regia*	Leaf	Shehong
C. godetiae	*J. regia*	Fruit	Aba
C. scovillei	*J. regia*	Leaf	Gaoxian
C. shehongense	*J. regia*	Petiole	Shehong
C. siamense	*J. regia*	Leaf	Yanting
Diaporthe citri	*J. regia*	Branch	Yibin
D. eres	*J. regia*	Branch	Luding
D. mianyangense	*J. regia*	Twig	Yanting
D. novem	*J. regia*	Branch	Panzhihua
D. pseudomangiferae	*J. regia*	Branch	Neijiang
D. ravennica	*J. regia*	Branch	Huili
D. tectonae	*J. regia*	Branch	Chongzhou
D. tulliensis	*J. regia*	Branch	Yanting
D. vawdreyi	*J. regia*	Branch	Guling
Diatrypella vulgaris	*J. regia*	Branch	Chongzhou
Dothiorella pugeense	*J. regia*	Branch	Puge
Eutypella microtheca	*J. regia*	Branch	Pingwu
Fusarium coffeatum	*J. regia*	Leaf	Neijiang
F. graminearum	*J. regia*	Branch	Panzhihua
F. incarnatum	*J. regia*	Branch	Shehong
F. lateritium	*J. regia*	Fruit	Bazhong
Helminthosporium juglandinum	*J. regia*	Branch	Yanting
H. velutinum	*J. regia*	Twig	Junlian
Hypoxylon perforatum	*J. regia*	Branch	Guangyuan
Juglanconis appendiculata	*J. sigillata*	Branch	Pingwu
J. mucosporium	*J. regia*	Branch	Beichuan
J. magnatum	*J. regia*	Branch	Chendu
J. juglandina	*J. regia*	Branch	Ganzi

Table 3 Continued.

Species	Host	Tissue	Geographical distribution
Kirschsteiniothelia yantingense	*J. regia*	twig	Yanting
Lecanicillium dimorphum	*J. regia*	Branch	Chongzhou
Lasiodiplodia chongzhouense	*J. regia*	Twig	Chongzhou, Yanting
L. juglans	*J. regia*	Twig	Puge
L. pseudotheobromae	*J. sigillata*	Branch	Chongzhou
L. theobromae	*J. regia*	Twig	Shehong
Microcera chrysomphaludis	*J. regia*	Trunk	Liangshan
Myrmaecium fulvopruinatum	*J. regia*	Branch	Chongzhou
Nectria fusiformispora	*J. regia*	Branch	Liangshang
N. pseudotrichia	*J. regia*	Branch	Luding
Neocosmospora solani	*J. regia*	Leaf	Neijiang
Neomelanconis juglandis	*J. regia*	Branch	Guling, Pingwu
Neopestalotiopsis chiangmaiensis	*J. regia*	Leaf	Luzhou
Neofusicoccum juglans	*J. regia*	Twig	Chongzhou
N. parvum	*J. regia*	Twig	Neijiang
N. sichuanense	*J. regia*	Twig	Guangyuan
N. wenchuanense	*J. regia*	Twig	Wenchuan
Ophiognomonia leptostyla	*J. sigillata*	Leaf	Ganzi
O. pseudopterocaryae	*J. regia*	petiole	Lixian
O. pterocaryae	*J. regia*	petiole	Huili
Palmiascoma qujingense	*J. regia*	Branch	Chongzhou
Paraeutypella citricola	*J. regia*	Branch	Shehong
P. neijiangense	*J. regia*	Branch	Neijiang
Paraphoma dioscoreae	*J. regia*	Petiole	Shehong
Penicillium citrinum	*J. regia*	Fruit	Guangyuan
Periconia byssoides	*J. regia*	Leaf	Bazhong
P. pseudobyssoides	*J. regia*	Petiole	Huili
P. thailandica	*J. regia*	Twig	Chongzhu
P. yantingense	*J. regia*	Twig	Yanting
Peroneutypa rubiformis	*J. regia*	Branch	Pingwu
Pestalotiopsis kenyana	*J. regia*	Branch	Yibin
P. vismiae	*Carya illinoensis*	Fruit	Chongzhou
Pseudochaetosphaeronema kunmingense	*J. sigillata*	Branch	Huili
Ragnhildiana diffusa	*J. regia*	Leaf	Chongzhou
Rhytidhysteron rufulum	*J. regia*	Twig	Shehong
R. sichuanensis	*J. regia*	Twig	Chongzhou
R. subrufulum	*J. regia*	Twig	Pinwu
Scopulariopsis pseudobrevicaulis	*J. sigillata*	Leaf	Neijiang
Sphaerulina juglandina	*J. regia*	Leaf	Neijiang
S. curvecylindrospora	*J. regia*	Leaf	Huili
Trichothecium downum	*J. regia*	Leaf	Chongzhou

Botryosphaeriaceae Theiss. & Syd

Botryosphaeriaceae was introduced by Theissen and Sydow (1918) to accommodate three genera, *Botryosphaeria*, *Dibotryon* and *Phaeobotryon*. Subsequently, *Neodeightonia* was introduced by Punithalingam (1969). Over decades of taxonomic revisions and updates based on morphology, the family has become increasingly complex. Initially, the family had been successively put into the orders *Dothideales* (von Arx & Müller 1954) and *Pleosporales* (Luttrell 1955), until Schoch et al. (2006) elevated *Botryosphaeriaceae* to the status of an order, as *Botryosphaeriales*. In this process, the number of genera in this family continuously either increased or reduced by various authors.

Currently, 24 genera are commonly accepted in *Botryosphaeriaceae* (Phillips et al. 2019, Hongsanan et al. 2020a, Wijayawardene et al. 2022a, Samarakoon et al. 2024).

Botryosphaeria Ces. & De Not., Comm. Soc. crittog. Ital. 1(fasc. 4): 211 (1863).

Botryosphaeria was introduced by Cesati & De Notaris (1863) based on the type species *B. dothidea*. This genus has undergone various revisions and updates over the years, at times encompassing a diverse range of morphologies. von Arx & Muller (1954) examined 183 taxa of *Botryosphaeriales* and reduced them to 11 species, with extensive synonymies under *B. dothidea* and *B. quercuum*, together with nine new combinations. In later studies these synonymies were not always accepted (Shoemaker 1964, Sivanesan 1984, Slippers et al. 2004). However, as the type material was immature, *B. dothidea* was epitypified by Slippers et al. (2004) based on morphology and phylogenetic data, which combined ITS, *tef*1-α and *tub*2 genes. Currently, Species Fungorum (2025) lists 242 epithets of *Botryosphaeria* species, but it is unclear, whether some of these would reside in *Diplodia*.

1. ***Botryosphaeria dothidea*** (Moug.) Ces. & De Not., Comm. Soc. crittog. Ital. 1(fasc. 4): 212 (1863) Fig. 2

Index Fungorum number: IF183247; Facesoffungi number: FoF03512

Associated with blight symptom on living branches of *Juglans regia*. Dead shoots can be observed in the lower branches or all over the affected tree. Affected branches or trunks show canker and some may have abundant resin flow. When the canker girdles the affected area, part of the tree above the canker dies. Sexual morph: *Ascostroma* 290–510 μm diam, black, circular or subglobose to globose, gregarious, uni- to multi-loculate, immersed to erumpent on host tissue, black dots with papillary protrusions, coriaceous, multiloculate, with 7–16 ascomata, with individual ostioles. *Ostiole* circular, central, papillate. *Peridium* composed of two-layered locules, outer layer composed of dark brown or brown thick-walled cells of *textura angularis*, inner layer composed of hyaline thin-walled cells of *textura angularis* lining the locule. *Pseudoparaphyses* 2.5–3.5 μm wide, hyphae-like, septate, no branch seen. *Asci* 78–132 × 17–23 μm ($\bar{x}$ = 108 × 21 μm, n = 40), 8-spored, bitunicate, fissitunicate, cylindrical to clavate, short pedicellatea, pically rounded with an ocular chamber. *Ascospores* 19–33 × 9–13 μm ($\bar{x}$ = 28 × 10.5 μm, n = 40), biseriate, hyaline, aseptate, fusoid to ovoid, sometimes with tapered ends, spindle-shaped, thin-walled, smooth with granular contents. Asexual morph: Not observed.

Cultural characteristics – Ascospores germinating on sterile water within 12 h and germ tubes produced from ends. Colonies on PDA reaching 60 mm diam., after 12 days at 25 ℃. The mycelium grows on the surface of the medium, forming circular colonies with well-developed aerial hyphae, fringed edges, a dense texture, and intact margins. Initially, the colonies are grayish-white, but they later turn dark brown to black. The reverse side appears black due to the production of black metabolites.

Material examined – China, Sichuan Province, Chengdu City, Chongzhou City (30°33′9.04″N 103°39′29.36″E, alt. 512 m), on living branches of *Juglans regia*, 16 May 2021, F.-H. Wang, WFH202105002 (SICAU 22-0114), living culture SICAUCC 22-0116.

GenBank numbers – SICAUCC 22-0116, OP964573 (LSU), OP963816 (ITS), OP962301 (SSU), OQ281399 (*tub*2), OQ281363 (*tef*1-α).

Note – This isolate is phylogenetically grouped with the type of *Botryosphaeria dothidea* (CBS 115476, ex-type) with strong statistical support (100% MLBS/1.00 BYPP) (Fig. 3). Morphologically, our strain shares similar morphology with the type of *Botryosphaeria dothidea* in having macronematous and overlap sized asci (78–132 × 17–23 μm vs. 96–144 × 18–25 μm), with biseriate, hyaline, aseptate, fusoid to ovoid, sometimes with tapered ends, thin-walled, similar sized ascospores (19–33 × 9–13 vs. 21–32 × 10–14 μm) (Jayawardena et al. 2022). Nucleotide comparisons of ITS, *tub*2, and *tef*1-α (SICAUCC 22-0116) also showed a high homology with the sequences of *B. dothidea* (CBS 115476), with a similarity of 100% (530/530, 0 gap), 100% (433/433, 0 gap), and 100% (283/283, 0 gap), respectively (Slippers et al. 2004). Based on morphological characters and

phylogenetic analyses, we determine our specimens as *B. dothidea*. *Botryosphaeria dothidea* is the type species of the genus, and was reported extensively from all around the world (Phillips et al. 2019).

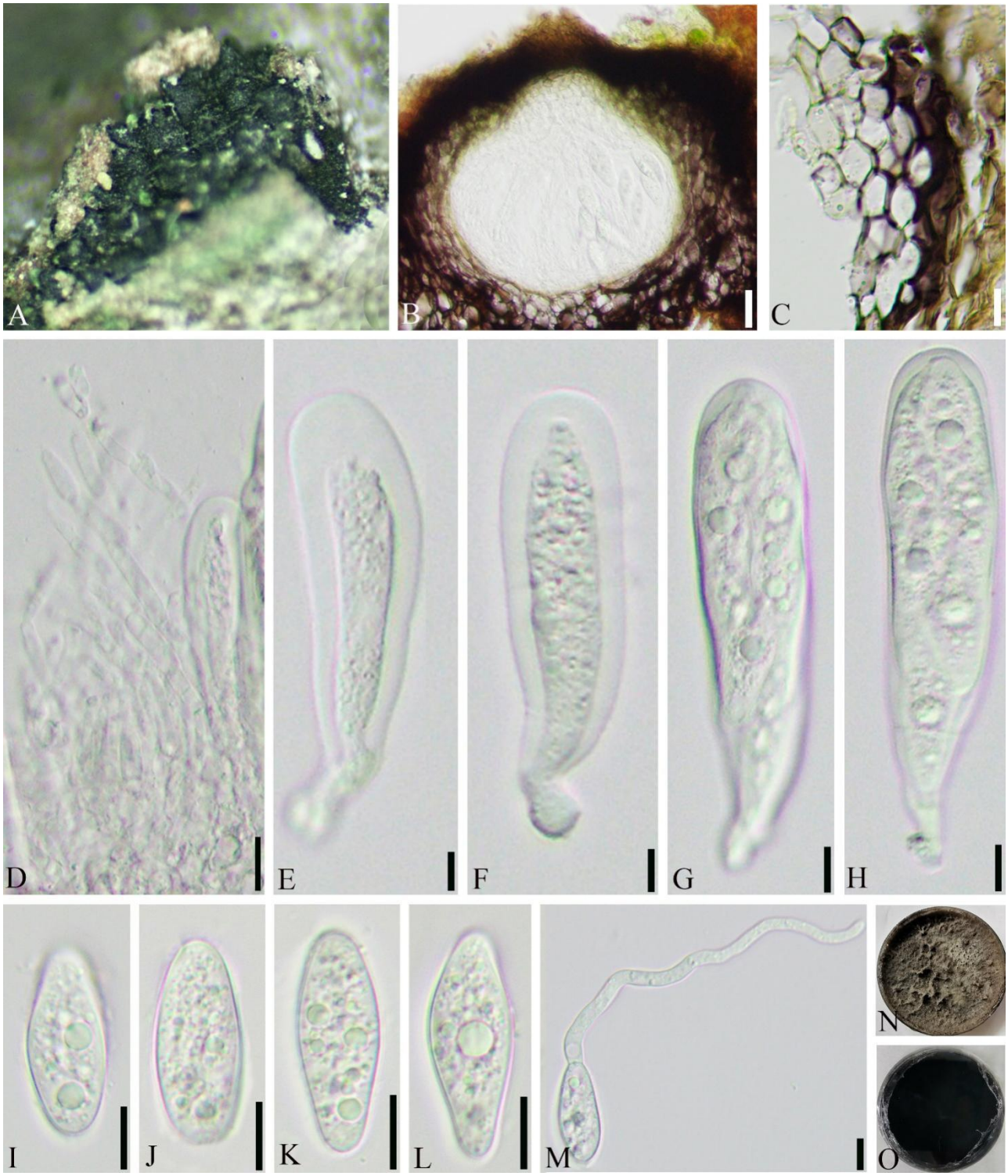


Figure 2 – *Botryosphaeria dothidea* (SICAU 22-0114). A Appearance of ascostroma on host substrate. B Section of ascoma. C Peridium. D Pseudoparaphyses and asci. E–H Asci. I–L Ascospores. M Germinating ascospore. N, O Colonies on PDA (N from above, O from below). Scale bars: B = 50 μm, D = 20 μm, C, E–M = 10 μm.

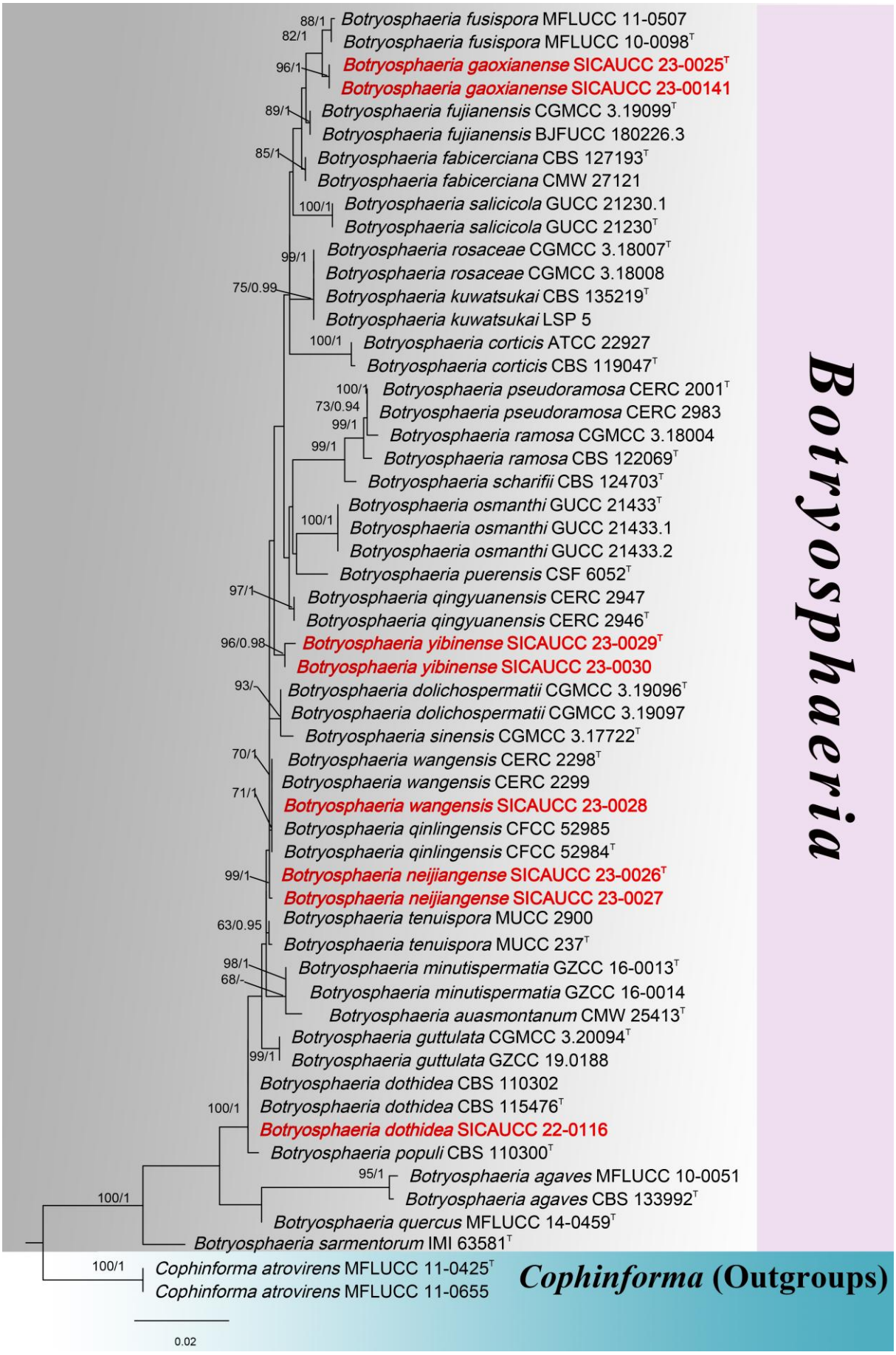


Figure 3 – Best scoring RAxML tree with a final likelihood value of -6,520.307172 based on combined ITS, *rpb*2, *tef*1-α and *tub*2 sequence data of related species. The tree is rooted with

Cophinforma atrovirens (MFLUCC 11-0425 and MFLUCC 11-0655). in *Botryosphaeriaceae*. Fifty-six strains were included in the analyses of the combined DNA loci and comprise 3,012 characters (990 characters for ITS, 938 characters for *rpb*2, 617 characters for *tef*1-α and 467 characters for *tub*2, including gaps). The matrix had 546 distinct alignment patterns with 52.10% undetermined characters and gaps. Estimated base frequencies were: A = 0.218600, C = 0.297627, G = 0.260903, T = 0.222870; substitution rates AC = 0.881817, AG = 3.223105, AT = 1.025336, CG = 0.911114, CT = 5.281710, GT = 1.000000; gamma distribution shape parameter α=0.161551. The Bayesian inference analyses was implemented by MrBayes v.3.2.2 with the best-fit model (HKY+I for ITS, *rpb*2, *tub*2; HKY+G for *tef*1-α) of evolution estimated with MrModeltest 2.2. The species determined in this study is indicated in red and bold. Bootstrap support values for maximum likelihood (MLBS, left) ⩾ 60% and Bayesian posterior probabilities (BYPP, right) ⩾ 0.90 are indicated at the nodes, respectively. Hyphens (-) represent support values less than 50% MLBS/0.90 BYPP. The ex-type superscript "T".

2. ***Botryosphaeria gaoxianense*** F.H. Wang & C.L. Yang, sp. nov. Fig. 4

Index Fungorum number: IF901556; Facesoffungi number: FoF15573

Etymology – Named after locality where the fungus was isolated for the first time.

Holotype – SICAU 23-0046.

Associated with branch blight on dead branches of *Juglans regia*. Symptoms include sudden wilting of small branches, yellowing of foliage, stunted growth, and premature defoliation. Olive-green to black streaks can be observed in the sapwood of infected branches. Sexual morph: Not observed. Asexual morph: *Conidiomata* 260–480 × 300–410 μm ($\bar{x}$ = 320 × 355 μm, n = 20), pycnidial, gregarious, uni- to multi-loculate, immersed to semi-immersed, raised, becoming erumpent through host epidermis, ostiolate. *Ostiole* central, circular, non-papillate. *Conidiomata wall* 18–32 μm wide, outer layer composed of thick-walled, dark brown cells of *textura angularis*, inner layer composed of thin-walled, hyaline to pale brown cells of *textura angularis*. *Conidiogenous cells* 6–12 × 3–5 μm wide ($\bar{x}$ = 9 × 4 μm, n = 20), holoblastic, hyaline, cylindrical, integrated, proliferating, producing a single apical conidium. *Conidia* 16–28 × 5–7 μm wide ($\bar{x}$ = 24 × 6 μm, n = 40), hyaline, aseptate, fusiform to ellipsoidal, sometimes irregular ellipsoidal, smooth, apex obtuse, base subtruncate or bluntly round, granular.

Culture characteristics – Conidia germinating on sterile water within 12 h and germ tubes produced from ends. Colonies on PDA reaching 60 mm diam., after 6 days at 25 ℃. The mycelium grows on the surface of the medium, forming circular colonies with well-developed aerial hyphae that are flocculent. The edges of the colonies are radiate and intact, initially white but later turning black. The reverse side of the colonies appears black, and not produced pigmentation on PDA media.

Material examined – China, Sichuan Province, Yibin City, Gaoxian County (28°28′56.38″N 104°38′59.27″E, alt. 531 m), on the dead branch of *Juglans regia*, 16 April 2022, F.-H. Wang, WFH202204047 (SICAU 23-0046, holotype), ex-type living culture SICAUCC 23-0025. *Ibid*., WFH202204047B (SICAU 23-0162), living culture SICAUCC 23-0141.

GenBank numbers – SICAUCC 23-0025, PP060641 (ITS), PP061110 (*rpb*2), PP061157 (*tub*2) and PP061125 (*tef*1-α); SICAUCC 23-0141, PP844869 (ITS), PP850046 (*rpb*2), PP850058 (*tub*2) and PP850050 (*tef*1-α).

Note – In the phylogenetic analyses of combined ITS, *rpb*2, *tef*1-α and *tub*2 sequence data, our strain (SICAUCC 23-0025 and SICAUCC 23-0141) formed a separate branch and clusters with strong statistical support (96% MLBS/1.00 BYPP). In the phylogenetic analyses, our strain (SICAUCC 23-0025 and SICAUCC 23-0141) clusters as sister to *B. fusispora* (MFLUCC 10-0098 and MFLUCC 11-0507) with statistical support (82% MLBS/0.98 BYPP) (Fig. 3) The conidia of both *B. fusispora* and *B. gaoxianense* are hyaline, aseptate, and exhibit shapes ranging from fusiform to ellipsoidal, sometimes irregularly ellipsoidal. They are smooth with obtuse apices and subtruncate or bluntly round bases that are granular. However, a distinguishing feature between the two is that *B. fusispora* forms solitary conidiomata, while *B. gaoxianense* forms clustered conidiomata. However, *B. gaoxianense* has larger but smaller conidiomata and smaller conidia than *B. fusispora* conidiomata

(260–480 × 300–410 µm vs. 140–180 × 160–210 µm), conidia (16–28 × 5–7 µm vs. 16–22 × 4–5.5 µm) (Liu et al.2012). Nucleotide comparisons reveal notable genetic dissimilarities between *B. gaoxianense* and *B. fusispora* (MFLUCC 10-0098, ex-type), viz. 0.2% (1/520, 1 gap), 2.3% (6/266, 2 gaps), 1.5% (11/718, 3 gaps), and 1.2% (5/429, 0 gap) in the ITS, *tef*1-α, *rpb*2, and *tub*2, respectively (Fig. 3). The PHI test revealed no significant recombination event between our strain and the closely related taxa (Φw = 0.37) (Fig. 4). Therefore, we introduce *B. gaoxianense* as a new species.

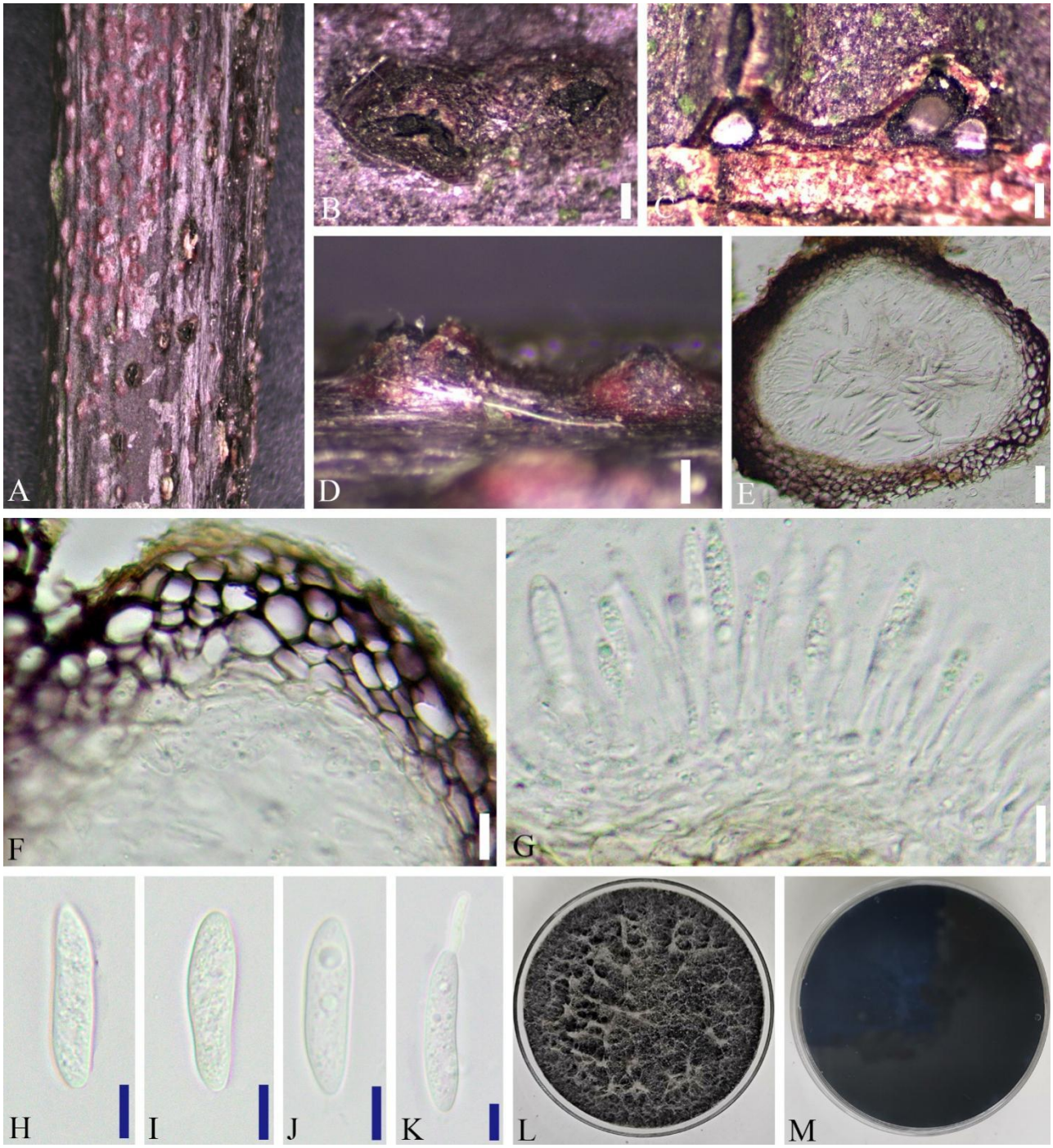


Figure 4 – *Botryosphaeria gaoxianense* (SICAU 23-0046, holotype). A, B, D Appearance of conidiomata on *Juglans regia*. C, E Vertical sections through conidiomata. F Section of conidiomata wall. G Conidiogenous cells and conidia. H–J conidia. K Geminating conidium. L, M Colonies on PDA (L from above, M from below). Scale bars: B–D = 200 µm, E = 50 µm, G = 20 µm, F, H–K = 10 µm.

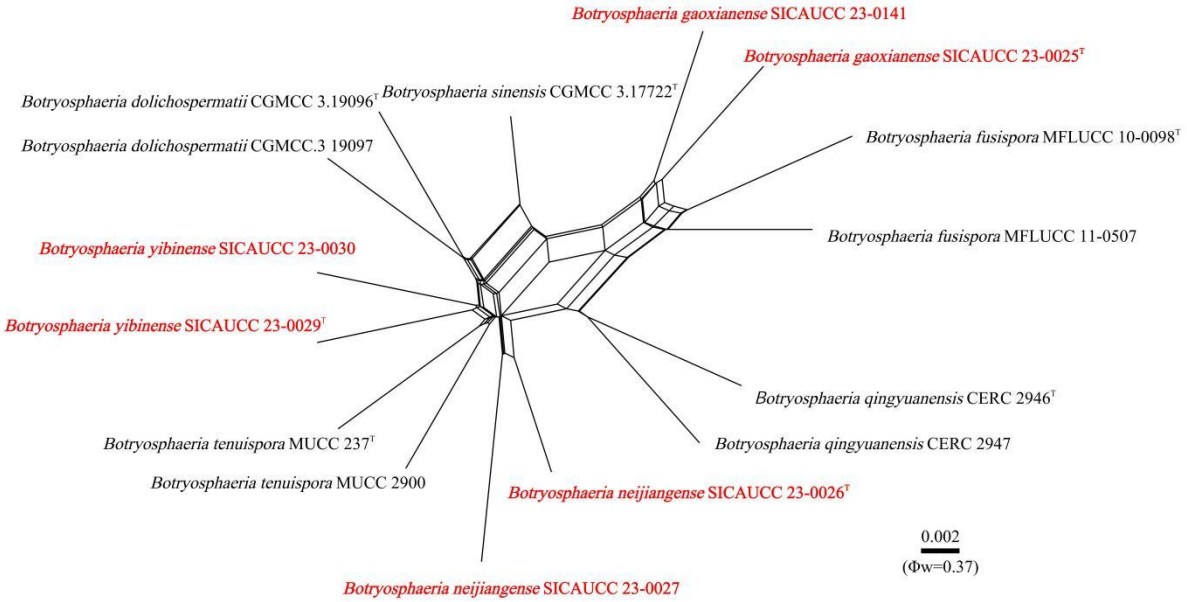


Figure 4 – The PHI test results for *Botryosphaeria gaoxianense*, *B. neijiangense*, *B. yibingense*, and closely related species were obtained using both LogDet transformation and splits decomposition methods. The PHI test did not find any statistically significant recombination (Φw = 0.37) in the data set. The new strains are represented in red and bold. "T" represents the type strain.

3. ***Botryosphaeria neijiangense*** F.H. Wang & C.L. Yang, sp. nov. Figs. 6, 7

Index Fungorum number: IF901557; Facesoffungi number: FoF15574

Etymology – Named after locality where the fungus was isolated for the first time.

Holotype – SICAU 23-0047.

Associated with branch blight on dead twigs of *Juglans regia*. Symptoms initially manifest as brown, elongated patches. Later, the branches turn brown, and the leaves fall off and dry up. In the later stages, the bark cracks and black, clustered stroma appear. Sexual morph: *Ascostromata* 600–1000 µm diam., comprising a botryose aggregate, black, circular or subglobose to globose, scattered, gregarious, uni- to multi-loculate, immersed to erumpent on host tissue, black dots with papillary protrusions. *Ascomata* individual globose to subglobose or fused, coriaceous, vertical to the host surface, with a central ostiole. *Ostiole* circular, central, papillate. *Peridium* comprising several layers of cells, 30–55 µm wide, outer layer composed of dark brown or brown thick-walled cells of *textura angularis*, inner layer composed of hyaline thin-walled cells of *textura angularis* lining the locule. *Pseudoparaphyses* 1.5–3 µm wide, hyphae-like, septate, numerous. *Asci* 90–109 × 14–21 µm ($\bar{x}$ = 97 × 17 µm, n = 20), 8-spored, bitunicate, fissitunicate, cylindrical-clavate, short pedicellate, apically rounded with an ocular chamber. *Ascospores* 22–29 × 8–11 µm ($\bar{x}$ = 25 × 10 µm, n = 40), biseriate, hyaline, aseptate, ellipsoid-oval, sometimes with tapered ends, usually wider in the middle, smooth-walled, smooth with granular contents. Asexual morph: *Conidiostromata* 300–800 × 240–760 µm. ($\bar{x}$ = 600 × 500 µm, n = 10) µm, epidermal, immersed, solitary or gregarious, brown to dark brown, globose to subglobose, unilocular to multilocular. *Conidiomata* 120–210 × 140–260 µm ($\bar{x}$ = 175 × 210 µm, n = 20), pycnidial, solitary, semi-immersed to immersed, dark brown to black walls. *Conidiomata wall* composed of thick-walled light brown cells of *textura angularis*, becoming hyaline towards the inner region. *Conidiogenous cells* 7–14 × 2–3 µm µm ($\bar{x}$ = 11 × 2.5 µm, n = 40), holoblastic, discrete, hyaline, cylindrical to lageniform, phialidic with periclinal thickening. *Paraphyses* not seen. *Conidia* 22–26 × 5–7 µm ($\bar{x}$ = 24 × 6 µm, n = 40), hyaline, thin-walled, smooth

with granular contents, unicellular, aseptate, narrowly fusiform to ellipsoidal, base subtruncate to bluntly rounded.

Cultural characteristics – Ascospores and conidia germinating on sterile water within 24 h and germ tubes produced from ends. Colonies on PDA reaching 60 mm diam., after 12 days at 25 ℃. The mycelium grows on the surface of the medium, forming circular colonies with well-developed aerial hyphae that are flocculent. The edges of the colonies are radiate and intact, initially white but later turning black. The reverse side of the colonies appears black, and not produced pigmentation on PDA media.

Material examined – China, Sichuan Province, Neijiang City, Dongxing District, Paifang Village (29°48′30.19″N 105°6′36.05″E, alt. 388 m), on the dead twigs of *Juglans regia*, 27 April 2022, F.-H. Wang, WFH202204085 (SICAU 23-0047, holotype), ex-type living culture SICAUCC 23-0026. Liangshan Yi Autonomous Prefecture, Huili City (26° 56′ 43.39′ ′ N 102° 16′ 26.87 ′ ′ E, alt. 2004 m), on the dead twigs of walnuts, 30 September 2022, F.-H. Wang, WFH202209010 (SICAU 23-0048), living culture SICAUCC 23-0027.

GenBank numbers – SICAUCC 23-0026, PP060642 (ITS), PP061111 (*rpb*2), PP061158 (*tub*2) and PP061126 (*tef*1-α); SICAUCC 23-0027, PP060643 (ITS), PP061112 (*rpb*2), PP061159 (*tub*2) and PP061127(*tef*1-α)

Note – In the phylogenetic analyses of combined ITS, *rpb*2, *tef*1-α and *tub*2 sequence data, our strain (SICAUCC 23-0026 and SICAUCC 23-0027) formed a separate branch and clusters with strong statistical support (99% MLBS/1.00 BYPP) (Fig. 3). *Botryosphaeria neijiangense* (SICAUCC 23-0026 and SICAUCC 23-0027) is phylogenetically closer to *B. tenuispora* (MUCC 237). Both *B. neijiangense* and *B. tenuispora* possess conidia that are hyaline, thin-walled, smooth with granular contents, unicellular, aseptate, narrowly fusiform to ellipsoidal. However, *B. gaoxianense* has smaller conidiomata than *B. tenuispora* (175 × 210 μm vs. 446 × 476 μm) (Hattori et al.2021). Nucleotide comparisons reveal notable genetic dissimilarities between *B. neijiangense rugae* and *B. tenuispora* (MUCC 237 ex-type), viz. 1.6% (8/509, 0 gap), 0 (0/576, 0 gap), 1.8% (7/398, 1 gap), and 2.2% (8/363, 0 gap) in the ITS, *rpb*2, *tub*2, and *tef*1-α, respectively. The PHI test revealed no significant recombination event between our strain and the closely related taxa (Φw = 0.37) (Fig. 4). Based on morphological characteristics and phylogenetic analyses, we determine our specimens as *B. neijiangense*. Thus, we identified our strain as a distinct new species as *B. neijiangense*.

4. ***Botryosphaeria wangensis*** G.Q. Li & S.F. Chen, Persoonia 40: 84 (2017) Fig. 8

Index Fungorum number: IF822325; Facesoffungi number: FoF16289

Associated with branch blight on dead twigs of *Juglans regia.* Symptoms manifest as irregular spots appearing on the branches, which gradually expand and envelop the entire branch, ultimately leading to its death. Sexual morph: *Ascostromata* 180–260 × 150−240 μm ($\bar{x}$ = 220 × 190 μm, n = 10), circular, blackened areas on host tissue, immersed to erumpent on host tissue, individual ascomata, gregarious, individually globose to subglobose. *Ostiole* circular, central, papillate. *Peridium* up to 16–40 μm wide, comprising several layers of brown to dark brown walled cells of *textura angularis*, broader at the base. *Pseudoparaphyses* 4–6 μm wide, hyphae-like, septate, constricted at the septa, inconspicuous branched and anastomosed at the apex, numerous. *Asci* 78−104 × 20−26 μm ($\bar{x}$ = 90 × 24 μm, n = 20), 8–spored, bitunicate fissitunicate, clavate to cylindro-clavate, upper end enlargement, short pedicellate, apically rounded with well developed ocular chamber. *Ascospores* 21–32 × 10–14 μm ($\bar{x}$ = 26.3 × 11.7 μm, n = 40), biseriate, hyaline, aseptate, during germination, a septum is formed, ellipsoidal to fusoid, or irregular in shape, sometimes with tapered ends, spindle-shaped, thin-walled, smooth with granular contents. Asexual morph: Not observed.

Cultural characteristics – Ascospores germinating on sterile water within 24 h and germ tubes produced from ends. Colonies on PDA reaching 60 mm diam., after 10 days at 25 ℃. The mycelium grows on the surface of the medium, forming circular colonies with well-developed aerial hyphae that have a velvet-like appearance and are radiate. The edges of the colonies are intact, initially white

but later turning black, and brown sclerotia are produced. The reverse side of the colonies appears black, and not produced pigmentation on PDA media.

Material examined – China, Sichuan Province, Suining City, Shehong City, Guangxing Town (30°57′22.78″N 105°18′54.17″E, alt. 406 m), on the dead twigs of *Juglans regia*, 17 May 2021, F.-H. Wang, WFH202105020 (SICAU 23-0049), living culture SICAUCC 23-0028.

GenBank numbers – SICAUCC 23-0028, PP060644 (ITS), PP061113(*rpb*2), PP061160(*tub*2) and PP061128(*tef*1-α)

Note – In the multi-loci phylogenetic analyses, our strain *Botryosphaeria wangensis* (SICAUCC 23-0028) clusters with the strains *B. wangensis* (CERC 2298 and CERC 2299), with 70% MLBS and 1.00 BYPP support for the cluster. The morphological characteristics of the asexual stage of this species have been reported thus far, with no information on its sexual stage. (Li et al. 2018). The nucleotide comparisons of ITS, *rpb*2, *tef*1-α, and *tub*2 from our isolate showed a high homology with the sequences of *B. wangensis* (CERC 2298, holotype), the similarities are 99.1% (532/537, 0 gap), 100% (718/718, 0 gap), 100% (284/284, 0 gap), and 99.1% (438/442, 0 gap), respectively (Li et al. 2018). In this article, the sexual morph of *B. wangensis* is described for the first time.

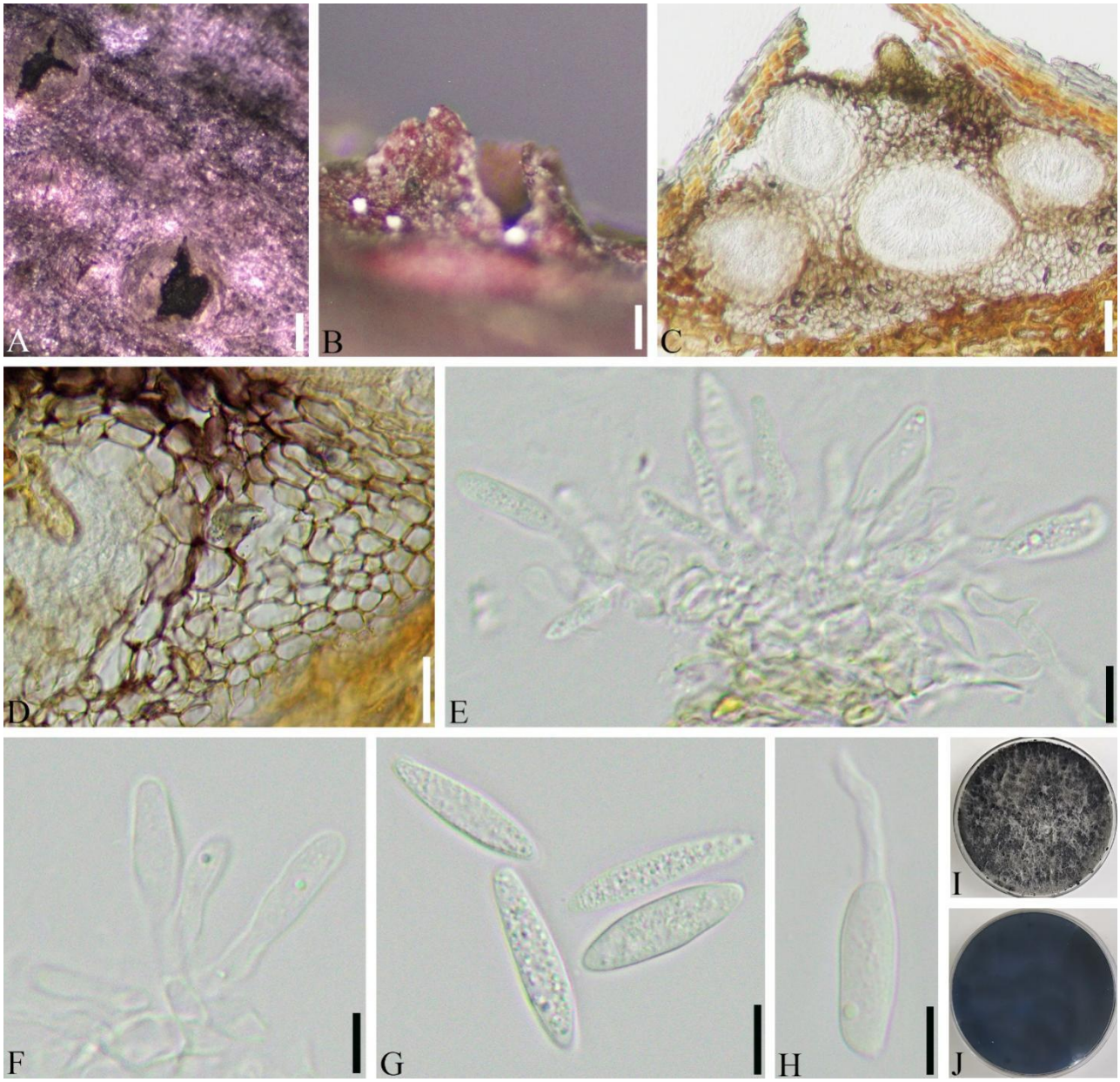


Figure 6 – Asexual morph of *Botryosphaeria neijiangense* (SICAU 23-0047, holotype). A, B Appearance of conidiostromata on *Juglans regia*. C Vertical section through conidiostromata. D

Section of conidiomata wall. E, F Conidiogenous cells and conidia. G Conidia. H Geminating conidium. I, J Colonies on PDA (I from above, J from below). Scale bars: A = 500 µm, B = 200 µm, C = 50 µm, D–H = 10 µm.

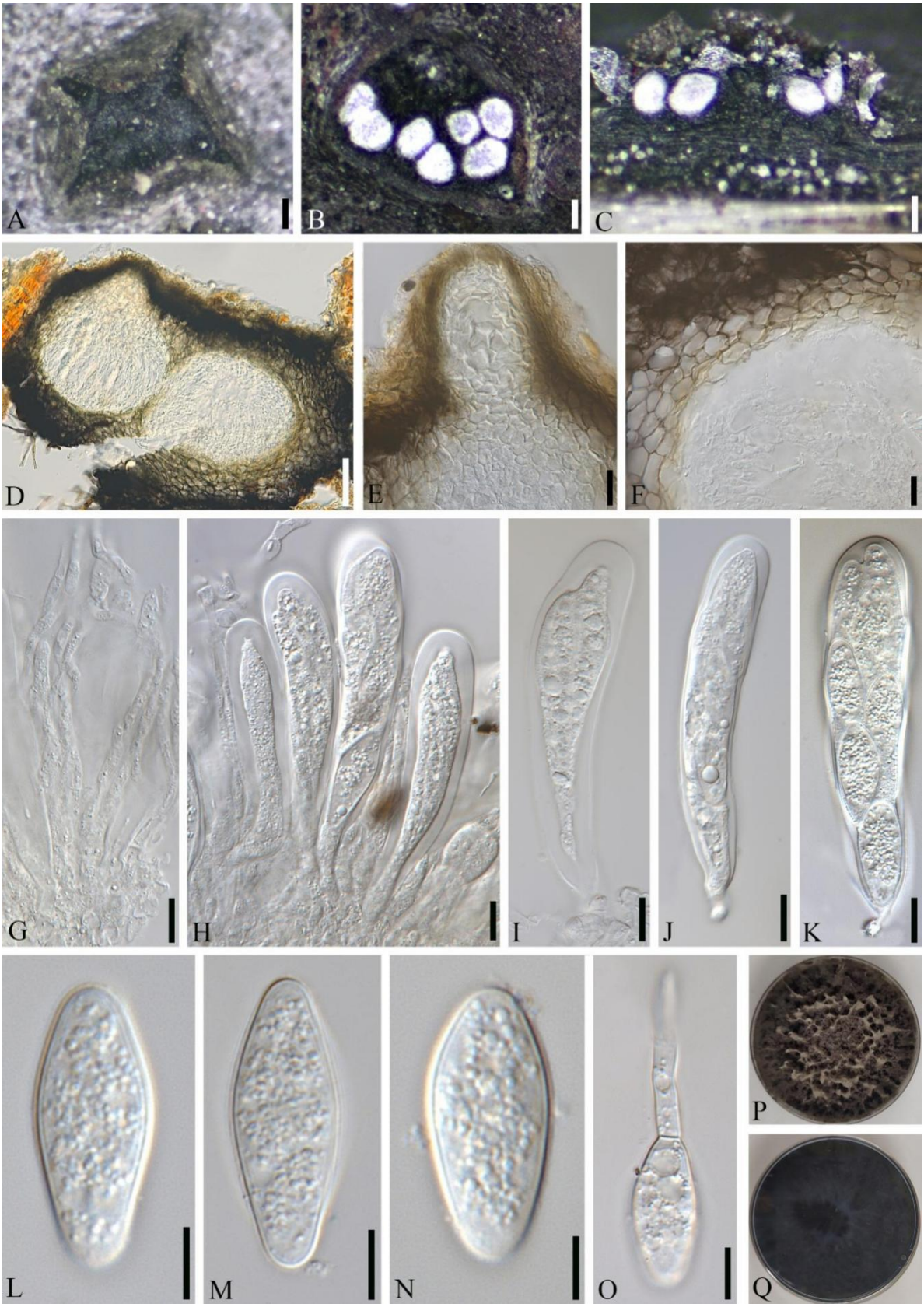


Figure 7 – Sexual morph of *Botryosphaeria neijiangense* (SICAU 23-0048). A Appearance of ascostroma on host substrate. B, C Longitudinal and transverse cutting diagram of ascostroma. D

ascostroma showing ascomata. E Papillate ostiole. F Peridium. G Pseudoparaphyses. H–K Asci. L–N Ascospores. O Germinating ascospore. P, Q Colonies on PDA (P from above, Q from below). Scale bars: B, C = 200 μm, D = 50 μm, H–K = 20 μm, E–G, O = 10 μm, L–N = 5 μm.

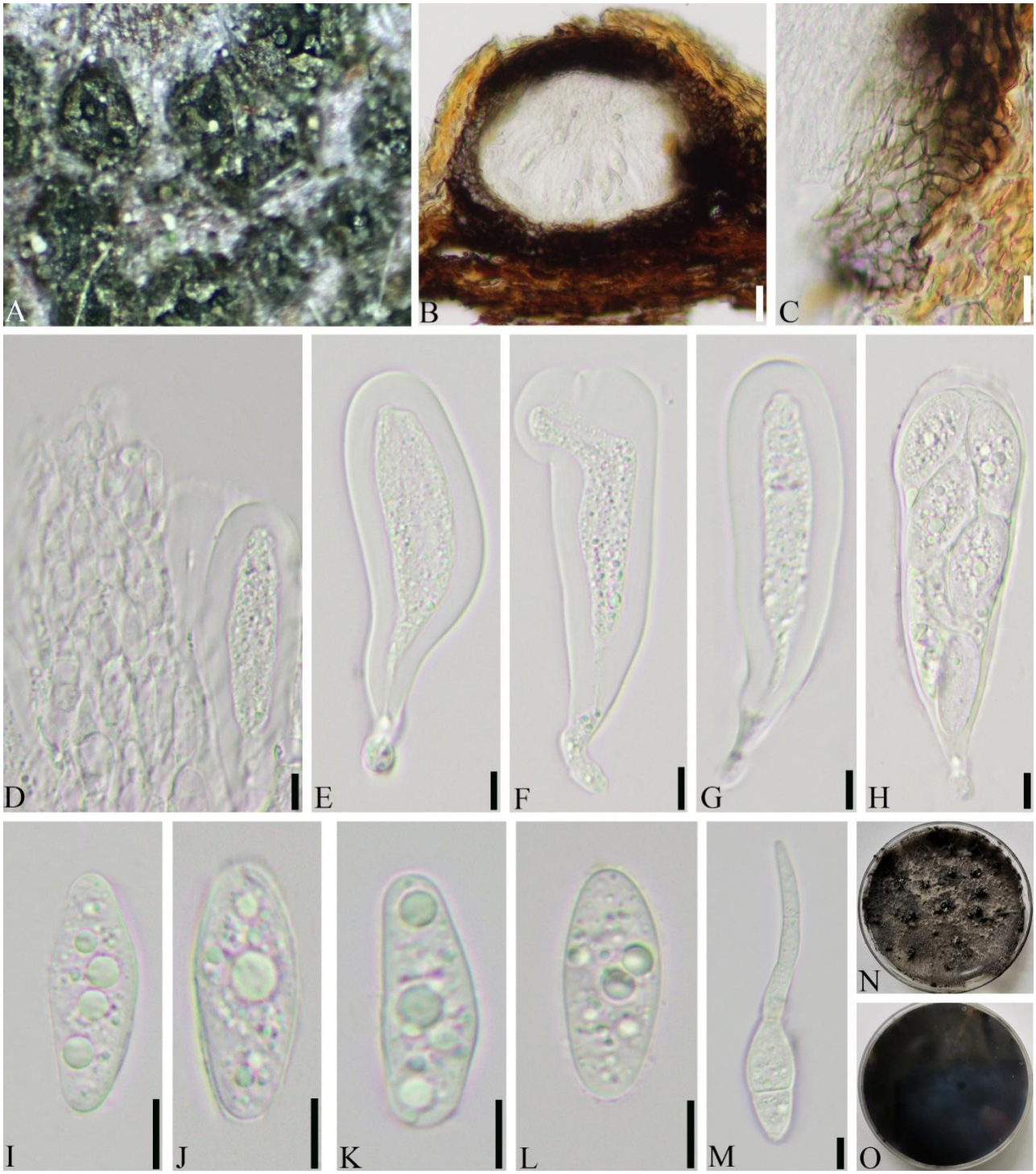


Figure 8 – *Botryosphaeria wangensis* (SICAU 23-0049). A Appearance of ascoma on host substrate. B Section of ascoma. C Peridium. D Pseudoparaphyses and asci. E–H Asci. I–L Ascospores. M Germinating ascospore. N–O Colonies on PDA (N from above, O from below). Scale bars: B = 50 μm, D = 20 μm, C, E–M = 10 μm.

5. ***Botryosphaeria yibinense*** F.H. Wang & C.L. Yang, sp. nov. Figs. 9, 10

Index Fungorum number: IF901558; Facesoffungi number: FoF15575

Etymology – Named after locality where the fungus was isolated for the first time.

Holotype – SICAU 23-0050.

Saprobic on dead twigs of *Juglans regia*. Sexual morph: *Ascostroma* 400–600 μm diam., black, immersed, aggregated or some clustered, scattered, composed of one or up to three ascomata in each ascostroma, developing in the substrate and erumpent through the bark at maturity, discoid to pulvinate or hemispherical, discrete or wide-spreading with surface slightly convex. *Ascomata* 210–280 × 200–260 μm ($\bar{x}$ = 240 × 230 μm, n = 20), when cut horizontally, ascomata visible with white contents, multiloculate, globose to subglobose, with thickened peridium, with a central ostiole. *Peridium* 40–70 μm wide, comprising several layers of brown-walled cells, the outer stratum of 1–3 cells comprising thick, dark brown walls *textura angularis*, the inner layer comprising pale brown to hyaline, thin-walled cells *textura angularis*. *Pseudoparaphyses* 2–4 μm wide, hyphae-like, numerous, septate, embedded in a gelatinous matrix. *Asci* 78–128 × 20–26 μm ($\bar{x}$ = 103 × 23 μm, n = 20), 8-spored, bitunicate, fissitunicate, cylindrical-clavate, short pedicellate, apically rounded with an ocular chamber. *Ascospores* 26–32 × 8–13 μm ($\bar{x}$ = 29 × 11 μm, n = 40), biseriate, hyaline, smooth, thin-walled, aseptate, fusoid-ellipsoidal to lageniform, sometimes with tapered ends, droplet object with oil inside. Asexual morph: *Conidiomata* formed on walnuts twigs spot, stromatic, brown to black, 300–500 μm diam, forming a botryose aggregate of up to 10 (sometimes solitary) globose with a central ostiole, semi-immersed to superficial, depressed globose or irregular subglobose, coriaceous locules. *Conidiophores* reduced to conidiogenous cells. *Conidiogenous cells* 3–7 × 2–4 μm ($\bar{x}$ = 5 × 3 μm, n = 20), holoblastic, discrete, hyaline, cylindrical to lageniform, phialidic with periclinal thickening. *Paraphyses* not seen. *Conidia* 22–28 × 5–7 μm ($\bar{x}$ = 26 × 6 μm, n = 40), hyaline, thin-walled, smooth with granular contents, aseptate, fusoid-ellipsoidal, widest in the middle, apex acute, base subtruncate to bluntly rounded.

Cultural characteristics – Ascospores and conidia germinating on sterile water within 24 h and germ tubes produced from ends. Colonies on PDA reaching 60 mm diam., after 8 days at 25 ℃. The mycelium grows on the surface of the medium, forming circular colonies with well-developed aerial hyphae that are fluffy and initially white, gradually turning olive-green, and then dark brown to black. The reverse side of the colonies appears black, and not produced pigmentation on PDA media.

Material examined – China, Sichuan Province, Yibin City, Junlian County (28°11′36.37″N 104°34′5.49″E, alt. 616 m), on the dead twigs of *Juglans regia*, 26 April 2022, F.-H. Wang, WFH202204051 (SICAU 23-0050, holotype), ex-type culture SICAUCC 23-0029. Yibin City, Junlian County (28°11′36.37″N 104°34′5.49″E, alt. 616 m), on the dead twigs of *Juglans regia*, 26 April 2022, F.-H. Wang, WFH202204054-1 (SICAU 23-0051), living culture SICAUCC 23-0030.

GenBank numbers – SICAUCC 23-0029, PP060645 (ITS), PP061114(*rpb*2), PP061161(*tub*2) and PP061129(*tef*1-α); SICAUCC 23-0030, PP060646 (ITS), PP061115(*rpb*2), PP061162(*tub*2) and PP061130(*tef*1-α)

Note – In the phylogenetic analyses of combined ITS, *rpb*2, *tef*1-α and *tub*2 sequence data, our strain (SICAUCC 23-0026 and SICAUCC 23-0027) formed a separate branch and clusters with strong statistical support (96% MLBS/0.98 BYPP) (Fig. 3). In terms of morphology, *B. yibinense*, *B. qingyuanensis*, *B. dolichospermatii*, and *B. sinensis* exhibit partially similar characteristics. (Zhou et al. 2016, Li et al. 2018, Chu et al. 2021). Nucleotide comparisons reveal notable genetic dissimilarities between *B. yibinense* and *B. qingyuanensis* (CERC 2946 ex-type), viz. 1% (5/521, 1 gap), 1.1% (5/710, 0 gap), 1.6% (7/430, 3 gaps), and 2.3% (6/257, 1 gap) in theITS, *rpb*2, *tub*2, and *tef*1-α, respectively. Nucleotide comparisons reveal notable genetic dissimilarities between *B. yibinense* and *B. dolichospermatii* (CGMCC 3.19096 ex-type), viz. 1.3% (7/521, 1 gap), 2.6% (11/430, 3 gaps), and 1.6% (4/256, 3 gaps) in the ITS, *tub*2, and *tef*1-α, respectively. The comparative analysis of sequences between (SICAUCC 23-0029) and *B. sinensis* (CGMCC 3.17722 ex-type) revealed a 98.1% similarity (521/531, 1 gap) in the ITS. Since *B. sinensis* (CGMCC 3.17722) only possesses ITS sequences and cannot be used for further comparisons, morphological comparison was conducted instead. Morphologically, *B. yibinense* differs from *B. sinensis* (CGMCC 3.17722) by larger ascostroma (400–600 μm vs. 140–260 μm). Comparisons of the asexual stages show that the species we collected have larger conidiomata (300–500 μm vs. 140–260 μm) and smaller conidiogenous cells (3–7 × 2–4 μm vs. 8–15 × 2–3 μm). The PHI test revealed no significant

recombination event between our strain and the closely related taxa (Φw = 0.37) (Fig. 4). Based on morphological characters and phylogenetic analyses, we determine our specimens as a new species, *B. yibinense.*

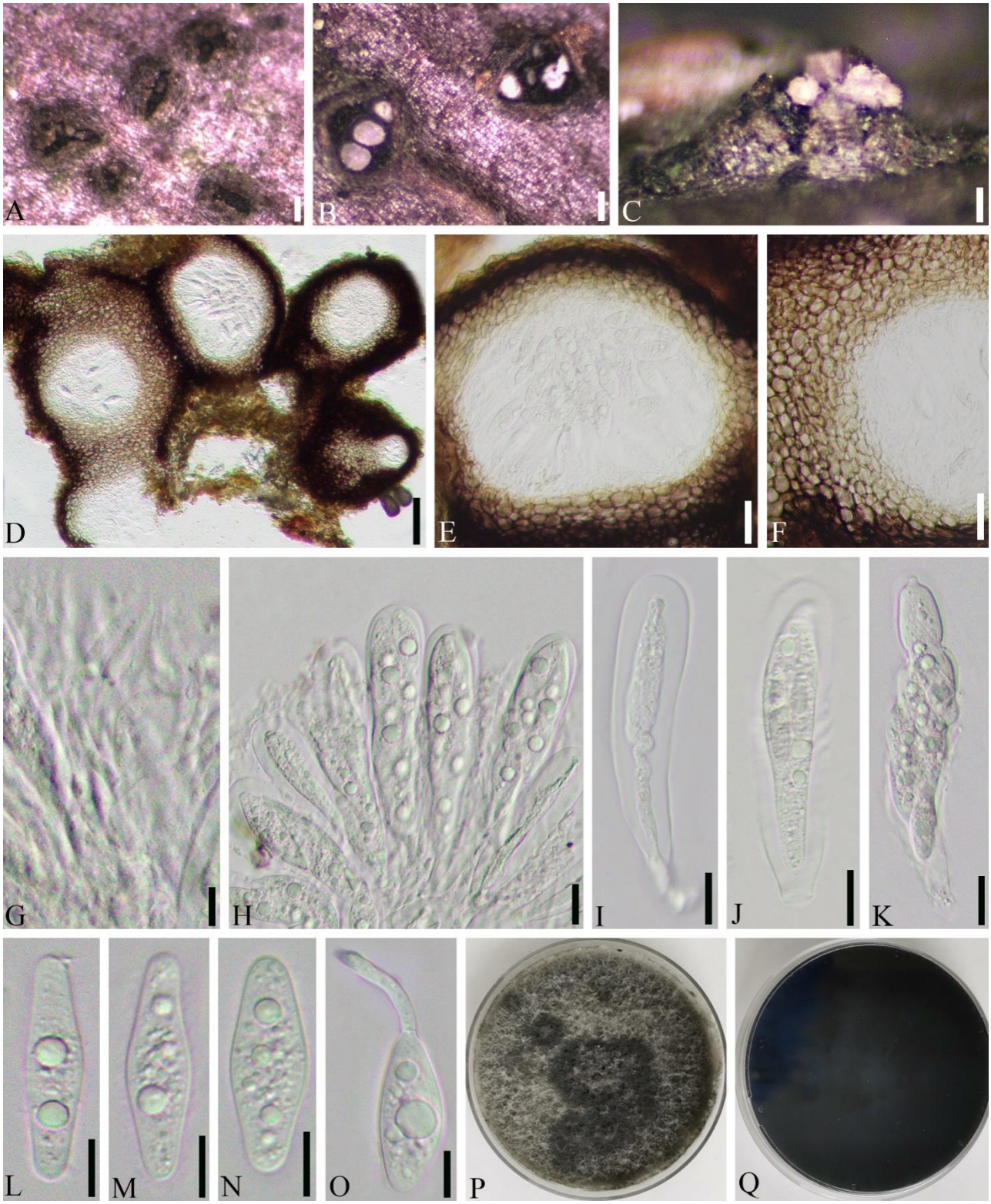


Figure 8 – Sexual morph of *Botryosphaeria yibingense* (SICAU 23-0050, holotype). A, C Appearance of ascostroma on host substrate. B Transverse cutting diagram of ascoma. D, E Sections of ascoma. F Peridium. G Pseudoparaphyses. H–K Asci. L–N Ascospores. O Germinating ascospore. P, Q Colonies on PDA (P from above, Q from below). Scale bars: A, B = 200 μm, C = 100 μm, D = 50 μm, E–K = 20 μm, L–O = 10 μm.

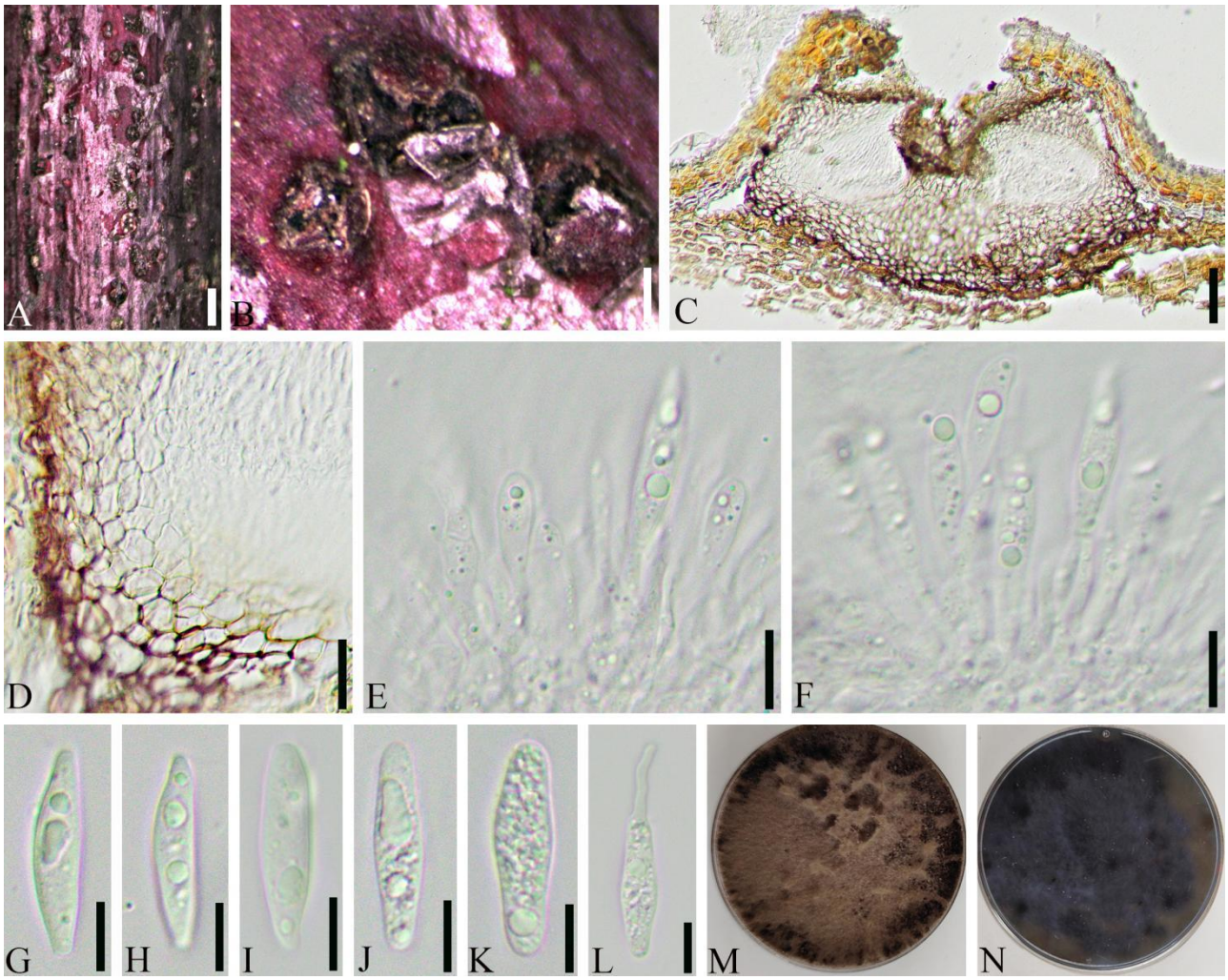


Figure 9 – Asexual morph of *Botryosphaeria yibingense* (SICAU 23-0051). A, B Appearance of conidiostromata on host substrate. C Vertical section through conidiostromata. D Section of conidiomata wall. E, F Conidiogenous cells and conidia. G–K Conidia. L Geminating conidium. M, N Colonies on PDA (M from above, N from below) Scale bars: A=500 µm, B=200 µm, C=50 µm, D–F=20 µm, G–L=10 µm.

Dothiorella Sacc., Michelia 2(no. 6): 5 (1880).

The type species, *Dothiorella pyrenophora* differs from *Diplodia* by conidia that are brown and 1-septate early in their development, while they are still attached to the conidiogenous cells (Phillips et al. 2013). Wide host ranges and morphological plasticity within the genus have made it impossible to identify species based only on morphology. Phillips et al. (2008) pointed out that *Dothiorella* has often been confused with *Spencermartinsia* in morphological characterizations (Hyde et al., 2019a). They have synonymized species of Spencermartinsia into the genus *Dothiorella*, because they found that apiculate ascospores were not reliable for separating these two genera. *Dothiorella* has 336 epithets listed in Species Fungorum (2025); however, only 60 species have available molecular data in GenBank. (Dissanayake et al. 2016, Hyde et al. 2024a, Zhang et al. 2025).

6. ***Dothiorella pugeense*** F.H. Wang & C.L. Yang, sp. nov. Fig. 11

Index Fungorum number: IF901559; Facesoffungi number: FoF15576

Etymology – Named after locality where the fungus was isolated for the first time.

Holotype – SICAU 23-0052.

Saprobic on the dead branches of *Juglans regia*. Sexual morph: *Ascostromata* 600–700 µm diam, immersed, erumpent, but still under host tissue, subglobose to ovoid, rough, multilocular, with 3–4 locules in one ascostroma, locules 240–360 µm diam, 270–410 µm high. *Ostiole* opening with a

pore, 60–84 μm long. *Peridium* 56–78 μm wide, two-layered, outer layer composed of brown to dark brown, thick-walled cells of *textura angularis*, inner layer composed of hyaline thin-walled cells of *textura angularis*. *Pseudoparaphyses* up to 3–5 μm wide, hyphae-like, cellular, numerous, embedded in a hyaline gelatinous matrix. *Asci* 70–98 × 16–22 μm ($\bar{x}$ = 85 × 18 μm, n = 20), 8−spored, bitunicate, fissitunicate, pedicellate, apically rounded with an ocular chamber. *Ascospores* 22–28 × 7–12 μm ($\bar{x}$ = 25 × 10 μm, n = 40), overlapping biseriate, ellipsoid to broad fusiform with broadly to narrowly rounded ends, hyaline when young, becoming pale brown or brown when mature,1-seriate, slightly constricted at septum. Asexual morph: Not established.

Cultural characteristics – Ascospores germinating on sterile water within 24 h and germ tubes produced from ends. Colonies on PDA reaching 60 mm diam., after 10 days at 25 ℃. The mycelium grows on the surface of the medium, forming circular, dense colonies with a coral fleece-like appearance. Initially white, the colonies gradually turn brown to dark brown. The reverse side of the colonies appears brown, and not produced pigmentation on PDA media.

Material examined – China, Sichuan Province, a walnut garden of Puge (27° 24′ 65′ ′ N, 102° 30′ 7′ ′ E), on the dead branches of *Juglans regia*, 24 August 2022, F.-H. Wang, WFH202208002 (SICAU 23-0052, holotype), ex-type culture SICAUCC 23-0031. *Ibid*., WFH202208002B (SICAU 23-0163), living culture SICAUCC 23-0142.

GenBank numbers – SICAUCC 23-0031: PP390175 (LSU), PP060647 (ITS), PV220916 (*tef*1-α) and PV220918 (*tub*2); SICAUCC 23-0142: PP862534 (LSU), PP844870 (ITS), PV220917 (*tef*1-α) and PV220918 (*tub*2).

Note – Sexual morphs of *Dothiorella* have pigmented, septate ascospores (Zhang et al. 2023a). However, the sexual stage of the species is rarely found in nature and has never been reported in culture (Hongsanan et al. 2020). Therefore, morphological comparison is impossible. *Dothiorella pugeense* is introduced as a new species based on its distinct morphology and phylogenetic results of a combined ITS, *tef*1-α and *tub*2 dataset. In the phylogenetic analyses, our strain (SICAUCC 23-0031 and SICAUCC 23-0142) clusters as sister to *D. tectonae* (MFLUCC 18-0232) with strong statistical support (97% MLBS/0.98 BYPP) (Fig. 12). Nucleotide comparisons reveal notable genetic dissimilarities between *D. pugeense* and *D. tectonae* (MFLUCC 18-0232), viz. 9.3% (52/560, 43 gaps), 2.7% (14/515, 0 gap), and 5.3% (23/435, 4 gaps) in the ITS, *tef*1-α and *tub*2, respectively. The PHI test revealed no significant recombination event between our strain and the closely related taxa (Φw = 1) (Fig. 13). Therefore, we designate our collection as a new *D. pugeense* species in *Dothiorella*.

Lasiodiplodia Ellis & Everh., Bot. Gaz. 21: 92. 1896.

Lasiodiplodia was introduced by Ellis (1894) with *L. tubericola* as the type species. Although Ellis did not describe it, Clendenin (1896) provided a description of the genus and the species, attributing both to Ellis & Everhardt. Griffin & Maublanc (1909) considered that on account of the pycnidia paraphyses, the cocoa pathogen, *Botryodiplodia theobromae*, was more suitably accommodated in *Lasiodiplodia*. *Lasiodiplodia theobromae* should be regarded as the type species of *Lasiodiplodia*. In earlier works on *Lasiodiplodia* and *Diplodia* it was considered that *Lasiodiplodia* could represent a possible synonym of *Diplodia* (Denman et al. 2000). However, in phylogenetic analyses, these two genera were clearly separated in two distinct clades (Zhou & Stanosz 2001, Slippers et al. 2004, Phillips et al. 2008). *Lasiodiplodia* is distinguished from *Diplodia* by striations on the conidia. (Sutton 1980, Phillips et al. 2008, Netto et al. 2014). Most species of this genus are plant pathogens. (Phillips et al. 2013, De Silva et al. 2019b). Both sexual and asexual morphs have been reported within the genus (Alves et al. 2008, Tennakoon et al. 2016). There are 92 records of *Lasiodiplodia* listed in Species Fungorum (2025). We follow the latest treatments and updated accounts of *Lasiodiplodia* in Tian et al. (2024).

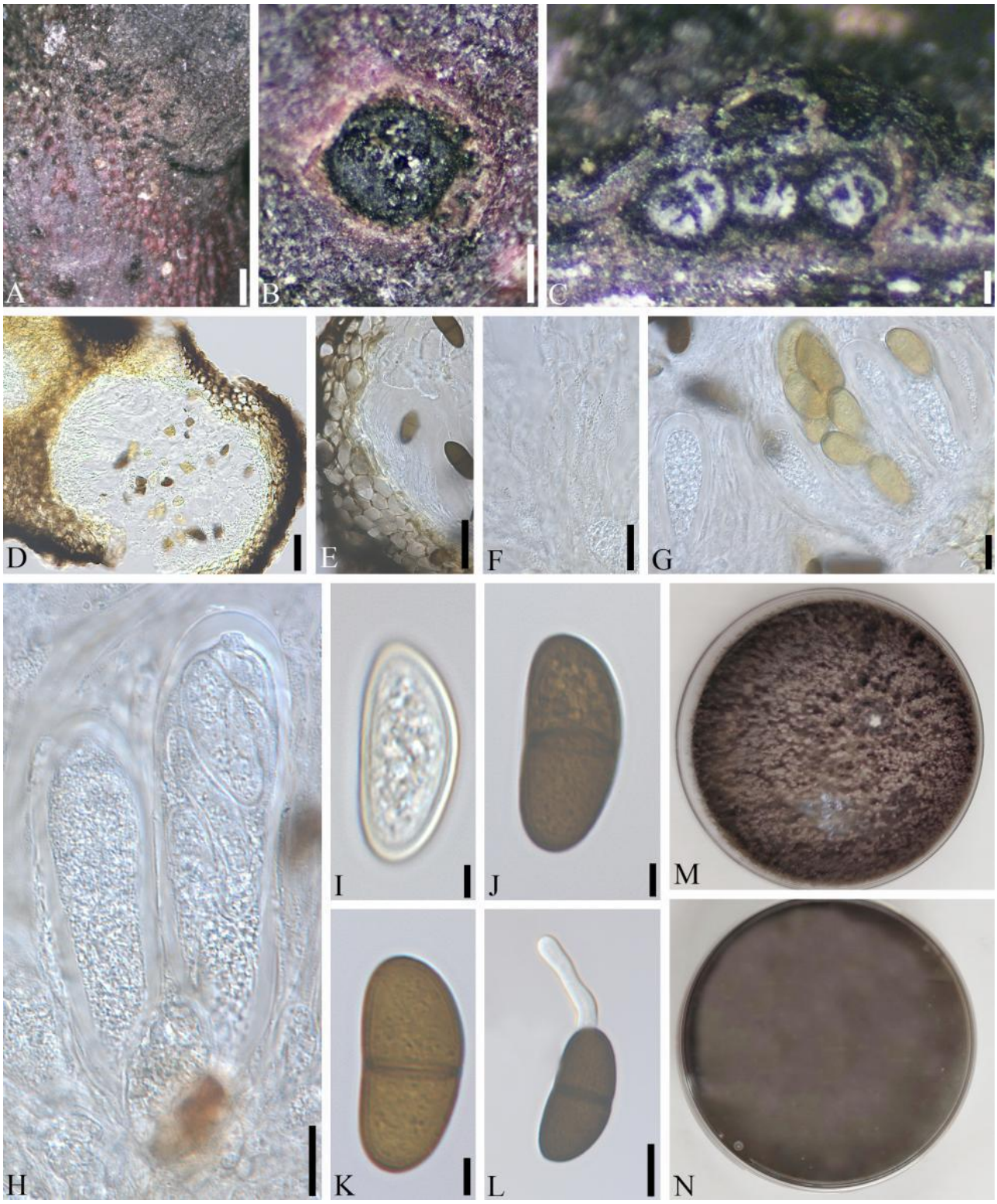


Figure 11 – *Dothiorella pugeense* (SICAU 23-0052, holotype). A Appearance of ascostroma on host substrate. B, C Longitudinal and transverse cutting diagram of ascomata. D Section of ascoma. E Peridium. F, G Paraphyses and asci. H Asci. I–K Ascospores. L Germinating ascospore. M, N Colonies on PDA (M from above, N from below). Scale bars: A = 1 mm, B = 500 μm, C = 100 μm, D = 50 μm, E–H = 20 μm, L = 10 μm, I–K = 5 μm.

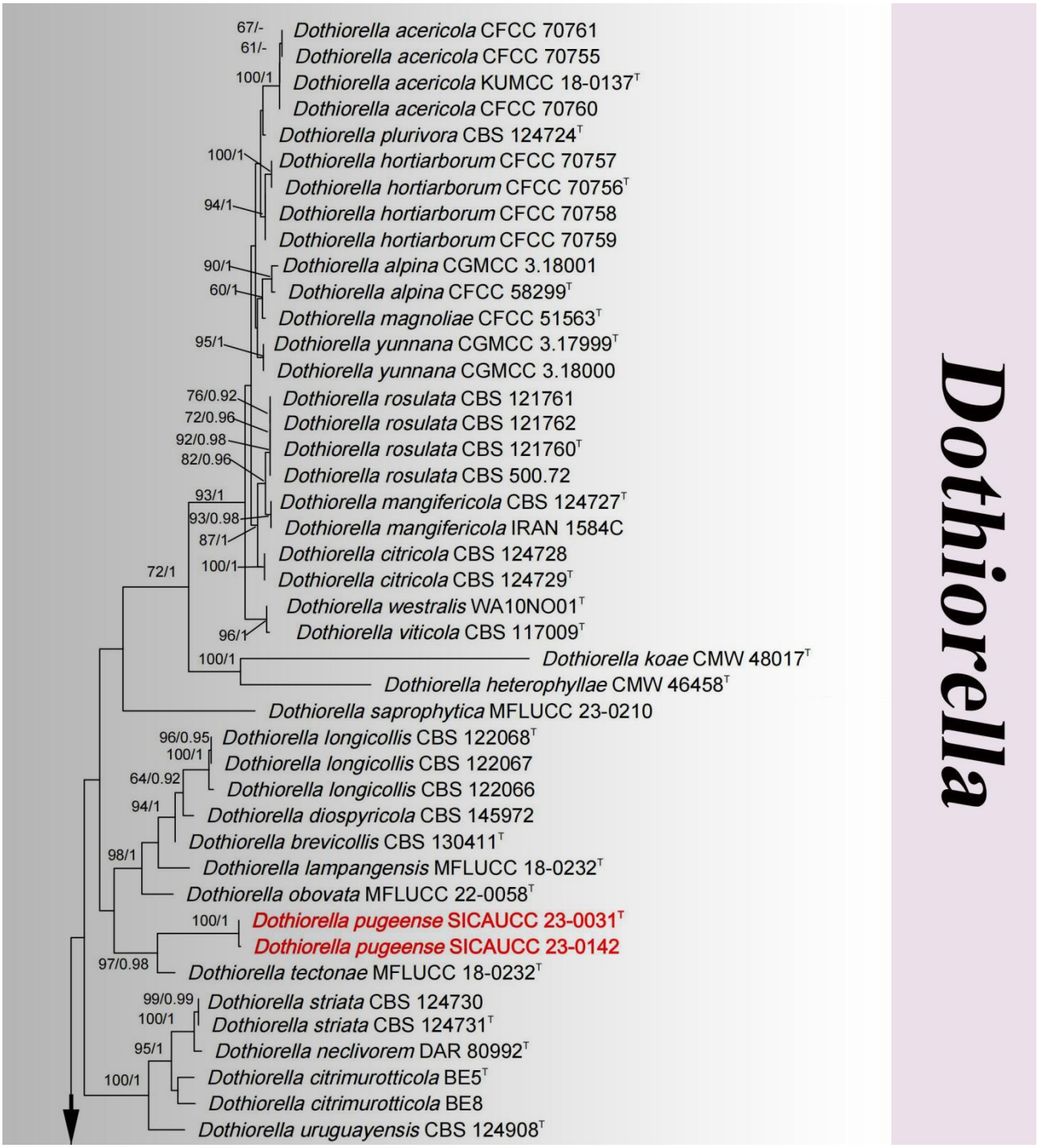
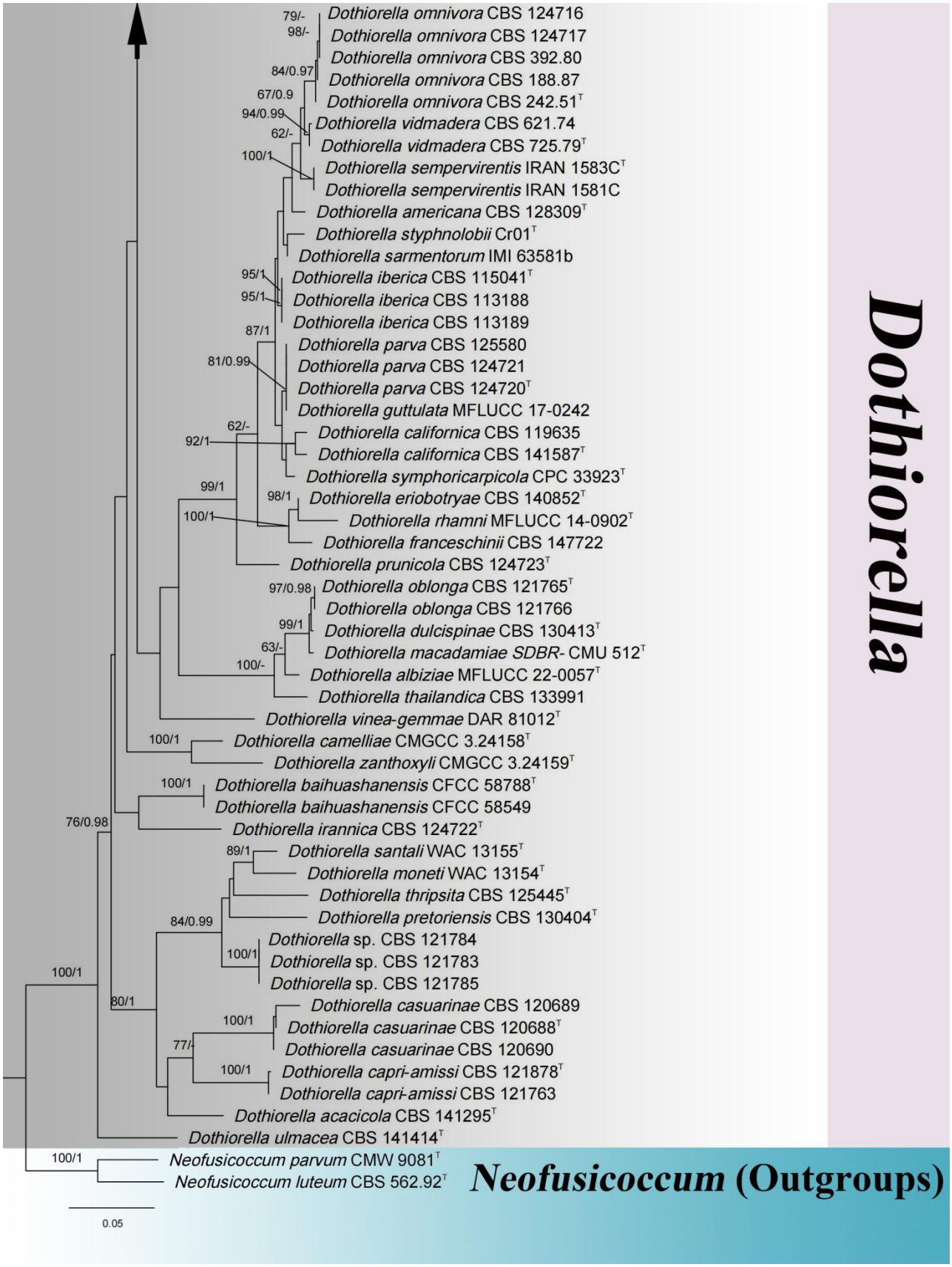


Figure 12 – Continued.

Figure 12 – The best scoring RAxML tree with a final likelihood value of -11,044.567005 based on ITS, *tef*1-α and *tub*2 sequence data for *Dothiorella* species. The topology and clade stability of the combined DNA analyses was compared to the single gene analyses. The tree is rooted with sequences of *Neofusicoccum luteum* (CBS 562.92) and *N. parvum* (CMW 9081) in *Neofusicoccum*. The tree from the maximum likelihood analyses had similar topology to the Bayesian analyses. Ninety-seven strains were included in the analyses of the combined DNA loci and comprise 1,813 characters (662 characters for ITS, 601 characters for *tef*1-α and 550 characters for *tub*2, including gaps). The matrix had 873 distinct alignment patterns, with 36.28% undetermined characters and gaps. Estimated base frequencies were as follows; A= 0.210060, C = 0.306988, G = 0.250847, T = 0.232106; substitution rates AC = 1.016911, AG = 2.242370, AT = 1.261001, CG = 1.145990, CT = 3.936644, GT=1.000000; gamma distribution shape parameter α = 0.249669. The GTR+I + G model was selected for every partition in Bayesian analyses. The species determined in this study is indicated in

red and bold. Bootstrap support values for maximum likelihood (MLBS, left) ⩾ 60% and Bayesian posterior probabilities (BYPP, right) ⩾ 0.90 are indicated at the nodes, respectively. Hyphens (-) represent support values less than 50% MLBS/0.90 BYPP. The ex-type superscript "T".



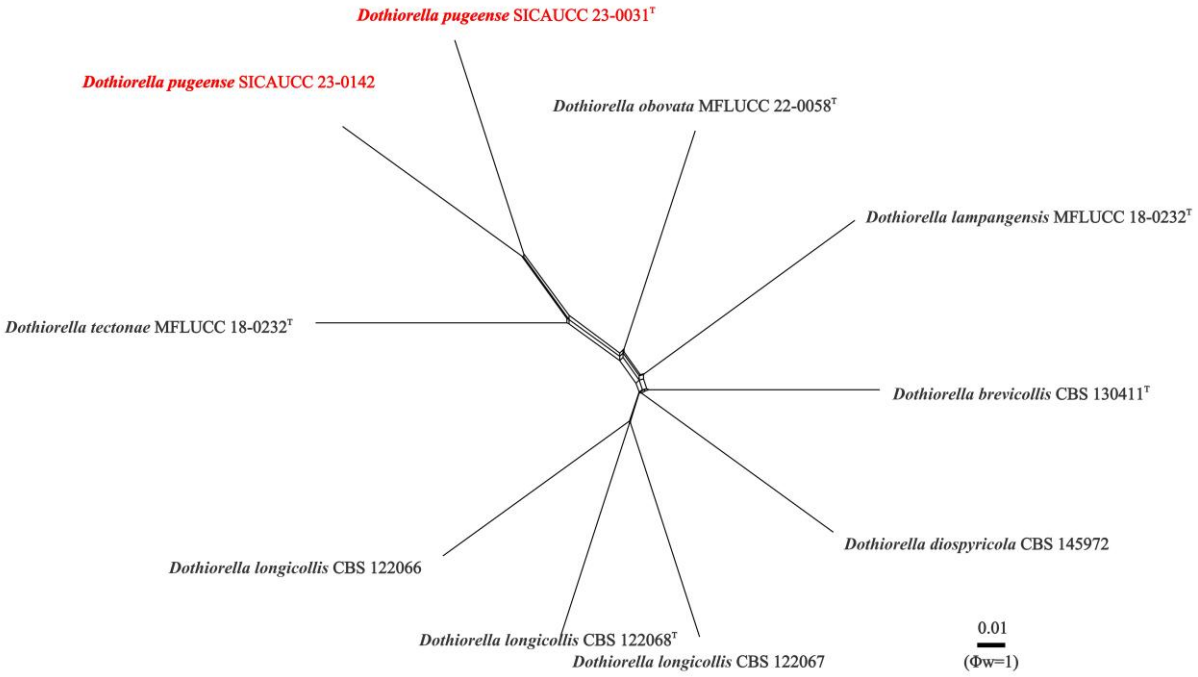


Figure 13 – Results of the PHI test of *Dothiorella pugeense* and closely related species using both LogDet transformation and splits decomposition. The PHI test did not find any statistically significant recombination (Φw = 1) in the data set. The new strains are represented in red and bold. "T" represents the type strain.

7. ***Lasiodiplodia chongzhouense*** F.H. Wang & C.L. Yang, sp. nov. Fig. 14

Index Fungorum number: IF901560; Facesoffungi number: FoF15577

Etymology – Named after locality where the fungus was isolated for the first time.

Holotype – SICAU 23-0053.

Associated with blight symptom on living twigs of *Juglans regia*. Symptoms include the development of brown lesions on the branches. Once these lesions encircle the infected branch, the portion of the branch above the lesion will wither and die. Sexual morph: Not observed. Asexual morph: *Conidiomata* 220–300 × 210–320 µm ($\bar{x}$ = 260 × 270 µm, n = 20), pycnidial, semi-immersed in the host, becoming erumpent at maturity, solitary or gregarious, brown to black, globose to subglobose, uniloculate. *Ostiole* not observed. *Conidiomata wall* 40–65 µm thick, composed of several layers of thin- and thick-walled, hyaline to brown to dark brown cells of *textura angularis* to *prismatica*. *Conidiophores* reduced to conidiogenous cells. *Conidiogenous cells* 6–14 × 1.5–5 µm ($\bar{x}$ = 10 × 3.5 µm, n = 40), hyaline, smooth, thin-walled, discrete, cylindrical, holoblastic, proliferating percurrently from hyaline inner conidiomata wall. *Paraphyses*, up to 60–90 µm long, 1.5–3 µm wide, numerous, filiform, aseptate, unbranched. *Conidia* 18–24 × 9–14 µm ($\bar{x}$ = 21 × 12 µm, n = 40), initially hyaline, thin-walled, smooth with granular contents, aseptate, oblong to ovoid, becoming mature 1-septate, pale brown to dark brown, straight, both ends broadly rounded, with guttules.

Culture characteristics – Conidia begin to germinate within 24 h in sterile water, with germ tubes emerging from both ends. Colonies on PDA reaching 60 mm diam., after 8 days at 25 ℃. The mycelium grows on the surface of the medium, forming circular, dense colonies with a coral fleece-like appearance. Initially white, the colonies gradually turn gray-green and then black, with well-developed aerial hyphae. The reverse side of the colonies appears black, and not produced pigmentation on PDA media.

Material examined – China, Sichuan Province, Chengdu City, Chongzhou City (30°33′9.04″N 103°39′29.36″E, alt. 512 m), on the living twigs of *Juglans regia*, 21 April 2021, F.-H. Wang,

WFH202204021 (SICAU 23-0053, holotype), ex-type culture SICAUCC 23-0032. *Ibid*., Mianyang City, Yanting County (31°5′25.88″N 105°27′36.27″E, alt. 365 m), on the living twigs of *J. regia*, 28 April 2022, F.-H. Wang, WFH202204104 (SICAU 23-0054), living culture SICAUCC 23-0033.

GenBank numbers – SICAUCC 23-0032: PP060648 (ITS), PP061131 (*tef*1-α) and PP061163 (*tub*2); SICAUCC 23-0033: PP060649 (ITS), PP061132 (*tef*1-α) and PP061164 (*tub*2).

Note – The new collection is a typical *Lasiodiplodia* species, with semi-immersed, erumpent conidiomata, hyaline, septate paraphyses and initially hyaline, aseptate, becoming mature 1-septate, pale brown to dark brown, oblong to ovoid conidia (Abdollahzadeh et al. 2010). *Lasiodiplodia chongzhouense* is phylogenetically closer to *L. citricola* (CBS 124706 and CBS 124707) and *L. mexicanensis* (AGQMy 00114 and AGQMy 00115) (Fig. 15). *Lasiodiplodia citricola* was associated with *Citrus* sp. leaves in Iran (Abdollahzadeh et al. 2010). Conidia of *L. chongzhouense* are smaller (21 × 12 µm) than those of *L. citricola* (25 × 15 µm). Paraphyses of *L. chongzhouense* are shorter (up to 55 µm) than those of *L. citricola* (up to 125 µm). Nucleotide comparisons reveal notable genetic dissimilarities between *L. chongzhouense* and *L. citricola* (CBS 124706, ex-type), viz. 0.4% (2/477, 0 gap), 1.8% (5/272, 1 gap), and 1.6% (7/424, 17 gaps) in the ITS, *tef*1-α, and *tub*2, respectively. *Lasiodiplodia mexicanensis* was associated with *Chamaedorea seifrizii* leaves in Mexico (Douanla-Meli & Scharnhorst 2021). Nucleotide comparisons reveal not obvious genetic dissimilarities between *L. chongzhouense* and *L. mexicanensis* (AGQMy 00115, ex-type), viz. 0.2% (1/477, 0 gap), 2% (6/272, 1 gap), and 1.1% (5/424, 9 gaps) in the ITS, *tef*1-α, and *tub*2, respectively. The PHI test revealed no significant recombination event between our strain and the closely related taxa (Φw = 1) (Fig. 16). Currently, there is no morphological description available for *L. mexicanensis*, and therefore, they are distinguished based on differences in their nucleotide bases. Therefore, we designate our collection as a new *L. chongzhouense* species in *Lasiodiplodia*.

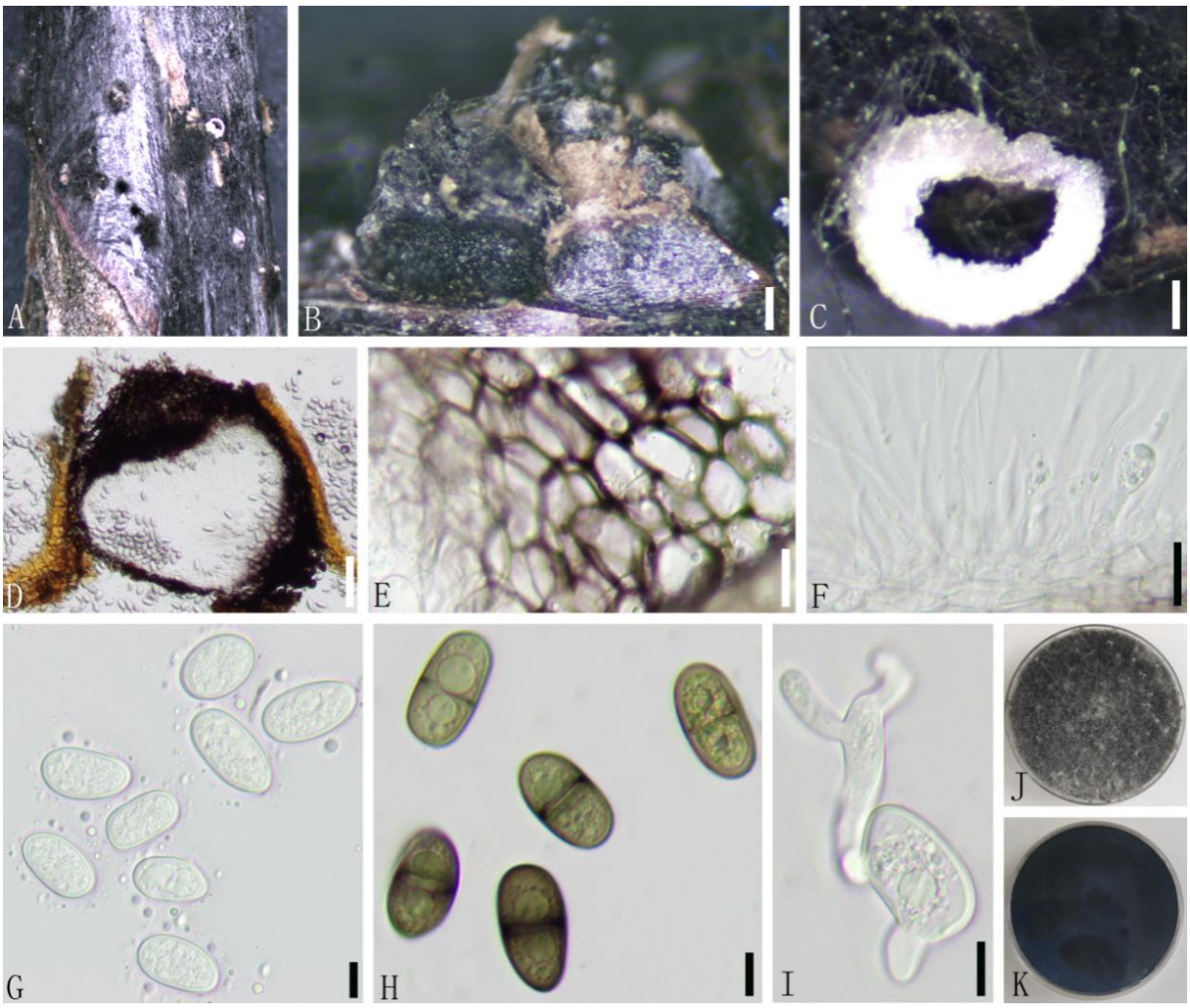


Figure 14 – *Lasiodiplodia chongzhouense* (SICAU 23-0053, holotype). A Habit of conidiostromata on twig. B Close-up of conidiostromata. C White conidial mass released. D Section of conidioma. E Conidiomata wall. F Conidiogenous cells embedded in paraphyses. G, H Conidia. I Germinating conidium. J, K Colonies from above on PDA (J from above, K from below). Scale bars: B = 200 µm, C = 100 µm, D = 50 µm, F = 20 µm, E, G–I = 10 µm.

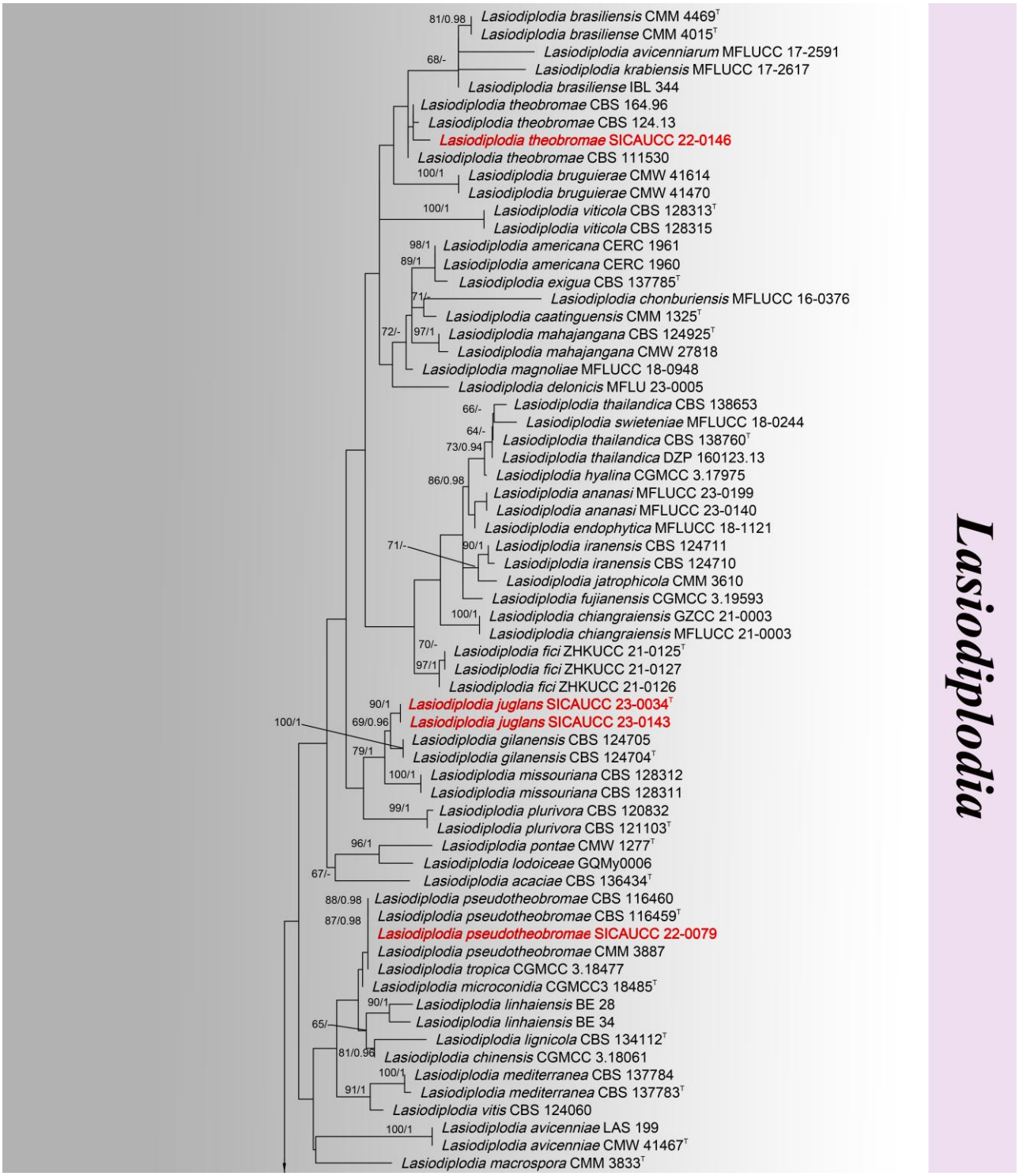


Figure 15 – Continued.

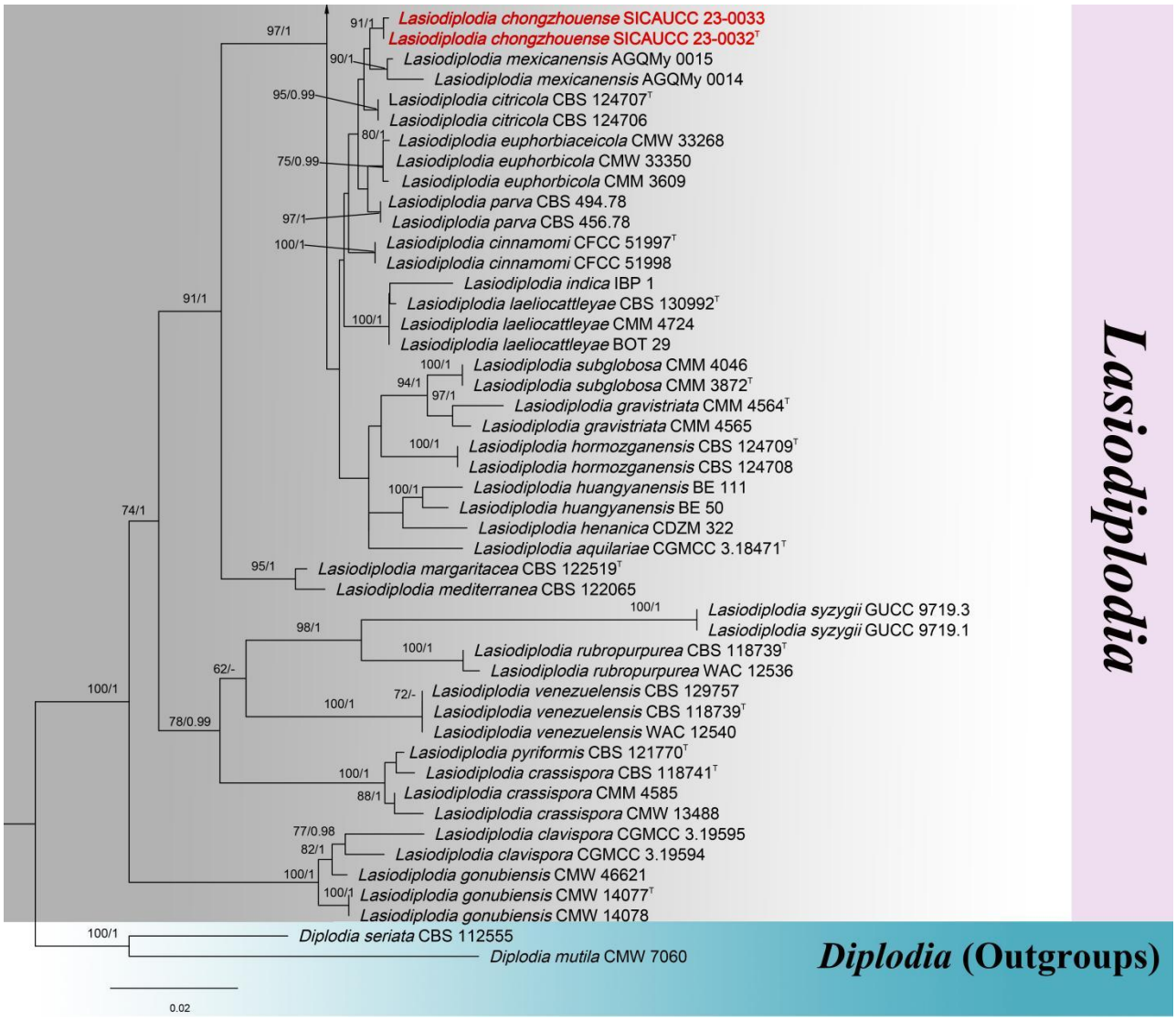


Figure 15 – Best scoring RAxML tree with a final likelihood value of -7,757.345383 based on combined ITS, *tef*1-α and *tub*2 sequence data of related species. The tree was rooted with *Diplodia mutila* CMW 7060 and *D. seriata* (CBS 112555). One hundred and thirteen strains were included in the combined analyses, which comprised 1,912 characters (636 characters for ITS, 812 characters for *tef*1-α and 464 characters for *tub*2, including alignment gaps). The matrix had 674 distinct alignment patterns, with 37.48% of undetermined characters and gaps. Estimated base frequencies were: A = 0.210848, C = 0.303990, G = 0.257216, T = 0.227946; substitution rates AC = 0.972200, AG = 3.536995, AT = 1.463692, CG = 1.142126, CT = 5.298252, GT = 1.000000; gamma distribution shape parameter α=0.216683. The Bayesian inference analyses was implemented by MrBayes v.3.2.2 with the best-fit model (K80+G for ITS; GTR+I+G for *tef*1-α; GTR+G for *tub*2) of evolution estimated with MrModeltest 2.2. The species determined in this study is indicated in red and bold. Bootstrap support values for maximum likelihood (MLBS, left) ⩾ 60% and Bayesian posterior probabilities (BYPP, right) ⩾ 0.90 are indicated at the nodes, respectively. Hyphens (-) represent support values less than 50% MLBS/0.90 BYPP. The ex-type superscript "T".

8. ***Lasiodiplodia juglans*** F.H. Wang & C.L. Yang, sp. nov. Fig. 16

Index Fungorum number: IF901561; Facesoffungi number: FoF15578

Etymology – Name refers to the host plant, *Juglans regia* L.

Holotype – SICAU 23-0055.

Associated with blight symptom on living branches of *Juglans regia*. Symptoms are not obvious in the early stages, with branches showing wilting leaves and dehydration leading to branch dieback. In later stages, the bark cracks, becoming rough and dry. Sexual morph: Not observed.

Asexual morph: Appearing as raised spots on the host. *Conidiomata* 290–390 × 320–430 µm ($\bar{x}$ = 320 × 380 µm, n = 20), stromatic, pycnidial, immersed, aggregated, unilocular or multilocular, globose to depressed globose. *Conidiomata wall* 55–95 µm wide, composed of 6–9-layers of pale brown to brown, smooth-walled cells of *textura angularis*. *Paraphyses* up to 45–72 µm long, 2–4 µm wide, aseptate, hyaline. *Conidiophores* reduced to conidiogenous cells. *Conidiogenous cells* 10–18 × 5–8 µm ($\bar{x}$ = 14 × 7 µm, n = 20), lining the pycnidial cavity, holoblastic, subcylindrical, hyaline, smooth-walled. *Conidia* 26–34 × 13–16 µm ($\bar{x}$ = 28 × 15 µm, n = 40) rarely subovoid to ellipsoid-ovoid, both ends are broadly rounded, hyaline, thick-walled, smooth-walled, becoming mature 1-septate, rough-walled, echinulate, pale brown to dark brown, oblong to ovoid, straight, not seen longitudinal striations.

Culture characteristics – Conidia begin to germinate within 24 hours in sterile water, with a germ tube emerging from the center. Colonies on PDA reaching 60 mm diam., after 9 days at 25 ℃. The mycelium grows on the surface of the medium, forming circular, fluffy colonies with a coral fleece-like appearance. Initially white, the colonies gradually turn brown to dark brown. The reverse side of the colonies appears brown, and not produced pigmentation on PDA media.

Material examined – China, Sichuan Province, Liangshan Yi Autonomous Prefecture Puge County (27°24′65″N, 102°30′7″E, alt. 1591 m), on the living branch of *Juglans regia*, 24 August 2021, F.-H. Wang, WFH202208004-1 (SICAU 23-0055, holotype), ex-type culture SICAUCC 23-0034. *Ibid*., WFH202208004-1B (SICAU 23-0164), living culture SICAUCC 23-0143.

GenBank numbers – SICAUCC 23-0034: PP060650 (ITS) and PP061165 (*tub*2); SICAUCC 23-0143: PP844871 (ITS) and PP850059 (*tub*2).

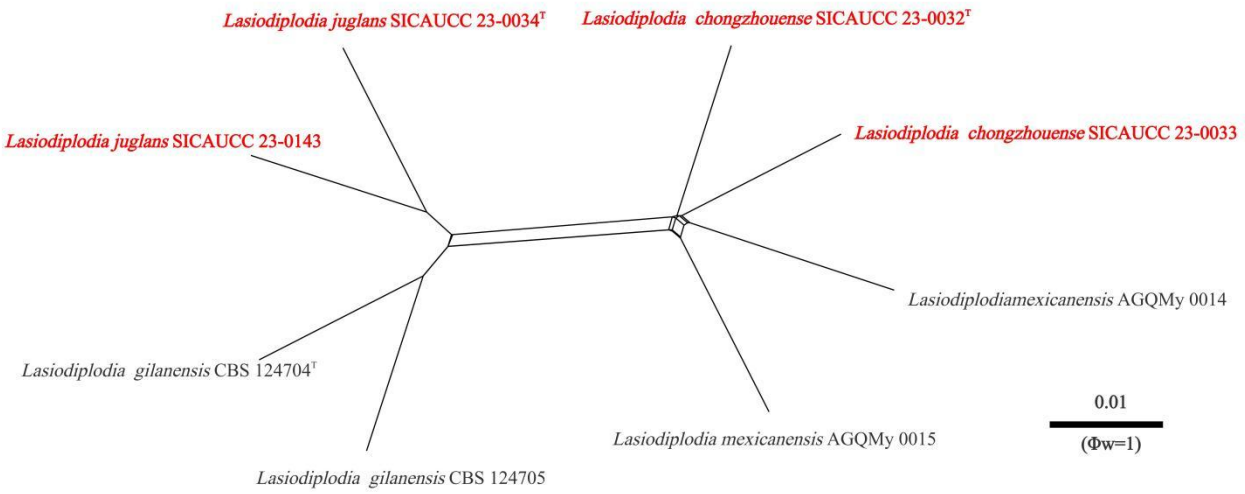


Figure 16 – The PHI test results for *Lasiodiplodia chongzhouense*, *L. juglans*, and closely related species were obtained using both LogDet transformation and splits decomposition methods. The PHI test did not find any statistically significant recombination (Φw = 1) in the data set. The new strains are represented in red and bold. "T" represents the type strain.

Note – *Lasiodiplodia chongzhouense* is characterized by stromatic, pycnidial, immersed, aggregated, unilocular or multilocular, globose to depressed globose conidiomata, hyaline, smooth, becoming mature 1-septate, rough-walled, echinulate, pale brown to dark brown, oblong to ovoid, straight, both ends broadly rounded, thin-walled, not seen longitudinal striations conidia *L. chongzhouense* is morphologically best fit *Lasiodiplodia* (Alves et al. 2008). *Lasiodiplodia*

chongzhouense is phylogenetically closer to *L. gilanensis* (CBS 124704 and CBS 124705) (Fig. 15). In the phylogeny analyses, *Lasiodiplodia juglans* groups sister to *L. gilanensis*. *Lasiodiplodia gilanensis* was associated with unknown woody plant. in Iran (Abdollahzadeh et al. 2010). The PHI test revealed no significant recombination event between our strain and the closely related taxa (Φw = 1) (Fig. 16). In morphology, our isolate (SICAUCC 23-0034) differs from *L. gilanensis* in having superficial, ered with dense mycelium, solitary, globose, thick-walled conidiomata,aseptate, ellipsoid to ovoid, with granular content, rounded at apex, base mostly truncate conidia. Our isolate has smaller conidiomata (320 × 380 µm vs. 900 × 980 µm). Therefore, we designate our collection as a new *L. juglans* species in *Lasiodiplodias*.

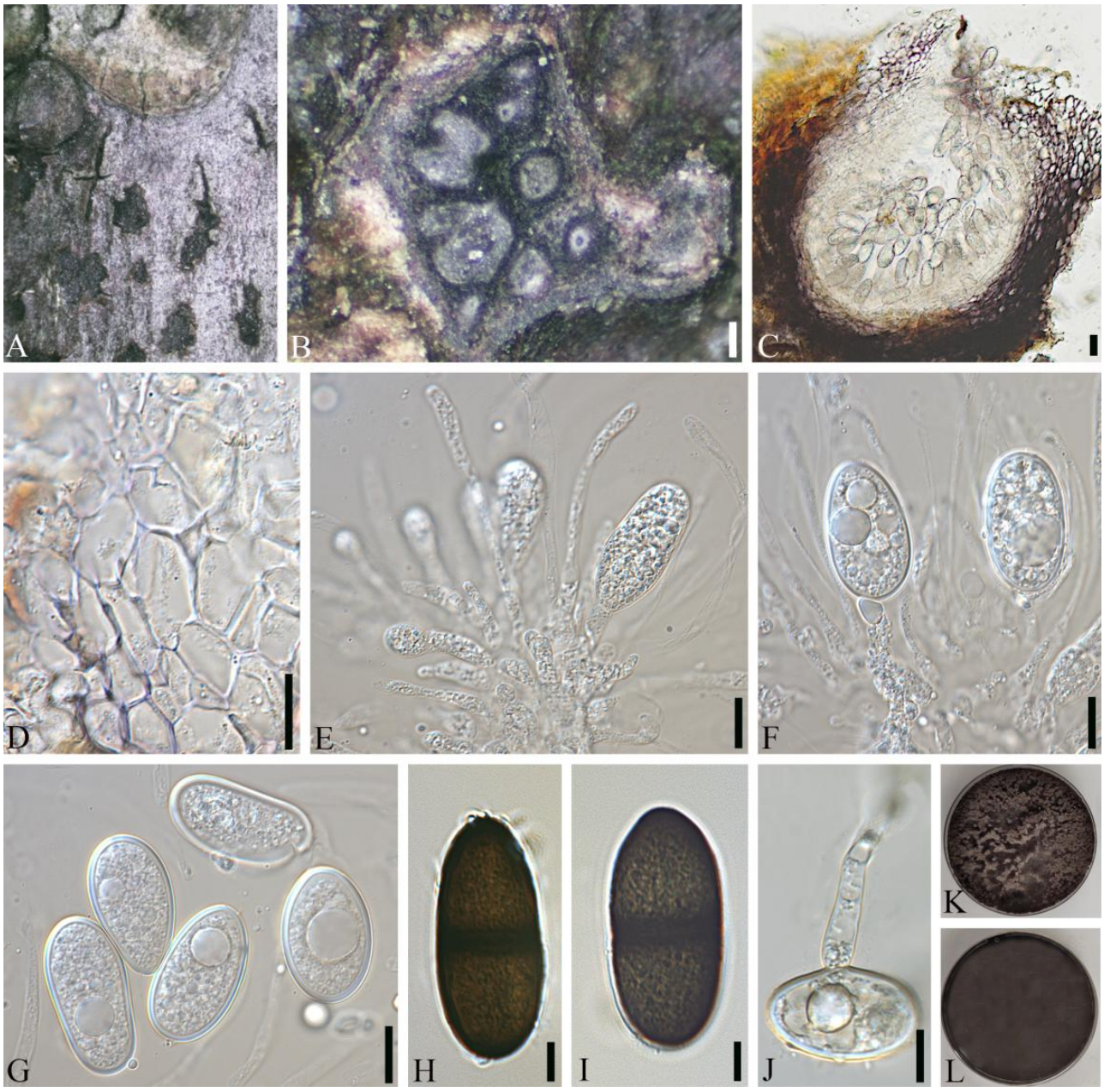


Figure 16 – *Lasiodiplodia juglans* (SICAU 23-0055, holotype). A Habit of conidiostromata on branch. B Transection section through conidiostromata. C Vertical section through conidioma. D Section of conidiomata wall. E, F Conidiogenous cells and conidia. G–I Conidia. J Geminating conidium. K, L Colonies on PDA (K from above, L from below). Scale bars: B = 200 µm, C = 20 µm, D–G, J = 10 µm, H, I = 5 µm.

9. ***Lasiodiplodia pseudotheobromae*** A.J.L. Phillips, A. Alves & Crous, Fungal Divers. 28: 8 (2008) Fig. 17

Index Fungorum number: IF510941; Facesoffungi number: FoF00166

Associated with blight symptom on living branches of *Juglans sigillata*. Symptoms manifest as brown patches appearing on the exterior of the branches and stems. These patches expand into larger areas, with longitudinal growth being faster than lateral growth. When the patches encircle the branches completely, it leads to the withering and death of the branches. Sexual morph: Not observed. Asexual morph: *Conidiomata* 160–280 × 140–190 μm ($\bar{x}$ = 220 × 165 μm, n = 20), formed on walnut branch in culture, uniloculate, dark brown to black, immersed in the host becoming erumpent when mature. *Paraphyses* hyaline, cylindrical, septate, no branched, ends rounded, up to 32–58 μm long, 3–4 μm wide arising amongst the conidiogenous cells. *Conidiogenous cells* hyaline, cylindrical, holoblastic. *Conidiomata wall* 32–58 μm wide, composed of 5–7 layers of brown to dark brown cells. *Conidia* 21.5–31 × 11.5–15.7 μm ($\bar{x}$ = 27 × 13.5 μm, n = 40), hyaline, globose to subglobose or ellipsoidal, with rounded apex and base, widest at the middle, thick-walled, and unicellular.

Culture characteristics – Conidia begin to germinate within 12 hours in sterile water, with a germ tube emerging from the center. Colonies on PDA reaching 60 mm diam., after 8 days at 25 ℃. The mycelium grows on the surface of the medium, forming circular colonies with well-developed aerial hyphae that are flocculent. Initially white, the colonies gradually turn olive green to black. The reverse side of the colonies appears black, and not produced pigmentation on PDA media.

Material examined – China, Sichuan Province, Chengdu City, Chongzhou City (30°40′6″N, 103°40′26″E, alt. 512 m), on the living branch of *Juglans sigillata*, 14 January 2021, F.-H. Wang, WFH202101011 (SICAU 22-0078), living culture SICAUCC 22-0079.

GenBank numbers – ON090365 (ITS), ON090418 (LSU), ON090406 (SSU), ON112377 (*tef*1-α) and ON112378 (*tub*2).

Note – In our phylogenetic analysis, new isolate (SICAUCC 22-0079) clustered with *Lasiodiplodia pseudotheobromae* in a well-supported clade (Fig. 15). Phylogenetic analysis showed that our new isolates clustered within *L. pseudotheobromae* clade. The sequence alignment of ITS, *tef*1-α, and *tub*2 with the ex-type strain *L. pseudotheobromae* (CBS 116459) shows no significant difference. Morphologically, our new isolates are similar to the description of *L. pseudotheobromae* (Phillips et al. 2013). Therefore, based on morphology and phylogeny, the isolate SICAUCC 22-0079 is identified as *L. pseudotheobromae*.

10. ***Lasiodiplodia theobromae*** (Pat.) Grif. & Maubl., Bull. Soc. Mycol. Fr. 25: 57 (1909) Fig. 18

Index Fungorum number: IF188476; Facesoffungi number: FoF00167

Associated with blight symptom on living twigs of *Juglans regia*. The symptoms appear at the tips of the branches, initially manifesting as water-soaked lesions, which later progress to rot and death. Sexual morph: Not observed. Asexual morph: *Conidiomata* 190–320 × 170–290 μm ($\bar{x}$ = 260 × 230 μm, n = 20), pycnidial, uniloculate, solitary or aggregated, globose to subglobose, immersed in the host becoming erumpent when mature. *Conidiomata wall*, unformed. *Paraphyses* hyaline, cylindrical, septate, occasionally branched, ends rounded, up to 50 μm long, 4–5 μm wide. *Conidiophores* reduced to conidiogenous cells. *Conidiogenous cells* 8–15 × 4–7 μm ($\bar{x}$ = 12 × 5 μm, n = 20) lining the pycnidial cavity, holoblastic, hyaline, subcylindrical, smooth-walled. *Conidia* 24–33 × 14–17 μm ($\bar{x}$ = 29 × 16 μm, n = 20), subovoid to ellipsoid-ovoid, apex broadly rounded, tapering to truncate base, widest in middle to upper third, thick-walled, contents granular, initially hyaline and aseptate, remaining hyaline for a long time, mature becoming dark brown, 1-septate.

Culture characteristics – Conidia begin to germinate within 12 hours in sterile water, with a germ tube emerging from the center. Colonies on PDA reaching 60 mm diam., after 7 days at 25 ℃. The mycelium grows on the surface of the medium, forming circular colonies with well-developed aerial hyphae that are flocculent in appearance. Initially white, the colonies gradually turn brown to black, and sclerotia are produced in the later stages. The reverse side of the colonies appears black, and not produced pigmentation on PDA media.

Material examined – China, Sichuan Province, Suining City, Shehong City, Guangxing Town (30°57′22.43″N 105°18′54.25″E, alt. 404 m), on the living twigs of *Juglans regia*, 17 May 2021, F.-H. Wang, WFH202105017 (SICAU 22-0144), living culture SICAUCC 22-0146.

GenBank numbers – OP963845 (ITS), OP964584 (LSU), OP962306 (SSU), OQ281383 (*tef*1-α) and OQ281420 (*tub*2).

Note – The phylogenetic result showed the strain SICAUCC 22-0146 clustered with the other strains of *Lasiodiplodia theobromae*. The sequence alignment of ITS, *tef*1-α, and *tub*2 with the ex-type strain *L. theobromae* (CBS 124.13) shows no significant difference. The morphological examination of this collection matched well with the holotype of *L. theobromae* (De Silva et al. 2022). *Lasiodiplodia theobromae* was previously collected in Thailand, while this is a record for China.

Neofusicoccum Crous, Slippers & A.J.L. Phillips, Studies in Mycology 55: 247 (2006).

Neofusicoccum is one of the species-rich genera in *Botryosphaeriaceae* and includes 71 epithets listed Species Fungorum (2024). *Neofusicoccum* was introduced by Crous et al. (2006a) to accommodate species that are similar to *Botryosphaeria*, but phylogenetically distinct. However, morphological characterisation of these species remains controversial (Abdollahzadeh et al. 2013, Tennakoon et al. 2021b). To resolve the species, multi-gene sequence data are essential. Species in *Neofusicoccum* have been reported as endophytes, pathogens and saprobes on a wide range of hosts (Li et al. 2018).

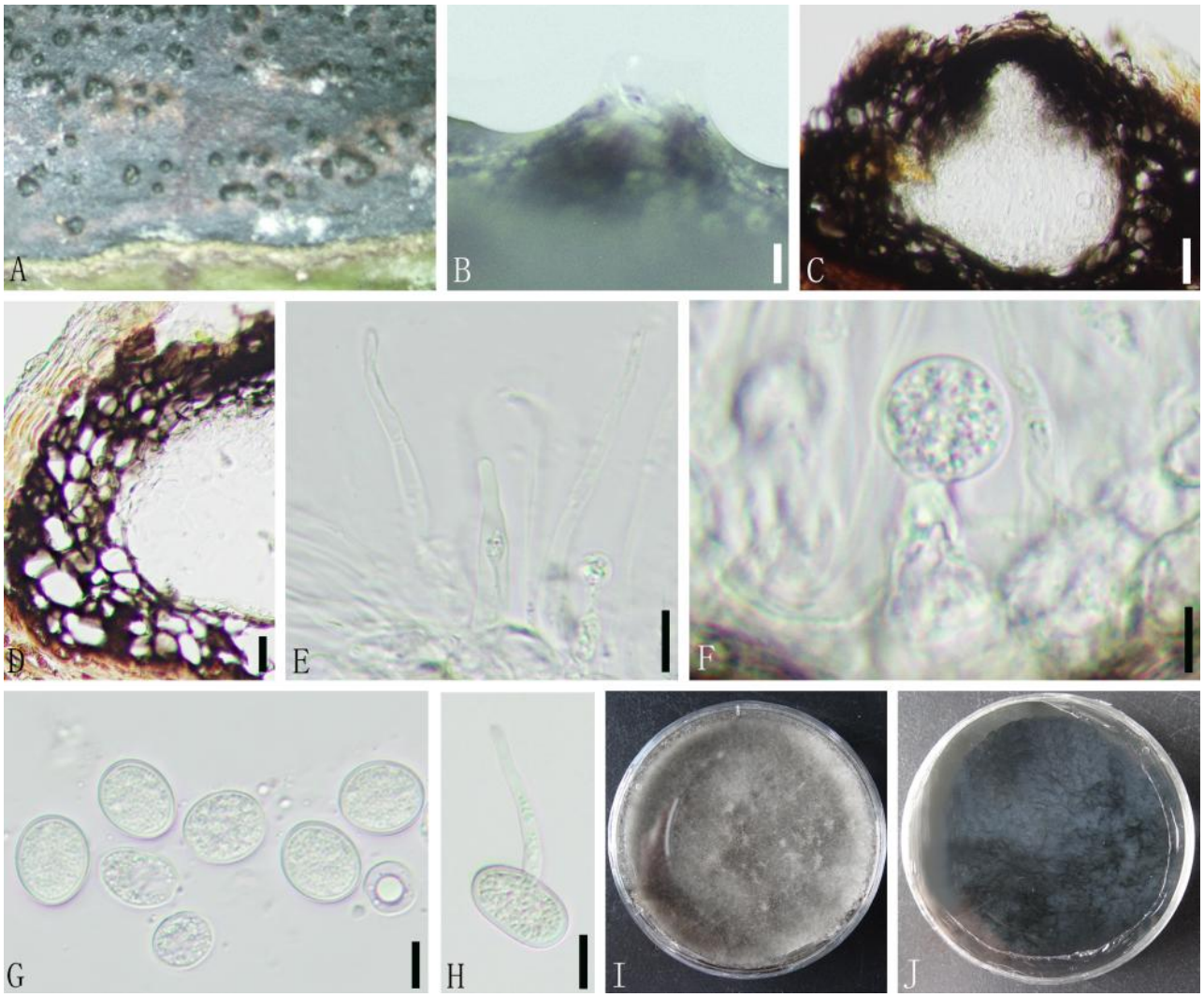


Figure 17 – *Lasiodiplodia pseudotheobromae* (SICAU 22-0078). A, B Habit of conidiomata on branch. C Vertical section through conidioma. D Section of conidiomata wall. E Paraphyses. F Conidiogenous cells and conidia. G Conidia. H Geminating conidium. I, J Colonies on PDA (I from above, J from below). Scale bars: B = 200 µm, C = 50 µm, D = 20 µm, E–H = 15 µm.

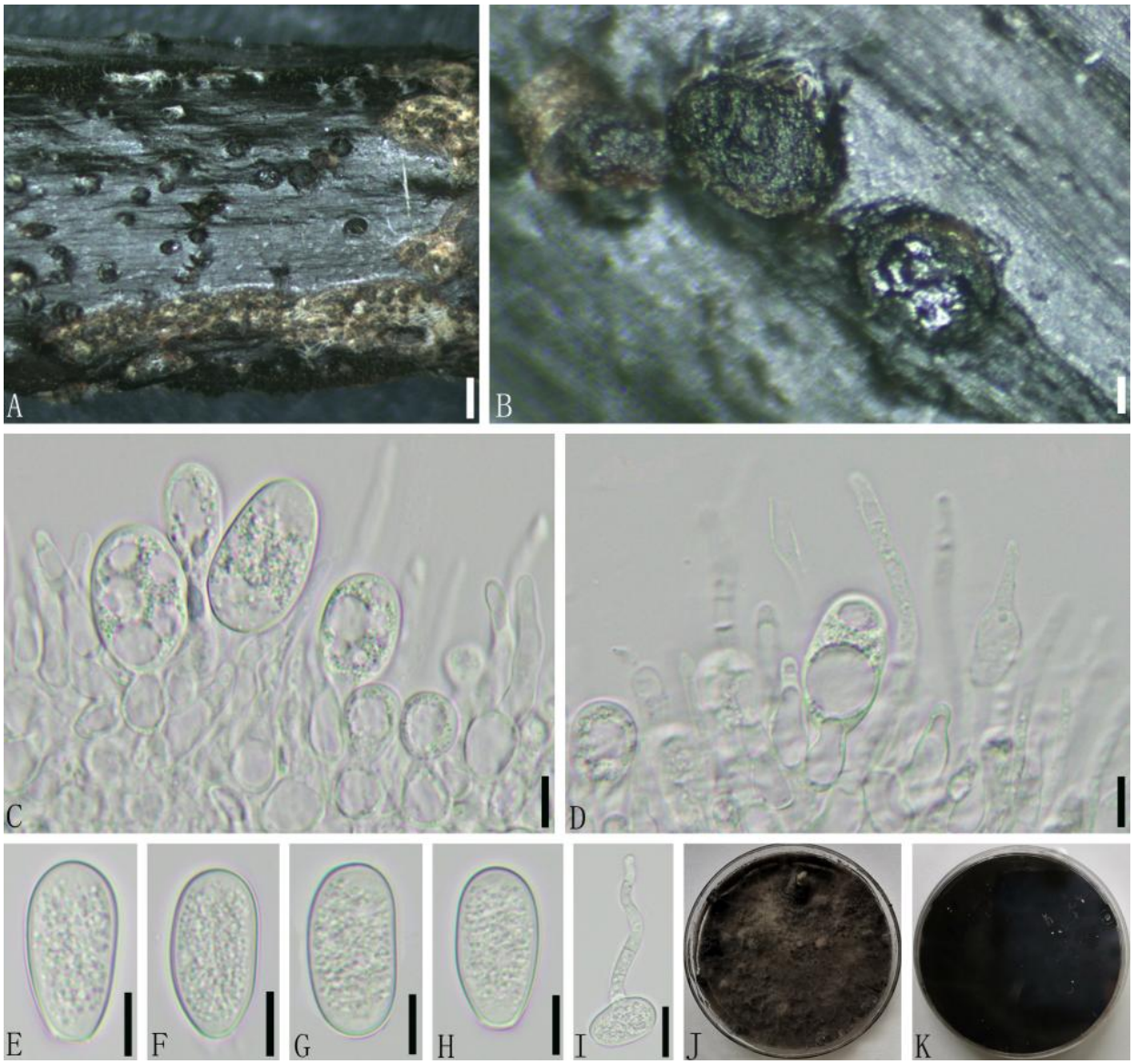


Figure 18 – *Lasiodiplodia theobromae* (SICAU 22-0144). A, B Habit of conidiomata on twig. C, D Conidiogenous cells and paraphyses. E–H Conidia. I Geminating conidium. J, K Colonies on PDA (J from above, K from below). Scale bars: A = 500 μm, B = 100 μm, I = 20 μm, C–H = 10 μm.

11. ***Neofusicoccum juglans*** F.H. Wang & C.L. Yang, sp. nov. Fig. 19

Index Fungorum number: IF901562; Facesoffungi number: FoF15579

Etymology – Name refers to the host plant, *Juglans regia.*

Holotype – SICAU 22-0056.

Associated with blight symptom on living twigs of *Juglans regia*. Death of shoot tips, twigs and branch tips can be observed. The infection progresses towards the main stem accompanied by a loss of foliage. Sexual morph: *Ascostromata* erumpent and well-developed, scattered or aggregated, 480–710 μm ($\bar{x}$ = 590 μm, n = 30), black, rounded to irregular, semi-immersed, and with multi-locule immersed in single stroma. *Ostiole* opening separately, usually papillate. *Locules* 198–330 diam., ($\bar{x}$ = 296 μm, n = 20), immersed in stroma, black, and circular to ovoid. *Peridium* comprising 4–7 layers of *textura angularis*, outer region of dark brown cells, a dinner region of hyaline cells lining the locule. *Pseudoparaphyses* 2–6 mm broad, filiform, septate, slightly constricted at septum. *Asci* 75–108 × 17–21 μm ($\bar{x}$ = 90 × 19 μm, n = 20), bitunicate, clavate, hyaline, with thin-walled, short pedicel, apically rounded, 8-spored, and forming among pseudoparaphyses. *Ascospores* 17–29 × 8–13 μm ($\bar{x}$ = 23 × 10 μm, n = 40), hyaline, 1–3-septate, thin-walled, fusoid to ellipsoid, sometimes with tapered ends, usually broadest in the middle, smooth, and granular. Asexual morph: Not observed.

Culture characteristics – Ascospores germinating on sterile water within 12 h and germ tubes produced from ends. Colonies on PDA reaching 60 mm diam., after 7 days at 25 ℃. The mycelium grows on the surface of the medium, forming circular colonies with flocculent hyphae. Initially, the colonies are white, fluffy, and moderately dense, with regular edges. They start out as white but gradually darken from the center. The reverse side of the colonies is dark black. Not produced pigmentation on PDA media.

Material examined – China, Sichuan Province, a walnut garden of Chongzhou (30° 40′ 6′′ N, 103° 40′ 20′′ E), on the living twigs of *Juglans regia*, 21 April 2022, F.-H. Wang, WFH202204013 (SICAU 23-0056, holotype), ex-type culture SICAUCC 23-0035. *Ibid*., WFH202204013B (SICAU 23-0165), living culture SICAUCC 23-0144.

GenBank numbers – SICAUCC 23-0035: PP060651 (ITS), PP061133 (*tef*1-α) and PP061166 (*tub*2); SICAUCC 23-0144: PP844872 (ITS), PP850051 (*tef*1-α) and PP850060 (*tub*2).

Note – *Neofusicoccum juglans* was collected from diseased branches of *Juglans regia* in China. In the phylogenetic analysis, *N. juglans* formed a monophyletic clade basal to *Neofusicoccum* species. *Neofusicoccum juglans* is phylogenetically closer to *N. sichuanense* (Fig. 20). However, *N. sichuanense* has aseptate ascospores, 12–19 × 4–7 µm, while *N. juglans* has 1–3 septate ascospores, 17–29 × 8–13 µm (Xu et al. 2022a). Nucleotide comparisons reveal notable genetic dissimilarities between *N. juglans* and *N. sichuanense* (SICAUCC 22-0099), viz. 1.4% (7/516, 0 gap), 3.0% (8/265, 0 gap), and 1.9% (8/424, 0 gap) in the ITS, *tef*1-α, and *tub*2, respectively. The PHI test revealed no significant recombination event between our strain and the closely related taxa (Φw = 1) (Fig. 21). Therefore, the new strain is introduced as a new species based on morphology evidence.

12. ***Neofusicoccum parvum*** (Pennycook & Samuels) Crous, Slippers & A.J.L. Phillips, Stud. Mycol. 55: 248 (2006) Fig. 22

Index Fungorum number: IF500879; Facesoffungi number: FoF00153

Associated with blight symptom on living twigs of *Juglans regia*. Symptoms on the branches appear as warts, the periderm around warts can become cracked, and the bark is roughened with a scaly periderm. During dry weather, these cankers expand and coalesce. Sexual morph: *Ascostromata* 600–1200 µm diam, 190–280 µm high (including the papilla), visible as minute black dots or papilla on host tissue, semi-immersed to erumpent under epidermis, individually globose to subglobose, solitary or clustered, longitudinal axis vertical to the host surface. *Locules* 190–280 × 180–290 µm ($\bar{x}$ = 240 × 260 µm, n = 20), nearly circular. *Ostiole* central, circular, papillate. *Peridium* of *locules* up to 20–55 µm wide, two-layered, outer layer composed of brown to dark brown, thick-walled cells of *textura angularis*, inner layer composed of hyaline thin-walled cells of *textura angularis*. *Pseudoparaphyses* 2–3.5 µm wide, hyphae-like, numerous, septate, slightly constricted at septum. *Asci* 78–116 × 13–17 µm ($\bar{x}$ = 96 × 15 µm, n = 20), 8–spored, bitunicate fissitunicate, clavate to cylindro-clavate, short pedicellate, apically rounded with well-developed ocular chamber. *Ascospores* 18–26 × 9–13 µm ($\bar{x}$ = 24 × 11 µm, n = 20), hyaline, aseptate, during germination, with a 1–2-septate, ellipsoidal to fusiform, usually wider in the center, thick and rough-walled. Asexual morph: Not observed.

Culture characteristics – Ascospores germinating on sterile water within 12 h and germ tubes produced from ends. Colonies on PDA reaching 60 mm diam., after 9 days at 25 ℃. The mycelium grows on the surface of the medium, filamentous, circular, flat with entire margin, from above brown to dark brown reticulation hyphae. The reverse side of the colonies is dark black. Not produced pigmentation on PDA media.

Material examined – China, Sichuan Province, Neijiang City, Dongxing District, Paifang Village (29°48′30.19″N 105°6′36.05″E, alt. 388 m), on the living twigs of *Juglans regia*, 17 May 2021, F.-H. Wang, WFH202105009 (SICAU 22-0150), living culture SICAUCC 22-0153.

GenBank numbers – OP963850 (ITS), OP964589 (LSU), OP962308 (SSU), OQ281388 (*tef*1-α) and OQ281422 (*tub*2).

Note – *Neofusicoccum parvum* has been reported on various woody hosts and is an important plant pathogen (Iturritxa et al. 2011, Liu et al. 2012, Abou-Mansour et al. 2015, Vakalounakis et al.

2019, Si et al. 2023). The sexual morph of *N. parvum* is characterized by uni- or multi-loculate ascostromata, cylindrical, to clavate asci and oval to broadly fusiform, hyaline, aseptate ascospores (Slippers et al. 2004). Nucleotide comparison of ITS, *tef*1-α, and *tub*2 (SICAUCC 22-0153) reveals high similarity to *N. parvum* (isolate MFLUCC 11-0184), the similarities are 100% (517/517, 0 gap), 99% (276/285, 0 gap), and 99.8% (430/434, 0 gap), respectively. We identified our isolate as *N. parvum* based on morphology and phylogeny.

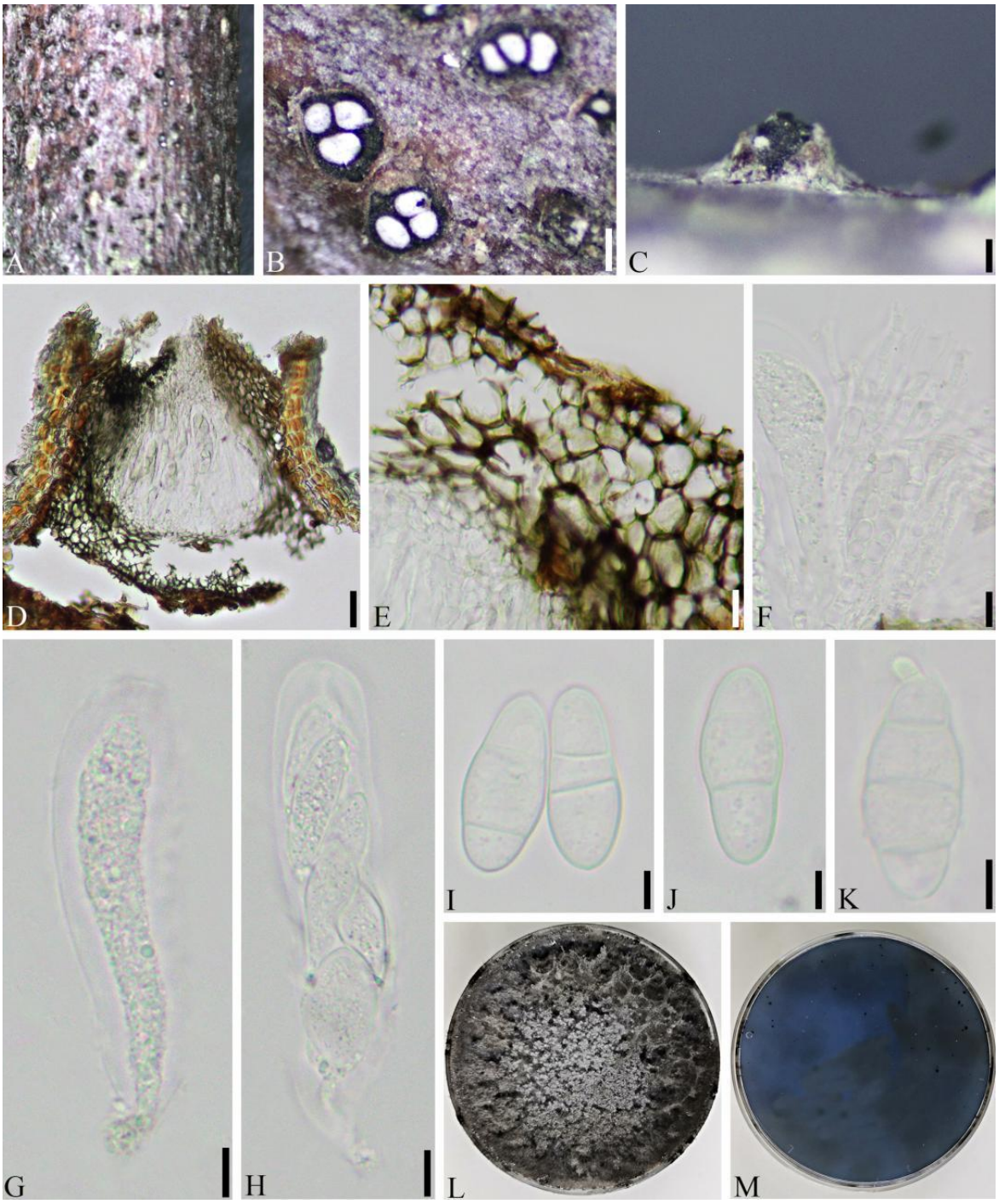


Figure 19 – *Neofusicoccum juglans* (SICAU 23-0056, holotype). A, C Appearance of ascostromata on host substrate. B Transverse cutting diagram of ascomata. D Section of ascoma. E Peridium. F Pseudoparaphyses and asci. G, H Asci. I, J Ascospores. K Germinating ascospore. L, M Colonies on PDA (L from above, M from below). Scale bars: B = 500 μm, C = 200 μm, D = 50 μm, F–H = 20 μm, E = 10 μm, I–K = 5 μm.

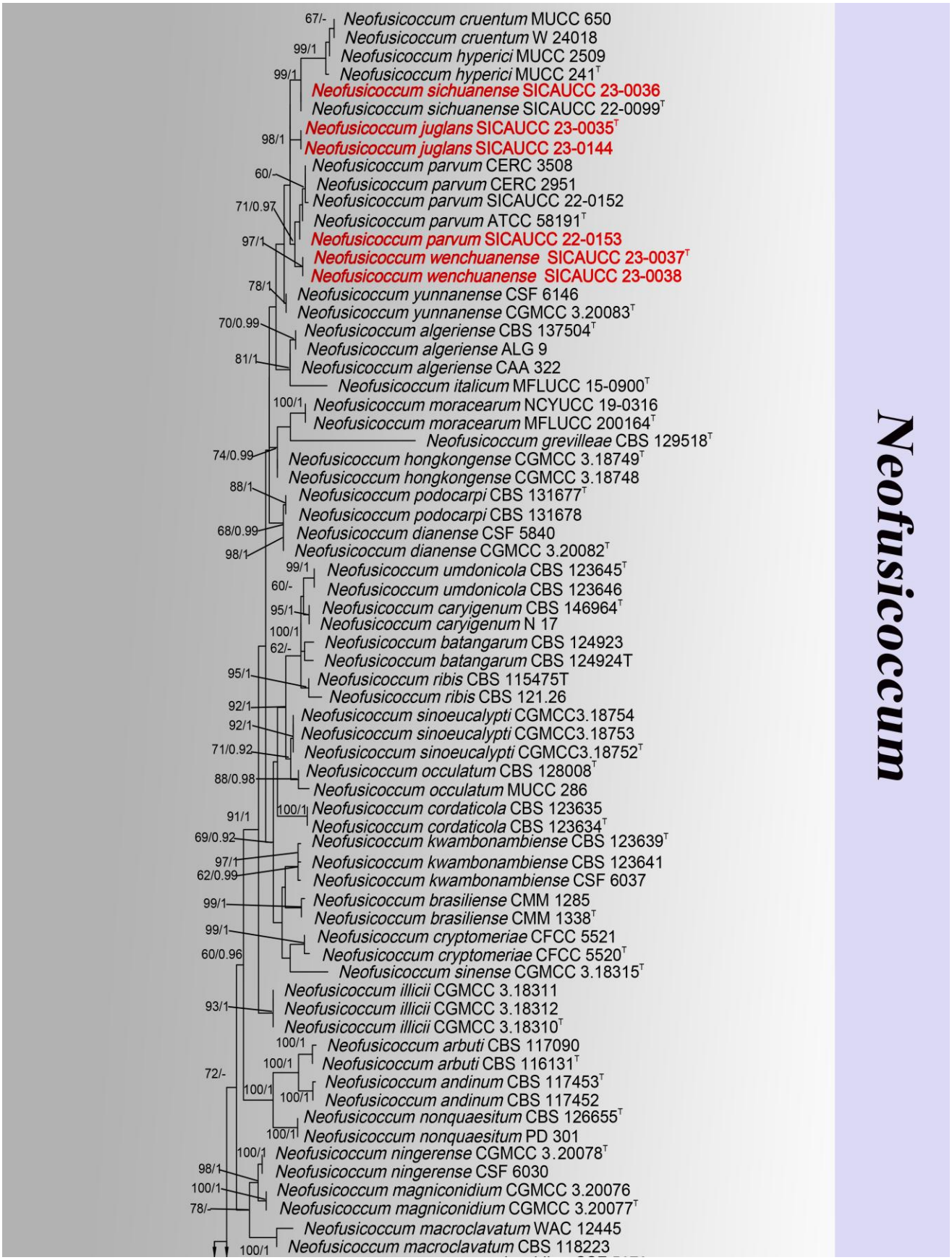


Figure 20 – Continued.

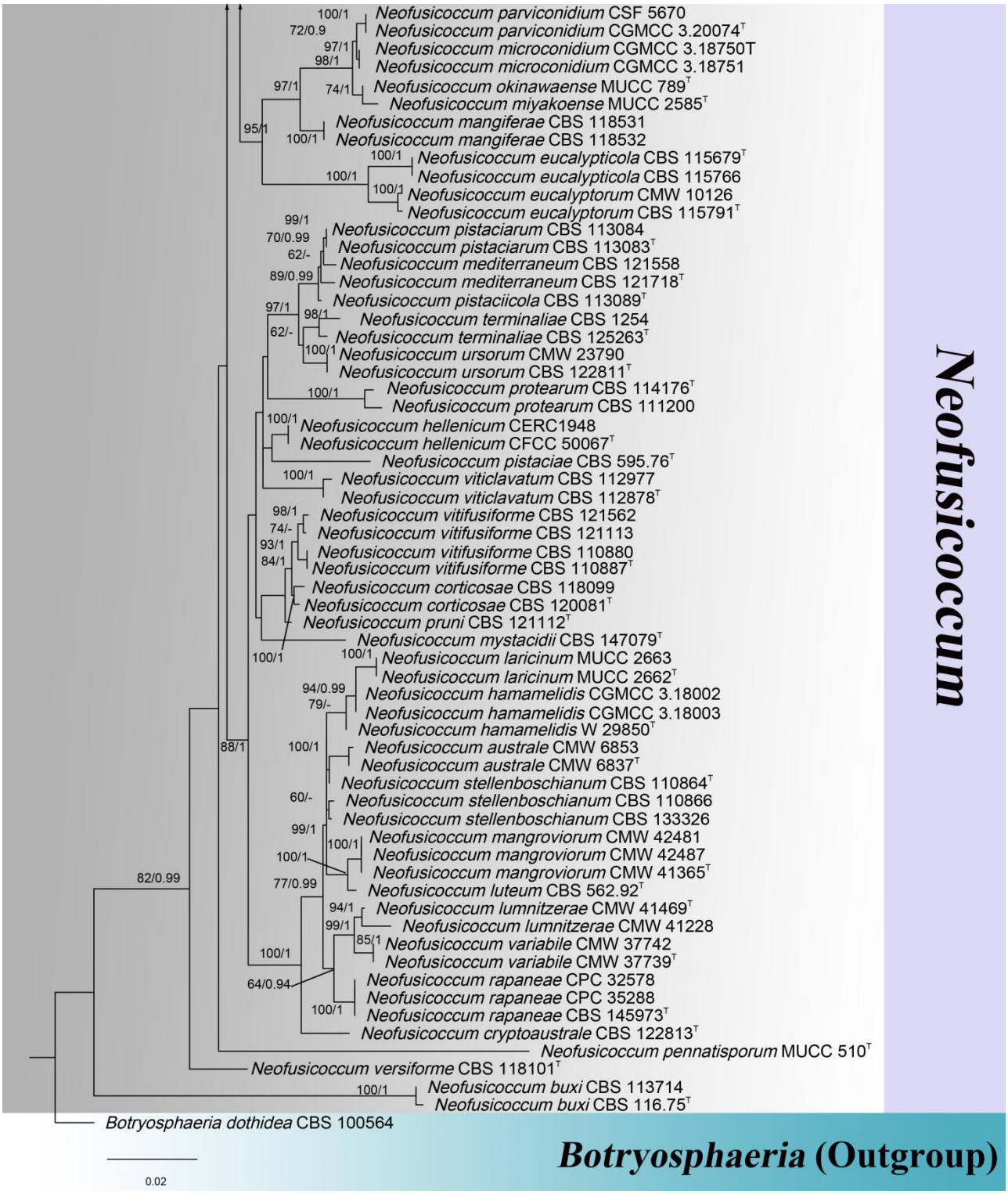


Figure 20 – Best scoring RAxML tree with a final likelihood value of -14,265.853033 based on combined ITS, *rpb*2, *tef*1-α and *tub*2 sequence data for *Neofusicoccum*. The tree is rooted with *Botryosphaeria dothidea* (CBS 100564). One hundred and thirty-one strains were included in the combined analyses which comprised 5,580 characters (2,319 characters for ITS, 1,108 characters for *rpb*2, 771 characters for *tef*1-α and 1,380 characters for *tub*2, including gap regions). The matrix had 1,000 distinct alignment patterns, with 69.57% undetermined characters and gaps. Estimated base frequencies were as follows; A = 0.218826, C = 0.291945, G = 0.271407, T = 0.217822; substitution rates AC = 1.003638, AG = 4.338911, AT = 0.954505, CG = 1.123794, CT = 8.272615, GT = 1.000000; gamma distribution shape parameter α=0.267434. The Bayesian inference analysis was implemented by MrBayes v.3.2.2 with the best-fit model (GTR+I+G for ITS, *tub*2; GTR+G for *rpb*2; HKY+I+G for *tef*1-α) of evolution estimated with MrModeltest 2.2. The species determined in this study is indicated in red and bold. Bootstrap support values for maximum likelihood (MLBS, left)

⩾ 60% and Bayesian posterior probabilities (BYPP, right) ⩾ 0.90 are indicated at the nodes, respectively. Hyphens (-) represent support values less than 60% MLBS/0.90 BYPP. The ex-type superscript "T".

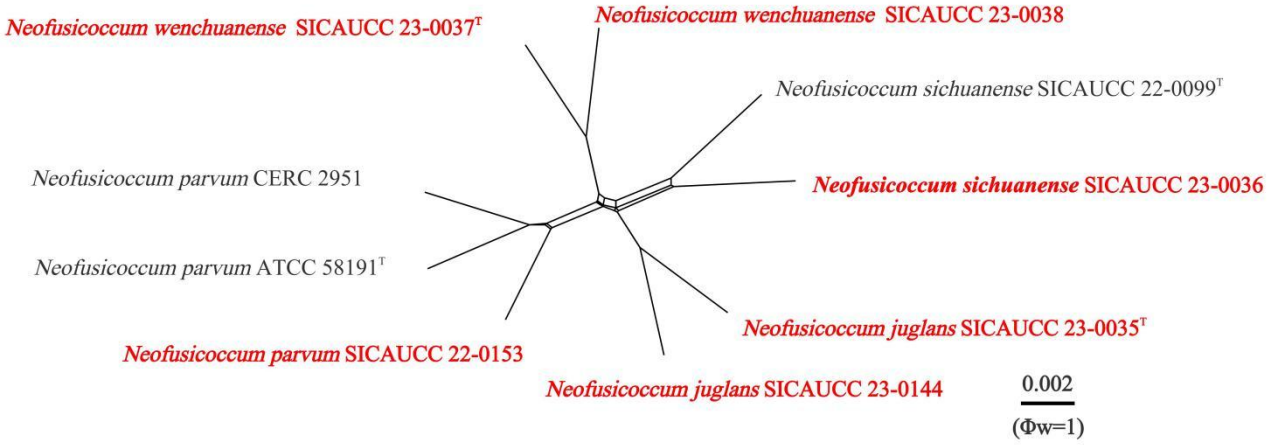


Figure 21 – The PHI test results for *Neofusicoccum juglans*, *N. sichuanense*, and closely related species were obtained using both LogDet transformation and splits decomposition methods. The PHI test did not find any statistically significant recombination (Φw = 1) in the dataset. The new strains are represented in red and bold. "T" represents the type strain.

13. ***Neofusicoccum sichuanense*** X.L. Xu & C.L. Yang, Front. Microbiol. 13(no. 1016548): 13 (2022)

Fig. 23

Index Fungorum number: 845074; Facesoffungi number: FoF 16289

Associated with blight symptom on living twigs of *Juglans regia*. Symptoms include the appearance of brown stripes on the bark of branches, veinal chlorosis, leaf wilting and shedding, ultimately leading to the dieback of twigs and branches. Sexual morph: Not observed. Asexual morph: *Conidiomata* pycnidial, epidermal, immersed, solitary or gregarious, brown to dark brown, globose to subglobose, uni- to multi-loculate, with a central ostiole, becoming erumpent and exuding conidia in a white mucoid mass, and each locule 180–255 × 140–230 µm ($\bar{x}$ = 200 × 190 µm, n = 10). *Conidiomata wall* up to 40–70 µm wide, composed of several layers of small, heavily pigmented, thick-walled cells of *textura angularis*, becoming hyaline and smaller towards the conidiogenous cells. *Conidiophores* reduced to conidiogenous cells. *Conidiogenous cells* 10–25 × 4–6 µm ($\bar{x}$ = 16 × 4 µm, n = 20), hyaline, terminal, subcylindrical, rarely ampulliform, proliferating near apex. *Conidia* 16–23 × 5–9 µm ($\bar{x}$ = 20 × 7 µm, n = 35), hyaline, thin-walled, aseptate, fusiform to narrowly ellipsoidal, straight or slightly curved, widest in the middle or near the apex of the conidium, apex subobtuse, base truncate, rough-walled.

Culture characteristics – Conidia germinating on sterile water within 12 h and germ tubes produced from ends. Colonies on PDA reaching 60 mm diam., after 12 days at 25 ℃. The mycelium grows on the surface of the medium, filamentous, circular, fimbriate, umbonate, surface rough, from above silver-white flocculent hyphae. The reverse side of the colonies is dark black. Not produced pigmentation on PDA media.

Material examined – China, Sichuan Province, Guangyuan City, Chaotian District (36°32′28.28″N 105°52′26.37″E, alt. 554 m), on the living twigs of *Juglans regia*, 21 April 2022, F.-H. Wang, WFH202105048-1 (SICAU 23-0057), living culture SICAUCC 23-0036.

GenBank numbers – PP060652 (ITS), PP061116 (*rpb*2), PP061134 (*tef*1-α) and PP061167 (*tub*2).

Note – In the phylogenetic tree, the new strain (SICAUCC 23-0036) is nested within *Neofusicoccum sichuanense* (SICAUCC 22-0099) strains with strong statistical support (99% MLBS/1.00 BYPP) (Fig. 7), and the specimen was similar to the description of *N. sichuanense* reported by Xu et al. (2022a). Nucleotide comparisons of ITS, *tef*1-α, *rpb*2 or *tub*2 from our collection (SICAUCC 23-0036) showed a high homology with the sequences of *N. sichuanense* (SICAUCC 22-0099), with a similarity of 100% (570/570, 0 gap), 99.7% (1/263, 0 gap), 100% (1310/1310, 0 gap) and 100% (1036/1036, 0 gap), respectively. Therefore, this species is introduced, collected from living twigs of *Juglans regia* and supported by phylogenetic analyses.

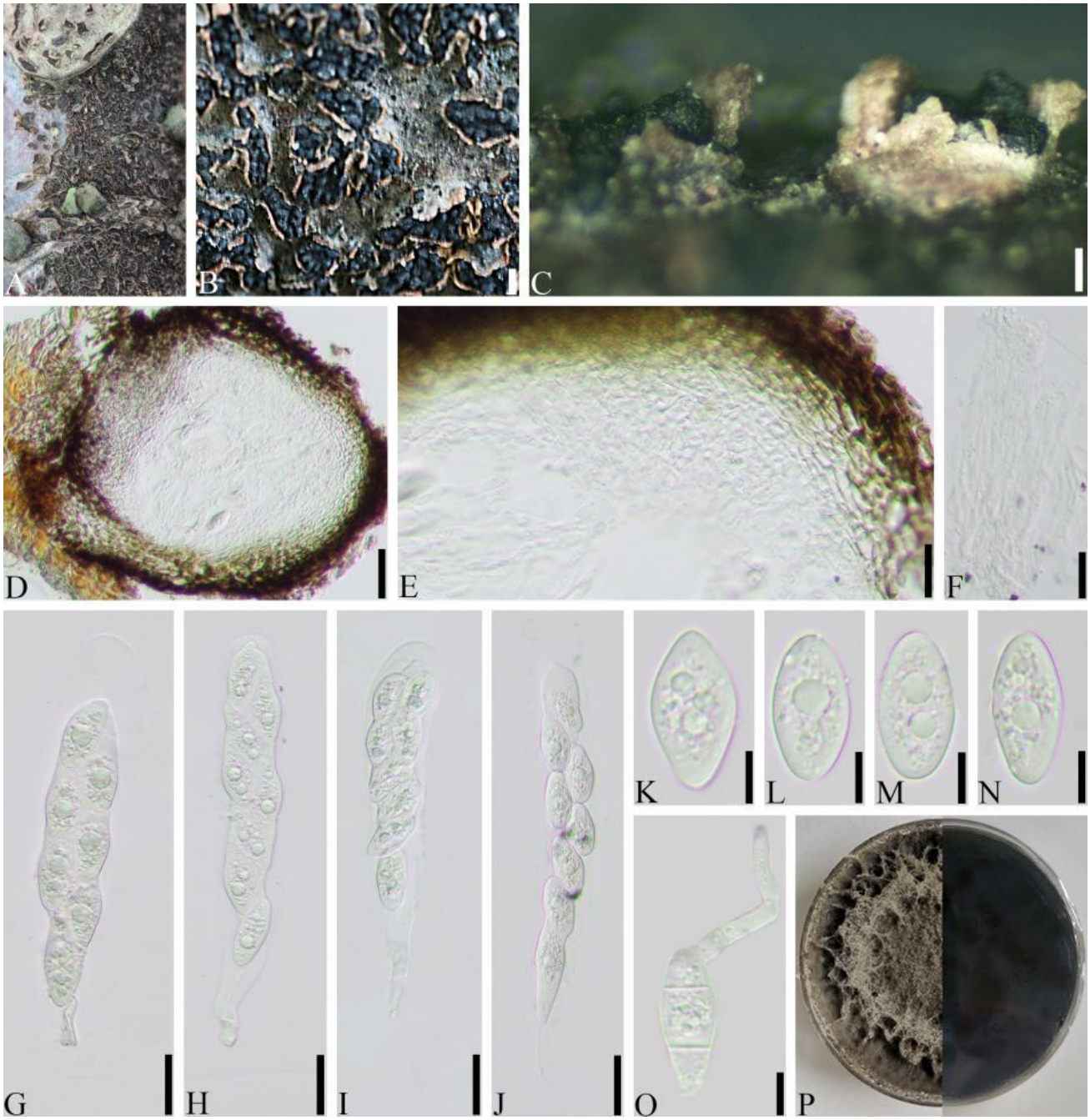


Figure 22 – *Neofusicoccum parvum* (SICAU 22-0150). A-C Appearance of ascostromata on host substrate. D Section of ascoma. E Peridium. F Paraphyses. G–J Asci. K–N Ascospores. O Germinating ascospore. P Colonies on PDA. Scale bars: B = 500 μm, C = 200 μm, D = 50 μm, E–J = 20 μm, K–O = 10 μm.

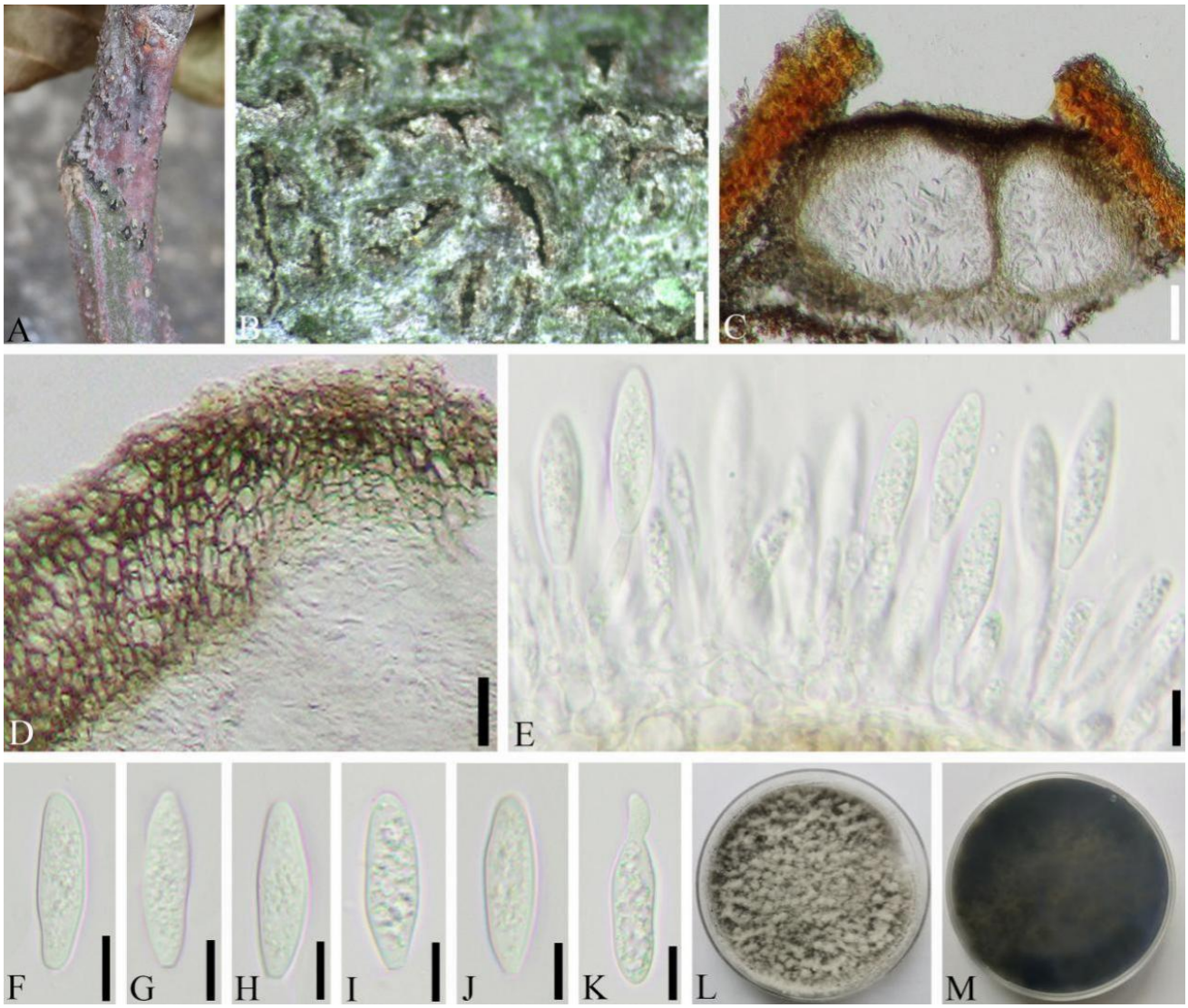


Figure 23 – *Neofusicoccum sichuanense* (SICAU 23-0057). A, B Appearance of conidiostromata on *Juglans regia*. C Vertical section through bi-loculate conidiostroma. D Section of conidiomata wall. E Conidiogenous cells and conidia. F–J Conidia. K Geminating conidium. L, M Colonies on PDA (L from above, M from below). Scale bars: B = 500 µm, C = 50 µm, D = 20 µm, E–H = 10 µm.

14. ***Neofusicoccum wenchuanense*** F.H. Wang & C.L. Yang, sp. nov. Figs. 24, 25

Index Fungorum number: IF901563; Facesoffungi number: FoF15580

Etymology – Named after locality where the fungus was isolated for the first time.

Holotype – SICAU 22-0058.

Associated with blight symptom on living twigs of *Juglans regia*. Symptoms include the appearance of brown stripes on the bark of branches, veinal chlorosis, leaf wilting and shedding, ultimately leading to the dieback of twigs and branches. Sexual morph: *Ascostromata* 380– 600 × 340–420 µm ($\bar{x}$ = 490 × 395 µm, n = 10), immersed to partially erumpent through the bark, gregarious or solitary, forming a botryose aggregate, black, multi-loculate, with 4–6 locules, individual locules, 170–275 × 150–240 µm ($\bar{x}$ = 235 × 185 µm, n = 20), sometimes with a central ostiole. *Peridium* 30–50 µm wide, two-layered, outer layer composed of dark brown, thick-walled cells of *textura angularis*, inner layer composed of lightly pigmented, thin-walled cells of *textura angularis* lining the locule. *Hamathecium* composed of 1–3 µm wide, hypha-like, septate paraphyses. *Asci* 86–120 × 15–20 µm ($\bar{x}$ = 98 × 18 µm, n = 20), 8-spored, bitunicate, fissitunicate, clavate, short pedicellate, apically rounded, with a small ocular chamber. *Ascospores* 10–16 × 19–26 µm ($\bar{x}$ = 13 × 23 µm, n = 40), hyaline, aseptate, thin-walled, fusoid to ellipsoid, sometimes with tapered ends, usually broadest in the middle, smooth, and granular. Asexual morph: *Conidiostromata* 490–670 × 270–480 µm ($\bar{x}$ =

540 × 390 μm, n = 40), immersed in host tissue, becoming superficial, solitary or gregarious, brown to dark brown, globose to subglobose, uni- to multi-loculate. *Locules* 400–620 × 230–410 μm ($\bar{x}$ = 490 × 330 μm, n = 40), round or pear-shaped. *Conidiomata wall* up to 30–50 μm wide, composed of 5–8 layers of small, the outer layer is brown and the inner layer is transparent, composed of isodiametric or sometimes irregular cells. *Conidiogenous cells* phialidic, hyaline, smooth, ampulliform, 7–14 × 3–6 μm ($\bar{x}$ = 12 × 4 μm, n = 20). *Conidia* 18–28 × 7–12 μm ($\bar{x}$ = 23 × 8 μm, n = 40), broadly fusoid to ellipsoidal, incidentally slightly curved, smooth- and thin-walled, hyaline, with many minute guttules.

Culture characteristics – Conidia and ascospores germinating on sterile water within 12 h and germ tubes produced from ends. Colonies on PDA reaching 60 mm diam., after 12 days at 25 ℃. The mycelium is white at first, and the surface is flocculent, becoming brown, when aged, villi form surface. The reverse side of the colonies is dark brown. Not produced pigmentation on PDA media.

Material examined – China, Sichuan Province, Aba Tibetan and Qiang Autonomous Prefecture, Wenchuan County (31°20′21.45″N 103°28′40.11″E, alt. 1660 m), on the living twigs of *Juglans regia*, 7 July 2022, F.-H. Wang, WFH202207017 (SICAU 23-0058, holotype), ex-type culture SICAUCC 23-0037. *Ibid*., Liangshan Yi Autonomous Prefecture, Huili City (26°56′43.17″N 102°16′26.36″E, alt. 2006 m), on the living twigs of *Juglans regia*, 30 September 2022, F.-H. Wang, WFH202209004 (SICAU 23-0059), living culture SICAUCC 23-0038.

GenBank numbers – SICAUCC 23-0037: PP060653 (ITS), PP061117 (*rpb*2), PP061135 (*tef*1-α) and PP061168 (*tub*2); SICAUCC 23-0038: PP060654 (ITS), PP061136 (*tef*1-α) and PP061169 (*tub*2).

Note – Phylogenetic analyses showed that *Neofusicoccum wenchuanense* (SICAUCC 23-0037 and SICAUCC 23-0038) formed an independent lineage within *Neofusicoccum*. *N. wenchuanense* is phylogenetically closer to *N. parvum* (ATCC 58191) (Fig. 18). Nevertheless, this new species differs from *N. sichuanense* in larger conidia and smaller ascospores (12–19 × 4–7 μm vs. 18–24 × 7–12 μm and 8–13 × 17–29 μm vs. 10–16 × 19–26), Larger conidiostromata (185 × 158 μmvs. 540 × 390 μm), whil also produce septa during germination (Xu et al. 2022a). Nucleotide comparisons reveal notable genetic dissimilarities between *N. wenchuanense* and *N. parvum* (ATCC 58191), viz. 0.8% (4/481, 0 gap), 4.8% (12/249, 4 gaps), 2.1% (8/370, 8 gaps), and 0.5% (3/592, 0 gap) in the ITS, *tub*2, *tef*1-α and *rpb*2, respectively. The PHI test revealed no significant recombination event between our strain and the closely related taxa (Φw = 1) (Fig. 21). *Neofusicoccum wenchuanense* and *N. hyperici* can be distinguished by base difference, but the difference between *N. wenchuanense* and *N. sichuanense* is not obvious. We recognize *N. wenchuanense* and *N. sichuanense* as distinct species based on morphological differences. However, further molecular evidence is needed to confirm their relationship.

Cladosporiales Abdollahz. & Crous.

This followed recent treatments by Hyde et al. (2024b).

Cladosporiaceae Chalm. & R.G. Archibald, Yearbook of Tropical Medicine and Hygiene: 25 (1915).

Nannizzi (1934) introduced the taxonomic unit of *Cladosporiaceae* to better accommodate the genus *Cladosporium*. Eight genera are currently accepted in this family, namely *Cladosporium*, *Cryoendolithus*, *Davidiellomyces*, *Graphiopsis*, *Neocladosporium*, *Rachicladosporium*, *Toxicocladosporium*, and *Verrucocladosporium* (Hongsanan et al. 2020a, Wijayawardene et al. 2020a, Hyde et al. 2024b).

Cladosporium Link, Mag. Gesell. naturf. Freunde, Berlin 7: 37 (1816)

Cladosporium was established by Link (1816) with *C. herbarum* as the type species, and is one of the largest genera of dematiaceous hyphomycetes. *Davidiella* was erected by Braun et al. (2003) to accommodate the sexual morph of *Cladosporium sensu stricto*. *Cladosporium* has priority over *Davidiella* at generic rank, and is also more commonly used in literatures (Bensch et al. 2012), therefore, *Davidiella* was recognized as a synonym of *Cladosporium*. Therefore, *Cladosporiaceae*

took preference over *Davidiellaceae* (Bensch et al. 2012). *Cladosporium* has a cosmopolitan distribution worldwide, and mainly includes many important pathogens causing leaf spots and stem rots on various plant hosts (Van Kan et al. 1991, Heuchert et al. 2005, Bensch et al. 2018, Tibpromma et al. 2019, Abdulla 2023), as well as in vertebrate hosts including humans (De Hoog et al. 2000, Sandoval-Denis et al. 2016a). In addition, *Cladosporium* species have also been recorded as endophytes, playing a positive effect on plant growth (Hamayun et al. 2009).

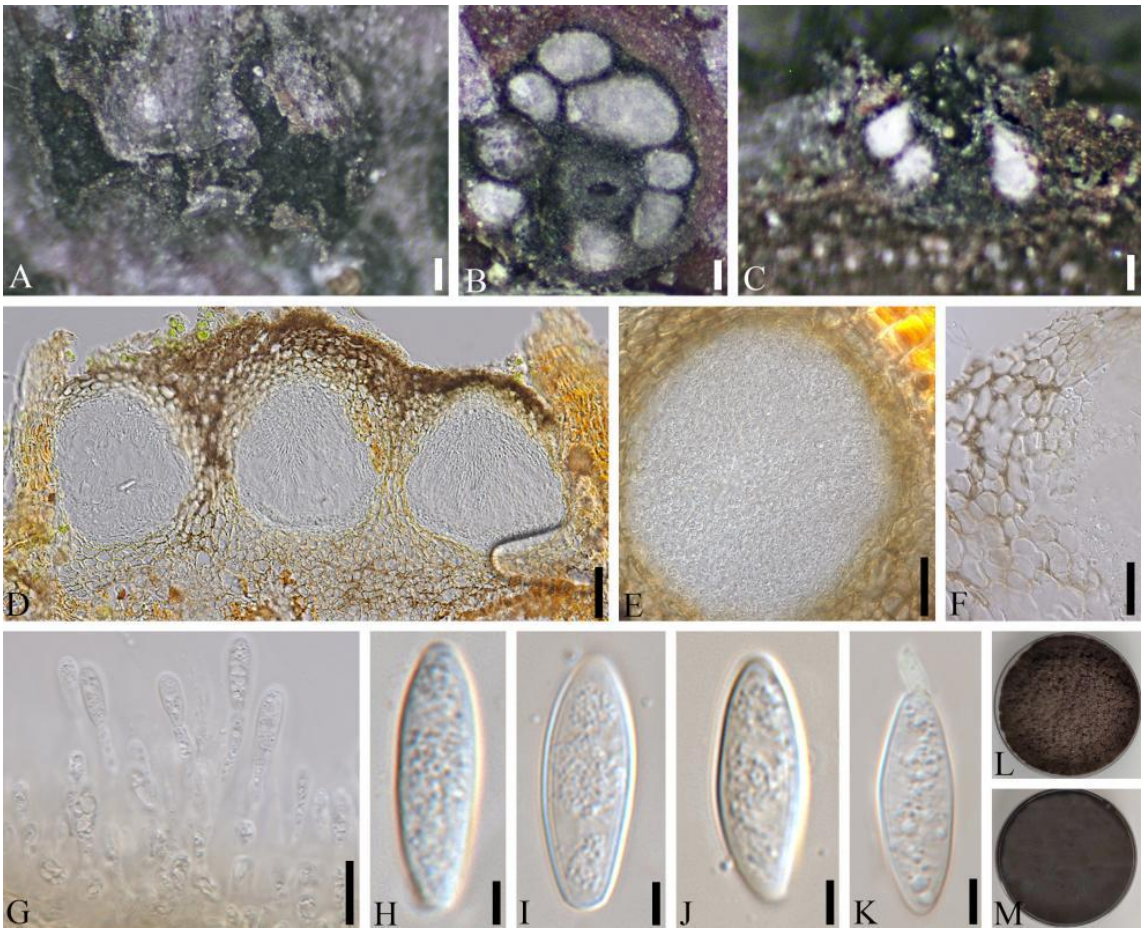


Figure 24 – Asexual morph of *Neofusicoccum wenchuanense* (SICAU 23-0058, holotype). A Appearance of conidiostromata on *Juglans regia*. B, C Longitudinal and transverse cutting diagram of conidiostromata. D, E Section of conidiomata wall. F Conidiomata wall. G Conidiogenous cells and conidia. H–J Conidia. K Geminating conidium. L, M Colonies on PDA (L from above, M from below). Scale bars: A–C = 100 µm, D = 50 µm, E, G = 20 µm, F = 10 µm, H–K = 5 µm.

15. ***Cladosporium cladosporioides*** (Fresen.) G.A. de Vries, Genus *Cladosporium*: 57. 1952. Fig. 26
Index Fungorum number: IF294915; Facesoffungi number: FoF06968

Associated with leaf spots on the living leaves of *Juglans regia*. Symptoms on the leaves are small, irregular yellow spots. As the spots enlarge, the central lesion becomes necrotic with the appearance of black dots, surrounded by brown concentric rings. Sexual morph: Not observed. Asexual morph: Hyphomycetous. *Colonies* greyish to dark brown, confluent. *Conidiophores* 90–200 × 4–11 µm ($\bar{x}$ = 120 × 7 µm, n = 40), solitary or in loose tufts, fasciculate, macronematous, arising terminally and laterally from swollen hyphae, erect, straight or flexuous, cylindrical-oblong, slightly attenuated toward the apex, subnodulose or nodulose, usually unbranched, occasionally once branched, 3–7-septate. *Micronematous conidiophores* reduced to conidiogenous cells. *Conidiogenous cells* 12–25 × 3–8 µm ($\bar{x}$ = 16 × 5 µm, n = 40), integrated, mainly terminal, cylindrical-oblong to subclavate, aseptate, sometimes uniseptate, sometimes geniculate, non-nodulose, polyblastic, with 1–4 apically crowed loci, 1–3 µm diam., central dome often not very

conspicuous, flat, somewhat thickened and darkened-refractive. *Ramoconidia* occasionally formed, up to 32 µm long, 4–5 µm wide, 1–2-septate, pale olivaceous, smooth, and base truncate. *Conidia* 8–14 × 4–7 µm ($\bar{x}$ = 11 × 5 µm, n = 40), numerous, catenate, forming short branched chains in all directions, aseptate. *Small terminal conidia* 4–8 × 3–6 µm ($\bar{x}$ = 5 × 4 µm, n = 40), globose, subglobose or ovoid to obovoid, and apex rounded or somewhat attenuated.

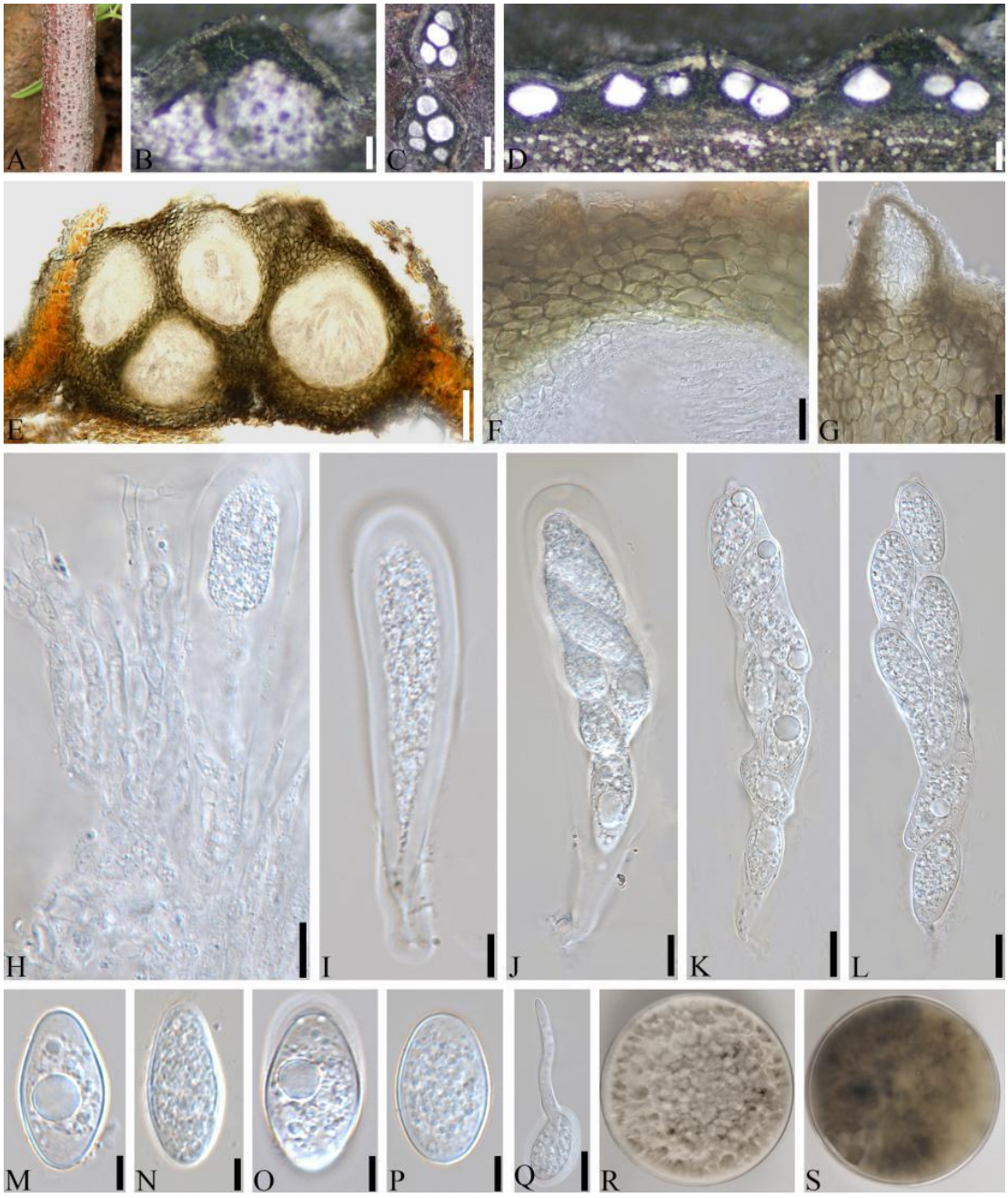


Figure 25 – Sexual morph of *Neofusicoccum wenchuanense* (SICAU 23-0059). A, B Appearance of ascostromata on host substrate. C, D Longitudinal and transverse cutting diagram of ascostromata. E Section of ascostromata. F Peridium. G Ostiole. H Pseudoparaphyses and asci. I–L Asci. M–P Ascospores. Q Germinating ascospore. R, S Colonies on PDA (R from above, S from below). Scale bars: B–D = 200 µm, E = 100 µm, F, G, Q = 20 µm, H–L = 10 µm, M–P = 5 µm.

Culture characteristics – Conidia germinating on sterile water within 12 h and germ tubes produced from ends. Colonies on PDA reaching 60 mm diam., after 14 days at 25 ℃. The mycelium grows on the surface of the medium, with parts embedded within, powdery to fluffy, sporulation

profuse, radially furrowed, without prominent exudates. Reverse, olivaceous, pale green to grayish white toward margins, and deep radial fissures. Not produced pigmentation on PDA media.

Material examined – China, Sichuan Province, Bazhong City, Nanjiang County, Gongshan Town (32°18′37.19″N 106°52′22.33″E, alt. 1006 m), on the living leaves of *Juglans regia*, 4 June 2022, F.-H. Wang, WFH202206004 (SICAU 22-0118), living culture SICAUCC 22-0120.

GenBank numbers – SICAUCC 22-0120: OP963820 (ITS), OQ281366 (*tef*1-α), OQ190485 (*act*).

Note – Given the overlapping of the key differential features on morphology, species identification of *Cladosporium* is currently based on multi-locus analysis. The preliminary phylogeny based on a concatenated ITS-*act*-*tef*1-α sequence matrix of the representative strain in *Cladosporium* indicates that our isolate belongs to the *C. cladosporioides* species complex. The phylograms from MLBS and BYPP analyses were similar in overall topologies. This isolate is phylogenetically grouped with the type of *C. cladosporioides* (CBS 112388 and CBS 113788) with strong statistical support (91% MLBS/1.00 BYPP) (Fig. 27). Nucleotide comparisons of ITS, *act*, and *tef*1-α (SICAUCC 23-0120) also showed a high homology with the sequences of *C. cladosporioides* (CBS 112388, ex-type), with a similarity of 99.6% (517/519, 0 gap), 99.5% (210/211, 0 gap), and 100% (376/376, 0 gap), respectively. Based on morphological characters and phylogenetic analyses, we determine our specimens as *C. cladosporioides*.

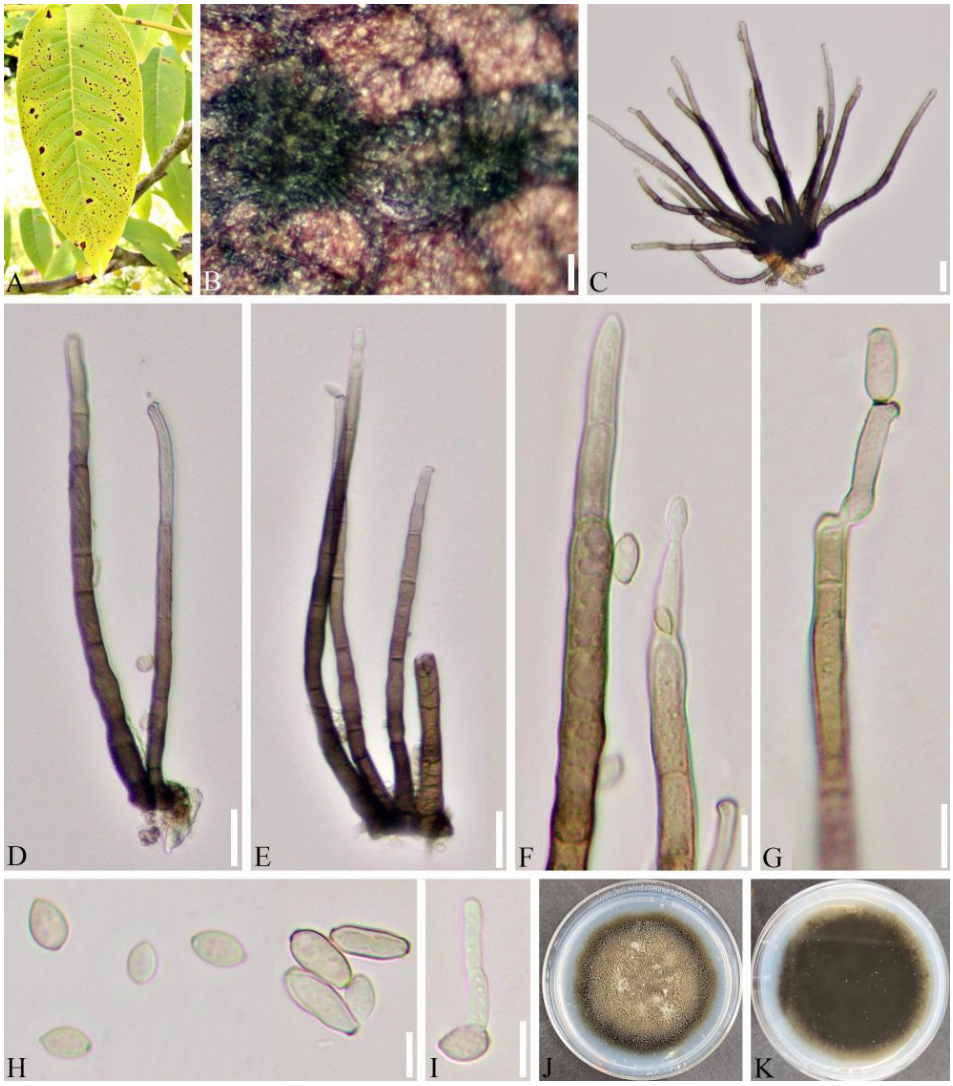


Figure 26 –*Cladosporium cladosporioides* (SICAU 22-0118). A Symptoms of necrotic lesions observed on host. B Appearance of colonies on substrate. C–E Conidiophores. F, G Conidiophores and conidiogenous cells with developing conidia. H Conidia. I Germinating conidium. J, K Colonies

on PDA (J from above, K from below). Scale bars: B = 500 µm, C = 100 µm, C–E = 20 µm, F–I = 10 µm.

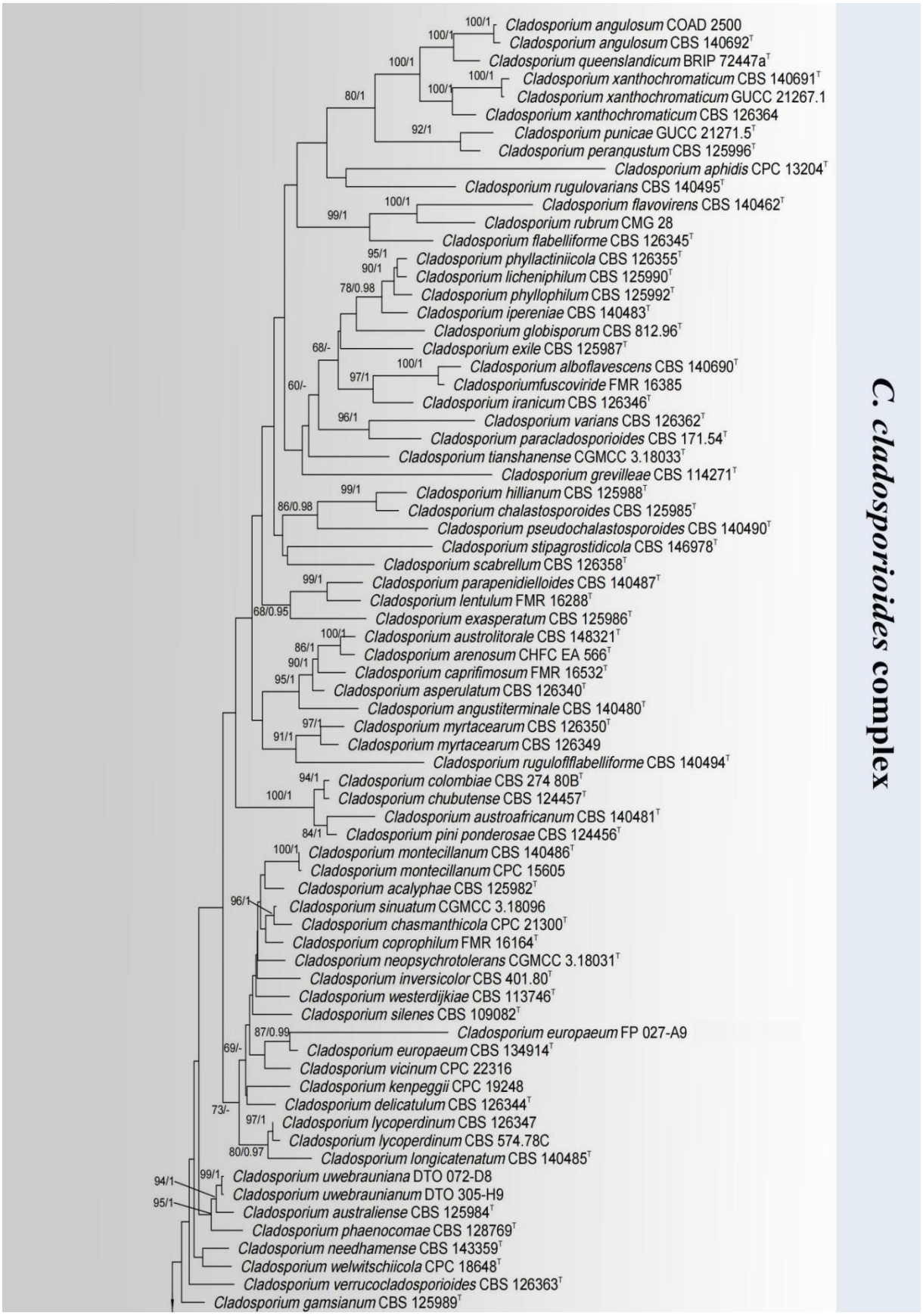


Figure 27 – Continued.

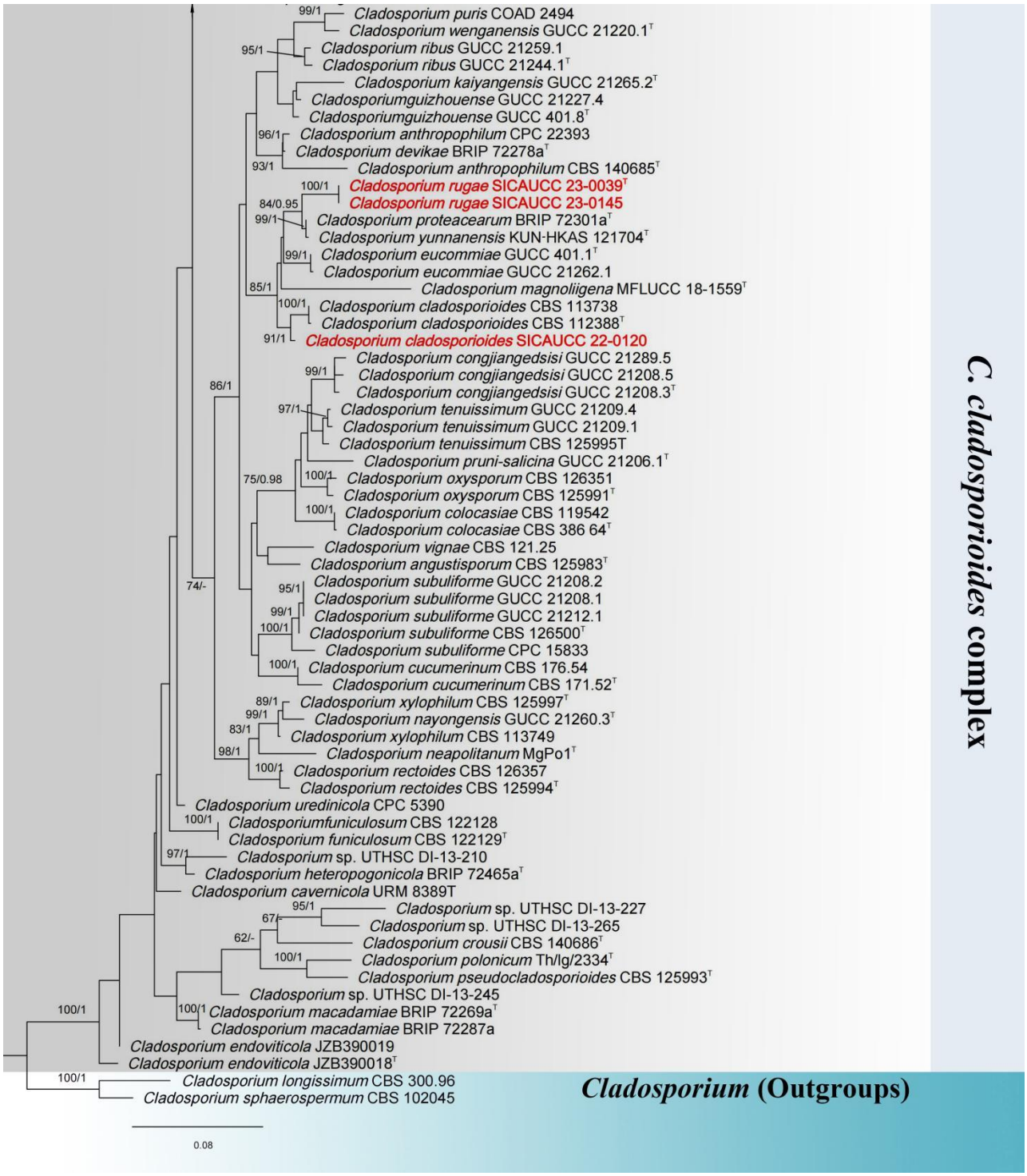


Figure 27 – Best scoring RAxML tree with a final likelihood value of -22,650.754894 based on combined ITS, *act* and *tef*1-α sequence data of related species. The tree is rooted with *Cladosporium sphaerospermum* (CBS 102045) and *C. longissimum* (CBS 300.96) in *C. cladosporioides* complex. One hundred and thirty-six strains were included in the combined analyses which comprised 3,487 characters (1,598 characters for ITS, 654 characters for *act* and 1,232 characters for *tef*1-α, including gap regions). The matrix had 1,183 distinct alignment patterns, with 66.84% undetermined characters and gaps. Estimated base frequencies were as follows; A = 0.233167, C = 0.289629, G = 0.249354, T = 0.227850; substitution rates AC = 1.882142, AG = 3.882533, AT = 1.936812, CG = 1.210193, CT = 6.375947, GT = 1.000000; gamma distribution shape parameter α = 0.246513. GTR+I+G model was used for each partition in Bayesian posterior analyses. The species determined in this study is indicated in red and bold. Bootstrap support values for maximum likelihood (MLBS, left) ⩾ 60%

and Bayesian posterior probabilities (BYPP, right) ⩾ 0.90 are indicated at the nodes, respectively. Hyphens (-) represent support values less than 60% MLBS/0.90 BYPP. The ex-type superscript "T".

16. ***Cladosporium rugae*** F.H. Wang & C.L. Yang, sp. nov. Fig. 28

Index Fungorum number: IF901564; Facesoffungi number: FoF15581

Etymology – *rugae*, referring to the wrinkles formed by colonies on the culture medium.

Holotype – SICAU 22-0060

Associated with leaf blight on living leaves of *Juglans regia*. symptoms manifest as chlorophyll loss on the leaf tips and edges, gradually leading to water loss and curling. As the curled area expands, black spots appear on the folds. Sexual morph: Not observed. Asexual morph: Hyphomycetous. *Mycelium* immersed and superficial, hyphae unbranched or once in a while branched, 2−3 µm wide, septate, sometimes constricted at septa, especially in wider ones, subhyaline to pale olivaceous or pale olivaceous brown, smooth, fertile hyphae minutely verruculose, mainly at the base of conidiophores. *Conidiophores* 80–150 × 4–8 µm ($\bar{x}$ = 115 × 6 µm, n = 20), solitary, erect, straight to slightly curved, cylindrical-oblong, unbranched or branched once or twice, branches often only as short denticle-like lateral outgrowths just below a septum, at the base often wider, somewhat attenuated towards the tip, 3−5-septate, sometimes slightly constricted at septa, medium to dark brown, paler towards the tip, smooth, occasionally rough-walled, wall somewhat thickened, but tips usually thin. *Conidiogenous cells* 10–18 × 3–5 µm ($\bar{x}$ = 14 × 4 µm, n = 20), integrated, terminal, sometimes intercalary, slightly attenuated, narrowly cylindrical-oblong, sometimes once geniculate, nodulose. *Ramoconidia* cylindrical-oblong, 19−27 × 3−5 µm ($\bar{x}$ = 23 × 4 µm, n = 20), pale olivaceous brown, smooth, base broadly truncate, 3−4 µm wide, unthickened or slightly thickened, sometimes slightly refractive. *Conidia* 5–13 × 3–5 µm ($\bar{x}$ = 9 × 4 µm, n = 30), catenate, in branched chains, pale olivaceous to olivaceous, subglobose, ellipsoid-ovoid, aseptate, smooth-walled. *Small terminal conidia* 4–10 × 3–4 µm ($\bar{x}$ = 6.5 × 4.5 µm, n = 30), obovoid, ovoid to limoniform or ellipsoid, sometimes subglobose.

Culture characteristics – Conidia germinating on sterile water within 12 h and germ tubes produced from ends. Colonies on PDA reaching 50 mm diam., after 28 days at 25 ℃. The mycelium grows on the surface of the medium, with parts embedded within, frontage, medium dense, circular, fat, slightly raised, colony wrinkled and folded, radially furrowed velvety to floccose, somewhat shiny, margins rhizoid, grey-olivaceous, aerial mycelium floccose, loose to dense, growth flat, without prominent exudates, sporulating. Reverse, olivaceous at the margin, brown in the center. Not produced pigmentation on PDA media.

Material examined – China, Sichuan Province, Aba Tibetan and Qiang Autonomous Prefecture, Lixian County (31°45′22″N 103°49′28″E, alt. 1521 m), on the living leaves of *Juglans regia*, 8 July 2022, F.-H. Wang, WFH202207041-1 (SICAU 23-0060, holotype), ex-type living culture SICAUCC 23-0039. *Ibid.*, WFH202207041-1B (SICAU 24-0031), living culture SICAUCC 23-0145.

GenBank numbers – SICAUCC 23-0039: PP060655 (ITS), PP061137 (*tef*1-α), PP061100 (*act*); SICAUCC 23-0145: PP844873 (ITS), PP850052 (*tef*1-α), PP850041 (*act*).

Note – Phylogenetic analyses showed that *Cladosporium rugae* (SICAUCC 23-0039, SICAUCC 23-0145) formed an independent lineage within *Cladosporium* (Fig. 24). *Periconia chiangraiensis* is phylogenetically closer to *C. proteacearum* (M50) and *C. yunnanensis* (KUN-HKAS 121704). Nucleotide comparisons reveal notable genetic dissimilarities between *C. rugae* and *C. proteacearum* (BRIP72301a), viz. 0% (0/536, 0 gap), 7.9% (18/229, 2 gaps), and 0% (0/211, 0 gap) in the ITS, *act* and *tef*1-α, respectively. Morphologically compared with *C. proteacearum* (M50), our isolates have slightly larger conidia (5–13 × 3–5 µm vs. 5–10 × 3–4 µm), our isolates have slightly larger small terminal conidia (4–10 × 3–4 µm vs. 4–5 × 2–3 µm), while the latter has longer conidiophore (80–150 × 4–8 µm vs. 150–500 × 2.5–4 µm). However, ramoconidia of *C. proteacearum* (BRIP72301a), subcylindrical, pale brown, smooth, 0–1-septate, hila thickened, darkened, refractive, without septa in the new species. Nucleotide comparisons reveal notable genetic dissimilarities between *C. rugae* and *C. proteacearum* (BRIP72301a), viz. 0% (0/466, 0 gap), 8.2% (19/232, 2 gaps), and 0% (0/211, 0 gap) in the ITS, *act* and *tef*1-α, respectively. Morphologically

compared with *C. yunnanensis* (KUN-HKAS 121704), our isolates have smaller conidia (5–13 × 3–5 µm vs. 7–19 × 5–7 µm), the morphology of small terminal conidia of *C. yunnanensis* (KUN-HKAS 121704). However, ramoconidia of *C. yunnanensis* (KUN-HKAS 121704), straight to slightly curved, cylindrical-oblong, 0–3-septate, pale to pale medium olivaceous-brown, without septa in the new species. We recognize *C. rugae* and *C. proteacearum* as distinct species based on morphological differences.

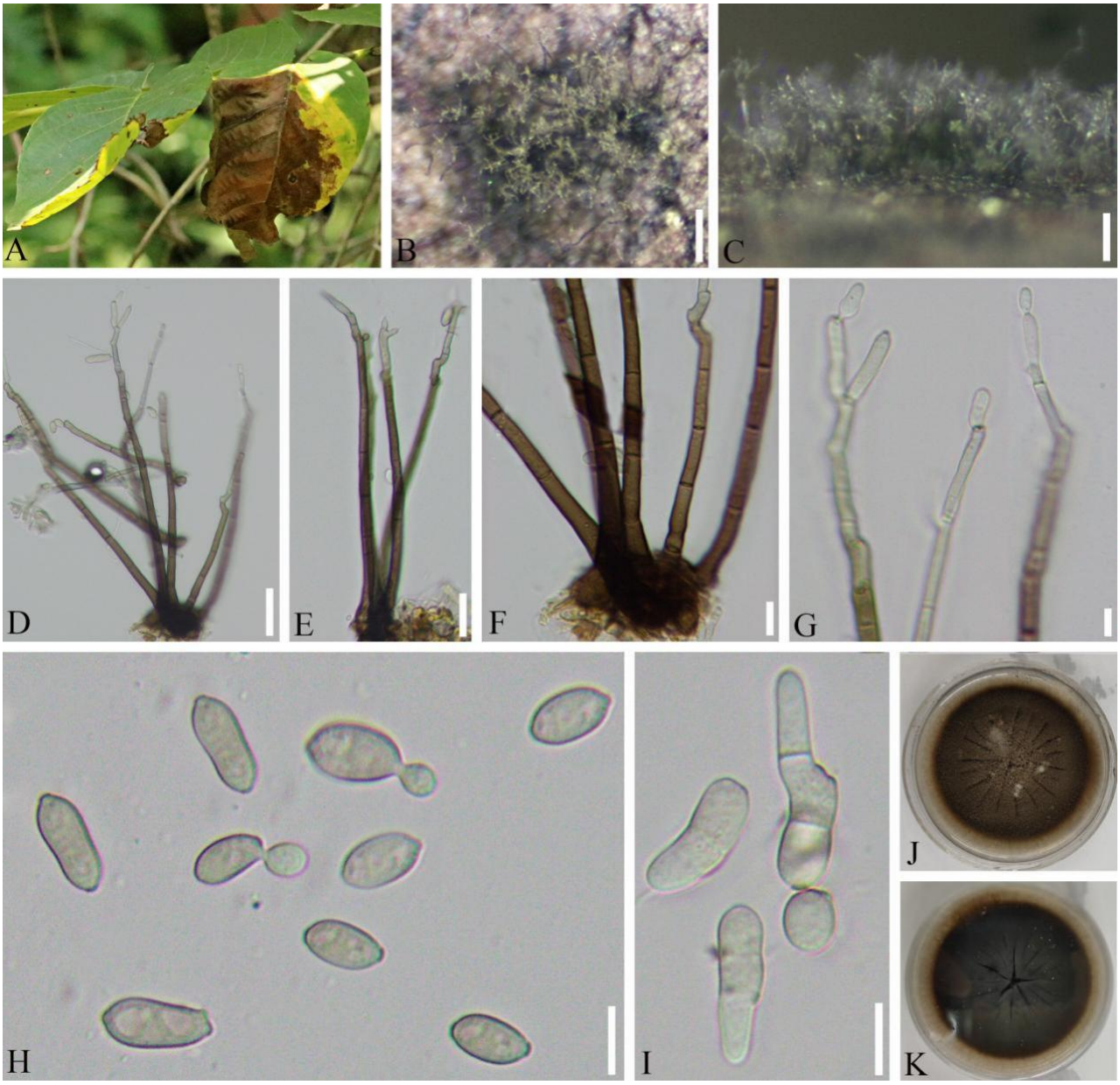


Figure 28 – *Cladosporium rugae* (SICAU 23-0060, holotype). A Symptoms of necrotic lesions observed on host. B, C Colonies on host substrate. D–F Conidiophores. G Conidiogenous cells with developing conidia. H Conidia. I Germinating conidia. J, K Colonies on PDA (J from above, K from below). Scale bars: B = 500 mm, C = 200 µm, D, E = 50 µm, F, G = 20 µm, H, I = 10 µm.

Hysteriales Lindau.

Hysteriales was introduced by Lindau (1897), and this includes single family *Hysteriaceae* that is characterised by hysteriform apothecia. Species in this order are mostly saprobic and widely distributed (Jayasiri et al. 2018, Hongsanan et al. 2020). In this study, we follow the updated accounts of *Hysteriales* in Raymundo et al. (2024), and the genus *Rhytidhysteron* from recent literatures

(Jayasiri et al. 2018, Kumar et al. 2019, Dayarathne et al. 2020, Xu et al. 2022b, Du et al. 2023, Senwanna et al. 2023).

Hysteriaceae Chevall.

Hysteriaceae was introduced by Chevallier (1826) which has been traditionally defined as specialized ascocarp termed the hysterothecium. The family has been classified in several orders such as *Pseudosphaeriales* (Nannfeldt 1932, Gäumann 1949), *Dothiorales* (Müller & Von Arx 1950, Von Arx & Müller 1954), *Dothideales* (Von Arx & Müller 1975) and presently, *Hysteriales*, which is closely related to the *Pleosporales* (Luttrell 1955, Kirk et al. 2008, Thambugala et al. 2016, Jayasiri et al. 2018, Wijayawardene et al. 2018, Hyde et al. 2024b, Manogaran et al. 2024). There are 13 genera in this family viz, *Actidiographium*, *Gloniella*, *Gloniopsis*, *Hysterium*, *Hysterobrevium*, *Hysterocarina*, *Hysterodifractum*, *Hysteroglonium*, *Oedohysterium*, *Ostreichnion*, *Pseudoscypha*, *Psiloglonium* and *Rhytidhysteron* (Hongsanan et al. 2020b). Taxa in this family are mostly found as saprobes on dead plant materials and characterised by erumpent or superficial, hysterothecial or navicular ascomata, sometimes branched or discoid. The *Exciple* is composed of cells of *textura angularis* and is carbonaceous, 2–4-layered, thick, stout, rarely thin. *Hamathecium* composed of pseudoparaphyses with tips sometimes darkened or branched above the asci. Asci are clavate to cylindrical, fissitunicate, with a distinct apical chamber. Ascospores are ellipsoid, fusoid or clavate, hyaline or brown, variously septate, smooth or ornamented, sometimes with a sheath. Asexual morphs are coelomycetes or hyphomycetes (Jaklitsch et al. 2016b, Jayasiri et al. 2018).

Rhytidhysteron Speg.

The genus was introduced by Spegazzini (1881), to accommodate two species, *Rhytidhysteron brasiliense* and *R. viride*. Clements & Shear (1931) named *R. brasiliense* as the type species (Dayarathne et al. 2020). Primitively, this genus was classified into *Patellariaceae* (Kutorga & Hawksworth 1997, Eriksson 2006, Lumbsch & Huhndorf 2010a). However, recent studies based on multi-gene analyses shown it should be placed in *Hysteriaceae* (Boehm et al. 2009a, b, De Almeida et al. 2014, Wijayawardene et al. 2014, Jayasiri et al. 2018, Wijayawardene et al. 2018, Kumar et al. 2019, Senwanna et al. 2023). Forty-one species are listed in Species Fungorum (http://www.speciesfungorum.org/Index.htm, September 2024). At present, sequences of 17 species are available in GenBank, viz. *R. bannaense*, *R. bruguierae*, *R. camporesii*, *R. chromolaenae*, *R. coffeae*, *R. hongheense*, *R. ligustrum*, *R. magnoliae*, *R. mengziense*, *R. neorufulum*, *R. rufulum*, *R. sichuanense*, *R. subrufulum, R. tectonae*, *R. thailandicum*, *R. xiaokongense*, and *R. yunnanense*. Taxa are characterised by hysterothecial ascomata, which are sometimes branched or discoid and erumpent or superficial. The exciple is composed of carbonaceous cells of *textura angularis* and hamathecium is composed of pseudoparaphyses and their tips are sometimes darkened or branched above asci. Asci are clavate to cylindrical, fissitunicate, with a distinct apical chamber. Ascospores are ellipsoid to fusoid, light brown to dark brown, septate and smooth or ornamented (Thambugala et al. 2016, Jayasiri et al. 2018). Recently, multiple species of this genus have been discovered in various locations, including China and Thailand. (Hyde et al. 2020a, Xu et al. 2022a, Senwanna et al. 2023). *Rhytidhysteron rufulum* is an emerging dematiaceous fungus detected as a human pathogen (Sharma et al. 2023).

17. ***Rhytidhysteron rufulum*** (Spreng.) Speg., Anal. Soc. Cient. Argent. 90(3-6): 177 (1921)

Fig. 29

Index Fungorum number: IF121714; Facesoffungi number: FoF01839

Saprobic on dead twigs of *Juglans regia*. Sexual morph: *Ascomata* 350–600 µm high, 500–1000 µm diam., ($\bar{x}$ = 360 × 720 µm, n = 10), labiates and elliptic or irregular in shape, navicular, superficial, with a carbonaceous rim, scattered, closed at first and opening at maturity, elongate, elliptic, dark brown to black with dark orange at the center, when dry folded at the margin. *Medullary excipulum* 28–48 µm ($\bar{x}$ = 36 µm, n = 10), composed of narrow, thin-walled, hyaline to brownish cells of *textura porrecta*. *Hymenium* hyaline. *Hamathecium* comprising 1–3 µm wide, cylindrical to filiform, septate

pseudoparaphyses, branched and forming a red epithecium above the asci, fused and slightly swollen at the apex and enclosed in a gelatinous matrix. *Asci* 96–170 × 9–15 µm ($\bar{x}$ = 150 × 12 µm, n = 10), 8-spored, bitunicate, 1-seriate, fissitunicate, cylindrical, straight or slightly curved, with a short pedicel, apically rounded with an ocular chamber. *Ascospores* 22–30 × 7–11 µm ($\bar{x}$ = 26 × 9 µm, n = 30), overlapping, uniseriate, hyaline when immature, becoming pale brown to brown when mature, broadly fusiform, 1-septate when immature, becoming 3-euseptate when mature, slightly constricted at the central septum, straight or slightly curved, without terminal appendages. Asexual morph: Not observed.

Culture characteristics – Ascospores germinating on sterile water within 24 h and germ tubes produced from ends. Colonies on PDA reaching 50 mm diam., after 18 days at 25 ℃. The mycelium grows on the surface of the medium, with parts embedded within, mycelium velvety, fluffy, undulate to filamentous, brown to dark brown, white aerial hyphae at the surface, there are fewer aerial hyphae, margin flat and circular. The reverse side of the colonies is dark black. Not produced pigmentation on PDA media.

Material examined – China, Sichuan Province, Suining City, Shehong City, Guangxing Town (30°57′22.43″N 105°18′54.25″E, alt. 404 m), dead twigs of *Juglans regia*, 28 May 2022, F.-H. Wang, WFH202204095 (SICAU 22-0159), living culture SICAUCC 22-0161.

GenBank numbers – SICAUCC 22-0161: OP980895 (ITS), OP964594 (LSU), OP962312 (SSU), OQ281397 (*tef*1-α).

Note – Our strain *Rhytidhysteron rufulum* (SICAUCC 22-0161) grouped with other *R. rufulum* (MFLUCC 12-0013) with strong statistical support (91% MLBS/1.00 BYPP) (Fig. 30). Our collection from *Juglans regia* from China is morphologically similar to *R. rufulum* in having 1–3-septate, brown, fusiform ascospores. Nucleotide comparisons of ITS, LSU, SSU, and *tef*1-α (SICAUCC 22-0161) also showed a high homology with the sequences of *R. rufulum* (MFLUCC 12-0013, ex-type), with a similarity of 99.6% (572/574, 2 gap), 100% (860/860, 0 gap), 100% (992/992, 0 gap), and 100% (780/780, 0 gap), respectively. Based on morphological characters and phylogenetic analyses, we determine our specimens as *R. rufulum*. This species is widely distributed all over the world (Xu et al. 2022b).

18. ***Rhytidhysteron sichuanense*** X.L. Xu & C.L. Yang [as '*sichuanensis*'], Cryptog. Mycol. 43(3): 70 (2022) Fig. 31

Index Fungorum number: IF660341; Facesoffungi number: FoF16290

Saprobic on dead twigs of *Juglans regia*. *Ascomata* 350–500 × 800–1300 µm ($\bar{x}$ = 460 × 900 µm, n = 10), hysterothecial, boat-shaped, scatter, superficial, brown-black, with exposed, lenticular to irregular, brown-black discs, folded along the margins when dry and forming an elongate slit, perpendicularly striate. *Medullary excipulum* 50–120 µm wide (n = 10), composed of dark brown to black, thick-walled cells of *textura angularis*. *Hamathecium* comprising 1–3 µm wide, cylindrical to filiform, septate pseudoparaphyses, branched and forming a brown epithecium above the asci, fused and slightly swollen at the apex and enclosed in a gelatinous matrix. *Asci* 88–160 × 10–14 µm ($\bar{x}$ = 148 × 12 µm, n = 15), 8-spored, bitunicate, cylindrical, with short, furcate pedicel, rounded at the apex, with distinct ocular chamber. *Ascospores* 20–27 × 7–11 µm ($\bar{x}$ = 21 × 9 µm, n = 40), uniseriate, slightly overlapping, hyaline when immature, becoming yellowish-brown to reddish-brown when mature, ellipsoidal to fusiform, rounded to slightly pointed at both ends, 1–3-septate, slightly constricted at the septa, with smooth wall, guttulate. Asexual morph: Not observed.

Culture characteristics – Ascospores germinating on PDA within 24 h. at room temperature and cells at both ends can produce germ tubes. Colonies on PDA, 60 mm diam., after 20 days. Colonies on PDA filamentous, mycelium velvety, fluffy, undulate to filamentous, brown to dark brown, white aerial hyphae at the surface, there are fewer aerial hyphae, margin flat and circular. The reverse side appears reddish brown due to the production of reddish-brown metabolites.

Material examined – China, Sichuan Province, Chengdu City, Chongzhou City (30°33′9.04″N 103°39′29.36″E, alt. 512 m), dead twigs of *Juglans regia*, 21 April 2022, F.-H. Wang, WFH202204007 (SICAU 23-0062), living culture SICAUCC 23-0041.

GenBank numbers – SICAUCC 23-0041: PP060657 (ITS), PP057950 (LSU), PP003818 (SSU), PP061138 (*tef*1-α).

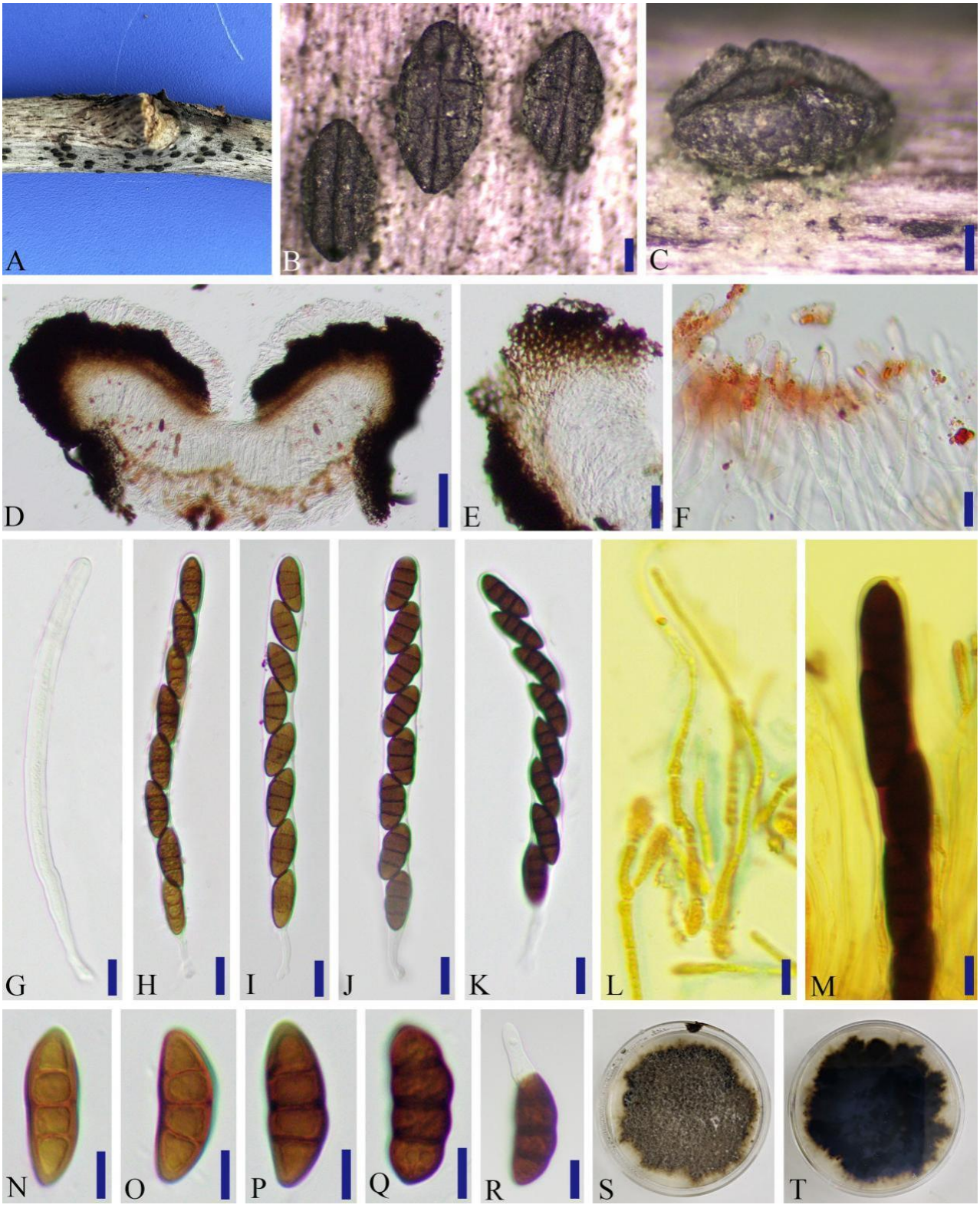


Figure 29 – *Rhytidhysteron rufulum* (SICAU 22-0159). A Substrate. B, C Ascomata on host. D Vertical section of ascoma. E Exciple. F Pseudoparaphyses with branched swollen reddish tips. G–K Asci. L, M Asci and pseudoparaphyses stained with Melzer's reagent. N–Q Ascospores. R Germinating ascospore. J, K Colonies on PDA (S from above, T from below). Scale bars: B, C = 200 µm, D, E = 50 µm, F–L = 20 µm, M–R = 10 µm.

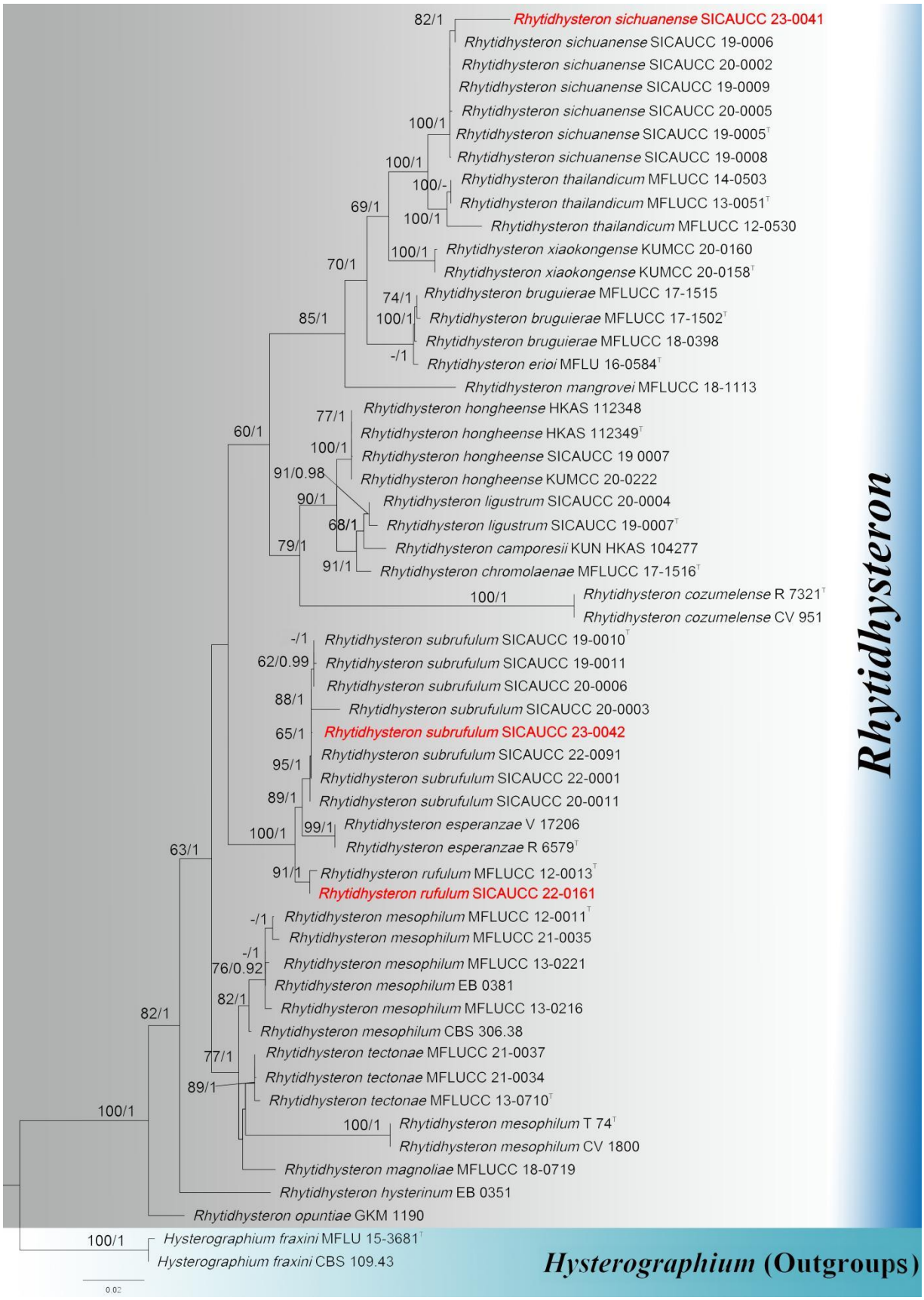


Figure 30 – Best scoring RAxML tree with a final likelihood value of -13,766.084922 based on combined LSU, ITS, SSU and *tef*1-α sequence data of related species. The tree is rooted with *Hysterographium fraxini* (MFLU 15-3681 and CBS 109.43) in *Pleosporomycetidae*. Fifty-five

strains were included in the combined gene analyses which comprised 4,274 characters (1,418 characters for LSU, 714 characters for ITS, 1,119 characters for SSU and 1,020 characters for *tef*1-α, including gap regions). The tree from the maximum likelihood analyses had similar topology to the Bayesian analyses. The matrix had 1,080 distinct alignment patterns with 32.64% undetermined characters or gaps. Estimated base frequencies were as follows: A = 0.241462, C = 0.248598, G = 0.274173, T = 0.235768; substitution rates AC = 1.356412, AG = 2.590524, AT = 1.135882, CG = 1.044583, CT = 5.338369, GT = 1.000000; gamma distribution shape parameter α = 0.200028. The Bayesian inference analyses was implemented by MrBayes v.3.2.2 with the best-fit model (HKY+I+G for LSU; GTR+I+G for ITS, SSU; GTR+G for *tef*1-α) of evolution estimated with MrModeltest 2.2. The species determined in this study is indicated in red and bold. Bootstrap support values for maximum likelihood (MLBS, left) ⩾ 60% and Bayesian posterior probabilities (BYPP, right) ⩾ 0.90 are indicated at the nodes, respectively. Hyphens (-) represent support values less than 60% MLBS/0.90 BYPP. The ex-type superscript "T".

Note – In the phylogenetic analysis, our taxon clustered together with strain of *Rhytidhysteron sichuanense* (SICAUCC 19-0006), having strong bootstrap support value (82% MLBS/1.00 BYPP) (Fig. 30). When comparing the morphology of *R. sichuanense*, our isolate shares similar morphology, and all of them were collected from walnuts (Xu et al. 2022b). Nucleotide comparisons of ITS, LSU, SSU, and *tef*1-α (SICAUCC 23-0041) also showed a high homology with the sequences of *R. sichuanense* (MFLUCC 19-0005 ex-type), with a similarity of 99.8% (517/518, 0 gap), 100% (777/777, 0 gap), 99.1% (997/1006, 0 gap), and 100% (957/957, 0 gap), respectively. Based on morphological characters and phylogenetic analyses, we determine our specimens as *R. sichuanense*.

19. ***Rhytidhysteron subrufulum*** X.L. Xu & C.L. Yang, Cryptog. Mycol. 43(3): 72 (2022) Fig. 32

Index Fungorum number: IF557216; Facesoffungi number: FoF16291

Saprobic on dead twigs of *Juglans regia.* Sexual morph: *Ascomata* 850–1360 × 1060–1580 μm ($\bar{x}$ = 1080 × 1388 μm, n = 10), hysterothecial with a longitudinal slit, black, solitary to aggregated, protrude from the epidermis, subiculum, coriaceous, rough surface with longitudinal stripes, bronzing at the center, when dry folded at the margin, forming an elongate slit. *Exciple* 82–123 μm, ($\bar{x}$ = 112, n = 20), composed of a *textura angularis*, comprising of two cell layers, outer layer comprising black to dark reddish, thick-walled cells, inner layer comprising hyaline, thin-walled cells. *Hamathecium* comprising 1.2–2 μm wide, dense, septate, pseudoparaphyses, filiform, forming epithecium above the asci and enclosed in a gelatinous matrix. *Asci* 150–180 × 9–13 μm ($\bar{x}$ = 170 × 12 μm, n = 15), 8-spored, bitunicate, subcylindrical to cylindrical, with a short furcate pedicel, apically rounded, apically rounded with well-developed ocular chamber. *Ascospores* 24–29 × 9–12 μm ($\bar{x}$ = 26 × 10μm, n = 40), uni-seriate, slightly overlapping, initially subglobose and 1-septate, hyaline to pale brown, becoming pale brown to dark brown with 2–3-septa, ellipsoidal to fusiform, slightly rounded or pointed at both ends, constricted at the central slightly septum, without a mucilaginous sheath, guttulate. Asexual morph: Not observed.

Culture characteristics – Ascospores germinating on PDA within 24 h. Both ends of ascospores can produce germ tubes. Colonies on PDA reaching 60 mm diam., after 18 days in the dark at 25 ℃. The mycelium is thin, fluffy, aerial, dense, sandy beige at the edge, grey at the center from above, the reverse side is light yellow. Not produced pigmentation on PDA media.

Material examined – China, Sichuan Province, Mianyang City, Pingwu County (32°12′59″N 104°50′15″E, alt. 727 m), dead twigs of *Juglans regia*, 9 July 2022, F.-H. Wang, WFH202207072 (SICAU 23-0063), living culture SICAUCC 23-0042.

GenBank numbers – SICAUCC 23-0042: PP060658 (ITS), PP057951 (LSU), PP003819 (SSU), PP061139 (*tef*1-α).

Note – In a BLASTn search of NCBI GenBank, the closest match of the *tef*1-α sequence of our strain with 99.9% similarity was *Rhytidhysteron subrufulum* (strains SICAUCC 19-0010, MT027606), while the closest match with the LSU, SSU and ITS sequences with 100%, 100% and 100% similarity, respectively, was *R. subrufulum* (strain SDBR-CMU475, OQ940378, OQ940382, OQ943972). In the present phylogenetic analysis *R. subrufulum* (SICAUCC 19-0010, SICAUCC 19-

0011, SICAUCC 20-0003, SICAUCC 20-0006, SICAUCC 22-0001, SICAUCC 22-0011 and SICAUCC 22-0091) clustering in the same clade. Our isolate exhibits morphological characteristics that are highly consistent with those of *R. subrufulum* (Xu et al. 2022b). Therefore, based on both morphological characteristics and phylogenetic analysis, we have identified the isolate as *R. subrufulum*.



Figure 31 – *Rhytidhysteron sichuanense* (SICAU 23-0062). A Substrate. B, C Ascomata on host. D Vertical sections of ascoma. E Exciple. F Pseudoparaphyses and asci. G, H Asci. I–L Ascospores. M Germinating ascospore. N, O Colonies on PDA (N from above, O from below). Scale bars: B, C = 200 µm, D = 100 µm, E, F = 50 µm, G, H, M = 20 µm, I–L = 10 µm.

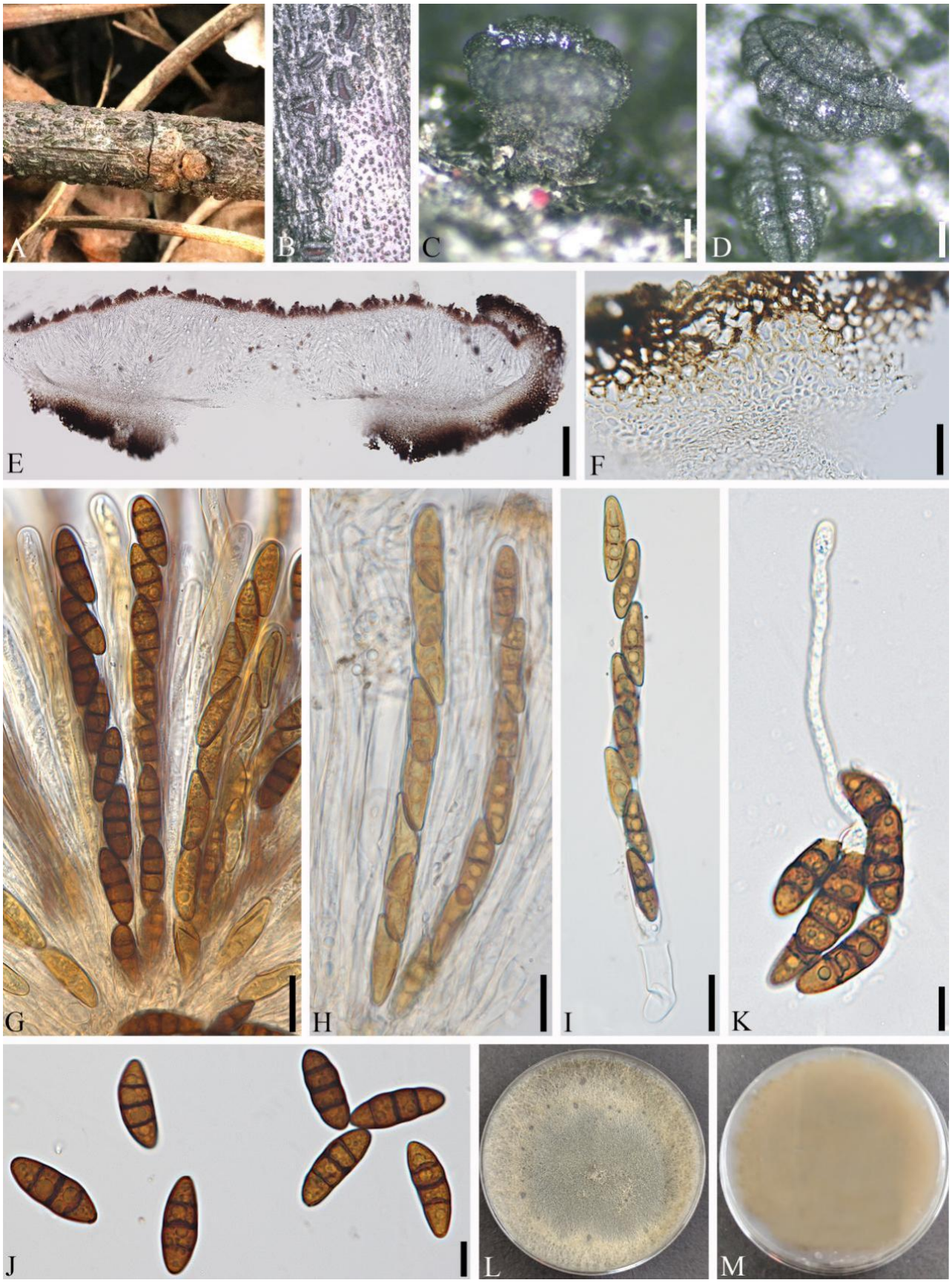


Figure 32 – *Rhytidhysteron subrufulum* (SICAU 23-0063). A, B Substrate. C, D Ascomata on host. E Vertical section of ascoma. F Exciple. G, H Pseudoparaphyses and asci. I Asci. J Ascospores. K Germinating ascospores. L, M Colonies on PDA (L from above, M from below). Scale bars: C, D = 500 µm, E = 200 µm, F–I = 20 µm, K, J = 10 µm.

Kirschsteiniotheliales Hern. -Restr., R.F. Castañeda, Gené & Crous.

Kirschsteiniotheliaceae Boonmee & K.D. Hyde, Mycologia 104(3): 705 (2012).

Kirschsteiniotheliaceae was introduced by Boonmee et al. (2012) to accommodate the holomorphic genus *Kirschsteiniothelia* based on the phylogeny inferred from combined LSU, SSU, and ITS gene regions. Taxa in the family are widely distributed and commonly saprobic on bark, dead twigs, branches, and stems from terrestrial and aquatic habitats. (Su et al. 2016, Mehrabi et al. 2017, Bao et al. 2018, Sun et al. 2021b). Currently, the family *Kirschsteiniotheliaceae* contains only one genus, namely Kirschsteiniothelia (Hyde et al. 2024b).

Kirschsteiniothelia D. Hawksw., Bot. J. Linn. Soc. 91: 182 (1985).

Kirschsteiniothelia was originally assigned in *Pleosporaceae* (Hawksworth 1985), but later Barr (1993) reported that *Kirschsteiniothelia* belongs to the *Pleomassariaceae* based on host, morphology and anamorph characters. The sexual stage characteristics is characterized by superficial, erumpent, globose to subglobose, dark brown to black, membraneaceous, scattered or loosely aggregated ascomata with or without a central papilla. A thick pseudoparenchymatous peridium consisting of thick-walled cells arranged in a pallisadic configuration at the base angles (*textura angularis*), a hamathecium comprising numerous, filiform, hyaline, pseudoparaphyses, bitunicate, fissitunicate, cylindrical-clavate, 8-spored. Asci with a long pedicel and an ocular apical chamber and bi- or triseriate ascospores, ellipsoidal, slightly curved, smooth-walled, olive brown to dark brown, 1 septate with a median or submedian septum, with or without a mucilaginous sheath (Hawksworth 1985, Boonmee et al. 2012, Hyde et al. 2013). The description of the asexual morphs of *Kirschsteiniothelia* is divided into two types: one with macronematous, apex-branching structures forming a stipe and head, colored brown to dark brown, and featuring determinate or apex-extending conidiophores that are mono- to polytretic, integrated, and terminal or lateral conidiogenous cells producing acrogenous, solitary or catenate, septate conidia; the other with macronematous, unbranched conidiophores that are integrated, terminal, monoblastic or monotretic, determinate or irregularly extending conidiogenous cells producing acrogenous, solitary or catenate, septate conidia, which may or may not be covered with a mucilaginous sheath. The former is referred to as the dendryphiopsis-like, while the latter is the sporidesmium-like (Mehrabi et al. 2017, Yang et al. 2023, Luo et al. 2025). We follow the latest treatment and updated accounts of *Kirschsteiniothelia* in Xiao et al. (2025)

20. ***Kirschsteiniothelia yantingense*** F.H. Wang & C.L. Yang, sp. nov. Fig. 33

Index Fungorum number: IF901566; Facesoffungi number: FoF15582

Etymology – Named after locality where the fungus was isolated for the first time.

Holotype – SICAU 23-0064.

Associated with twig blight on living twigs of *Juglans regia*. Symptoms consists of red discoloration strands in the xylem of branches, veinal chlorosis, wilt and shedding of leaves resulting in ultimate dieback of twigs and branches. Sexual morph: *Ascomata* 128–156 μm high, 230–285 μm ($\bar{x}$ = 138 × 265 μm, n = 10), black, scattered, subglobose to globose or slightly conical in appearance, superficial with apical papilla or plane, base remaining immersed, usually flattened. *Peridium* laterally 28–36 μm wide, composed of 3-6 layers of *textura angularis*, with dark brown outer layer cells and inner layers pale brown, cells around the ostiole with small lumina, reduced at the base, of 1–2 layers of cells. *Pseudoparaphyses* 1.5–2 μm wide, branched, embedded in a gelatinous matrix. *Asci* 68–106 × 12–19 μm ($\bar{x}$ = 96 × 16 μm, n = 10), 8-spored, cylindrical-clavate, straight or slightly curved, apically rounded, with a short pedicellate up to 5 μm long. *Ascospores* 14–20 × 4.5–6 μm ($\bar{x}$ = 18 × 5 μm, n = 36), brown, 1–2-seriate, ellipsoid, rounded or slightly pointed at the ends, 1-septate, septum submedian and constricted, upper cell broader than the lower cell, each cell containing a distinct large guttule, smooth-walled. Asexual morph: Not observed.

Culture characteristics – Ascospores germinating on PDA within 24 h. Colonies on PDA reaching 20 mm diam., after 15 days at 25 ℃. The surface covered with a white mat of aerial hyphae

in first week, then becoming brown to dark brown, with gray white, dense aerial mycelium on the central surface, sparse mycelium on the entire margin, dark brown in reverse. Not produced pigmentation on PDA media.

Material examined – China, Sichuan Province, Mianyang City, Yanting County (31°5′25.88″N 105°27′36.27″E, alt. 365 m), living twigs of *Juglans regia*, 18 May 2021, F.-H. Wang, WFH202105034 (SICAU 23-0064, holotype), ex-type living culture SICAUCC 23-0043. *Ibid*., living twigs of *Juglans regia*, 28 April 2022, F.-H. Wang, WFH202204110 (SICAU 23-0065), living culture SICAUCC 23-0044.

GenBank numbers – SICAUCC 23-0043: PP060659 (ITS), PP057952 (LSU), PP003820 (SSU); SICAUCC 23-0044: PP060660 (ITS), PP057953 (LSU), PP003821 (SSU).

Note – Phylogenetic analyses showed that *Kirschsteiniothelia yantingense* (SICAUCC 23-0043 and SICAUCC 23-0044) formed an independent lineage within *Kirschsteiniothelia* (Fig. 35). *Kirschsteiniothelia yantingense* is phylogenetically closer to *K. cangshanensesis* (MFLU 16-1350). However, we could not compare their morphology as *K. cangshanensesis* is only represented by a coelomycetous asexual morph (Bao et al. 2018). Nucleotide comparisons between *K. yantingense* (SICAUCC 23-0043) and *K. cangshanensis* (MFLU 16-1350) revealed differences of 2.7% (20/732, 1 gap), 0.5% (4/820, 0 gap), and 4.2% (42/1005, 2 gaps) in the ITS, LSU, and SSU regions, respectively. The PHI test revealed no significant recombination event between our strain and the closely related taxa (Φw = 1) (Fig. 34). Hence, based on the phylogenetic analysis differences, we introduce a new species, *K. yantingense* in *Kirschsteiniothelia*.

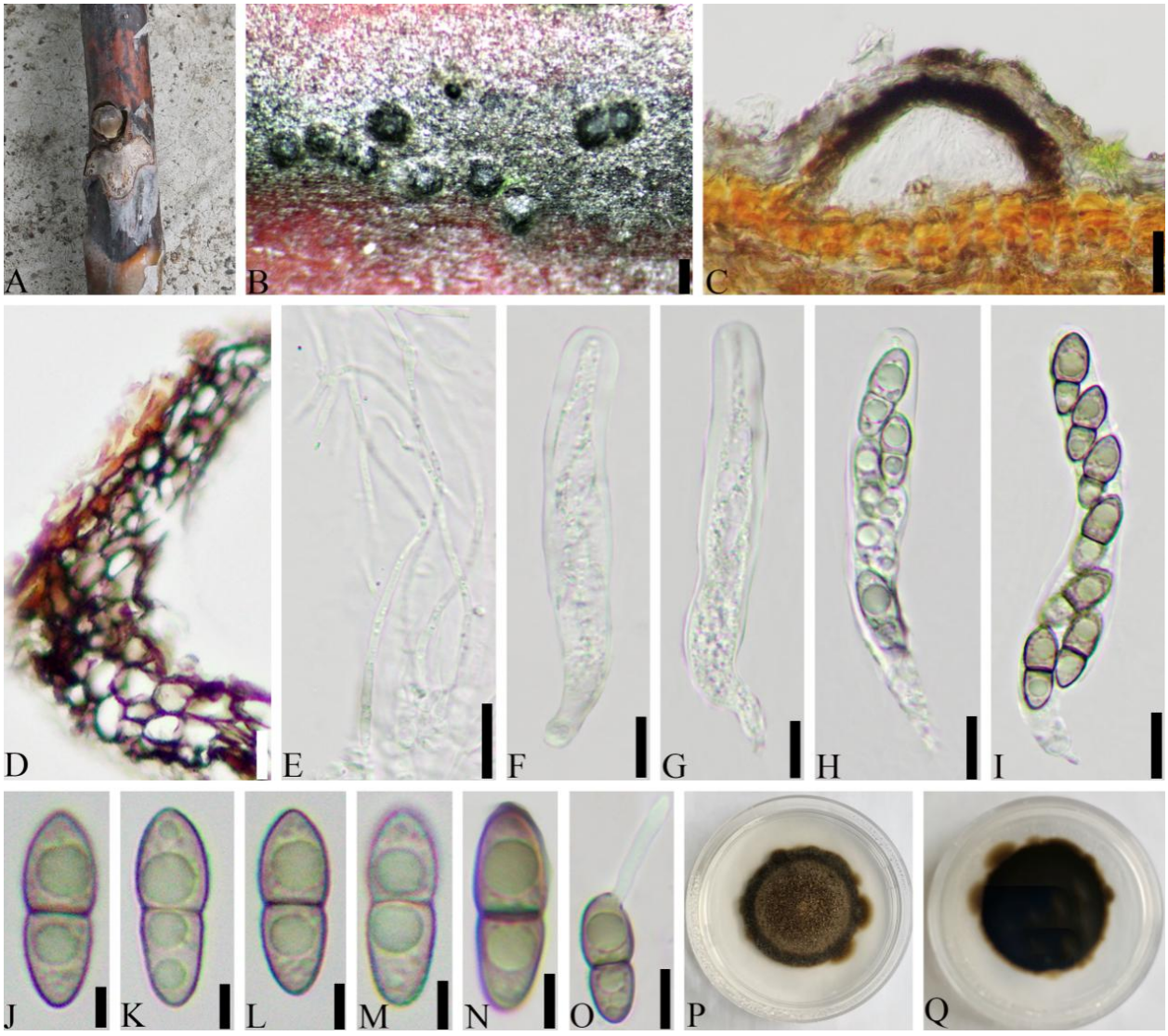


Figure 33 – *Kirschsteiniothelia yantingense* (SICAU 23-0064, holotype). A Symptoms of necrotic lesions observed on host. B Ascomata on host. C Vertical section through the ascoma. D Peridium. E Pseudoparaphyses. F–I Asci. J–N Ascospores. O Germinating ascospore. P, Q Colonies on PDA (P from above, Q from below). Scale bars: B = 200 μm, C = 100 μm, E–I = 20 μm, D, O = 10 μm, J–N = 5 mm.

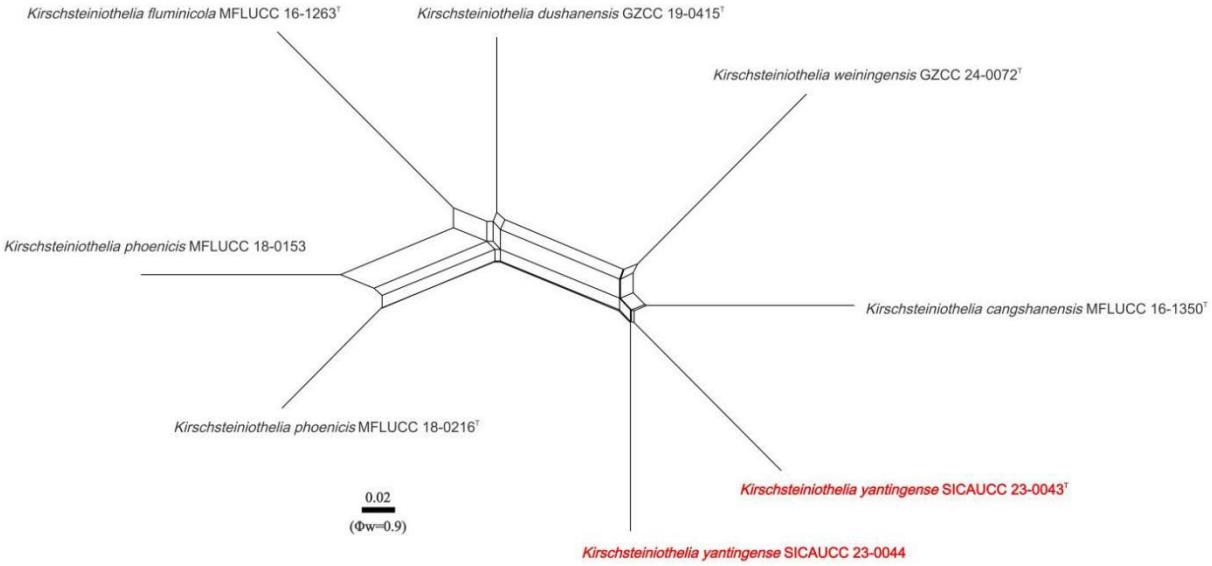


Figure 34 – Results of the PHI test of *Kirschsteiniothelia yantingense* and closely related species using both LogDet transformation and splits decomposition. The PHI test did not find any statistically significant recombination (Φw = 0.9) in the dataset. The new strains are represented in red and bold. "T" represents the type strain.

Mycosphaerellales (Nannf.) P.F. Cannon

Hawksworth et al. (1995) introduced *Mycosphaerellaceae* in the *Dothideales*, while Kirk et al. (2001) elevated this family to the order *Mycosphaerellales*, and Schoch et al. (2006) and Kirk et al. (2008) again placed it as a family in the *Capnodiales*. Despite high support values obtained in subsequent phylogenetic studies (Crous et al. 2009, Schoch et al. 2009a, Suetrong et al. 2009, Hyde et al. 2013), the *Mycosphaerellales* was never resurrected, and the *Capnodiales* was applied in a broad sense beyond the original concept presented by Woronichin (1926) to accommodate the sooty moulds. Abollahzadeh et al. (2020), based on LSU, *tef*1-α and *rpb*2 sequence data revalidated *Mycosphaerellales* as a separate order. *Mycosphaerellales* include species that are saprobes, ectomycorrhizae, plant pathogens and lichenised fungi (Jayawardena et al. 2022). This order includes eleven families viz. *Aeminiaceae*, *Cystocoleaceae*, *Dissoconiaceae*, *Extremaceae, Mycosphaerellaceae*, *Neodevriesiaceae*, *Phaeothecoidiellaceae*, *Phillipsiellaceae*, *Schizothyriaceae*, *Teratosphaeriaceae* and *Xenodevriesiaceae* (Zhang et al. 2024a, Hyde et al. 2024b).

Mycosphaerellaceae Lindau, Nat. Pflanzenfamilien: 421(1897)

Mycosphaerellaceae was established by Lindau (1897) with *Mycosphaerella* as the type genus. This is one of the largest families including asexual morphs, asexual holomorphs or species with *Mycosphaerella* like sexual morphs. The majority of them are parasitic or saprobic on plants, fungi and lichens (Hyde et al. 2013, Wijayawardeneet al. 2022). The family *Mycosphaerellaceae* currently accommodates 135 genera (Hyde et al. 2024b).

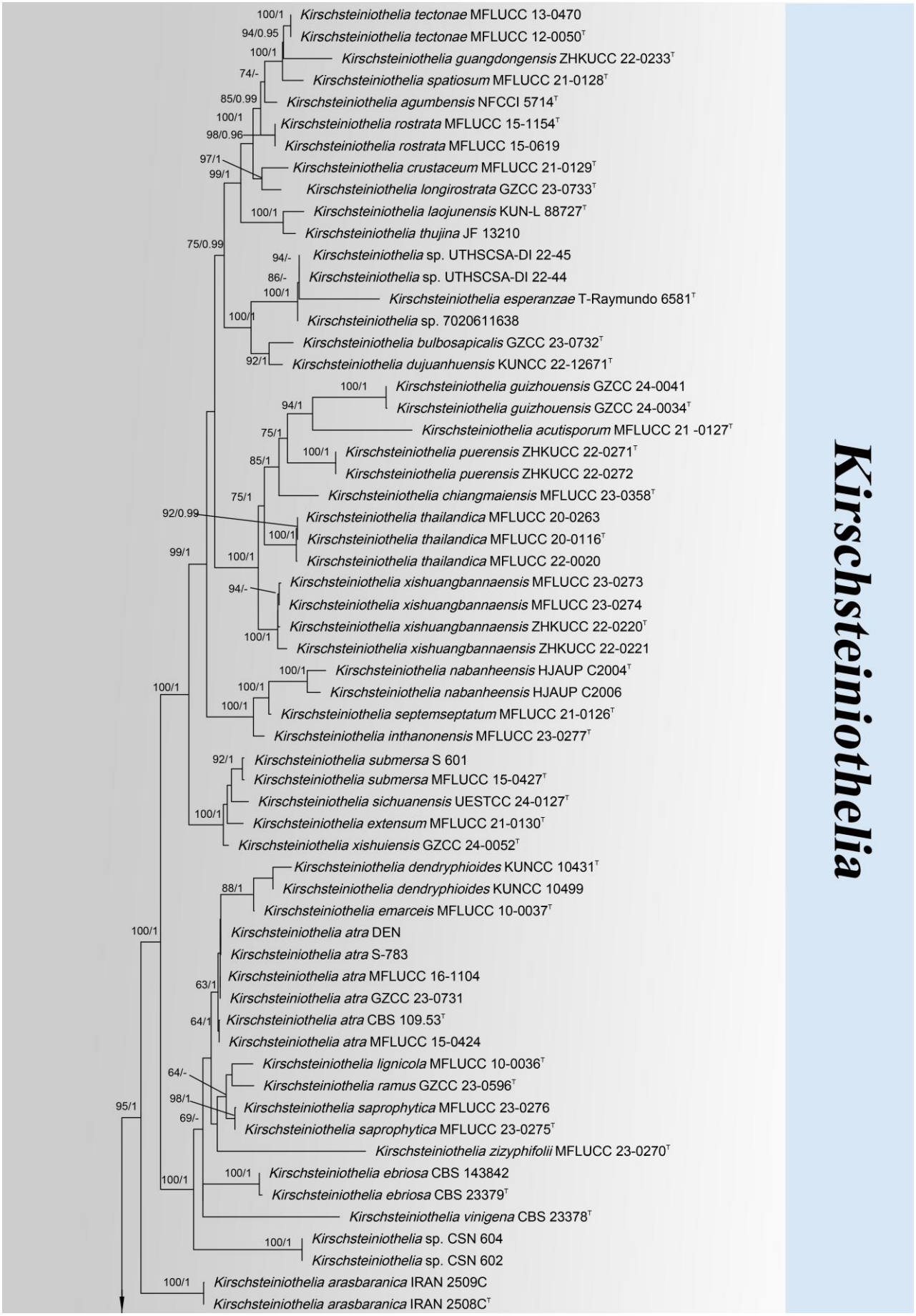

Kirschsteiniothelia tectonae MFLUCC 13-0470
Kirschsteiniothelia tectonae MFLUCC 12-0050T
Kirschsteiniothelia guangdongensis ZHKUCC 22-0233T
Kirschsteiniothelia spatiosum MFLUCC 21-0128T
Kirschsteiniothelia agumbensis NFCCI 5714T
Kirschsteiniothelia rostrata MFLUCC 15-1154T
Kirschsteiniothelia rostrata MFLUCC 15-0619
Kirschsteiniothelia crustaceum MFLUCC 21-0129T
Kirschsteiniothelia longirostrata GZCC 23-0733T
Kirschsteiniothelia laojunensis KUN-L 88727T
Kirschsteiniothelia thujina JF 13210
Kirschsteiniothelia sp. UTHSCSA-DI 22-45
Kirschsteiniothelia sp. UTHSCSA-DI 22-44
Kirschsteiniothelia esperanzae T-Raymundo 6581T
Kirschsteiniothelia sp. 7020611638
Kirschsteiniothelia bulbosapicalis GZCC 23-0732T
Kirschsteiniothelia dujuanhuensis KUNCC 22-12671T
Kirschsteiniothelia guizhouensis GZCC 24-0041
Kirschsteiniothelia guizhouensis GZCC 24-0034T
Kirschsteiniothelia acutisporum MFLUCC 21 -0127T
Kirschsteiniothelia puerensis ZHKUCC 22-0271T
Kirschsteiniothelia puerensis ZHKUCC 22-0272
Kirschsteiniothelia chiangmaiensis MFLUCC 23-0358T
Kirschsteiniothelia thailandica MFLUCC 20-0263
Kirschsteiniothelia thailandica MFLUCC 20-0116T
Kirschsteiniothelia thailandica MFLUCC 22-0020
Kirschsteiniothelia xishuangbannaensis MFLUCC 23-0273
Kirschsteiniothelia xishuangbannaensis MFLUCC 23-0274
Kirschsteiniothelia xishuangbannaensis ZHKUCC 22-0220T
Kirschsteiniothelia xishuangbannaensis ZHKUCC 22-0221
Kirschsteiniothelia nabanheensis HJAUP C2004T
Kirschsteiniothelia nabanheensis HJAUP C2006
Kirschsteiniothelia septemseptatum MFLUCC 21-0126T
Kirschsteiniothelia inthanonensis MFLUCC 23-0277T
Kirschsteiniothelia submersa S 601
Kirschsteiniothelia submersa MFLUCC 15-0427T
Kirschsteiniothelia sichuanensis UESTCC 24-0127T
Kirschsteiniothelia extensum MFLUCC 21-0130T
Kirschsteiniothelia xishuiensis GZCC 24-0052T
Kirschsteiniothelia dendryphioides KUNCC 10431T
Kirschsteiniothelia dendryphioides KUNCC 10499
Kirschsteiniothelia emarceis MFLUCC 10-0037T
Kirschsteiniothelia atra DEN
Kirschsteiniothelia atra S-783
Kirschsteiniothelia atra MFLUCC 16-1104
Kirschsteiniothelia atra GZCC 23-0731
Kirschsteiniothelia atra CBS 109.53T
Kirschsteiniothelia atra MFLUCC 15-0424
Kirschsteiniothelia lignicola MFLUCC 10-0036T
Kirschsteiniothelia ramus GZCC 23-0596T
Kirschsteiniothelia saprophytica MFLUCC 23-0276
Kirschsteiniothelia saprophytica MFLUCC 23-0275T
Kirschsteiniothelia zizyphifolii MFLUCC 23-0270T
Kirschsteiniothelia ebriosa CBS 143842
Kirschsteiniothelia ebriosa CBS 23379T
Kirschsteiniothelia vinigena CBS 23378T
Kirschsteiniothelia sp. CSN 604
Kirschsteiniothelia sp. CSN 602
Kirschsteiniothelia arasbaranica IRAN 2509C
Kirschsteiniothelia arasbaranica IRAN 2508CT
Kirschsteiniothelia

Figure 35 – Continued.

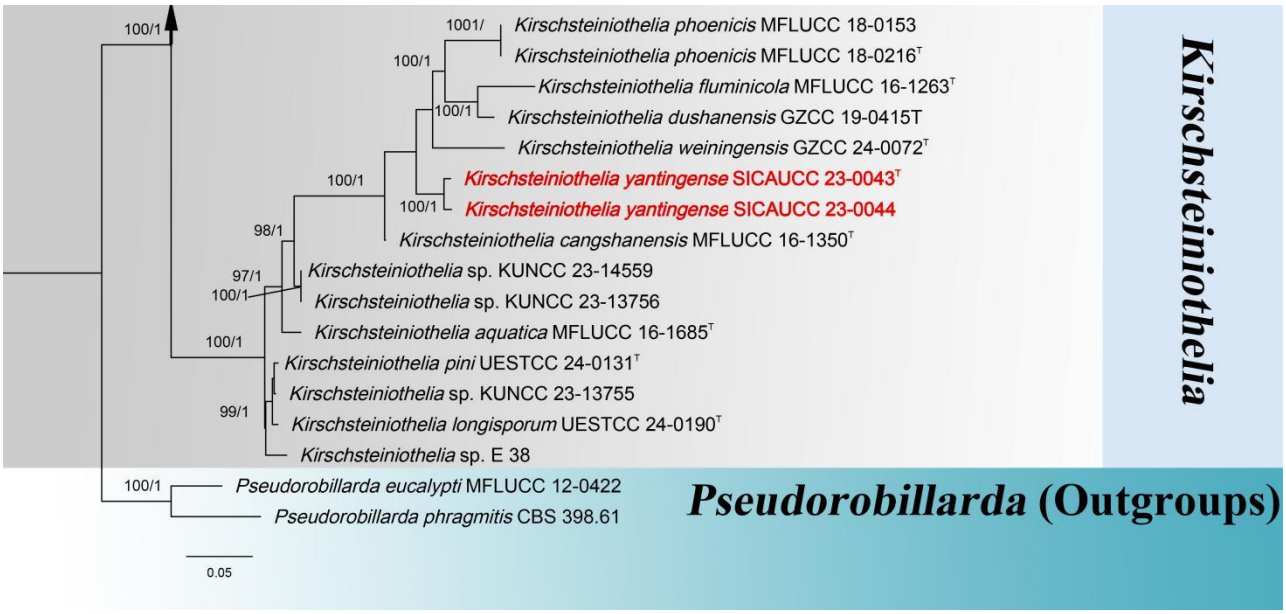


Figure 35 – Best scoring RAxML tree with a final likelihood value of -27,515.039680 based on combined LSU, ITS and SSU sequence data of related species. The tree is rooted with *Pseudorobillarda phragmitis* (CBS 398.61) and *P. eucalypti* (MFLUCC 12-0422) in *Pleosporales*. Seventy-seven strains were included in the combined gene analyses which comprised 3,818 characters (1,462 characters for LSU, 1,191 characters for ITS and 1,163 characters for SSU, including gap regions). The tree from the maximum likelihood analyses had similar topology to the Bayesian analyses. The matrix had 2,074 distinct alignment patterns with 49.31% undetermined characters or gaps. Estimated base frequencies were as follows: A = 0.228642, C = 0.256742, G = 0.302121, T = 0.212495; substitution rates AC = 1.183479, AG = 2.265099, AT = 0.930592, CG = 1.141938, CT = 4.750704, GT = 1.000000; gamma distribution shape parameter α = 0.386413. The Bayesian inference analyses was implemented by MrBayes v.3.2.2 with the best-fit model (GTR+I+G for ITS, LSU; GTR+G for SSU) of evolution estimated with MrModeltest 2.2. The species determined in this study is indicated in red and bold. Bootstrap support values for maximum likelihood (MLBS, left) ⩾ 60% and Bayesian posterior probabilities (BYPP, right) ⩾ 0.90 are indicated at the nodes, respectively. Hyphens (-) represent support values less than 60% MLBS/0.90 BYPP. The ex-type superscript "T".

Cercospora Fresen. ex Fuckel

Cercospora was established by Fresenius (1863) according to *C. apii* as the type species, and most species of this genus are plant pathogens. *Cercospora* is widely distributed in the world, as an important pathogenic fungus, which can cause leaf spot on many plants. (Meghvansi et al. 2013, Bakhshi et al. 2015, Park et al. 2017). Species of *Cercospora* were conventionally identified based on the ecological species criterion namely after the host from which they were isolated (Ellis 1971, To-anun et al. 2011). For morphological identification, the primary criteria include the size and various characteristics of the conidia such as length, breadth, base shape, and tip morphology, along with whether they are pigmented, occur singly, or in chains. Additionally, the morphology of the mycelium, conidiogenous cells, and conidiophores serves as essential basis for identification. (Pollack 1987, Crous & Braun 2003, Bakhshi et al. 2015, 2018, Senwanna et al. 2022). When utilizing polygenic phylogenetic data for the classification and identification of *Cercospora* species, it was found that calmodulin can significantly differentiate interspecific variations. (Montenegro-Calderón et al. 2011, Groenewald et al. 2013, Chen et al. 2022a)

21. ***Cercospora nicotianae*** Ellis & Everh., Proc. Acad. Nat. Sci. Philad. 45: 170 (1893) Fig. 36

Index Fungorum number: IF155078; Facesoffungi number: FoF16292

Associated with leaf spots on the living leaves of *Juglans regia*. *Leaf spots* amphigenous, pale brown to brown, margin indefinite, elongated to irregular. Caespituli amphigenous, punctiform, brown. *Stromata* substomatal to intraepidermal, brown, 27–50 μm high, 32–60 μm wide. *Conidiophores* 53−198 × 4−6 μm ($\bar{x}$ = 178 × 5 μm, n = 30), fasciculate, pale olivaceous, paler and narrower towards the apex, unbranched or occasionally a branch, main portion straight, subcylindrical, only conidiogenous cells distinctly geniculate. *Conidiogenous cells* 30−54 × 2−5 μm ($\bar{x}$ = 42 × 4 μm, n = 30), proliferating sympodially 1−6 times, integrated, terminal and intercalary, conidiogenous loci conspicuous, thickened and darkened, multilocal, formed apical or on shoulders caused by proliferation. *Conidia* 87−152 × 2−4 μm ($\bar{x}$ = 134 × 4 μm, n = 30), solitary, hyaline, thin-walled, smooth, acicular to somewhat obclavate, subobtuse at the apex, truncate to slightly obconically truncate at the base, indistinctly 2–7-septate, hila slightly thickened, darkened and refractive, 1−3 μm diam.

Culture characteristics – Conidia germinate within 24 h in sterile water, and each cell is capable of producing germ tubes. Colonies on PDA reaching 50 mm diam., after 21 days at 25 ℃. The mycelium spreading, convex, with sparse to moderate aerial mycelium, entire margin and folded surface. On PDA surface whitish, pale grey at the center with no pigment surrounding the colony. Reverse, olivaceous-black. Not produced pigmentation on PDA media.

Material examined – China, Sichuan Province, Bazhong City, Nanjiang County, Gongshan Town (32°18′37.45″N 106°52′22.53″E, alt. 1011 m), on the living leaves of *Juglans regia*, 29 June 2022, F.-H. Wang, WFH202206004-1 (SICAU 22-0115), living culture SICAUCC 22-0117.

GenBank numbers – SICAUCC 22-0117: OP963817 (ITS), OQ190497 (*cal*).

Note – *Cercospora* are commonly isolated from leaves of diseased herbal hosts (Almeida et al. 2005, Albu et al. 2016, Park et al. 2017). There are few reports in woody plants. *C. nicotianae* can cause soybean and tobacco leaf spot (Sautua et al. 2020, Zhao et al. 2020). In our study, we collected the asexual morph on a Walnut leaf in China, which has same morphology with the type. Our collection forms a clade with two strains of *C. nicotianae*, including the type strain (CBS131.32) in the phylogeny tree (Fig. 37) with high bootstrap support (100% MLBS/1.00 BYPP). Nucleotide comparisons of ITS, and *cal* (SICAUCC 22-0117) also showed a high homology with the sequences of *C. nicotianae* (CBS131.32 ex-type), with a similarity of 100% (506/506, 0 gap), and 100% (290/290, 0 gap), respectively. Based on morphological characters and phylogenetic analyses, we determine our specimens as *C. nicotianae*.

Ragnhildiana Solheim, Mycologia 23(5): 402 (1931).

Ragnhildiana was formally established by Solheim (1931), and the type species is *R. agerati*. Most members of this genus are plant pathogens that can cause cankers. Most of them are distributed on plant leaves. (Crous et al. 2013, Poletto et al. 2017, Videira et al. 2017). Currently, there are a total of 10 valid species within this genus (Hyde et al. 2024b).

22. ***Ragnhildiana diffusa*** (Heald & F.A. Wolf) Videira & Crous, Stud. Mycol. 87: 342 (2017) Fig. 38

Index Fungorum number: IF822788; Facesoffungi number: FoF16293

Associated with leaf spots on the living leaves of *Juglans regia*. Leaf spots tiny and reddish to brown, subcircular to irregular, with a yellowish halo appeared dispersedly on the leaves. *Mycelium* internal and external, composed of pale brown to brown hyphae, that are septate and smooth to verruculose. *Conidiophores* 46–75 × 4–6 μm ($\bar{x}$ = 59 × 5 μm, n = 30) were in fascicles or independent, 0–3-septate, emerging from stromata, brown to pale brown, paler towards apex, smooth to verruculose, straight to sinuous-geniculate, simple or branched, and sometimes reduced to conidiogenous cells, with prominent, thickened and darkened conidiogenous loci. *Conidiogenous cells* terminal and intercalary, polyblastic, proliferating sympodially, with rim-like conidiogenous loci, thickened and darkened, 2–3 μm diam. *Conidia* 20–120 × 3–5 μm ($\bar{x}$ = 76 × 5 μm, n = 40), solitary, hyaline to pale olivaceous brown, obovoid, cylindrical, tapered toward the distal end, straight

or curved, base obconicaly truncate, apex rounded, 0–8-septate, occasionally constricted at the septa, hila thickened and darkened.

Culture characteristics – Conidia germinating from all round. Colonies on PDA growing slow, reaching 15 mm diam., after 40 days at 25 ℃, black in the center and reddish brown in the periphery, the colonies raised like a tumor. The color of the colonies on the reverse side of the petri dish was constant, with all the isolates having a similar reddish-brown color. However, a red pigmentation diffused into the culture medium around the colonies, pigment is obvious.

Material examined – China, Sichuan Province, Chengdu City, Chongzhou City (30°33′10.04″N 103°39′29.18″E, alt. 512 m), on the living leaves of *Juglans regia*, 10 September 2021, F.-H. Wang, WFH202109007 (SICAU 22-0077), living culture SICAUCC 22-0077.

GenBank numbers – SICAUCC 22-0077: ON409525 (ITS), ON409559 (LSU), ON417473 (*rpb*2).

Note – In Mexico, South Africa, and the United States, *Ragnhildiana diffusa* has been reported as causing brown leaf spots in pecan trees (Chupp 1954, Crous & Braun 2003). Additionally, in Brazil, this disease was first observed in pecan trees in 2016 (Poletto et al. 2017), leading to leaf spots and subsequent defoliation. In the phylogenetic analysis *R. diffusa* strain (SICAUCC 22-0077) and *R. diffusa* (CBS 106.14) formed a distinct clade (Fig. 39). The asexual morph of our taxon was not obtained from culture. Sequence comparisons reveal a high similarity in their ITS (100%, 532/532, 0 gap) LSU (100%, 850/850, 0 gap), and *rpb*2 (100%, 861/861, 0 gap) signifying their close genetic relationship. The collection SICAU 22- 0077 is therefore identified as *R. diffusa*.

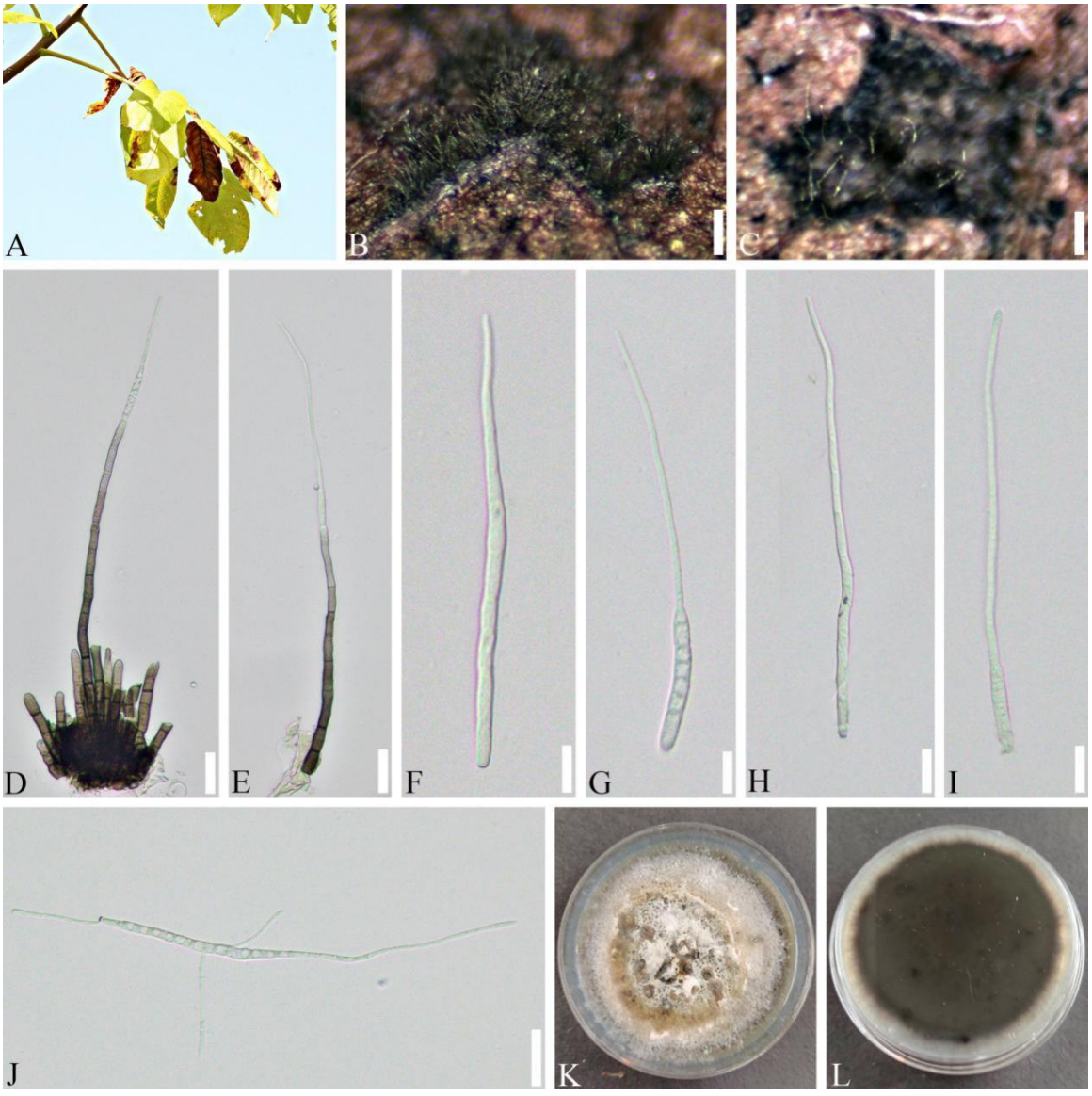


Figure 36 – *Cercospora nicotianae* (SICAU 22-0115). A Symptoms of necrotic lesions observed on host. B, C Conidiophore fascicles. D, E Conidiophores. F–I Conidia. J Germinating conidium. K, L Colonies on PDA (K from above, L from below). Scale bars: B = 1 mm, C = 500 µm, D, E = 50 µm, F, G = 20 µm, H, I = 10 µm.

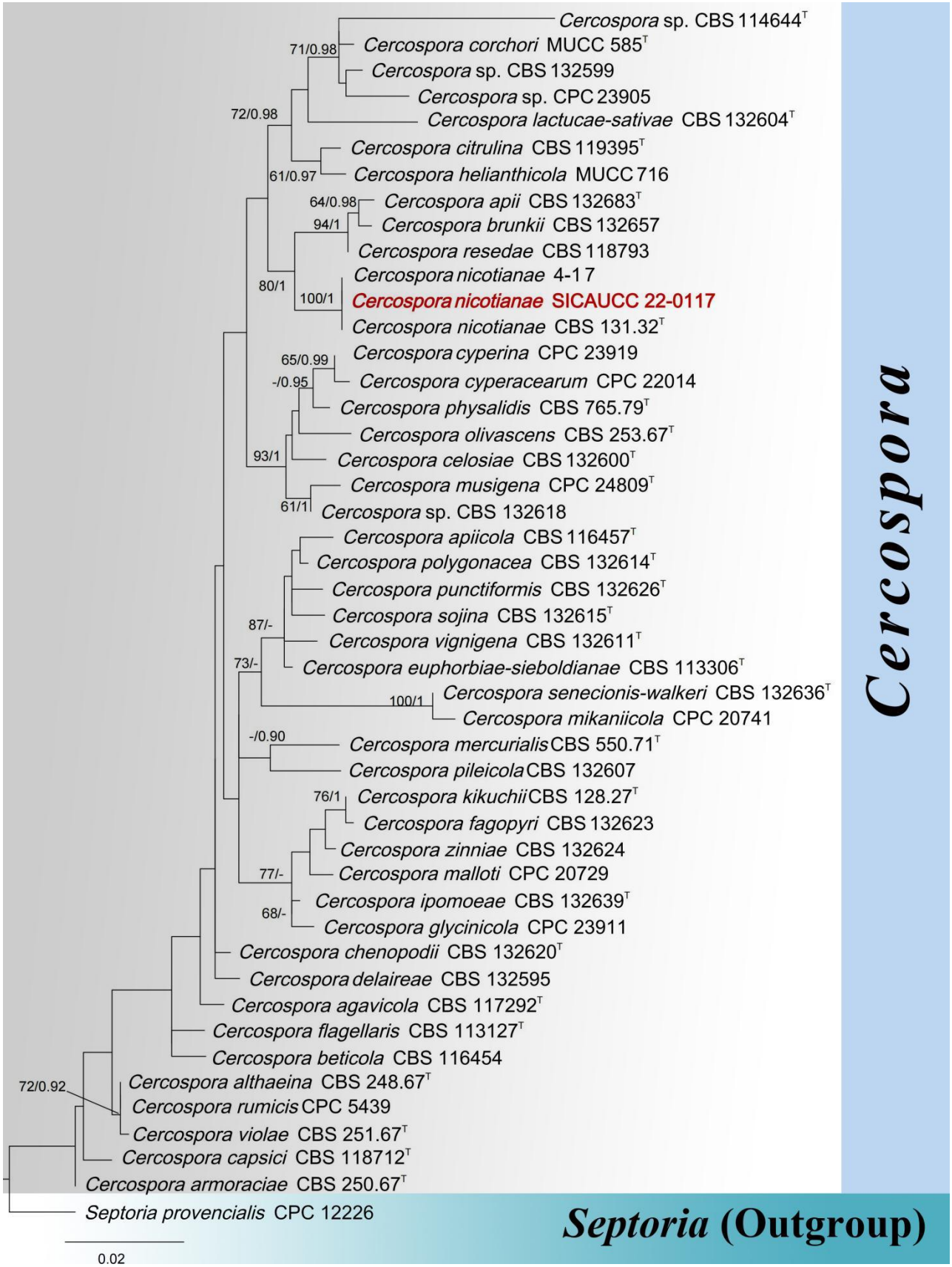


Figure 37 – Best scoring RAxML tree with a final likelihood value of -3,699.112363 based on combined *cal* and ITS sequence data of related species. The tree is rooted with *Septoria provencialis* (CPC 12226) in *Mycosphaerellaceae*. Forty-seven strains were included in the combined gene analyses which comprised 1,180 characters (475 characters for *cal* and 704 characters for ITS, including gap regions). The matrix had 274 distinct alignment patterns with 28.39% undetermined characters or gaps. Estimated base frequencies were as follows: A = 0.239683, C = 0.277979, G = 0.262142, T = 0.220195; substitution rates AC = 2.389580, AG = 6.037874, AT = 1.685113, CG = 1.383162, CT = 10.522307, GT = 1.000000; gamma distribution shape parameter α = 0.116251. The Bayesian inference analysis was implemented by MrBayes v.3.2.2 with the best-fit model (GTR+I+G for CAL; K80+I for ITS) of evolution estimated with MrModeltest 2.2. The species determined in this study is indicated in red and bold. Bootstrap support values for maximum likelihood (MLBS, left) ⩾ 60% and Bayesian posterior probabilities (BYPP, right) ⩾ 0.90 are indicated at the nodes, respectively. Hyphens (-) represent support values less than 60% MLBS/0.90 BYPP. The ex-type superscript "T".

Sphaerulina Sacc., Michelia 1(no. 4): 399. 1878.

Sphaerulina was chiefly separated from *Mycosphaerella* on the basis of ascospore septation (Crous et al. 2011). *Sphaerulina* is a heterothallic ascomycete that exhibits both asexual and sexual morphs (Tabima et al. 2020). Most species of this genus are pathogenic fungi, among which the poplar canker caused by *S. musiva* has been reported more (Bier 1939, Feau et al. 2010, Dhillon et al. 2015). Early studies lacked molecular data, and most species were later revised. Therefore, extensive collection and cultivation of species within this genus are crucial for current research (Ujat & Nakashima 2024).

23. ***Sphaerulina curvecylindrospora*** F.H. Wang & C.L. Yang, sp. nov. Fig. 40

Index Fungorum number: IF901565; Facesoffungi number: FoF15583

Holotype – SICAU 22-0061

Etymology – refers to its curved cylindrical conidia.

Associated with leaf spots on the living leaves of *Juglans regia*. *Symptoms* clear, small brown dots at the beginning, scattered or in clusters, in the center black, silver gray surrounding, somewhat elevated zone, the junction of disease and health is reddish brown. *Conidiomata* pycnidial, a large number, semi-immersed, disperse or gather, white or light brown, spherical to ellipsoidal, 80 μm diam. *Stromatal* base 4–8 μm thick, and composed of several layers of cells of hyaline. *Conidiophores* branched at the base, doliiform, cylindrical, or ampuliform, hyaline, holoblastic, proliferating percurrently with one to several, or sympodially, sometimes both types of proliferation occurring in a single conidiogenous cell. *Conidiogenous cells* 14–28 × 2–4 μm ($\bar{x}$ = 23 × 3 μm, n = 20), hyaline, discrete or integrated in simple, short, 0–2-septate. *Conidia* 19–36 × 2.5–4.5 μm ($\bar{x}$ = 28 × 3 μm, n = 40), cylindrical, curved or flexuous, broadly rounded at the apex which is provided with a cap of mucilaginous material, attenuated gradually to a broadly or more narrowly truncate base which often is also provided with an amorphous mass of mucilaginous material, hyaline, 0–5-septate, slightly constricted at the septum, sometimes at one or more septa also some amorphous mucilaginous material may be present, contents with numerous small oil droplets.

Culture characteristics – Conidia germinate within 24 hours in sterile water, and each cell is capable of producing germ tubes. Colonies on PDA reaching 10 mm diam., after 30 days at 25 ℃, slow growth, irregular shape, rough margin, white at first, ash to greenish black after 2 weeks, obvious bulge, flat on the surface, aerial mycelium is scarce. Reverse, black. Not produced pigmentation on PDA media.

Material examined – China, Sichuan Province, Liangshan Yi Autonomous Prefecture, Huili City (26°56′43.22″N 102°16′26.06″E, alt. 2001 m), on the living leaves of *Juglans regia*, 30 September 2021, F.-H. Wang, WFH202209002 (SICAU 23-0061, holotype), ex-type living culture SICAUCC 23-0040. *Ibid*., WFH202209002B (SICAU 24-0032), living culture SICAUCC 23-0146.

GenBank numbers – SICAUCC 23-0040: PP060656 (ITS), PP057949 (LSU), PP061118 (*rpb*2), PP061170 (*tub*2); SICAUCC 23-0146: PP844874 (ITS), PP826164 (LSU), PP850047 (*rpb*2), PP850061 (*tub*2).

Note – In the phylogenetic analysis, *Sphaerulina curvecylindrospora* (SICAUCC 23-0040 and SICAUCC 23-0146) forms a distinct lineage basal to *S. juglandina* (SICAUCC 22-0109), *S. juglandin* (SICAUCC 22-0108) and *S. juglandina* (SICAUCC 22-0162) with 72% MLBS support (Fig. 41). *Sphaerulina curvecylindrospora* (SICAUCC 23-0040) is morphologically and phylogenetically distinct from *S. juglandina* on *Juglans regia*, conidia 1–4-septate, 26–49 × 2–4 µm (Xu et al 2022a). Nucleotide comparisons revealed notable genetic dissimilarities between *S. curvecylindrospora* (SICAUCC 23-0040) and *S. juglandina* (SICAUCC 22-0108), viz. 5.4% (24/443, 5 gaps), 0.4% (3/809, 0 gap), 14% (138/983, 0 gap), and 29.3% (129/440, 21 gaps) in the ITS, LSU, *rpb*2, and *tub*2, respectively. The PHI test revealed no significant recombination event between our strain and the closely related taxa (Φw = 1) (Fig. 42). Therefore, we consider *S. curvecylindrospora* (SICAUCC 23-0040) to be a new species.



Figure 38 – *Ragnhildiana diffusa* (SICAU 22-0077). A Symptoms of necrotic lesions observed on host. B Conidiophore fascicles. C Conidiophores. D–K Conidia. L Germinating conidium. M, N Colonies on PDA (M from above, N from below). Scale bars: B = 1 mm, C–L = 20 µm, D–K = 10 µm.

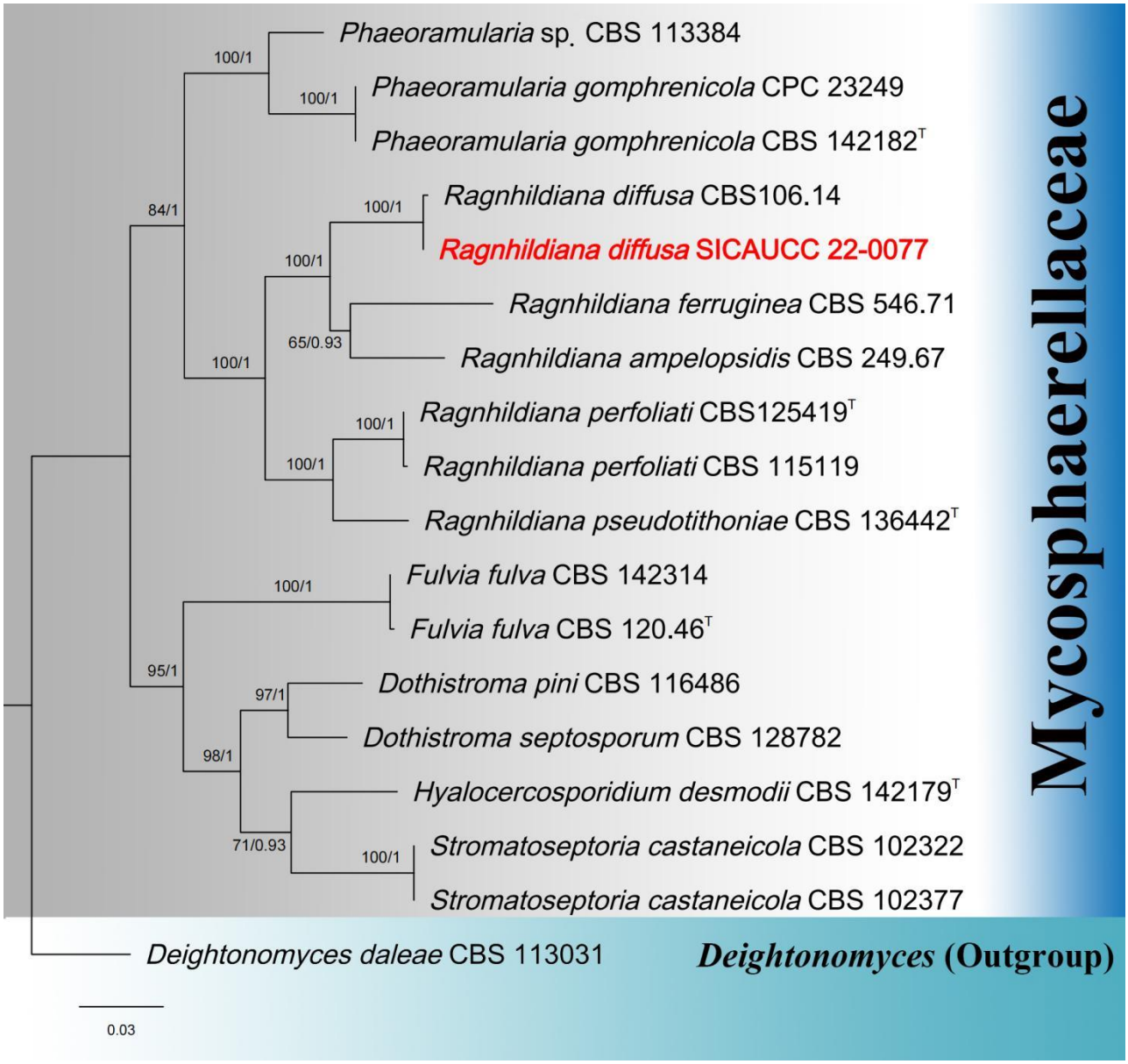


Figure 39 – Best scoring RAxML tree with a final likelihood value of -11,138.053715 based on combined ITS, LSU and *rpb2* sequence data of related species. The tree is rooted with *Deightonomyces daleae* (CBS 113031). Eighteen strains were included in the combined analyses which comprised of 3,548 characters (1,526 characters for ITS, 880 characters for LSU and 1,134 characters for *rpb2*, including gap regions). The matrix had 636 distinct alignment patterns, with 37.12% of undetermined characters and gaps. Estimated base frequencies were as follows; A = 0.246490, C = 0.247214, G = 0.286834, T = 0.219462; substitution rates AC = 1.559804, AG = 3.343436, AT = 0.759963, CG = 0.993238, CT = 6.587645, GT = 1.000000; gamma distribution shape parameter α = 0.138851. In our analysis, GTR+I+G model was used for each partition in Bayesian posterior analysis. The species determined in this study is indicated in red and bold. Bootstrap support values for maximum likelihood (MLBS, left) ⩾ 60% and Bayesian posterior

probabilities (BYPP, right) ⩾ 0.90 are indicated at the nodes, respectively. Hyphens (-) represent support values less than 60% MLBS/0.90 BYPP. The ex-type superscript "T".

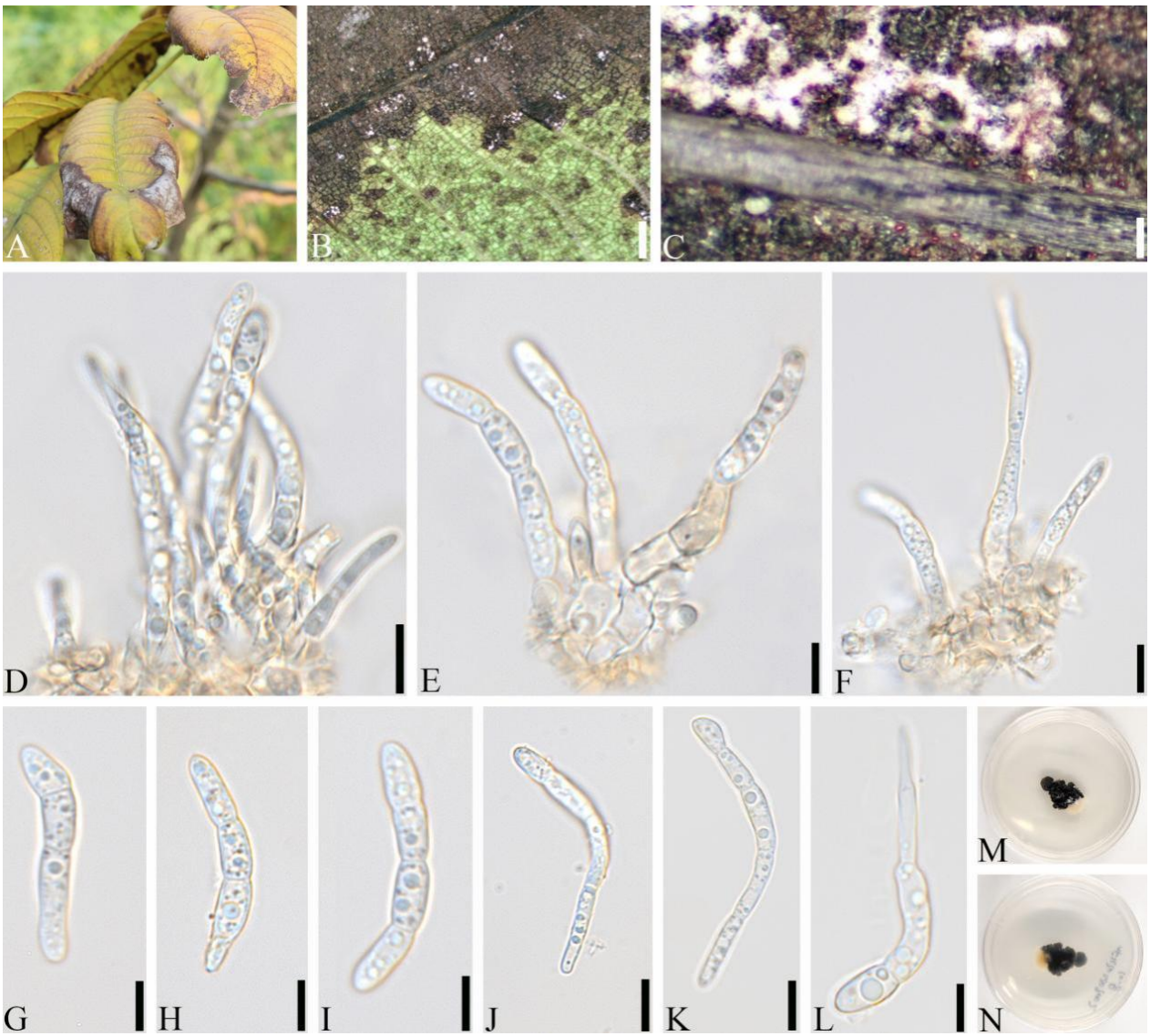


Figure 40 – *Sphaerulina curvecylindrospora* (SICAU 23-0061, holotype). A Symptoms of necrotic lesions observed on host. B, C Conidiophore fascicles. D–F Conidiogenous cells. G–K Conidia. L Germinating conidium. M, N Colonies on PDA (M from above, N from below). Scale bars: B = 1 mm, C = 200 µm, D–L = 10 µm.

24. ***Sphaerulina juglandina*** X.L. Xu & C.L. Yang, Front. Microbiol. 13(no. 1016548): 19 (2022) Fig. 43

Index Fungorum number: IF845075; Facesoffungi number: FoF16294

Associated with leaf spots on the living leaves of *Juglans regia*. Symptom firstly 3–4 mm diam., appearing as small specks on leaf, later merging, up to 7–8 mm diam. *Conidiomata*, dark brown, up to 120 µm diam, flat stromatic, amphigenous, solitary, scattered, initially immersed, finally erumpent, usually broke through the upper epidermis and extravasated conidia, tiny dots though epiphyllous, lacte. *Stromata* base 3–10 µm thick, composed of several layers of cells of hyaline. *Conidiophores* reduced to conidiogenous cells or giving rise to several terminal conidiogenous cells, hyaline, cylindrical, smooth-walled, and aseptate. *Conidiogenous cells* 4–10 × 2–4 µm ($\bar{x}$ = 7 × 3 µm, n = 20), hyaline, subcylindrical, sometimes slightly tapered toward the apex, monophialidic, and with apical loci indistinctly. *Conidia* 24–45 × 2–4 µm ($\bar{x}$ = 35 × 3 µm, n = 40), cylindrical, mostly

curved or flexuous, apex narrowly or broadly rounded, narrowed slightly to the truncate base, 1–4-septate, not or slightly constricted around the septum, hyaline, and contents with few oil droplets and minute granules in each cell.

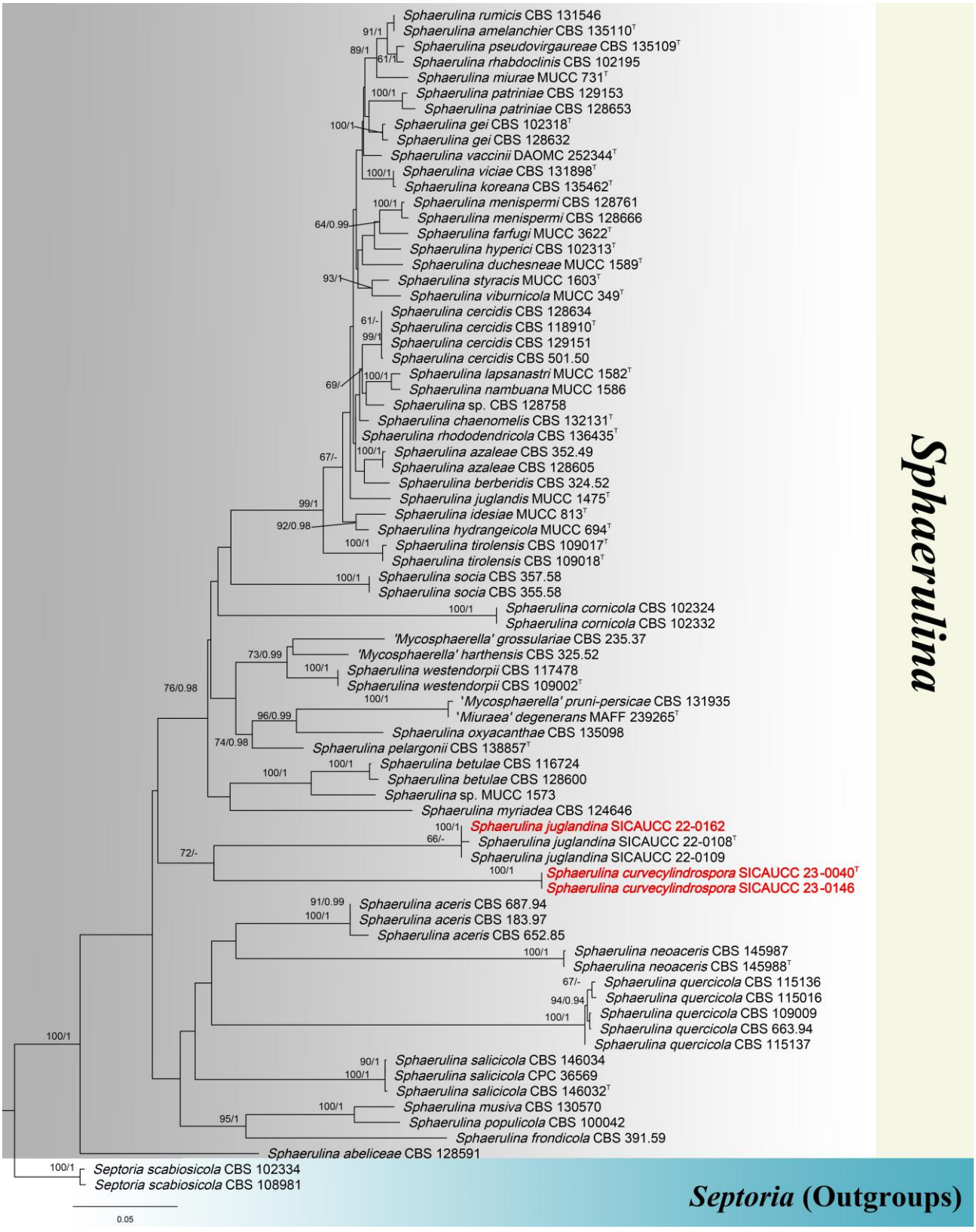


Figure 41 – Best scoring RAxML tree with a final likelihood value of -24,795.125540 based on combined ITS, LSU, *rpb*2, *tef*1-α and *tub*2 sequence data of related species. The tree is rooted with

Septoria scabiosicola (CBS 102334 and CBS 108981). in *Mycosphaerellaceae*. Seventy-six strains were included in the combined gene analyses which comprised 4,657 characters (1,104 characters for ITS, 893 characters for LSU, 1,159 characters for *rpb*2, 996 characters for *tef*1-α and 501 characters for *tub*2, including gap regions). The matrix had 1,683 distinct alignment patterns with 49.20% undetermined characters or gaps. Estimated base frequencies were as follows: A = 0.242374, C = 0.253452, G = 0.281722, T = 0.222452; substitution rates AC = 1.395825, AG = 3.111175, AT = 1.049953, CG = 0.900636, CT = 6.167769, GT = 1.000000; gamma distribution shape parameter α = 0.219371. The Bayesian inference analyses was implemented by MrBayes v.3.2.2 with the best-fit model (GTR+I+G for ITS, LSU, *rpb*2; K80+I for *tef*1-α; HKY+I+G for *tub*2) of evolution estimated with MrModeltest 2.2. The species determined in this study is indicated in red and bold. Bootstrap support values for maximum likelihood (MLBS, left) ⩾ 50% and Bayesian posterior probabilities (BYPP, right) ⩾ 0.90 are indicated at the nodes, respectively. Hyphens (-) represent support values less than 50% MLBS/0.90 BYPP. The ex-type superscript "T".

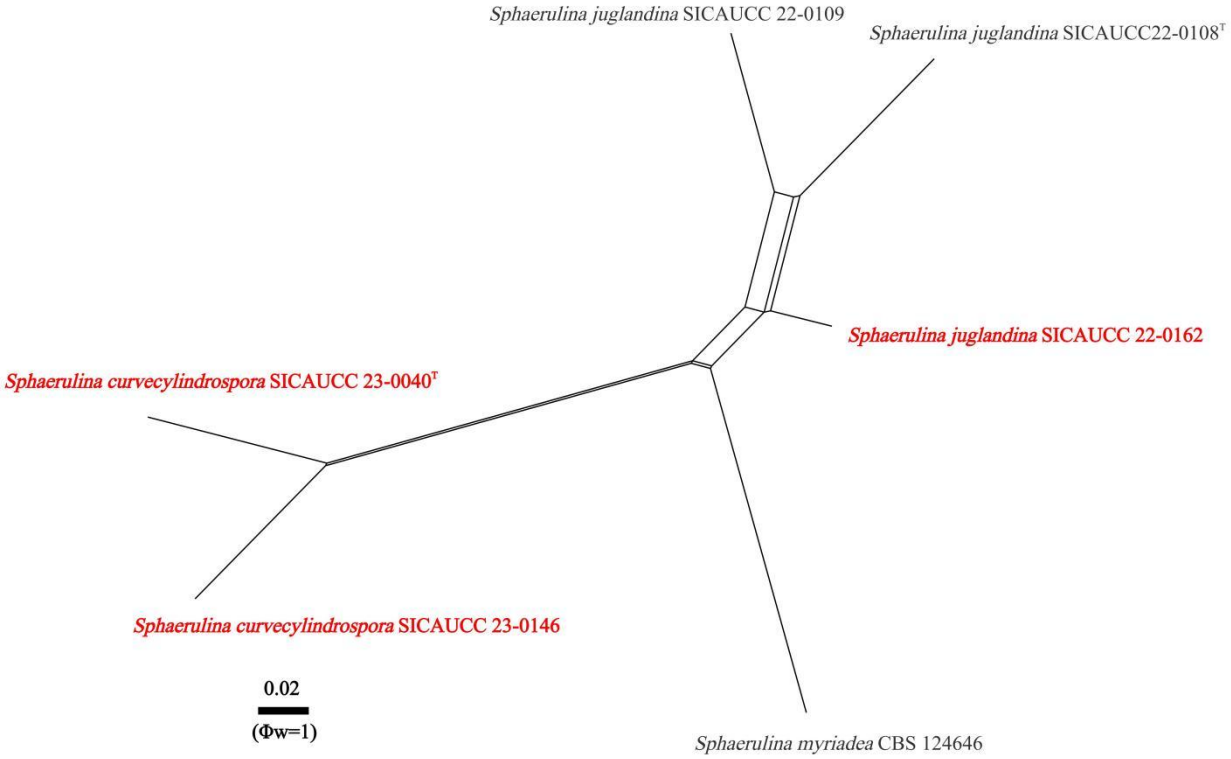


Figure 42 – Results of the PHI test of *Sphaerulina curvecylindrospora* and closely related species using both LogDet transformation and splits decomposition. The PHI test did not find any statistically significant recombination (Φw = 1) in the data set. The new strains are represented in red and bold. "T" represents the type strain.

Culture characteristics – Conidia germinate within 24 hours in sterile water, and each cell is capable of producing germ tubes. Colonies on PDA reaching 20 mm diam., after 30 days at 25 ℃, slow-growing, subcircular, raised, irregular edge, the edge grayish white wheel-like, raised part white, and reverse dark brown to black. Not produced pigmentation on PDA media.

Material examined – China, Sichuan Province, Neijiang City, Dongxing District, Paifang Village (29°48′30.19″N 105°6′36.05″E, alt. 388 m), on the living leaves of *Juglans regia*, 27 April 2021, F.-H. Wang, WFH202204069 (SICAU 22-0160), living culture SICAUCC 22-0162.

GenBank numbers – SICAUCC 22-0162: OP980896 (ITS), OQ436577 (*tef*1-α), OQ436578 (*tub*2).

Note – *Sphaerulina juglandina* (SICAUCC 22-0162) tallies with the generic concept of *Sphaerulina* in having immersed, flat stromatic, amphigenous, solitary, scattered conidiomata, hyaline, cylindrical, septate, curved or flexuous, not or slightly constricted around the septum conidia (Quaedvlieg et al. 2013). Phylogeny indicates that our collection grouped with *S. juglandina* (SICAUCC 22-0109) with strong statistical support (100% MLBS/1.00 BYPP) (Fig. 41). Nucleotide comparisons of ITS, LSU, *tef*1-α, and *tub*2 (SICAUCC 22-0162) also showed a high homology with the sequences of *S. juglandina* (SICAUCC 22-0108 ex-type), with a similarity of 100% (900/900, 0 gap), 99.8% (547/548, 0 gap), and 100% (441/441, 0 gap), respectively. Both isolates *S. juglandina* (SICAUCC 22-0109) and *S. juglandina* (SICAUCC 22-0162), share similar size ranges of conidiogenous cells (4–10 × 2–4 µm vs 3–9 × 2–4 µm) and conidia (24–45 × 2–4 µm vs 26–49 × 2–4 µm). Based on morphological characters and phylogenetic analyses, we determine our specimens as *S. juglandina*. *Sphaerulina juglandina* was introduced by Xu et al. (2022a), from leaves of *Juglans regia* in China.

Pleosporales Luttrell ex M.E. Barr.

Pleosporales was introduced by Luttrell (1955). The order is highly diverse with more than 75 families (Wijayawardene et al. 2018). We follow the latest treatments and updated accounts of *Pleosporales* in Hongsanan et al. (2020b) and Wijayawardene et al. (2022) together with recent relevant literature for updated accounts of each family (Jayawardena et al. 2022, Hyde et al. 2024d).

Bambusicolaceae D.Q. Dai & K.D. Hyde, Fungal Divers. 63: 49 (2013)

Hyde et al. (2013) established the family *Bambusicolaceae* to accommodate *Bambusicola* on account of its coelomycetous asexual morph different from that of *Trematosphaeriaceae* (hyphomycetous asexual morph), as well as a multi-gene (SSU, LSU, *rpb*2 and *tef*1-α) phylogeny. *Palmiascoma* (Liu et al. 2015), *Leucaenicola* (Jayasiri et al. 2019), and *Corylicola* (Wijesinghe et al. 2020) were subsequently added to this family based on morph-phylogenetic evidence. *Bambusicolaceae* are characterized by solitary, scattered, immersed, semi-immersed to erumpent and conical or globose to subglobose ascomata, anastomosing, branching interascal filaments, cylindrical to clavate asci with a short furcate or rounded to obtuse pedicel and slightly broad-fusiform or clavate to ellipsoidal, hyaline or yellowish to brown, single-septate ascospores with a gelatinous sheath (Hyde et al. 2013, Liu et al. 2015, Dai et al. 2015, 2017, Phookamsak et al. 2024). Asexual morphs are characterized by having pycnothyrial conidiomata, and holoblastic, annelidic or phialidic conidiogenous cells, producing cylindrical, globose or oblong to ellipsoidal, pale to dark brown, aseptate or 1–3-septate conidia (Wijesinghe et al. 2020, Phukhamsakda et al. 2022).

Palmiascoma Phook. & K.D. Hyde, Fungal Divers. 72: 65 (2015)

Palmiascoma was introduced by Liu et al. (2015) and is typified by *P. gregariascomum* collected from a dead frond of a palm. *Palmiascoma* is similar to *Didymosphaeria* in having didymosporous, brown, and echinulate ascospores, but differs in phylogeny. Monkai et al. (2021) introduced the second species into the genus as *P. qujingense* isolated from dead twigs of *Fagaceae* sp. in Yunnan, China. Li et al. (2023a) introduced the third species into the genus as *P. acericola* isolated from dead twigs of *Acer truncatum* in Sichuan, China.

25. ***Palmiascoma qujingense*** Monkai & Phookamsak, Mycol. Progr. 20: 727 (2021) Fig. 44

Index Fungorum number: IF556132; Facesoffungi number: FoF09505

Associated with blight symptom on living twigs of *Juglans regia*. Symptom small branches wither, the leaves turn yellow, growth is hindered, and premature defoliation occurs. On the bark of infected branches, brown stripes can be observed. In later stages, pinpoint dark spots appear. Sexual morph: *Ascomata* 270–340 × 180–280 µm ($\bar{x}$ = 310 × 260 µm, n = 10), immersed to erumpent, gregarious to dense, crowded, less commonly solitary, compressed globose, with flat base, brown to

dark brown. *Ostiole* 36.5–48 µm wide, central, papillate, with a crest-like apex and a pore-like opening, filled with hyaline periphyses. *Peridium* 26–38 µm thick, composed of 3–5 layers of brown-walled cells of *textura angularis*. *Hamathecium* comprising 2.2–2.8 µm wide, cylindrical, hyaline, septate, branched pseudoparaphyses. *Asci* 63–69 × 9.5–11 µm ($\bar{x}$ = 66 × 10 µm, n = 20), 8-spored, bitunicate, fissitunicate, cylindric-clavate, elongated and cylindrical pedicellate, with a furcate base, apically rounded. *Ascospores* 11–15 × 4–6 µm ($\bar{x}$ = 14 × 5 µm, n = 40), biseriate, fusiform to ellipsoid, with rounded ends, uniseptate, slightly constricted at the septum, rough-walled, guttulate. Asexual morph: Not observed.

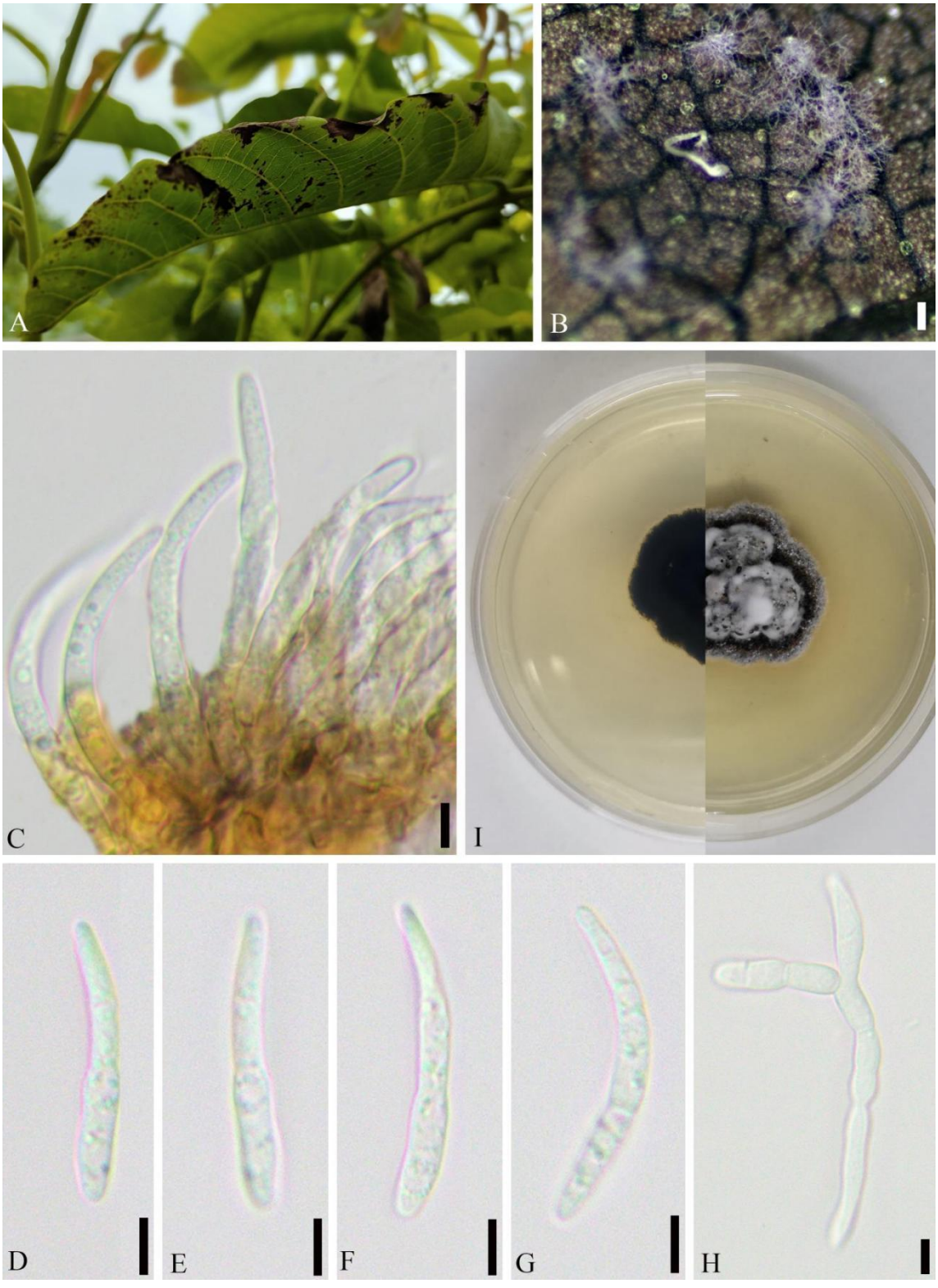


Figure 43 – *Sphaerulina juglandina* (SICAU 22-0160). A Symptoms of necrotic lesions observed on host. B Conidiophore fascicles. C Conidiophores. D–G Conidia. I Germinating conidium. J, K Colonies on PDA. Scale bars: B = 1 mm, C–H = 10 μm.

Culture characteristics – Ascospores germinating on sterile water within 24 h and germ tubes produced from ends. Colonies on PDA fast growing, 40 mm diam., after 15 days at 25 ℃, medium dense, circular, convex, surface slightly rough with entire edge, effuse, velvety to hairy, margin well defined, colony from both above and below: white to greyish at the margin, white in the center. Not produced pigmentation on PDA media.

Material examined – China, Sichuan Province, Chengdu City, Chongzhou City (30°33′9.54″N 103°39′29.36″E, alt. 512 m), living twigs of *Juglans regia*, 10 September 2020, F.-H. Wang, WFH202009004 (SICAU 21-0012), living culture SICAUCC 21-0013.

GenBank numbers – SICAUCC 21-0013: MZ951112 (ITS), MZ983549 (LSU), MZ959419 (SSU), MZ818772 (*rpb*2).

Note – Our new collection of *Palmiascoma qujingense* (SICAUCC 21-0013) is described on living twigs of *Juglans regia* species from China. We found the sexual morph of the taxon with a similar range of ascomata (270–340 × 180–280 μm vs. 280–400 × 200–300 μm) and ascospores (11–15 × 4–6 μm vs. 12−16 × 4.5−5.5) in morphologies compared to the type species *P. qujingense* (KUMCC 19-0201). In multigene phylogeny, our strain clusters with KUMCC 19-0201 with strong statistical support (94% MLBS/0.99 BYPP) (Fig. 45). Nucleotide comparisons of ITS, LSU, SSU, and *rpb*2 (SICAUCC 21-0013) also showed a high homology with the sequences of *P. qujingense* (KUMCC 19-0201), with a similarity of 99.4% (467/470, 0 gap), 100% (848/848, 0 gap), 100% (940/940, 0 gap), and 100% (884/884, 0 gap), respectively. Based on morphological characters and phylogenetic analyses, we determine our specimens as *P. qujingense*.

Pseudochaetosphaeronema Punith., Nova Hedwigia 31(1-3): 126 (1979).

Pseudochaetosphaeronema was introduced by Punithalingam (1979) based on *Pseudochaetosphaeronema larense*. Currently, only morphological descriptions of the asexual stages of species within this genus are available (Zhang et al. 2016; Hyde et al. 2020a). The members of the genus can act as human pathogens, endophytes and saprobes (Ahmed et al. 2014, 2015, Zhang et al. 2016, Hyde et al. 2020a). Species epithets are listed in Species Fungorum (http://www.speciesfungorum.org/Index.htm, September 2024). In this study, we introduce a novel species of *Pseudochaetosphaeronema* collected from Thailand, and it is the first report of the sexual morph of the genus. The tree topology of our multigene phylogenetic analyses is similar to the latest analysis performed by Xu et al. (2024)

26. ***Pseudochaetosphaeronema kunmingense*** D.P. Wei, Wanas. & K.D. Hyde, Fungal Divers. 100: 75 (2020) Fig. 46

Index Fungorum number: IF557019; Facesoffungi number: FoF07078

Saprobic on decaying *Juglans sigillata* twig. Sexual morph: *Ascomata* 170–315 × 210–340 μm ($\bar{x}$ = 265 × 280 μm, n = 10), immersed, erumpent, aggregated, clustered, globose to subglobose, uniloculate, dark brown to black. *Peridium* 10–28 μm ($\bar{x}$ = 18μm, n = 20) wide, comprising several layers of dark brown cells of *textura angularis*. *Hamathecium* comprising 1–2 μm wide, cylindrical, filamentous, rarely branched, inconspicuously septate, anastomosed, hyaline pseudoparaphyses. *Asci* 50–88 × 7–11 μm ($\bar{x}$ = 65 × 9 μm, n = 20), 8-spored, bitunicate, cylindric-clavate to clavate, slightly curved, bulbous pedicellate, apically rounded. *Ascospores* 14–16 × 4–6 μm ($\bar{x}$ = 15 × 5 μm, n = 20), overlapping uni- to bi-seriate, ellipsoid to obovoid, slightly curved, light brown to brown, 1–3-septate, strongly constricted and darkened at the septa, guttulate, smooth-walled. Asexual morph: Coelomycetous. *Conidiomata* 180–250 μm diam., ($\bar{x}$ = 221 μm, n = 5), pycnidial, erumpent to superficial, globose to subglobose scattered, black, glabrous, solitary, uni-loculate, without papilla. *Conidiomata wall* 15–50 μm ($\bar{x}$ = 30 μm, n = 30), outer layers comprised of thick-walled, brown cells of *textura angularis*, inner layers comprised of hyaline, thin-walled cells of *textura angularis*.

Conidiophores reduced to conidiogenous cells. *Conidiogenous cells* 3–9 × 1–2.5 µm ($\bar{x}$ = 6 × 1.3 µm, n = 20), produced from inner stromatic tissue, monophialidic, cylindrical or ampulliform, integrated, hyaline, smooth-walled. *Conidia* 10–15 × 4–6 µm ($\bar{x}$ = 13 × 5 µm, n = 50), hyaline when immature, becoming brown at maturity, typically fusiform with round ends, occasionally oval, smooth-walled, 3-septate, slightly constricted at the septa. (Hyde et al. 2020b)

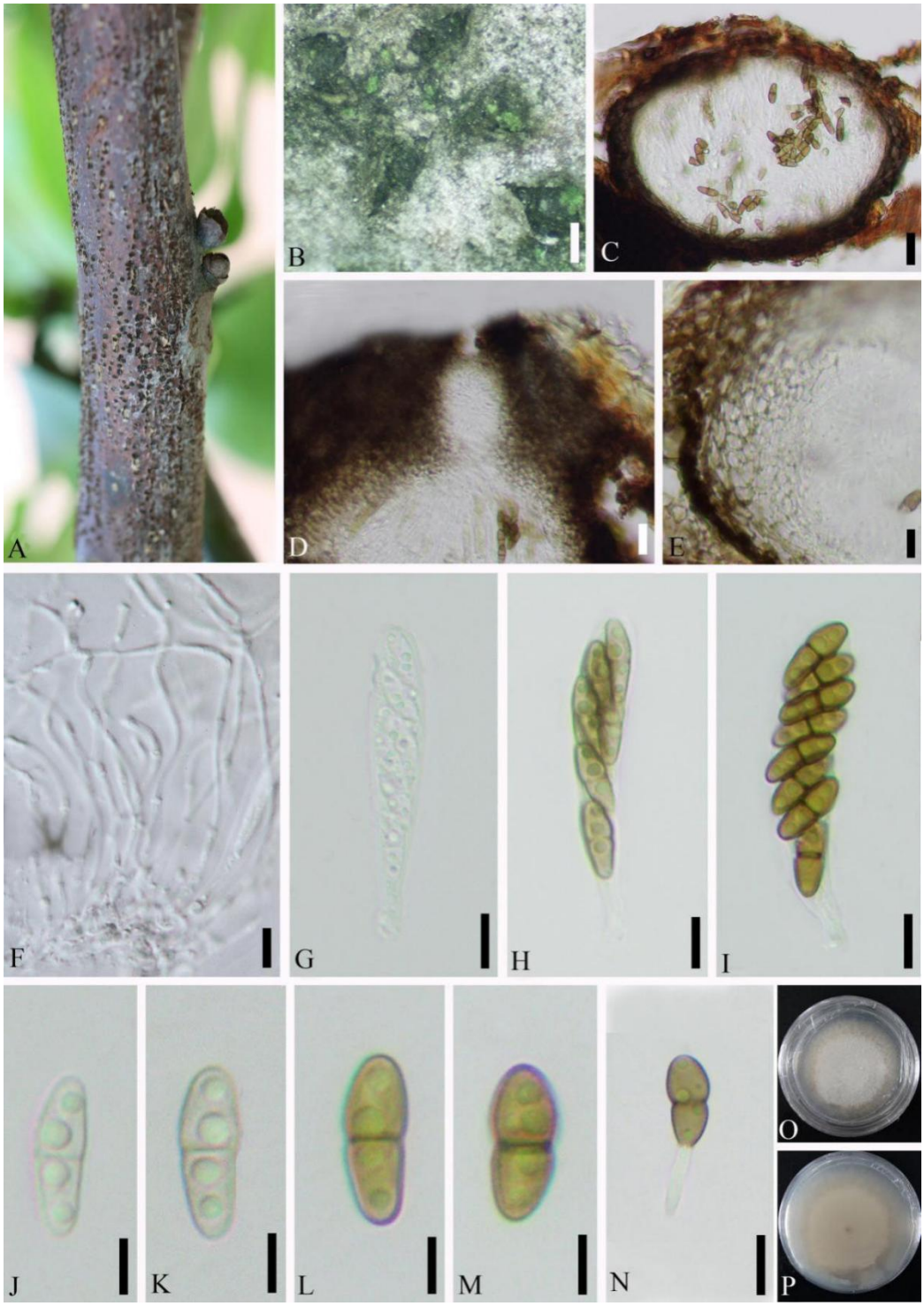


Figure 44 – *Palmiascoma qujingense* (SICAU 21-0012). A Disease-sensitive necrotic branches. B Appearance of ascostroma on host. C Vertical section through the ascoma. D ostiole. E Peridium. F Pseudoparaphyses. G–I Asci. J–M Ascospores. N Germinating ascospore. O, P Colonies on PDA (O from above, P from below). Scale bars: B = 200 µm, C–E = 20 µm, F–I, N = 10 µm, J–M = 5 µm.

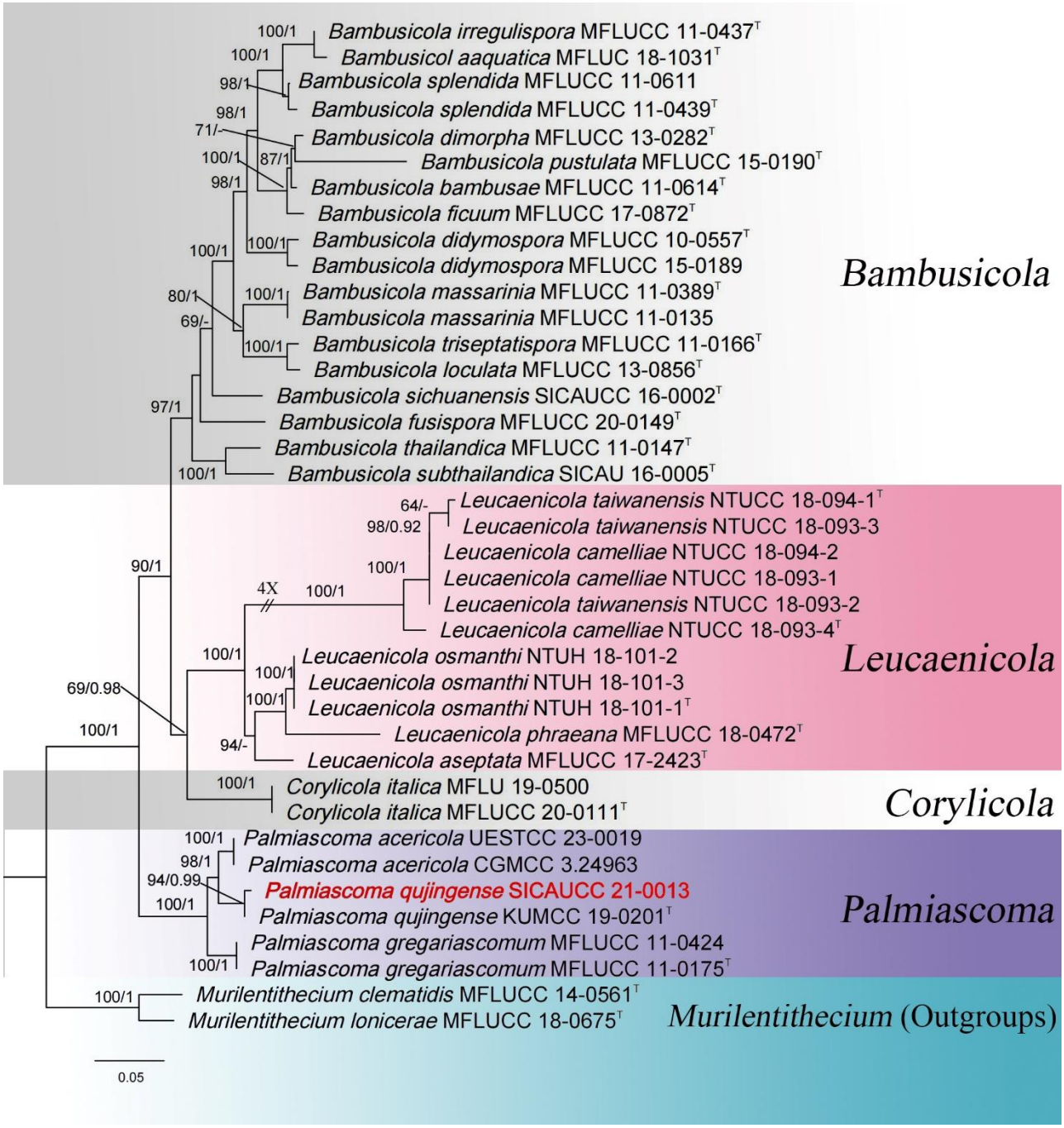


Figure 45 – Best scoring RAxML tree with a final likelihood value of -22,382.961359 based on combined ITS, LSU, *rpb*2 and SSU sequence data of related species. The tree is rooted with *Murilentithecium clematidis* (MFLUCC 14-0561) and *M. lonicerae* (MFLUCC 18-0675) in *Lentitheciaceae*. Thirty-seven strains were included in the combined gene analyses which comprised 4,673 characters (1,130 characters for ITS, 933 characters for LSU, 1,254 characters for *rpb*2 and 1,353 characters for SSU, including gap regions). The matrix had 1,576 distinct alignment patterns with 30.40% undetermined characters or gaps. Estimated base frequencies were as follows: A = 0.249109, C = 0.243031, G = 0.274745, T = 0.233114; substitution rates AC = 1.268642, AG = 2.817958, AT = 1.041382, CG = 1.112572, CT = 5.355396, GT = 1.000000; gamma distribution shape parameter α = 0.251882. The Bayesian inference analyses was implemented by MrBayes v.3.2.2 with the best-fit model (GTR+G for ITS, *rpb*2; GTR+I+G for LSU; HKY+I for SSU) of evolution estimated with MrModeltest 2.2. The species determined in this study is indicated in red and bold. Bootstrap support values for maximum likelihood (MLBS, left) ⩾ 60% and Bayesian

posterior probabilities (BYPP, right) ⩾ 0.90 are indicated at the nodes, respectively. Hyphens (-) represent support values less than 60% MLBS/0.90 BYPP. The ex-type superscript "T".

Macrodiplodiopsidaceae Voglmayr, Jaklitsch & Crous, IMA Fungus 6(1): 178 (2015).

Macrodiplodiopsidaceae was introduced by Crous et al. (2015a) to accommodate *Macrodiplodiopsis* and *Pseudochaetosphaeronema* in the suborder *Massarineae*. Tanaka et al. (2015) accepted the asexual genera *Camarographium*, *Macrodiplodiopsis* and *Pseudochaetosphaeronema* and Ariyawansa et al. (2015) introduced *Pseudomonodictys*. However, *Macrodiplodiopsis* and *Pseudochaetosphaeronema* are currently accepted in *Macrodiplodiopsidaceae* (Wijayawardene et al. 2020a). In this study, the sequences for phylogenetic analyses were downloaded from GenBank by following the latest treatment in Hyde et al. (2020) and results of BLAST searches in NCBI. Our phylogenetic analysis is similar to that of Xu et al. (2024).

Culture characteristics – Conidia germinating on PDA and germ tubes produced from conidium within 24 h. Colonies growing on PDA, circular, with fat surface, edge entire, cotton, reaching 20 mm diam., in 14 days at 25℃, gray upper and reverse view with white to light gray margin on PDA medium. Not produced pigmentation on PDA media.

Material examined – China, Sichuan Province, Liangshan Yi Autonomous Prefecture, Huili City (26°56′43.39″N 102°16′26.87″E, alt. 2004 m), dead branches of *Juglans sigillata*, 30 September 2022, F.-H. Wang, WFH202209023 (SICAU 23-0074), living culture SICAUCC 23-0053.

GenBank numbers – SICAUCC 23-0053: PP060669 (ITS), PP057961 (LSU), PP003826 (SSU), PP061146 (*tef*1-α).

Note – In the phylogenetic tree, our isolate *Pseudochaetosphaeronema kunmingense* (SICAUCC 23-0053) was sister to the ex-type strain of *P. kunmingense* (KUMCC 19-0215) with strong statistical support (100% MLBS/1.00 BYPP) (Fig. 47). Nucleotide comparisons of ITS, LSU, SSU, and *tef*1-α (SICAUCC 23-0053) also showed a high homology with the sequences of *P. kunmingense* (KUMCC 19-0215 ex-type), with a similarity of 100% (509/509, 0 gap), 100% (817/817, 0 gap), 100% (999/999, 0 gap), and 100% (853/853, 0 gap), respectively. However, *P. kunmingense* (SICAUCC 23-0053) is a sexual morph and cannot be compared with *P. kunmingense* reported to have only an asexual morph (Hyde et al. 2020b). Based on the molecular evidence, we recognize they are the same species. In this study, we identify our collection as the sexual morph of *P. kunmingense* phylogenetically and report a new host record of the species in China.

Massarinaceae Munk.

We follow the latest treatment and updated accounts of *Massarinaceae* in Chen et al. (2022b).

Helminthosporium Link.

Helminthosporium was introduced by Link (1809) with *H. velutinum* as the type species. *Helminthosporium* is a polyphyletic genus in *Massarinaceae* (*Pleosporales*). It is a species-rich genus with a worldwide distribution. *Helminthosporium* includes mostly saprobes and pathogens on a wide range of hosts and has a worldwide distribution (Voglmayr & Jaklitsch 2017a, Tian et al. 2017, Zhao et al. 2018). Hongsanan et al. (2020a) stated there were 223 *Helminthosporium* names, however many species are identified only based on morphological studies, and only 25 species have sequence data. In addition, there are 779 epithets of *Helminthosporium* (http://www.speciesfungorum.org/Index.htm, September 2024), whereas many of them are not congeneric with the generic type and were reclassified into other groups in subsequent studies Chen et al. (2022b).

27. ***Helminthosporium juglandinum*** Voglmayr & Jaklitsch, Stud. Mycol. 87: 59 (2017) Fig. 48

Index Fungorum number: IF821199; Facesoffungi number: FoF16295

Saprobic on dead branches. Sexual morph: Not observed. Asexual morph: Hyphomycetous. *Colonies* 730–1284 μm diam., effuse, dark brown to black, hairy. *Mycelium* immersed, forming stroma-like aggregations of dark brown pseudoparenchymatous cells. *Conidiophores* 420–970 × 7–

11 ($\bar{x}$ = 810 × 9 µm, n = 20), mononematous, macronematous, caespitose, erect, cylindrical, straight to slightly flexuous, wide at the base, unbranched, dark brown, with apical pore, multi-septate, with dark scars, smooth-walled. *Conidiogenous cells* mono- to polytretic, integrated, terminal and intercalary, cylindrical, cicatrized, with dark scars, with distinct pores. *Conidia* 54–120 × 12–18 ($\bar{x}$ = 90 × 16 µm, n = 40), solitary, obclavate, straight to slightly curved, wider below than apex, truncate and with dark scar at base, upper cell tapering towards long apex, cylindrical, apically rostrate and pale brown, 6–12-distoseptate, smooth-walled. *Conidial secession* schizolytic.

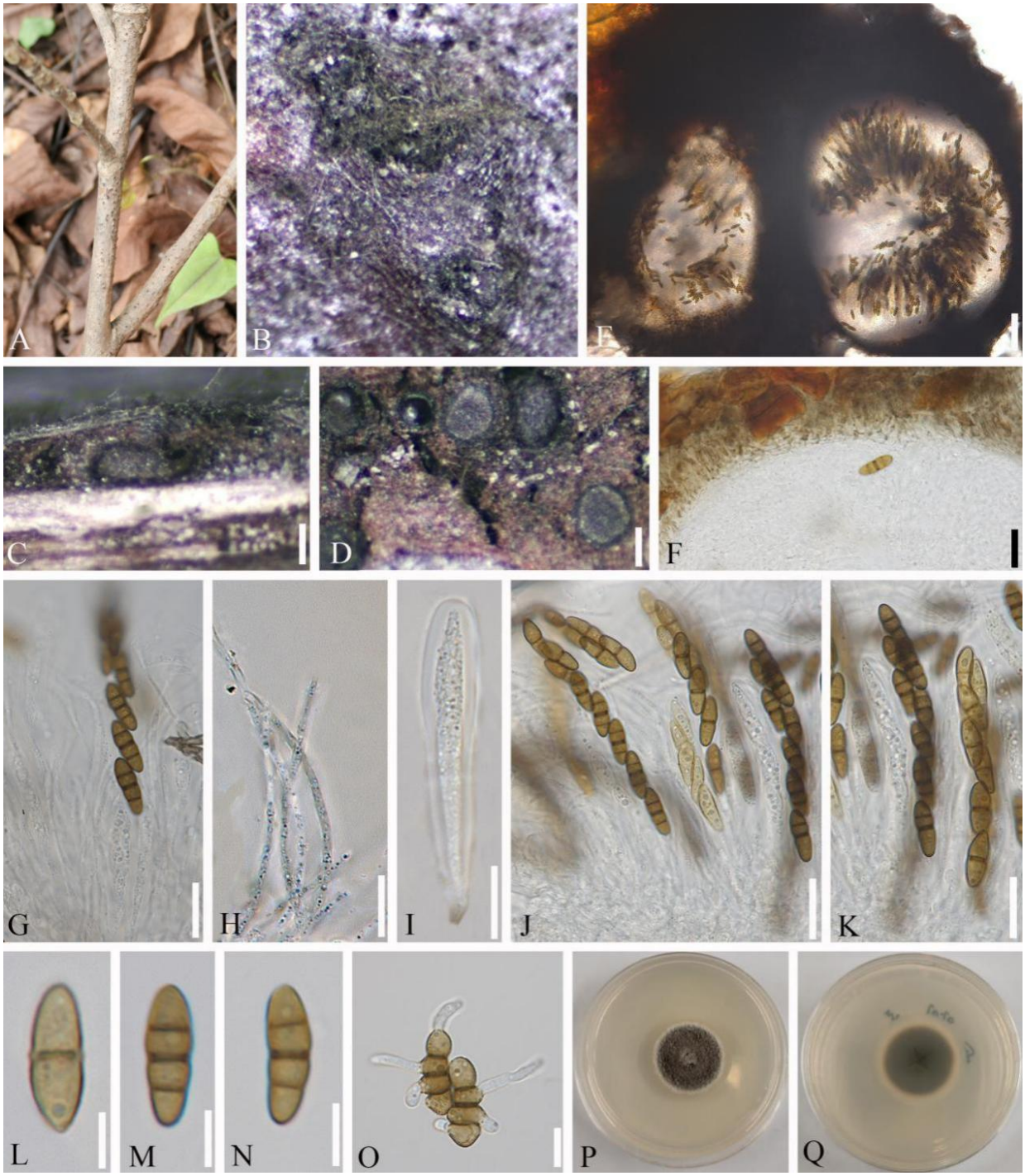


Figure 46 – *Pseudochaetosphaeronema kunmingense* (SICAU 23-0074). A, B Appearance of ascostroma in host substrate. C, D Vertical and horizontal sections of ascoma. E Section through ascoma. F Peridium. G–K Pseudoparaphyses and asci. L–N Ascospores. O germinating ascospores in sterile water. P, Q Colonies on PDA (P from above, Q from below). Scale bars: C, D = 300 µm, E = 50 µm, F–K = 20 µm, L–O = 10 µm.

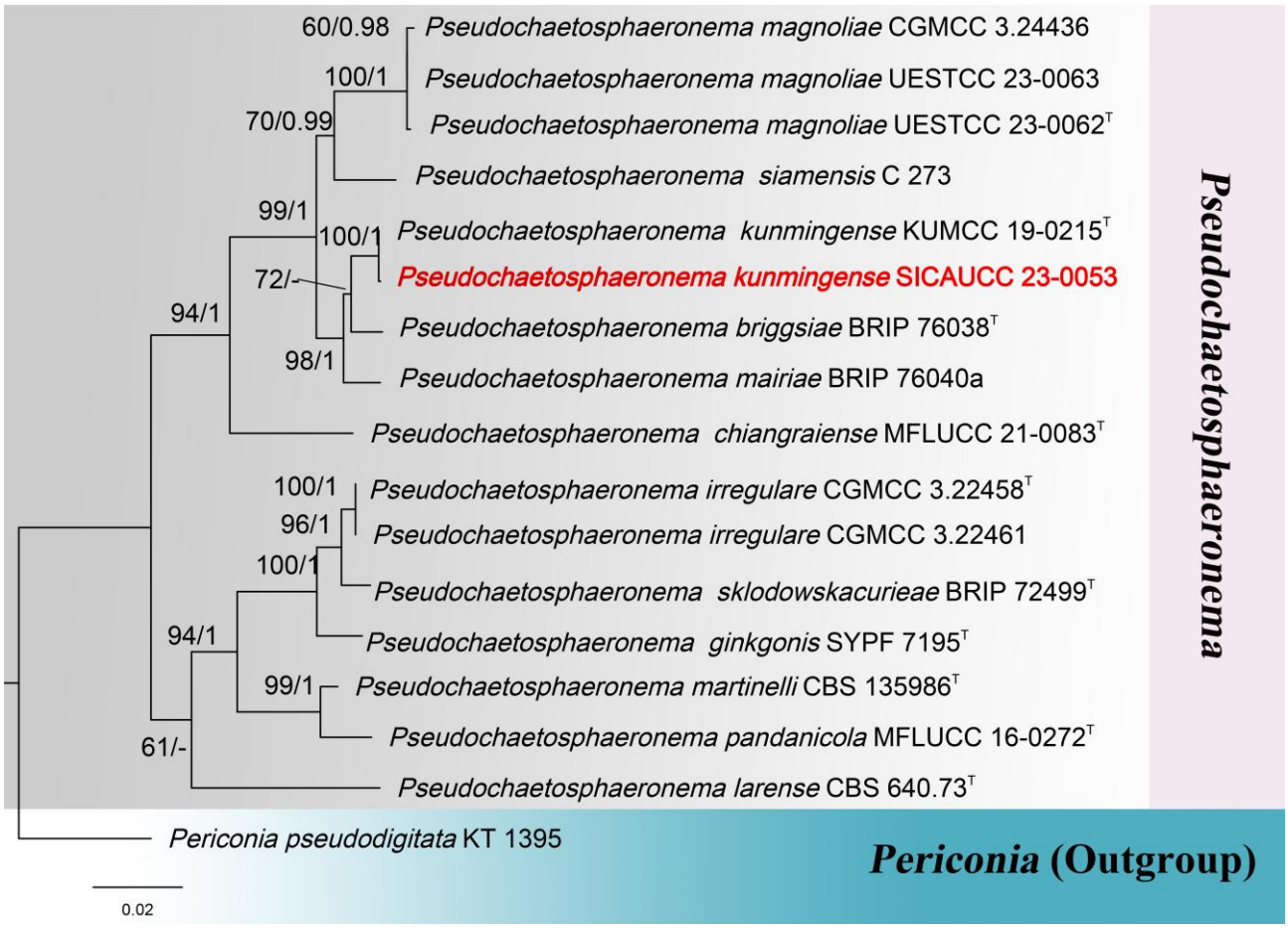


Figure 47 – Best scoring RAxML tree with a final likelihood value of -11,185.944704 based on combined LSU, ITS, SSU and *tef*1-α sequence data of related species. The tree is rooted with *Periconia pseudodigitata* (KT 1395) in *Pleosporales*. Fourteen strains were included in the combined gene analyses which comprised 5,432 characters (1,429 characters for LSU, 744 characters for ITS, 1,772 characters for SSU and 1,484 characters for *tef*1-α, including gap regions). The matrix had 559 distinct alignment patterns with 51.52% undetermined characters or gaps. Estimated base frequencies were as follows: A = 0.240377, C = 0.245422, G = 0.271235, T = 0.242966; substitution rates AC = 1.403949, AG = 4.029143, AT = 2.564941, CG = 1.079738, CT = 12.033684, GT = 1.000000; gamma distribution shape parameter α = 0.020000. The Bayesian inference analysis was implemented by MrBayes v.3.2.2 with the best-fit model (GTR+I+G for LSU, *tef*1-α; GTR+G for ITS; HKY+I for SSU) of evolution estimated with MrModeltest 2.2. The species determined in this study is indicated in red and bold. Bootstrap support values for maximum likelihood (MLBS, left) ⩾ 60% and Bayesian posterior probabilities (BYPP, right) ⩾ 0.90 are indicated at the nodes, respectively. Hyphens (-) represent support values less than 60% MLBS/0.90 BYPP. The ex-type superscript "T".

Culture characteristics – Conidia germinating on PDA within 24 h and germ tubes produced from top ends. Colonies on PDA reaching 30 mm diam., in 13 days at room temperature, within a month covering the petri dish, effuse, hairy, mycelium radiating outwards, fimbriate edge, dense, white. Mycelium superficial and partly immersed, grayish brown, the edge of the reverse side is white and the center is grayish brown. Not produced pigmentation on PDA media.

Material examined – China, Sichuan Province, Mianyang City, Yanting County (31°5′25.32″N 105°27′36.68″E, alt. 369 m), dead branches of *Juglans regia*, 18 May 2021, F.-H. Wang, WFH202205026 (SICAU 22-0140), living culture SICAUCC 22-0142.

GenBank numbers – SICAUCC 22-0142: OP963841 (ITS), OP964580 (LSU), OP962303 (SSU), OQ281352 (*rpb*2), OQ281380 (*tef*1-α).

Note – Our isolate is in a well-clustered clade together with five other strains of *Helminthosporium juglandinum*. Phylogenetic analysis of the combined ITS, LSU, SSU *rpb*2 and *tef*1-α sequence data of *Helminthosporium* taxa, our strain *H. juglandinum* (SICAUCC 22-0142) clusters with the strain *H. juglandinum* (MFLUCC 17-0241, CBS 136922, CBS 136911, CBS 136912, SICAUCC 22-0090) with strong statistical support (100% MLBS/1.00 BYPP) (Fig. 49). The sequence comparison indicates a 100% (550/550, 0 gap) similarity in the ITS with *H. juglandinum* (SICAUCC 22-0090), a 99.8% (889/891, 0 gap) similarity in the LSU with *H. juglandinum* (CBS 136911), a 99.9% (997/998, 0 gap) similarity in the SSU with *H. juglandinum* (CBS 136911), a 100% (1047/1047, 0 gap) similarity in the *rpb*2 with *H. juglandinum* (SICAUCC 22-0090), and 100% (919/919, 0 gap) similarity in the *tef*1-α with *H. juglandinum* (SICAUCC 22-0090). Based on morphological characters and phylogenetic analyses, we determine our specimens as *H. juglandinum*. *Helminthosporium juglandinum* appears to be the most common of the three species known on *Juglans* in Europe and is apparently confined to that host.



Figure 47 – *Helminthosporium juglandinum* (SICAU 22-0140). A Colonies in face view. B Stromata cells in section. C Stromata in side view. D Conidiomata in side view with column-like subcortical Stromata. E Conidiophores. F, G Conidiophore apices with apical conidia. H–J Conidia. K Germinating conidium. L, M Colonies on PDA (L from above, M from below). Scale bars: A = 1000 µm, B, C = 500 µm, E = 100 µm, G = 50 µm, H–K = 20 µm.

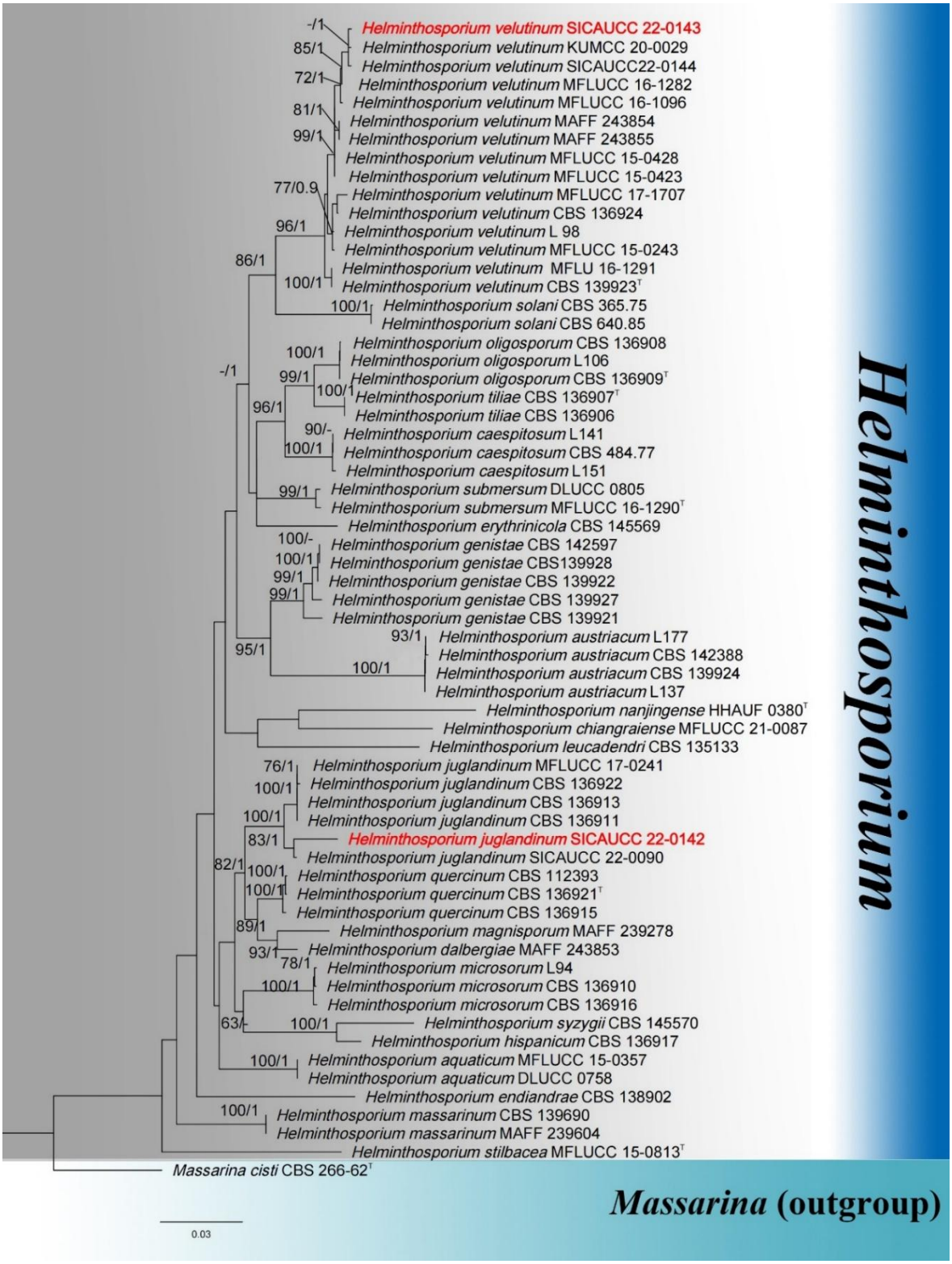


Figure 49 – Best scoring RAxML tree with a final likelihood value of -27,192.518421 based on combined ITS, LSU, *rpb*2, SSU, and *tef*1-α sequence data of related species. The tree is rooted with *Massarina cisti* (CBS 266-62) in *Massarinaceae*. Sixty-three strains were included in the combined gene analyses which comprised 8,275 characters (1,675 characters for ITS, 2,089 characters for LSU, 1,148 characters for *rpb*2, 1,792 characters for SSU and 1,568 characters for *tef*1-α, including gap regions). The matrix had 1,654 distinct alignment patterns with 45.16% undetermined characters or gaps. Estimated base frequencies were as follows: A = 0.238164, C = 0.252478, G = 0.272146, T = 0.237212; substitution rates AC = 1.614323, AG = 4.142570, AT = 1.640893, CG = 1.273504, CT = 9.596153, GT = 1.000000; gamma distribution shape parameter α = 0.111145. The Bayesian inference analysis was implemented by MrBayes v.3.2.2 with the best-fit model (GTR+I+G for ITS, LSU, *tef*1-α; HKY+I+G for *rpb*2; HKY+I for SSU) of evolution estimated with MrModeltest 2.2. The species determined in this study is indicated in red and bold. Bootstrap support values for maximum likelihood (MLBS, left) ⩾ 60% and Bayesian posterior probabilities (BYPP, right) ⩾ 0.90 are indicated at the nodes, respectively. Hyphens (-) represent support values less than 60% MLBS/0.90 BYPP. The ex-type superscript "T".

28. ***Helminthosporium velutinum*** Link [as '*Helmisporium*'], Berlin 3(1-2): 10 (1809) Fig. 50

Index Fungorum number: IF250075; Facesoffungi number: FoF01053

Saprobic on dead twigs. Sexual morph: Not observed. Asexual morph: Colony on walnut substrate effuse, black, hairy. *Mycelium* immersed, composed of unbranched, septate, thick-walled hyphae. *Colonies* discrete, punctiform, sometimes confluent, usually in large groups, black, and effuse. *Conidiophores* 310–890 × 9–16 ($\overline{x}$ = 760 × 14 μm, n = 20), tapering to 7–13 μm near the apex, arising solitary or in fascicles from the stroma cells, simple, straight or flexuous, cylindrical, thick-walled, smooth, brown to dark brown. *Conidia* 40–108 × 9–17 μm ($\overline{x}$ = 86 × 13 μm, n = 40), gradually tapering to 4–8 μm at the distal end, with a 2–4 μm wide, blackish-brown to black scar at the base, straight or flexuous, obclavate to rostrate, smooth-walled, pale golden brown to brown, 6–14-distoseptate, with angular lumina; wall up to 3 μm thick.

Culture characteristics – Conidia germinated on PDA within 12 h, germ tubes produced at both ends. Colonies grew slow on PDA, reached 50 mm in diam., after 18 days at 25℃. Colony was originally white, then olive, the center is slightly protruding, and the surface is covered with white hyphae, the center of the reverse side is black and the edge is light olive. Not produced pigmentation on PDA media.

Material examined – China, Sichuan Province, Yibin City, Junlian County (28°11′36″N 104°34′5″E, alt. 616 m), dead twigs of *Juglans regia*, 26 April 2022, F.-H. Wang, WFH202204041 (SICAU 22-0141), living culture SICAUCC 22-0143.

GenBank numbers – SICAUCC 22-0143: OP963842 (ITS), OP964581 (LSU), OP962304 (SSU), OQ281353 (*rpb*2), OQ281381 (*tef*1-α).

Note – The multi-gene phylogenetic result (Fig. 44) clearly showed that our collection nested with *Helminthosporium velutinum* (KUMCC 20-0029). In addition, each gene region between *H. velutinum* (CBS 139923) and our new collection was compared, there is no difference between LSU, SSU, ITS, *rpb*2, and *tef*1-α. We recognize our collection as *H. velutinum* based on the available evidence. The type species of the *Helminthosporium* genus, *H. velutinum* is characterized by solitary, cylindrical, unbranched, brown conidiophores that produce obclavate, distoseptate conidia (Luttrell 1957, 1963, 1964, Hughes 1980). *Helminthosporium velutinum* is by far the most commonly recorded and best-known species of the genus. Remarkably, it has been recorded world-wide from a wide range of woody and herbaceous substrates; more than 100 hosts are listed in Farr & Rossman (2024).

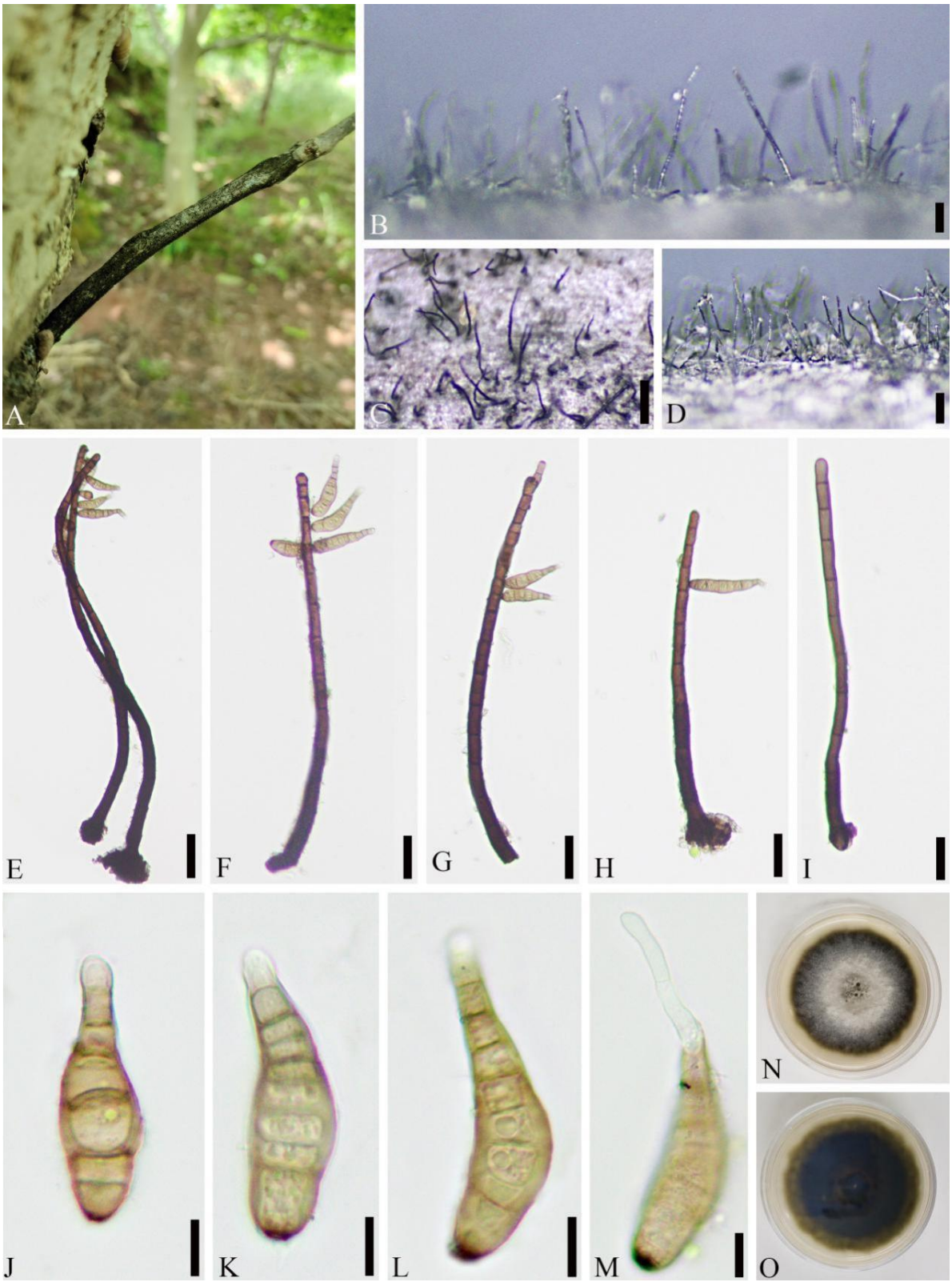


Figure 50 – *Helminthosporium velutinum* (SICAU 22-0141). A Symptoms of dead twig observed on host. B, D Conidiophores lateral in side view. C Colonies in face view. E–I Conidiophores with apical and lateral conidia and pores. J–L. Conidia. M Germinating conidium. N, O Colonies on PDA (N from above, O from below). Scale bars: C, D = 500 µm, B = 200 µm, E–I = 50 µm, J–M = 20 µm.

Periconiaceae Nann.

Nannizzi (1934) introduced *Periconiaceae* to accommodate *Periconia* as the type genus. This family has long been placed as a member of *Massarinaceae*, but Tanaka et al. (2015) revised

Massarineae and placed it as a distinct family based on phylogeny. Phukhamsakda et al. (2016) showed *Periconiaceae* diverging in the late cretaceous period. Two genera (viz. *Flavomyces* and *Periconia*) are accepted with endophytic, saprobic and pathogenic nutritional modes (Sarkar et al. 2019, Samarakoon et al. 2020, Hongsanan et al. 2020b, Wijayawardene et al. 2022, Yang et al. 2022, Su et al. 2023, Phookamsak et al. 2024, Hyde et al. 2024b). We follow the latest treatment and updated accounts of *Periconiaceae* (Hongsanan et al. 2020b, Hyde et al. 2020, Tennakoon et al. 2021b, Jayawardena et al. 2022, De Silva et al. 2022, Yang et al. 2022, Su et al. 2023, Phookamsak et al. 2024, Liao et al. 2024, Shen et al. 2024).

Periconia Tode.

Periconia was introduced by Tode (1791) and typified by *P. lichenoides*. Sexual morph: characterized by having solitary to gregarious, scattered to clustered, immersed to erumpent, dark brown to black, globose to subglobose, or conical, ostiolate, papillate ascomata; peridium composed of several layers of thin- or thick-walled, brown to dark brown pseudoparenchymatous cells of textura angularis to textura prismatica. numerous, cellular, hyaline, septate, branched, anastomosed pseudoparaphyses. 8-spored, bitunicate, fissitunicate, cylindrical, with short, rounded or furcate pedicel, apically rounded with a shallow ocular chamber ascus. overlapping 1–2-seriate, hyaline, fusiform, 1-septate, with guttules, smooth-walled, with an entire sheath ascospores. Asexual morph: macronematous, unbranched to branched, stiff, light to dark brown conidiophores with a spherical apex, monoblastic or polyblastic, discrete conidiogenous cells and verruculose or echinulate, pale to dark brown, unicellular which are catenate, usually sphaerical to subsphaerical conidia (Ellis 1971, Tanaka et al. 2015, Thambugala et al. 2017a, Phookamsak et al. 2019, Hongsanan et al. 2020a, Yang et al. 2022). Both sexual and asexual morphs are recorded in this genus (Tanaka et al. 2015, Liu et al. 2017a). There are 172 epithets listed in Species Fungorum (http://www.speciesfungorum.org/Index.htm, September 2024). *Periconia* has been reported as a plant pathogen, endophyte and a common saprobe in terrestrial and aquatic habitats with a cosmopolitan distribution (Ellis 1961, 1976, Markovskaja & Kačergius 2014, Tanaka et al. 2015, Liu et al. 2017a, Yang et al. 2022, Phookamsak et al. 2024, Liao et al. 2024, Shen et al. 2024).

29. ***Periconia byssoides*** Pers., Syn. meth. fung. (Göttingen) 2: 686 (1801) Fig. 51

Index Fungorum number: IF144538; Facesoffungi number: FoF 09319

Associated with leaf spots on the living leaves of *Juglans regia.* Symptoms include wilting, mild to severe, of either all leaves or just the lowest leaves in the canopy, premature death of the oldest leaves or a general decline of the tree. Sexual morph: Not observed. Asexual morph: *Colonies* on substrate numerous, effuse, dark brown to black, floccose. *Conidiophores* 260–310 × 13–18 µm ($\overline{x}$ = 280 × 15 µm, n = 10), macronematous, mononematous, unbranched, straight or slightly flexuous, verruculose, initially subhyaline to brownish, septate, thick-walled. *Conidiogenous cells* discrete determinate, terminal or lateral, subglobose, polyblastic. *Conidia* 7–14 × 8–13 µm ($\overline{x}$ = 13 × 11 µm, n = 30), solitary, subglobose to globose, light brown to dark brown, finely verruculose, aseptate.

Culture characteristics – Conidia germinate within 24 hours in sterile water, producing germ tubes from all around. Colonies on PDA reaching 20 mm diam., after 7 days at 25℃, dense, circular, fat, slightly raised, margin entire, fluffy to velvety with smooth aspects, cream. Reverse, light brown at the margin, dark brown to black in the center, light brown pigmentation produced in media.

Material examined – China, Sichuan Province, Bazhong City, Nanjiang County, Gongshan Town (32°18′37.27″N 106°52′22.45″E, alt. 1009 m), dead leaves of *Juglans regia*, 29 June 2021, F.-H. Wang, WFH202206011 (SICAU 22-0156), living culture SICAUCC 22-0158.

GenBank numbers – SICAUCC 22-0158: OP963856 (ITS), OP964593 (LSU), OP962312 (SSU), OQ281394 (*tef*1-α).

Note – Multi-gene phylogeny also indicates that our collection clusters with other *Periconia byssoides* (SICAUCC 22-0158) with strong statistical support (97% MLBS/1.00 BYPP) (Fig. 52). Nucleotide comparisons of ITS, LSU, SSU, and *tef*1-α (SICAUCC 22-0158) also showed a high homology with the sequences of *P. byssoides* (MAFF 243873), with a similarity of 100% (522/522,

0 gap), 99.3% (859/865, 0 gap), 99.8% (990/992, 2 gaps), and 100% (930/930, 0 gap), respectively. The morphological characteristics of our collection resembles *P. byssoides* in having macronematous, mononematous, unbranched, erect, light brown to dark brown conidiophores and globose to subglobose, light brown to dark brown, verruculose, aseptate conidia (Persoon 1801, Jayasiri et al. 2019). Based on morphological characters and phylogenetic analyses, we determine our specimens as *P. byssoides*. Previous studies have been described and illustrated in detail, and it is found that the host plants of this species are diverse and widely distributed (Wang et al. 2008, Markovskaja & Kačergius 2014, Jayasiri et al. 2019, Tennakoon et al. 2021b, Jayawardena et al. 2022, De Silva et al. 2022).

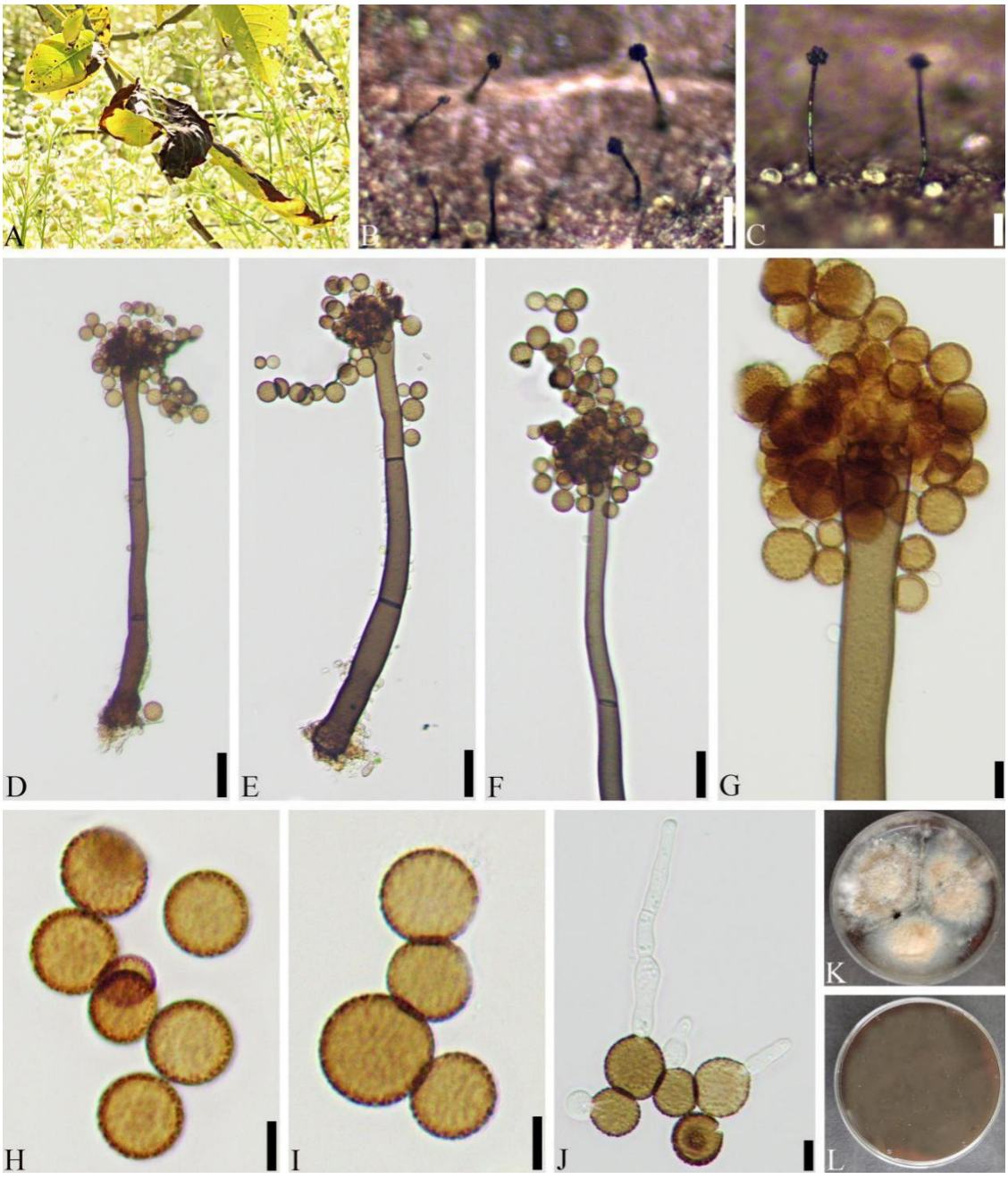


Figure 51 – *Periconia byssoides* (SICAU 22-0156). A Symptoms of necrotic lesions observed on host. B, C Conidiogenesis. D–F Conidiophores. G Close view of the conidial head showing conidia and phialides. H, I Conidia. J Germinating conidia. K, L Colonies on PDA (K from above, L from below). Scale bars: B = 200 μm, C = 100 μm, D–F = 40 μm, G–J = 10 μm.

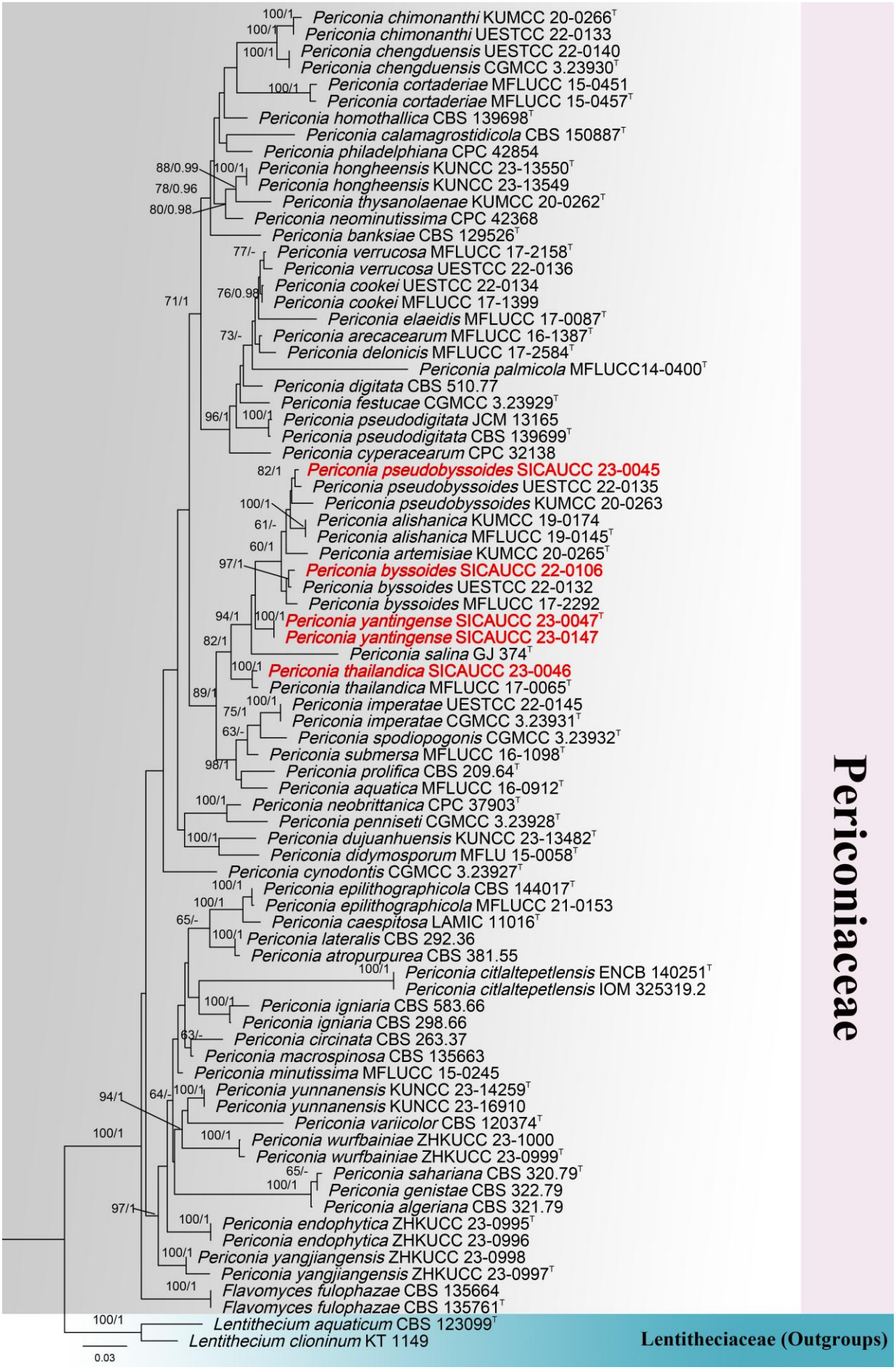

Periconia chimonanthi KUMCC 20-0266T
Periconia chimonanthi UESTCC 22-0133
Periconia chengduensis UESTCC 22-0140
Periconia chengduensis CGMCC 3.23930T
Periconia cortaderiae MFLUCC 15-0451
Periconia cortaderiae MFLUCC 15-0457T
Periconia homothallica CBS 139698T
Periconia calamagrostidicola CBS 150887T
Periconia philadelphiana CPC 42854
Periconia hongheensis KUNCC 23-13550T
Periconia hongheensis KUNCC 23-13549
Periconia thysanolaenae KUMCC 20-0262T
Periconia neominutissima CPC 42368
Periconia banksiae CBS 129526T
Periconia verrucosa MFLUCC 17-2158T
Periconia verrucosa UESTCC 22-0136
Periconia cookei UESTCC 22-0134
Periconia cookei MFLUCC 17-1399
Periconia elaeidis MFLUCC 17-0087T
Periconia arecacearum MFLUCC 16-1387T
Periconia delonicis MFLUCC 17-2584T
Periconia palmicola MFLUCC14-0400T
Periconia digitata CBS 510.77
Periconia festucae CGMCC 3.23929T
Periconia pseudodigitata JCM 13165
Periconia pseudodigitata CBS 139699T
Periconia cyperacearum CPC 32138
Periconia pseudobyssoides SICAUCC 23-0045
Periconia pseudobyssoides UESTCC 22-0135
Periconia pseudobyssoides KUMCC 20-0263
Periconia alishanica KUMCC 19-0174
Periconia alishanica MFLUCC 19-0145T
Periconia artemisiae KUMCC 20-0265T
Periconia byssoides SICAUCC 22-0106
Periconia byssoides UESTCC 22-0132
Periconia byssoides MFLUCC 17-2292
Periconia yantingense SICAUCC 23-0047T
Periconia yantingense SICAUCC 23-0147
Periconia salina GJ 374T
Periconia thailandica SICAUCC 23-0046
Periconia thailandica MFLUCC 17-0065T
Periconia imperatae UESTCC 22-0145
Periconia imperatae CGMCC 3.23931T
Periconia spodiopogonis CGMCC 3.23932T
Periconia submersa MFLUCC 16-1098T
Periconia prolifica CBS 209.64T
Periconia aquatica MFLUCC 16-0912T
Periconia neobrittanica CPC 37903T
Periconia penniseti CGMCC 3.23928T
Periconia dujuanhuensis KUNCC 23-13482T
Periconia didymosporum MFLU 15-0058T
Periconia cynodontis CGMCC 3.23927T
Periconia epilithographicola CBS 144017T
Periconia epilithographicola MFLUCC 21-0153
Periconia caespitosa LAMIC 11016T
Periconia lateralis CBS 292.36
Periconia atropurpurea CBS 381.55
Periconia citlaltepetlensis ENCB 140251T
Periconia citlaltepetlensis IOM 325319.2
Periconia igniaria CBS 583.66
Periconia igniaria CBS 298.66
Periconia circinata CBS 263.37
Periconia macrospinosa CBS 135663
Periconia minutissima MFLUCC 15-0245
Periconia yunnanensis KUNCC 23-14259T
Periconia yunnanensis KUNCC 23-16910
Periconia variicolor CBS 120374T
Periconia wurfbainiae ZHKUCC 23-1000
Periconia wurfbainiae ZHKUCC 23-0999T
Periconia sahariana CBS 320.79T
Periconia genistae CBS 322.79
Periconia algeriana CBS 321.79
Periconia endophytica ZHKUCC 23-0995T
Periconia endophytica ZHKUCC 23-0996
Periconia yangjiangensis ZHKUCC 23-0998
Periconia yangjiangensis ZHKUCC 23-0997T
Flavomyces fulophazae CBS 135664
Flavomyces fulophazae CBS 135761T
Lentithecium aquaticum CBS 123099T
Lentithecium clioninum KT 1149
0.03
Periconiaceae
Lentitheciaceae (Outgroups)

Figure 52 – Best scoring RAxML tree with a final likelihood value of -23,159.235368 based on combined ITS, LSU, SSU and *tef*1-α sequence data of related species. The tree is rooted with *Morosphaeria ramunculicola* (NBRC 107813) and *M. velatispora* (NBRC 107813) in *Morosphaeriaceae*. Eighty strains were included in the combined gene analyses which comprised 4,870 characters (1,420 characters for LSU, 788 characters for ITS, 1,540 characters for SSU and 1,118 characters for *tef*1-α, including gap regions). The matrix had 1,507 distinct alignment patterns with 45.59% undetermined characters or gaps. Estimated base frequencies were as follows: A = 0.239001, C = 0.256014, G = 0.268897, T = 0.236088; substitution rates AC = 1.435259, AG = 2.446969, AT = 1.438725, CG = 1.113033, CT = 7.001848, GT = 1.000000; gamma distribution shape parameter α = 0.190868. The Bayesian inference analyses was implemented by MrBayes v.3.2.2 with the best-fit model (GTR+I+G for ITS, *tub*2; GTR+G for *tef*1-α) of evolution estimated with MrModeltest 2.2. The species determined in this study is indicated in red and bold. Bootstrap support values for maximum likelihood (MLBS, left) ⩾ 60% and Bayesian posterior probabilities (BYPP, right) ⩾ 0.90 are indicated at the nodes, respectively. Hyphens (-) represent support values less than 60% MLBS/0.90 BYPP. The ex-type superscript "T".

30. ***Periconia pseudobyssoides*** Markovsk. & A. Kačergius, Mycol. Prog. 13(2): 293 (2013)

Fig. 53

Index Fungorum number: IF804763; Facesoffungi number: FoF03857

Saprobic on dead petiole of *Juglans regia*. Sexual morph: Not observed. Asexual morph: Hyphomycetous. *Colonies* on substrate numerous, effuse, dark brown to black, floccose. *Conidiophores* 260–390 × 17–22 μm ($\bar{x}$ = 340 × 19 μm, n = 10), macronematous, mononematous, unbranched, erect, straight or slightly flexuous, single, light brown to dark brown, 0–2-septate, thick-walled. *Conidiogenous cells* polyblastic, discrete. *Conidia* 8–16 × 7–14 μm ($\bar{x}$ = 14 × 12 μm, n = 40), solitary, globose, light brown to dark brown, finely verruculose, aseptate.

Culture characteristics – Conidia germinate within 24 hours in sterile water, producing germ tubes from all around. Colonies on PDA, 50 mm diam., after 28 days. Colonies from above: medium dense, circular, fat, slightly raised, surface smooth, crenate edge, cotton-like, light grey to white at the margin, white in the center. Reverse, light brown at the margin, dark brown to black in the center, light brown pigmentation produced in media.

Material examined – China, Sichuan Province, Liangshan Yi Autonomous Prefecture, Huili City (26°56′43.37″N 102°16′26.41″E, alt. 2006 m), dead petiole of *Juglans regia*, 30 September 2022, F.-H. Wang, WFH202209009 (SICAU 23-0066), living culture SICAUCC 23-0045.

GenBank numbers – SICAUCC 23-0045: PP060661 (ITS), PP057954 (LSU), PP003822 (SSU), PP061140 (*tef*1-α).

Note – The morphological characteristics of the strain discovered in this study are highly consistent with those of *Periconia pseudobyssoides*. Phylogeny also indicates that our collection clusters with other *P. pseudobyssoides* isolates in a same clade, in particular, close to *P. pseudobyssoides* (MAFF 243868) with strong statistical support (82% MLBS/1.00 BYPP) (Fig. 52). Nucleotide comparisons of ITS, LSU, SSU, and *tef*1-α (SICAUCC 23-0045) also showed a high homology with the sequences of *P. pseudobyssoides* (MAFF 243868), with a similarity of 99.8% (442/443, 1 gap), 100% (817/817, 0 gap), 99.8% (1026/1027, 1 gaps), and 99.8% (910/912, 0 gap), respectively. Based on morphological characters and phylogenetic analyses, we determine our specimens as *P. pseudobyssoides*. Therefore, we introduce our collection as a new host record of *P. pseudobyssoides* from dead twigs of *J. regia* in China.

31. ***Periconia thailandica*** N.G. Liu, K.D. Hyde & Hongsanan, Phytotaxa 323(3): 257 (2017)

Fig. 54

Index Fungorum number: IF552956; Facesoffungi number: FoF03115

Saprobic on dead twigs of *Juglans regia*. Sexual morph: Not observed. Asexual morph: *Colonies* on substrate numerous, effuse, dark brown to black, floccose. *Conidiophores* 190–310 × 14–21 μm ($\bar{x}$ = 280 × 17 μm, n = 10), macronematous, mononematous, single, cylindrical, brown to

dark brown, erect, or curved, 1–3-septate, thick-walled, and smooth. *Conidiogenous cells* monoblastic, proliferating, hyaline, terminal, blunt end, ovoid to globose, thick-walled, sometimes swollen region partly, and discrete on stipe. *Conidia* 11–18 × 9–14 µm ($\bar{x}$ = 14 × 11 µm, n = 40) solitary, globose, aseptate, initially hyaline to pale-brown, brown to dark brown upon maturity, thin-walled, and verruculose.

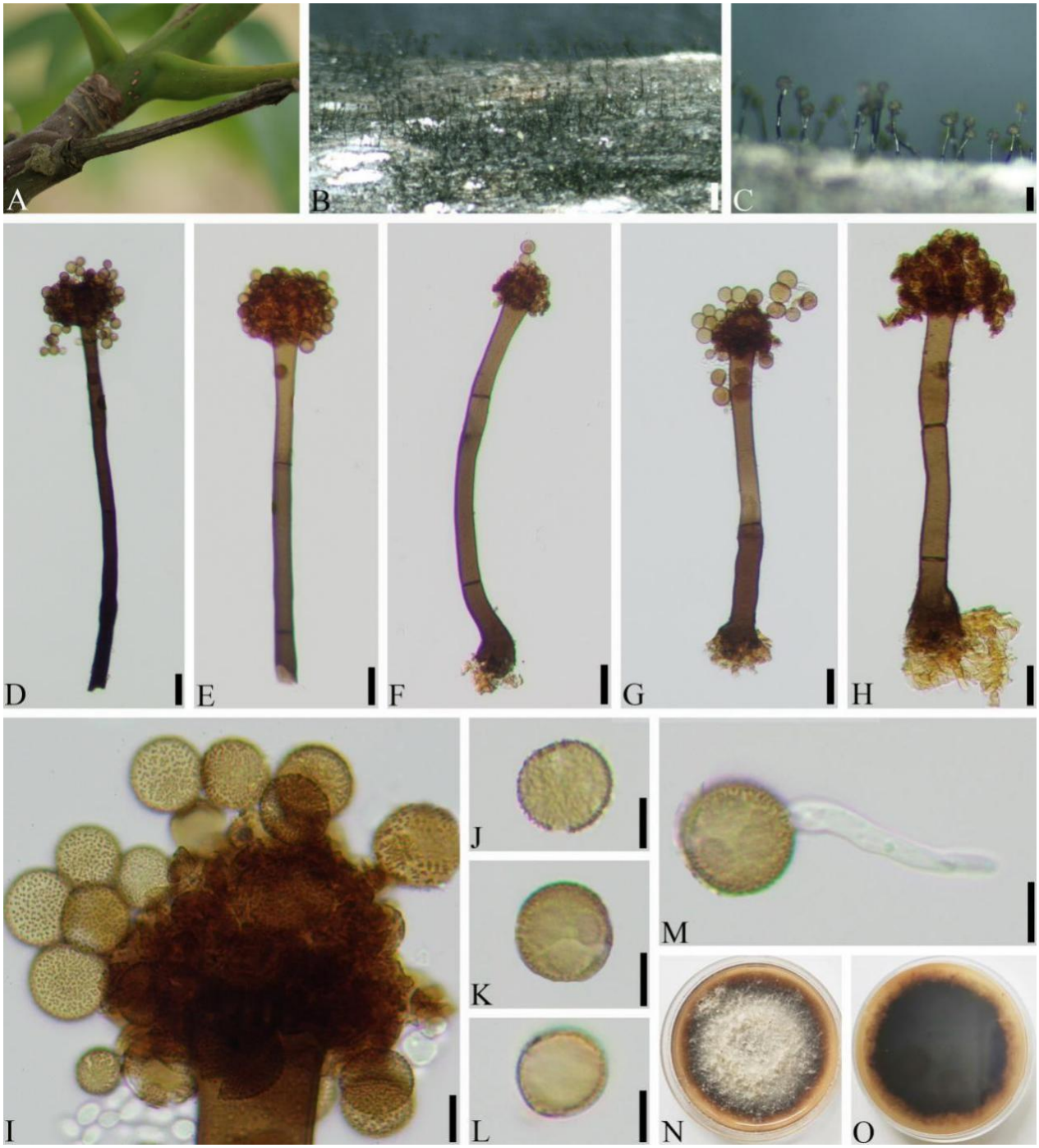


Figure 53 – *Periconia pseudobyssoides* (SICAU 23-0066). A, B Appearance of colonies in host substrate. C Conidiophores lateral in side view. D–H Conidiophores. I Close view of the Conidial head showing Conidia and phialides. J–L Conidia. M Germinating conidium. N, O Colonies on PDA (N from above, O from below). Scale bars: B = 500 µm, C = 200 µm, D–H = 30 µm, I–M = 10 µm.

Culture characteristics – Conidia germinate within 24 hours in sterile water, producing germ tubes from all around. Colonies on PDA reach 30 mm in diam., after 20 days, medium dense, initially

circular and white, later undulate, with orderly margin, gray white, floccose, generating sandy beige pigment inside the medium, and initially reverse gray white but later black. Not produced pigmentation on PDA media.

Material examined – China, Sichuan Province, Chendu City, Chongzhou City (30°40′6″N 103°40′20″E, alt. 512 m), dead twigs of *Juglans regia*, 28 July 2022, F.-H. Wang, WFH202107022 (SICAU 23-0067), living culture SICAUCC 23-0046.

GenBank numbers – SICAUCC 23-0046: PP060662 (ITS), PP057955 (LSU), PP003823 (SSU), PP061141 (*tef*1-α).

Note – Based on BLASTn search results of ITS, LSU, SSU and *tef*1-α sequence data, *Periconia thailandica* (SICAUCC 23-0046), showed high similarity to *P. thailandica* (MFLUCC 17-0065) as follows; ITS = 99.6%, LSU = 99.8%, SSU = 99.9%, *tef*1-α = 99.7%. Our new collection is similar to the holotype of *P. thailandica*, except the length and the shape of the conidiophores (190–310 × 14–21 µm vs. 400–1100 × 10–20 µm), 4–7-septate, smooth to minutely verruculose (Liu et al. 2017b). There is no significant difference in the nucleotide base pair comparison of our strain with the ex-type strain. In our multigene phylogeny, *P. thailandica* (SICAUCC 23-0046) grouped with *P. thailandica* (MFLUCC 17-0065) with strong statistical support (MLBS = 100%, BYPP = 1.00) (Fig. 52). In this study, we identify our new collection as *P. thailandica*, from *Juglans regia*, from China for the first time as a new geographical record.

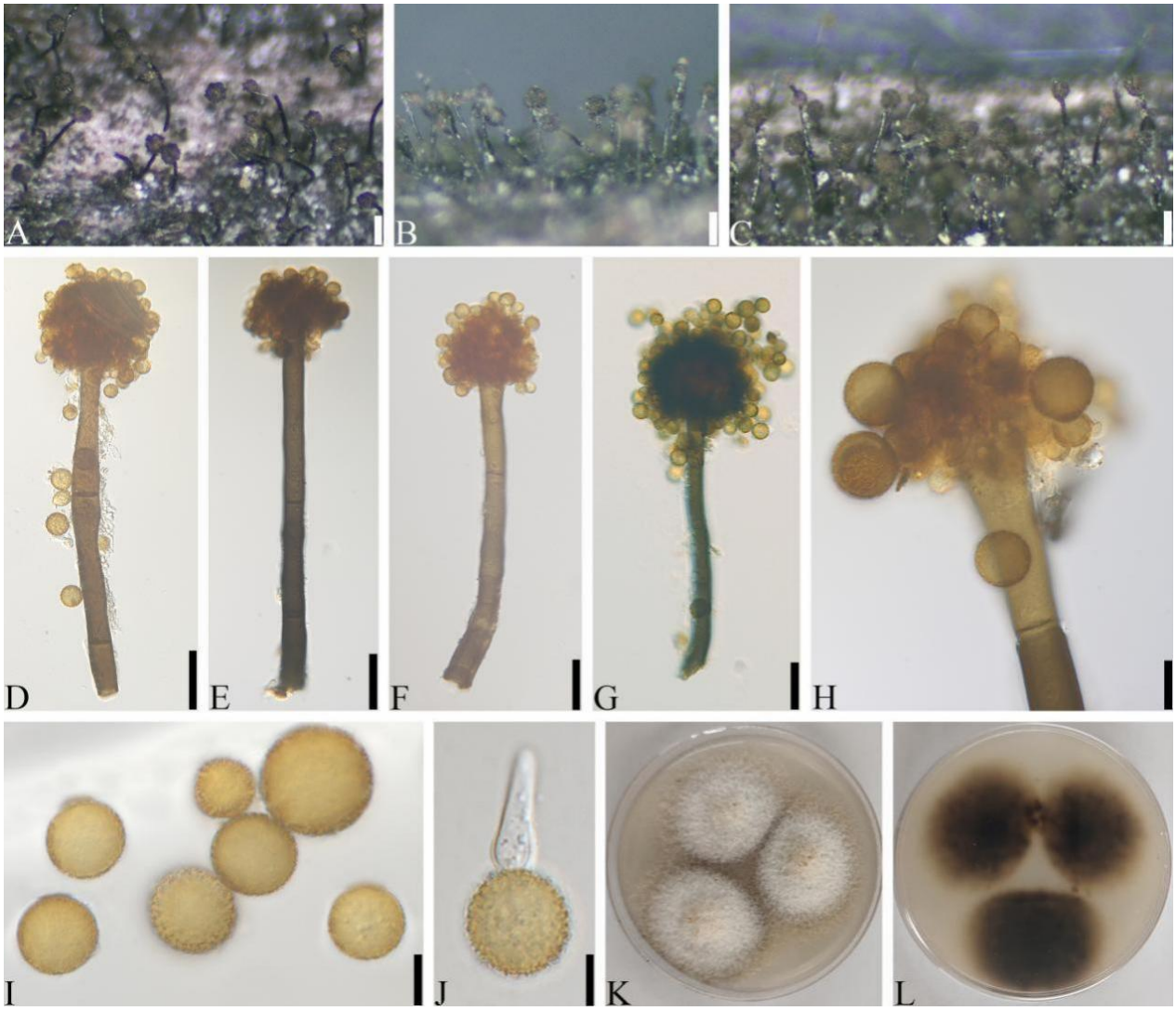


Figure 54 – *Periconia thailandica* (SICAU 23-0067). A–C Appearance of colonies in host substrate. D–G Conidiophores. H Close view of the conidial head showing conidia and phialides. I Conidia. J

Germinating conidium. K, L Colonies on PDA (K from above, L from below). Scale bars: A–C = 200 μm, D–G = 50 μm, H = 20 μm, I, J = 10 μm.

32. ***Periconia yantingense*** F.H. Wang & C.L. Yang, sp. nov. Fig. 55

Index Fungorum number: IF901567; Facesoffungi number: FoF15584

Etymology – Named after locality where the fungus was isolated for the first time.

Holotype – SICAU 23-0068.

Saprobic on dead twigs of *Juglans regia*. Sexual morph: Not observed. Asexual morph: Hyphomycetous. *Colonies* on substrate numerous, effuse, dark brown to black, floccose. *Conidiophores* 210–300 × 7–15 μm ($\bar{x}$ = 284 × 12 μm, n = 10), macronematous, mononematous, unbranched, erect or slightly flexuous, single, greyish brown to dark brown, 1–3-septate, smooth to minutely verruculose, thick-walled. *Conidiogenous cells* monoblastic, proliferating, hyaline, terminal, blunt end, ovoid to globose, thick-walled. *Conidia* 7–17 × 8–16 μm ($\bar{x}$ = 12 × 13 μm, n = 40), solitary, subglobose to globose, light brown to dark brown, verruculose, aseptate.

Culture characteristics – Conidia germinate within 24 hours in sterile water, producing germ tubes from all around. Colonies on PDA, 60 mm diam., after 28 days, colonies from above: dense, irregular, fat, obvious bulge, surface hyphae flocculent, crenate edge, initially circular and white, later undulate, with irregular margin, flocculent, late dark brown. Reverse, gray white at the margin, dark brown to black in the center. Not produced pigmentation on PDA media.

Material examined – China, Sichuan Province, Mianyang City, Yanting County (31°5′25.11″N 105°27′36.53″E, alt. 363 m), dead twigs of *Juglans regia*, 18 May 2021, F.-H. Wang, WFH202105025 (SICAU 23-0068, holotype), ex-type living culture SICAUCC 23-0047. *Ibid.*, WFH202105025B (SICAUCC 24-0033), living culture SICAUCC 23-0147.

GenBank numbers – SICAUCC 23-0047: PP060663 (ITS), PP057956 (LSU), PP003824 (SSU), PP061142 (*tef*1-α); SICAUCC 23-0147: PP844875 (ITS), PP826165 (LSU), PP853378 (SSU), PP850053 (*tef*1-α).

Note – Our new collection fits well with the generic concept of *Periconia* in having macronematous, mononematous, brown conidiophores, polyblastic, ovoid to globose conidiogenous cells, verruculose or subglobose to globose conidia. In our phylogenetic analyses, our new collection of *P. yantingense* (SICAUCC 23-0047) was placed within *Periconia,* closely related to *P. salina* (MFLUCC 19-1235) (Fig. 52). Nucleotide comparisons revealed notable genetic dissimilarities between *P. yantingense* (SICAUCC 23-0047) and *P. salina* (MFLUCC 19-1235), with sequence divergences of 1.7% (9/534, 7 gaps), 5.4% (46/854, 10 gaps), and 3.4% (29/851, 1 gap) in the ITS, LSU, and SSU, respectively. *Periconia yantingense* (SICAUCC 23-0047) resembles *P. salina* (MFLUCC 19-1235) in the shape of the conidiophores, and conidia (subglobose to globose conidia, and erect or slightly flexuous conidiophores) (Dayarathne et al. 2020). However, *P. yantingense* (SICAUCC 23-0047) differs from *P. salina* (MFLUCC 19-1235) by its darker and longer conidiophores (210–300 × 7–15 μm vs. 384–500 × 20–25 μm). Hence, based on both morphology and phylogeny, we introduce our collection as a new species of *P. yantingense*.

Phaeosphaeriaceae M.E. Barr.

Phaeosphaeriaceae has been subjected to various taxonomic changes since its establishment by Barr (1987). The inception of multi-gene phylogenetic analyses coupled with morphology has greatly resolved many taxonomic inconsistencies along with the introduction of several novel taxa (Phookamsak et al. 2014, 2017, Li et al. 2015, 2016b, Crous et al. 2018, Phookamsak et al. 2019, Hyde et al. 2020b, c). Members of *Phaeosphaeriaceae* are cosmopolitan and exhibit diverse life modes, mainly as saprobes, endophytes and pathogens of economically important plants as well humans (Phookamsak et al. 2014, 2017, Hongsanan et al. 2020a). However, confusion in the placement of many taxa in the family still remains uncertain and problematic (Hongsanan et al. 2020a). Apart from their cosmopolitan distribution, the family is morphologically and phylogenetically highly diverse. Thus, currently 87 genera are accommodated in this family (Hongsanan et al. 2020a, Hyde et al. 2024b).

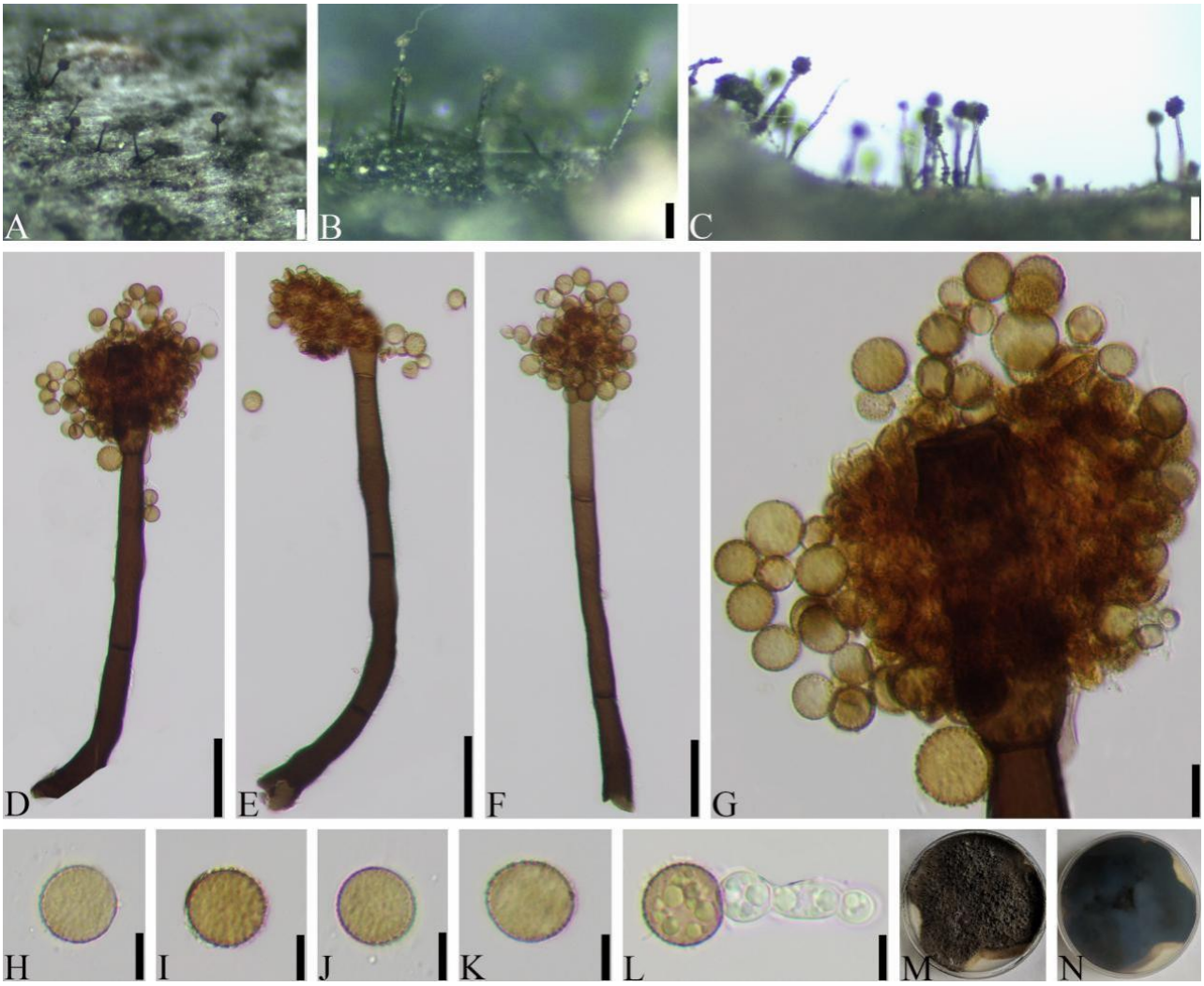


Figure 55 – *Periconia yantingense* (SICAU 23-0068, holotype). A, B Appearance of colonies on host substrate. C Conidiophores lateral in side view. D–F Conidiophores. G Close view of the conidial head showing conidia and phialides. H–K Conidia. L Germinating conidium. M, N Colonies on PDA (M from above, N from below). Scale bars: A = 200 μm, B, C = 100 μm, D–F = 50 μm, G–L = 10 μm.

Paraphoma Morgan-Jones & J.F. White, Mycotaxon 18(1): 58 (1983).

Paraphoma as typified by *P. radicina* was previously treated in *Pyrenochaeta* by McAlpine (1902) and later, Boerema & Dorenbosch (1979) transferred the species to *Phoma*. Morgan-Jones & White (1983) introduced the new genus *Paraphoma* in order to accommodate phoma-like species with setose conidiomata. However, the genus was later treated at section level within *Phoma* by Boerema (1997). De Gruyter et al. (2010) reinstated the genus, and placed it into the family *Phaeosphaeriaceae* based on a phylogenetic analysis. At present, there are 15 species of this genus (http://www.speciesfungorum.org/Index.htm, September 2024), and there is no report on the sexual morphology of this genus.

33. ***Paraphoma dioscoreae*** Quaedvl., H.D. Shin, Verkley & Crous, Stud. Mycol. 75: 370 (2013) Fig. 56

Index Fungorum number: IF804445; Facesoffungi number: FoF16296

Saprobic on dead petiole of *Juglans regia*. Sexual morph: *Ascomata* 180–318 × 145–238 μm ($\bar{x}$ = 265 × 210 μm, n = 10), scattered or sometimes clustered, immersed, visible as raised, black dots on the host surface, uni to bi-loculate, subglobose, brown to dark brown, ostiolate. *Ostiole* central,

papillate. *Peridium* composed of multiple layers of thick-walled, composed of black, brittle carbonaceous textura prismatica. *Pseudoparaphyses* of 2–4 μm wide, cellular, hyaline, septate, unbranched, anastomosing mostly above the asci and embedded in a mucilaginous matrix. *Asci* 72–124 × 7–11 μm ($\bar{x}$ = 92 × 9 μm, n = 10), 8-spored, bitunicate, fissitunicate, broadly cylindrical or cylindric-clavate, sessile to subsessile, apically rounded with an ocular chamber. *Ascospores* 18–34 × 3–6μm ($\bar{x}$ = 28 × 5 μm, n = 40), overlapping uni to bi-seriate, fusiform, second cell from the top inflate, yellowish-brown to brown, 3–4-septate, slightly constricted at the central septum, straight to curved, rough-walled, lacking a mucilaginous sheath. Asexual morph: Not observed.

Culture characteristics – Ascospores germinating on sterile water within 24 h and germ tubes produced from ends. Colonies on PDA, reaching 50 mm diam., after 28 days at 25℃. Culture brown radiating sandy beige toward the edge, with dense mycelia, circular, flat, dull, fimbriate, and slightly covered with white aerial mycelium, cotton-like. Reverse, black with radiating brown mycelium. Not produced pigmentation on PDA media.

Material examined – China, Sichuan Province, Suining City, Shehong City, Guangxing Town (30°57′22.18″N 105°18′54.24″E, alt. 406 m), dead petiole of *Juglans regia*, 27 April 2022, F.-H. Wang, WFH202204096 (SICAU 23-0069), living culture SICAUCC 23-0048.

GenBank numbers – SICAUCC 23-0048: PP060664 (ITS), PP061143 (*tef*1-α).

Note – In our study, a strain from a sexually reproductive fungus formed a monophyletic clade with the type strain of *Paraphoma dioscoreae* (CBS 135100) and the other two strains *P. dioscoreae* (CPCS 11355, CPCS 11361) with strong statistical support (100% MLBS/1.00 BYPP) (Fig. 57). Nucleotide comparisons of ITS and *tef*1-α (SICAUCC 23-0048) also showed a high homology with the sequences of *P. dioscoreae* (CBS 135100 ex-type), with a similarity of 99.4% (511/514, 0 gap) and 99.3% (528/532, 0 gap), respectively. Unfortunately, no sexual morph from the type strain is available. Instead of introducing a new species, we propose considering the sequence similarities to link these asexual and sexual forms as a single species. Therefore, we revised the species description to update the characteristics of its sexual form. This finding represents a new host record of this fungus from *Juglans regia*. At the same time, it also provides sexual morphological characteristics for the genus.

Pleosporaceae Nitschke, Verh. Naturhist. Vereines Preuss.Rheinl.: 74 (1869)

This family consists of endophytes, pathogens and saprobes and has a worldwide distribution (Hongsanan et al. 2020a). Twenty-three taxa are accepted in this family (Wijayawardene et al. 2022). We follow the latest treatments and updated accounts of *Pleosporacea*e in Jayawardena et al. (2022).

Alternaria Nees, System der Pilze und Schwamme: 72 (1817)

Alternaria was introduced by Nees (1816), based on *A. tenuis*, which has dark-coloured phaeodictyospores in chains, and a beak of tapering apical cells (Woudenberg et al. 2013). Species of *Alternaria* are saprobic, endophytic or pathogenic, which are associated with a wide variety of substrates including seeds, plants, agriculture products, animals, soil and the atmosphere (Woudenberg et al. 2015, Ariyawansa et al. 2015, Thambugala et al. 2017a, Chethana et al. 2019, Nishikawa & Nakashima 2020, Li et al. 2022, Li et al. 2023d, Schmey et al. 2023, He et al. 2024, Nwe et al. 2024, Alasadi et al. 2024, Bessadat et al. 2025). Currently this is one of the species rich genera in *Pleosporales* having about 450 accepted species epithets listed in Species Fungorum (http://www.speciesfungorum.org/Index.htm, September 2024).

34. ***Alternaria alternata*** (Fr.) Keissl., Abt. 2 29: 434 (1912) Fig. 58

Index Fungorum number: IF119834; Facesoffungi number: FoF03825.

Associated with leaf spots on the living leaves of *Juglans regia*. Infection and lesion formation initially occur on older leaves before progressing to newer ones. Small, brown fecks develop with a reddish border, expanding to circular spots with an ashy-grey centre. Concentric rings may be observed as individual lesions expand. Sexual morph: Not observed. Asexual morph: *Mycelium* subhyaline to pale olivaceous, branched, smooth. *Conidiophores* 18–82 × 3–6 μm ($\bar{x}$ = 52 × 5 μm, n

= 20), single, simple, straight or flexuous, pale, olivaceous or brown, smooth, septate, sometimes slightly swollen at the apex, with one or several apical conidiogenous cells. *Conidiogenous cells* 9–12 × 9–13 μm ($\bar{x}$ = 10× 11 μm, n = 30), mono- to polytretic, integrated, terminal, determinate or percurrent, cylindrical, subhyaline to pale yellowish, doliiform at apex, with 1–2 conidiogenous loci, smooth, thin-walled. *Conidia* 14–58 × 6–12 μm ($\bar{x}$ = 32 × 9 μm, n = 40), simple or branched chains, obclavate, obpyriform, ovoid or ellipsoidal, pale to dark brown, muriform, up to 3–6 transverse and some cells have longitudinal or oblique septa, slightly constricted near some septa, smooth.

Culture characteristics – Conidia germinate within 12 hours in sterile water, and each cell is capable of producing germ tubes. Colonies on PDA, 60 mm diam., after 3 weeks, medium dense, cottony, circular, entire edge, olivaceous to gray at the margin, light brown to brown in the center, white film on the surface. Reverse, brown at the margin, light brown to grey in the center. Not produced pigmentation on PDA media.

Material examined – China, Sichuan Province, Suining City, Shehong City, Guangxing Town (30°57′21.89″N 105°18′54.32″E, alt. 408 m), dead leaves of *Juglans regia*, 17 May 2021, F.-H. Wang, WFH202105015 (SICAU 22-0111), living culture SICAUCC 22-0113.

GenBank numbers – SICAUCC 22-0113: OP963813 (ITS), OQ281343 (*rpb*2), OQ281360 (*tef*1-α), OQ214943 (*gapdh*).

Note – In the phylogeny (Fig. 59), this species clustered with the type species, *Alternaria alternata* (Schoch et al. 2006). Nucleotide comparisons of ITS, *gapdh*, *tef*1-α, and *rpb*2 (SICAUCC 22-0113) also showed a high homology with the sequences of *A. alternata* (CBS916.96 ex-type), with a similarity of 100% (531/531, 0 gap), 99.7% (580/582, 0 gap), 100% (241/241, 0 gap), and 100% (754/754, 0 gap), respectively. *Alternaria alternata* is known as the cause of leaf spot and other diseases in over 100 host species of plants (Rotem 1994), but also as postharvest disease in various crops (Coates & Johnson 1997) and of upper respiratory tract infections and asthma in humans (Kurup et al. 2000). The morphology of our collection resembles *A. alternata* in having similar size ranges of conidiophores (18–82 × 3–6 μm vs. 15–93 × 3–5 μm) and obclavate, obpyriform, ovoid or ellipsoidal, pale to dark brown, muri form conidia (14–58 × 6–12 μm vs. 11–50 × 7–18 μm) (Nishikawa et al. 2020). Based on morphological characters and phylogenetic analyses, we determine our specimens as *A. alternata*. This is the first record from *Juglans regia* in Sichuan.

35. ***Alternaria doliconidium*** J.F. Li, Camporesi & K.D. Hyde, Fungal Divers. 89: 147 (2018)

Fig. 60

Index Fungorum number: IF554202; Facesoffungi number: FoF04041

Associated with leaf spots on the living leaves of *Juglans regia*. Common symptoms include small, brown lesions that develop with a reddish border, eventually expanding to larger circular or angular spots. Concentric rings may be observed as individual lesions expand. The tissue becomes thin and brittle, and often drops out, leaving a ragged hole. Severely affected leaves wither and die from coalescing lesions. Sexual morph: Not observed. Asexual morph: *Mycelium* superficial on the substrate, composed of septate, branched, smooth, thin-walled, white to light pink-coloured hyphae. *Conidiophores* 76–128 × 3–6 μm ($\bar{x}$ = 94 × 5 μm, n = 20), macronematous, mononematous, light brown to brown, thick-walled, smooth, septate, branched on base, straight or flexuous, cylindrical. *Conidiogenous cells* 11–32 × 5–12 μm ($\bar{x}$ = 18 × 7 μm, n = 20), monoblastic, holoblastic, integrated, terminal, determinate or percurrent, cylindrical, doliiform, subhyaline, smooth, colourless, thin-walled, with 1-2 conidiogenous loci. *Conidia* 14–75 × 11–19 μm ($\bar{x}$ = 56 × 14 μm, n = 40) acrogenous, solitary, brown to dark brown, 3–7-septate, dry, simple, straight, curved, fusiform, obpyriform or obturbinate, subglobose, borne in chain, sometimes rostrate, unsmooth, thin-walled.

Culture characteristics – Conidia germinating on sterile water within 12 h and all cells can produce germ tubes. Colonies on PDA reaching 60 mm diam., after 17 days at 25 ℃. Mycelium superficial, hairy or cottony, white to light brown, effuse, with regular edge, white to light pink-coloured hyphae. Not produced pigmentation on PDA media.

GenBank numbers – SICAUCC 23-0147: PP060665 (ITS), PP057957 (LSU), PP061104 (*gapdh*).

Note – *Alternaria doliconidium* was introduced by Wanasinghe et al. (2018), from diseased dead aerial of *Rosa canina* in Italy. The morphology of our collection *A. doliconidium* (SICAUCC 23-0049) shares similarities with *A. doliconidium* (MFLUCC 17-0263) in having overlapped size ranges of conidia and obpyriform to obclavate, light brown, muriform conidia (10–26 × 5–10 µm vs. 16–30.2 × 5–13 µm). Phylogeny indicates that our collection *A. doliconidium* (SICAUCC 23-0049), clustered with *A. doliconidium* (MFLUCC 17-0263, KUN-HKAS 1100840) with strong statistical support (98% MLBS/1.00 BYPP) (Fig. 59). Nucleotide comparisons of ITS, LSU, and *gapdh* (SICAUCC 21-0013) also showed a high homology with the sequences of *A. doliconidium* (MFLUCC 17-0063), with a similarity of 99.4% (531/534, 3 gaps), 99.3% (850/856, 6 gaps), and 100% (584/584, 0 gap), respectively. Hence, based on both morphology and phylogeny, we introduce our collection as a new host record of *A. doliconidium* from *Juglans regia*.

Material examined – China, Sichuan Province, Bazhong City, Nanjiang County, Gongshan Town (32°18′37.22″N 106°52′22.48″E, alt. 1003 m), dead leaves of *Juglans regia*, 29 June 2022, F.-H. Wang, WFH202206005 (SICAU 23-0070), living culture SICAUCC 22-0049.

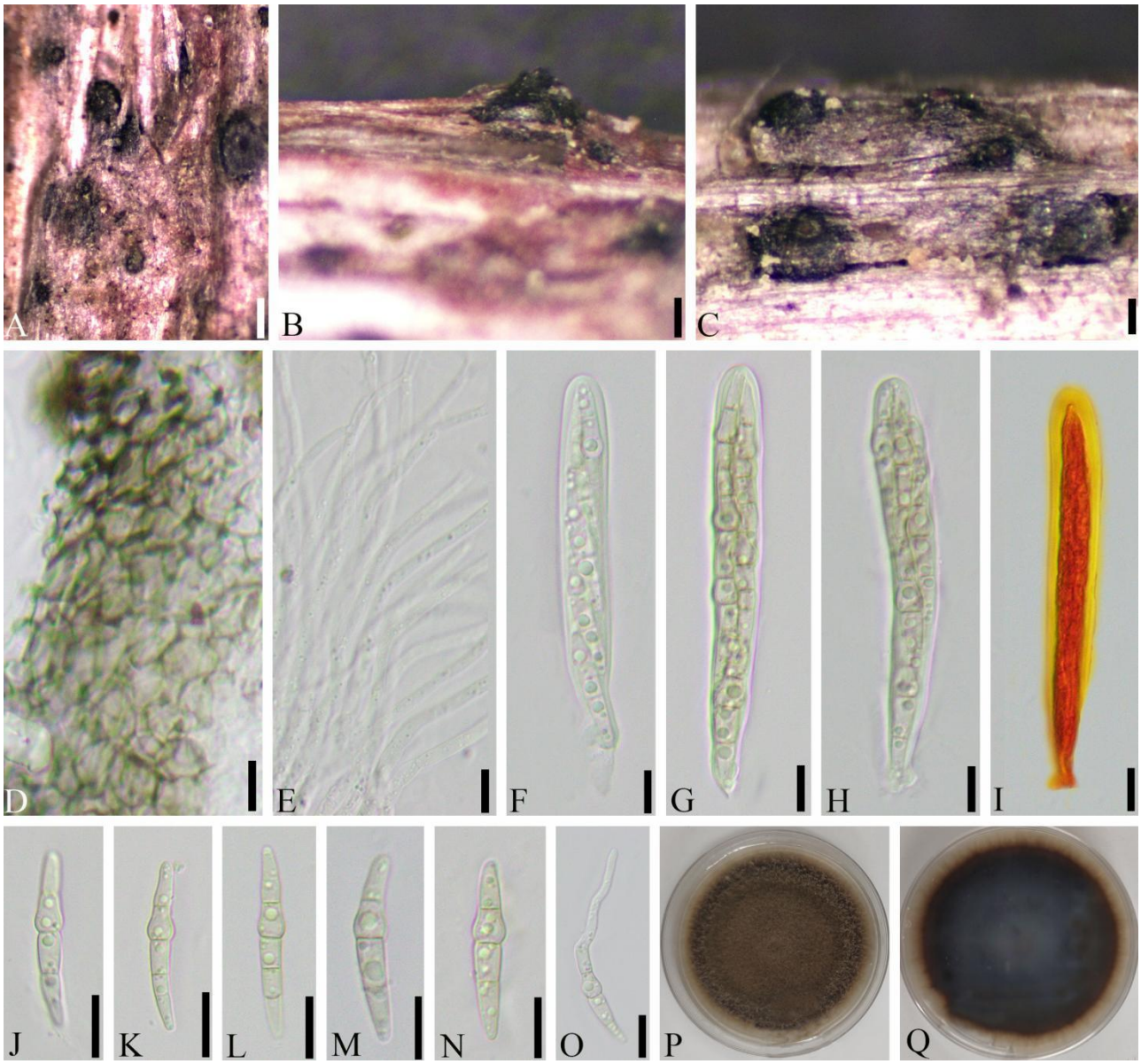


Figure 56 – *Paraphoma dioscoreae* (SICAU 23-0069). A–C Appearance of ascostroma in host substrate. D Peridium. E Pseudoparaphyses. F–H Asci. I Asci stained with Melzer's reagent. J–N Ascospores. O Germinating ascospore. P, Q Colonies on PDA (P from above, Q from below). Scale bars: A = 300 µm, B, C = 200 µm, E–I, O = 20 µm, D, J–N = 15 µm.

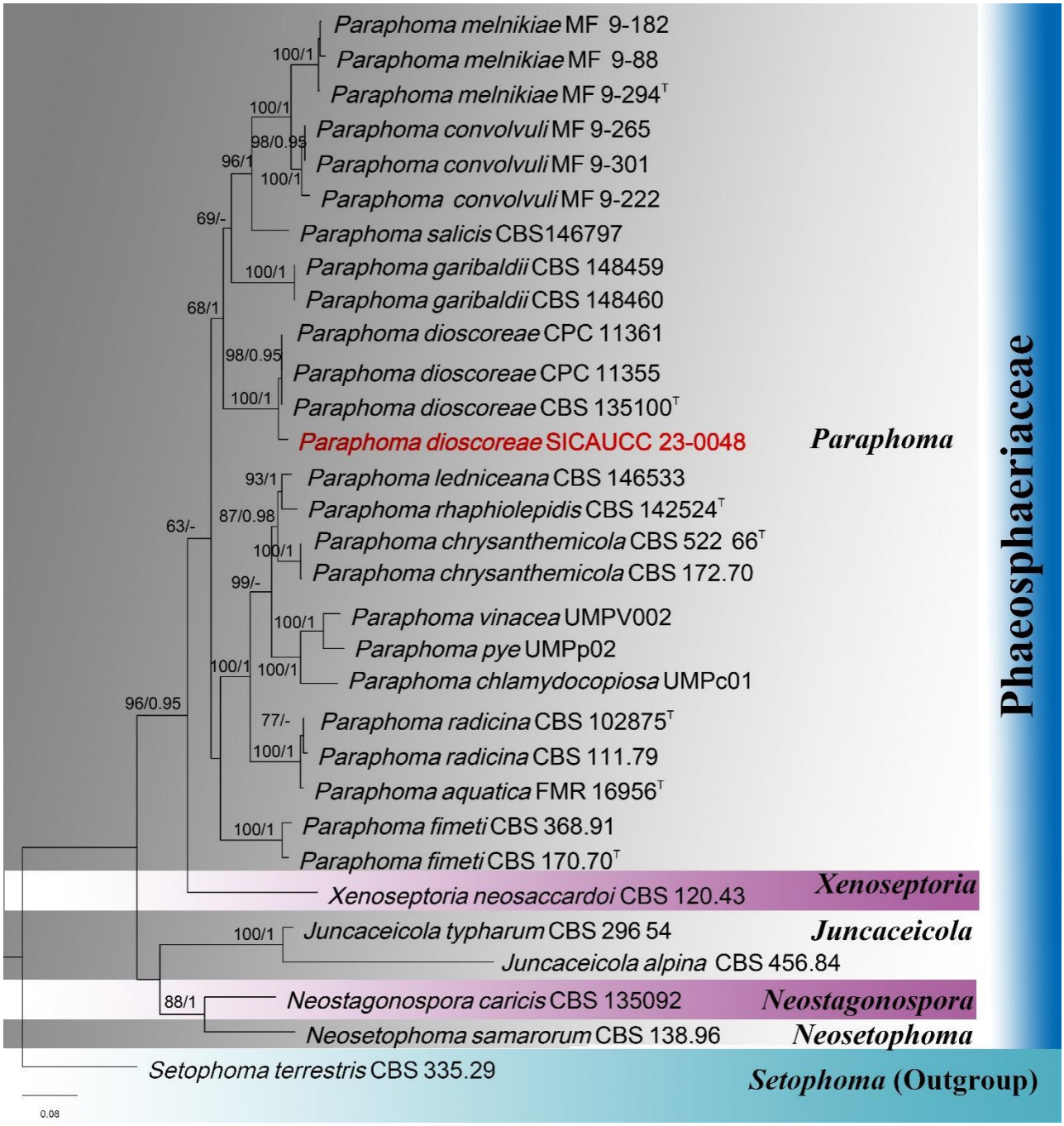


Figure 57 – Best scoring RAxML tree with a final likelihood value of -10,988.037210 based on combined ITS, *tef*1-α and *tub*2 sequence data of related species. The tree is rooted with *Setophoma terrestris* (CBS 335.29) in *Phaeosphaeriaceae*. Thirty-one strains were included in the combined gene analyses which comprised 1,830 characters (621 characters for ITS, 617 characters for *tef*1-α and 590 characters for *tub*2, including gap regions). The matrix had 924 distinct alignment patterns with 37.48% undetermined characters or gaps. Estimated base frequencies were as follows: A = 0.227740, C = 0.268027, G = 0.241785, T = 0.262448; substitution rates AC = 1.120325, AG = 2.473024, AT = 1.536456, CG = 0.969217, CT = 3.780474, GT = 1.000000; gamma distribution shape parameter α = 0.428550. The Bayesian inference analysis was implemented by MrBayes v.3.2.2 with the best-fit model (GTR+I+G for ITS, *tub*2; GTR+G for *tef*1-α) of evolution estimated with MrModeltest 2.2. The species determined in this study is indicated in red and bold. Bootstrap support values for maximum likelihood (MLBS, left) ⩾ 60% and Bayesian posterior probabilities

(BYPP, right) ⩾ 0.90 are indicated at the nodes, respectively. Hyphens (-) represent support values less than 60% MLBS/0.90 BYPP. The ex-type superscript "T".

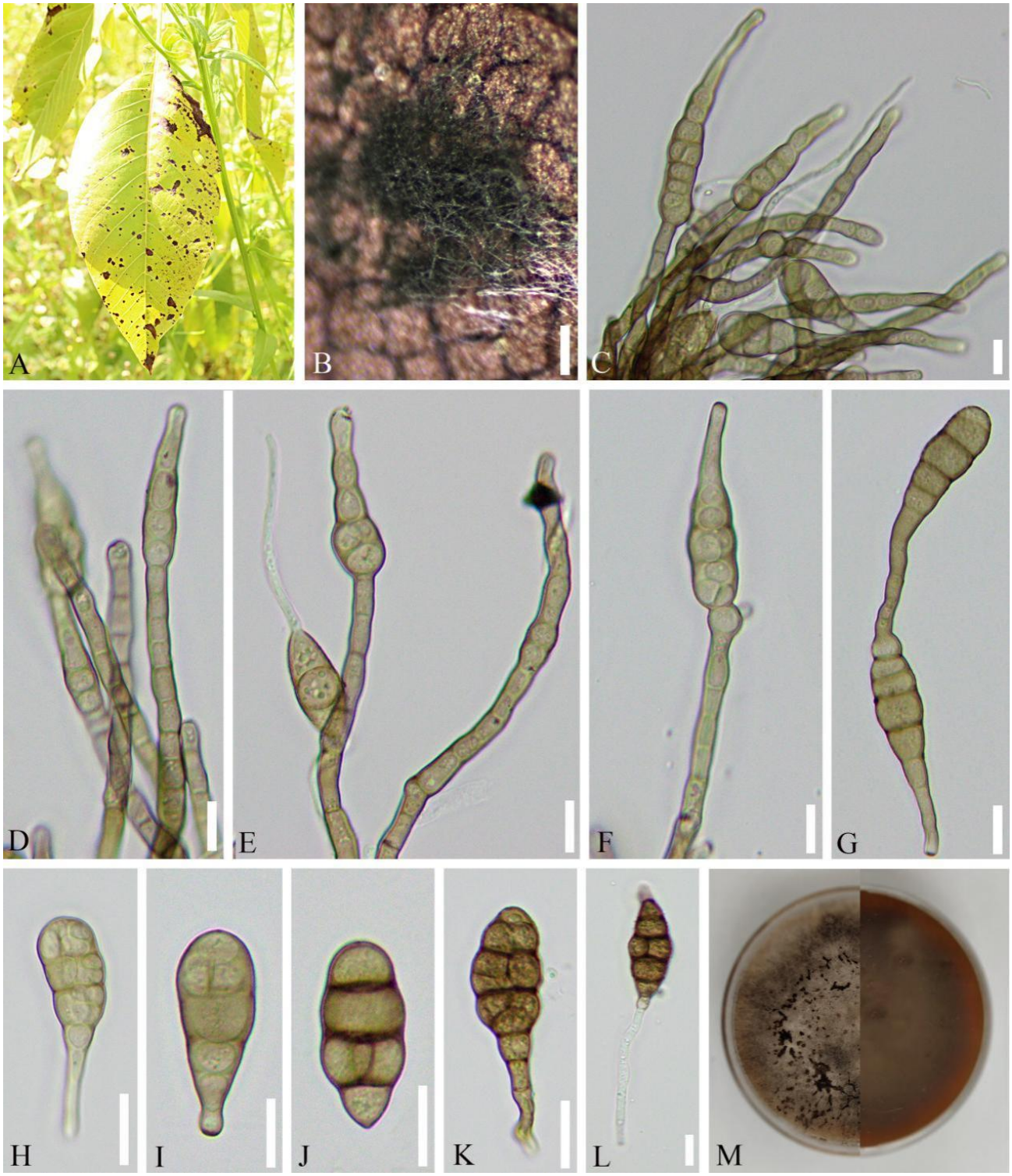


Figure 58 – *Alternaria alternata* (SICAU 22-0111). A Symptoms of necrotic lesions observed on host. B Colony on host. C–F Conidiophores. G Chain conidia. H–K Conidia N. Germinating conidium. M Colonies on PDA. Scale bars: B = 500 µm, C–K = 20 µm, L = 10 µm.

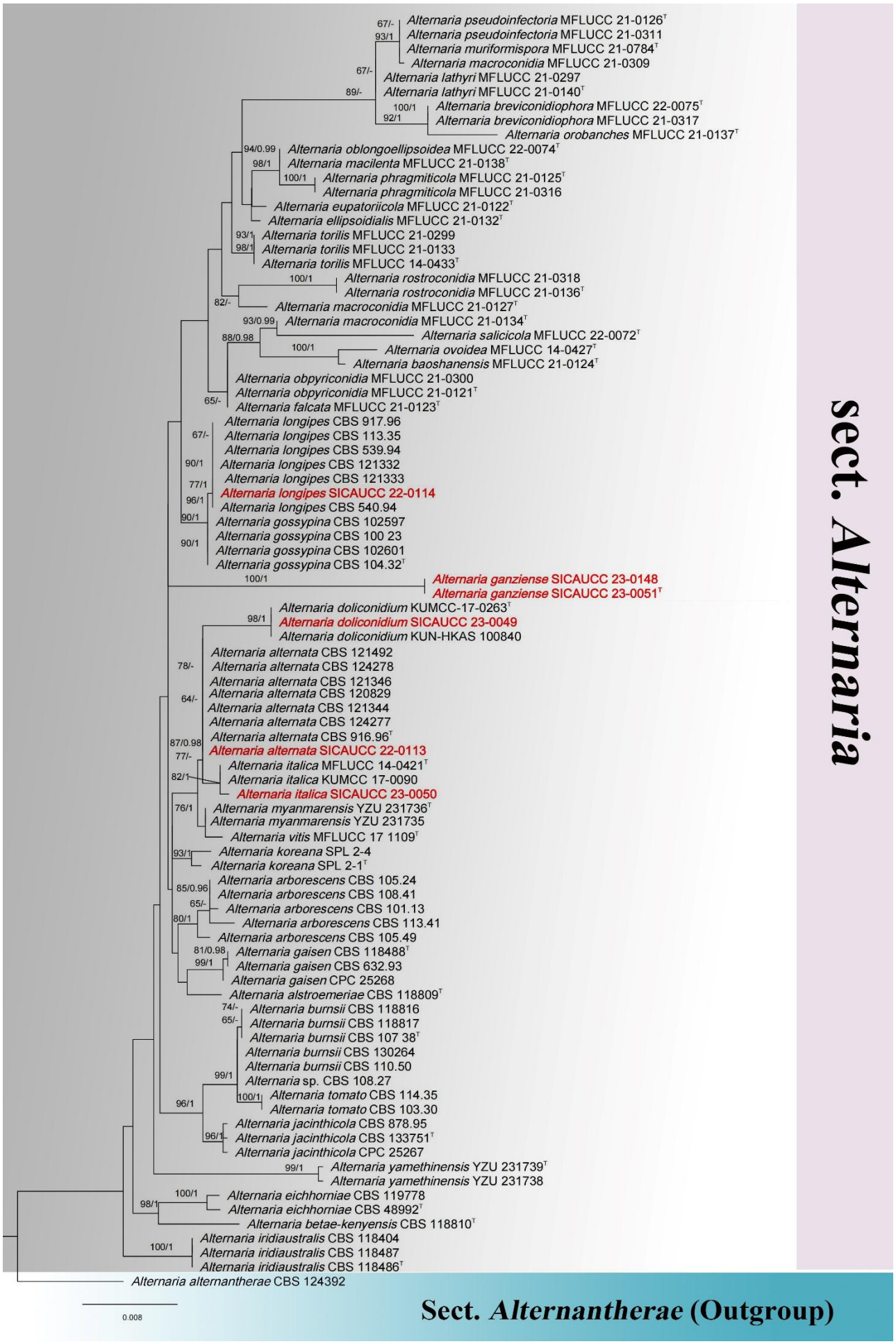

Alternaria pseudoinfectoria MFLUCC 21-0126T
Alternaria pseudoinfectoria MFLUCC 21-0311
Alternaria muriformispora MFLUCC 21-0784T
Alternaria macroconidia MFLUCC 21-0309
Alternaria lathyri MFLUCC 21-0297
Alternaria lathyri MFLUCC 21-0140T
Alternaria breviconidiophora MFLUCC 22-0075T
Alternaria breviconidiophora MFLUCC 21-0317
Alternaria orobanches MFLUCC 21-0137T
Alternaria oblongoellipsoidea MFLUCC 22-0074T
Alternaria macilenta MFLUCC 21-0138T
Alternaria phragmiticola MFLUCC 21-0125T
Alternaria phragmiticola MFLUCC 21-0316
Alternaria eupatoriicola MFLUCC 21-0122T
Alternaria ellipsoidialis MFLUCC 21-0132T
Alternaria torilis MFLUCC 21-0299
Alternaria torilis MFLUCC 21-0133
Alternaria torilis MFLUCC 14-0433T
Alternaria rostroconidia MFLUCC 21-0318
Alternaria rostroconidia MFLUCC 21-0136T
Alternaria macroconidia MFLUCC 21-0127T
Alternaria macroconidia MFLUCC 21-0134T
Alternaria salicicola MFLUCC 22-0072T
Alternaria ovoidea MFLUCC 14-0427T
Alternaria baoshanensis MFLUCC 21-0124T
Alternaria obpyriconidia MFLUCC 21-0300
Alternaria obpyriconidia MFLUCC 21-0121T
Alternaria falcata MFLUCC 21-0123T
Alternaria longipes CBS 917.96
Alternaria longipes CBS 113.35
Alternaria longipes CBS 539.94
Alternaria longipes CBS 121332
Alternaria longipes CBS 121333
Alternaria longipes SICAUCC 22-0114
Alternaria longipes CBS 540.94
Alternaria gossypina CBS 102597
Alternaria gossypina CBS 100 23
Alternaria gossypina CBS 102601
Alternaria gossypina CBS 104.32T
Alternaria ganziense SICAUCC 23-0148
Alternaria ganziense SICAUCC 23-0051T
Alternaria doliconidium KUMCC-17-0263T
Alternaria doliconidium SICAUCC 23-0049
Alternaria doliconidium KUN-HKAS 100840
Alternaria alternata CBS 121492
Alternaria alternata CBS 124278
Alternaria alternata CBS 121346
Alternaria alternata CBS 120829
Alternaria alternata CBS 121344
Alternaria alternata CBS 124277
Alternaria alternata CBS 916.96T
Alternaria alternata SICAUCC 22-0113
Alternaria italica MFLUCC 14-0421T
Alternaria italica KUMCC 17-0090
Alternaria italica SICAUCC 23-0050
Alternaria myanmarensis YZU 231736T
Alternaria myanmarensis YZU 231735
Alternaria vitis MFLUCC 17 1109T
Alternaria koreana SPL 2-4
Alternaria koreana SPL 2-1T
Alternaria arborescens CBS 105.24
Alternaria arborescens CBS 108.41
Alternaria arborescens CBS 101.13
Alternaria arborescens CBS 113.41
Alternaria arborescens CBS 105.49
Alternaria gaisen CBS 118488T
Alternaria gaisen CBS 632.93
Alternaria gaisen CPC 25268
Alternaria alstroemeriae CBS 118809T
Alternaria burnsii CBS 118816
Alternaria burnsii CBS 118817
Alternaria burnsii CBS 107 38T
Alternaria burnsii CBS 130264
Alternaria burnsii CBS 110.50
Alternaria sp. CBS 108.27
Alternaria tomato CBS 114.35
Alternaria tomato CBS 103.30
Alternaria jacinthicola CBS 878.95
Alternaria jacinthicola CBS 133751T
Alternaria jacinthicola CPC 25267
Alternaria yamethinensis YZU 231739T
Alternaria yamethinensis YZU 231738
Alternaria eichhorniae CBS 119778
Alternaria eichhorniae CBS 48992T
Alternaria betae-kenyensis CBS 118810T
Alternaria iridiaustralis CBS 118404
Alternaria iridiaustralis CBS 118487
Alternaria iridiaustralis CBS 118486T
Alternaria alternantherae CBS 124392
0.008
sect. Alternaria
Sect. Alternantherae (Outgroup)

Figure 59 – Best scoring RAxML tree with a final likelihood value of -9,414.713376 based on combined ITS, *gapdh*, LSU, *rpb*2 and *tef*1-α sequence data of related species. The tree is rooted with Sect. *Alternantherae* (CBS 124392) in *Alternaria*. Eighty-nine strains were included in the combined gene analyses which comprised 3,538 characters (649 characters for ITS, 594 characters for *gapdh*, 937 characters for LSU, 1,068 characters for *rpb*2 and 285 characters for *tef*1-α, including gap regions). The matrix had 651 distinct alignment patterns with 23.86% undetermined characters or gaps. Estimated base frequencies were as follows: A = 0.246716, C = 0.256155, G = 0.260998, T = 0.236131; substitution rates AC = 0.861906, AG = 2.223271, AT = 1.072667, CG = 0.846976, CT = 3.933572, GT = 1.000000; gamma distribution shape parameter α = 0.329439. The Bayesian inference analyses was implemented by MrBayes v.3.2.2 with the best-fit model (GTR+I+G for ITS, LSU, *rpb*2; HKY+I+G for *gapdh*; GTR+G for *tef*1-α) of evolution estimated with MrModeltest 2.2. The species determined in this study is indicated in red and bold. Bootstrap support values for maximum likelihood (MLBS, left) ⩾ 60% and Bayesian posterior probabilities (BYPP, right) ⩾ 0.90 are indicated at the nodes, respectively. Hyphens (-) represent support values less than 60% MLBS/0.90 BYPP. The ex-type superscript "T".

36. ***Alternaria ganziense*** F.H. Wang & C.L. Yang, sp. nov. Fig. 61

Index Fungorum number: IF901568; Facesoffungi number: FoF15585

Etymology – The specific epithet reflects Ganzi state in Sichuan, where the species was collected.

Holotype – SICAU 23-0072

Associated with leaf spots on the living leaves of *Juglans regia*. Initial symptoms of the leaves are small, irregular, brown spots. Generally, the spots gradually lighten and eventually become greyish as they become necrotic and dry. When severe, yellow spots can be seen throughout all leaves of the plant and the heavily infected leaves die. Sexual morph: Not observed. Asexual morph: *Mycelium*, consisting of branched, septate, smooth, hyaline hyphae. *Conidiophores* 22–84 × 3–5 μm ($\bar{x}$ = 68 × 4 μm, n = 20), macronematous, mononematous, erect, solitary or in fascicles, pale brown, becoming paler towards the apex, 3–6-septate, branched, smooth-walled, cylindrical. *Conidiogenous cells* 12–28 × 3–7 μm ($\bar{x}$ = 21 × 5 μm, n = 20) polytretic, integrated, terminal or intercalary, determinate, subhyaline to pale brown, cylindrical, proliferating sympodially, with pores for tretic sporulation. *Conidia* 15–40 × 6–12 μm ($\bar{x}$ = 32 × 7 μm, n = 40), acropleurogenous, chain-typed, pale brown, obclavate, rostrate, straight, or slightly curved, up to 1–6-septate, tapering towards the rounded base, truncate at the base, blackish-brown scar at the base, constricted at the septa, smooth-walled.

Culture characteristics – Conidia germinating on sterile water within 12 h and germ tubes can produce from every cell. Colonies on PDA reaching 20 mm diam., after 14 days at 25 ℃. The mycelium grows on the surface of the medium, circular, with fluffy, dense, dark grayish mycelium on the surface, in reverse dark brown with entire margin. Not produced pigmentation on PDA media.

Material examined – China, Sichuan Province, Garze Tibetan Autonomous Prefecture, Luding County, Kuiwu Village (29°40′32.17″N 102°11′34.13″E, alt. 1306 m), dead leaves of *Juglans regia*, 8 July 2022, F.-H. Wang, WFH202207035 (SICAU 23-0072, holotype), ex-type living culture SICAUCC 23-0051. *Ibid*., WFH202207035B (SICAU 24-0034), living culture SICAUCC 23-0148.

GenBank numbers – SICAUCC 23-0051: PP060667 (ITS), PP057959 (LSU), PP061120 (*rpb*2), PP061145 (*tef*1-α), PP061105 (*gapdh*); SICAUCC 23-0148: PP844876 (ITS), PP826166 (LSU), PP850048 (*rpb*2), PP850054 (*tef*1-α), PQ213083 (*gapdh*).

Note – Phylogenetic analyses showed that *Alternaria ganziensis* (SICAUCC 23-0051 and SICAUCC 23-0148) formed an independent lineage within *Alternaria* (Fig. 59). The NCBI BLASTn search of our new collection matched *A. vitis* (MFLUCC 17-1108) with 99.76% similarity in ITS sequences. *Alternaria ganziensis* (SICAUCC 23-0051) acropleurogenous, chain-typed, pale brown, obclavate conidia, while *A. vitis* (MFLUCC 17-1108) usually producing single conidia, single conidia, the conidia of *A. vitis* (MFLUCC 17-1108) is wider than that of *A. ganziensis*(SICAUCC

23-0051) (25–66 × 10–18 vs. 15–40 × 6–12) (Jayawardena et al. 2018). *Alternaria vitis* (MFLUCC 17-1108) is commonly a pathogen of *Vitis vinifera*. *Alternaria ganziensis* (SICAUCC 23-0051) was a saprobe on *Juglans regia* (Fig. 33). At present, only ITS sequences of *A. vitis* (MFLUCC 17-1108) are available for reference (1.8%, 9/495, 2 gaps), making further comparison impossible. Therefore, collecting and updating a large number of sequences will be the key in the future. We recognize our collection as a distinct species based on the morphology, but further molecular data are required to confirm their relationship.

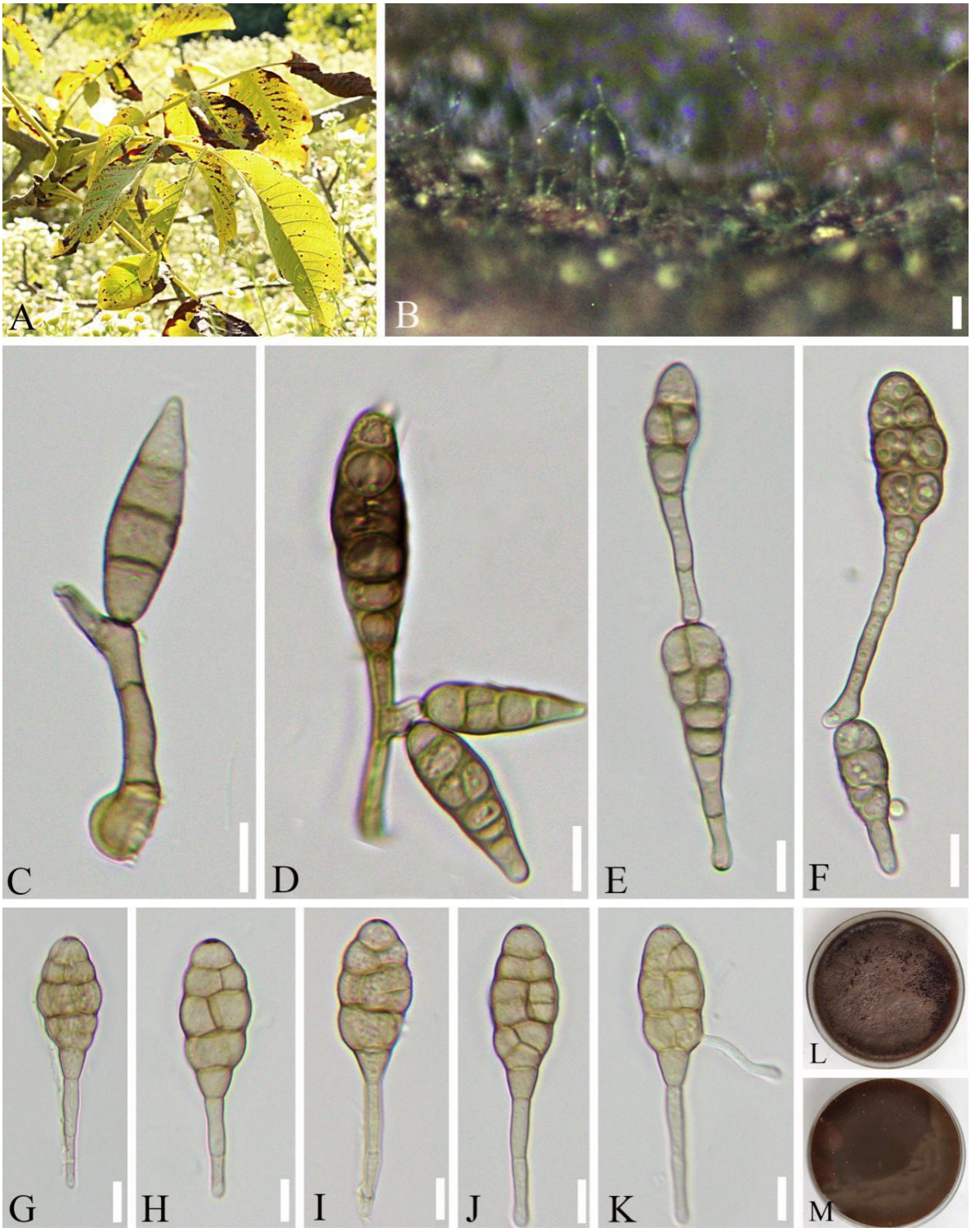


Figure 60 – *Alternaria doliconidium* (SICAU 23-0070). A. Symptoms of necrotic lesions observed on host. B. Colony on host. C, D Conidiophores. E, F chain conidia. G–J Conidia K. Germinating

conidium. L, M Colonies on PDA (L from above, M from below). Scale bars: B = 200 µm, C, D = 20 µm, E–K = 15 µm.



Figure 61 – *Alternaria ganziense* (SICAU 23-0072, holotype). A Symptoms of necrotic lesions observed on host. B, C Colony on host. D–F Conidiophores. G, H chain Conidia. I–N Conidia. O

Germinating conidium. P, Q Colonies on PDA (P from above, Q from below). Scale bars: B, C = 200 μm, D–O = 10 μm.

37. ***Alternaria italica*** J.F. Li, Camporesi & K.D. Hyde, Mycosphere 9(1): 43 (2018) Fig. 62

Index Fungorum number: IF553987; Facesoffungi number: FoF03880

Associated with leaf spots on the living leaves of *Juglans regia*. On leaves, the pathogen causes small, blackish concentric lesions. The initial symptoms can be observed on the leaf margin, however, as the disease progresses lesions may also develop in leaves as well. Lesions may coalesce and severely affected leaves may turn blackish giving a scorched appearance. Sexual morph: Not observed. Asexual morph: *Mycelium* mostly immersed, composed of pale to dark brown, septate, branched, smooth, hyaline to subhyaline hyphae. *Conidiophores* 40–290 × 4–7 μm ($\bar{x}$ =118 × 5 μm, n = 20), macronematous, mononematous, light brown to brown, thick-walled, smooth, septate, partly branched, straight or flexuous, cylindrical. *Conidiogenous cells* 14–21 × 9–15 μm ($\bar{x}$ = 17 × 12 μm, n = 20), cicatrized, monoblastic, integrated, terminal, determinate or percurrent, cylindrical, doliiform, subhyaline, smooth, thin-walled. *Conidia* 42–98 × 13–19 μm ($\bar{x}$ = 69 × 15 μm, n = 40), acrogenous, holoblastic, solitary, light grey to brownish grey, 5–9-septate or more, dry, simple, straight, curved, fusiform, obpyriform, obturbinate or subglobose, catenate, sometimes rostrate, smooth, thin-walled.

Culture characteristics – Conidia germinating on sterile water within 24 h and germ tubes produced from all cells. Colonies growing on PDA, hairy or cottony, brown to dark brown, reaching 60 mm in 20 days at 25ºC. Mycelium superficial, effuse, radially striate, with irregular edge, brown to dark brown hyphae, there are flocculent grey white aerial hyphae in the center. Reverse, grey at the margin, light brown to grey in the center. Not produced pigmentation on PDA media.

Material examined – China, Sichuan Province, Aba Tibetan and Qiang Autonomous Prefecture, Wenchuan County (31°20′21.45″N 103°28′40.11″E, alt. 1660 m), dead leaves of *Juglans regia*, 7 July 2022, F.-H. Wang, WFH202207016 (SICAU 23-0071), living culture SICAUCC 23-0050.

GenBank numbers – SICAUCC 23-0050: PP060666 (ITS), PP057958 (LSU), PP061119 (*rpb*2), PP061144 (*tef*1-α).

Note – We recognized our collection as *Alternaria italica*, because phylogenetically it clustered with other *A. italica* strains. Nucleotide comparisons of ITS, LSU, and *rpb*2 (SICAUCC 25-0050) also showed a high homology with the sequences of *A. italica* (MFLUCC 14-0421 ex-type), with a similarity of 99.8% (496/497, 0 gap), 100% (905/905, 0 gap), and 100% (807/807, 0 gap), respectively. Our strain is morphologically identical to *A. italica*. *Alternaria italica* is a pathogen in plant due it causing leaf blights. Based on morphology, Jayawardena et al. (2018) and Liao et al. (2023) reported this species from Italy and China. In this study we identified this species as a pathogen of *Juglans regia* based on morphology as well as sequence data.

38. ***Alternaria longipes*** (Ellis & Everh.) E.W. Mason, Mycol. 2(1): 19 (1928) Fig. 63

Index Fungorum number: IF269712; Facesoffungi number: FoF14360,

Associated with leaf spots on the living leaves of *Juglans regia*. In the early stage of infection, symptoms appear as small blighted areas on leaves that enlarge rapidly to cover most of the leaf blade. Affected leaves dry out and fade to a bleached straw colour, appearing as irregular-shaped patches on blighted leaves. Sexual morph: Not observed. Asexual morph: *Mycelium* superficial to immersed in media, branched, septate, smooth. *Conidiophores* 32–118 × 3–6 μm ($\bar{x}$ = 64 × 4 μm, n = 20), solitary to fascicular, subcylindrical, unbranched or basal branch, straight or sometimes geniculate, thin. *Conidiogenous cells* 12–19 × 6–9 μm ($\bar{x}$ = 15 × 8 μm, n = 20), cicatrized, monoblastic, integrated, terminal, determinate or percurrent, short to long, cylindrical, doliiform, subhyaline, smooth, thin-walled. *Conidia* 40–140 × 10–17 μm ($\bar{x}$ = 96 × 15 μm, n = 40) either solitary, or in short chains of 3–4 conidia without lateral branches, with a long handle, vary in size and appear as distorted, ovoid, ellipsoid to broadly obclavate, or sometimes beakless small oval, pale brown to yellowish brown, with 3–16 transverse and 0–1 longitudinal septum, constricted at some transverse septa, commonly with distosepta-like internal wall structure.

Culture characteristics – Conidia germinating on sterile water within 24 h and germ tubes produced from all cells. Colonies on PDA, 60 mm diam., after 20 days at 25ºC. The mycelium grows on the surface of the medium, dense, cottony, circular, edge irregular, light brown to brown at the margin, dark grey to black in the center. Reverse grey at the margin, dark brown to black in the center. Not produced pigmentation on PDA media.

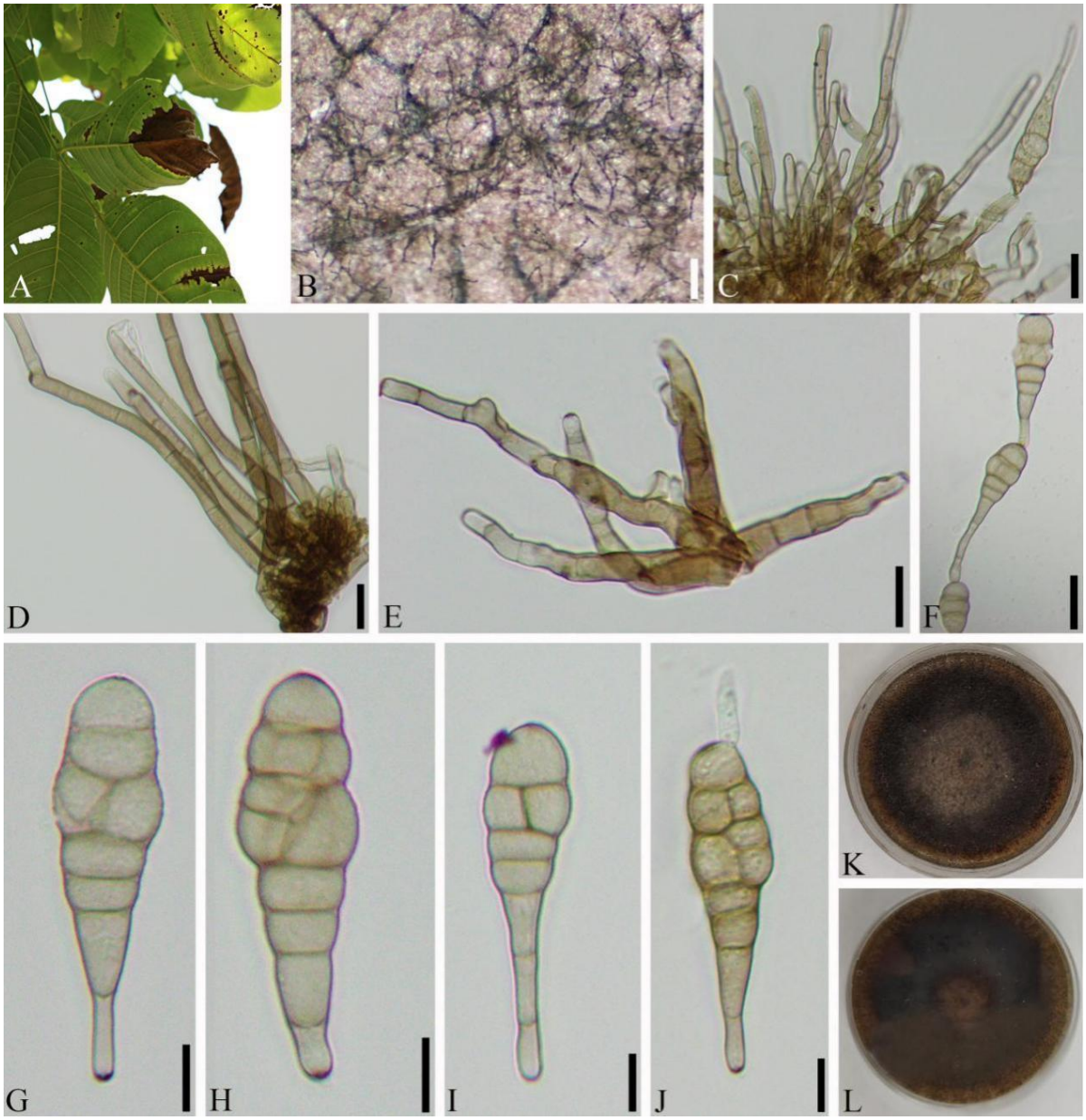


Figure 62 – *Alternaria italica* (SICAU 23-0071). A Symptoms of necrotic lesions observed on host. B Colony on host. C–E Conidiophores. F chain conidia. G–I Conidia. J Germinating conidium. K, L Colonies on PDA (K from above, L from below). Scale bars: B = 500 µm, C–F = 50 µm, G–J = 20 µm.

Material examined – China, Sichuan Province, Garze Tibetan Autonomous Prefecture, Luding County, Kuiwu Village (29°40′32.46″N 102°11′34.28″E, alt. 1309 m), dead leaves of *Juglans regia*, 18 July 2021, F.-H. Wang, WFH202107009 (SICAU 22-0112), living culture SICAUCC 22-0114.

GenBank numbers – SICAUCC 22-0114: OP963814 (ITS), OQ281344 (*rpb*2), OQ281361 (*tef*1-α), OQ214944 (*gapdh*).

Note – Phylogenetic analysis revealed that SICAU 22-0114 forms a sister clade with *Alternaria longipes* (CBS 917.96 and CBS 539.94) with strong statistical support (96% MLBS/1.00 BYPP) (Fig.

59), specifically with *Alternaria longipes* (CBS 917.96 and CBS 539.94). Sequence comparisons reveal a high similarity in their ITS (99.8%, 515/516, 1 gap), *rpb*2 (99.1%, 754/754, 0 gap), *tef*1-α (99.6%, 241/242, 0 gap), and *gapdh* (100%, 579/579, 0 gap), signifying their close genetic relationship. *Alternaria longipes* is a globally recognized pathogenic fungus with a broad range of host plants. It can cause leaf rot in tobacco, resulting in a decline in tobacco leaf quality or even death, which leads to economic losses. Studies have also found that *A. longipes* serves as an endophyte and saprophyte within tobacco plants. Furthermore, it is a fungus that is pathogenic to humans as well. (Vintal et al. 2002, Maiti et al. 2007, Long et al. 2009, Suwannarach et al. 2015, Hou et al. 2016, Ranganathan et al. 2019). This study is the first record of *A. longipes* on *Juglans regia* species.



Figure 63 – *Alternaria longipes* (SICAU 22-0112). A, B Symptoms of necrotic lesions observed on host. C Conidiogenesis. D-F Conidiophores. G–I Conidia J Germinating conidium. K Colonies on PDA. Scale bars: C = 1000, D-J = 20 μm.

Teichosporaceae M.E. Barr, Mycotaxon 82: 374 (2002) Synonym. *Floricolaceae* Thambug., Kaz. Tanaka & K. D. Hyde, Fungal Divers. 74: 244 (2015).

Teichosporaceae is considered as a species rich family in *Pleosporales*, whose members are morphologically, ecologically and phylogenetically diverse (Barr 2002, Hongsanan et al. 2020b). This family was introduced by Barr (2002) to accommodate eight genera, namely *Bertiella*, *Byssothecium*, *Chaetomastia*, *Immotthia*, *Loculohypoxylon*, *Moristroma*, *Sinodidymella* and the type genus *Teichospora* by using morphological characteristics. These genera were previously included in *Decampiaceae* (Barr 1987) based on their *Peridium* structure, ascus morphology and different trophic states (saprotrophic species). Most of *Dacampiaceae* species are lichenicolous and thus, Barr introduced *Teichosporaceaein* order to separate some saprobic species in woody stems from *Dacampiaceae* (Barr 2002). Jaklitsch et al. (2016b) synonymized *Floricolaceae* with *Teichosporaceae* and transferred all the genera, which were previously included in *Floricolaceae* (Thambugala et al. 2015) to *Teichosporaceae*. Therefore, all genera which were accepted in Thambugala et al. (2015) in *Floricolaceae*, became synonyms of *Teichospora*. Based on the combination of morphological and phylogenetic studies, Tennakoon et al. (2021a) opposed the generalized genus concept of *Teichosporaceae*, and 9 genera have been restored. Ascomata non-stromatic but sometimes surrounded or overlain by brown hyphae, immersed, erumpent to superficial, dark brown to black, perithecioid. Ostiolar necks papillate to elongate, pore rounded, interior periphysate, apex variously coloured. Peridium pseudoparenchymatous, 2–3 layered, brown. Hamathecium comprising paraphyses and pseudoparaphyses. Asci 4–8-spored, bitunicate, fissitunicate, cylindrical to subclavate. Ascospores brown, less commonly hyaline, ellipsoid, oblong, fusoid or clavate, symmetric or asymmetric, usually septate, rarely with a gelatinous sheath. Asexual morphs coelomycetous, forming pycnidial that contain brown septate or brown, rarely hyaline non-septate conidia.

Aurantiascoma Thambugala & K.D. Hyde, Fungal Divers. 74: 249 (2015).

Aurantiascoma was introduced by Thambugala et al. (2015), to accommodate *A. minimum* as the type species. *A. minimum* was previously known as *Misturatosphaeria minima*, which was collected from decorticated woody branches and named based on smaller ascomata (Mugambi & Huhndorf 2009). Jaklitsch et al. (2016a) synonymized *Aurantiascoma* under *Teichospora* and erected *Misturatosphaeria minima* as *T. parva*. The morphological characters of *A. minimum* are distinctly different from the type species of *Teichospora*, viz. *A. minimum* has hyaline, fusiform, 1–3-septate ascospores with one of the central cells broader than others, constricted at the central septum and a thin mucilaginous sheath, whereas *T. trabicola* has brown, rarely hyaline, muriform ascospores which are not or slightly constricted at the septa (Mugambi & Huhndorf 2009, Jaklitsch et al. 2016b). *A. minimum* shares similarities with the type species of *Misturatosphaeria* (*M. aurantiinotata*) in having superficial ascomata, with an orange ostiolar area, and 3-septate, fusiform ascospores (Thambugala et al. 2015). Tennakoon et al. (2021a) resumed the genus *Aurantiascoma*, and there are currently three species in this genus, namely *A. minimum*, *A. nephelii* and *A. quercus*.

39. ***Aurantiascoma juglandis*** F.H. Wang & C.L. Yang, sp. nov. Fig. 64

Index Fungorum number: IF901569; Facesoffungi number: FoF15586

Etymology – Name refers to *Juglans*, the host genus from which this fungus was collected.

Holotype – SICAU 23-0073

Saprobic on dead *Juglans sigillata* branches. Sexual morph: *Ascomata* 278–352μm × 173–286μm ($\bar{x}$ = 320 × 235μm, n = 10), solitary or scattered, immersed, papilla usually erumpent, black, subglobose to globose, coriaceous, uniloculate, ostiolate. *Ostiole* central, rounded, compressed, periphysate, with a pore-like opening. *Peridium* 18–50μm ($\bar{x}$ = 36μm, n = 20) wide, 6-9-layered, composed of small, dark brown to lightly pigmented cells of textura globulosa to *textura angularis*, fusing at the outside with the host tissues. *Hamathecium* comprising 1.5–2.5 μm wide, numerous, filamentous, distinct septate, non-constricted at the septa, sparsely anastomosing, cellular. *Pseudoparaphyses*, embedded in a gelatinous matrix. *Asci* 68–93 × 7–11μm ($\bar{x}$ = 80 × 9μm, n = 20),

8-spored, bitunicate, fissitunicate, cylindrical, with a short pedicel, rounded at the apex, with an ocular chamber. *Ascospores* 17–28 × 3–6 µm ($\bar{x}$ = 24 × 4.5µm, n = 40), overlapping bi-seriate, hyaline, fusiform to cylindrical, usually 1-septate, constricted at the septum, surrounded by a thin mucilaginous sheath, filled with small guttules when immature. Asexual morph: Not observed.

Culture characteristics – Ascospores germinating on sterile water within 12 h and germ tubes produced from both ends. Colonies on PDA growing slowly, reaching 30 mm diam., after 28 days at 25℃, circular, entire edge, pale olivaceous-grey in outer region, spreading with moderate aerial mycelium, and even, smooth margins. Reverse olivaceous-grey, white at the margin. Not produced pigmentation on PDA media.

Material examined – China, Sichuan Province, Liangshan Yi Autonomous Prefecture, Huili City (26°56′43.17″N 102°16′26.36″E, alt. 2006 m), dead branches of *Juglans sigillata*, 30 September 2022, F.-H. Wang, WFH202209022 (SICAU 23-0073, holotype), ex-type living culture SICAUCC 23-0052. *Ibid*., WFH202209022B (SICAU 24-0035), living culture SICAUCC 23-0149.

GenBank numbers – SICAUCC 23-0052: PP060668 (ITS), PP057960 (LSU), PP003825 (SSU), PP061121 (*rpb*2); SICAUCC 23-0149: PP844877 (ITS), PP826167 (LSU), PP853379 (SSU), PP850049 (*rpb*2).

Note – The genus *Aurantiascoma* was treated in detail by Tennakoon et al. (2021a) and includes several generic synonyms. Phylogeny herein indicates that of all *Aurantiascoma juglandis* strains cluster together with strong statistical support (99% MLBS/1.00 BYPP) and the clade is sister to *A. minimum* (GKM 169) with strong statistical support (88% MLBS/0.90 BYPP) (Fig. 65). The morphological characters of *A. juglandis* (SICAUCC 23-0052) resemble *A. minimum* (GKM 169) in immersed, dark brown ascomata, a multi-layered, brown peridium, cylindric-clavate, short pedicellate asci and hyaline, fusiform, septate ascospores, which constricted at the central septum, with mucilaginous sheath (Mugambi & Huhndorf 2009). There are also significant differences in the pseudoparaphysess between *A. juglandis* (SICAUCC 23-0052) and *A. minimum* (GKM 169), with *A. juglandis* (SICAUCC 23-0052) being aseptate while *A. minimum* (GKM 169) is septate, asci (68–93 × 7–11 µm vs. 72–112 × 8–11 µm) and ascospores (17–28 × 3–6 µm vs. 18–22 × 8–9 µm) dimensions. Currently, only LSU sequences are available for reference for *A. minimum* (SICAUCC 23-0052) (1.6%, 13/809, 0 gap), and this genus is still surrounded by extensive controversies (Tennakoon et al 2021a). The PHI test revealed no significant recombination event between our strain and the closely related taxa (Φw = 1) (Fig. 66). Given the morphological differences, we define *A. juglandis* as a new species within the genus *Aurantiascoma*.

Valsariales Jaklitsch, K.D. Hyde & Voglmayr, Fungal Divers. 73: 167 (2015).

Valsariales was introduced by Jaklitsch et al. (2015) based on multi-gene phylogeny analyses to accommodate the single family *Valsariaceae*. *Valsariales* species possess perithecioid ascomata that are immersed in either eu- or pseudostromata. These ascomata contain bitunicate asci, which lack obvious fissitunicate dehiscence, and produce dark brown, biseriate ascospores. Member of *Valsariales* have a worldwide distribution on various substrates as saprobes, plant pathogens or necrotrophs (Ju et al. 1996a, Jaklitsch et al. 2015). There are only three genera with molecular data. The divergence time for *Valsariales* is estimated as 224 MYA (stem age, Hongsanan et al. 2020b).

Valsariaceae Jaklitsch, K.D. Hyde & Voglmayr, Fungal Divers. 73: 167 (2015).

Valsariaceae was introduced by Jaklitsch et al. (2015) with *Valsaria insitiva* as the type species. Members of *Valsariaceae* have a worldwide distribution on various substrates as saprobes, plant pathogens or necrotrophs. Three genera, *Bambusaria*, *Myrmaecium* and *Valsaria* are accepted in this family. The spore ornamentation is an important character to differentiate genera within *Valsariaceae*, while the number of guttules and wall development has been used to segregate species of *Valsaria* (Pem et al. 2019).

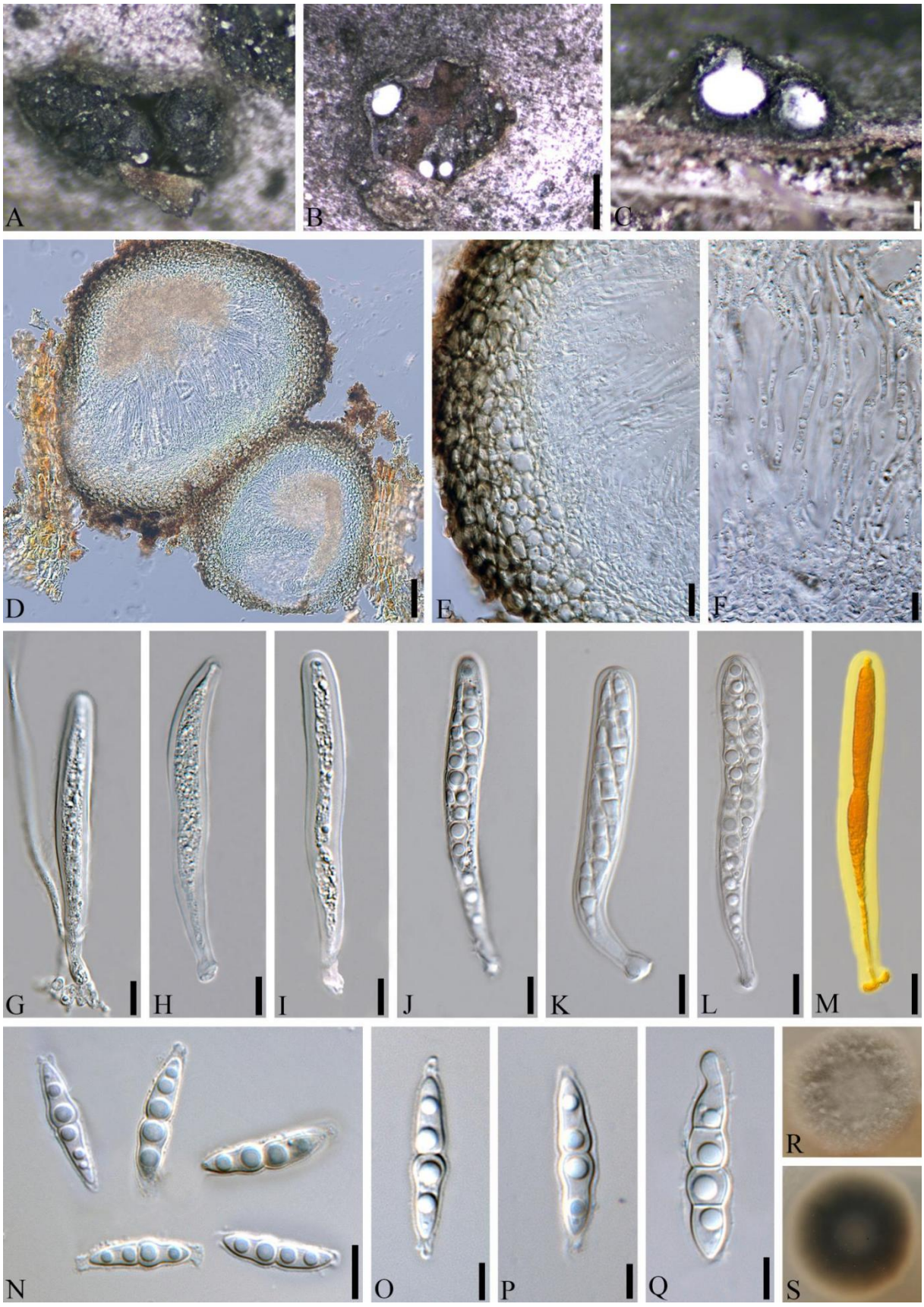


Figure 64 – *Aurantiascoma juglandis* (SICAU 23-0073, holotype). A Appearance of ascostroma in host substrate. B, C Vertical and horizontal section of ascoma. D Section through ascoma. E Peridium. F Pseudoparaphyses. G–L Immature and mature asci. M Asci in Melzer's reagent. N–P Ascospores. Q Germinating ascospore. R, S Colonies on PDA (R from above, S from below). Scale bars: B = 1000 µm, C = 200 µm, D = 50 µm, E = 20 µm, F–N = 10 µm, O-Q = 5 µm.

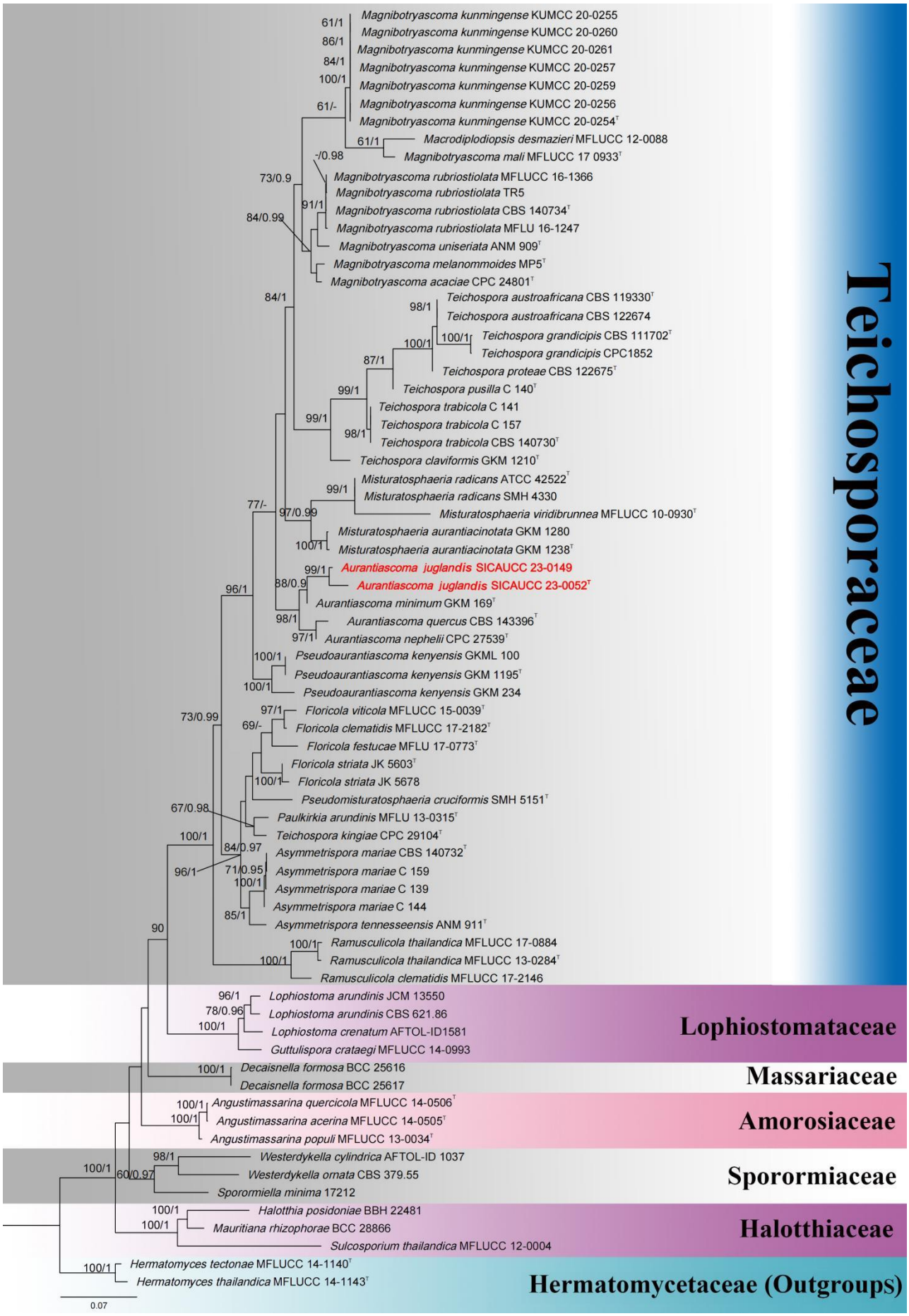

Magnibotryascoma kunmingense KUMCC 20-0255
Magnibotryascoma kunmingense KUMCC 20-0260
Magnibotryascoma kunmingense KUMCC 20-0261
Magnibotryascoma kunmingense KUMCC 20-0257
Magnibotryascoma kunmingense KUMCC 20-0259
Magnibotryascoma kunmingense KUMCC 20-0256
Magnibotryascoma kunmingense KUMCC 20-0254T
Macrodiplodiopsis desmazieri MFLUCC 12-0088
Magnibotryascoma mali MFLUCC 17 0933T
Magnibotryascoma rubriostiolata MFLUCC 16-1366
Magnibotryascoma rubriostiolata TR5
Magnibotryascoma rubriostiolata CBS 140734T
Magnibotryascoma rubriostiolata MFLU 16-1247
Magnibotryascoma uniseriata ANM 909T
Magnibotryascoma melanommoides MP5T
Magnibotryascoma acaciae CPC 24801T
Teichospora austroafricana CBS 119330T
Teichospora austroafricana CBS 122674
Teichospora grandicipis CBS 111702T
Teichospora grandicipis CPC1852
Teichospora proteae CBS 122675T
Teichospora pusilla C 140T
Teichospora trabicola C 141
Teichospora trabicola C 157
Teichospora trabicola CBS 140730T
Teichospora claviformis GKM 1210T
Misturatosphaeria radicans ATCC 42522T
Misturatosphaeria radicans SMH 4330
Misturatosphaeria viridibrunnea MFLUCC 10-0930T
Misturatosphaeria aurantiacinotata GKM 1280
Misturatosphaeria aurantiacinotata GKM 1238T
Aurantiascoma juglandis SICAUCC 23-0149
Aurantiascoma juglandis SICAUCC 23-0052T
Aurantiascoma minimum GKM 169T
Aurantiascoma quercus CBS 143396T
Aurantiascoma nephelii CPC 27539T
Pseudoaurantiascoma kenyensis GKML 100
Pseudoaurantiascoma kenyensis GKM 1195T
Pseudoaurantiascoma kenyensis GKM 234
Floricola viticola MFLUCC 15-0039T
Floricola clematidis MFLUCC 17-2182T
Floricola festucae MFLU 17-0773T
Floricola striata JK 5603T
Floricola striata JK 5678
Pseudomisturatosphaeria cruciformis SMH 5151T
Paulkirkia arundinis MFLU 13-0315T
Teichospora kingiae CPC 29104T
Asymmetrispora mariae CBS 140732T
Asymmetrispora mariae C 159
Asymmetrispora mariae C 139
Asymmetrispora mariae C 144
Asymmetrispora tennesseensis ANM 911T
Ramusculicola thailandica MFLUCC 17-0884
Ramusculicola thailandica MFLUCC 13-0284T
Ramusculicola clematidis MFLUCC 17-2146
Lophiostoma arundinis JCM 13550
Lophiostoma arundinis CBS 621.86
Lophiostoma crenatum AFTOL-ID1581
Guttulispora crataegi MFLUCC 14-0993
Decaisnella formosa BCC 25616
Decaisnella formosa BCC 25617
Angustimassarina quercicola MFLUCC 14-0506T
Angustimassarina acerina MFLUCC 14-0505T
Angustimassarina populi MFLUCC 13-0034T
Westerdykella cylindrica AFTOL-ID 1037
Westerdykella ornata CBS 379.55
Sporormiella minima 17212
Halotthia posidoniae BBH 22481
Mauritiana rhizophorae BCC 28866
Sulcosporium thailandica MFLUCC 12-0004
Hermatomyces tectonae MFLUCC 14-1140T
Hermatomyces thailandica MFLUCC 14-1143T
0.07
Teichosporaceae
Lophiostomataceae
Massariaceae
Amorosiaceae
Sporormiaceae
Halotthiaceae
Hermatomycetaceae (Outgroups)

Figure 65 – Best scoring RAxML tree with a final likelihood value of -39,604.048873 based on combined LSU, ITS, *rpb*2, SSU and *tef*1-α sequence data of related species. The tree is rooted with *Hermatomyces tectonae* (MFLUCC 14-1140^{T}) and *H. thailandica* (MFLUCC 14-1143^{T}) in *Hermatomyces*. Seventy-two strains were included in the combined gene analyses which comprised 8,884 characters (2,111 characters for LSU, 1,656 characters for ITS, 1,869 characters for *rpb*2, 1,766 characters for SSU and 1,478 characters for *tef*1-α, including gap regions). The tree from the maximum likelihood analyses had similar topology to the Bayesian analyses. The matrix had 2,669 distinct alignment patterns with 64.98% undetermined characters or gaps. Estimated base frequencies were as follows: A = 0.244520, C = 0.251028, G = 0.276268, T = 0.228185; substitution rates AC = 1.212614, AG = 2.528984, AT = 1.418002, CG = 1.121102, CT = 6.707751, GT = 1.000000; gamma distribution shape parameter α = 0.310078. The GTR+I+G model was selected for every partition in Bayesian analyses. The species determined in this study is indicated in red and bold. Bootstrap support values for maximum likelihood (MLBS, left) ⩾ 60% and Bayesian posterior probabilities (BYPP, right) ⩾ 0.90 are indicated at the nodes, respectively. Hyphens (-) represent support values less than 60% MLBS/0.90 BYPP. The ex-type superscript "T".

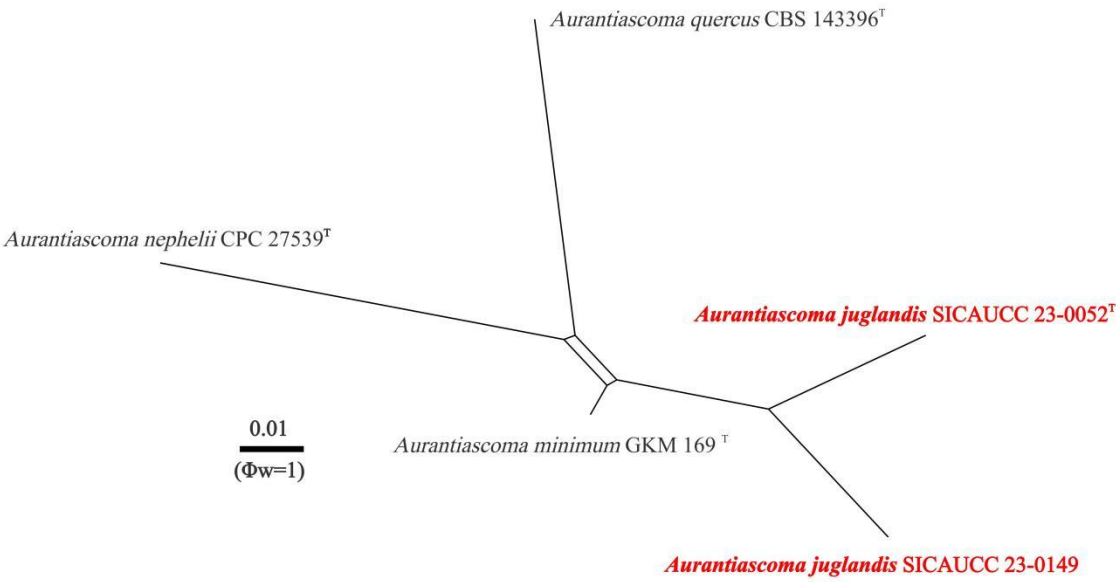


Figure 66 – Results of the PHI test of *Aurantiascoma juglandis* and closely related species using both LogDet transformation and splits decomposition. The PHI test did not find any statistically significant recombination (Φw = 1) in the data set. The new strains are represented in red and bold. "T" represents the type strain.

Myrmaecium Nitschke ex Fuckel, Jb. Nassau. Ver. Naturk. 23–24: 227 (1870); non Myrmaecium Sacc., Michelia 2: 138 (1880).

Myrmaecium (*Valsariaceae*, *Valsariales*) is a genus traditionally treated as a synonym of *Valsaria*, but resolved by Jaklitsch et al. (2015) to comprise *M. fulvopruinatum*, *M. rubricosum* and *M. rubrum*.

40. ***Myrmaecium fulvopruinatum*** (Berk.) Jaklitsch & Voglmayr, Fungal Divers. 73: 190 (2015)

Fig. 67

Index Fungorum number: IF811904; Facesoffungi number: FoF00614

Associated with trunk rot on living trunk of *Juglans regia*. Affected branches or trunks show canker and some may have abundant resin flow. When the canker girdles the affected area, part of the tree above the canker dies. Sexual morph: *Stromata* eustromatic, immersed to erumpent, causing small bumps in bark, subpulvinate, labiate or ring-like, often longish, separate, 0.7–3 × 0.5–2 mm ($\bar{x}$ = 2 × 1.5 mm, n = 20), aggregated in linear rows. *Ascomata* are 180–410 × 160–350 μm ($\bar{x}$ = 350 × 280 μm, n = 20), arranged monostichously in valsoid groups of 4–8 at near basal position or in the stroma middle, less commonly in diatrypoid configuration just below the stroma surface, flask-shaped to subglobose. *Peridium* 15–25 μm ($\bar{x}$ = 19 μm, n = 20) wide, composed of a thin outer layer of flattened dark brown cells and an inner layer of flattened hyaline cells. *Ostiole necks* converging into a common neck, less commonly separate, 190–380 × 90–150 μm ($\bar{x}$ = 320 × 120 μm, n = 20), black, smooth; apices at the surface usually with distinct circular outline, flush with the stroma surface or projecting to 120 μm, periphysate. *Paraphyses* filiform, unbranched, apically free, up to 150 μm long, 1–5 μm wide, attenuated upwards, slightly enlarged at the tip. *Asci* 72–96 × 8–12 μm ($\bar{x}$ = 80 × 11 mm, n = 20), numerous, cylindrical to subclavate, containing 8 uniseriate ascospores, bitunicate, fissitunicate, small ocular chamber, thick apex, apical ring absent or thin. *Ascospores* 12–20 × 6–9 μm ($\bar{x}$ = 16 × 7 mm, n = 20), ellipsoid, septate, slightly constricted at the septum, 2-celled, dark brown to black. Asexual morph: Not observed.

Culture characteristics – Ascospores germinating on sterile water within 12 h and germ tubes produced from ends. Colonies on PDA reaching 60 mm diam., after 7 days at 25 ℃. Colonies zonate, with sparse mycelium on the surface, pale yellow in the middle, bronzing at the edge. Reverse yellow in the middle, the reverse side is the same as the front side. Not produced pigmentation on PDA media.

Material examined – China, Sichuan Province, Chengdu City, Chongzhou City (30°33′9.17″N 103°39′28.56″E, alt. 512 m), dead trunk of *Juglans regia*, 16 October 2021, F.-H. Wang, WFH202110003 (SICAU 22-0146), living culture SICAUCC 22-0148.

GenBank numbers – SICAUCC 22-0148: ON287043 (ITS), ON287044 (LSU), ON315871 (*rpb*2), ON315870 (*tef*1-α).

Note – Our collection *Myrmaecium fulvopruinatum* (SICAUCC 22-0148) grouped with *M. fulvopruinatum* (CFCC 52769, CFCC 52770, CFCC 52771, CFCC 52772, CFCC 52773, CFCC 52774, VFJ1CBS 139057, CBS 139058 and CBS 139059) as a sister taxon with strong statistical support (100% MLBS/1.00 BYPP) (Fig. 68). Comparisons of the ITS, LSU, *rpb*2 and *tef*1-α sequences of our specimen and the ex-type strain of *M. fulvopruinatum* (VFJ1) revealed 100%, 100%, 98.9% and 99.3% similarity, respectively.

Eurotiomycetes O.E. Erikss. & Winka, Myconet 1: 6 (1997).

Eurotiomycetes was established by Eriksson & Winka (1997) and presently consists of six subclasses: *Chaetothyriomycetidae*, *Coryneliomycetidae*, *Cryptocaliciomycetidae*, Misturatosphaeria minima, *Mycocaliciomycetidae*, and *Sclerococcomycetidae* (Hibbett et al. 2007, Wood et al. 2016, Geiser et al. 2017, Réblová et al. 2017, Prieto et al. 2021). The *Microcolonies* of *Eurotiomycetes* formed under natural conditions do not have much morphological differences leading to difficulty morphologically in distinguishing species. The incorporation of molecular techniques in the fungal taxonomy made the classification of fungi more objective, accurate, and comprehensive (Wood et al. 2016, Réblová et al. 2017, Luo et al. 2019, Wijayawardene et al. 2020b, Dong et al. 2020, Prieto et al. 2021). Wijayawardene et al. (2020b) provided an outline of the classification of the fungi and fungus-like taxa, and counted all legally published species, with a total of 3,994 *Eurotiomycetes* species.

Eurotiales G.W. Martin ex Benny & Kimbr., Mycotaxon 12 (1): 23 (1980).

Eurotiales comprises some of the most commonly encountered microfungi, including the well-known genera *Aspergillus* and *Penicillium*, some species of which can survive at extreme

environments, such as deep water and high temperature (Geiser et al. 2015). We follow the latest treatment and updated accounts of *Aspergillacea*e in Zhang et al. (2021)

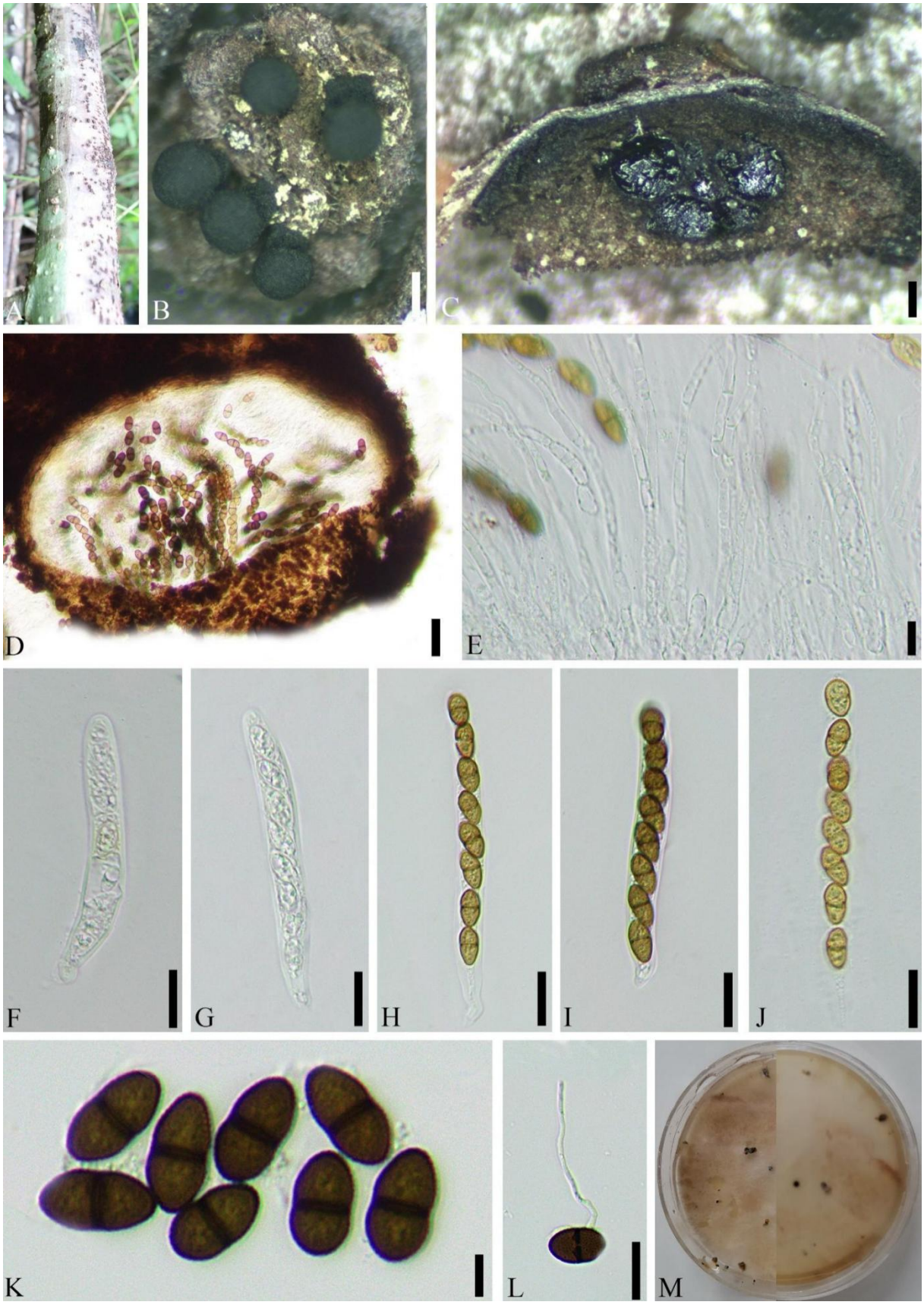


Figure 67 – *Myrmaecium fulvopruinatum* (SICAU 22-0146). A Appearance of ascostroma in host substrate. B Ectostromata in face view. C, D Vertical sections of ascomata. E Pseudoparaphyses. F–

J Immature and mature asci. K Ascospores. L Germinating ascospore. M Colonies on PDA. Scale bars: B = 500 µm, C = 200 µm, D = 50 µm, F–J, L = 20 µm, E = 15 µm, K = 10 µm.

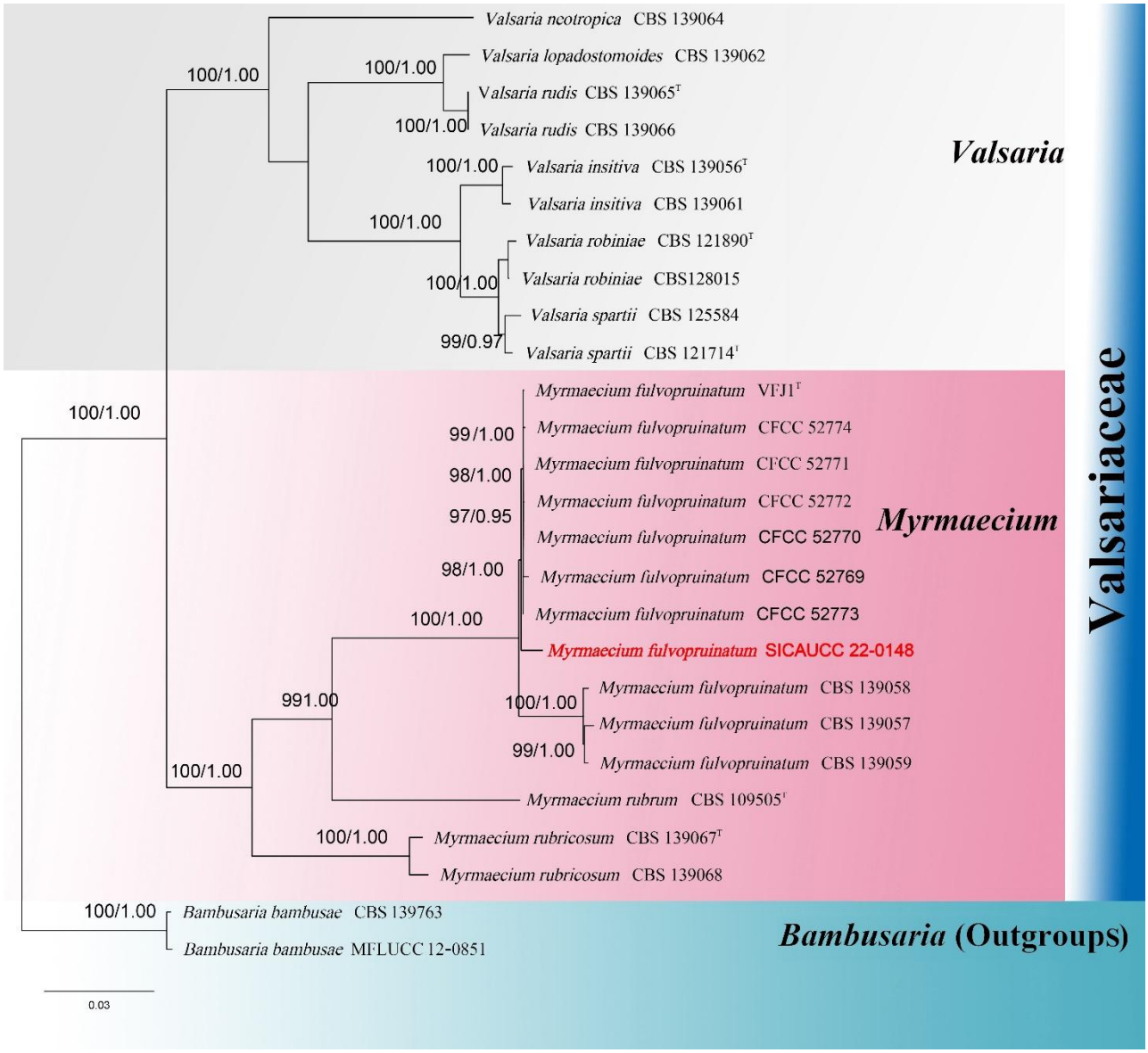


Figure 68 – Best scoring RAxML tree with a final likelihood value of -22,636.671919 based on combined ITS, LSU, *rpb*2 and *tef*1-α sequence data of related species. The tree is rooted with *Bambusaria bambusae* (MFLUCC 12-0851 and CBS 139763) in *Bambusaria.* Twenty-six strains were included in the combined analyses which comprised 6,674 characters (2,020 characters for ITS, 2,018 characters for LSU, 1,205 characters for *rpb*2 and 1,428 characters for *tef*1-α, including gap regions). The matrix had 1,412 distinct alignment patterns, with 24.56% undetermined characters and gaps. Estimated base frequencies were as follows; A = 0.242006, C = 0.265530, G = 0.278302, T = 0.214162; substitution rates AC = 1.273395, AG = 3.224359, AT = 1.290426, CG = 1.098891, CT = 8.579267, GT = 1.000000; gamma distribution shape parameter α = 0.185627. The Bayesian inference analyses was implemented by MrBayes v.3.2.2 with the best-fit model (GTR+I+G for ITS, LSU, *tef*1-α; SYM+I+G for *rpb*2) of evolution estimated with MrModeltest 2.2. The species determined in this study is indicated in red and bold. Bootstrap support values for maximum likelihood (MLBS, left) ⩾ 60% and Bayesian posterior probabilities (BYPP, right) ⩾ 0.90 are indicated at the nodes, respectively. Hyphens (-) represent support values less than 60% MLBS/0.90 BYPP. The ex-type superscript "T".

Aspergillaceae Link (= *Monascaceae* J. Schröt.).

We follow the latest treatment and updated accounts of *Aspergillaceae* in Zhang et al. (2021).

Penicillium Link, Magazin der Gesellschaft Natur forschenden Freunde Berlin 3 (1): 16 (1809).

The genus *Penicillium* (*Trichocomaceae*, *Eurotiales*) was first described in 1,809 by Johann Heinrich Friedrich Link. *Penicillium* species are of major importance in natural environments as well as food and drug production. The genus is found worldwide in various habitats, especially soil, vegetation, air, indoor environments, and contaminated foodstuff (Frisvad et al. 2004, Samson et al. 2010, Pangging et al. 2021). We follow the latest treatment and updated accounts of *Penicillium* in Alinta et al. (2025).

41. ***Penicillium citrinum*** Thom, Bureau Animal Industry 118: 61 (1910) Fig. 69

Index Fungorum number: IF165293; Facesoffungi number: FoF10546

Associated with rot disease on the green husks of the fruits of *Juglans regia*. Small, circular, dark spots with a brown-purple border can be seen on fruits, spots gradually enlarge and form brown depressions, causing the lesions to crack and resulting in premature fruit drop. Sexual morph: Not observed. Asexual morph: *Conidiophores* 28–69 × 3–7 μm ($\bar{x}$ = 46 × 5 μm, n = 20), mostly biverticillate, sometimes tri-verticillate; stipes smooth, monoverticillate, stipes smooth, vary greatly in length, septate. phialides ampulliform, 4–8 per verticil. *Conidia*, 2–6 × 2–5 μm ($\bar{x}$ = 4 × 3.5 μm, n = 50), finely rough to rough-walled, moderately, globose, often in chains.

Culture characteristics – Conidia germinate within 24 hours in sterile water, producing germ tubes from all around. Colonies on PDA reaching 30 mm diam., after 7 days at 25 ℃. The mycelium grows on the surface of the medium, initially compact and round, becoming widely effused, aerial mycelium with an undulated edge, white, sparse on surface, turn gray in the later stage. Reverse, same. Not produced pigmentation on PDA media.

Material examined – China, Sichuan Province, Guangyuan City, Chaotian District (36°32′28.28″N 105°52′26.37″E, alt. 554 m), on the green peel of rotten *Juglans regia* fruits, 19 May 2021, F.-H. Wang, WFH202105050 (SICAU 23-0075), living culture SICAUCC 23-0054.

GenBank numbers – SICAUCC 23-0054: PP060670 (ITS), PP057962 (LSU), PP003827 (SSU), PP061171 (*tub*2).

Note – *Penicillium citrinum* is a commonly occurring filamentous fungus with a worldwide distribution and it may well be one of the most commonly occurring eukaryotic life forms on earth (Pitt 1979, Houbrakenet et al. 2010, Mathew et al. 2010). In this study, our new isolates *P. citrinum* (SICAUCC 23-0054) clustered together with the strain of *P. citrinum* (RCEF 7060) with strong statistical support (100% MLBS/1.00 BYPP) (Fig. 70). We recognized our collection as *P. citrinum* because it clustered with the strain of *P. citrinum* (RCEF 7060) and was identical in morphology and molecular data. *Penicillium citrinum* has been reported as a plant pathogen causing fruit rot. This species has been isolated from various substrates such as soil, (tropical) cereals, spices and indoor environments (Samson et al. 2004). This is the first report of *P. citrinum* from *Juglans regia*.

Leotiomycetes O.E. Erikss. & Winka.

We follow the latest treatment and updated accounts of *Leotiomycetes* in Wu et al. (2023)

Helotiales Nannf.

The order *Helotiales* represents one of the largest groups of inoperculate discomycetes, comprising species of diverse lifestyle and morphology (Wang et al. 2006). However, the delimitation and relationships among most *Helotiales* families are obscure. (Schoch et al. 2009a 2009b, Lantz et al. 2011, Crous et al. 2014, Johnston et al. 2014, Chethana et al. 2021).

Sclerotiniaceae Whetzel, Mycologia 37(6): 652 (1945).

We follow the latest treatment and updated accounts of *Sclerotiniaceae* in Pärtel et al. (2017)

Botrytis P. Micheli ex Pers., Neues Mag. Bot. 1: 120 (1794).

We follow the latest treatment and updated accounts of *Botrytis* in Hou et al. (2022)

42. ***Botrytis cinerea*** Pers., Syn. meth. fung. (Göttingen) 2: 690 (1801) Fig. 71

Index Fungorum number: IF217312; Facesoffungi number: FoF03832

Associated with rot disease on the green husks of the fruits of *Juglans regia.* Small, circular, dark spots with a brown-purple border can be seen on fruits, in later stages, the lesions expand to form protruding scars, impeding the growth of the fruit. Sexual morph: Not observed. Asexual morph: *Hyphae* hyaline to pale brown, septate, 4–7 µm wide. *Conidiophores* 80–215 × 3–8 µm ($\bar{x}$ = 160 × 6 µm, n = 20), branched at top, erect, septate, subhyaline to pale brown. *Conidiogenous cells* 6–12 × 4–9 µm ($\bar{x}$ = 9 × 7 µm, n = 20), swollen at the apex. *Conidia* 7–13 × 3–7 µm ($\bar{x}$ = 9 × 6 µm, n = 20), in hyphae apex, elliptical to ovoid, unicellular, hyaline to pale brown.

Culture characteristics – Conidia germinate within 24 hours in sterile water, producing germ tubes from all around. Colonies on PDA reaching 30 mm diam., after 10 days at 25 ℃. The mycelium grows on the surface of the medium, pale grey, abundant aerial mycelium in dark grey irregular tufts that cover most of the surface. Reverse pale grey to buff brown. Not produced pigmentation on PDA media.

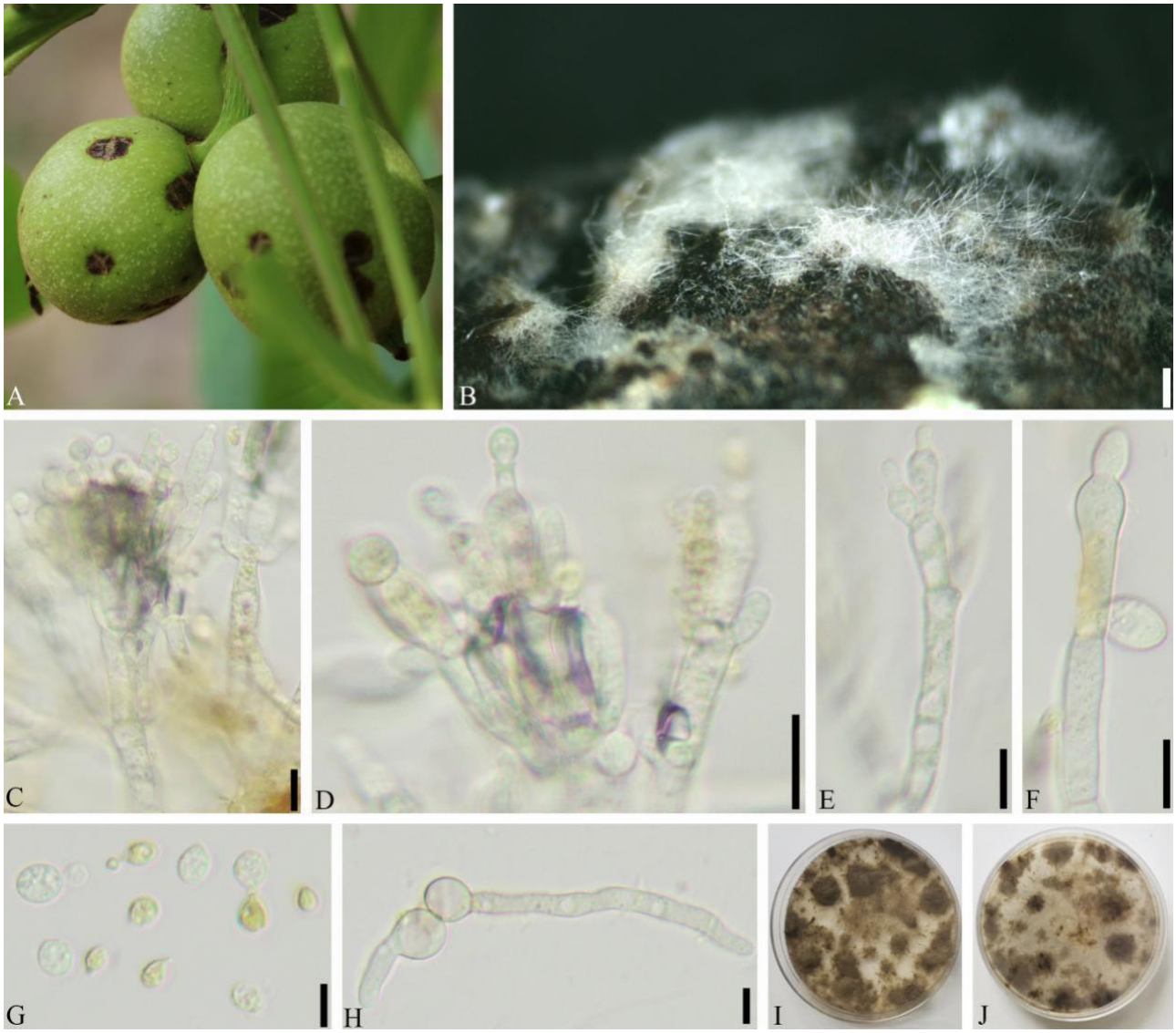


Figure 69 – *Penicillium citrinum* (SICAU 23-0075). A Symptoms of necrotic lesions observed on host. B Colonies on substrate. C–F Conidiophores. G Conidia. H Germinating conidia. I, J Colonies on PDA (I from above, J from below). Scale bars: B = 1000 µm, C–G = 10 µm, H = 5 µm.

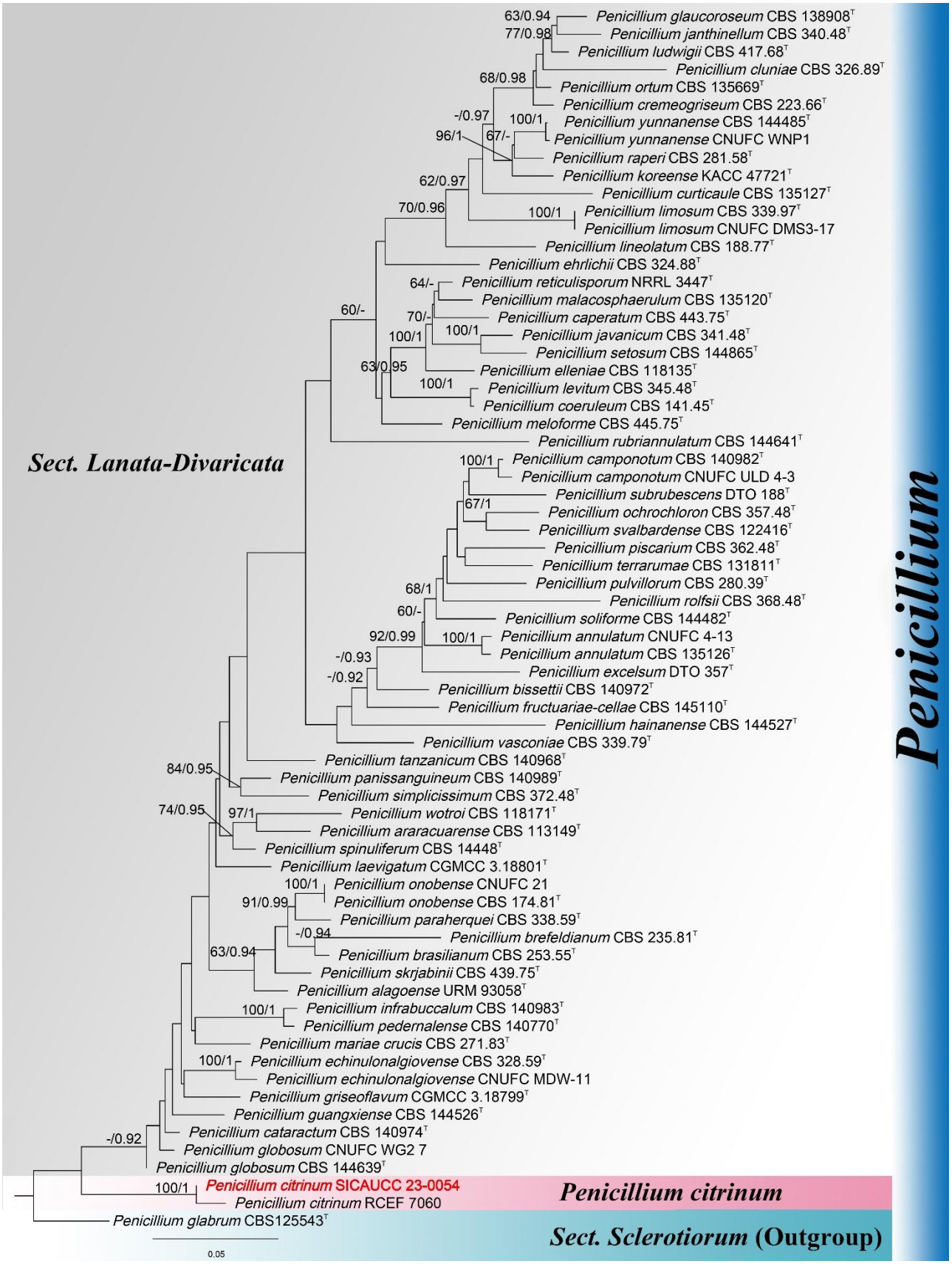


Figure 70 – Best scoring RAxML tree with a final likelihood value of -17,245.700588 based on combined ITS, *CaM* and *tub*2 sequence data of related species. The tree is rooted with *Penicillium glabrum* (CBS 125543^{T}) in *Penicillium*. Sixty-nine strains were included in the combined analyses which comprised 2,391 characters (1,185 characters for ITS, 652 characters for *CaM* and 552

characters for *tub*2, including gap regions). The matrix had 924 distinct alignment patterns, with 37.76% undetermined characters and gaps. Estimated base frequencies were as follows; A = 0.216288, C = 0.298027, G = 0.262393, T = 0.223292; substitution rates AC = 1.048595, AG = 2.984905, AT = 1.299914, CG = 0.621119, CT = 3.985777, GT = 1.000000; gamma distribution shape parameter α = 0.228620. The Bayesian inference analysis was implemented by MrBayes v.3.2.2 with the best-fit model (GTR+I+G for ITS, CAMD; HKY+I+G for *tub*2) of evolution estimated with MrModeltest 2.2. The species determined in this study is indicated in red and bold. Bootstrap support values for maximum likelihood (MLBS, left) ⩾ 60% and Bayesian posterior probabilities (BYPP, right) ⩾ 0.90 are indicated at the nodes, respectively. Hyphens (-) represent support values less than 60% MLBS/0.90 BYPP. The ex-type superscript "T".

Material examined – China, Sichuan Province, Dazhou City, Wanyuan City (32°1′41.09″N 108°7′32″E, alt. 932 m), On the green peel of rotten *Juglans regia* fruits, 20 May 2021, F.-H. Wang, WFH202105058 (SICAU 23-0076), living culture SICAUCC 23-0055.

GenBank numbers – SICAUCC 23-0055: PP060671 (ITS), PP003828 (SSU), PP061122 (*rpb*2), PP061106 (*gapdh*), PP061107 (*hsp*60).

Note – Our new isolates *Botrytis cinerea* (SICAUCC 23-0055) was placed in a strongly supported clade with *B. cinerea* (MUCL87) with strong statistical support (97% MLBS/0.99 BYPP) (Fig. 72). Nucleotide comparisons of *rpb*2, *gapdh*, and *hsp*60 (SICAUCC 23-0055) showed a high homology with the sequences of *B. cinerea* (MUCL 87), with a similarity of 99.8% (1093/1095, 0 gap), 100% (825/825, 0 gap), and 100% (603/603, 0 gap), respectively. Our strain is morphologically identical to *B. cinerea*. Based on morphological characters and phylogenetic analyses, we determine our specimens as *B. cinerea*. This is the first report of *B. cinerea* from *Juglans regia* in China.

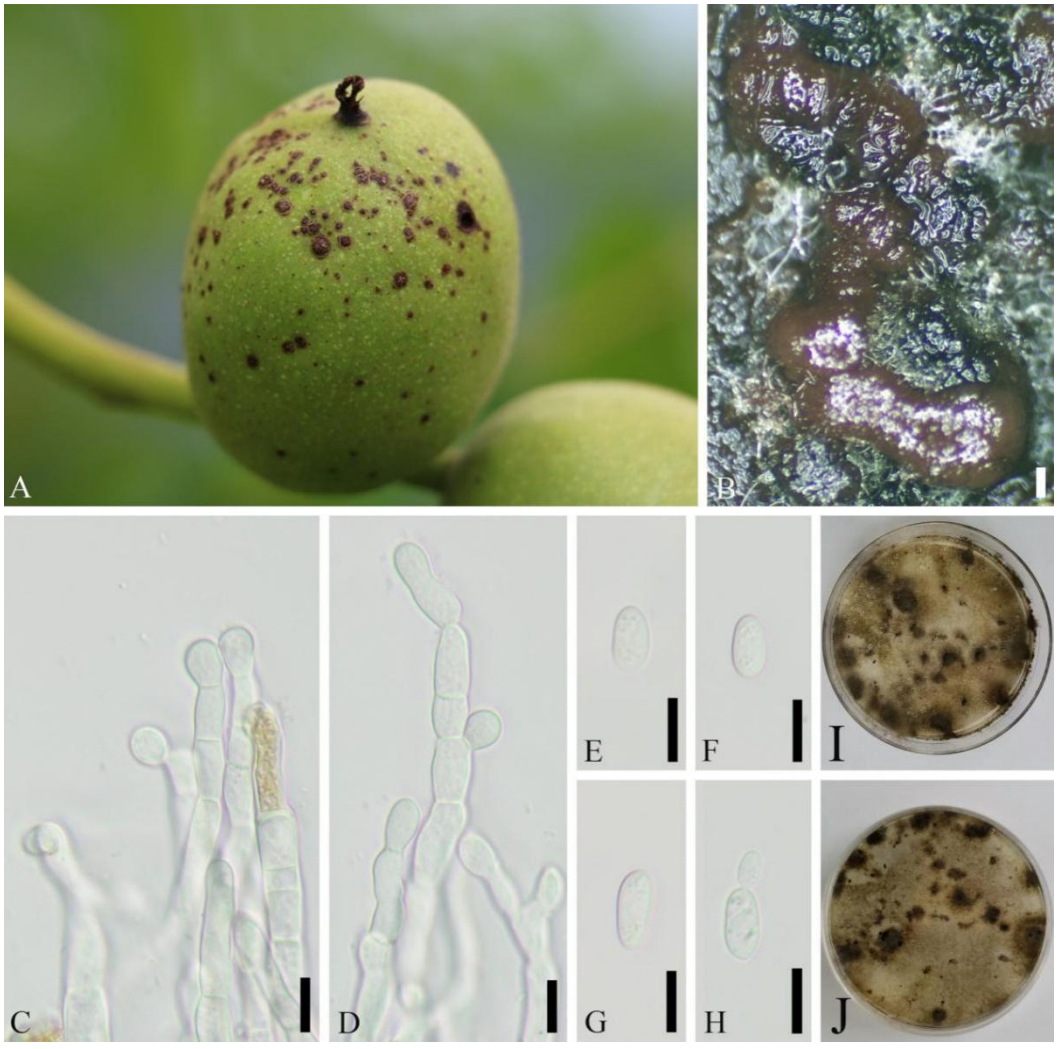


Figure 71 – *Botrytis cinerea* (SICAU 23-0076). A Symptoms of necrotic lesions observed on host. B Colonies on substrate. C, D Conidiophores. E–G Conidia. H Germinating conidium. I, J Colonies on PDA (I from above, J from below). Scale bars: B = 500 µm, C–H = 10 µm.

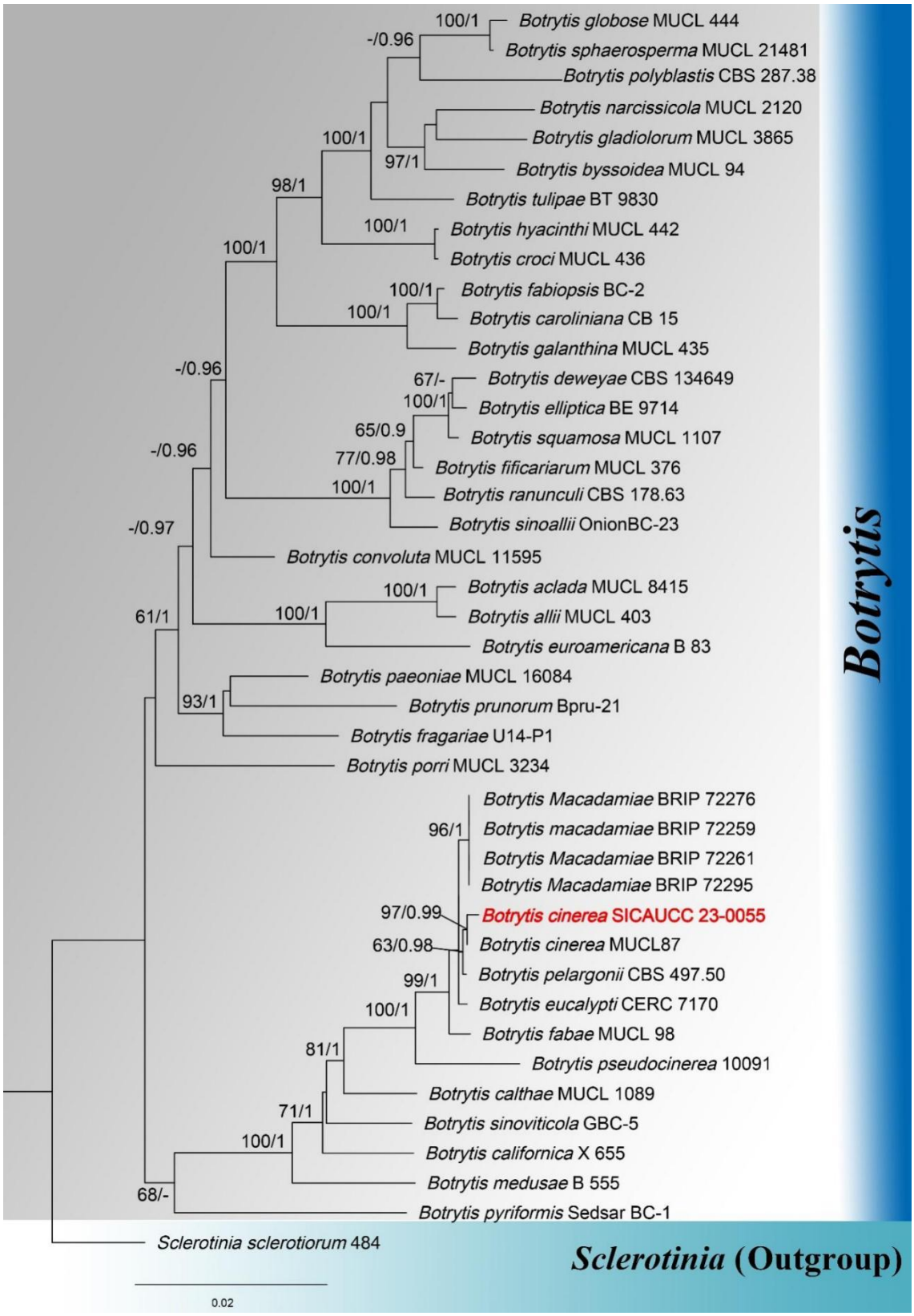


Figure 72 – Best scoring RAxML tree with a final likelihood value of -11,693.149716 based on combined *gapdh*, *hsp*60 and *rpb*2 sequence data of related species. The tree is rooted with *Sclerotinia*

sclerotiorum (484) in *Sclerotinia*. Forty-two strains were included in the combined analyses which comprised. 3,096 characters (956 characters for *gapdh*, 987 characters for *hsp*60 and 1,152 characters for *rpb*2, including gap regions). The matrix had 639 distinct alignment patterns, with 5.38% undetermined characters and gaps. Estimated base frequencies were as follows; A = 0.271893, C = 0.237149, G = 0.235491, T = 0.255468; substitution rates AC = 1.541607, AG = 4.269044, AT = 1.143021, CG = 0.578382, CT = 11.345111, GT = 1.000000; gamma distribution shape parameter α = 0.224463. The Bayesian inference analysis was implemented by MrBayes v.3.2.2 with the best-fit model (SYM+I+G for *gapdh*, *hsp*60; GTR+I+G for *rpb*2) of evolution estimated with MrModeltest 2.2. The species determined in this study is indicated in red and bold. Bootstrap support values for maximum likelihood (MLBS, left) ⩾ 60% and Bayesian posterior probabilities (BYPP, right) ⩾ 0.90 are indicated at the nodes, respectively. Hyphens (-) represent support values less than 60% MLBS/0.90 BYPP. The ex-type superscript "T".

Sordariomycetes O.E. Erikss. & Winka.
Amphisphaeriales D. Hawksw. & O.E. Erikss.

Amphisphaeriales was recently accepted with 21 families, including several genera in *Amphisphaeriales* genera incertae sedis (Wijayawardene et al. 2017, 2022, Hyde et al. 2020b, Samarakoon et al. 2022). The divergence time of this order has been estimated at 133 Mya (Hyde et al. 2020b).

Sporocadaceae Corda.

Sporocadaceae was introduced by Corda (1842) to accommodate *Sporocadus* as the type genus. *Sporocadaceae* species typically possess appendage bearing conidia and are important as endophytes, saprobes or pathogens on leaves, twigs, branches, fruits of flowering plants and gymnosperms, and as parasites on humans and animals (Liu et al. 2019, Hyde et al. 2020b). Following recent revision of the morphology and multigene phylogeny, there are 35 genera in *Sporocadaceae*, with the divergence time of *Sporocadaceae* estimated at 52.22 Mya (Wijayawardene et al. 2017, 2022, Hyde et al. 2020b).

Neopestalotiopsis Maharachch., K.D. Hyde & Crous, Stud. Mycol. 79: 135 (2014).

Neopestalotiopsis species are important plant pathogens, causing post-harvest diseases, fruit rots, and leaf blights in plants worldwide (Gualberto et al. 2021, Prasannath et al. 2021, Sun et al. 2021a). *Pestalotiopsis* was divided into three genera by Maharachchikumbura et al. (2014), *Pestalotiopsis* and *Pseudopestalotiopsis* are very similar to *Neopestalotiopsis* in morphology but can be distinguished based on conidial pigmentation and molecular phylogeny. Currently, 92 records are listed in Species Fungorum (http://www.speciesfungorum.org/Index.htm, September 2024).

43. ***Neopestalotiopsis chiangmaiensis*** Tibpromma & K.D. Hyde, Fungal Divers. (2018)

Fig. 73

Index Fungorum number: IF554515; Facesoffungi number: FoF04525

Associated with leaf spots on the living leaves of *Juglans regia*. Leaves distal to the infection turn light green in the interveinal areas and turn scorch brown colour from the margins. Sexual morph: Not observed. Asexual morph: *Conidiomata* 84–175 × 62–128 μm ($\bar{x}$ = 154 × 84 μm, n = 20), acervuli, with basal stroma and lateral wall of 1–2 layers, thin, wall cells pale brown, *textura angularis*. *Conidiophores* reduced to conidiogenous cells. *Conidiogenous cells* enteroblastic, discrete, simple, short, filiform. *Conidia* 16–23 × 6–9 μm ($\bar{x}$ = 21 × 7 μm, n = 20), fusiform to ellipsoid, straight to slightly curved, 4-septate, three median cells doliiform or subcylindrical, wall verruculose, versicoloured, septa darker than the rest of the cell basal cell conic, hyaline, thin and smooth-walled, with 2–3 tubular apical appendages (mostly 3).

Culture characteristics – Conidia germinate within 12 h in sterile water, and each cell is capable of producing germ tubes. Colonies on PDA reaching 60 mm diam., after 14 days at 25 ℃ The mycelium grows on the surface of the medium, dense, aerial mycelium on surface fat or raised, effuse

with floccose texture, margin crenate and filamentous, white to cream at the margin, white in the center, slightly convex, form a ring shape. Reverse, cream to faint yellow at the margin, cream in the center and obvious yellow rings. Not produced pigmentation on PDA media.

Material examined – Sichuan Province, Luzhou City, Guling County (27°56′49″N 105°51′28″E, alt. 1090 m), on leaves of *Juglans regia*, 25 April 2022, F.-H. Wang, WFH202204029 (SICAU 22-0154), living culture SICAUCC 22-0156.

GenBank numbers – SICAUCC 22-0156: OP963854 (ITS), OQ281392 (*tef*1-α), OQ281426 (*tub*2).

Note – In this study, our isolate *Neopestalotiopsis chiangmaiensis* (SICAUCC 22-0156) shares overlapped size range of conidia (24–28 × 6–9 μm vs. 18–22 × 8–11 μm) with the type of *N. chiangmaiensis* (MFLUCC 18-0113) (Tibpromma et al. 2018a). Phylogeny also shows that our collection grouped with *N. chiangmaiensis* (MFLUCC 18-0113) with strong statistical support (93% MLBS/1.00 BYPP) (Fig. 74). Nucleotide comparisons of *tef*1-α and *tub*2 (SICAUCC 22-0156) also showed a high homology with the sequences of *N. chiangmaiensis* (MFLUCC 18-0113 ex-type), with a similarity of 100% (482/482, 0 gap) and 99.6% (447/449, 2 gaps), respectively. Based on morphological characters and phylogenetic analyses, we determine our specimens as *N. chiangmaiensis*. Therefore, we introduce our isolate as a new host record of *N. chiangmaiensis* from dead leaves of *Juglans regia*.

Pestalotiopsis Steyaert, Bull. Jard. bot. État Brux. 19: 300 (1949).

Pestalotiopsis was erected by Steyaert (1949) with *P. guepinii* (Desm.) Steyaert as the type species. Species with 5-celled conidia (4-septate) were grouped within *Pestalotiopsis*. *Pestalotiopsis* is a complex genus and has considerable phenotypic diversity (Maharachchikumbura et al. 2014). *Pestalotiopsis* species have a cosmopolitan distribution worldwide, as saprobes, endophytes or opportunistic pathogens on economically important plants, as well as ornamental crops (Maharachchikumbura et al. 2014, 2016a, Crous et al. 2017, Ariyawansa & Hyde 2018, Razaghi et al. 2024). There are 384 epithets listed in Species Fungorum (http://www.speciesfungorum.org/Index.htm, September 2024).

44. ***Pestalotiopsis kenyana*** Maharachch., K.D. Hyde & Crous, Stud. Mycol. 79: 166 (2014) Fig. 75

Index Fungorum number: IF809741; Facesoffungi number: FoF06981

Associated with blight symptom on living twigs of *Juglans regia*. Symptoms manifest as black necrosis on the current year's new branches, with small black bumps protruding from the bark. When moist, these bumps release black conidia. Sexual morph: Not observed. Asexual morph: *Conidiophores* 12–30 × 2–4 μm ($\bar{x}$ = 20 × 3 μm, n = 40), unbranched, reduced to conidiogenous cells. *Conidiogenous cells* discrete, holoblastic, simple, filiform, smooth, thin-walled, hyaline. *Conidia* 20–28 × 5–9 μm ($\bar{x}$ = 24 × 7 μm, n = 40), fusoid to ellipsoid, straight to slightly curved, 4-septate, basal cell conic to obconic with obtuse end, hyaline, thin-walled, verruculose, 3–6 μm long($\bar{x}$ = 4 μm), three median cells, doliiform, concolorous, hyaline becoming brown with age, together 12–17 μm long ($\bar{x}$ = 14 μm), second cell from base 4–6 μm long ($\bar{x}$ = 5 μm); third cell 4–6 μm long ($\bar{x}$ = 4.5 μm); fourth cell 4–5 μm long ($\bar{x}$ = 4 μm); apical cell hyaline, conic 3–6 μm long ($\bar{x}$ = 5 μm), with 2(–3) tubular apical appendages; appendages arising from the apex of the apical cell, unbranched, 9–14 μm long ($\bar{x}$ = 12 μm); single basal appendage usually present, 3–6 μm long ($\bar{x}$ = 4 μm), tubular, unbranched, centric.

Culture characteristics – Conidia germinate within 12 h in sterile water, and each cell is capable of producing germ tubes. Colonies on PDA reaching 60 mm diam., after 9 days at 25 ℃ The mycelium grows on the surface of the medium, with irregular edge, whitish to pale yellow-coloured, with sparse aerial mycelium on the central surface and dark brown to black conidial masses. Reverse, cream to faint yellow at the margin, cream in the center and obvious yellow rings. Not produced pigmentation on PDA media.

Material examined – China, Sichuan Province, Yibin City, Junlian County (28°11′36.37″N 104°34′5.49″E, alt. 616 m), on living twigs of *Juglans regia*, 26 April 2022, F.-H. Wang, WFH202204045 (SICAU 22-0157), living culture SICAUCC 22-0159.

GenBank numbers – SICAUCC 22-0159: OP963857 (ITS), OQ281395 (*tef*1-α), OQ281427 (*tub*2).

Note – Phylogeny shows that our collection *Pestalotiopsis kenyana* (SICAUCC 22-0159) clusters with the type *P. kenyana* (CBS 442.67) with strong statistical support (95% MLBS/0.99 BYPP) (Fig. 76). Nucleotide comparisons of ITS, *tef*1-α and *tub*2 (SICAUCC 22-0159) also showed a high homology with the sequences of *P. kenyana* (CBS 442.67 ex-type), with a similarity of 99.8% (542/543, 0 gap), 100% (481/481, 0 gap) and 100% (448/448, 0 gaps), respectively. Both isolates share similar morphology in having overlapped size range of conidia (20–28 × 5–9 µm vs. 23–28 × 7–9 µm) (Maharachchikumbura et al. 2014). Therefore, we introduce our collection as a new host record of *P. kenyana* from living leaves of *Juglans regia*. *Pestalotiopsis kenyana* was initially introduced by Maharachchikumbura et al. (2014) from branch of *Coffea* sp. in Kenya.

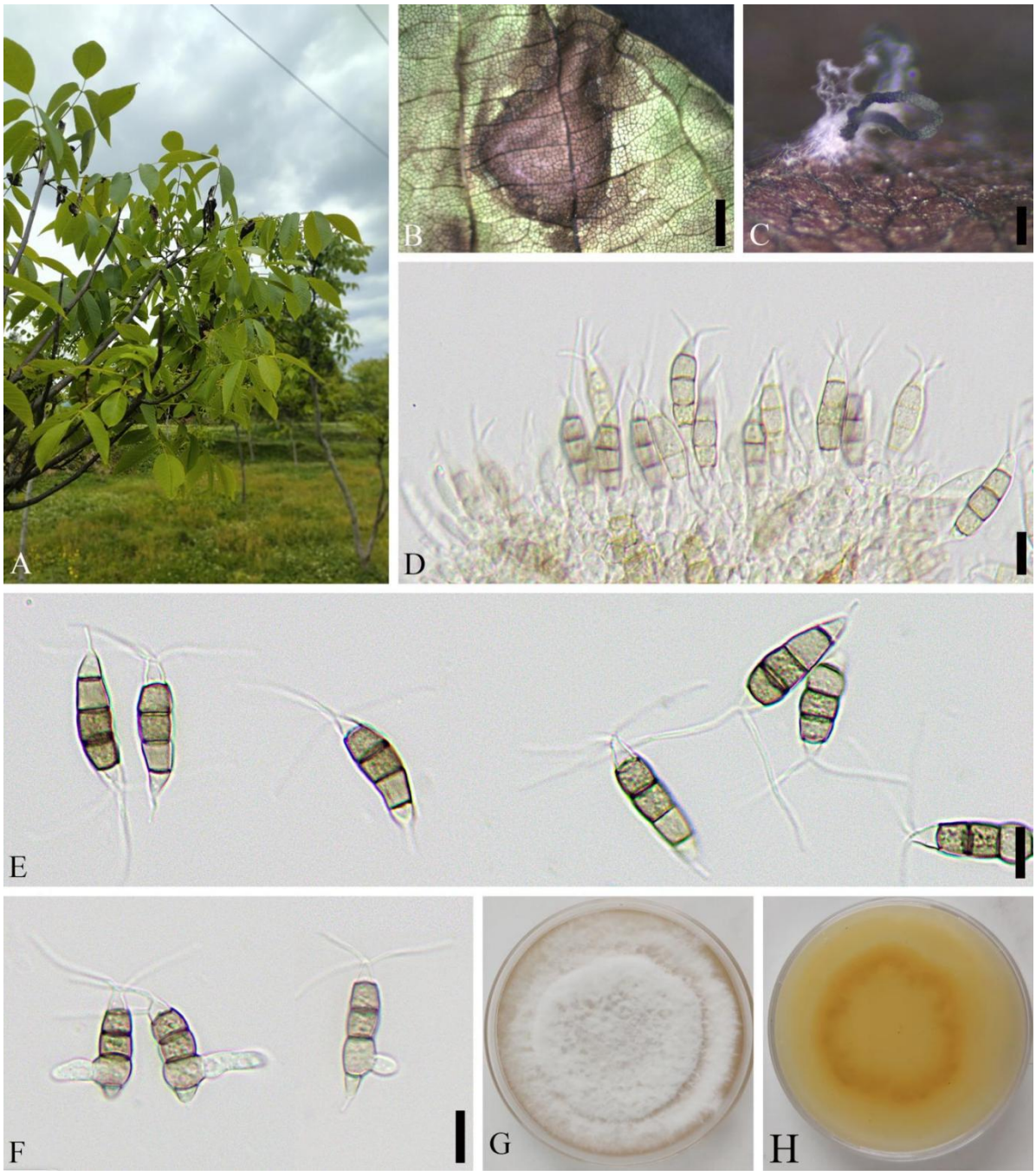


Figure 73 – *Neopestalotiopsis chiangmaiensis* (SICAU 22-0154). A, B Symptoms of leaf spots observed on host. C Black conidial mass released. D Conidiogenous cells and conidia. E Conidia. F Germinating conidia. G, H Colonies on PDA (G from above, H from below). Scale bars: B = 5 mm, C = 1000 µm, D, F = 15 µm, E = 10 µm.

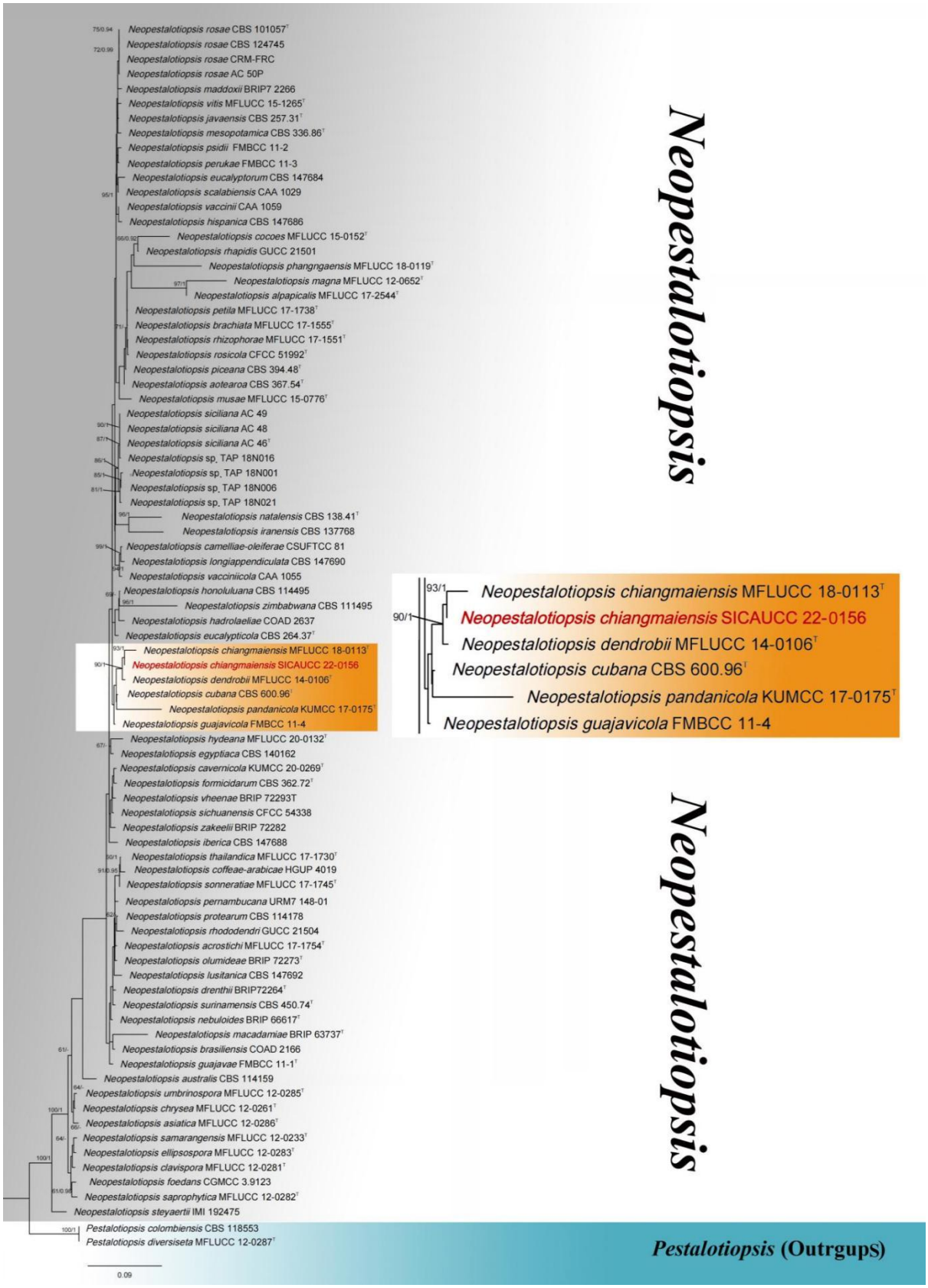


Figure 74 – Best scoring RAxML tree with a final likelihood value of -18,011.330038 based on combined ITS, *tef*1-α and *tub*2 sequence data of related species. The tree is rooted with *Pestalotiopsis colombiensis* (CBS 118553) and *P. diversiseta* (MFLUCC 12-0287) in *Pestalotiopsis*. Eighty-three strains were included in the combined analyses which comprised 3,841 characters (1,176 characters for *tef*1-α, 1,483 characters for ITS and 1,180 characters for *tub*2, including gap regions). The matrix had 1,512 distinct alignment patterns, with 55.08% undetermined characters and gaps. Estimated base frequencies were as follows; A = 0.237696, C = 0.270360, G = 0.222566, T = 0.269378; substitution rates AC = 0.954248, AG = 2.541582, AT = 1.015054, CG = 0.986206, CT = 2.669358, GT = 1.000000; gamma distribution shape parameter α = 1.756115. The Bayesian inference analysis was implemented by MrBayes v.3.2.2 with the best-fit model (GTR+G for *tef*1-α; SYM+I+G for ITS; K80+G for *tub*2) of evolution estimated with MrModeltest 2.2. The species determined in this study is indicated in red and bold. Bootstrap support values for maximum likelihood (MLBS, left) ⩾ 60% and Bayesian posterior probabilities (BYPP, right) ⩾ 0.90 are indicated at the nodes, respectively. Hyphens (-) represent support values less than 60% MLBS/0.90 BYPP. The ex-type superscript "T".

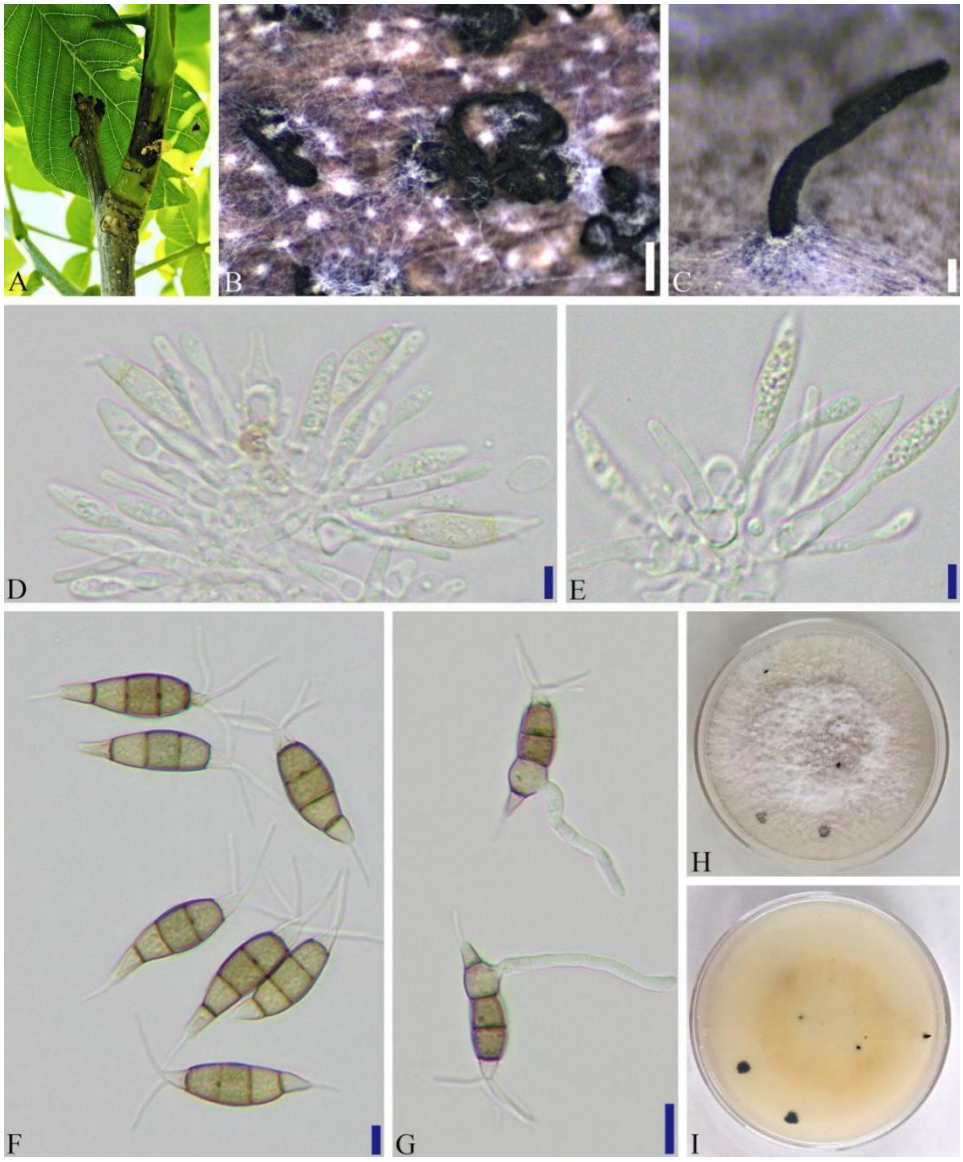


Figure 75 – *Pestalotiopsis kenyana* (SICAU 22-0157). A Symptomatic manifestation on host plants. B, C Black conidial mass released. D, E Conidiogenous cells with conidiophores and conidia. F Conidia. G Germinating conidia in sterile water. H, I Colonies on PDA (H from above, I from below). Scale bars: B = 1000 μm, C = 500 μm, G = 10 μm, D-F = 5 μm.

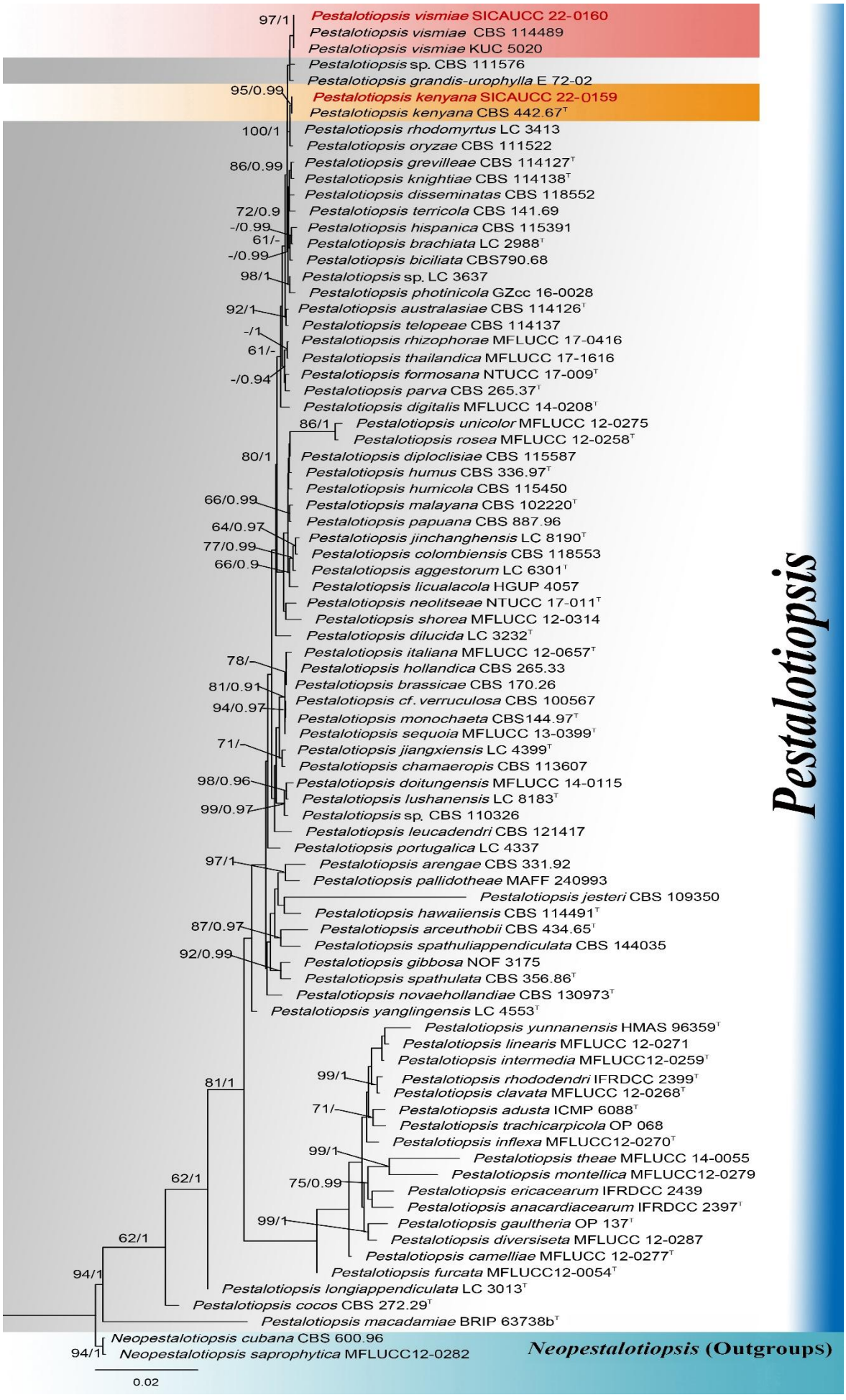

Pestalotiopsis vismiae SICAUCC 22-0160
Pestalotiopsis vismiae CBS 114489
Pestalotiopsis vismiae KUC 5020
Pestalotiopsis sp. CBS 111576
Pestalotiopsis grandis-urophylla E 72-02
Pestalotiopsis kenyana SICAUCC 22-0159
Pestalotiopsis kenyana CBS 442.67T
Pestalotiopsis rhodomyrtus LC 3413
Pestalotiopsis oryzae CBS 111522
Pestalotiopsis grevilleae CBS 114127T
Pestalotiopsis knightiae CBS 114138T
Pestalotiopsis disseminatas CBS 118552
Pestalotiopsis terricola CBS 141.69
Pestalotiopsis hispanica CBS 115391
Pestalotiopsis brachiata LC 2988T
Pestalotiopsis biciliata CBS790.68
Pestalotiopsis sp. LC 3637
Pestalotiopsis photinicola GZcc 16-0028
Pestalotiopsis australasiae CBS 114126T
Pestalotiopsis telopeae CBS 114137
Pestalotiopsis rhizophorae MFLUCC 17-0416
Pestalotiopsis thailandica MFLUCC 17-1616
Pestalotiopsis formosana NTUCC 17-009T
Pestalotiopsis parva CBS 265.37T
Pestalotiopsis digitalis MFLUCC 14-0208T
Pestalotiopsis unicolor MFLUCC 12-0275
Pestalotiopsis rosea MFLUCC 12-0258T
Pestalotiopsis diploclisiae CBS 115587
Pestalotiopsis humus CBS 336.97T
Pestalotiopsis humicola CBS 115450
Pestalotiopsis malayana CBS 102220T
Pestalotiopsis papuana CBS 887.96
Pestalotiopsis jinchanghensis LC 8190T
Pestalotiopsis colombiensis CBS 118553
Pestalotiopsis aggestorum LC 6301T
Pestalotiopsis licualacola HGUP 4057
Pestalotiopsis neolitseae NTUCC 17-011T
Pestalotiopsis shorea MFLUCC 12-0314
Pestalotiopsis dilucida LC 3232T
Pestalotiopsis italiana MFLUCC 12-0657T
Pestalotiopsis hollandica CBS 265.33
Pestalotiopsis brassicae CBS 170.26
Pestalotiopsis cf. verruculosa CBS 100567
Pestalotiopsis monochaeta CBS144.97T
Pestalotiopsis sequoia MFLUCC 13-0399T
Pestalotiopsis jiangxiensis LC 4399T
Pestalotiopsis chamaeropis CBS 113607
Pestalotiopsis doitungensis MFLUCC 14-0115
Pestalotiopsis lushanensis LC 8183T
Pestalotiopsis sp. CBS 110326
Pestalotiopsis leucadendri CBS 121417
Pestalotiopsis portugalica LC 4337
Pestalotiopsis arengae CBS 331.92
Pestalotiopsis pallidotheae MAFF 240993
Pestalotiopsis jesteri CBS 109350
Pestalotiopsis hawaiiensis CBS 114491T
Pestalotiopsis arceuthobii CBS 434.65T
Pestalotiopsis spathuliappendiculata CBS 144035
Pestalotiopsis gibbosa NOF 3175
Pestalotiopsis spathulata CBS 356.86T
Pestalotiopsis novaehollandiae CBS 130973T
Pestalotiopsis yanglingensis LC 4553T
Pestalotiopsis yunnanensis HMAS 96359T
Pestalotiopsis linearis MFLUCC 12-0271
Pestalotiopsis intermedia MFLUCC12-0259T
Pestalotiopsis rhododendri IFRDCC 2399T
Pestalotiopsis clavata MFLUCC 12-0268T
Pestalotiopsis adusta ICMP 6088T
Pestalotiopsis trachicarpicola OP 068
Pestalotiopsis inflexa MFLUCC12-0270T
Pestalotiopsis theae MFLUCC 14-0055
Pestalotiopsis montellica MFLUCC12-0279
Pestalotiopsis ericacearum IFRDCC 2439
Pestalotiopsis anacardiacearum IFRDCC 2397T
Pestalotiopsis gaultheria OP 137T
Pestalotiopsis diversiseta MFLUCC 12-0287
Pestalotiopsis camelliae MFLUCC 12-0277T
Pestalotiopsis furcata MFLUCC12-0054T
Pestalotiopsis longiappendiculata LC 3013T
Pestalotiopsis cocos CBS 272.29T
Pestalotiopsis macadamiae BRIP 63738bT
Neopestalotiopsis cubana CBS 600.96
Neopestalotiopsis saprophytica MFLUCC12-0282
0.02
Pestalotiopsis
Neopestalotiopsis (Outgroups)

Figure 76 – Best scoring RAxML tree with a final likelihood value of -22,688.445061 based on combined ITS, *tef*1-α and *tub*2 sequence data of related species. The tree is rooted with *Neopestalotiopsis cubana* (CBS 600.96) and *N. saprophytica* (MFLUCC 12-0282) in *Neopestalotiopsis*. Eighty-three strains were included in the combined analyses which comprised 2,849 characters (651 characters for ITS, 1,098 characters for *tef*1-α and 1,100 characters for *tub*2, including gap regions). The matrix had 1,607 distinct alignment patterns, with 39.43% undetermined characters and gaps. Estimated base frequencies were as follows; A = 0.240374, C = 0.289196, G = 0.221500, T = 0.248929; substitution rates AC = 0.987536, AG = 3.146388, AT = 1.192239, CG = 0.991335, CT = 4.033263, GT = 1.000000; gamma distribution shape parameter α = 0.469395. The Bayesian inference analyses was implemented by MrBayes v.3.2.2 with the best-fit model (SYM+I+G for ITS; GTR+I+G for *tef*1-α; HKY+G for *tub*2) of evolution estimated with MrModeltest 2.2. The species determined in this study is indicated in red and bold. Bootstrap support values for maximum likelihood (MLBS, left) ⩾ 60% and Bayesian posterior probabilities (BYPP, right) ⩾ 0.90 are indicated at the nodes, respectively. Hyphens (-) represent support values less than 60% MLBS/0.90 BYPP. The ex-type superscript "T".

45. ***Pestalotiopsis vismiae*** (Petr.) J. Xiang Zhang & T. Xu, Mycotaxon 85: 96 (2003) Fig. 77

Index Fungorum number: IF373612; Facesoffungi number: FoF16297

Associated with fruits rot of *Carya illinoensis.* Initially, brown spots form on the epidermis of fruits, which later expand to cause epidermal decay. Sexual morph: Not observed. Asexual morph: *Conidiophores* reduced to conidiogenous cells. *Conidiogenous cells* discrete, holoblastic, simple, filiform, smooth, thin-walled, hyaline, and long. *Conidia* 19–25 × 4–7 μm ($\bar{x}$ = 22 × 5.5 μm, n = 40), fusoid to ellipsoid, straight to slightly curved, 4-septate, basal cell conic to obconic with obtuse end, hyaline, thin and verruculose, 2–4 μm long ($\bar{x}$ = 3 μm), with three median cells, doliiform, concolorous, yellow to pale brown, together 11–15 μm long ($\bar{x}$ = 14 μm); second cell from base, pale brown, 3–5 μm long ($\bar{x}$ = 4 μm); third cell, pale brown, 4–6 μm long ($\bar{x}$ = 5 μm); fourth cell, pale brown, 4–5 μm long ($\bar{x}$ = 4.5 μm), apical cell hyaline, conic to sometimes cylindrical, 3–5 μm long ($\bar{x}$ = 4 μm), with (2–)3 tubular apical appendages; appendages arising from apex of the apical cell, unbranched, 3–8 μm long ($\bar{x}$ = 6 μm); basal appendage present, 2–5 μm long ($\bar{x}$ = 4 μm), single, tubular, centric.

Culture characteristics – Conidia germinate within 12 h in sterile water, and each cell is capable of producing germ tubes. Colonies on PDA reaching 60 mm diam., after 8 days at 25 ℃ The mycelium grows on the surface of the medium, with irregular edge, circular, edge entire, whitish to sandy beige, with dense, aerial mycelium on surface, fruiting bodies black. Reverse of culture whitish to sandy beige. Not produced pigmentation on PDA media.

Material examined – China, Sichuan Province, Chengdu City, Chongzhou City (30°33′8.70″N 103°39′29.13″E, alt. 512 m), on green peel of *Carya illinoensis*, 6 September 2021, F.-H. Wang, WFH202109001 (SICAU 22-0158), living culture SICAUCC 22-0160.

GenBank numbers – SICAUCC 22-0160: OP963858 (ITS), OQ281396 (*tef*1-α), OQ281428 (*tub*2).

Note – As morphology largely overlaps with that of *Pestalotiopsis vismiae*, we therefore report our collection as a new record of *P. vismiae* from fruit rot of *Carya illinoensis* (*Juglandaceae*). Phylogeny, also indicates that our collection *P. vismiae* (SICAUCC 22-0160), clusters with *P. vismiae* (KUC 5020) and *P. vismiae* (CBS 114489) with strong statistical support (97% MLBS/1.00 BYPP) (Fig. 76). And was nearly identical to *P. vismiae* in the ITS, *tef*1-α and *tub*2 gene sequences. In particular, conidiogenous cells and conidial same shape that the two strains are the same species. This is the first report of *P. vismiae* from *Carya illinoensis* (*Juglandaceae*).

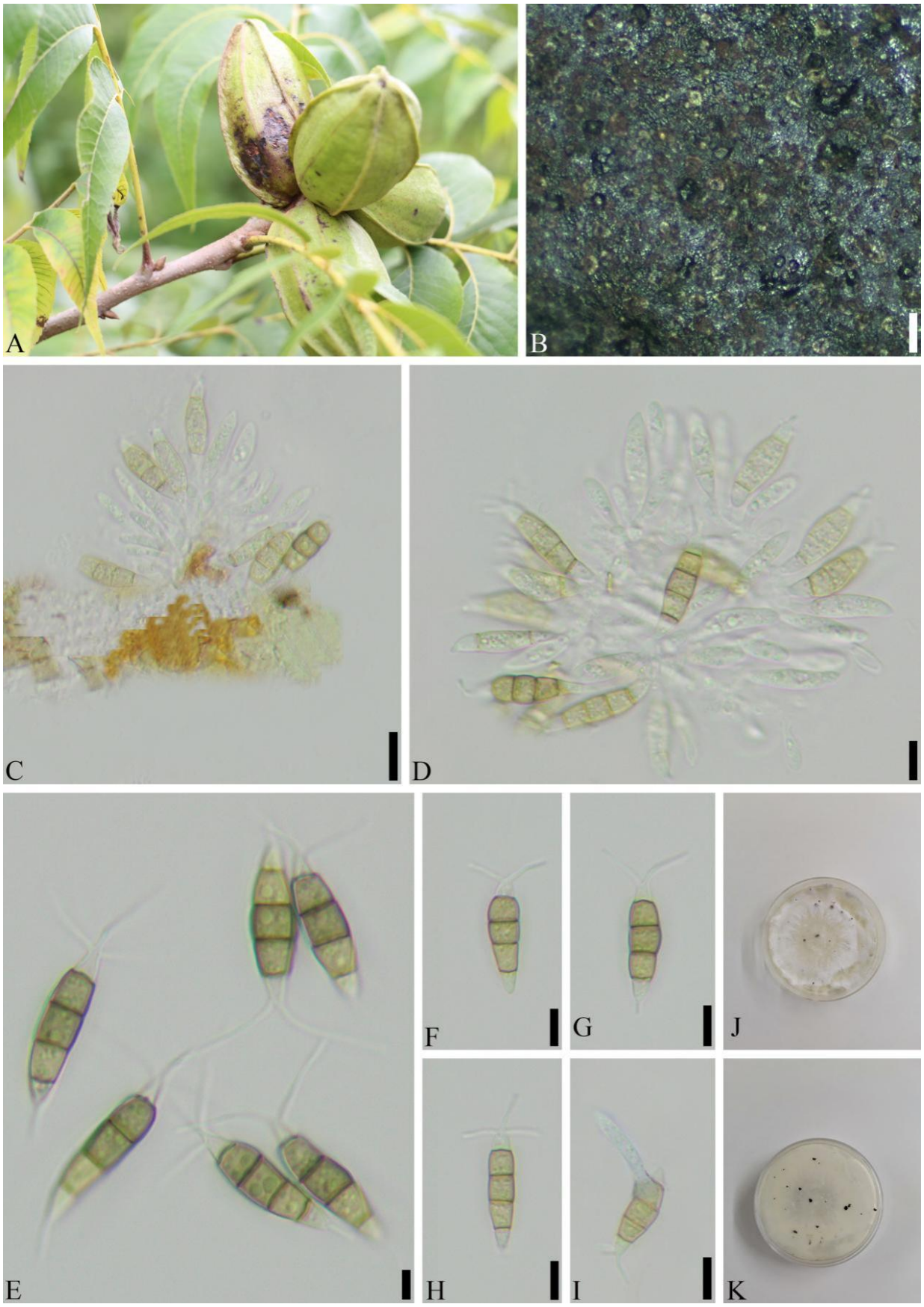


Figure 77 – *Pestalotiopsis vismiae* (SICAU 22-0158). A Symptoms of necrotic lesions observed on host. B Appearance of conidiomata on host substrate. C, D Conidiogenous cells with conidiophores and conidia. E–H Conidia. I Germinating conidium. J, K Colonies on PDA (J from above, K from below). Scale bars: B = 500 µm, C = 20 µm, D, F–I = 10 µm, E = 5 µm.

Diaporthales Nannf.

Diaporthaceae Höhn. ex Wehm., Am. J. Bot. 13: 638. 1926.

The family *Diaporthaceae* encompasses a diverse array of endophytic and phytopathogenic fungal species, as highlighted by Udayanga et al. (2011). This family was introduced and classified within the order *Diaporthales* by Von Höhnel (1917), further expanding our understanding of the fungal kingdom (Von Höhnel 1917, Udayanga et al. 2011, Dissanayake et al. 2017, Senanayake et al. 2017a). It is the second largest family in *Diaporthales*, containing 15 genera with over 500 species (Hyde et al. 2020a, b, c, Jayawardena et al. 2022).

Diaporthe Nitschke, Pyrenomyc. Germ. 2: 240 (1870).

Diaporthe is the type genus of *Diaporthaceae*, and it was established by Nitschke (1867). *Diaporthe* belongs in *Diaporthaceae*, *Diaporthales*, *Diaporthomycetidae*, *Sordariomycetes*, *Ascomycota* (Wijayawardene et al. 2022), and is a widely distributed genus with diverse ecological roles. *Diaporthe* species comprise pathogens, endophytes, and saprobes, and are associated with a wide range of hosts (Udayanga et al. 2011, 2012, 2014, Manawasinghe et al. 2019; Abeywickrama et al. 2020, Aumentado & Balendres 2024). *Diaporthe* is a large and taxonomically complex genus, with nearly a thousand epithets listed in Species Fungorum (http://www.speciesfungorum.org/Index.htm, September 2024).

46. ***Diaporthe citri*** (H.S. Fawc.) F.A. Wolf, Washington 33(7): 625 (1926) Fig. 78

Index Fungorum number: IF260952; Facesoffungi number: FoF16298

Saprobic on dead aerial branch of *Juglans regia*. Sexual morph: Not observed. Asexual morph: *Conidiomata* 210–370 × 190–280 μm ($\bar{x}$ = 320 × 250 μm, n = 10), pycnidial, initially immersed, erμmpent at maturity, globose to pyriform, black. *Conidiomata wall* parenchymatous, consisting of 3–4 layers of me dark brown *textura angularis*. *Conidiophores* 10–17 × 2–3 μm ($\bar{x}$ = 14 × 2.5 μm, n = 30), ampulliform, straight to sinuous, unbranched, hyaline, smooth. *Conidiogenous cells* phialidic, cylindrical, terminal, slight tapering towards apex, 1–2 μm diam. *Paraphyses* abundant among *conidiophores*, 18–37 × 1–2 μm ($\bar{x}$ = 30 × 2 μm, n = 30). *Alpha-conidia* 5–8 × 2–4 μm ($\bar{x}$ = 7 × 3 μm, n = 40), aseptate, hyaline, smooth, ovate to ellipsoidal, guttulate. *Beta-conidia* not observed.

Culture characteristics – Conidia germinating on sterile water within 12 h and germ tubes produced from both ends. The mycelium grows on the surface of the medium, with orderly edge, near circular growth, whitish to pale grey, cotton-like aerial mycelium on the central surface and dark brown to black conidial masse. Reverse side similar. Not produced pigmentation on PDA media.

Material examined – China, Sichuan Province, Yibin City, Junlian County (28°11′36.36″N 104°34′5.23″E, alt. 618 m), on dead aerial branch of *Juglans regia*, 26 April 2022, F.-H. Wang, WFH202204043 (SICAU 22-0127), living culture SICAUCC 22-0129.

GenBank numbers – SICAUCC 22-0129: OP963829 (ITS), OQ281367 (*tef*1-α), OQ281408 (*tub*2), OQ190498 (*cal*).

Note – *Diaporthe citri* (SICAUCC 22-0129) was recovered from a dead aerial branch of *Juglans regia* in China. Morphologically, our strain is similar to the ex-type strain of *D. citri* (CBS 135422). In the multigene phylogenetic analyses, our strain clustered with the ex-type strain of *D. citri* (CBS 135422) with strong statistical support (100% MLBS/1.00 BYPP). Nucleotide comparisons of ITS, *tef*1-α, *tub*2 and *cal* (SICAUCC 22-0129) also showed a high homology with the sequences of *D. citri* (CBS 135422 ex-type), with a similarity of 99.8% (572/573, 1 gap), 99.7% (344/345, 0 gap), 100% (519/519, 0 gap), and 100% (506/506, 0 gap), respectively. Based on morphological characters and phylogenetic analyses, we determine our specimens as *D. citri*. This study presents the first report of *D. citri* from a *J. regia* from China.

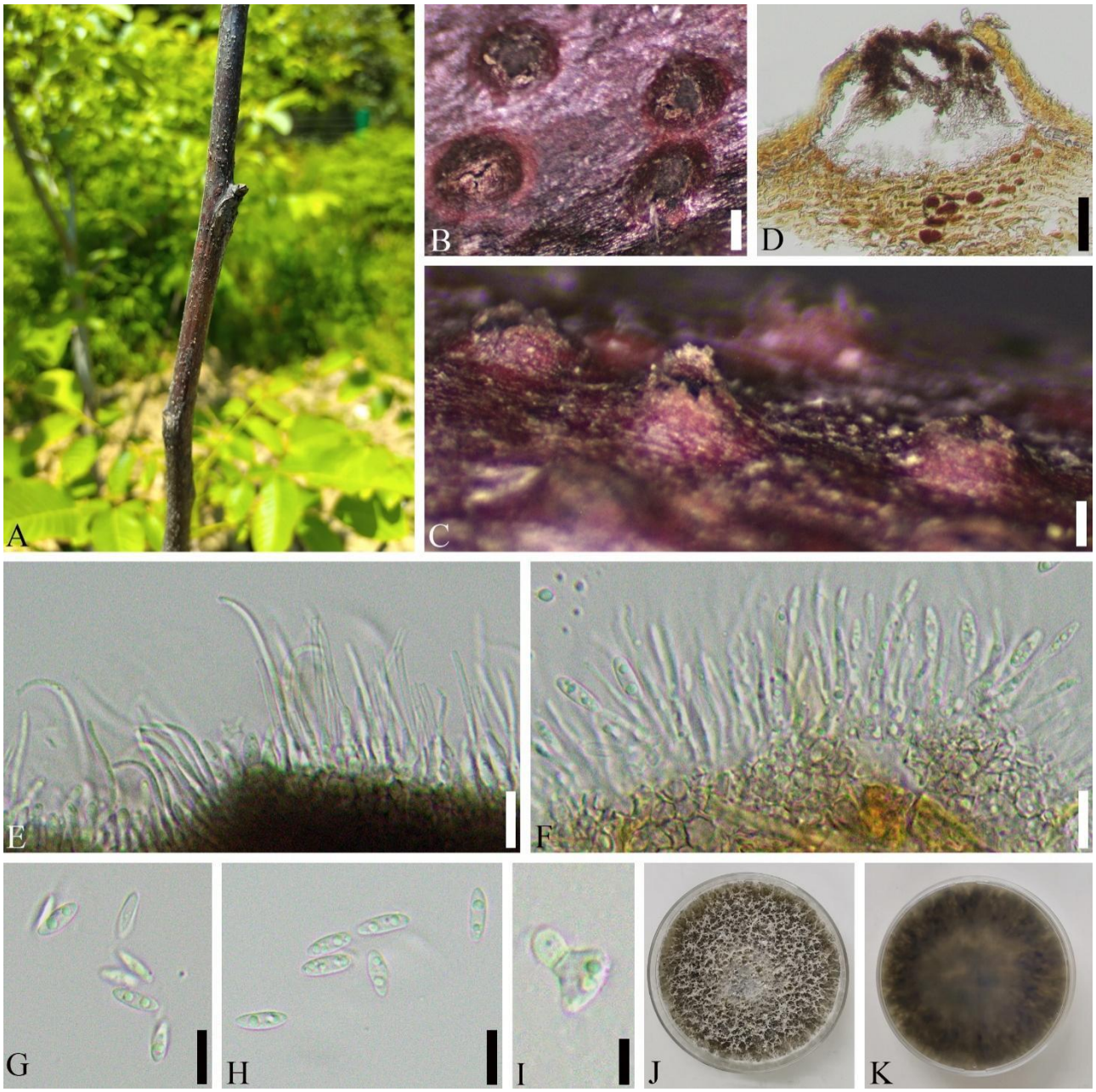


Figure 78 – *Diaporthe citri* (SICAU 22-0127). A *Juglans regia* branch affected by *D. citri*. B, C Conidiomata on the host. D Section through the conidiomata. E, F Conidiophores, paraphyses and conidiogenous cells. G, H Alpha-conidia. I Germinating alpha-conidium. J, K Colonies on PDA (J from above, K from below). Scale bars: B, C = 200 µm, D = 50 µm, E–I = 10 µm.

47. ***Diaporthe eres*** Nitschke, Pyrenomyc. Germ. 2: 245 (1870) Fig. 80

Index Fungorum number: IF172054; Facesoffungi number: FoF02182

Associated with blight symptom on living branches of *Juglans regia*. Symptoms include the development of brown spots on the branches of trees, which can lead to damage to twigs and branches, ultimately causing the branches to wither and die when the lesions encircle them completely. Sexual morph: Not observed. Asexual morph: *Conidiomata* 140–300 × 120–170 µm ($\bar{x}$ = 240 × 150 µm, n = 10), pycnidial, solitary, gregarious or confluence, semi-immersed, unilocular, globose, dark brown, ostiolate. *Ostiole* papillate. *Conidiomata wall* 10–30 µm ($\bar{x}$ = 24 µm, n = 20) wide, composed of thick-walled, brown, cells of *textura rectangle*. *Conidiophores* reduced to conidiogenous cells. *Conidiogenous cells* 10–24 × 1–2 µm ($\bar{x}$ = 17 × 2 µm; n = 20), densely aggregated, smooth, cylindrical, subulate, mostly straight, phialidic, simple, hyaline, *Alpha-conidia* 5–8 × 2–4 µm ($\bar{x}$ = 7 × 3 µm; n = 40), aseptate, hyaline, fusoid to ellipsoidal, 2- guttulate, smooth-

walled, asymmetrical, aseptate, truncate at the base, tapering towards both ends, mostly straight. *Beta-conidia* 15–27 × 0.5–1.5 μm ($\bar{x}$ = 21 × 1 μm; n = 40), aseptate, hyaline, smooth, apex and base bluntly rounded, slightly curved.

Culture characteristics – Conidia germinating on sterile water within 12 h and germ tubes produced from both ends. Colonies on PDA reaching 50 mm diam., after 14 days at 25 ℃. The mycelium grows on the surface of the medium surface with white or pale white thin aerial mycelium, initially appearing white and light yellow becoming chartreuse or olive from the center with age. After 16 days, exuding dark green to black conidial masses. Reverse white to pale yellow to light olive. Not produced pigmentation on PDA media.

Material examined – China, Sichuan Province, Garze Tibetan Autonomous Prefecture, Luding County, Kuiwu Village (29°40′32.27″N 102°11′34.56″E, alt. 1303 m), on dead aerial branch of *Juglans regia*, 18 July 2021, F.-H. Wang, WFH202107006 (SICAU 22-0128), living culture SICAUCC 22-0130.

GenBank numbers – SICAUCC 22-0130: OP963830 (ITS), OQ281368 (*tef*1-α), OQ281409 (*tub*2), OQ190499 (*cal*).

Note – *Diaporthe eres* was first introduced from *Ulmus* sp. in Germany (Udayanga et al. 2014, Guo et al. 2020). The species was reported as causing branch canker, leaf blight, and root rot on a wide range of hosts and distributions (Dissanayake et al. 2017c, Guo et al. 2020, Chaisiri et al. 2021, Du et al. 2021). *Diaporthe eres* has been used to be the name of the second largest species complex in *Diaporthe*. Our isolate *D. eres* (SICAUCC 22-0130) share close phylogenetic relationships to *D. eres* (CBS 200.39 and CBS587.79) in a monophyletic cladewith strong statistical support (96% MLBS/1.00 BYPP) (Fig. 79). Nucleotide comparisons of ITS, *tef*1-α, *tub*2 and *cal* (SICAUCC 22-0130) also showed a high homology with the sequences of *D. eres* (CBS 200.39 ex-type), with a similarity of 98.8% (575/582, 7 gaps), 100% (347/347, 0 gap), 100% (701/701, 0 gap), and 99.8% (462/463, 0 gap), respectively. This relationship morphologically fits as both species possess alpha and Beta-conidia. Also, the papillate ostiole, hyaline, smooth, unbranched, cylindrical, straight to sinuous conidiophores and phialidic, cylindrical, terminal conidiogenous cells support their close affinity. Based on morphological characters and phylogenetic analyses, we determine our specimens as *D. eres*.

48. ***Diaporthe mianyangense*** F.H. Wang & C.L. Yang, sp. nov. Fig. 81

Index Fungorum number: IF901572; Facesoffungi number: FoF15587

Etymology – Named after locality where the fungus was isolated for the first time.

Holotype – SICAU 23-0080.

Associated with blight symptom on living twigs of *Juglans regia*. Dead shoots can be observed in the lower branches or all over the affected tree. Affected branches or trunks show canker. When the canker girdles the affected area, part of the tree above the canker dies. Sexual morph: Not observed. Asexual morph: *Conidiomata* 185–310 × 150–280 μm ($\bar{x}$ = 260 × 200 μm, n = 10), light to dark brown, scattered, ellipsoidal patches on the host, pycnidial, pyriform, initially immersed, erumpent at maturity, globose to pyriform, reddish brown, coriaceous, ostiolate. *Ostiole* papillate. *Conidiomata wall* 10–108 μm wide, consisting of 4–5 layers of pale brown, thick-walled cells of *textura angularis*, usually thickened at the top. *Conidiophores* 7–11 × 1–2 μm ($\bar{x}$ = 9 × 1.5 μm, n = 20), septate, straight, branched, sometimes reduced to conidiogenous cells, hyaline, smooth. *Alpha-conidia* 4–7 × 2–3 μm ($\bar{x}$ = 6 × 2.5 μm, n = 40), aseptate, hyaline, smooth, often biguttulate, ovate to ellipsoidal, base subtruncate. *Beta-conidia* not observed.

Culture characteristics – Conidia germinating on sterile water within 12 h and germ tubes produced from both ends. Colonies on PDA reaching 50 mm diam., after 14 days at 25 ℃. The mycelium grows on the surface of the medium, circular, dense, flat, slightly raised, dull with entire edge, fluffy to floccose, with regular edge; white at the margin, becoming greyish at the center with black droplets, forming black pycnidial at the whole plane. Reverse, white to cream at the margin, greenish-grey at middle, black irregular plaque. Not produced pigmentation on PDA media.

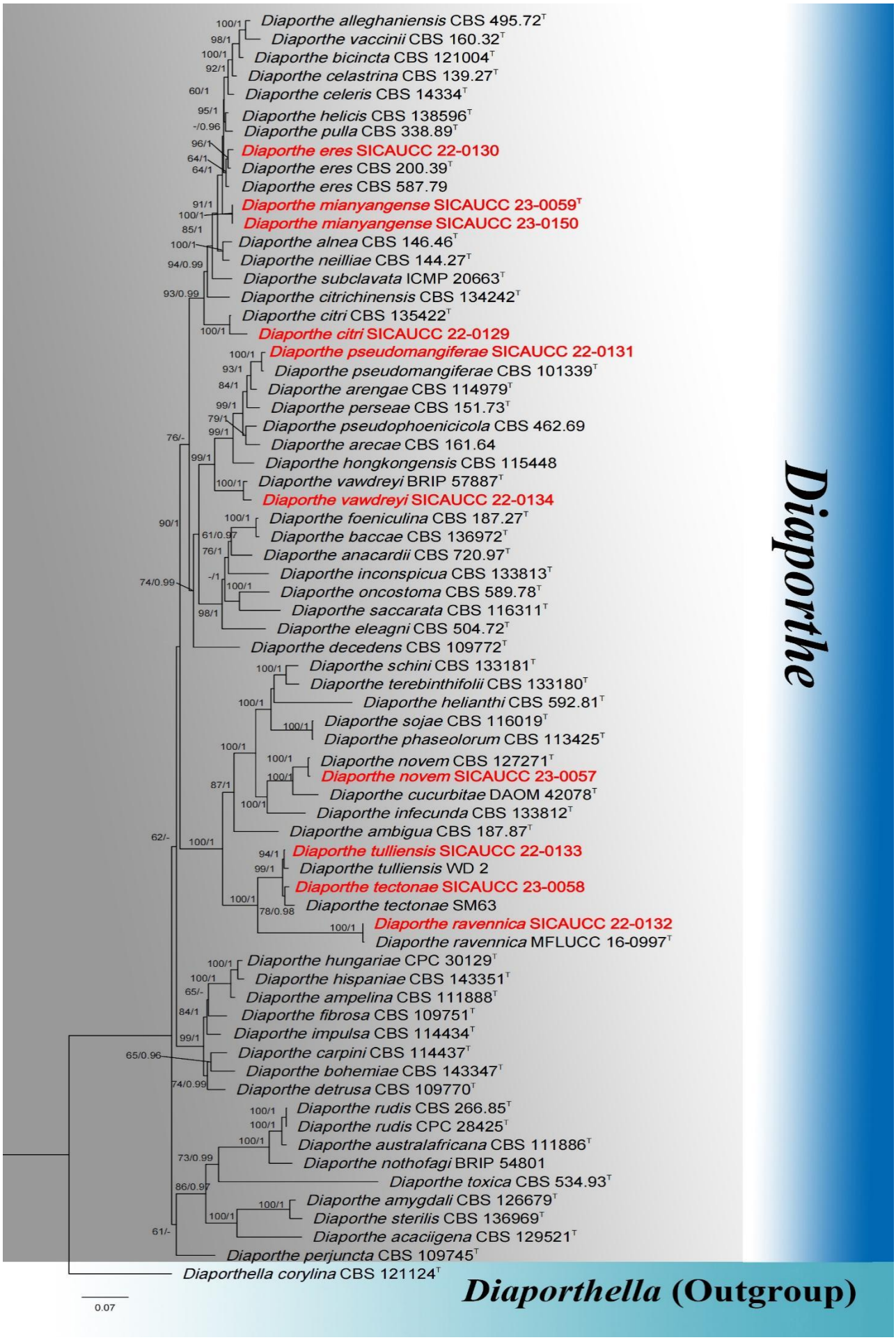

Diaporthe alleghaniensis CBS 495.72T
Diaporthe vaccinii CBS 160.32T
Diaporthe bicincta CBS 121004T
Diaporthe celastrina CBS 139.27T
Diaporthe celeris CBS 14334T
Diaporthe helicis CBS 138596T
Diaporthe pulla CBS 338.89T
Diaporthe eres SICAUCC 22-0130
Diaporthe eres CBS 200.39T
Diaporthe eres CBS 587.79
Diaporthe mianyangense SICAUCC 23-0059T
Diaporthe mianyangense SICAUCC 23-0150
Diaporthe alnea CBS 146.46T
Diaporthe neilliae CBS 144.27T
Diaporthe subclavata ICMP 20663T
Diaporthe citrichinensis CBS 134242T
Diaporthe citri CBS 135422T
Diaporthe citri SICAUCC 22-0129
Diaporthe pseudomangiferae SICAUCC 22-0131
Diaporthe pseudomangiferae CBS 101339T
Diaporthe arengae CBS 114979T
Diaporthe perseae CBS 151.73T
Diaporthe pseudophoenicicola CBS 462.69
Diaporthe arecae CBS 161.64
Diaporthe hongkongensis CBS 115448
Diaporthe vawdreyi BRIP 57887T
Diaporthe vawdreyi SICAUCC 22-0134
Diaporthe foeniculina CBS 187.27T
Diaporthe baccae CBS 136972T
Diaporthe anacardii CBS 720.97T
Diaporthe inconspicua CBS 133813T
Diaporthe oncostoma CBS 589.78T
Diaporthe saccarata CBS 116311T
Diaporthe eleagni CBS 504.72T
Diaporthe decedens CBS 109772T
Diaporthe schini CBS 133181T
Diaporthe terebinthifolii CBS 133180T
Diaporthe helianthi CBS 592.81T
Diaporthe sojae CBS 116019T
Diaporthe phaseolorum CBS 113425T
Diaporthe novem CBS 127271T
Diaporthe novem SICAUCC 23-0057
Diaporthe cucurbitae DAOM 42078T
Diaporthe infecunda CBS 133812T
Diaporthe ambigua CBS 187.87T
Diaporthe tulliensis SICAUCC 22-0133
Diaporthe tulliensis WD 2
Diaporthe tectonae SICAUCC 23-0058
Diaporthe tectonae SM63
Diaporthe ravennica SICAUCC 22-0132
Diaporthe ravennica MFLUCC 16-0997T
Diaporthe hungariae CPC 30129T
Diaporthe hispaniae CBS 143351T
Diaporthe ampelina CBS 111888T
Diaporthe fibrosa CBS 109751T
Diaporthe impulsa CBS 114434T
Diaporthe carpini CBS 114437T
Diaporthe bohemiae CBS 143347T
Diaporthe detrusa CBS 109770T
Diaporthe rudis CBS 266.85T
Diaporthe rudis CPC 28425T
Diaporthe australafricana CBS 111886T
Diaporthe nothofagi BRIP 54801
Diaporthe toxica CBS 534.93T
Diaporthe amygdali CBS 126679T
Diaporthe sterilis CBS 136969T
Diaporthe acaciigena CBS 129521T
Diaporthe perjuncta CBS 109745T
Diaporthella corylina CBS 121124T
0.07
Diaporthe
Diaporthella (Outgroup)

Figure 79 – Best scoring RAxML tree with a final likelihood value of -40,430.771816 based on combined ITS, *cal*, *his*, *tef*1-α and *tub*2 sequence data of related species. The tree is rooted with *Diaporthella corylina* (CBS 121124^{T}) in *Diaporthella*. Sixty-nine strains were included in the combined analyses which comprised 4,667 characters (659 characters for ITS, 849 characters for *cal*, 585 characters for *his*, 1,098 characters for *tef*1-α and 1,098 characters for *tub*2, including gap regions). The matrix had 2,285 distinct alignment patterns, with 44.60% undetermined characters and gaps. Estimated base frequencies were as follows; A = 0.216956, C = 0.327799, G = 0.237822, T = 0.217422; substitution rates AC = 1.013269, AG = 2.971518, AT = 1.149405, CG = 0.848195, CT = 4.265418, GT = 1.000000; gamma distribution shape parameter α = 0.366988. The Bayesian inference analysis was implemented by MrBayes v.3.2.2 with the best-fit model (GTR+I+G for ITS, *his*; SYM+I+G for *cal*; GTR+G for *tef*1-α; HKY+I+G for *tub*2) of evolution estimated with MrModeltest 2.2. The species determined in this study is indicated in red and bold. Bootstrap support values for maximum likelihood (MLBS, left) ⩾ 60% and Bayesian posterior probabilities (BYPP, right) ⩾ 0.90 are indicated at the nodes, respectively. Hyphens (-) represent support values less than 60% MLBS/0.90 BYPP. The ex-type superscript "T".

Material examined – China, Sichuan Province, Mianyang City, Yanting County (31°5′25.43″N 105°27′36.23″E, alt. 367 m), on dead aerial twig of *Juglans regia*, 28 April 2022, F.-H. Wang, WFH202204103-1 (SICAU 23-0080, holotype), ex-type living culture SICAUCC 23-0059. *Ibid*., WFH202204103-1B (SICAU 24-0036), living culture SICAUCC 23-0150.

GenBank numbers – SICAUCC 23-0059: PP060675 (ITS), PP061149 (*tef*1-α), PP061174 (*tub*2); SICAUCC 23-0150: PP844878 (ITS), PP850055 (*tef*1-α), PP850062 (*tub*2).

Note – The symptoms were observed on twig of walnut. Initial symptoms appeared as small lesions, more or less circular, later elongated, blackish-brown lesions, eventually pycnidial developed. Phylogenetic analysis of *Diaporthe* based on the combined ITS, *tef*1-α, *cal*, *his*, and *tub*2 sequence data, *D. mianyangense* (SICAUCC 23-0059) an independence branch of the *Diaporthe* clade with strong statistical support (100% MLBS/1.00 BYPP) (Fig. 79). According to the morphological comparisons, our novel species can be distinguished from closely related species. *Diaporthe mianyangense* (SICAUCC 23-0059) differs from *D. eres* (CBS 200.39) by its smaller conidiophores (7–11 × 1–2 μm vs. 10–24 μm × 1–2 μm), smaller conidia (4–7 × 2–3 μm vs. 5–8 μm × 2–4 μm). *Diaporthe mianyangense* (SICAUCC 23-0059) shares similar morphological characteristics with *D. alnea* (CBS 146.46) in the size, shape, color of conidiophores, but difer in conidial size (4–7 × 2–3 μm vs. 8–10 μm × 2–3 μm). However, *D. neilliae* (CBS 144.27) only describes the sexual stage morphology. Nucleotide comparisons revealed sequence differences of 1.3% (7/571, 1 gap), 4.08% (17/417, 0 gap), and 0.6% (2/346, 0 gap) in the ITS, *tef*1-α, and *tub*2 regions, respectively, between *D. mianyangense* (SICAUCC 23-0059) and *D. eres* (CBS 200.39). Similarly, the sequence differences between *D. mianyangense* and *D. alnea* in the ITS, *tef*1-α, and *tub*2 regions were 4% (23/575, 6 gaps), 5.3% (22/417, 0 gap), and 8.1% (28/346, 8 gaps), respectively. Lastly, the sequence differences between *D. mianyangense* and *D. neilliae* (CBS 144.27) in the same regions were also 3.8% (22/572, 6 gaps), 5.52% (23/417, 0 gap), and 6.2% (34/552, 13 gaps), respectively. Therefore, the new strain is introduced as a new species based on morphology and phylogenetic evidence.

49. ***Diaporthe novem*** J.M. Santos, Vrandečić & A.J.L. Phillips, Persoonia 27: 14 (2011) Fig. 82

Index Fungorum number: IF518521; Facesoffungi number: FoF14582

Associated with blight symptom on living branches of *Juglans regia*. First appear as water-soaked lesions turning tan to dark brown, circular or irregular in shape surrounded by a red, dark brown or purple border with a chlorotic zone. In later stages, it turns black, leading to the death of the branches. Sexual morph: Not observed. Asexual morph: *Conidiomata* 140–210 × 170–260 μm ($\bar{x}$ = 170 × 220 μm, n = 10), visible as black dots up, superficial, solitary, scattered on host, oval to round, black. *Conidiomata wall* 15–40 μm thick, inner layer composed of hyaline to light brown textura circle, outer layer composed of dark brown to black *textura angularis*. *Paraphyses* not

observed. *Conidiophores* 4–10 × 1–2 µm ($\bar{x}$ = 8 × 1.5 µm, n = 30), long, hyaline, smooth, densely aggregated, unbranched, cylindrical, straight. *Conidiogenous cells* 2–4 × 1–3 µm, phialidic, cylindrical, terminal, slightly tapering towards apex, hyaline, formed from the inner layer of pycnidium wall. *Alpha-conidia* with 1–2 guttules per cell, 6–8 × 2–3 µm ($\bar{x}$ = 7 × 2 µm, n = 30) µm, hyaline, fusiform or oval. *Beta-conidia*, filiformis, ad pycnidial, tubulineus, 31–52 µm long.

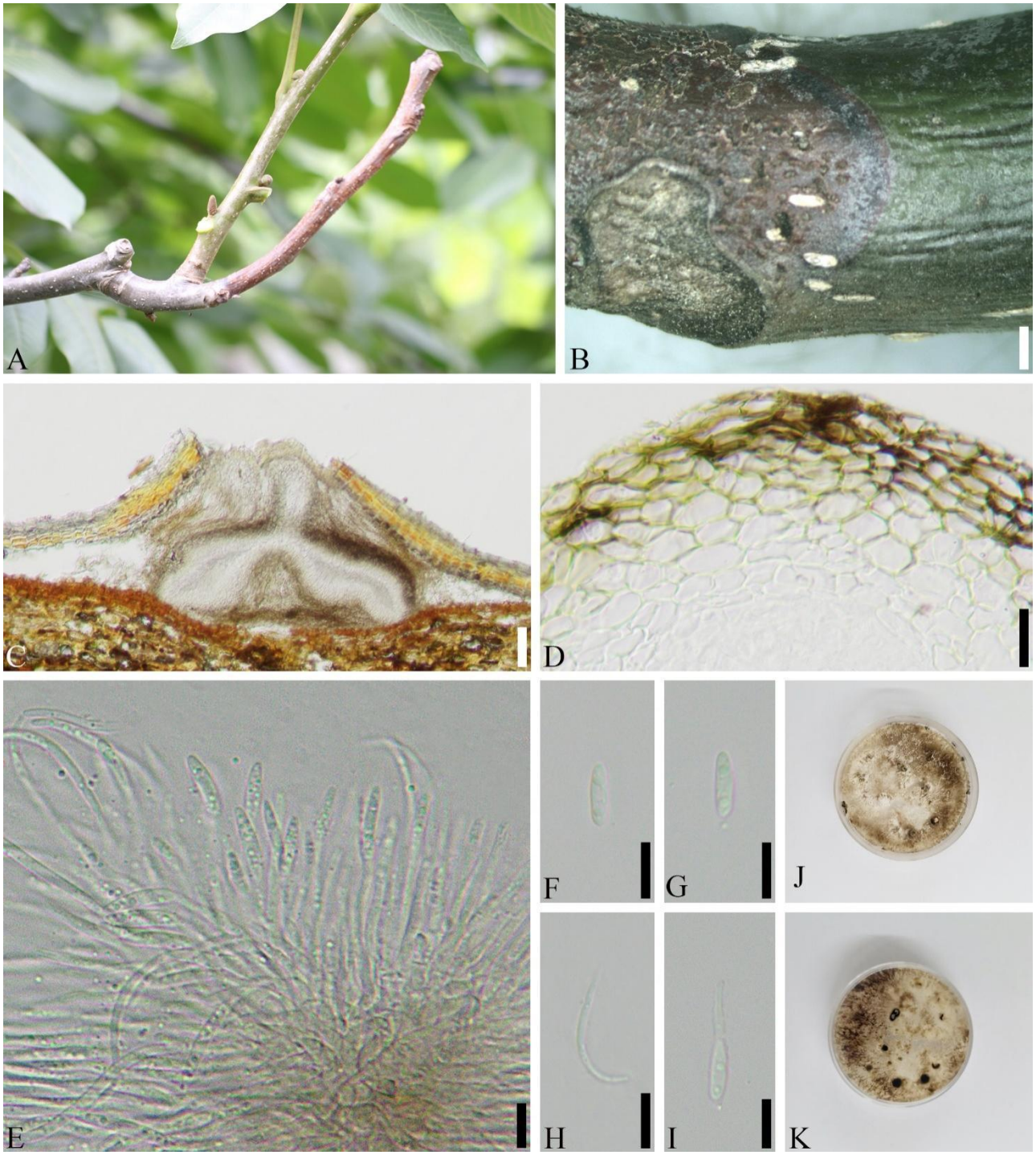


Figure 80 – *Diaporthe eres* (SICAU 22-0128). A *Juglans regia* branch affected by *D. citri*. B Conidiomata on the host. C Section through the Conidiomata. D Sections of Peridium. E. Conidiophores, paraphyses and Conidiogenous cells. F, G Alpha-conidia. H Beta-conidia. I Germinating alpha-conidium. J, K Colonies on PDA (J from above, K from below). Scale bars: B = 2 mm, C = 50 µm, E, H = 20 µm, D, F, G, I = 10 µm.

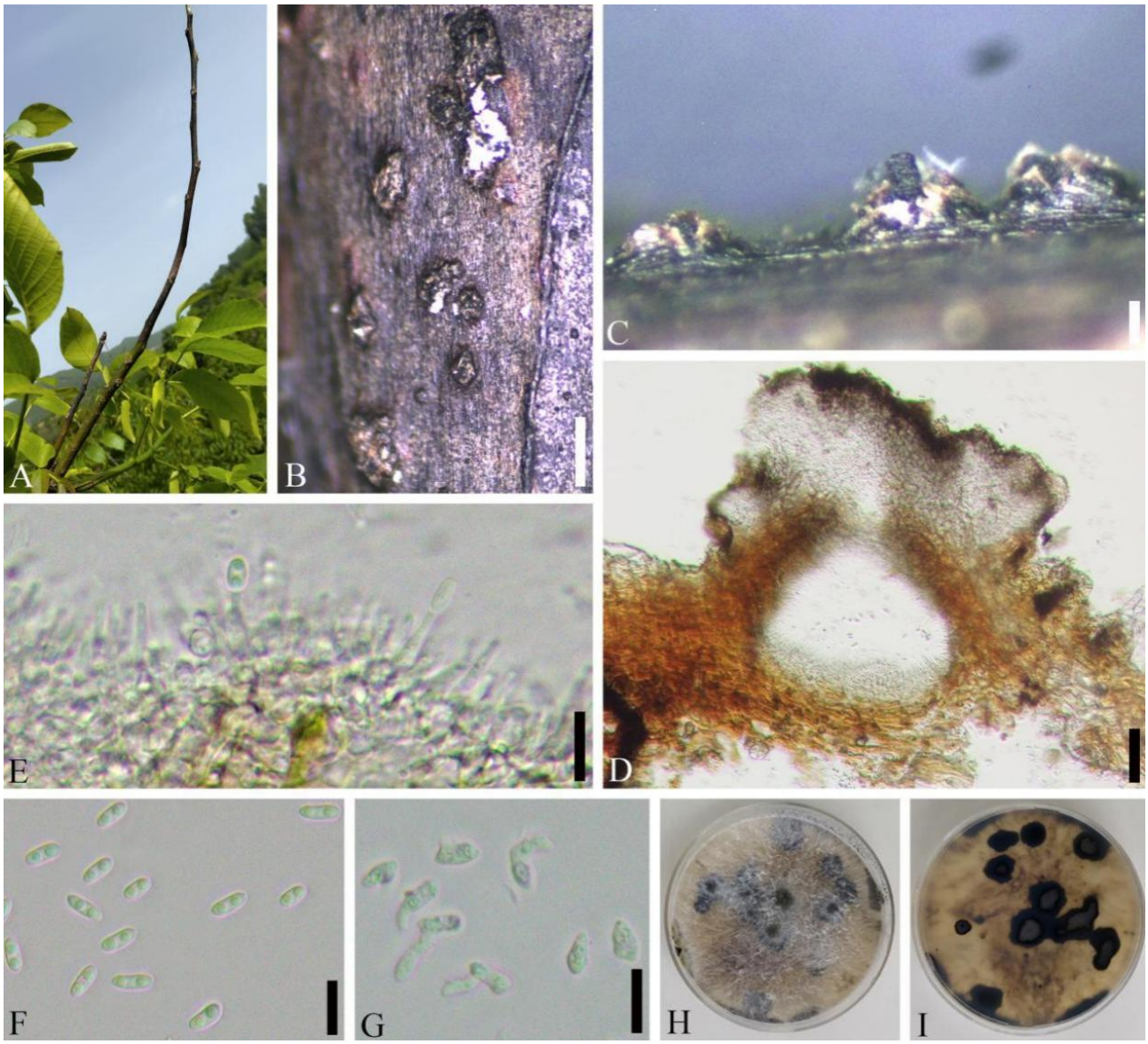


Figure 81 – *Diaporthe mianyangense* (SICAU 23-0080, holotype). A *Juglans regia* branch affected by *D. mianyangense*. B, C Conidiomata on the host. D Section through the conidiomata. E Conidiophores, paraphyses and conidiogenous cells. F Alpha-conidia. G Germinating alpha-conidium. H, I Colonies on PDA (H from above, I from below). Scale bars: B = 1000 μm, C = 200 μm, D = 50 μm, E = 15 μm, F, G = 10 μm.

Culture characteristics – Conidia germinating on sterile water within 12 h and germ tubes produced from both ends. Colonies on PDA reaching 50 mm diam., after 28 days at 25 ℃. The mycelium grows on the surface of the medium, white, radiating to the edge, margin undulate, medium dense, fat or umbonate, late center is black. Reverse, cream, radiating faint yellow outwardly.

Material examined – China, Sichuan Province, Panzhihua City, Renhe District, Ala Township (26°16′22.29″N 101°38′51.41″E, alt. 1686 m), on dead aerial branch of *Juglans regia*, 24 August 2021, F.-H. Wang, WFH202108003 (SICAU 23-0078), living culture SICAUCC 23-0057.

GenBank numbers – SICAUCC 23-0057: PP060673 (ITS), PP061147 (*tef*1-α), PP061172 (*tub*2).

Note – In the phylogenetic analysis our new collection (SICAUCC 23-0057) clusters with the ex-type strain of *Diaporthe novem* (CBS 127271) and they form a subclade with strong statistical support (100% MLBS/1.00 BYPP) (Fig. 79). And was nearly identical to *D. novem* in the ITS, *tef*1-α and *tub*2 gene sequences. Morphologically, they are similar in having hyaline, fusiform or oval

septate filiformis Alpha-conidia with an ad pycnidial, tubulineus beta-conidia. Based on morphological characters and phylogenetic analyses, we determine our specimens as *D. novem*. Therefore, our new specimen is identified as *D. novem*, and reported as a new geographical record for China.

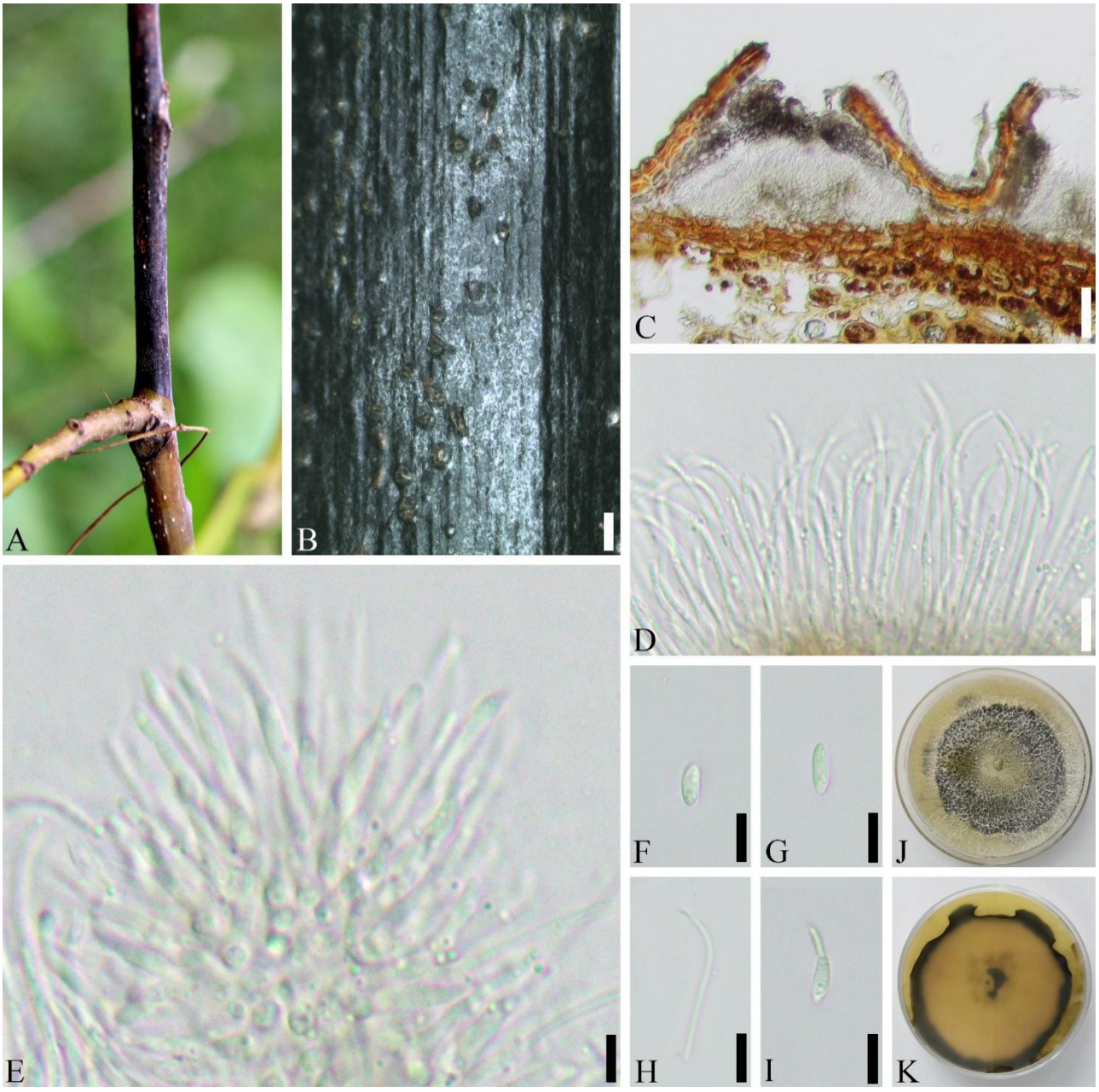


Figure 82 – *Diaporthe novem* (SICAU 23-0078). A *Juglans regia* branch affected by *D. novem*. B Conidiomata on the host. C Section through the conidiomata. D, E Conidiophores, paraphyses and conidiogenous cells. F, G Alpha-conidia. H Beta-conidia. I Germinating alpha-conidia. J, K Colonies on PDA (J from above, K from below). Scale bars: B = 500 µm, C = 50 µm, D, H = 20 µm, E, G, I = 10 µm, K-M = 5 µm.

50. ***Diaporthe pseudomangiferae*** R.R. Gomes, Glienke & Crous, Persoonia 31: 30 (2013) Fig. 83

Index Fungorum number: IF802945; Facesoffungi number: FoF16299

Saprobic on *Juglans regia*. Sexual morph: Not observed. Asexual morph: *Conidiomata* pycnidial, erumpent to superficial on branch, globose, 180 µm diam., with elongated necks with central ostioles. *Conidiomata wall* of 6–8 layers of brown *textura angularis*. *Conidiophores* 4–12 × 1–2 µm ($\bar{x}$ = 9 × 1.5 µm, n = 30) hyaline, smooth, 1–2-septate, unbranched, densely aggregated, cylindrical, straight to sinuous. *Conidiogenous cells* 4–7 × 1–2 µm ($\bar{x}$ = 5 × 1.5 µm, n = 30), phialidic,

cylindrical, terminal and lateral with slight apical taper. Paraphyses not seen. *Alpha-conidia* 4–8 × 1–2 µm ($\bar{x}$ = 6 × 2 µm, n = 30), aseptate, hyaline, smooth, guttulate to granular, fusiform, tapering towards both ends, apex acutely rounded, base truncate. *Beta-conidia* not seen.

Culture characteristics – Conidia germinating on sterile water within 12 h and germ tubes produced from both ends. Colonies on PDA reaching 50 mm diam., after 28 days at 25 ℃. The mycelium grows on the surface of the medium, with moderate aerial mycelium, surface iron-grey, with patches of dirty white. Reverse, iron-grey with patches of dirty white. Not produced pigmentation on PDA media.

Material examined – China, Sichuan Province, Neijiang City, Dongxing District, Paifang Village (29°48′30.37″N 105°6′36.26″E, alt. 384 m), on dead branch of *Juglans regia*, 17 May 2021, F.-H. Wang, WFH202105001 (SICAU 22-0129), living culture SICAUCC 22-0131.

GenBank numbers – SICAUCC 22-0131: OP963831 (ITS), OQ281369 (*tef*1-α), OQ281410 (*tub*2), OQ190500 (*cal*).

Note – We newly collected specimens *Diaporthe pseudomangiferae* (SICAUCC 23-0131) are phylogenetically related to *D. pseudomangiferae* (CBS 101339) (Fig. 79). Sequence comparison for the ITS, *tef*1-α, *tub*2 and *cal* region between our isolate (SICAUCC 23-0131) and *D. pseudomangiferae* (CBS 101339) showed no significant base pair differences. Morphologically, they correspond to *D. pseudomangiferae* with an overlap in dimensions of microscopic structures *Conidiophores* (4–12 × 1–2 vs. 10–15 × 2–2.5 µm) and conidial (4–8 × 1–2 µm vs. 7–9 × 2–3 µm) (Gomes et al. 2013). Hence, these new collections are identified as *D. pseudomangiferae*, and which has been reported as an important plant pathogen on a wide range host (Serrato-Diaz et al. 2014, Serrato-Diaz et al. 2022).

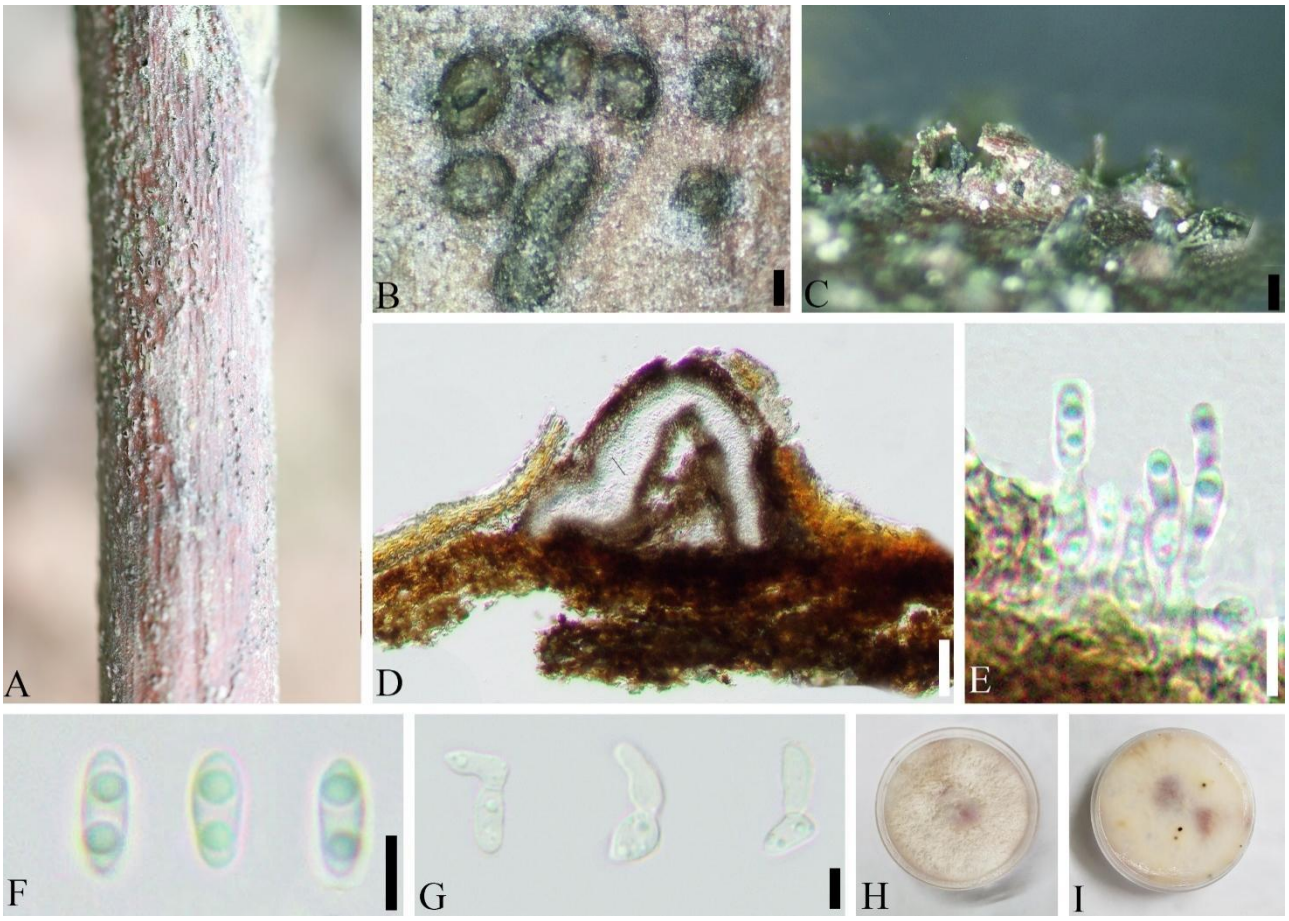


Figure 83 – *Diaporthe pseudomangiferae* (SICAU 22-0129). A Saprobic on *Juglans regia*. B, C Conidiomata on the host. D Section through the Conidiomata. E Conidiophores, and Conidiogenous

cells. F Alpha-conidia. G Germinating alpha-conidium. H, I Colonies on PDA (H from above, I from below). Scale bars: B = 200 μm, C = 100 μm, D = 50 μm, E = 10 μm, F, G = 5 μm.

51. ***Diaporthe ravennica*** Thambug., Camporesi & K.D. Hyde, Fungal Divers. (2016) Fig. 84

Index Fungorum number: IF552100; Facesoffungi number: FoF02171

Associated with blight symptom on living twigs of *Juglans regia*. Symptoms manifest as initial brown stripes, which, when encircling the branch, lead to the withering of the upper part of the branch, leaf shedding, and a noticeable depression at the junction between the healthy and affected areas. Sexual morph: Not observed. Asexual morph: *Conidiomata* pycnidial 240 μm diam., scattered, immersed to slightly erumpent, multi-loculate, black, subglobose or irregular, with or without an ostiole. *Conidiomata wall* comprising 4-6 layers of lightly pigmented to light brown cells of *textura angularis*, becoming hyaline towards the inner region. *Paraphyses* not observed. *Conidiophores* 12–24 × 1–2.5 μm ($\bar{x}$ = 17 × 1.5 μm, n = 40), hyaline, smooth, once in a while branched, cylindrical, straight to sinuous. *Conidiogenous cells* phialidic, cylindrical, terminal, slightly tapering towards the apex. *Alpha-conidia* 5–8 × 1.5–3 μm ($\bar{x}$ = 6.5 × 2.5 μm, n = 40), aseptate, hyaline, ellipsoidal or fusiform, two or many guttules, smooth-walled. *Beta-conidia* not observed.

Culture characteristics – Conidia germinating on sterile water within 12 h and germ tubes produced from both ends. Colonies on PDA reaching 50 mm diam., after 12 days at 25 ℃. The mycelium grows on the surface of the medium, irregular, flat, moderately dense, surface white, with slightly undulate edge, producing conidia after 14 days frequently at the margin and center. Reverse, iron-grey with patches of dirty white. Not produced pigmentation on PDA media.

Material examined – China, Sichuan Province, Liangshan Yi Autonomous Prefecture, Huili City (26°56′43.32″N 102°16′26.16″E, alt. 2001 m), on living twigs of *Juglans regia*, 30 September 2022, F.-H. Wang, WFH202209001 (SICAU 22-0130), living culture SICAUCC 22-0132.

GenBank numbers – SICAUCC 22-0132: OP963832 (ITS), OQ281370 (*tef*1-α), OQ281411 (*tub*2), OQ190501 (*cal*).

Note – *Diaporthe ravennica* has been found on *Tamarix* and *Clematis vitalba* (Thambugala et al. 2017b, Phukhamsakda et al. 2020). Phylogenetically, our new collection (SICAUCC 22-0132) also clustered with D. ravennica (MFLUCC 16-0997) with strong statistical support (100% MLBS/1.00 BYPP). The nucleotide comparisons showed that our strain (SICAUCC 22-0132) is not significantly different from the type strain o f *D. ravennica* (MFLUCC 16-0997) in ITS, *tef*1-α, *cal* and *tub*2, which indicated that they are the same species (Fig. 79). Thus, the new specimen is identified as *D. ravennica*, and reported here as a new host record for China.

52. ***Diaporthe tectonae*** Doilom, Dissan. & K.D. Hyde, Fungal Divers. (2016) Fig. 85

Index Fungorum number: IF551976; Facesoffungi number: FoF01871

Saprobic on dead branch of *Juglans regia*. Sexual morph: *Ascomata* 190–270 × 170–250 μm ($\bar{x}$ = 240 × 215 μm, n = 10), immersed to erumpent throughout the host surface, scattered, solitary to gregarious, depressed globose to subglobose, dark brown to black, coriaceous, ostiolate. *Ostiole* central, with a long neck that emerging through cracks in the substrate. *Peridium* 19–31 μm ($\bar{x}$ = 23μm, n = 20) wide, composed of several layers of cells arranged in *textura angularis*, hyaline and thin inwardly, becoming brown and thick-walled outwardly. *Hamathecium* not observed. *Asci* 32–50 × 5–9 μm ($\bar{x}$ = 42 × 7 μm, n = 20), 8-spored, unitunicate, cylindric-clavate, sessile, apex blunt with a apical ring. *Ascospores* 7–12 × 2–4 μm ($\bar{x}$ = 9 × 3 μm, n = 40), hyaline, randomly arranged, oval shape, round and blunt to the ends, 1-septate, constricted at the septum, guttulate, without any gelatinous/mucilaginous appendages. Asexual morph: Not observed.

Culture characteristics – Ascospores germinating on sterile water within12 h and germ tubes produced from both ends. Colonies on PDA reaching 50 mm diam., after 21 days at 25 ℃. The mycelium grows on the surface of the medium, white, radiating to the edge, margin undulate, medium dense, cotton-like aerial mycelium. Reverse cream, radiating white outwardly. Not produced pigmentation on PDA media.

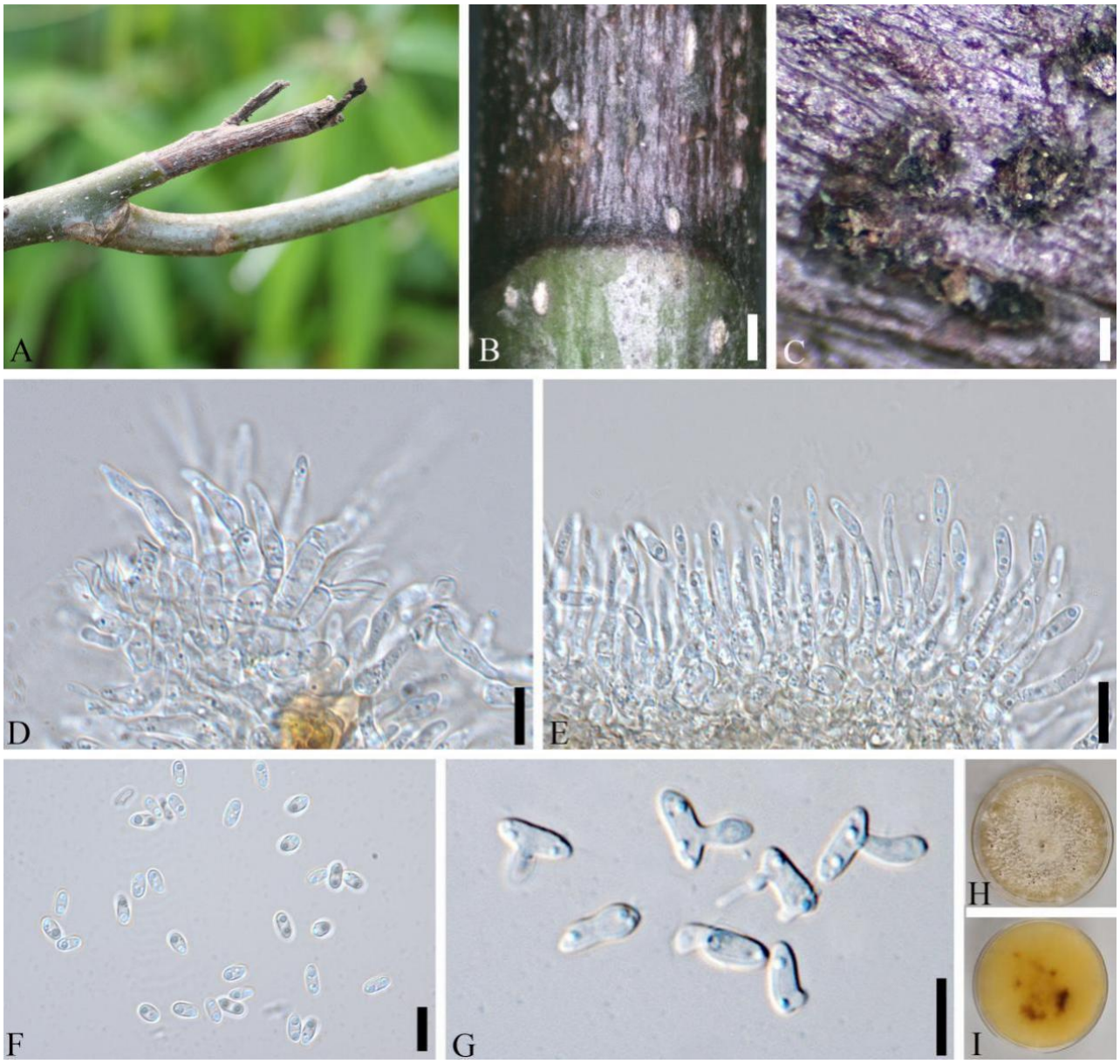


Figure 84 – *Diaporthe ravennica* (SICAU 22-0130). A *Juglans regia* branch affected by *D. ravennica*. B, C Conidiomata on the host. D, E Conidiophores and conidiogenous cells. F Alpha-conidia. G Germinating alpha-conidia. H, I Colonies on PDA (H from above, I from below). Scale bars: B = 500 μm, C = 200 μm, D–G = 10 μm.

Material examined – China, Sichuan Province, Chengdu City, Chongzhou City (30°33′9.44″N 103°39′29.76″E, alt. 512 m), on dead branch of *Juglans regia*, 21 April 2022, F.-H. Wang, WFH202204005 (SICAU 23-0079), living culture SICAUCC 23-0058.

GenBank numbers – SICAUCC 23-0058: PP060674 (ITS), PP061148 (*tef*1-α), PP061173 (*tub*2).

Note – *Diaporthe tectonae* (SICAUCC 23-0058) is a close relative to *D. tectonae* (SM 63) based on multi gene phylogenetic analysis (Fig. 79). Following the recommendations by (Chethana et al. 2021), the nucleotide comparisons showed that our strain (SICAUCC 23-0058) is not significantly different from the strain of *D. tectonae* (SM 63) in ITS, *tef*1-α and *tub*2, which indicated that they are the same species. Morphologically, *D. tectonae* at present, only the morphological characteristics of asexual stage are described. Thus, our discovery fills the gap in the understanding of the sexual morph of *D. tectonae*. This is the first report of *D. tectonae* from *Juglans regia* in China.

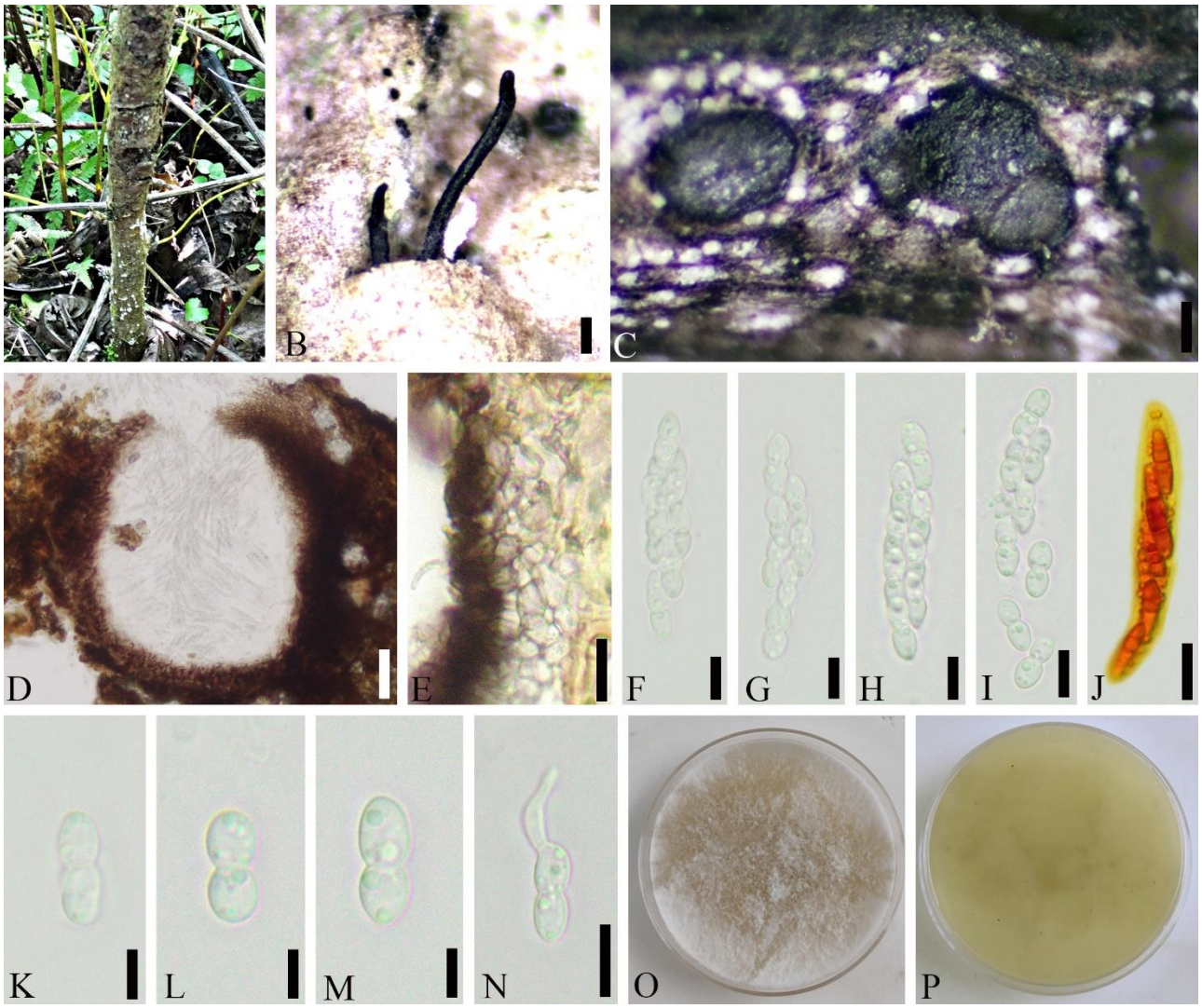


Figure 85 – *Diaporthe tectonae* (SICAU 23-0079). A, B Appearance of stroma on the substrate. C, D Vertical section of ascoma. E Peridium. F–I Asci. J Asci in Melzer's reagent. K–M Ascospores. N. Germinating ascospore. O, P Colonies on PDA (O from above, P from below). Scale bars: B = 200 μm, C = 100 μm, D = 50 μm, E–G, N = 10 μm, K–M = 5 μm.

53. ***Diaporthe tulliensis*** R.G. Shivas, Vawdrey & Y.P. Tan, Persoonia 35: 301 (2015) Fig. 86

Index Fungorum number: IF812896; Facesoffungi number: FoF16300

Associated with blight symptom on living branches of *Juglans regia*. Symptoms include the appearance of red discoloration stripes on the bark of branches, veinal chlorosis, leaf wilting and shedding, ultimately leading to the dieback of branches and twigs. Sexual morph: Not observed. Asexual morph: *Conidiomata* pycnidial 169–308 × 170–246 μm ($\bar{x}$ = 231 × 182 μm, n = 10), scattered or aggregated, black, subglobose or variable in shape. *Conidiomata wall* composed of a *textura angularis*, comprising of two cell layers, outer layer; black to brown, thick-walled, inner layer; hyaline, thin-walled. *Conidiophores* 10–19 × 1–2 μm ($\bar{x}$ = 14 × 1.5 μm, n = 30), hyaline, unbranched, cylindrical, septate, smooth, occurring in dense clusters, straight or slightly curved, tapering towards the apex, wider at base. *Conidiogenous cells* 2–5 × 0.5–1.5 μm ($\bar{x}$ = 3 × 1 μm, n = 30), phialidic, cylindrical, terminal, with slight tapering towards apex. *Alpha-conidia* 3–6 × 1–2.5 μm ($\bar{x}$ = 5 × 2 μm, n = 40), with 1–2-guttulate, mostly bi-guttulate, hyaline, oblong to ellipsoid, apex bluntly rounded, base obtuse to subtruncate, smooth. *Beta-conidia* 9–20 × 0.5–1.6 μm ($\bar{x}$ = 16 × 1.2 μm, n = 10), aseptate, cylindrical, flexuous, hamate, apex rounded, base subtruncate, hyaline, rare, smooth.

Culture characteristics – Conidia germinating on sterile water within 12 h and germ tubes produced from ends. Colonies on PDA reaching 60 mm diam., after 14 days at 25 ℃. The mycelium

is white at first, flat with a small quantity of aerial mycelium, white, producing conidia after 16 days frequently at the margin. Reverse, off-white. Not produced pigmentation on PDA media.

Material examined – China, Sichuan Province, Mianyang City, Yanting County (31°5′25.88″N 105°27′36.22″E, alt. 366 m), on dead branch of *Juglans regia*, 27 April 2022, F.-H. Wang, WFH202204104-1 (SICAU 22-0131), living culture SICAUCC 22-0133.

GenBank numbers – SICAUCC 22-0133: OP963833 (ITS), OQ281371 (*tef*1-α), OQ281412 (*tub*2) and OQ190502 (*cal*)

Note – *Diaporthe tulliensis* in having scattered or aggregated, subglobose or variable conidiomata, cylindrical conidiophores, ellipsoid alpha-conidia (Crous et al. 2015b). The strain SICAUCC 22-0133 clustered with the strain *D. tulliensis* (WD 2) with strong statistical support (94% MLBS/1.00 BYPP) (Fig. 79). Nucleotide comparisons of ITS, *tef*1-α, *tub*2, and *cal* (SICAUCC 23-0001) showed a high homology with the sequences of *D. tulliensis* (WD 2), with a similarity of 98.9% (572/578, 6 gaps), 100% (343/343, 0 gap), 100% (514/514, 0 gap), and 99.5% (414/416, 2 gaps), respectively. Based on morphological characters and phylogenetic analyses, we determine our specimens as *D. tulliensis*. The first record of *D. tulliensis* was from Queensland, Australia. while our collection was found in the Sichuan part of China, it has been found in other parts of China before. This species is reported as a variety of plant pathogenic fungi (Bai et al. 2017, Wu et al. 2021, Huang et al. 2021). This is the first record of *D. tulliensis* on *Juglans regia* species.

54. ***Diaporthe vawdreyi*** Y.P. Tan & R.G. Shivas, Persoonia 35: 303 (2015) Fig. 87

Index Fungorum number: IF812895; Facesoffungi number: FoF16301

Saprobic on dead branch of *Juglans regia*. Sexual morph: Not observed. Asexual morph: *Conidiomata* pycnidial 197–296 × 120–198 μm ($\bar{x}$ = 245 × 153 μm, n = 10), scattered, aggregated, subglobose, ostiolate. *Conidiomata wall* consisting of 7–12 layers of medium light brown *textura angularis*, the outer layer is dark and the inner layer is transparent. *Conidiophores* 9–18 × 1–2.5 μm ($\bar{x}$ = 13 × 1.6 μm, n = 20) formed from the inner layer of the locular wall, cylindrical to lageniform, mostly reduced to conidiogenous cells or, hyaline. *Alpha-conidia* 5–9 × 1.5–2.8 μm ($\bar{x}$ = 5.9 × 2.3 μm, n = 40), cylindrical, abundant, rounded at the apex, sometimes tapered towards the base, hyaline. *Beta-conidia* not observed.

Culture characteristics – Ascospores germinating on sterile water within 24 h and germ tubes produced from both ends. Colonies on PDA reaching 20 mm diam., after 7 days at 25 ℃. The mycelium grows on the surface of the medium, flat with sparse aerial mycelium, margin undulate, off white to dirty white, stroma produced in 18 days old culture. Reverse, irregularly zonate, pale hazel at margin becoming darker towards center. Not produced pigmentation on PDA media.

Material examined – China, Sichuan Province, Luzhou City, Guling County (27°56′49.28″N 105°51′28.14″E, alt. 1090 m), on dead branch of *Juglans regia*, 25 April 2022, F.-H. Wang, WFH202204028 (SICAU 22-0132), living culture SICAUCC 22-0134.

GenBank numbers – SICAUCC 22-0134: OP963834 (ITS), OQ281372 (*tef*1-α), OQ281413 (*tub*2), OQ190503 (*cal*).

Note – Although *Diaporthe vawdreyi* was isolated from a specimen of rotted fruit, it is not known whether this fungus is a pathogen, opportunistic saprobe or endophyte (Crous et al. 2015b). In the phylogenetic tree, our isolate *D. vawdreyi* (SICAUCC 23-0053) was sister to the ex-type strain of *D. vawdreyi* (BRIP 57887) with strong statistical support (100% MLBS/1.00 BYPP). Morphologically, they correspond to *D. vawdreyi* (BRIP 57887) with an overlap in dimensions of microscopic structures. Therefore, our new specimen is identified as *D. vawdreyi*, and reported as a new host record for China.

Gnomoniaceae G. Winter [as '*Gnomonieae*'], Rabenh. Krypt. -Fl., Edn 2 (Leipzig) 1.2: 570. 1886.

Species within *Gnomoniaceae* have narrow host ranges, sometimes specific on a single host species, and the family is primarily known from North America and Europe, with a few species in Asia (Kobayashi 1970, Monod 1983, Mejía et al. 2008, 2011a, b, 2012, Walker et al. 2012a). The host diversity of *Gnomoniaceae* is high. (Walker et al. 2010, Mejía et al. 2011a, 2012). Some species

of *Gnomoniaceae* are also important plant pathogens. (Ostry 1997, Castlebury et al. 2002, Sinclair & Lyon 2005, Sogonov et al. 2008, Mejía et al. 2008, 2011a, 2012, Tian et al. 2015). The asexual morphs of this family are generally coelomycetes, which have acervular or pycnidial conidiomata with a broad opening, phialidic conidiogenous cells, and pallid, diverse Conidia. (Monod 1983, Mejía et al. 2012, Visentin et al. 2012, Senanayake et al. 2017b)

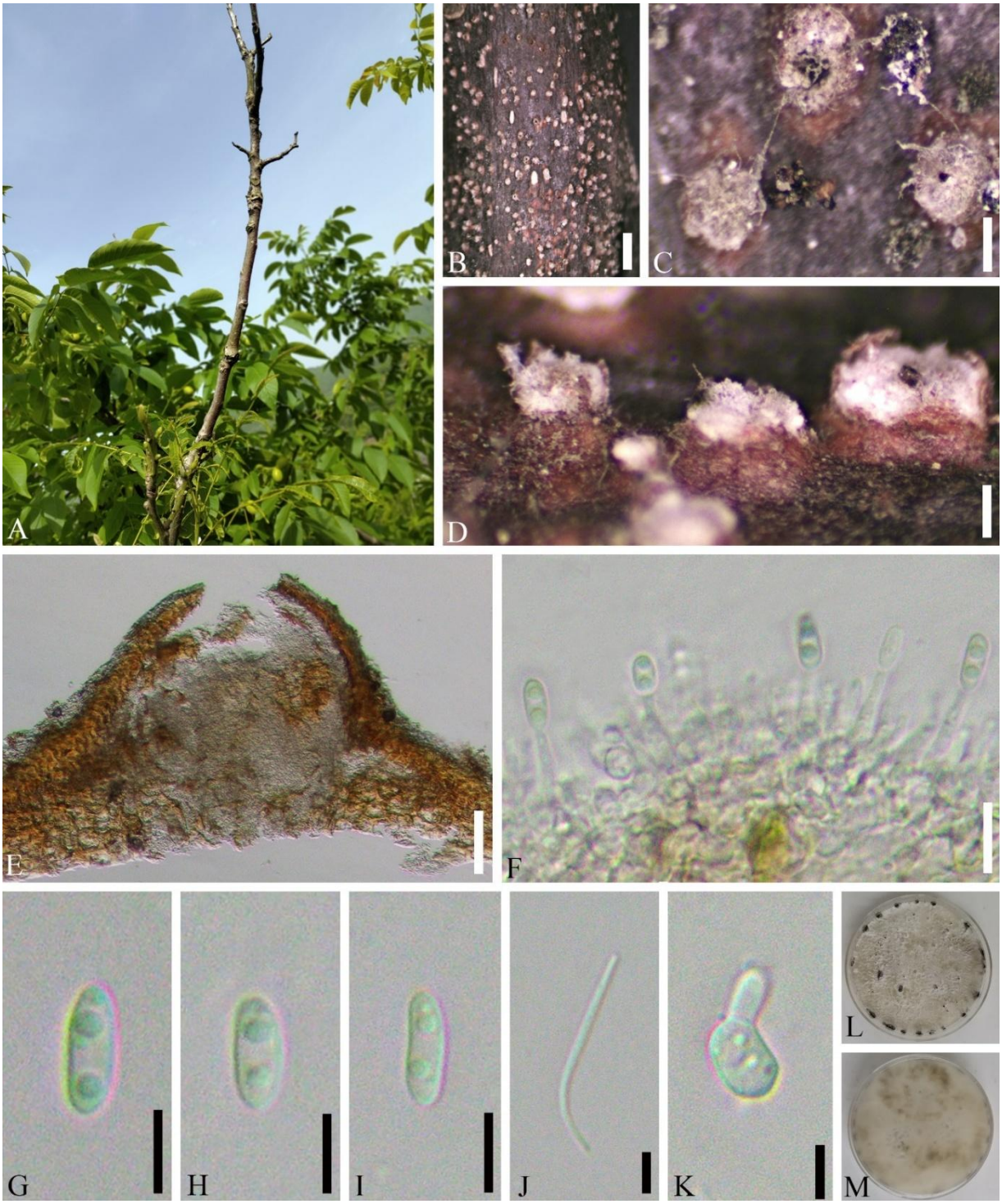


Figure 86 – *Diaporthe tulliensis* (SICAU 22-0131). A Saprobic on *Juglans regia*. B–D Conidiomata on the host. E Section through the conidioma. F Conidiophores, and conidiogenous cells. G-I Alpha-conidia. J Beta-conidia. k Germinating alpha-conidium. L, M Colonies on PDA (L from above, M from below). Scale bars: B = 2 mm, C = 300 µm, D = 200 µm, E = 50 µm, F = 20 µm, G–K = 5 µm.

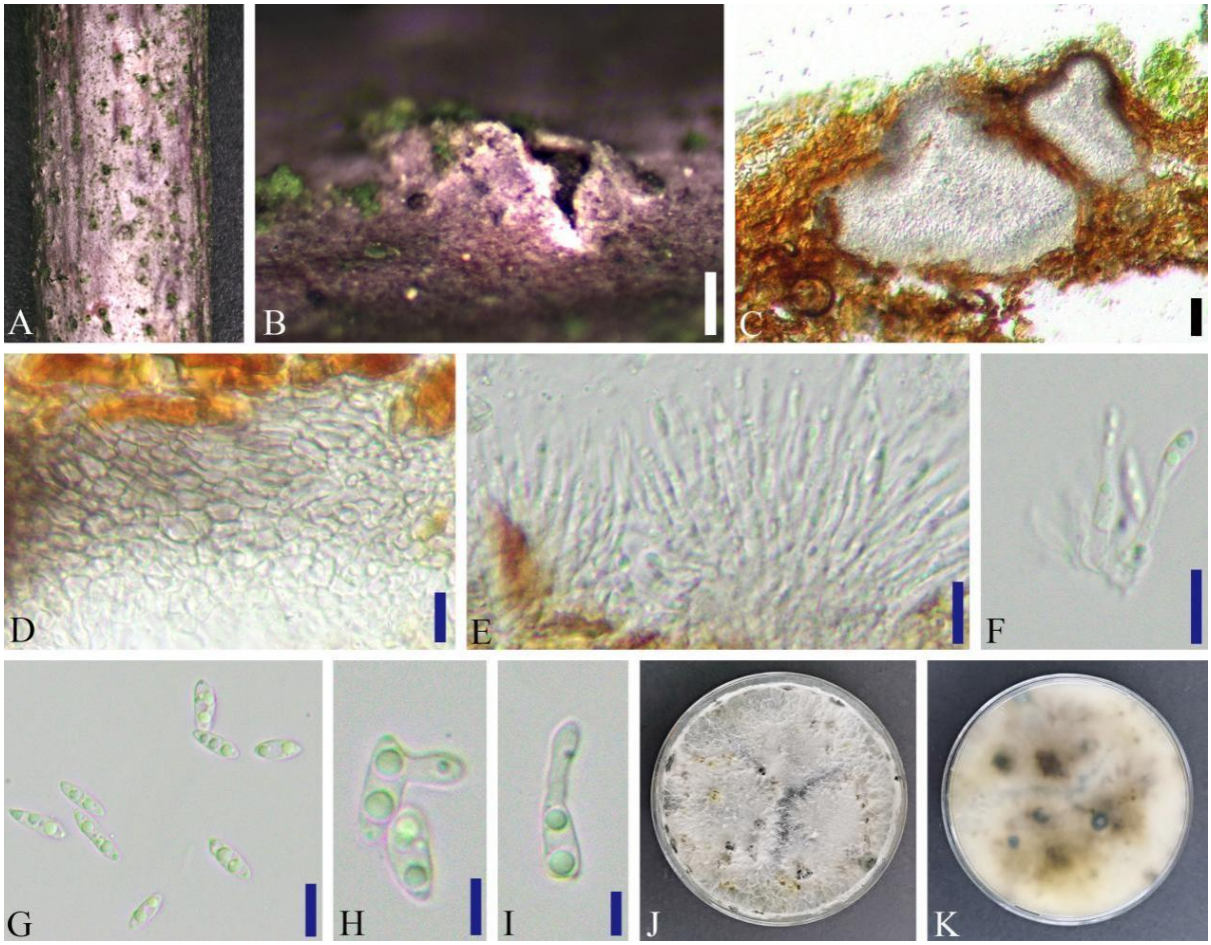


Figure 87 – *Diaporthe vawdreyi* (SICAU 22-0132). A, B Conidiomata on the host. C Section through the conidiomata. D Sections of peridium. E, F Conidiophores, and conidiogenous cells. G Alpha-conidia. H, I Germinating alpha-conidium. J, K Colonies on PDA (J from above, K from below). Scale bars: B = 200 μm, C = 50 μm, E, F = 20 μm, D, G = 10 μm, H–I = 5 μm.

Neomelanconis F.H. Wang & C.L. Yang, gen. nov.

Index Fungorum number: IF901570; Facesoffungi number: FoF15588

Etymology – Named after its morphological similarity to melanconis.

Type species: *Neomelanconis juglandis* F.H. Wang & C.L. Yang, sp. nov

Saprobic on dead walnut culms. Sexual morph: Not observed. Asexual morph: *Conidiomata* consisting of an inconspicuous, erumpent, light to dark coloured ectostromatic disc causing a more or less pustulate bark surface. *Ectostromatic* disc convex, flat or concave, greyish to brownish, surrounded by bark flaps. Central column beneath the disc more or less conical. The marginal part of the central column comprises conidiophores and their basal cell layers. *Conidiophores* unbranched, aseptate, cylindrical, hyaline to pale brown, smooth-walled, sometimes reduced to conidiogenous cells. *Conidiogenous cells* annellidic, sometimes with apical collarette. *Conidia* hyaline when immature, non-septate, becoming brown at maturity, ellipsoid to oblong, 1-septate, 2-celled, multi-guttulate, without sheath.

Note – *Neomelanconis* is phylogenetically placed in a distinct clade within the family *Gnomoniaceae*, where it is closely related to *Amphiporthe* (Fig. 88). *Neomelanconis* was classified as a new genus in *Gnomoniaceae* throughout molecular data and the characteristics of asexual morph. Morphologically, it is distinguished from other genera in conidiomata by without sheath and septate conidia. Hence, we establish it as a new genus to accommodate the type species *Neomelanconis juglandis*, based on the morpho-phylogenetic evidence.

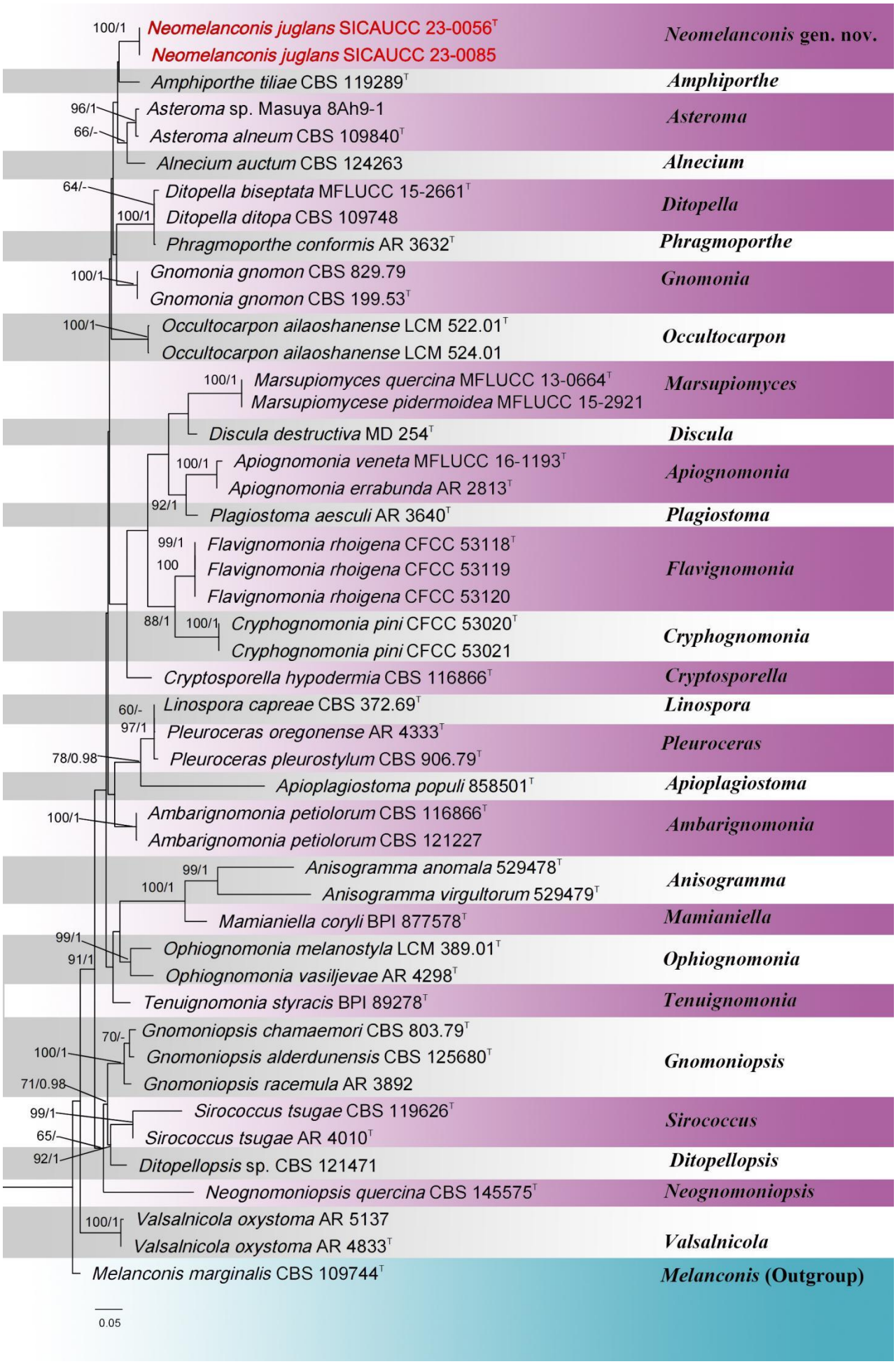

100/1
Neomelanconis juglans SICAUCC 23-0056T
Neomelanconis juglans SICAUCC 23-0085
Neomelanconis gen. nov.
Amphiporthe tiliae CBS 119289T
Amphiporthe
96/1
66/-
Asteroma sp. Masuya 8Ah9-1
Asteroma alneum CBS 109840T
Asteroma
Alnecium auctum CBS 124263
Alnecium
64/-
100/1
Ditopella biseptata MFLUCC 15-2661T
Ditopella ditopa CBS 109748
Ditopella
Phragmoporthe conformis AR 3632T
Phragmoporthe
100/1
Gnomonia gnomon CBS 829.79
Gnomonia gnomon CBS 199.53T
Gnomonia
100/1
Occultocarpon ailaoshanense LCM 522.01T
Occultocarpon ailaoshanense LCM 524.01
Occultocarpon
100/1
Marsupiomyces quercina MFLUCC 13-0664T
Marsupiomycese pidermoidea MFLUCC 15-2921
Marsupiomyces
Discula destructiva MD 254T
Discula
100/1
Apiognomonia veneta MFLUCC 16-1193T
Apiognomonia errabunda AR 2813T
Apiognomonia
92/1
Plagiostoma aesculi AR 3640T
Plagiostoma
99/1
100
Flavignomonia rhoigena CFCC 53118T
Flavignomonia rhoigena CFCC 53119
Flavignomonia rhoigena CFCC 53120
Flavignomonia
88/1
100/1
Cryphognomonia pini CFCC 53020T
Cryphognomonia pini CFCC 53021
Cryphognomonia
Cryptosporella hypodermia CBS 116866T
Cryptosporella
Linospora capreae CBS 372.69T
Linospora
60/-
97/1
Pleuroceras oregonense AR 4333T
Pleuroceras pleurostylum CBS 906.79T
Pleuroceras
78/0.98
Apioplagiostoma populi 858501T
Apioplagiostoma
100/1
Ambarignomonia petiolorum CBS 116866T
Ambarignomonia petiolorum CBS 121227
Ambarignomonia
99/1
100/1
Anisogramma anomala 529478T
Anisogramma virgultorum 529479T
Anisogramma
Mamianiella coryli BPI 877578T
Mamianiella
99/1
91/1
Ophiognomonia melanostyla LCM 389.01T
Ophiognomonia vasiljevae AR 4298T
Ophiognomonia
Tenuignomonia styracis BPI 89278T
Tenuignomonia
70/-
100/1
Gnomoniopsis chamaemori CBS 803.79T
Gnomoniopsis alderdunensis CBS 125680T
Gnomoniopsis racemula AR 3892
Gnomoniopsis
71/0.98
99/1
65/-
Sirococcus tsugae CBS 119626T
Sirococcus tsugae AR 4010T
Sirococcus
92/1
Ditopellopsis sp. CBS 121471
Ditopellopsis
Neognomoniopsis quercina CBS 145575T
Neognomoniopsis
100/1
Valsalnicola oxystoma AR 5137
Valsalnicola oxystoma AR 4833T
Valsalnicola
Melanconis marginalis CBS 109744T
Melanconis (Outgroup)
0.05

Figure 88 – Best scoring RAxML tree with a final likelihood value of -30,404.140489 based on combined ITS, LSU, *tef*1-α and *rpb*2 sequence data of related species. The tree is rooted with *Melanconis marginalis* (CBS 109744) in *Melanconidaceae*. Forty-seven strains were included in the combined analyses which comprised 9,451 characters (3,201 characters for ITS, 3,647 characters for LSU, 1,404 characters for *tef*1-α and 1,196 characters for *rpb*2, including gap regions). The matrix had 1,554 distinct alignment patterns, with 76.03% of undetermined characters and gaps. Estimated base frequencies were as follows; A = 0.255130, C = 0.244436, G = 0.266943, T = 0.233491; substitution rates AC = 1.318429, AG = 2.535617, AT = 1.179650, CG = 1.019766, CT = 5.903115, GT = 1.000000; gamma distribution shape parameter α = 0.222968. In our analyses, GTR+I+G model was used for each partition in Bayesian posterior analyses. The species determined in this study is indicated in red and bold. Bootstrap support values for maximum likelihood (MLBS, left) ⩾ 60% and Bayesian posterior probabilities (BYPP, right) ⩾ 0.90 are indicated at the nodes, respectively. Hyphens (-) represent support values less than 60% MLBS/0.90 BYPP. The ex-type superscript "T".

55. ***Neomelanconis juglandis*** F.H. Wang & C.L. Yang, sp. nov. Fig. 89

Index Fungorum number: IF901571; Facesoffungi number: FoF15589

Etymology – Name refers to *Juglans*, the host genus from which this fungus was collected.

Holotype – SICAU 23-0077

Saprobic on dead branch of *Juglans regia*. Sexual morph: Not observed. Asexual morph: *Conidiomata*, 500–1200 × 400–1000 μm ($\bar{x}$ = 800 × 700 μm, n = 20), acervular, immersed in host bark to erumpent, covered by blackish conidial masses at maturity. Central column beneath the disc more or less conical. *Conidiophores* 18–30 × 1.5–3 μm ($\bar{x}$ = 24 × 2.4 μm, n = 20), unbranched, aseptate, cylindrical, hyaline to pale brown, smooth-walled. *Conidiogenous cells* enteroblastic, annellidic, with distinct annellations and collarettes. *Conidia* 13–19 × 3–6 μm ($\bar{x}$ = 16 × 5 μm, n = 40), hyaline when immature, Smooth wall, becoming greyish sepia to brown, ellipsoid to oblong, multi-guttulate, straight to slightly curved, 1-septate, 2-celled, without sheath.

Culture characteristics – Conidia do not germinate in sterile water. Conidia germinating on PDA within 32 h and germ tubes produced from one or both ends, slow growth. Colonies on PDA reaching 30 mm diam., after 35 days at 25 ℃. The mycelium grows on the surface of the medium, slightly convex, irregular edge, without aerial mycelium, at the beginning white, tan to and black after 20 days, producing conidia after 30 days frequently at the margin. Reverse, be similar. Not produced pigmentation on PDA media.

Material examined – China, Sichuan Province, Luzhou City, Guling County (27°56′49.17″N 105°51′28.28″E, alt. 1091 m), on dead branch of *Juglans regia*, 25 April 2022, F.-H. Wang, WFH202204034 (SICAU 23-0077, holotype), ex-type living culture SICAUCC 23-0056. *Ibid*., Mianyang City, Pingwu County (32°12′59.03″N 104°50′15.58″E, alt. 727 m), on dead branch of *Juglans regia*, 9 July 2022, F.-H. Wang, WFH202207053 (SICAU 23-0106), living culture SICAUCC 23-0085.

GenBank numbers – SICAUCC 23-0056: PP060672 (ITS), PP057963 (LSU), PV289225 (*tef*1-α), PV289227 (*rpb*2); SICAUCC 23-0085: PP060701 (ITS), PP057980 (LSU), PV289226 (*tef*1-α), PV289228 (*rpb*2).

Note – The characteristics of *Neomelanconis juglandis* include its stroma being embedded within the bark, which upon maturity protrudes from the surface and is covered with a black mass of conidia. Beneath the disc lies a conical central column. Conidiophores are unbranched, aseptate, cylindrical, transparent to pale brown in color, and have smooth walls. The conidiogenous cells are of the endophiallic type, displaying a distinct annulus and collarette at their apices. The conidia, when immature, are transparent with smooth walls, but mature into grayish-brown to brown, elliptical to oblong shapes, containing multiple oil droplets. They are either straight or slightly curved, possess a single septum, are bicellular, and lack a sheath. Two strains of *N. juglandis* are sister taxa to *Amphiporthe tiliae* (CBS 119289) within the *Gnomoniaceae* order (Fig. 89). The genera within the *Gnomoniaceae* family exhibit remarkable morphological diversity, particularly in the forms of their ascospores and conidia, which can make identification based solely on morphology challenging.

However, nucleotide sequence comparisons reveal specific differences between *N. juglandis* and its related species. Specifically, the sequence divergences between *N. juglandis* (SICAUCC 23-0056) and *Amphiporthe tiliae* (CBS 119289) in the ITS, LSU *tef*1-α and *rpb*2 regions are 7.8% (39/499, 10 gaps), 0.7% (5/760, 0 gap), 3.8% (18/471, 10 gap), and 1.7% (18/1081, 1 gap), respectively. These findings provide valuable insights into the genetic relationships and differences among these species.

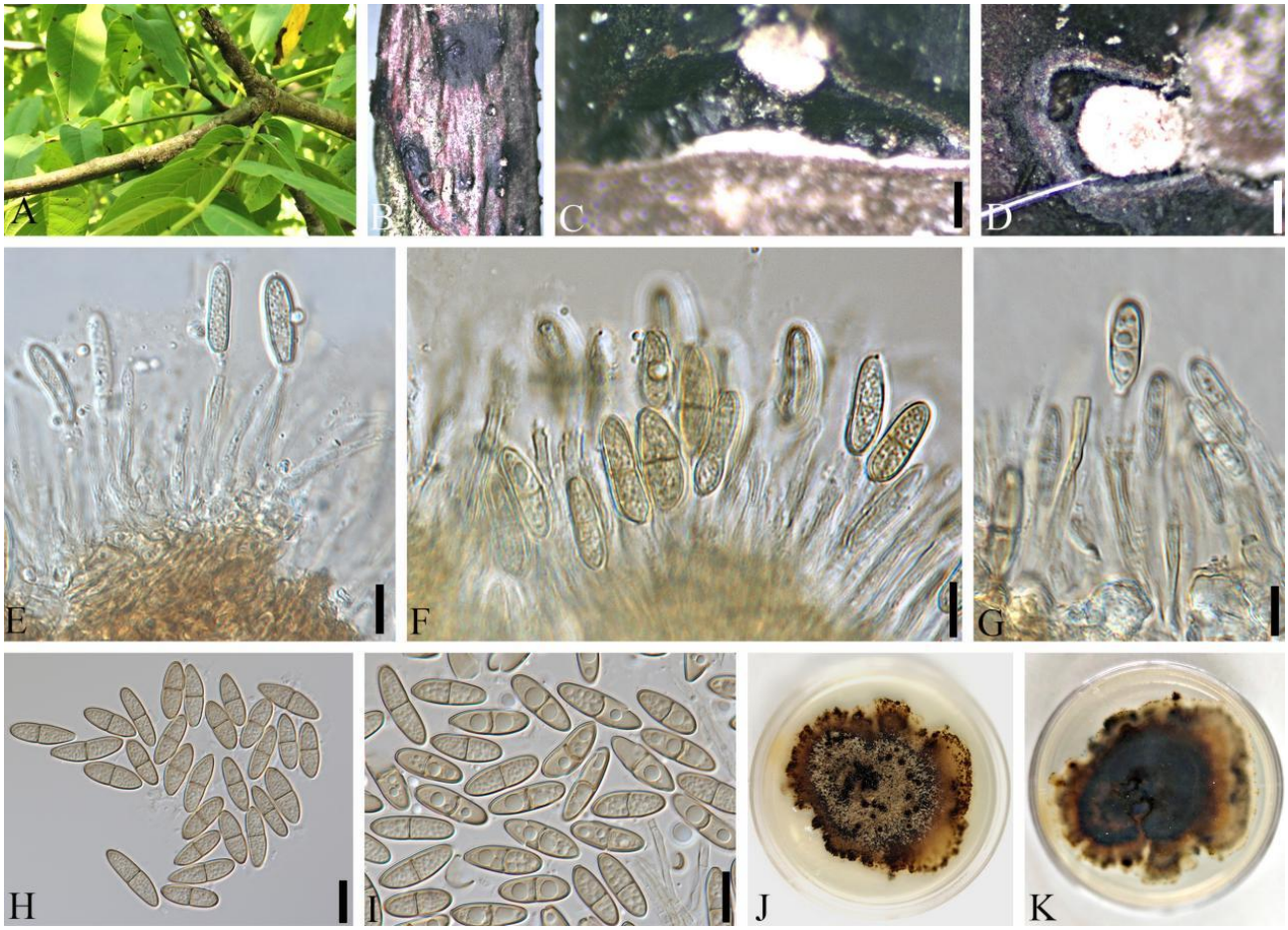


Figure 89 – *Neomelanconis juglandis* (SICAU 23-0077, holotype). A, B Appearance of Conidiomata in host substrate. C, D Transverse and vertical sections through Conidiomata. D. Developing conidia attached to conidiogenous cells. H, I Conidia. J, K Colonies on PDA (J from above, K from below). Scale bars: D = 500 μm, C = 200 μm, E–I = 10 μm.

Ophiognomonia (Sacc.) Speg., Revta Fac. Agron. Vet. Univ. nac. La Plata 2(19): 231 (1896).

Prior to Sogonov et al. (2008) considerable confusion existed about the generic concept of *Ophiognomonia*. *Ophiognomonia melanostyla* was originally described in the genus *Sphaeria* and then transferred to *Cryptoderis*, *Gnomonia*, and *Gnomoniella* before being designated as the type species of *Ophiognomonia* in 1899 (Sogonov et al. 2008). Members of this genus are distributed worldwide and reported as important pathogens causing canker and dieback disease of a wide range of plants. Many new taxa were discovered in recent studies. (Broderset al. 2011, Walker et al. 2012a, Gong et al. 2017, Senanayake et al. 2018, Xu et al. 2022a)

56. ***Ophiognomonia leptostyla*** (Fr.) Sogonov, Stud. Mycol. 62: 62 (2008) Fig. 90

Index Fungorum number: IF512187; Facesoffungi number: FoF16302

Associated with leaf spots on the living leaves of *Juglans sigillata*. Symptoms initially spread inward from the leaf edges, with lesions appearing as light brown. In later stages, the leaves wilt and die, and small, raised black spots appear on the leaf surface. Sexual morph: Not observed. Asexual morph: *Conidiomata* 90–280 × 70–190 μm ($\bar{x}$ = 178 × 124 μm, n = 30), growing under the leaf

epidermis, rupturing when mature, dark brown to black, usually with an opening, discoid, and single-chambered. *Conidiophores* reduced to conidiogenous cells. *Conidiogenous cells* 7–17 × 2–6 µm ($\bar{x}$ = 14 × 4 µm, n = 30), hyaline, cylindrical or ampulliform, monophialidic, rarely branch-like phialidic, and enteroblastic. *Conidia* 14–38 × 4–8 µm ($\bar{x}$ = 30 × 6 µm, n = 50), lunate, reniform, basal cell rounded, base truncation, apical cell with acute end, uniseptate, occasionally 1-septate, sometimes constricted at septum, and hilum usually conspicuous.

Culture characteristics – Conidia do not germinate in sterile water. Conidia germinating on PDA within 24 h and germ tubes produced from one or both ends, slow growth. Colonies on PDA reaching 40 mm diam., after 28 days at 25 ℃. The mycelium grows on the surface of the medium, subcircular, crenated, obvious bulge, initially white, with a circular ring shape, gradually turning yellowish with black spots with abundant sporulation, aerial mycelia developed and fluffy. Reverse, pale yellow or brown, and pale yellow at the margin. Not produced pigmentation on PDA media.

Material examined – China, Sichuan Province, Aba Tibetan and Qiang Autonomous Prefecture, Mao County (31°45′22.18″N 103°49′28.76″E, alt. 2002 m), on living leaves of *Juglans sigillata*, 8 July 2022, F.-H. Wang, WFH202207038 (SICAU 22-0155), living culture SICAUCC 22-0157.

GenBank numbers – SICAUCC 22-0157: OP963855 (ITS), OQ281393 (*tef*1-α), OQ214951 (*ms*204).

Note – We recognized our collection as *Ophiognomonia leptostyla*, because phylogenetically it clustered with other *O. leptostyla* strains. And it has formed an independent branch with a high statistical support (100% MLBS/1.00 PBYP) (Fig. 91). In addition, each gene region between *O. leptostyla* and our new collection was compared, there is no difference between ITS, *tef*1-α and *ms*204. The morphology of the new isolate is similar to the description of *O. leptostyla* provided by Walker et al. (2012a). Therefore, these new specimens are identified as *O. leptostyla*, which has been reported from America, Europe, and Asia (Juhásová et al. 2006, Belisario et al. 2008, Yang et al. 2021a, b, Xu et al.2022a).

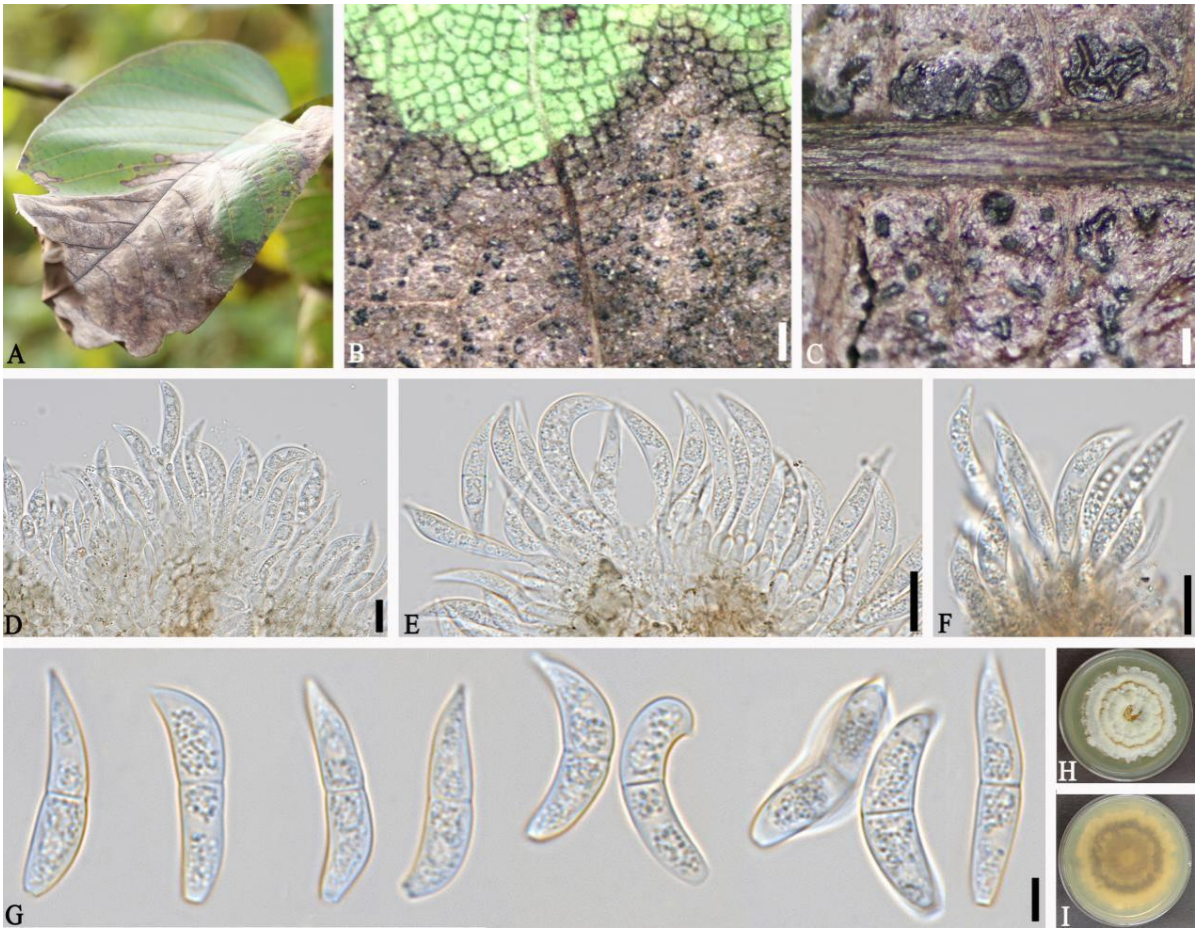


Figure 90 – *Ophiognomonia leptostyla* (SICAU 22-0155). A, B Symptoms of leaf spots observed on host. C Close-up of acervulus conidiomata. D-E Conidiophores, conidiogenous cells, and developing conidia. G Conidia. H, I Colonies on PDA (H from above, I from below). Scale bars: B = 1000 μm, C = 300 μm, D-F = 20 μm, G = 10 μm.

57. ***Ophiognomonia pseudopterocaryae*** F.H. Wang & C.L. Yang, sp. nov. Fig. 92

Index Fungorum number: IF901573; Facesoffungi number: FoF15590

Etymology – Refers to the similarity to *Ophiognomonia pterocaryae*.

Holotype – SICAU 23-0082

Saprobic on petioles. Sexual morph: *Ascomata* 240–320 × 200–280 μm ($\bar{x}$ = 260 × 230 μm, n = 30), immersed, causing host tissue to swell, rupture, and expose bases, on petioles, solitary, glossy black, globose to subglobose. central necks 590–780 × 29–40 μm ($\bar{x}$ = 649 × 32 μm, n = 30), black, sometimes slightly flexuous. *Asci* 36–48 × 8–11 μm ($\bar{x}$ = 40 × 9 μm, n = 30), with smooth walls, 8 ascospores, arranged irregularly in parallel or multiseriate rows, fusiform, with straight to curved stipe and conspicuous apical ring. *Ascospores* 19–28 × 2.5–3 μm ($\bar{x}$ = 25 × 2.5 μm, n = 40), elongated fusiform with narrow ends, straight or slightly curved, not obvious septum, slightly constricted at septum, each cell with not obvious guttules. Asexual morph: Not observed.

Culture characteristics – Ascospores germinating on sterile water within 32 h and germ tubes produced from ends. Colonies on PDA reaching 40 mm diam., after 50 days at 25 ℃. The mycelium grows on the surface of the medium, with knobbed center and flat margin, sometimes radially furrowed; aerial mycelium felty to woolly, orange-white, whitish or greyish brown, margin well-defined, irregular, white, colony surface sometimes covered by droplets of clear exudates. Reverse pale orange to greyish brown. Not produced pigmentation on PDA media.

Material examined – China, Sichuan Province, Aba Tibetan and Qiang Autonomous Prefecture, Lixian County (31°33′40.49″N 103°23′50.07″E, alt. 1521 m), on dead petioles of *Juglans regia*, 7 July 2022, F.-H. Wang, WFH202207021 (SICAU 23-0082, holotype), ex-type living culture SICAUCC 23-0061. *Ibid*., WFH202207021B (SICAU 24-0037), living culture SICAUCC 23-0151.

GenBank numbers – SICAUCC 23-0061: PP060677 (ITS), PP061151 (*tef*1-α), PP061109 (*ms*204); SICAUCC 23-0151: PP844879 (ITS), PP850056 (*tef*1-α), PP850045 (*ms*204).

Note – In the phylogenetic analysis *Ophiognomonia pseudopterocaryae* (SICAUCC 23-0061) forms an independent clade sister to *O. pterocaryae* (CBS131359) (Fig. 91). The two species resemble each other in having ascomata immersed, solitary, glossy black, globose to subglobose, and with a long central neck, 8-spored, with smooth walls, fusiform asci and septate ascospores (Walker et al. 2012a). However, *O. pterocaryae* (CBS131359) has longer asci than *O. pseudopterocaryae* (SICAUCC 23-0061) (39–59 × 16–17 μm vs. 36–48 × 8–11 μm), but short ascospores (19–28 × 2.5–3 μm vs. 15–18 × 3–4 μm) (Walker et al. 2012a). A comparison of each gene region between these two taxa was processed based on the recommendations of Jeewon & Hyde (2016), and the results show that there are 2.4% (14/586, 0 gaps), 3.3% (36/1089, 0 gap) and 12.9% (46/356, 0 gap) base pair differences (including gaps) in ITS, *ms*204 and *tub*2, respectively. The PHI test revealed no significant recombination event between our strain and the closely related taxa (Φw = 0.57) (Fig. 93). Based on the above evidence, *O. pseudopterocaryae* is therefore introduced as a new species.

58. ***Ophiognomonia pterocaryae*** D.M. Walker, Fungal Divers. 57(1): 132 (2012) Fig. 94

Index Fungorum number: IF901573; Facesoffungi number: FoF16303

Saprobic on petioles. Sexual morph: *Ascomata* 220–410 × 300–460 μm ($\bar{x}$ = 310 × 380 μm, n = 40), immersed to erumpent, occasionally causing host tissue to swell, on petioles, and rachises, hypophyllous, solitary, loosely aggregated, or clusters, glossy black, subglobose. Necks central 519–700 × 24–31 μm ($\bar{x}$ = 590 × 29 μm, n = 20), marginal, or lateral, straight to curved. *Asci* 19–57 × 14–19 μm ($\bar{x}$ = 45 × 17 μm, n = 20), clavate to fusiform, apex rounded to papillate, stipe acute to long tapering, ascospores arranged uniseriate to irregularly multiseriate. *Ascospores* 11–17 × 2–3.5 μm ($\bar{x}$ = 15 × 2.5 μm, n = 40), fusiform with rounded ends, straight to slightly curved, uniseptate, median to indistinctly sub- or supramedian, not constricted at septum. Asexual morph: Not observed.

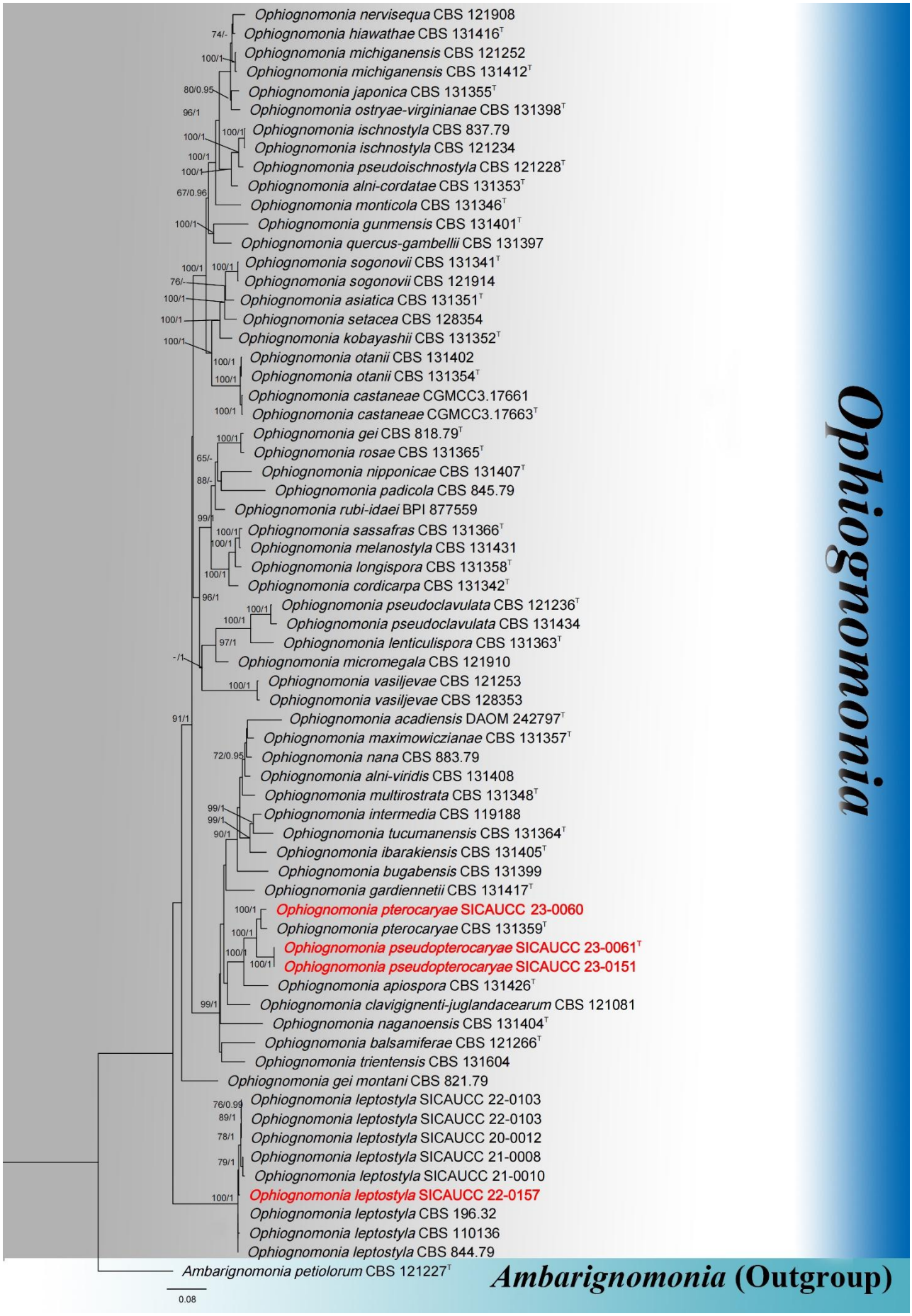

Ophiognomonia nervisequa CBS 121908
Ophiognomonia hiawathae CBS 131416T
Ophiognomonia michiganensis CBS 121252
Ophiognomonia michiganensis CBS 131412T
Ophiognomonia japonica CBS 131355T
Ophiognomonia ostryae-virginianae CBS 131398T
Ophiognomonia ischnostyla CBS 837.79
Ophiognomonia ischnostyla CBS 121234
Ophiognomonia pseudoischnostyla CBS 121228T
Ophiognomonia alni-cordatae CBS 131353T
Ophiognomonia monticola CBS 131346T
Ophiognomonia gunmensis CBS 131401T
Ophiognomonia quercus-gambellii CBS 131397
Ophiognomonia sogonovii CBS 131341T
Ophiognomonia sogonovii CBS 121914
Ophiognomonia asiatica CBS 131351T
Ophiognomonia setacea CBS 128354
Ophiognomonia kobayashii CBS 131352T
Ophiognomonia otanii CBS 131402
Ophiognomonia otanii CBS 131354T
Ophiognomonia castaneae CGMCC3.17661
Ophiognomonia castaneae CGMCC3.17663T
Ophiognomonia gei CBS 818.79T
Ophiognomonia rosae CBS 131365T
Ophiognomonia nipponicae CBS 131407T
Ophiognomonia padicola CBS 845.79
Ophiognomonia rubi-idaei BPI 877559
Ophiognomonia sassafras CBS 131366T
Ophiognomonia melanostyla CBS 131431
Ophiognomonia longispora CBS 131358T
Ophiognomonia cordicarpa CBS 131342T
Ophiognomonia pseudoclavulata CBS 121236T
Ophiognomonia pseudoclavulata CBS 131434
Ophiognomonia lenticulispora CBS 131363T
Ophiognomonia micromegala CBS 121910
Ophiognomonia vasiljevae CBS 121253
Ophiognomonia vasiljevae CBS 128353
Ophiognomonia acadiensis DAOM 242797T
Ophiognomonia maximowiczianae CBS 131357T
Ophiognomonia nana CBS 883.79
Ophiognomonia alni-viridis CBS 131408
Ophiognomonia multirostrata CBS 131348T
Ophiognomonia intermedia CBS 119188
Ophiognomonia tucumanensis CBS 131364T
Ophiognomonia ibarakiensis CBS 131405T
Ophiognomonia bugabensis CBS 131399
Ophiognomonia gardiennetii CBS 131417T
Ophiognomonia pterocaryae SICAUCC 23-0060
Ophiognomonia pterocaryae CBS 131359T
Ophiognomonia pseudopterocaryae SICAUCC 23-0061T
Ophiognomonia pseudopterocaryae SICAUCC 23-0151
Ophiognomonia apiospora CBS 131426T
Ophiognomonia clavigignenti-juglandacearum CBS 121081
Ophiognomonia naganoensis CBS 131404T
Ophiognomonia balsamiferae CBS 121266T
Ophiognomonia trientensis CBS 131604
Ophiognomonia gei montani CBS 821.79
Ophiognomonia leptostyla SICAUCC 22-0103
Ophiognomonia leptostyla SICAUCC 22-0103
Ophiognomonia leptostyla SICAUCC 20-0012
Ophiognomonia leptostyla SICAUCC 21-0008
Ophiognomonia leptostyla SICAUCC 21-0010
Ophiognomonia leptostyla SICAUCC 22-0157
Ophiognomonia leptostyla CBS 196.32
Ophiognomonia leptostyla CBS 110136
Ophiognomonia leptostyla CBS 844.79
Ambarignomonia petiolorum CBS 121227T
0.08
Ophiognomonia
Ambarignomonia (Outgroup)

Figure 91 – Best scoring RAxML tree with a final likelihood value of -30,052.537578 based on combined ITS, *ms*204 and *tef*1-α sequence data of related species. The tree is rooted with *Ambarignomonia petiolorum* (CBS 121227) in *Ambarignomonia*. Sixty-six strains were included in the combined analyses which comprised 3,409 characters (648 characters for ITS, 1,313 characters for *ms*204 and 1,446 characters for *tef*1-α, including gap regions). The matrix had 1,790 distinct alignment patterns, with 30.92% undetermined characters and gaps. Estimated base frequencies were as follows; A = 0.227984, C = 0.300892, G = 0.235041, T = 0.236083; substitution rates AC = 1.167492, AG = 2.426422, AT = 1.277453, CG = 0.910593, CT = 4.052388, GT = 1.000000; gamma distribution shape parameter α = 0.363600. In our analysis, GTR+I+G model was used for each partition in Bayesian posterior analysis. The species determined in this study is indicated in red and bold. Bootstrap support values for maximum likelihood (MLBS, left) ⩾ 60% and Bayesian posterior probabilities (BYPP, right) ⩾ 0.90 are indicated at the nodes, respectively. Hyphens (-) represent support values less than 60% MLBS/0.90 BYPP. The ex-type superscript "T".

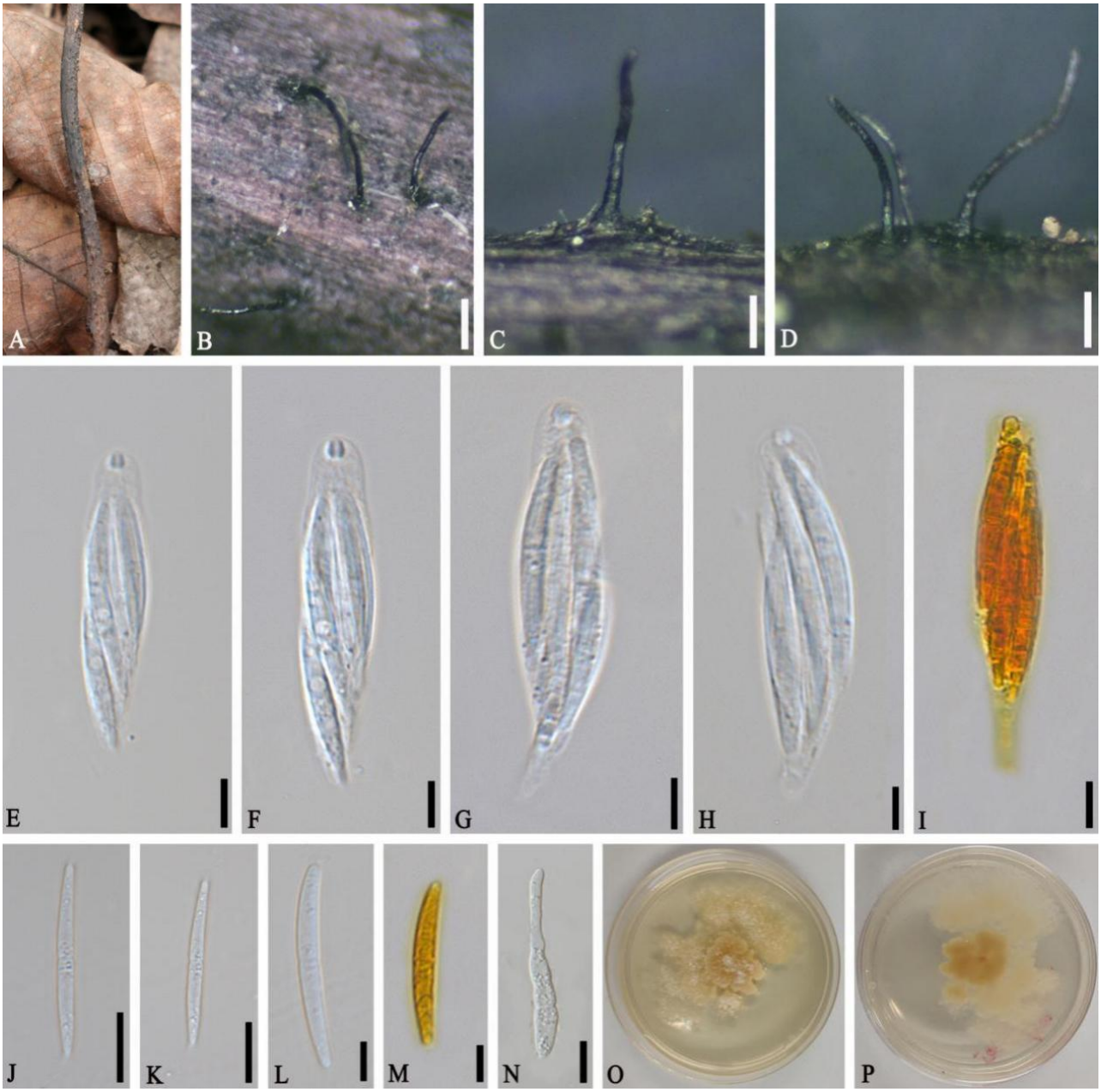


Figure 92 – *Ophiognomonia pseudopterocaryae* (SICAU 23-0082, holotype). A Walnut petiole. B–D Mature ascomata. E-H Asci. I Asci in Melzer's reagent. J–L Ascospores. M Ascospores in Melzer's

reagent N. Germinating ascospore. O, P Colonies on PDA (O from above, P from below). Scale bars: B = 500 µm, C, D = 200 µm, E–K, N = 10 µm, L, M = 5 µm.

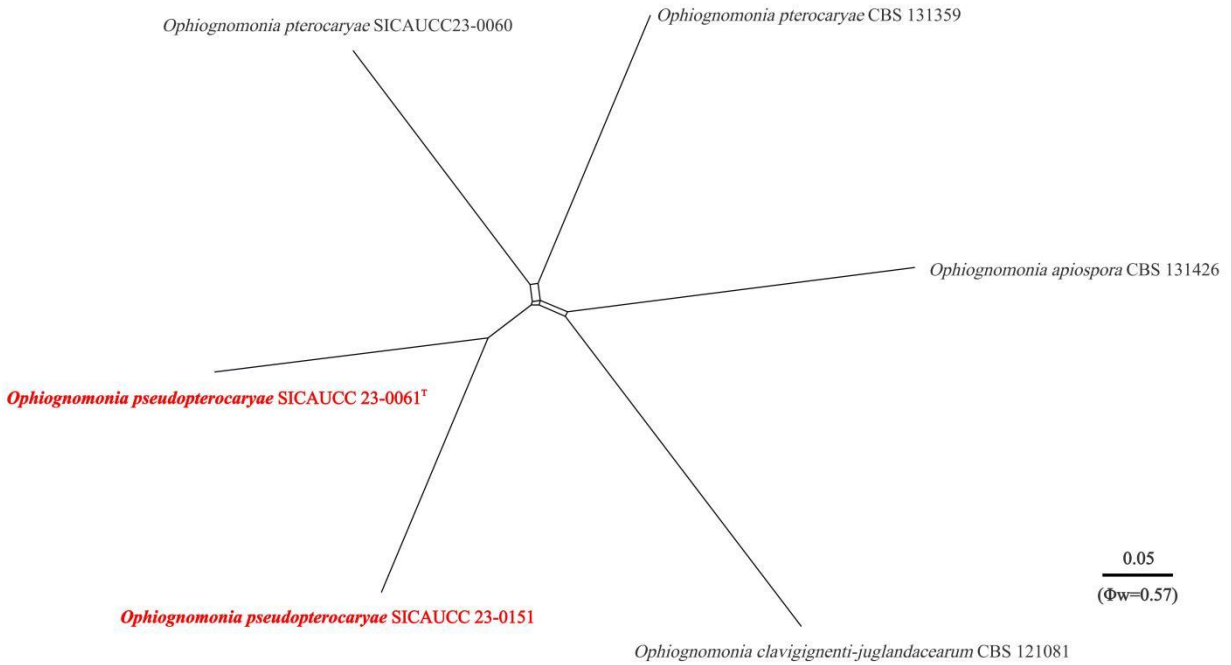


Figure 93 – Results of the PHI test of *Ophiognomonia pseudopterocaryae* and closely related species using both LogDet transformation and splits decomposition. The PHI test did not find any statistically significant recombination (Φw = 0.57) in the data set. The new strains are represented in red and bold. "T" represents the type strain.

Culture characteristics – Ascospores do not germinate in sterile water. Ascospores germinating on PDA within 36 h and germ tubes produced from one or both ends, slow growth. Colonies on PDA reaching 60 mm diam., after 30 days at 25 ℃. The mycelium grows on the surface of the medium, with bump center and flat margin, sometimes radially furrowed; aerial mycelium felty to woolly, orange-white, whitish or greyish brown, nearly round growth with irregular edges, white. Reverse, yellowish brown.

Material examined – China, Sichuan Province, Liangshan Yi Autonomous Prefecture, Huili City (26°56′43.49″N 102°16′26.76″E, alt. 2008 m), on dead petioles of *Juglans regia*, 30 September 2022, F.-H. Wang, WFH202209005 (SICAU 23-0081), living culture SICAUCC 23-0060.

GenBank numbers – SICAUCC 23-0060: PP060676 (ITS), PP061150 (*tef*1-α), PP061108 (*ms*204).

Note – A phylogenetic analysis placed our new collection *Ophiognomonia pterocaryae* (SICAUCC 23-0060) within *Ophiognomonia* and it clustered with *O. pterocaryae* (CBS131359) with strong statistical support (100% MLBS/1.00 BYPP) (Fig. 91). Nucleotide comparisons of ITS, *tef*1-α, and *ms*204 (SICAUCC 21-0013) also showed a high homology with the sequences of *O. pterocaryae* (CBS131359 ex-type), with a similarity of 99.8% (511/512, 1 gap), 100% (365/365, 0 gap), and 99.4% (1092/1099, 1 gap), respectively. Morphologically, the gross characteristics of this new specimen correspond to *O. pterocaryae* as described by Walker et al. (2012a) including the measurements of ascomata, asci and ascospores. Therefore, the new specimen is identified as *O. pterocaryae* and it is reported as a new geographical record for China, previously having been found in Japan (Walker et al. 2012a).

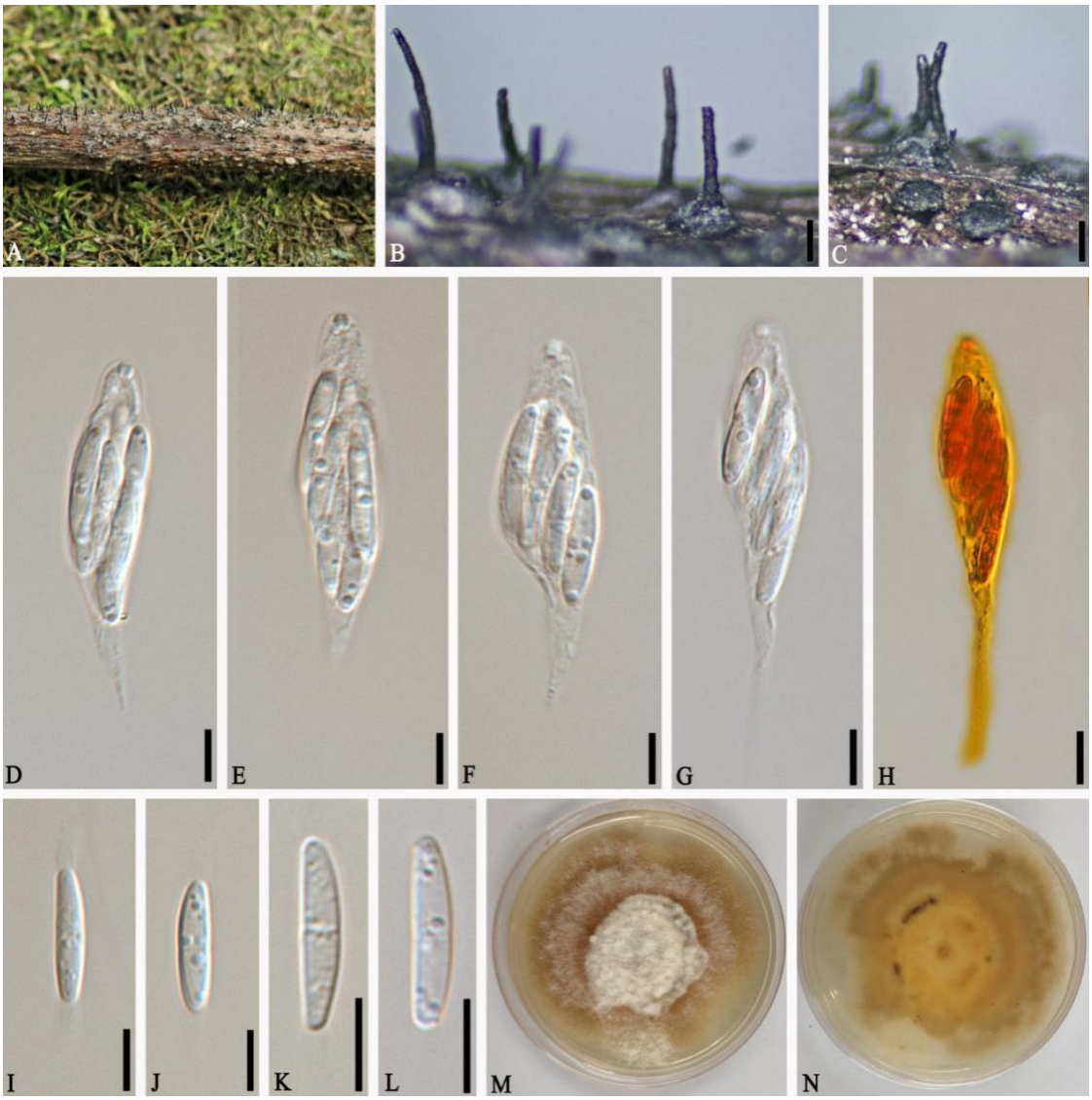


Figure 94 – *Ophiognomonia pterocaryae* (SICAU 23-0081). A Walnut petiole. B Mature perithecia. C Vertical section of ascomata. D–G Asci. H Asci in Melzer's reagent. I–L Ascospores. M, P Colonies on PDA (M from above, N from below). Scale bars: B, C = 500 μm, D–L = 10 μm.

Juglanconidaceae Voglmayr & Jaklitsch, Persoonia 38: 142. 2017.

Description: See Voglmayr et al. (2017b).

Type genus: *Juglanconis* Voglmayr & Jaklitsch.

Amniculicolaceae was introduced by Voglmayr et al. (2017b). At present, there is only the genus *Juglanconis*, based on morphological and molecular data. *Juglanconidaceae* is morphologically restricted to the melanconium-like species occuring on *Juglandaceae*. Most *Juglanconidaceae* are pathogenic causing black pustular dieback disease.

Juglanconis Voglmayr & Jaklitsch, Persoonia 38: 142 (2017).

Voglmayr et al. (2017a) recently described the new genus *Juglanconis* for four *Melanconis* species on hosts of tribe *Juglandinae*, viz. three species (*Juglanconis appendiculata, J. juglandina, J. oblonga*) on various *Juglans* species and one (*J. pterocaryae*) from *Pterocarya* spp. Recently, Voglmayr et al. (2019) and others rediscovered a species on *Pterocarya rhoifolia*. At present, there are 5 species in this genus.

59. ***Juglanconis appendiculata*** Voglmayr & Jaklitsch, Persoonia 38: 144 (2017) Figs. 95, 96

Index Fungorum number: IF819583; Facesoffungi number: FoF16304

Associated with blight symptom on living branches of *Juglans sigillata*. Symptoms manifest as chlorophyll loss and dehydration in the branches, leading to wilting and subsequent leaf drop. Sexual morph: *Pseudostromata* 1–3 mm diam., typically distinct, circular, slightly projecting, without perithecial bumps. *Ectostromatic disc* 0.5–1.2 mm diam., distinct, circular or oblong, dark grey, brown or black, often covered by densely arranged ostioles, pulvinate. *Central column* yellowish to brownish grey. *Entostroma* indistinct. *Ostioles* several per disc, plane or slightly papillate, black, sometimes covered by distinct white crust. *Perithecia* 380–490 × 540–660 µm ($\bar{x}$ = 420 × 560 µm, n = 10), arranged in various configurations. *Asci* 120–145 × 19–26 µm ($\bar{x}$ = 133 × 23 µm, n = 20), 8-spored, clavate to fusoid, with distinct funnel-shaped apical. *Ascospores* 22–30 × 9–13 µm ($\bar{x}$ = 27 × 11 µm, n = 20), hyaline, ellipsoid or broadly fusoid, symmetric to slightly asymmetric, distinctly constricted at the septum, with indistinct appendages. Asexual morph: *Conidiomata* acervular, 0.5–1.4 mm diam., black, scattered or occasionally confluent, with central or eccentric stromatic column, at maturity covered by black discharged conidial masses, usually conspicuous. *Conidiophores* 26–39 × 3–6 µm ($\bar{x}$ = 32 × 4 µm, n = 20), narrowly cylindrical to lageniform, simple or branched at the base, smooth, subhyaline to pale brown. *Conidiogenous cells* annellidic with distinct annellations, integrated. *Conidia* 20–28 × 7–11 µm ($\bar{x}$ = 25 × 9 µm, 4 = 20), unicellular, hyaline when immature, brown when mature, broadly ellipsoid to broadly pip-shaped, truncate with distinct scar at the base, densely multi-guttulate, thick-walled, wall ornamented on the inside with irregular confluent verrucae and with gelatinous sheath.

Material examined – China, Sichuan Province, Mianyang City, Pingwu County (32°12′59.24″N 104°50′15.65″E, alt. 726 m), on dead branches of *Juglans sigillata*, 9 July 2022, F.-H. Wang, WFH202207057 (SICAU 23-0083), living culture SICAUCC 23-0062. *Ibid*., Mianyang City, Pingwu County (32°12′59.24″N 104°50′15.65″E, alt. 726 m), on dead branches of *Juglans regia*, 9 July 2022, WFH202207065 (SICAU 23-0084), living culture SICAUCC 23-0063.

GenBank numbers – SICAUCC 23-0062: PP060678 (ITS), PP057964 (LSU); SICAUCC 23-0063: PP060679 (ITS), PP057965 (LSU).

Note – In the phylogenetic analysis our newly collected specimen (SICAUCC 23-0062 and SICAUCC 23-0063) clusters with *Juglanconis appendiculata* (D96) with strong statistical support (100% MLBS/1.00 BYPP) (Fig. 97). Nucleotide comparisons of ITS and LSU (SICAUCC 23-0062) showed a high homology with the sequences of *J. appendiculata* (D96, ex-type), with a similarity of 99.8% (566/567, 1 gap), and 100% (800/800, 0 gap). Nucleotide comparisons of ITS and LSU (SICAUCC 23-0063) showed a high homology with the sequences of *J. appendiculata* (D96, ex-type), with a similarity of 99.8% (566/567, 1 gap), and 100% (776/776, 0 gap). Morphologically our new specimen matches *J. appendiculata* based on the synopsis that provided by Voglmayr et al. (2017b). Based on morphological characters and phylogenetic analyses, we determine our specimens as *J. appendiculata*.

60. ***Juglanconis magnatum*** F.H. Wang & C.L. Yang, sp. nov. Fig. 98

Index Fungorum number: IF901574; Facesoffungi number: FoF15592

Etymology – Referring to larger conidia.

Holotype – SICAU 23-0085

Saprobic on dead twigs and branches of *Juglans regia*. Sexual morph unknown. Asexual morph: *Conidiomata* acervular, 0.4–0.7 mm diam, dark brown to blackish, flat, inconspicuous, scattered, with small central or eccentric whitish to light grey stromatic column, at maturity sometimes covered by brown to blackish discharged conidial masses. *Conidiophores* 14–36 × 2–4 µm ($\bar{x}$ = 27 × 3.5 µm, n = 20), cylindrical to lageniform, simple, rarely branched at the base, smooth, subhyaline to pale brown. *Conidiogenous cells* annellidic with distinct annellations, integrated. *Conidia* 9–14 × 5–8 µm ($\bar{x}$ = 12 × 6.5 µm, n = 40), unicellular, hyaline when immature, brown to dark brown when mature, ellipsoid, sometimes slightly allantoid, truncate with distinct scar at the base, densely multi-guttulate, thick-walled, thin gelatinous sheath.

Culture characteristics – Conidia germinating on sterile water within 36 h and germ tubes produced from ends. Colonies on PDA reaching 50 mm diam., after 35 days at 25 ℃. The mycelium

grows on the surface of the medium, grey with white, dense, irregular, marginal hyphae are radial pattern, later gradually turned black. Reverse, sameness. Not produced pigmentation on PDA media.

Material examined – China, Sichuan Province, Chengdu City, Chongzhou City (30°33′9.44″N 103°39′29.76″E, alt. 512 m), on dead branches of *Juglans regia*, 21 April 2022, F.-H. Wang, WFH202204004 (SICAU 23-0085 holotype), ex-type living culture SICAUCC 23-0064. *Ibid*., WFH202204004B (SICAU 24-0038), living culture SICAUCC 23-0152.

GenBank numbers – SICAUCC 23-0064: PP060680 (ITS), PP057966 (LSU), PP061175 (*tub*2); SICAUCC 23-0152: PP844880 (ITS), PP826168 (LSU), PP850063 (*tub*2).

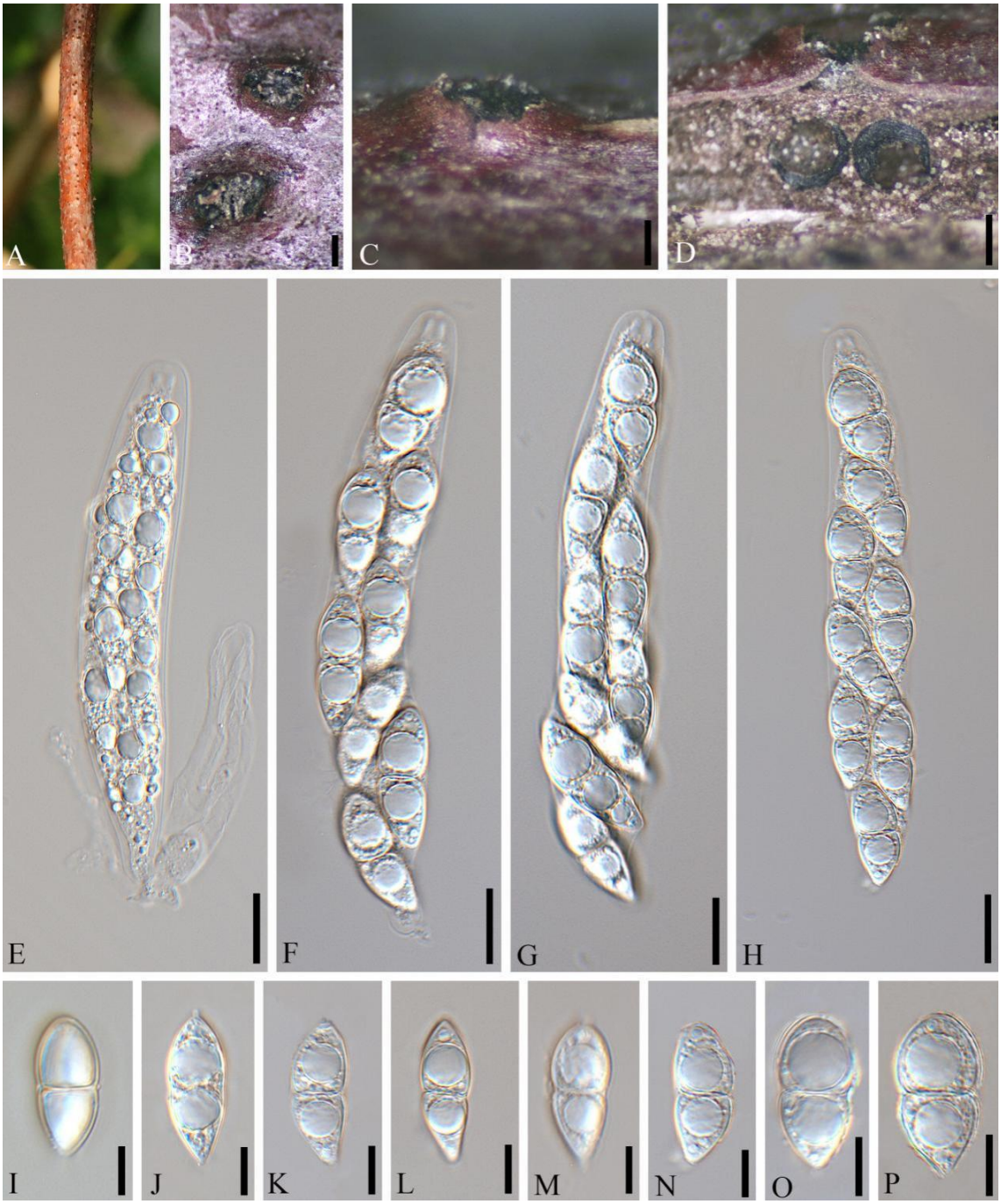


Figure 95 – Sexual morph of *Juglanconis appendiculata* (SICAU 23-0084). A Branch dieback covered by acervuli of *J. appendiculata*. B, C Appearance of ascostroma on the substrate. D Vertical section of ascomata. E–H Asci. I–P Ascospores. Scale bars: B = 1 mm, C, D = 500 μm, E–H = 20 μm, I–P = 10 μm.

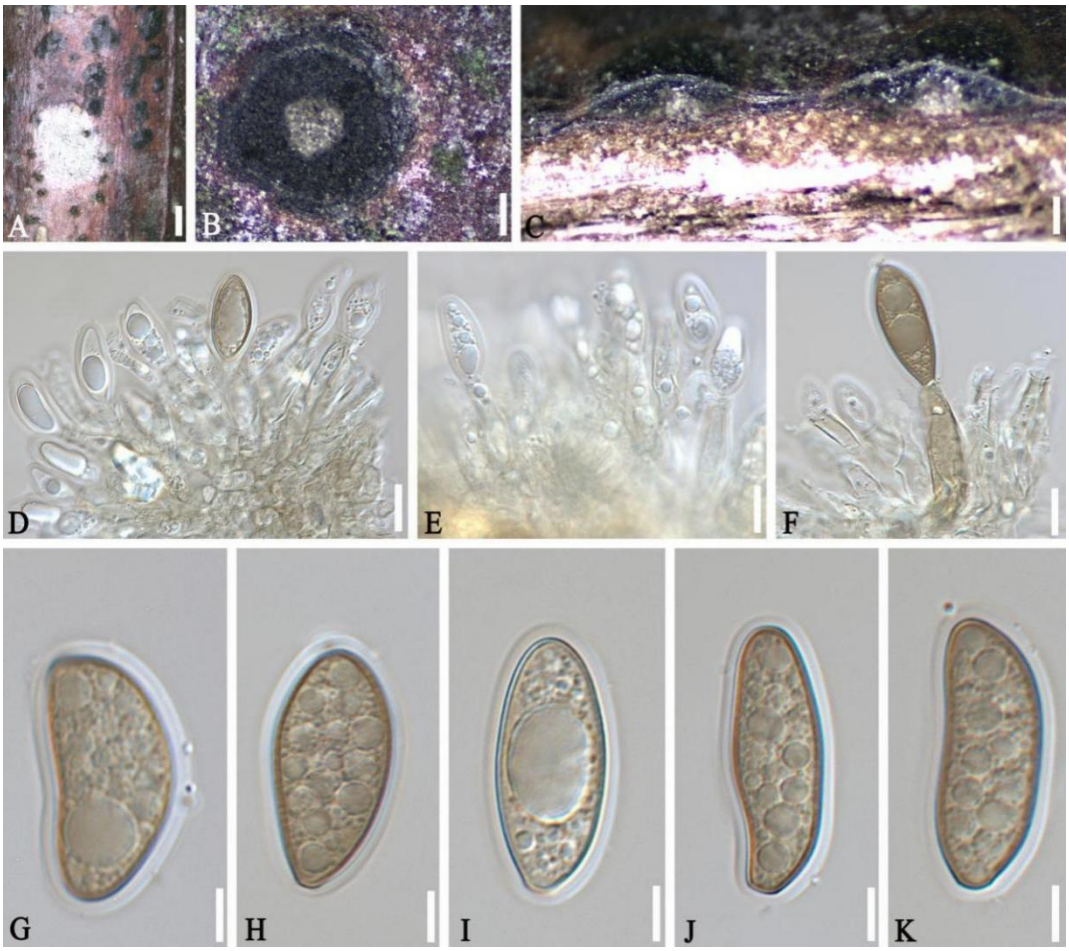


Figure 96 – Asexual morph of *Juglanconis appendiculata* (SICAU 23-0083). A Habit of conidiomata on a branch. B Transverse section of conidiomata. C Longitudinal section through conidiomata. D–F Conidiogenous cells attached with conidia. G–K Conidia. Scale bars: A = 5 mm, B, C = 500 μm, D–F = 20 μm, G–K = 5 μm.

Note – *Juglanconis magnatum* (SICAUCC 23-0064) is introduced based on both morphological and phylogenetic evidence (Fig. 97). The morphology of *J. oblonga* (ME14) is similar to *J. magnatum* (SICAUCC 23-0064), but distinguishable by the characters of the conidia (Voglmayr et al. 2017b). *Juglanconis magnatum* (SICAUCC 23-0064) has smaller conidia (18–22 × 9–12 vs. 9–14 × 5–8 μm) (Voglmayr et al. 2017a). In the phylogenetic analysis, *J. magnatum* (SICAUCC 23-0064) forms a related lineage with *J. pterocaryae* (MAFF 410079), *J. japonica* (ME20) and *J. appendiculata* (D96) with moderate support (88% MLBS/1.00 BYPP). In a BLASTn search of GenBank, the closest match of the ITS sequence of SICAUCC 23-0064 was *J. japonica* (FPH 2623) with 99.49% similarity to, while the closest match with the LSU sequence was *J. oblonga* (E14) with 99.76% similarity to, while the closest match with the *tub*2 sequence was *J. oblonga* (E14) with 96.55%. Specifically, the sequence divergences between *J. magnatum* (SICAUCC 23-0064) and *J. japonica* (ME20) in the ITS, LSU and *tub*2 regions are 0.57% (3/530, 1 gap), 0.35% (3/849, 1 gap), and 4.6% (41/899, 23 gaps), respectively. In contrast, the sequence divergences between *J. magnatum* (SICAUCC 23-0064) and *J. pterocaryae* (MAFF 410079) in the same regions are 1.5% (9/592, 2 gaps), 0.47% (4/849, 1 gap), and 4.6% (41/899, 23 gaps), respectively. In contrast, the sequence divergences between *J. magnatum* (SICAUCC 23-0064) and *J. appendiculata* (D 96) in the same regions are 2.2% (13/592, 5 gaps), 0.47% (4/849, 1 gap), and 7.9% (71/899, 27 gaps), respectively. The PHI test revealed no significant recombination event between our strain and the closely related taxa (Φw = 0.96) (Fig. 99). Thus, *J. magnatum* is introduced and described as a new species.

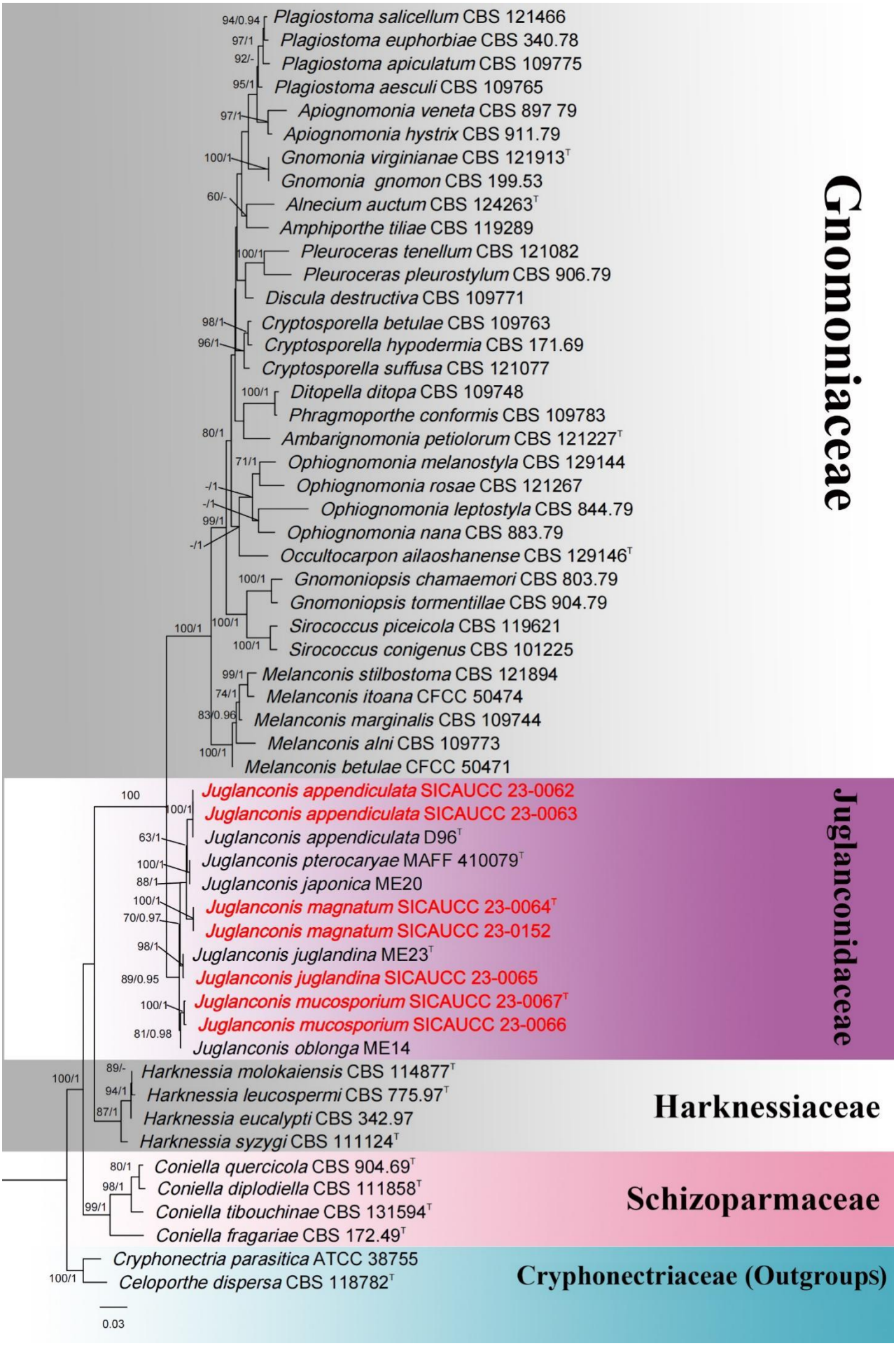

Gnomoniaceae
Plagiostoma salicellum CBS 121466
Plagiostoma euphorbiae CBS 340.78
Plagiostoma apiculatum CBS 109775
Plagiostoma aesculi CBS 109765
Apiognomonia veneta CBS 897 79
Apiognomonia hystrix CBS 911.79
Gnomonia virginianae CBS 121913T
Gnomonia gnomon CBS 199.53
Alnecium auctum CBS 124263T
Amphiporthe tiliae CBS 119289
Pleuroceras tenellum CBS 121082
Pleuroceras pleurostylum CBS 906.79
Discula destructiva CBS 109771
Cryptosporella betulae CBS 109763
Cryptosporella hypodermia CBS 171.69
Cryptosporella suffusa CBS 121077
Ditopella ditopa CBS 109748
Phragmoporthe conformis CBS 109783
Ambarignomonia petiolorum CBS 121227T
Ophiognomonia melanostyla CBS 129144
Ophiognomonia rosae CBS 121267
Ophiognomonia leptostyla CBS 844.79
Ophiognomonia nana CBS 883.79
Occultocarpon ailaoshanense CBS 129146T
Gnomoniopsis chamaemori CBS 803.79
Gnomoniopsis tormentillae CBS 904.79
Sirococcus piceicola CBS 119621
Sirococcus conigenus CBS 101225
Melanconis stilbostoma CBS 121894
Melanconis itoana CFCC 50474
Melanconis marginalis CBS 109744
Melanconis alni CBS 109773
Melanconis betulae CFCC 50471
Juglanconidaceae
Juglanconis appendiculata SICAUCC 23-0062
Juglanconis appendiculata SICAUCC 23-0063
Juglanconis appendiculata D96T
Juglanconis pterocaryae MAFF 410079T
Juglanconis japonica ME20
Juglanconis magnatum SICAUCC 23-0064T
Juglanconis magnatum SICAUCC 23-0152
Juglanconis juglandina ME23T
Juglanconis juglandina SICAUCC 23-0065
Juglanconis mucosporium SICAUCC 23-0067T
Juglanconis mucosporium SICAUCC 23-0066
Juglanconis oblonga ME14
Harknessiaceae
Harknessia molokaiensis CBS 114877T
Harknessia leucospermi CBS 775.97T
Harknessia eucalypti CBS 342.97
Harknessia syzygi CBS 111124T
Schizoparmaceae
Coniella quercicola CBS 904.69T
Coniella diplodiella CBS 111858T
Coniella tibouchinae CBS 131594T
Coniella fragariae CBS 172.49T
Cryphonectriaceae (Outgroups)
Cryphonectria parasitica ATCC 38755
Celoporthe dispersa CBS 118782T
0.03

Figure 97 – Best scoring RAxML tree with a final likelihood value of -14,782.194798 based on combined ITS, LSU and *tub*2 sequence data of related species. The tree is rooted with *Celoporthe dispersa* (CBS 118782) and *Cryphonectria parasitica* (ATCC 38755) in *Diaporthales*. Fifty-five strains were included in the combined analyses which comprised 4,790 characters (1,715 characters for LSU, 2,129 characters for LSU and 595 characters for *tub*2, including gap regions). Thistree includes selected taxa of *Diaporthales* and rooted with *Celoporthe dispersa* (CBS 118782) and *Cryphonectria parasitica* (ATCC 38755) in *Diaporthales*. The matrix had 760 distinct alignment patterns, with 58.34% of undetermined characters and gaps. Estimated base frequencies were as follows; A = 0.255219, C = 0.235299, G = 0.272557, T = 0.236924; substitution rates AC = 1.481507, AG = 2.559980, AT = 1.917538, CG = 0.741930, CT = 6.096012, GT = 1.000000; gamma distribution shape parameter α = 0.134118. The Bayesian inference analyses was implemented by MrBayes v.3.2.2 with the best-fit model (SYM+I+G for ITS; GTR+I+G for LSU; GTR for *tub*2) of evolution estimated with MrModeltest 2.2. The species determined in this study is indicated in red and bold. Bootstrap support values for maximum likelihood (MLBS, left) ⩾ 60% and Bayesian posterior probabilities (BYPP, right) ⩾ 0.90 are indicated at the nodes, respectively. Hyphens (-) represent support values less than 60% MLBS/0.90 BYPP. The ex-type superscript "T"

61. ***Juglanconis mucosporium*** F.H. Wang & C.L. Yang, sp. nov. Figs. 100, 101

Index Fungorum number: IF901575; Facesoffungi number: FoF15591

Etymology – Conidia with gelatinous sheaths.

Holotype – SICAUCC 23-0066

Saprobic on dead twigs and branches of *Juglans regia*. Sexual morph: *Pseudostromata* 1–2.5 mm diam, usually distinct, circular, projecting up to 0.3 mm, without perithecial bumps. *Ectostromatic disc* indistinct, usually circular, greyish to brownish or black, 0.4–1.3 mm diam, commonly concealed by densely arranged ostioles, often pulvinate. Central column white, grey to brownish grey. *Entostroma* indistinct. *Ostioles* 440–680 × 45–67 µm ($\bar{x}$ = 530 × 52 µm, n = 20), 1–9 per disc, papillate, carbonaceous, black. *Perithecia* 524–700 × 480–670 µm ($\bar{x}$ = 610 × 530 µm, n = 20), arranged in various configurations. *Asci* 96–114 × 14–19 µm ($\bar{x}$ = 107 × 16 µm, n = 20), clavate to cylinder-shaped, containing 8 uni- to irregularly biseriate ascospores, ring cylindrical to funnel-shaped. *Ascospores* 20–28 × 8–12 µm ($\bar{x}$ = 24 × 10 µm, n = 20), hyaline, ellipsoid, broadly ellipsoid or broadly fusoid, usually the upper cell is larger than the lower cell, straight, rarely slightly curved, constricted at the septum, without appendages, with large guttules in each cell. Asexual morph. *Conidiomata* acervular, 1–2 mm diam, blackish, scattered or occasionally confluent, with central or eccentric stromatic column; at maturity covered by black discharged conidial masses. *Conidiophores* 24–34 × 2–5 µm ($\bar{x}$ = 31 × 3.5 µm, n = 20), cylindrical to lageniform, simple, rarely branched at the base, smooth, subhyaline to pale brown. *Conidiogenous cells* annellidic with distinct annellations, integrated. *Conidia* 17–26 × 10–13 µm ($\bar{x}$ = 20 × 11 µm, n = 40), unicellular, hyaline when immature, brown to blackish when mature, ellipsoid, elongate to pip-shaped, sometimes slightly allantoid, truncate with distinct scar at the base, densely multi-guttulate, thick-walled, with 0.6–1.1 µm wide gelatinous sheath.

Culture characteristics – Conidia do not germinate in sterile water. Conidia germinating on PDA within 36 h and germ tubes produced from one or both ends, slow growth. Colonies on PDA reaching 40 mm diam., after 34 days at 25 ℃. The mycelium grows on the surface of the medium, edge undulate, white to pale yellow, aerial mycelium with black fruiting bodies, dense, circular, fat, dull. Reverse, of culture, yellow to pale orange. Not produced pigmentation on PDA media.

Material examined – China, Sichuan Province, Aba Tibetan and Qiang Autonomous Prefecture, Beichuan County (31°45′12.33″N 104°1′5.89″E, alt. 1107 m), on dead branches of *Juglans regia*, 8 July 2022, F.-H. Wang, WFH202207048 (SICAU 23-0087, holotype), ex-type living culture SICAUCC 23-0066. *Ibid*., Mianyang City, Pingwu County (32°12′59.17″N 104°50′15.43″E, alt. 724 m), on dead branches of *Juglans regia*, 9 July 2022, F.-H. Wang, WFH202207063 (SICAU 23-0088), living culture SICAUCC 23-0067.

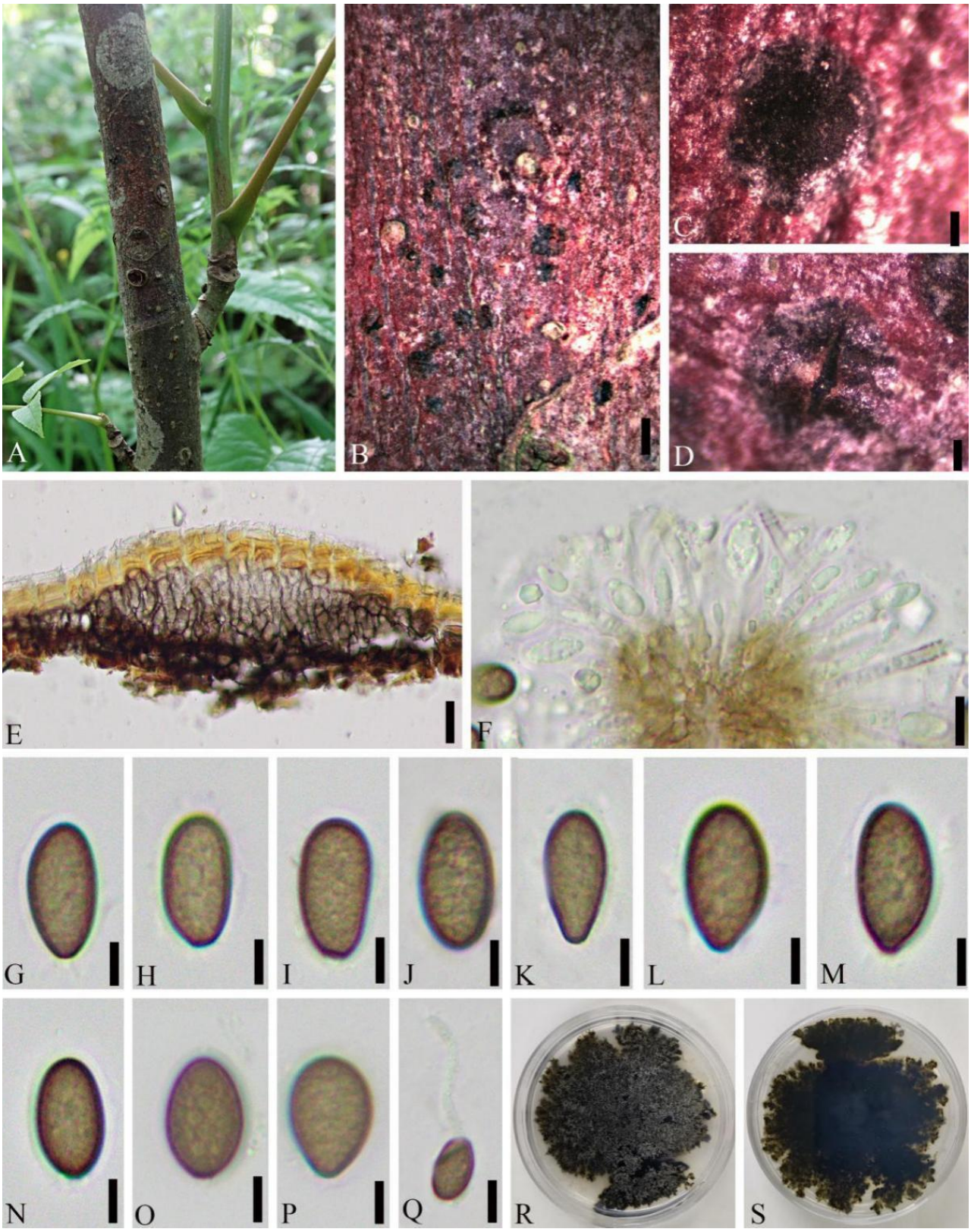


Figure 98 – *Juglanconis magnatum* (SICAU 23-0085, holotype). A Habit of conidiomata on a branch. B Appearance of conidiomata in host substrate. C Longitudinal section through conidiomata. F Conidiogenous cells attached with conidia. J–P Conidia. Q Germinating conidium. R, S Colonies on PDA (R from above, S from below). Scale bars: B = 500 µm, C, D = 200 µm, E = 50 µm, F, Q = 10 µm, G–P = 5 µm.

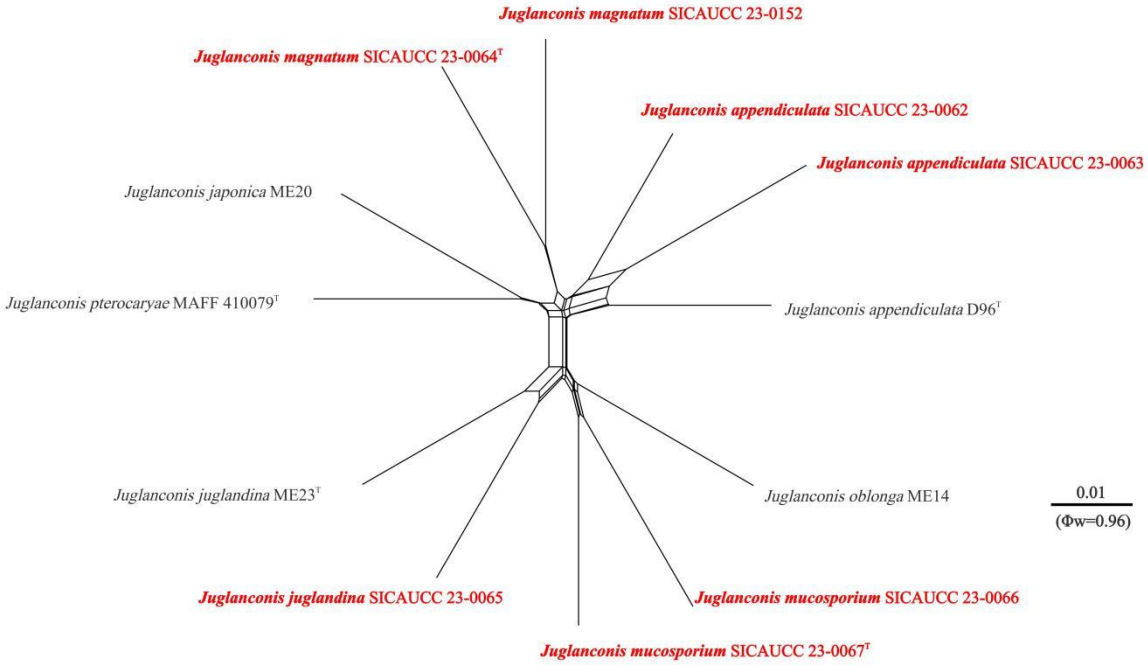


Figure 99 – Results of the PHI test of *Juglanconis magnatum*, *J. mucosporium*, and closely related species using both LogDet transformation and splits decomposition. The PHI test did not find any statistically significant recombination (Φw = 0.96) in the data set. The new strains are represented in red and bold. "T" represents the type strain.

GenBank numbers – SICAUCC 23-0066: PP060682 (ITS), PP057968 (LSU), PP061177 (*tub*2); SICAUCC 23-0067: PP060683 (ITS), PP057969 (LSU), PP061178 (*tub*2).

Note – *Juglanconis mucosporium* (SICAUCC 23-0066) is phylogenetically close to *J. oblonga* (E14) (Fig. 97). It is typical of *Juglanconis* in having immersed to erumpent, oblong or fusoid, octosporous asci, hyaline, ellipsoid, straight to curved, bicellular, with septum ascospores and brown, variable in shape conidia. However, *J. mucosporium* differs from *J. oblonga* (ME14) by having smaller conidiophores (24–34 × 2–5 µm vs. 28–44 × 4.8–6.5 µm) and larger conidia (17–26 × 10–13 µm vs. 18–22 × 9–12 µm) (Voglmayr et al. 2017a). In the phylogenetic analysis, *J. mucosporium* (SICAUCC 23-0066) forms a related lineage with *J. oblonga* (ME14) with moderate support (81% MLBS/0.98 BYPP). Specifically, the sequence divergences between *J. mucosporium* (SICAUCC 23-0066) and *J. oblonga* (ME14) in the ITS, LSU and *tub*2 regions are 1.6% (9/568, 4 gaps), 0.63% (5/799, 0 gap), and 5.2% (47/899, 21 gaps), respectively. The PHI test revealed no significant recombination event between our strain and the closely related taxa (Φw = 0.96) (Fig. 99). Hence, *J. mucosporium* is introduced as a new species in this study

62. ***Juglanconis juglandina*** (Kunze) Voglmayr & Jaklitsch, Persoonia 38: 144. 2017 Fig. 102

Index Fungorum number: IF819584; Facesoffungi number: FoF04446

Saprobic on dead twigs and branches of *Juglans regia*. Sexual morph unknown. Asexual morph. *Conidiomata* acervular, 1–3.5 mm diam, blackish, scattered or occasionally confluent, with central or eccentric stromatic column; at maturity covered by black discharged many conidial masses, usually conspicuous. *Conidiophores* 24–40 × 4–6 µm ($\bar{x}$ = 27 × 3.5 µm, n = 20), cylindrical to lageniform, simple, rarely branched at the base, smooth, subhyaline to pale brown. *Conidiogenous cells* annellidic with distinct annellations, integrated. *Conidia*17–26 × 10–15 µm ($\bar{x}$ = 21 × 13 µm, n = 20), unicellular, hyaline when immature, brown to blackish when mature, broadly ellipsoid to

broadly pip-shaped, truncate with distinct scar at the base, densely multi-guttulate, thick-walled, with 0.5–1.0 µm wide gelatinous sheath.

Culture characteristics – Conidia germinating on sterile water within 36 h and germ tubes produced from ends. Colonies on PDA reaching 60 mm diam., after 30 days at 25 ℃. The mycelium grows on the surface of the medium, grey with white, dense, circular, slightly convex. Reverse, dark olive. Not produced pigmentation on PDA media.

Material examined – China, Sichuan Province, Aba Tibetan and Qiang Autonomous Prefecture, Mao County (31°45′22.38″N 103°49′28.24″E, alt. 2009 m), on dead branches of *Juglans regia*, 8 July 2022, F.-H. Wang, WFH202207036 (SICAU 23-0086), living culture SICAUCC 23-0065.

GenBank numbers – SICAUCC 23-0065: PP060681 (ITS), PP057967 (LSU), PP061176 (*tub*2).

Note – Phylogenetic analysis shows that out new collections (SICAUCC 23-0065) cluster together with the ex-type strain of *Juglanconis juglandina* (ME23) with strong statistical support (98% MLBS/1.00 BYPP) (Fig. 97). Nucleotide comparisons of ITS, LSU, and *tub*2 (SICAUCC 23-0065) also showed a high homology with the sequences of *J. juglandina* (ME23 ex-type), with a similarity of 99.3% (587/591, 4 gap), 100% (797/797, 0 gap), and 100% (874/874, 0 gap), respectively. Morphologically, our new specimens match the description of *J. juglandina* (ME23) including overlap measurements of microscopic structures (Voglmayr et al. 2017a). Therefore, this species identified as *J. juglandina*, a species which has been reported from Asia and Europe (Voglmayr et al. 2017a, Fan et al. 2018b, Ma et al. 2019).

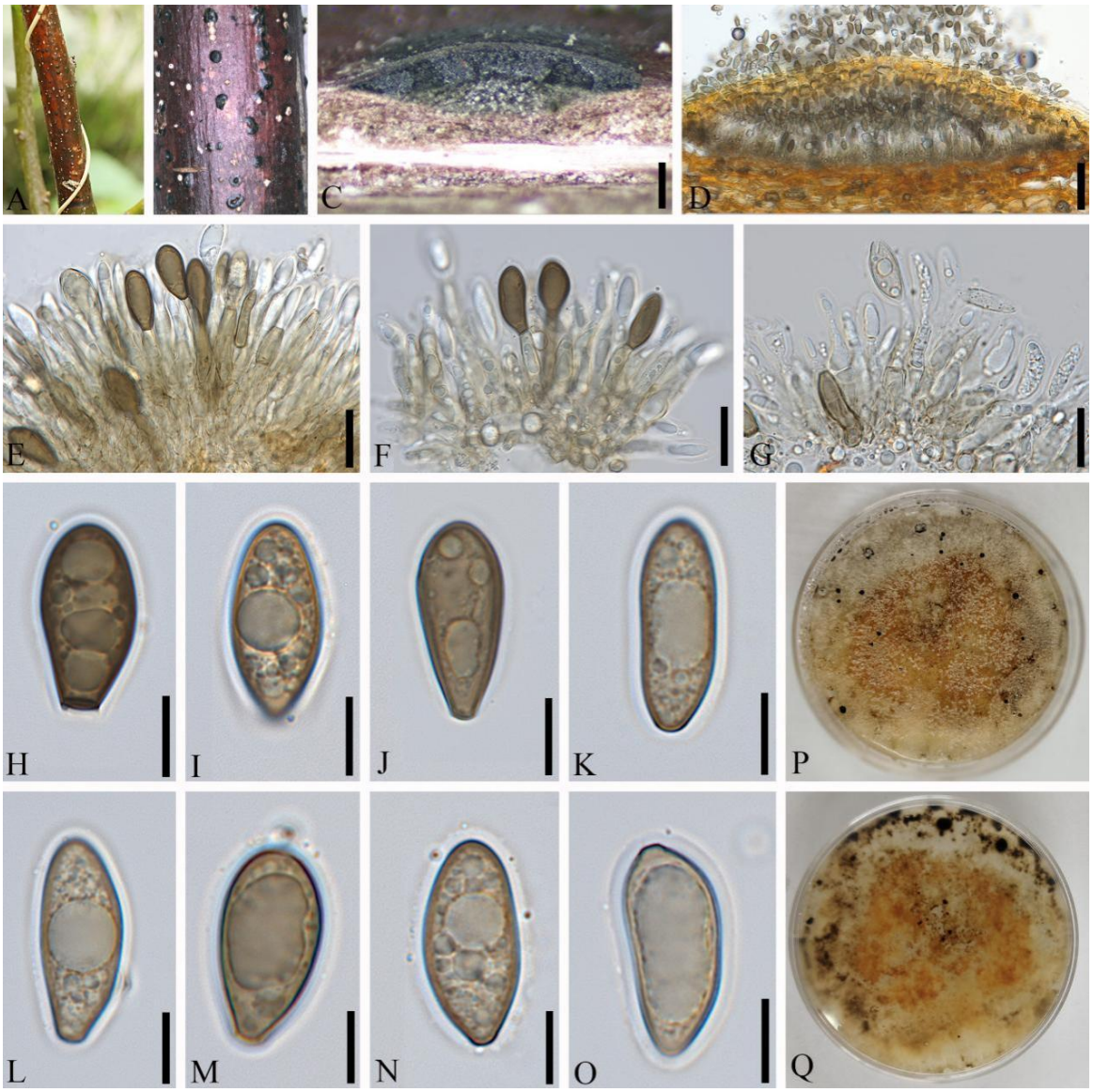


Figure 100 – Asexual morph of *Juglanconis mucosporium* (SICAU 23-0087, holotype). A Habit of conidiomata on a branch. B Appearance of conidiomata in host substrate. C, D Longitudinal section through conidiomata. E, G Conidiogenous cells attached with conidia. H–O Conidia. P, Q Colonies on PDA (P from above, Q from below). Scale bars: C = 100 μm, D = 60 μm, E–G = 20 μm, H–O = 10 μm.



Figure 101 – Sexual morph of *Juglanconis mucosporium* (SICAU 23-0088). A Branch dieback covered by acervuli of *J. mucosporium*. B, C Appearance of ascostroma on the substrate. D Vertical section of ascomata. E–H Asci. I Asci in Melzer's reagent. J–M Ascospores. N, O Colonies on PDA (N from above, O from below). Scale bars: B = 5 mm, C = 1000 μm, D = 500 μm. E–I = 10 μm, J–M = 5 μm.

Glomerellales Chadef. ex Réblová, W. Gams & Seifert, Stud. Mycol. 68: 170 (2011).

Glomerellales was proposed by Réblová et al. (2011) to accommodate *Australiascaceae*, *Glomerellaceae* and *Reticulascaceae* based on both morphology and phylogeny. Subsequently,

Maharachchikumbura et al. (2016b) and Tibpromma et al. (2018b) introduced *Plectosphaerellaceae* and *Malaysiascaceae* respectively in *Glomerellales*. Five families are currently accepted in *Glomerellales*, namely *Australiascaceae*, *Glomerellaceae*, *Malaysiascaceae*, *Plectosphaerellaceae* and *Reticulascaceae*.

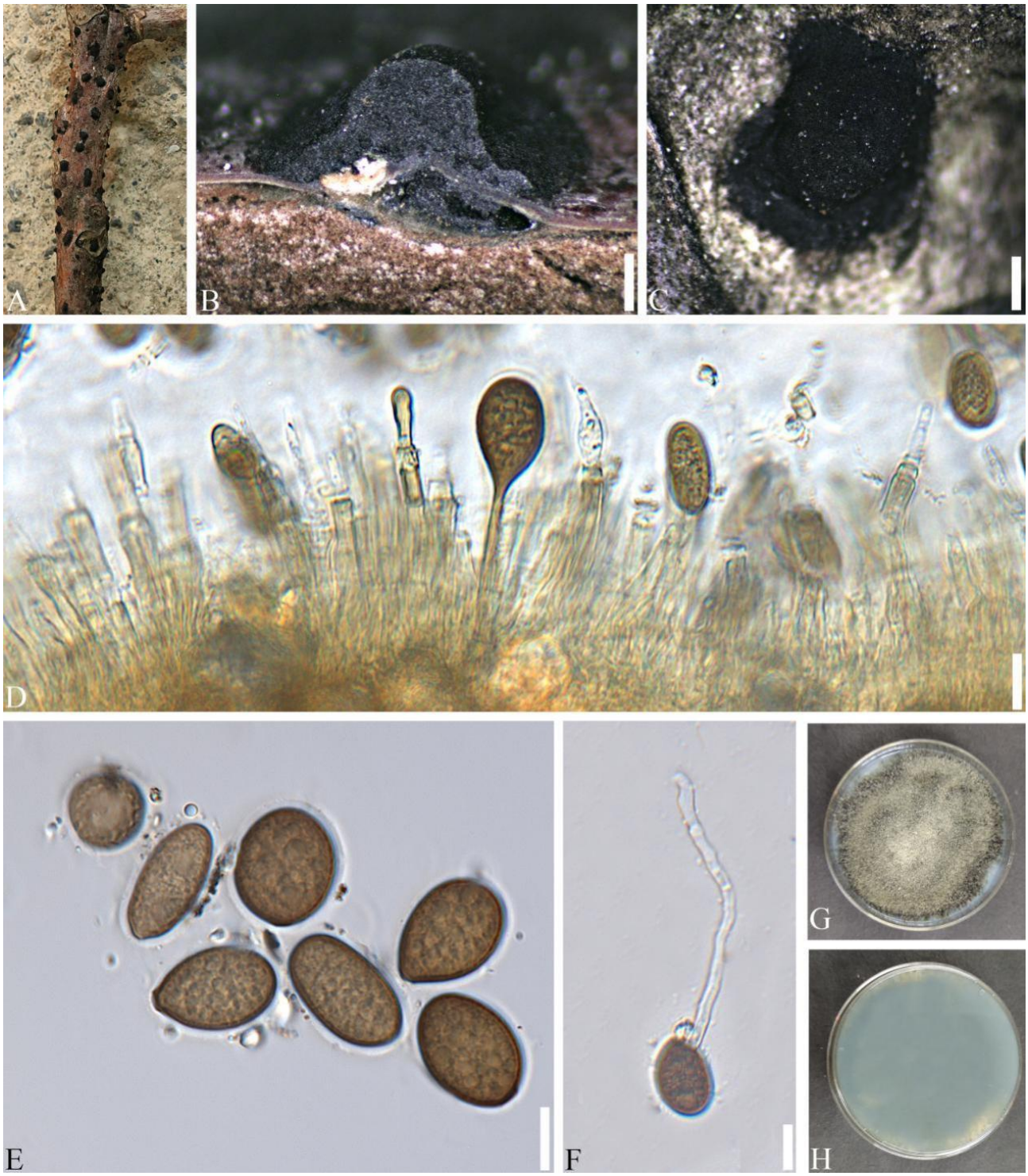


Figure 102 – *Juglanconis juglandina* (SICAU 23-0086). A Appearance of conidiomata in host substrate. B vertical sections of conidiomata. C Conidiomata in surface view. D Conidiogenous cells attached with conidia. E Conidia. F Germinating conidium. G, H Colonies on PDA (G from above, H from below). Scale bars: B, C = 2 mm, F = 20 μm, D, E = 10 μm.

Glomerellaceae Locq. ex Seifert & W. Gams.

Glomerellaceae was informally erected by Locquin (1984) as *Glomerella* Spauld. & H. Schrenk as type genus. Uecker (1994) showed that *Colletotrichum* does not belong in the same order as *Phyllachora* based on preliminary sequence-based studies. Thus, Kirk et al. (2001) placed *Glomerellaceae* in an uncertain position in *Sordariomycetidae*. Zhang et al. (2006) validated the family *Glomerellaceae* with a Latin description placing this family in *Hypocreomycetidae*. Afterwards, validated by Réblová et al. (2011) and Maharachchikumbura et al. (2016b) provided phylogenetic position of *Glomerellaceae* within *Glomerellales*. *Glomerellaceae* comprises pathogens, endophytes and saprobes (Udayanga et al. 2013, Jayawardena et al. 2016, Maharachchikumbura et al. 2016b).

Colletotrichum Corda, in Sturm, Deutschl. Fl., 3 Abt. (Pilze Deutschl.) 3(12): 41 (1831).

Colletotrichum was established by Corda (1831) to accommodate *C. lineola* as the type species (Damm et al. 2009). *Colletotrichum* comprises important plant pathogens, endophytes and saprobes as well as human and animal pathogens (Cannon et al. 2012, Jayawardena et al. 2021, Talhinhas & Baroncelli 2021). Bhunjun et al. (2021) demonstrated that coalescent approaches and multi-locus phylogeny are vital in establishing species boundaries in *Colletotrichum*. Liu et al. (2022) accepted 280 species in 16 species complexes and 15 singleton species and established a genome tree comprising 94 species. Further 13 species were added by Alizadeh et al. (2022), Hassan et al. (2022) and Zheng et al. (2022). New species groups are constantly being discovered (Sui et al. 2024, Vieira t al. 2024).

63. ***Colletotrichum beichuanense*** F.H. Wang & C.L. Yang, sp. nov. Fig. 103

Index Fungorum number: IF901577; Facesoffungi number: FoF15593

Etymology – Name reflects the location from which it was collected, Beichuan, China.

Holotype – SICAU 23-0090

Associated with leaf spots on the living leaves of *Juglans regia*. Leaves of infected sheaths usually turn yellow and die. Sexual morph: Not observed. Asexual morph: *Conidiomata* (on host), without setae, globose to subglobose, solitary or aggregated, semi-immersed to erumpent, pale brown to black, 70–130 μm diam., exuding globose, at maturity pale brown to yellowish conidial masses. *Conidiophores* 8–20 × 1.5–3 μm ($\bar{x}$ = 14 × 2 μm, n = 40), hyaline, cylindrical or clavate, septate, unbranched, smooth-walled, simple, occurring in densely arranged clusters. *Conidiogenous cells* 6–11 × 2.5–4 μm ($\bar{x}$ = 9 × 3 μm, n = 40), hyaline, enteroblastic, cylindrical or ampulliform, smooth. *Conidia* 13–19 × 4–6 μm ($\bar{x}$ = 15 × 5 μm, n = 40), hyaline, smooth, aseptate, subcylindrical, straight, two-end circle, containing oil-drop particles, part of the center is slightly curved. *Appressoria* not observed.

Culture characteristics – Conidia germinating on sterile water within 12 h. Colonies on PDA, 60 mm diam., after 12 days. The mycelium grows on the surface of the medium, initially white, becoming brown with age, dense, circular, with raised entire edge, velvety, black in reverse, with smooth margin. Not produced pigmentation on PDA media.

Material examined – China, Sichuan Province, Aba Tibetan and Qiang Autonomous Prefecture, Beichuan County (31°45′12.23″N 104°1′5.38″E, alt. 1103 m), on living leaves of *Juglans regia*, 8 July 2022, F.-H. Wang, WFH202207055 (SICAU 23-0090, holotype), ex-type living culture SICAUCC 23-0069. *Ibid*., WFH202207055B (SICAU 24-0039), living culture SICAUCC 23-0154.

GenBank numbers – SICAUCC 23-0069: PP060685 (ITS), PP061101 (*act*), PP061103 (*chs*-1), PV397444 (*tub*2); SICAUCC 23-0154: PP844882 (ITS), PP850042 (*act*), PP850044 (*chs*-1), PV397445 (*tub*2).

Note – Phylogenetic analyses showed that *Colletotrichum beichuanense* (SICAUCC 23-0069 and SICAUCC 23-0154) formed an independent lineage within Gloeosporioides complex, with medium statistical support (97% MLBS/1.00 BYPP) (Fig 104). The strains we isolated are closely related to *C. chrysophilum* (URM 7368). *Colletotrichum beichuanense* (SICAUCC 23-0069) is typical of *Colletotrichum* in having oval, solitary, gregarious conidiomata, unitunicate, simple,

hyaline to pale brown, smooth-walled *conidiophores* that hyaline, smooth-walled, aseptate, straight, cylindrical to fusiform conidia (Damm et al. 2009, Hyde et al. 2009). Morphologically, our new specimen resembles *C. chrysophilum* with overlapping size of conidia (Willie et al. 2018). However, the morphological description of *C. chrysophilum* (URM 7368) indicates that it was cultivated on various indoor media, and there are certain differences in the size of conidia among these different media. *Colletotrichum chrysophilum* (URM 7368) is capable of producing appressoria, whereas the strains collected in this study did not exhibit appressoria. *Colletotrichum chrysophilum* (URM 7368) possesses setae, whereas the strains collected in this study did not show the presence of setae. Nucleotide comparisons revealed notable genetic dissimilarities between *C. chrysophilum* (URM 7368) and *C. beichuanense* (SICAUCC 23-0069), viz. 0% (0/570, 0 gap), 6.2% (16/260, 7 gaps), 2.3% (14/599, 2 gaps) and 0% (0/230, 0 gap) in the ITS, *chs*-1, *tub*2 and *act*, respectively. Therefore, *C. beichuanense* is identified as a new species based on the recommendations of Jeewon & Hyde et al. (2016).

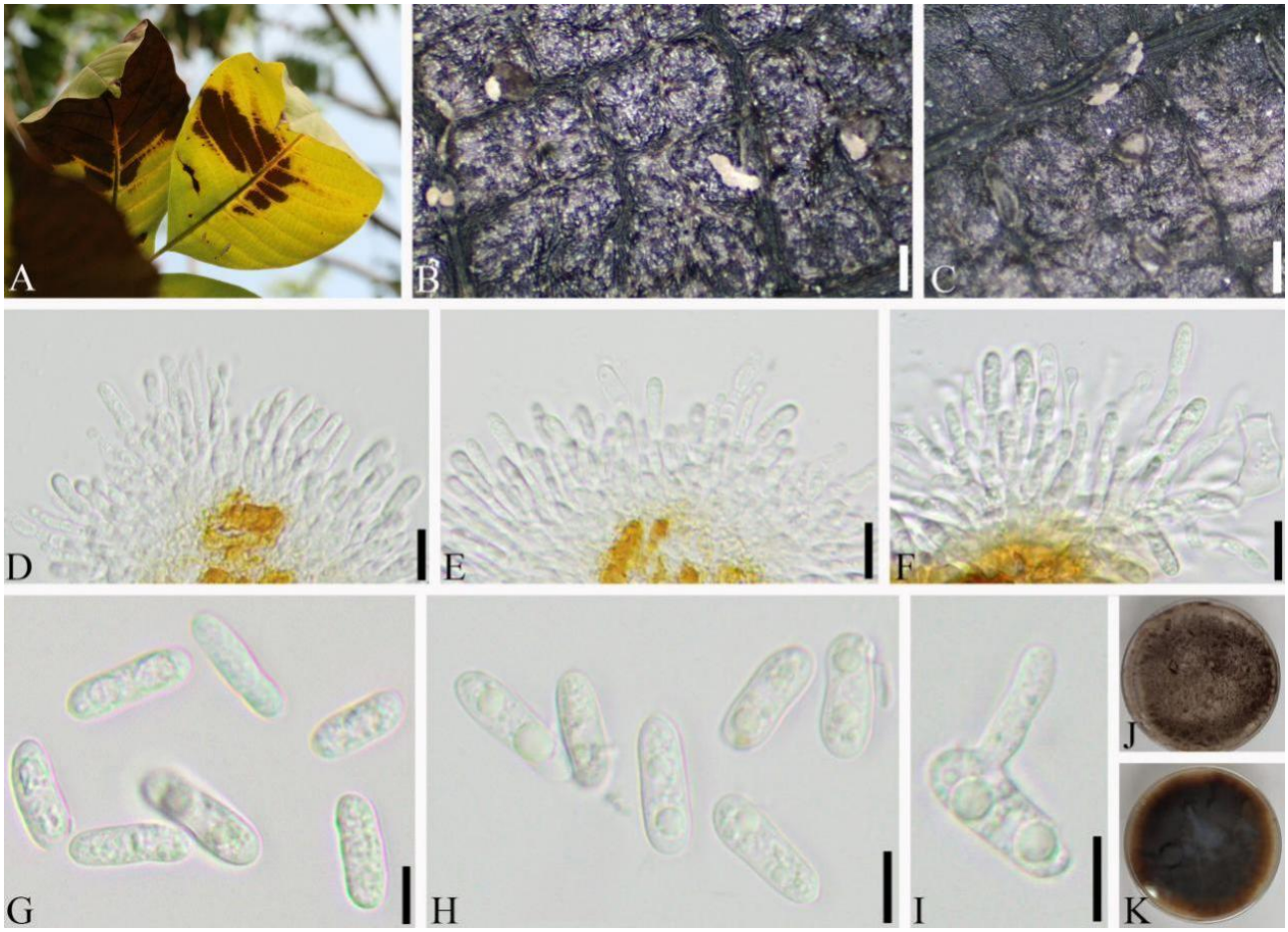


Figure 103 – *Colletotrichum beichuanense* (SICAU 23-0090, holotype). A Appearance of conidiomata on host. B, C Conidia in mass. D–F Conidiophores and conidiogenous cells. G, H Conidia. I Germinating conidium. J, K Colonies on PDA (J from above, K from below). Scale bars: B, C = 500 μm, D–F = 15 μm, G–I = 10 μm.

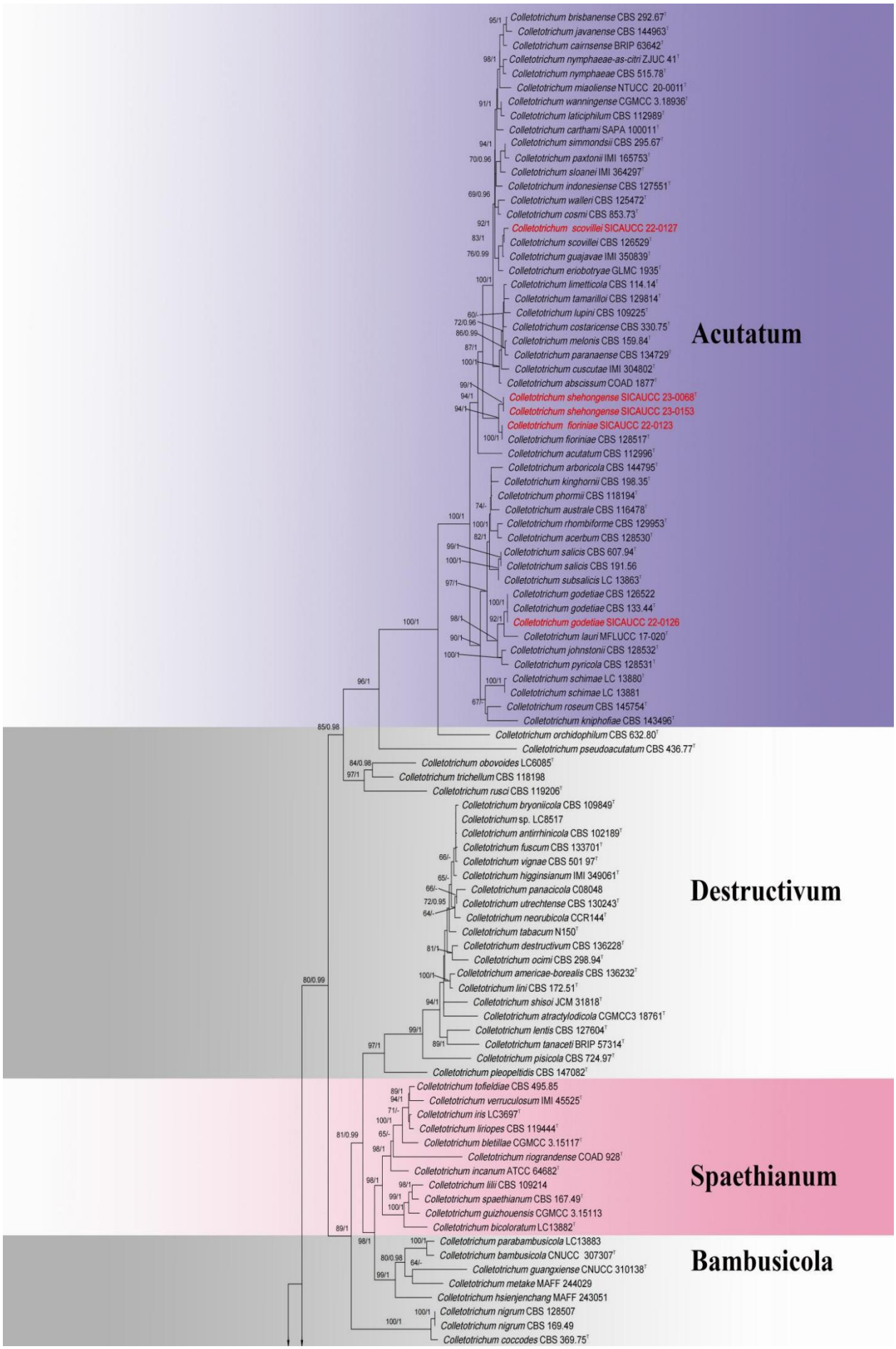


Figure 104 – Continued

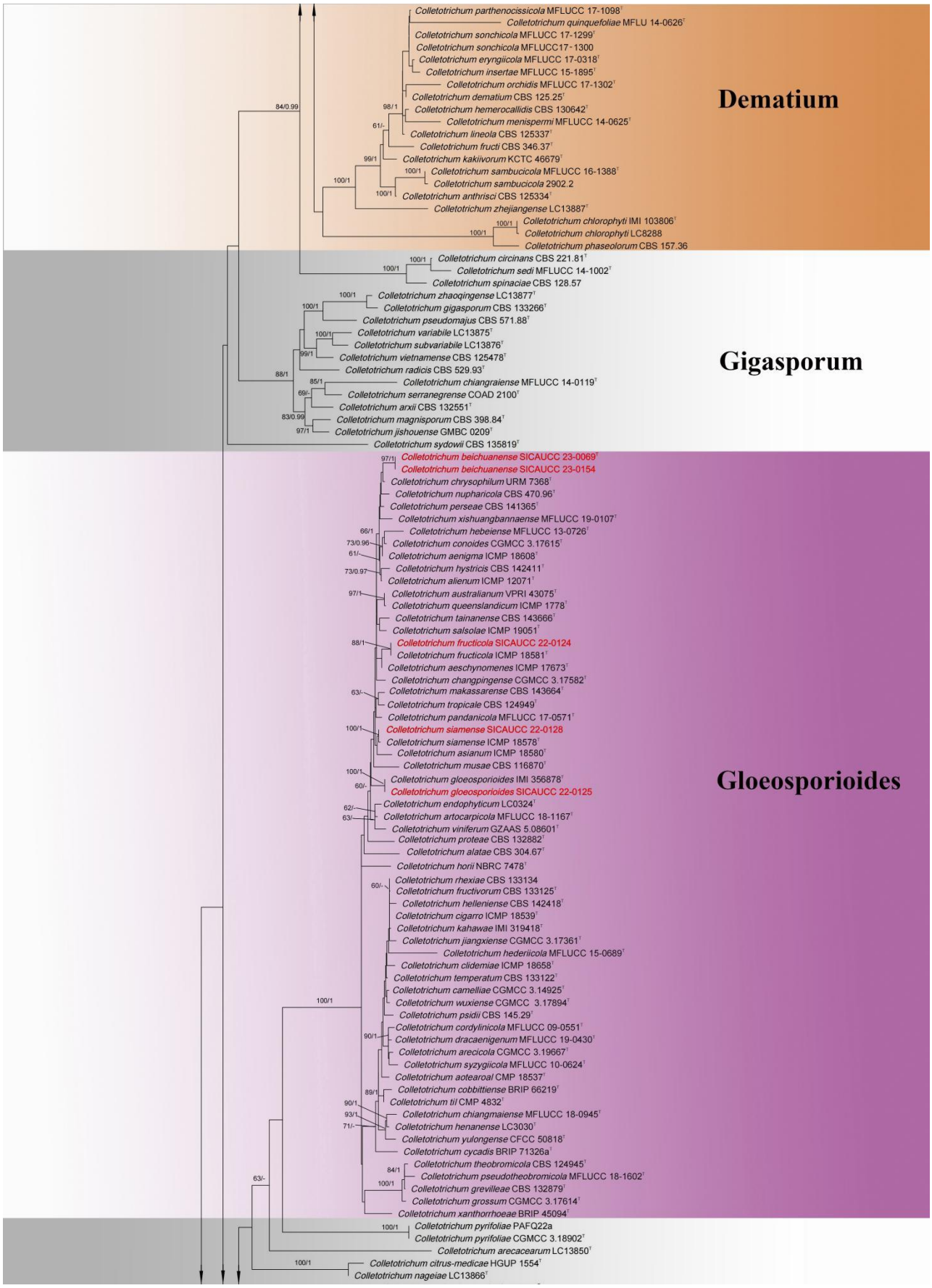


Figure 104 – Continued.

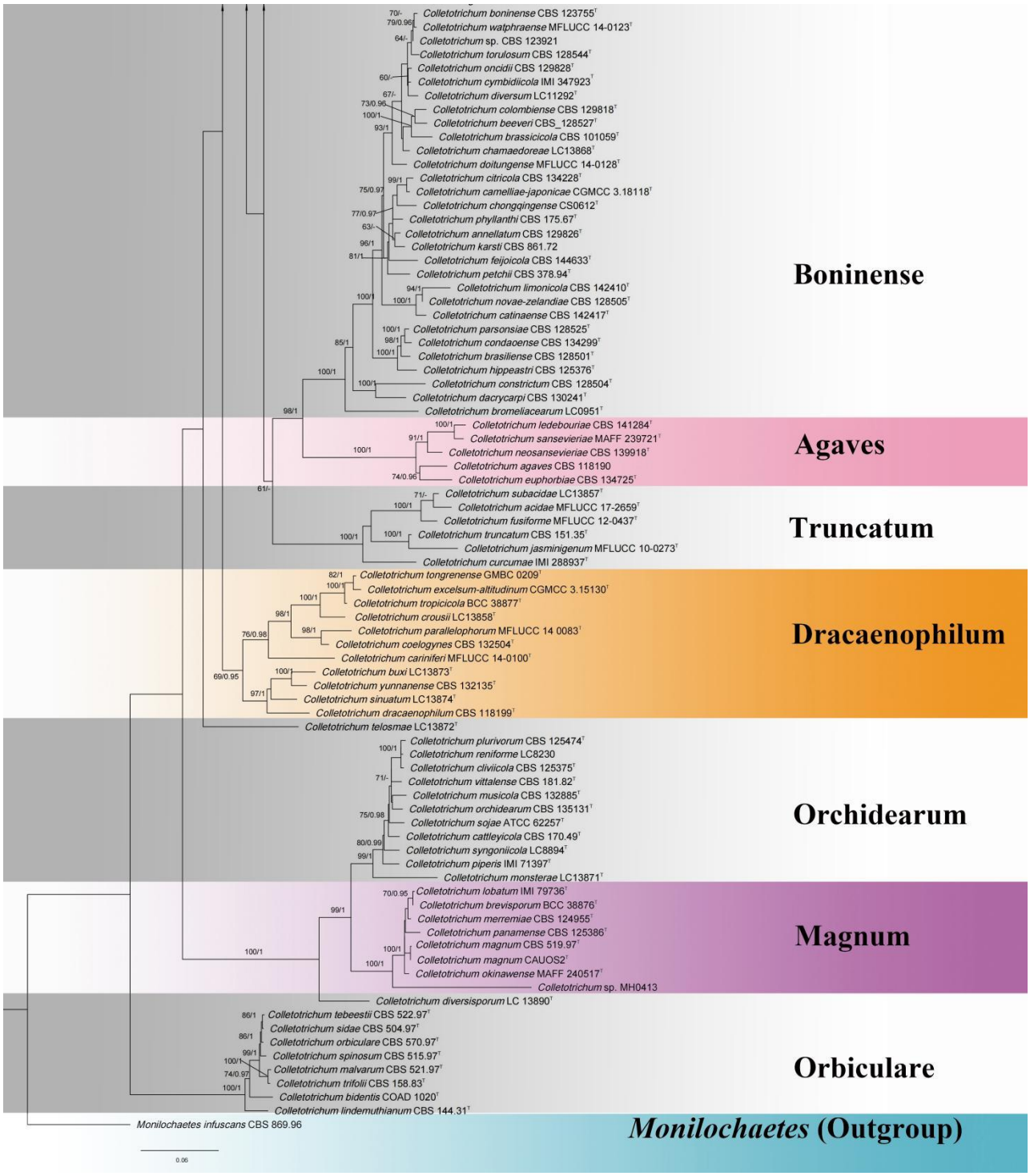


Figure 104 – Best scoring RAxML tree with a final likelihood value of -47,881.604955 based on combined *act*, *chs*-1, ITS and *tub*2 sequence data of related species. The tree is rooted with *Monilochaetes infuscans* (CBS 869.96) in *Monilochaetes*. Two hundred and eighty strains were included in the combined analyses which comprised 2,394 characters (387 characters for *act*, 322 characters for *chs*-1, 725 characters for ITS and 960 characters for *tub*2, including gap regions). The matrix had 1,795 distinct alignment patterns, with 34.70% undetermined characters and gaps. Estimated base frequencies were as follows; A = 0.225106, C = 0.293947, G = 0.253524, T = 0.227422; substitution rates AC = 1.111399, AG = 3.502852, AT = 1.326744, CG = 0.982896, CT = 5.015359, GT = 1.000000; gamma distribution shape parameter α = 0.440106. The Bayesian inference analysis was implemented by MrBayes v.3.2.2 with the best-fit model (GTR+G for *act*; GTR+I+G for *chs*-1, ITS; HKY+I+G for *tub*2) of evolution estimated with MrModeltest 2.2. The species determined in this study is indicated in red and bold. Bootstrap support values for maximum

likelihood (MLBS, left) ⩾ 60% and Bayesian posterior probabilities (BYPP, right) ⩾ 0.90 are indicated at the nodes, respectively. Hyphens (-) represent support values less than 60% MLBS/0.90 BYPP. The ex-type superscript "T".

64. ***Colletotrichum fioriniae*** (Marcelino & Gouli) Pennycook, Mycotaxon 132(1): 150 (2017) Fig. 105

Index Fungorum number: IF553097; Facesoffungi number: FoF02891

Associated with leaf spots on the living leaves of *Juglans regia*. Leaves distal to the infection turn light green in the interveinal areas and turn scorch brown colour from the margins. Sexual morph: Not observed. Asexual morph: *Conidiomata* 90–180 × 80–170 μm ($\bar{x}$ = 140 × 130 μm, n = 20), black, acervulus, globose, oval, solitary, gregarious, when mature, the surface is covered with pale yellow conidia. *Conidiophores* 18–50 × 2–3 μm ($\bar{x}$ = 30 × 2.5 μm, n = 20), hyaline to pale brown, smooth-walled, septate, branched. *Conidiogenous cells* 10–15 × 2–4 μm ($\bar{x}$ = 13 × 3 μm, n = 20), hyaline to pale brown, smooth-walled, cylindrical. *Conidia* 12–17 × 3–5 μm ($\bar{x}$ = 15 × 4 μm, n = 20), hyaline, smooth-walled, aseptate, straight, cylindrical to ellipse, with one end round and one end slightly acute. *Appressoria* not observed.

Culture characteristics – Conidia germinating on sterile water within 12 h. Colonies on PDA 60 mm diam., after 7 days at 25℃. The mycelium grows on the surface of the medium, edge radial, white to light purple, aerial mycelium cluster distribution, orange conidial masses, dense. Reverse, of culture, center is black, light purple, with brown rings. Not produced pigmentation on PDA media.

Material examined – China, Sichuan Province, Guangyuan City, Chaotian District (36°32′28.29″N 105°52′26.01″E, alt. 556 m), on living leaves of *Juglans regia*, 19 May 2022, F.-H. Wang, WFH202105038 (SICAU 22-0119), living culture SICAUCC 22-0123.

GenBank numbers – SICAUCC 22-0123: OP963821 (ITS), OQ281400 (*tub*2), OQ190486 (*act*), OQ214935 (*chs*-1).

Note – *Colletotrichum fioriniae* was described from a scale insect, *C. fioriniae* externa and has been also recorded as a pathogen on *Ailanthus altissima*, *Persea americana*, as well as an endophyte from *Mangifera indica* (Damm et al. 2012, Hyde et al. 2017). The strain SICAUCC 22-0123 clustered with the strain *C. fioriniae* (CBS 128517) with strong statistical support (100% MLBS/1.00 BYPP) (Fig. 104). Morphologically, our new specimen resembles *C. fioriniae* with overlapping size of conidia (Pennycook. 2017). Nucleotide comparisons of ITS, *tub*2, *act*, and *chs*-1 (SICAUCC 22-0125) showed a high homology with the sequences of *C. fioriniae* (CBS 128517), with a similarity of 100% (540/540, 0 gap), 99.8% (406/407, 1 gap), 100% (245/245, 0 gap), and 100% (282/282, 0 gap), respectively. We recognized our collection as *C. fioriniae*, because it clustered with the strain of *C. fioriniae* (CBS 128517), and was identical in morphology and molecular data.

65. ***Colletotrichum fructicola*** Prihast., L. Cai & K.D. Hyde, Fungal Divers. 39: 96 (2009) Fig. 106

Index Fungorum number: IF515409; Facesoffungi number: FoF06767

Associated with leaf spots on the living leaves of *Juglans regia*. On leaves lesions are marginal, irregular with various shaded brown centers. Light brown specks gradually become reddish-brown larger specks causing wilting and dieback. Sexual morph: Not observed. Asexual morph: *Conidiomata* 70–160 × 60–150 μm ($\bar{x}$ = 120 × 110 μm, n = 20), black, globose, oval, solitary, gregarious. *Conidiophores* 10–24 × 1.5–3 μm ($\bar{x}$ = 18 × 2 μm, n = 20), hyaline, smooth-walled to verruculose, aseptate, branched. *Conidia* 8–13 × 4–6 μm ($\bar{x}$ = 11 × 4.5 μm, n = 50), formed from the tip of the conidiophore, one-celled, cylindrical with rounded ends, contents appearing, granular, *Appressoria* not observed.

Culture characteristics – Conidia germinating on sterile water within 12 h. Colonies on PDA 60 mm diam., after 6 days at 25℃. The mycelium grows on the surface of the medium, grey to green, edge white, regular. Reverse, dark grey or light yellow, white edge with black conidial masses. Not produced pigmentation on PDA media.

Material examined – China, Sichuan Province, Suining City, Shehong City, Guangxing Town (30°57′22.21″N 105°18′54.19″E, alt. 410 m), on living leaves of *Juglans regia*, 26 August 2021, F.-H. Wang, WFH202108009 (SICAU 22-0122), living culture SICAUCC 22-0124.

GenBank numbers – SICAUCC 22-0124: OP963824 (ITS), OQ281403 (*tub*2), OQ190489 (*act*), OQ214938 (*chs*-1).

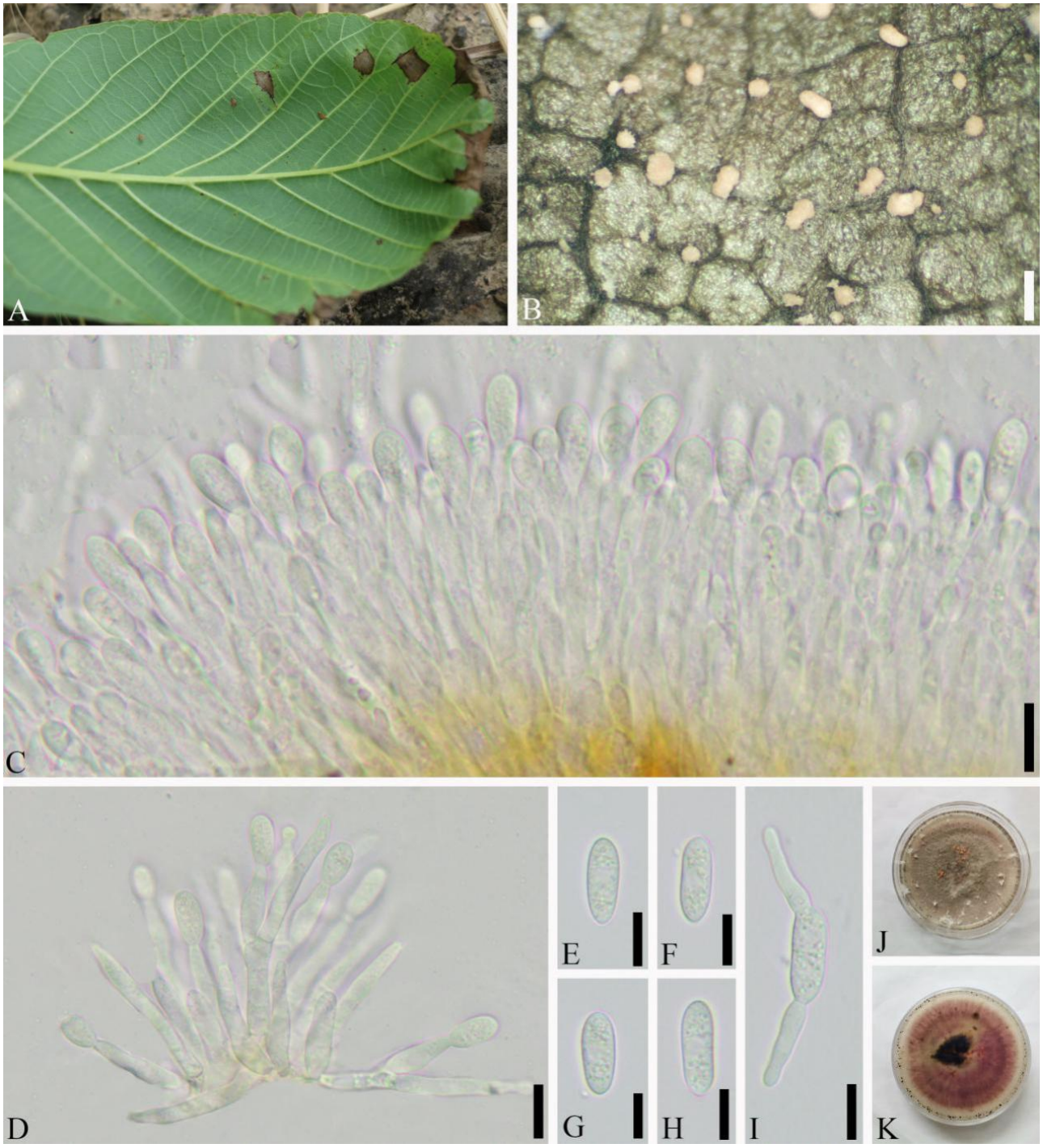


Figure 105 – *Colletotrichum fioriniae* (SICAU 22-0119). A Appearance of conidiomata on host. B Conidia in mass. C, D Conidiophores and conidiogenous cells. E–H Conidia. I Germinating conidium. J, K Colonies on PDA (J from above, K from below). Scale bars: B = 500 μm, C, D = 20 μm, E–I = 8 μm.

Note – The strain *C. fructicola* (SICAUCC 22-0124) clustered with the strain *C. fructicola* (ICMP 18581) with strong statistical support (88% MLBS/1.00 BYPP) (Fig. 104). Nucleotide

comparisons of ITS, *tub*2, *act*, and *chs*-1 (SICAUCC 22-0124) showed a high homology with the sequences of *C. fructicola* (ICMP 18581), with a similarity of 99.6% (568/570, 0 gap), 99.5% (436/438, 0 gap), 95.8% (230/240, 0 gap), and 99.6% (246/247, 0 gap), respectively. A comparison of the ITS, *tub*2, *act* and *chs*-1 sequence data revealed no significant difference between our new collection and the *C. fructicola*. There are no significant morphological differences compared to *C. fructicola* (ICMP 18581) (Prihastuti et al. 2009). Studies have found that *C. fructicola* is a variety of plant pathogens (Manawasinghe et al. 2022, Peng et al. 2023). This is the discovery of a new geographical record.

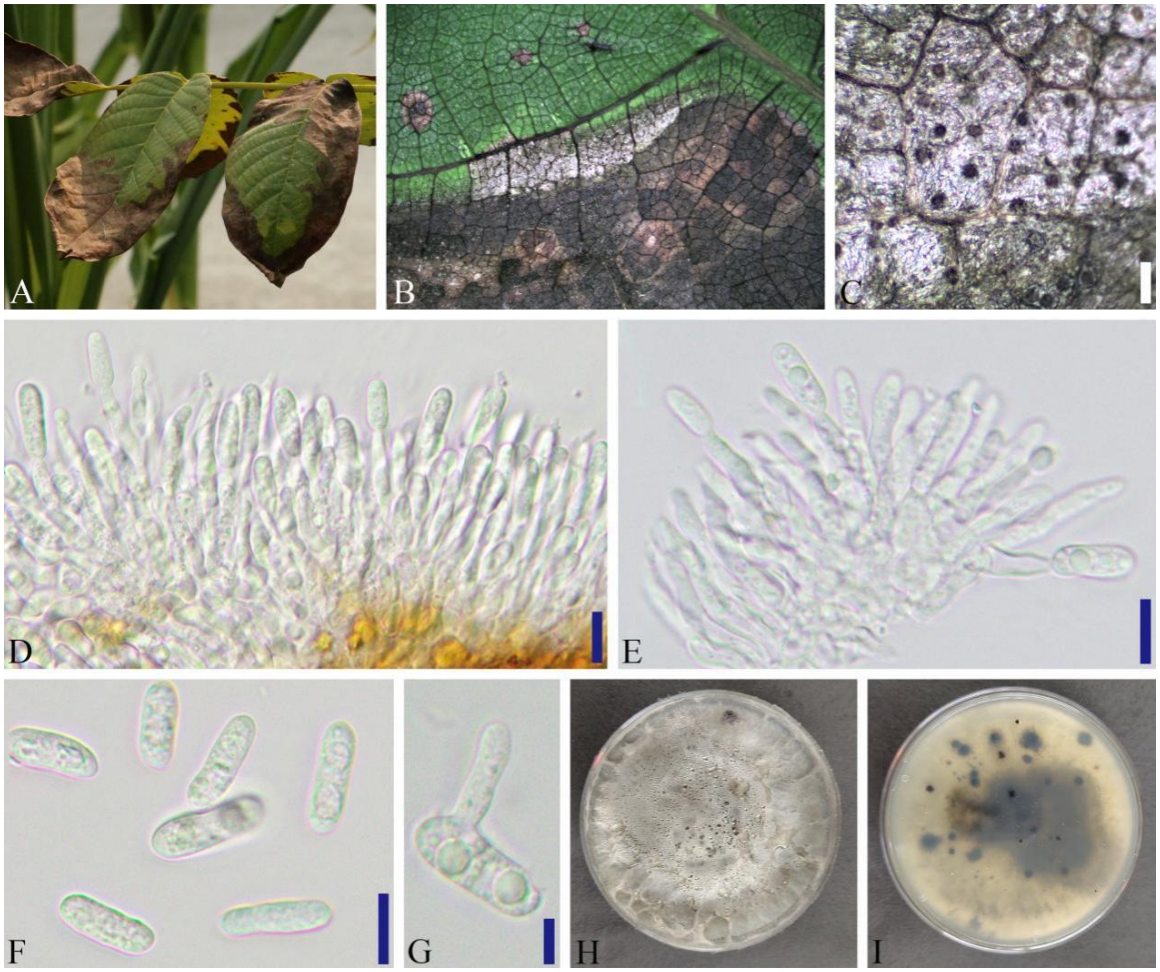


Figure 106 – *Colletotrichum fructicola* (SICAU 22-0122). A–C Appearance of conidiomata on host. D, E Conidiophores and conidiogenous cells. F Conidia. G Germinating conidium. H, I Colonies on PDA (H from above, I from below). Scale bars: C = 1000 μm, D–E = 20 μm, F = 10 μm, G = 5 μm.

66. ***Colletotrichum gloeosporioides*** (Penz.) Penz. & Sacc, Sér. 6 2(5): 670 (1884) Fig. 107

Index Fungorum number: IF158410; Facesoffungi number: FoF09424

Associated with leaf spots on the living leaves of *Juglans regia*. Symptoms start as small brown spots, which later expand continuously to form irregular lesions. The center of these lesions loses water, turns white, and ruptures, forming holes. Sexual morph: not observed. Asexual morph: *Conidiomata* 110–140 × 90–130 μm ($\bar{x}$ = 120 × 108 μm, n = 20), black, acervulus, globose, oval, solitary, gregarious. *Conidiophores* 15–37 × 2.5–4 μm ($\bar{x}$ = 32 × 3 μm, n = 20), hyaline, barrel shaped, smooth-walled, aseptate. *Conidiogenous cells* 9–14 × 4–5 μm ($\bar{x}$ = 11 × 4.5 μm, n = 20), hyaline, cylindrical. *Conidia* 11–16 × 5–7 μm ($\bar{x}$ = 13 × 6 μm, n = 40), aseptate, hyaline, smooth-walled, cylindrical, straight to slightly curved, mostly rounded ends, rarely obtuse at one end. *Appressoria* not observed.

Culture characteristics – Conidia germinating on sterile water within 12 h. Colonies on PDA 60 mm diam., after 6 days at 25℃. The mycelium grows on the surface of the medium, circular with entire edge, grey in the central and white at the margin and become black with age, velvety, black conidial masses. Reverse, be similar. Not produced pigmentation on PDA media.

Material examined – China, Sichuan Province, Suining City, Shehong City, Guangxing Town (30°57′22.18″N 105°18′54.24″E, alt. 406 m), on living leaves of *Juglans regia*, 17 May 2021, F.-H. Wang, WFH202105022 (SICAU 22-0123), living culture SICAUCC 22-0125.

GenBank numbers – SICAUCC 22-0125: OP963825 (ITS), OQ281404 (*tub*2), OQ190490 (*act*), OQ214939 (*chs*-1).

Note – The *Colletotrichum gloeosporioides* species complex is an important group of plant pathogenic fungi (Weir et al. 2012, Jayawardena et al. 2018, Bhunjun et al. 2021). *C. gloeosporioides* (SICAUCC 22-0125) shows a close phylogenetic affinity to *C. gloeosporioides* (IMI356878) with strong statistical support (100% MLBS/1.00 BYPP) (Fig. 104). Nucleotide comparisons of ITS, *tub*2, *act*, and *chs*-1 (SICAUCC 22-0125) showed a high homology with the sequences of *C. gloeosporioides* (IMI356878), with a similarity of 100% (515/515, 0 gap), 100% (351/351, 0 gap), 99.6% (253/254, 0 gap), and 100% (280/281, 0 gap), respectively. Based on morphological characters and phylogenetic analyses, we determine our specimens as *C. gloeosporioides.* This represents the discovery of a new geographical record.

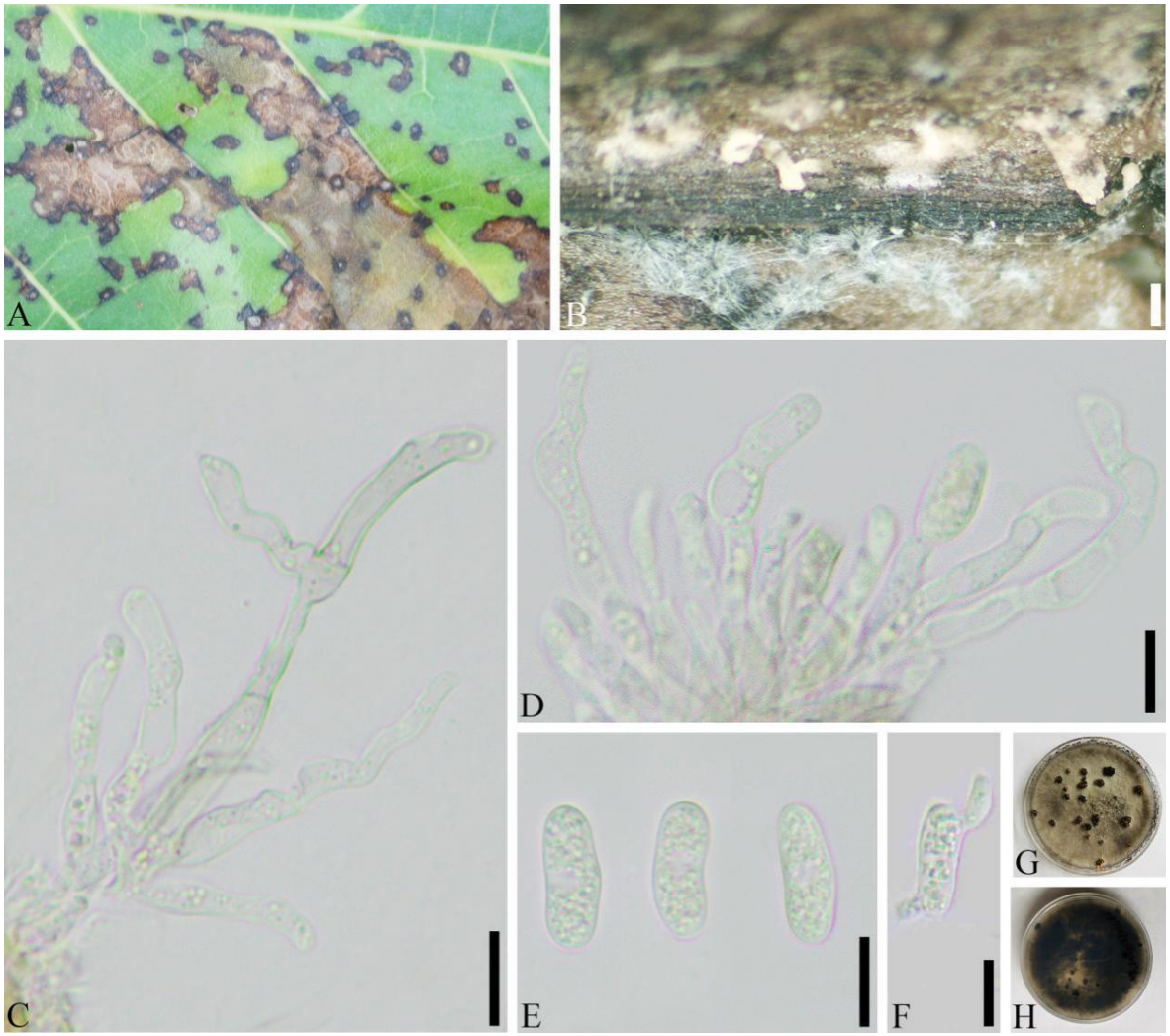


Figure 107 – *Colletotrichum gloeosporioides* (SICAU 22-0123). A Appearance of conidiomata on host. B Conidia in mass. C, D Conidiophores and conidiogenous cells. E Conidia. F Germinating conidium. G, H Colonies on PDA (G from above, H from below). Scale bars: B = 500 μm, C, D = 20 μm, E, F = 10 μm.

67. ***Colletotrichum godetiae*** Neerg., Friesia 4(1-2): 72 (1950) Fig. 108

Index Fungorum number: IF440864; Facesoffungi number: FoF03881

Associated with fruits rot on *Juglans regia*. Fruits may shrivel and change colour to brown. Sexual morph: not observed. Asexual morph: *Vegetative hyphae* 2–4 μm diam, hyaline to pale brown, smooth-walled, septate, branched. *Chlamydospores* not observed. *Conidiomata* absent, conidiophores formed directly on hyphae. *Setae* not observed. *Conidiophores* 9–18 × 2–4 μm ($\bar{x}$ = 11 × 3 μm, n = 20), hyaline, smooth-walled, simple. *Conidiogenous cells* 5–13 × 4–6 μm ($\bar{x}$ = 9 × 4.5 μm, n = 20), hyaline, smooth-walled, cylindrical, often with only short necks, periclinal thickening observed. *Conidia* 8–15 × 4–6 μm ($\bar{x}$ = 12 × 5.5 μm, n = 40), hyaline, smooth-walled, aseptate, straight, cylindrical with both ends round.

Culture characteristics – Conidia germinating on sterile water within 12 h. Colonies on PDA reaching 60 mm diam., after 6 days at 25 ℃. The mycelium grows on the surface of the medium, cottony, circular, slightly raised and depressed in the center, Aerial mycelia white and medium in dense. Reverse, dark grey or light yellow, white edge with black conidial masses. Not produced pigmentation on PDA media.

Material examined – China, Sichuan Province, Aba Tibetan and Qiang Autonomous Prefecture (30°23′40″N 102°17′11″E, alt. 2276 m), on fruits rot of *Juglans regia*, 29 July 2022, F.-H. Wang, WFH202207081 (SICAU 22-0124), living culture SICAUCC 22-0126.

GenBank numbers – SICAUCC 22-0126: OP963826 (ITS), OQ281405 (*tub*2), OQ190491 (*act*), OQ214940 (*chs*-1).

Note – *Colletotrichum godetiae* was first reported on the seeds of Godetia hybrid in Denmark by Neergaard (1943), and given detailed identification seven years later. *C. godetiae* was also recovered from fruits of *Fragaria* × *ananassa*, *Prunus cerasus*, *Solanum Betaceum*, *Citrus aurantium*, and *Olea europaea*, leaves of *Laurus nobilis* and *Mahonia aquifolium*, twigs of *Ugni molinae,* and canes of *Rubus idaeus* (Prihastuti et al. 2009, Yang et al. 2011b, Weir et al. 2012, Schena et al. 2017). Phylogenetic analysis based on a combined *act*, *chs*-1, ITS and *tub*2 sequence data indicated that our isolate and *C. godetiae* (CBS133.44) clustered together with strong statistical support (100% MLBS/1.00 BYPP) (Fig. 104). Nucleotide comparisons of ITS, *tub*2, *act*, and *chs*-1 (SICAUCC 22-0125) showed a high homology with the sequences of *C. gloeosporioides* (IMI356878), with a similarity of 100% (538/538, 0 gap), 100% (490/490, 0 gap), 100% (282/282, 0 gap), and 100% (247/247, 0 gap), respectively. We recognized our collection as *C. godetiae*, because it clustered with the ex-type strain of *C. godetiae* (CBS133.44) and was identical in morphology and molecular data. In this study, the isolates were obtained from walnut fruit and could infect both the peach fruit.

68. ***Colletotrichum scovillei*** Damm, P.F. Cannon & Crous, Stud. Mycol. 73: 100 (2012) Fig. 109

Index Fungorum number: IF800512; Facesoffungi number: FoF16305

Associated with leaf spots on the living leaves of *Juglans regia*. Symptoms are characterized by scattered small black spots on the leaves, often appearing along the leaf veins. As these black spots enlarge, they cause the leaves to wilt and die. Sexual morph: Not observed. Asexual morph: *Conidiomata* 100–170 × 80–120 μm ($\bar{x}$ = 140 × 100 μm, n = 20), acervular, without setae, yellow to orange. *Setae* not observed. *Conidiophores* 10–29 × 90–130 μm ($\bar{x}$ = 19 × 4 μm, n = 20), hyaline to pale, smooth-walled to verruculose, septate, 1-3 branched. *Conidiogenous cells* 7–12 × 3–5 μm ($\bar{x}$ = 9 × 3.5 μm, n = 20), hyaline smooth-walled, cylindrical, to slightly inflated, periclinal thickening conspicuous. *Conidia* 10–15 × 3–6 μm ($\bar{x}$ = 12 × 4 μm, n = 20), hyaline, smooth-walled, aseptate, straight, cylindrical to oval shape.

Culture characteristics – Conidia germinating on sterile water within 12 h. Colonies on PDA reaching 60 mm diam., after 6 days at 25 ℃. The mycelium grows on the surface of the medium, appeared white to pink with abundant aerial mycelium, round, regular edge, center color is darker. Reverse, be similar. There is purple pigmentation within the PDA.

Material examined – China, Sichuan Province, Yibin City, Gaoxian County (28°28′56.38″N 104°38′59.27″E, alt. 531 m), on leaves rot of *Juglans regia*, 26 April 2022, F.-H. Wang, WFH202204049-1 (SICAU 22-0125), living culture SICAUCC 22-0127.

GenBank numbers – SICAUCC 22-0127: OP963827 (ITS), OQ281406 (*tub*2), OQ190492 (*act*), OQ214941 (*chs*-1).

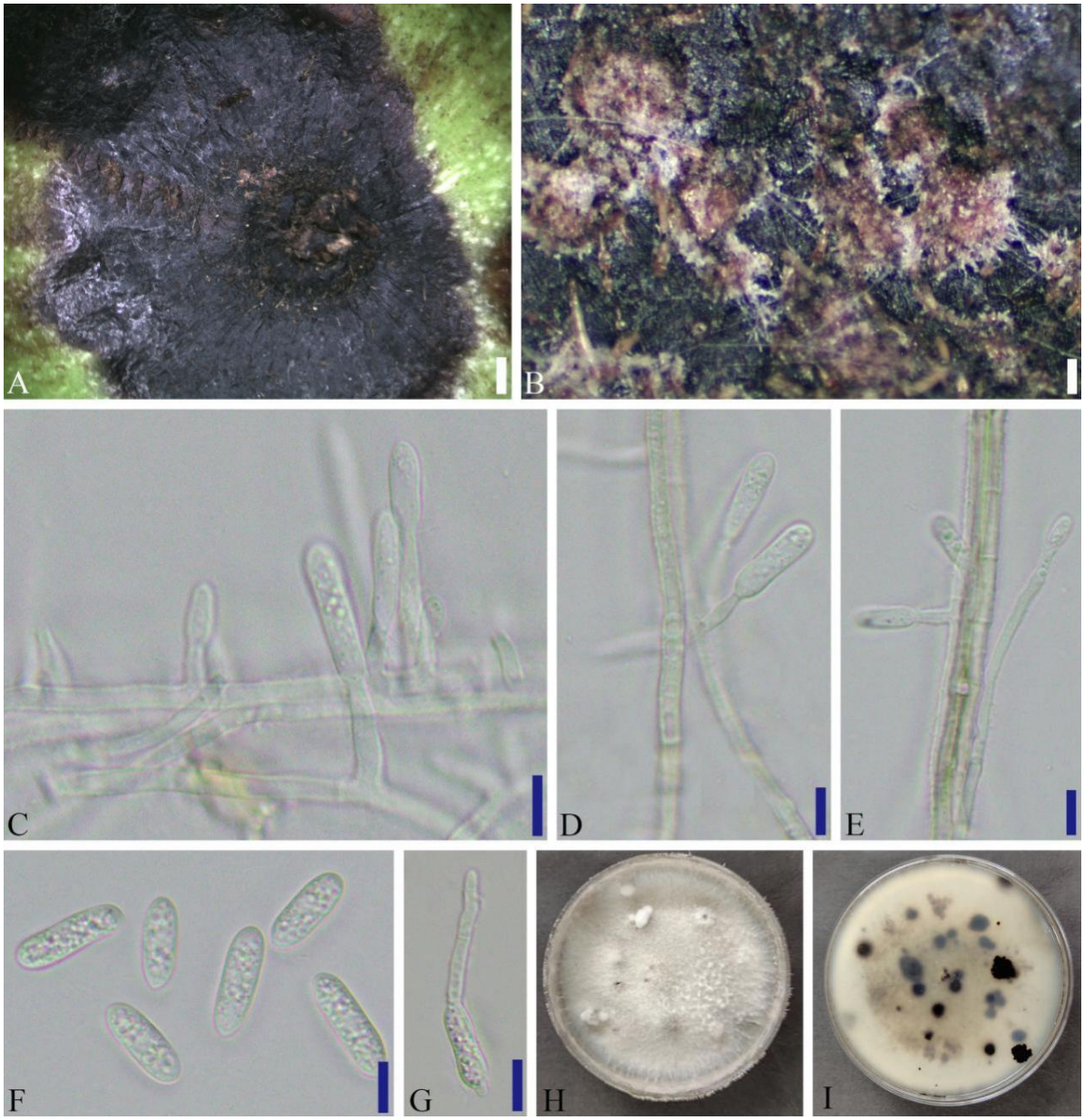


Figure 108 – *Colletotrichum godetiae* (SICAU 22-0124). A, B Appearcance of conidiomata on host. C–E Vegetative hyphae, conidiophores and conidiogenous cells. F Conidia. G Germinating conidium. H, I Colonies on PDA (H from above, I from below). Scale bars: A = 1000 μm, G = 8 μm, C–F = 5 μm.

Note – Multi-gene phylogenetic analysis including the ITS, *tub*2, *act,* and *chs*-1 sequence data showed that our collection clustered with reference specimens of *Colletotrichum scovillei*. This species is located in the Acutatum complex and clusters with the ex-type strain, *C. scovillei* (CBS126529) with strong statistical support (92% MLBS/1.00 BYPP) (Fig. 104). Nucleotide comparisons of ITS, *tub*2, *act*, and *chs*-1 (SICAUCC 22-0127) showed a high homology with the sequences of *C. scovillei* (CBS126529 ex-type), with a similarity of 100% (540/540, 0 gap), 100% (490/491, 0 gap), 100% (246/246, 0 gap), and 99.6% (282/283, 0 gap), respectively. Our strain is

morphologically identical to *C. scovillei.* Based on morphological characters and phylogenetic analyses, we determine our specimens as *C. scovillei*. Damm et al. (2012) introduced *C. scovillei* from a stem lesion of *Capsicum* sp. *Colletotrichum scovillei* is a common phytopathogen known to cause anthracnose in leaves. (De Silva et al. 2019a). We report our collection as a new host of *C. scovillei* on living leaves of *Juglans regia*.

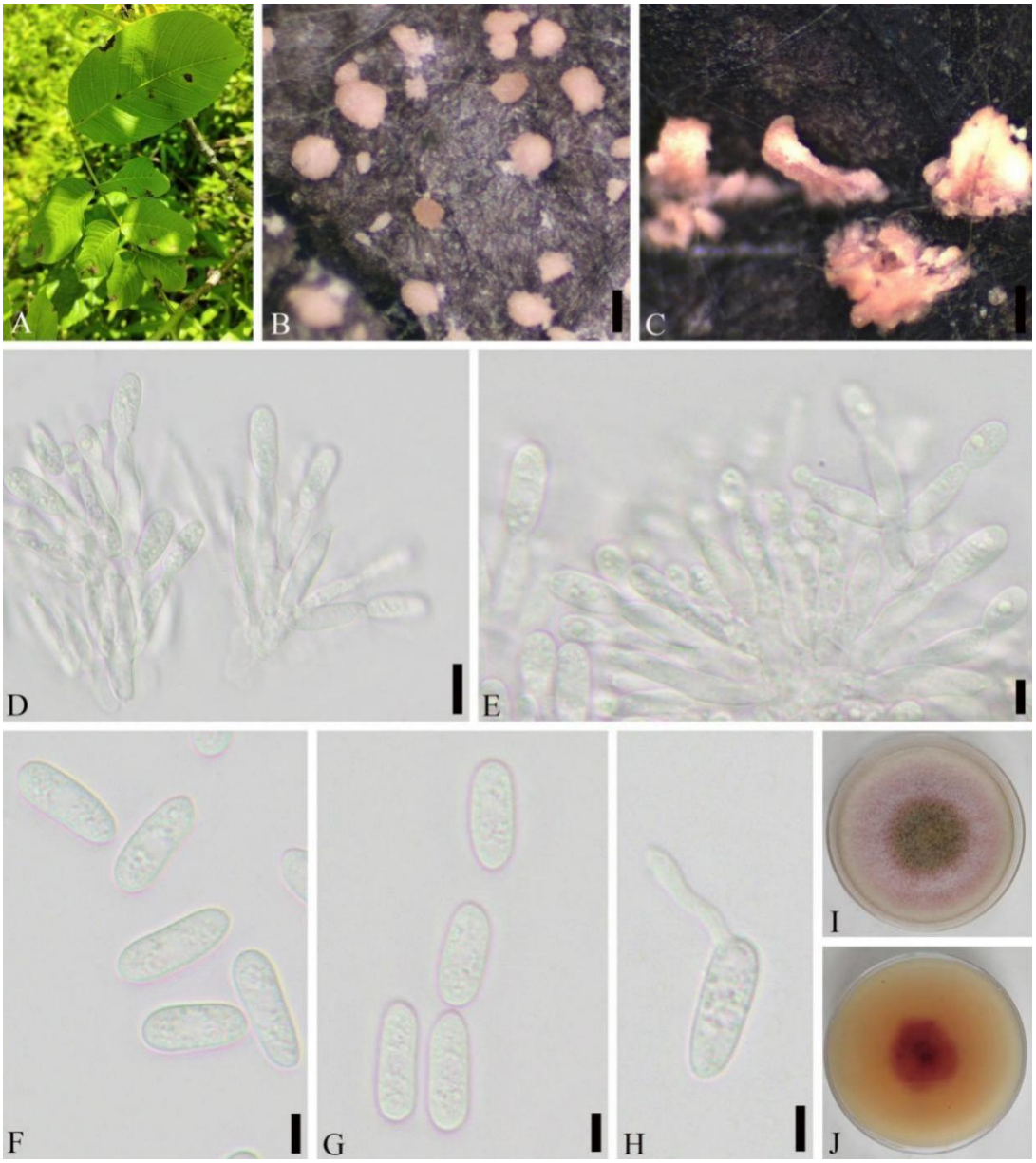


Figure 109 – *Colletotrichum scovillei* (SICAU 22-0125). A Appearcance of conidiomata on host. B, C Conidia in mass. D, E Conidiophores and conidiogenous cells. F, G Conidia. H Germinating conidium. I, J Colonies on PDA (I from above, J from below). Scale bars: B = 500 μm, C = 200 μm, D = 10 μm, E = 80 μm, F–H = 5 μm.

69. ***Colletotrichum shehongense*** F.H. Wang & C.L. Yang, sp. nov. Fig. 110

Index Fungorum number: IF901576; Facesoffungi number: FoF15594

Etymology – Name reflects the location from which it was collected, Shehong, China.

Holotype – SICAU 23-0089

Associated with petiole rot on the petiole of *Juglans regia*. The symptoms present as brown spots covering the surface of the leaves. In later stages, these spots enlarge and connect, resulting in the entire leaf wilting and dying. Sexual morph: Not observed. Asexual morph: *Conidiomata* 160–

200 × 130–190 μm ($\bar{x}$ = 180 × 150 μm, n = 20), black, acervulus, oval, solitary, gregarious. *Setae* not observed with unaided eye. *Conidiophores* 10–23 × 1.5–3 μm ($\bar{x}$ = 17 × 2.5 μm, n = 20), simple, hyaline to pale brown, smooth-walled, unbranched. *Conidiogenous cells* 5–10 × 3–5.5 μm ($\bar{x}$ = 7 × 4 μm, n = 20), hyaline, smooth-walled, cylindrical to slightly inflated, often with short necks, opening 1–2 μm wide, collarette or periclinal thickening observed. *Conidia* 8–17 × 3–6 μm ($\bar{x}$ = 12 × 4 μm, n = 20), hyaline, smooth-walled, aseptate, straight, cylindrical to fusiform, with both ends acute or one end round and one end slightly acute. *Appressoria* 4–7 × 2–5 μm ($\bar{x}$ = 5 × 3 μm, n = 20), solitary, medium brown, smooth-walled, subglobose, ellipsoidal to obovate, entire margin.

Culture characteristics – Conidia germinating on sterile water within 12 h. Colonies on PDA reaching 60 mm diam., after 7 days at 25 ℃. The mycelium grows on the surface of the medium, sparse, circular, raised, surface smooth, entire edge, fluffy to velvety with smooth aspects, white to French grey at the margin, white in the center. Reverse, white at the margin, white to pale brown in the center. Light purple on PDA after 2 weeks incubation period in 12/12 dark, at 25℃.

Material examined – China, Sichuan Province, Suining City, Shehong City, Guangxing Town (30°57′22.27″N 105°18′54.34″E, alt. 407 m), on petiole rot of *Juglans regia*, 26 August 2021, F.-H. Wang, WFH202108018 (SICAU 23-0089, holotype), ex-type living culture SICAUCC 23-0068. *Ibid*., WFH202108018B (SICAU 24-0040), living culture SICAUCC 23-0153.

GenBank numbers – SICAUCC 23-0068: PP060684 (ITS), PQ152162 (*act*), PP061102 (*chs*-1), PV397446 (*tub*2); SICAUCC 23-0153: PP844881 (ITS), PQ152163(*act*), PP850043 (*chs*-1), PV397447 (*tub*2).

Note – Phylogeny indicates that *Colletotrichum shehongense* (SICAUCC 23-0068) constitutes an independent lineage with close affinity to *C. fioriniae* with strong statistical support (94% MLBS/1.00 BYPP) (Fig. 104). Morphologically, *C. shehongense* SICAUCC 23-0068 is typical of *Colletotrichum* in oval, solitary, gregarious conidiomata, unitunicate, simple, hyaline to pale brown, smooth-walled conidiophores that hyaline, smooth-walled, aseptate, straight, cylindrical to fusiform conidia (Damm et al. 2009, Hyde et al. 2009). There are certain morphological differences in the conidiomata (160–200 × 130–190 vs. 90–180 × 80–170 μm), shorter conidiophores (10–23 × 1.5–3 vs. 18–50 × 2–3 μm). Moreover, *C. shehongense* (SICAUCC 23-0068) exhibits distinct appressoria, whereas *C. fioriniae* (CBS 128517) does not show any. However, nucleotide sequence comparisons reveal specific differences between *C. shehongense* (SICAUCC 23-0068) and its related species. Nucleotide comparisons revealed notable genetic dissimilarities between *C. fioriniae* (CBS 128517) and *C. shehongense* (SICAUCC 23-0068), viz. 0.2% (1/540, 0 gap), 0.8% (2/241, 0 gap), 8.7% (21/241, 2 gaps), and 5.1% (25/492, 2 gaps) in the ITS, *chs*-1 *act* and *tub*2, respectively. Therefore, the new strain is introduced as a new species based on morphology and phylogenetic evidence.

70. ***Colletotrichum siamense*** Prihast., L. Cai & K.D. Hyde, Fungal Divers. 39: 98 (2009) Fig. 111

Index Fungorum number: IF515410; Facesoffungi number: FoF03599

Associated with leaf spots on the living leaves of *Juglans regia*. Symptoms start as small brown spots, which later expand continuously to form irregular lesions. The center of these lesions loses water, turns white, and ruptures, forming holes. Sexual morph: Not observed. Asexual morph: *Conidiomata* 70–123 × 60–110 μm ($\bar{x}$ = 100 × 90 μm, n = 20), acervular, without setae, black. *Conidiophores* 8–20 × 1–3 μm ($\bar{x}$ = 14 × 2 μm, n = 20), hyaline to subhyaline, branched, smooth-walled, aseptate. *Conidiogenous cells* 12–19 × 2–4 μm ($\bar{x}$ = 16 × 3 μm, n = 20), hyaline to subhyaline, smooth-walled, phialidic, cylindrical, with distinct collarette. *Conidia* 16–24 × 3–6 μm ($\bar{x}$ = 20 × 4 μm, n = 40), hyaline, aseptate, smooth-walled, long ellipse to cylindrical, both ends bluntly rounded. Appressoria 4–7 × 5–7 μm ($\bar{x}$ = 5.5 × 6 μm, n = 20), dark brown, solitary, circular.

Culture characteristics – Conidia germinating on sterile water within 24 h and germ tubes produced from both ends. Colonies on PDA reaching 50 mm diam., after 9 days at 25 ℃. The mycelium grows on the surface of the medium, circular with entire edge, grey in the central and white at the margin and become black with age, velvety. Not produced pigmentation on PDA media.

Material examined – China, Sichuan Province, Mianyang City, Yanting County (31°5′25.06″N 105°27′36.33″E, alt. 368 m), on leaf spots of *Juglans regia*, 28 April 2022, F.-H. Wang, WFH202204112 (SICAU 22-0126), living culture SICAUCC 22-0128.

GenBank numbers – SICAUCC 22-0128: OP963828 (ITS), OQ281407 (*tub*2), OQ190493 (*act*), OQ214942 (*chs*-1).

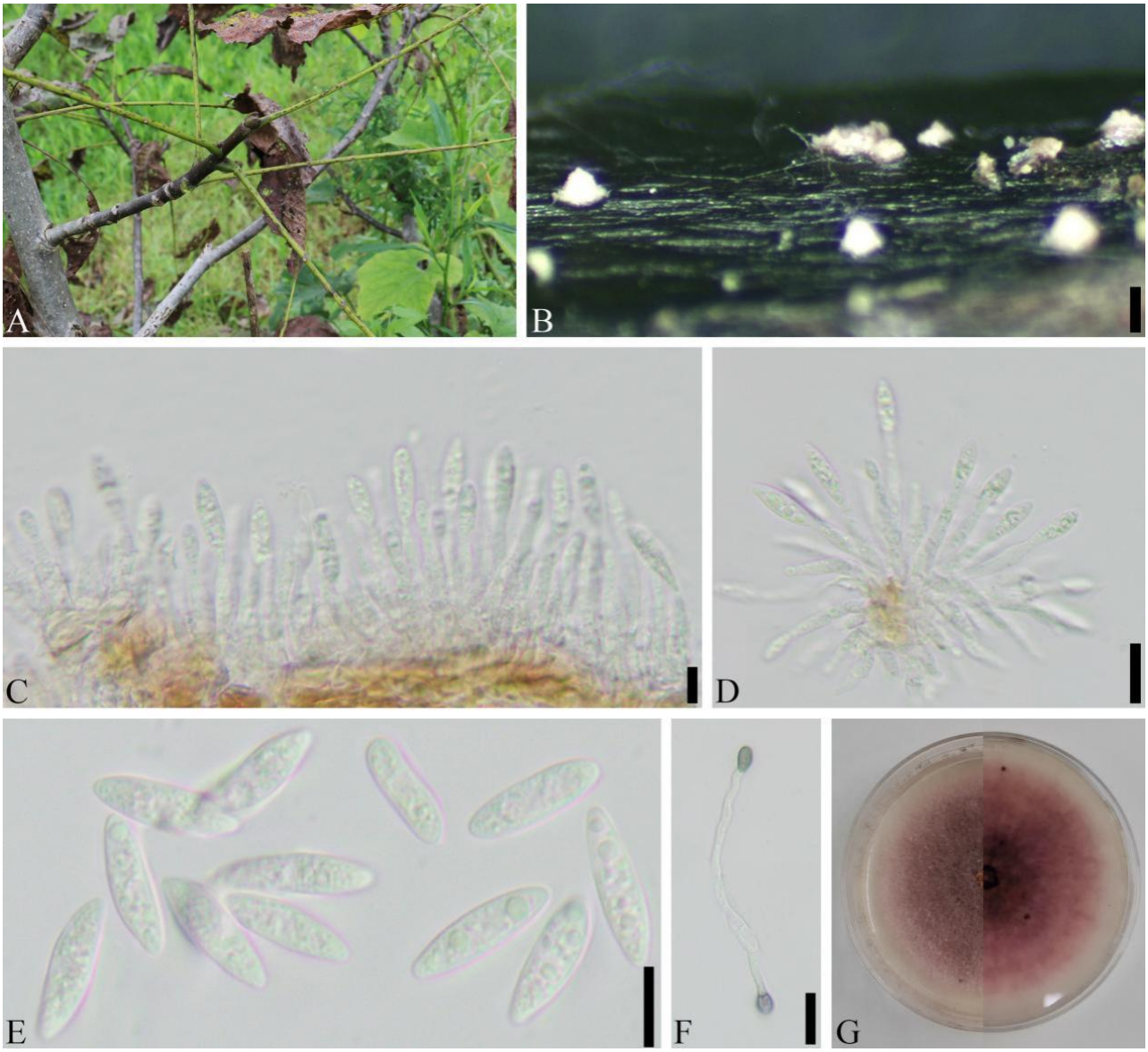


Figure 110 – *Colletotrichum shehongense* (SICAU 23-0089, holotype). A Appearance of Conidiomata on host. B Conidia in mass. C, D Conidiophores and conidiogenous cells. E Conidia. F Germinating conidium. G Colonies on PDA. Scale bars: B = 200 μm, B, C = 500 μm, D, F = 20 μm, C, E = 10 μm.

Note – Phylogenetic analysis revealed that SICAUCC 23-0128 forms a sister clade with *Colletotrichum siamense* (ICMP 18578) with strong statistical support (100% MLBS/1.00 BYPP) (Fig. 104), specifically with *C. siamense* (BPDI 2 and BPDI 4). Sequence comparisons reveal a high similarity in their ITS (100%, 502/502, 0 gap), *tub*2 (99.8%, 405/406, 0 gap), *act* (99.6%, 283/284, 0 gap), and *chs*-1 (100%, 300/300, 0 gap), signifying their close genetic relationship. Morphological characteristics are similar to *C. siamense* described by Prihastuti et al. (2009). Herein we identified our strain as a new geographical record of *C. siamense*.

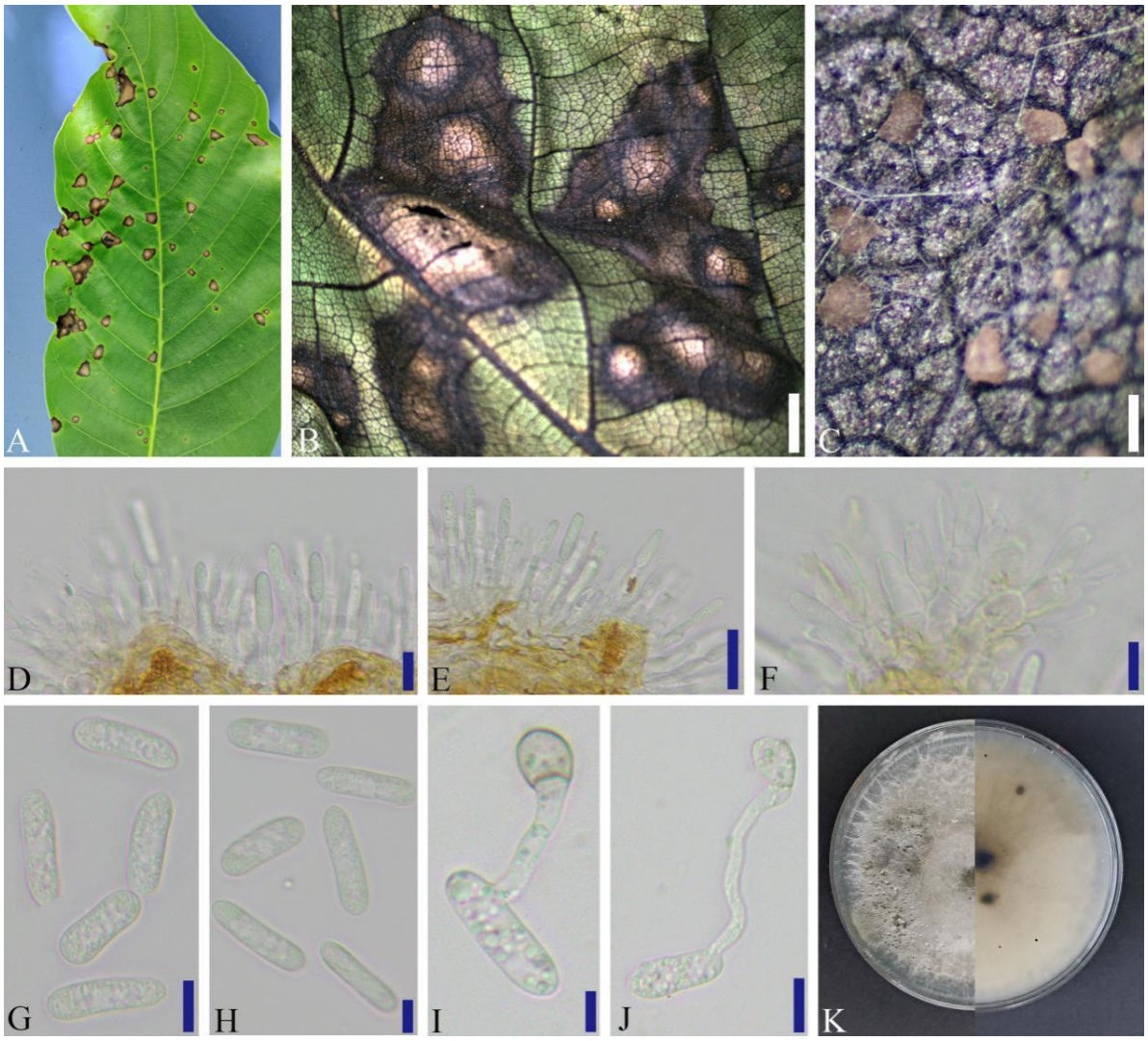


Figure 111 – *Colletotrichum siamense* (SICAU 22-0126). A, B Appearance of conidiomata on host. C Conidia in mass. D–F Conidiophores and conidiogenous cells. G, H Conidia. I, J Germinating conidia. K Colonies on PDA. Scale bars: B = 2 mm, C = 200 µm, E, J = 20 µm, D, F G = 10 µm, H, I = 5 µm.

Hypocreales Lindau, in Engler & Prantl, Nat. Pfanzenfam., Teil. I (Leipzig) 1(1): 343 (1897).

Hypocrea was introduced by Fries (1825) and was classified in the order *Sphaeriaceae*. Fries (1849) accepted *Hypocrea* with a narrow sense. Lindau (1897) introduced the family *Hypocreaceae* based on *Hypocrea* and introduced the order *Hypocreales* to accommodate *Hypocreaceae* as the only family. Taxonomic revision of *Hypocreales* by Rossman et al. (1999) recognised five families: *Clavicipitaceae*, *Hypocreaceae*, *Nectriaceae*, *Niessliaceae* and the new family *Bionectriaceae*. Earlier, Hyde et al. (2020) placed *Cylindriaceae* in *Xylariomycetidae*. This was later confirmed by the analysis of Samarakoon et al. (2022). Hence, *Cylindriaceae* should be excluded from *Hypocreales* and placed in *Xylariomycetidae*. The most recent treatment of *Hypocreales* was provided by Wijayawardene et al. (2022). Xiao et al. (2023) recently introduced a new family *Polycephalomycetaceae* to *Hypocreales*. Perera et al. (2023) provided an updated phylogenetic analysis of combined gene analysis of ITS, LSU, *rpb*2, *tef*1-α and *tub*2 for *Hypocreales* and accepted 17 families, including three new families (*Ijuhyaceae*, *Stromatonectriaceae* and *Xanthonectriaceae*) Bao et al. (2023) will *Pseudoacremonium* and *Sedecimiella* are transferred to *Bionectriaceae* and *Nectriaceae*, respectively. *Emericellopsis* was excluded from *Myrotheciomycetaceae* and placed in *Hypocreales* genera incertae sedis.

Bionectriaceae Samuels & Rossman.

Rossman et al. (1999) established *Bionectriaceae* in (*Hypocreales*) and placed 26 genera in the family. Based on LSU phylogeny, Rossman et al. (2001) confirmed the monophyletic nature of *Bionectriaceae* and, revealed that the family is distinct from other families of *Hypocreales* (*Hypocreaceae*, *Clavicipitaceae* and *Nectriaceae*). The classification of *Bionectriaceae* has been revised and refined by several studies based on phylogenetic analyses (Maharachchikumbura et al. 2015, 2016b, Wijayawardene et al. 2018). The recent treatment of *Bionectriaceae* was provided by Bao et al. (2023) and Perera et al. (2023), with the acceptance of 47 genera.

Acremonium Link.

Acremonium accommodates saprobic species, including important plant pathogens and agents of opportunistic infections in humans (Gams 1971, Kiyuna 2011). *Acremonium* species are difficult to distinguish on morphological characters because they are poorly differentiated in asexual morphs. Molecular phylogenetic analyses have demonstrated that this genus is polyphyletic (Summerbell et al. 2011, Hou et al. 2023).

71. ***Acremonium hennebertii*** W. Gams, Cephalosporium-artige Schimmelpilze (Stuttgart): 79 (1971)

Fig. 112

Index Fungorum number: IF308156; Facesoffungi number: FoF16306

Associated with tip blight on the branch tip of *Juglans regia*. Symptoms manifest as yellowing leaves, with scorching starting from the edges, ultimately leading to the complete withering and death of the leaves in later stages. Sexual morph: Not observed. Asexual morph: Hyphomycetous. *Colonies* effuse, white to light grey, velvety. Mycelium mostly immersed, partly superficial, consisting of septate, branched, thin-walled, white racquet hyphae. *Conidiophores* 9–14 × 1–3 μm ($\bar{x}$ = 12 × 2 μm, n = 10) micronematous, ampulliform, subhyaline, smooth, thin-walled. *Conidiogenous cells* 2–5 × 1–3 μm ($\bar{x}$ = 3 × 2 μm, n = 5), phialidic, globose, subhyaline, smooth. *Conidia* 3.5–6 × 1.5–3.5 μm ($\bar{x}$ = 5 × 2.5 μm, n = 50), catenate, in branched chains, abundant, ellipsoid-fusiform, narrow and truncate at both ends, hyaline to green-yellow, smooth, thick-walled, aseptate.

Culture characteristics – Ascospores germinating on sterile water within 24 h and germ tubes produced from ends. Colonies on PDA reaching 20 mm diam., after 14 days at 25 ℃. The mycelium grows on the surface of the medium, hairy, pale white, mycelium partly superficial, partly immersed, slightly effuse, radially striate, with regular edge, pale white. center of the reverse side is yellowish. Not produced pigmentation on PDA media.

Material examined – China, Sichuan Province, Neijiang City, Dongxing District, Paifang Village (29°48′30.18″N 105°6′36.42″E, alt. 385 m), on tip blight of *Juglans regia*, 17 May 2021, F.-H. Wang, WFH202105008 (SICAU 22-0110), living culture SICAUCC 22-0112.

GenBank numbers – SICAUCC 22-0112: OP963812 (ITS), OP964571 (LSU), OP962299 (SSU), OQ281342 (*rpb*2), OQ281359 (*tef*1-α).

Note – *Acremonium hennebertii* fits well within the *Acremonium* genus, characterized by having ampulliform conidiophores with phialidic conidiogenous cells and bearing conidia in chains. In phylogenetic tree based on ITS, LSU, SSU, *tef*1-α and *rpb*2 gene, *A. hennebertii* (SICAUCC 22-0112) forms a separated clade sister to *A. citrinum* (CBS 384.96), *A. cavaraeanum* (CBS 758.69) and *A. hennebertii* (CBS 768.69) in *Acremonium* sensu lato (*Bionectriaceae*) with strong statistical support (100% MLBS/1.00 BYPP) (Fig. 113). Nucleotide comparisons of ITS and LSU (SICAUCC 22-0112) showed a high homology with the sequences of *A. hennebertii* (CBS 768.69 ex-type), with a similarity of 99.8% (553/554, 1 gap) and 100% (774/774, 0 gap), respectively. The morphological differences between *A. hennebertii* (SICAUCC 22-0112) and *A. hennebertii* (CBS 768.69) are indistinguishable. Based on the morpho-molecular analyses, we conclude that our new collection is another record of *A. hennebertii* and also a new host record on *Juglans regia* in China.

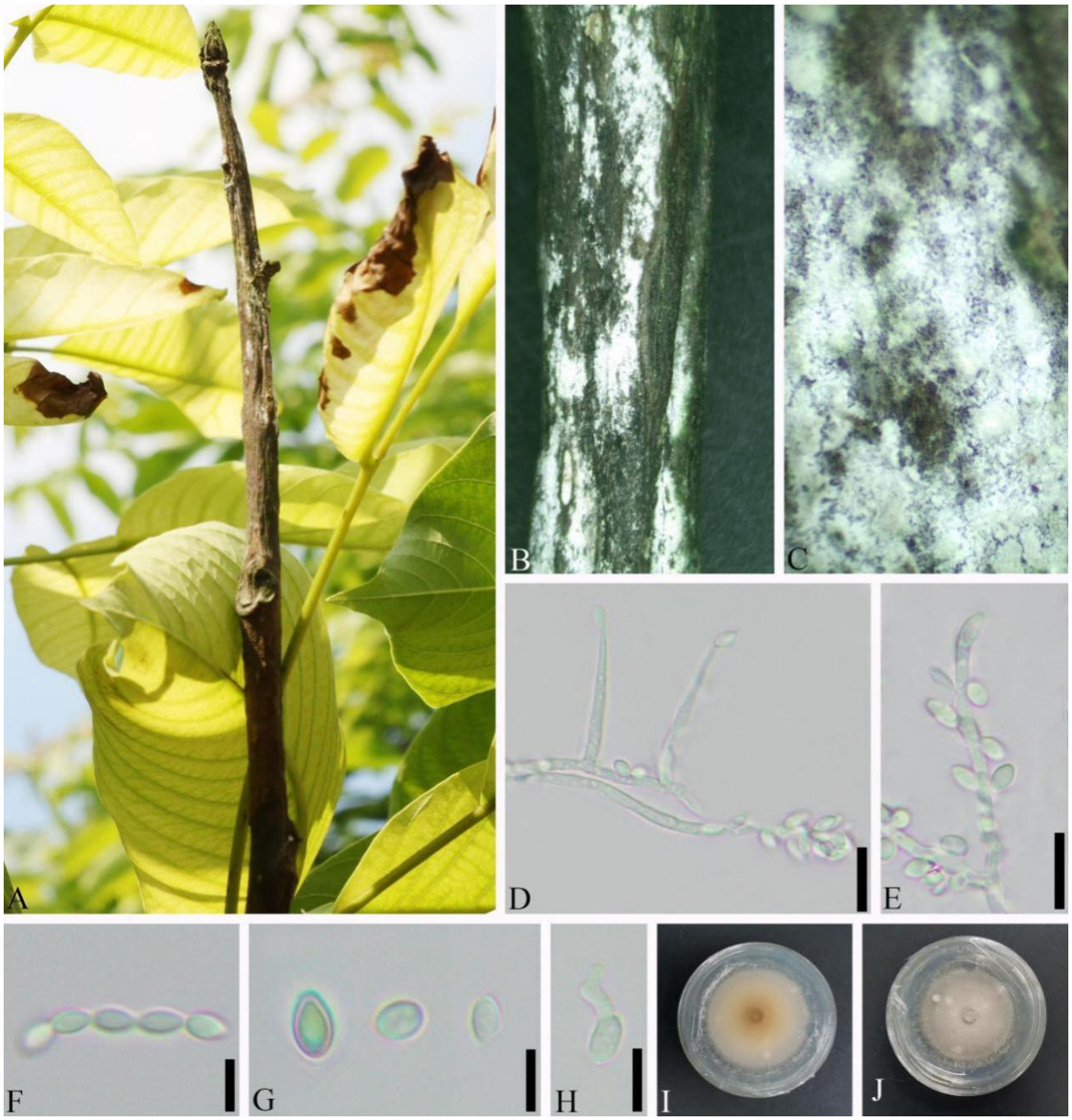


Figure 112 – *Acremonium hennebertii* (SICAU 22-0110). A Symptoms of walnut tender shoot infection. B, C Colonies on branch tip. D, E Conidiophores with conidiogenous cells. F Conidia in chains. G Conidia. H Germinating conidium. I, J Colonies on PDA (I from above, J from below). Scale bars: D, E = 20 µm, F–H = 10 µm.

Clonostachys Corda, Pracht-Fl. Eur. Schimmelbild.: 31 (1839).

Corda (1839) introduced *Clonostachys* based on *Clonostachys araucaria* (current name *Clonostachys rosea*). However, no type material of *C. araucaria* is currently available, but only original descriptions and drawings (Schroers et al. 1999). Based on morphological similarity Schroers et al. (1999) recognised *C. rosea* as the asexual morph of *Bionectria ochroleuca*, and it was confirmed in the phylogenetic studies by Schroers (2011). *Clonostachys* species are characterized by sexual morphs with globose to subglobose ascomata, narrowly clavate asci with ellipsoidal ascospores. The conidiophores are verticillate or penicillate, phialides arranged in whirls producing typically hyaline, less commonly greenish to olivaceous or green conidia (Schroers 2011). Rossman et al. (2013) linked sexual morphic genus *Bionectria* to *Clonostachys* by giving priority to older and frequently used name *Clonostachys*. *Clonostachys* has a worldwide distribution and is commonly found in tropical and subtropical regions (Drummond et al. 2007). Species in the genus are saprobes, endophytes, plant pathogens and mycoparasites from various habitats including soil (Toledo et al. 2006, Zhang et al.

2008, Moreira et al. 2016). There are more than 123 records of *Clonostachys* listed in Species Fungorum (http://www.speciesfungorum.org/Index.htm, September 2024) of which 65 species are commonly accepted (Lombard et al. 2015, Dao et al. 2016, Prasher & Chauhan 2017, Lechat & Fournier 2018, 2019, 2020, Zeng & Zhuang 2022, Bao et al. 2023, Perera et al. 2023).

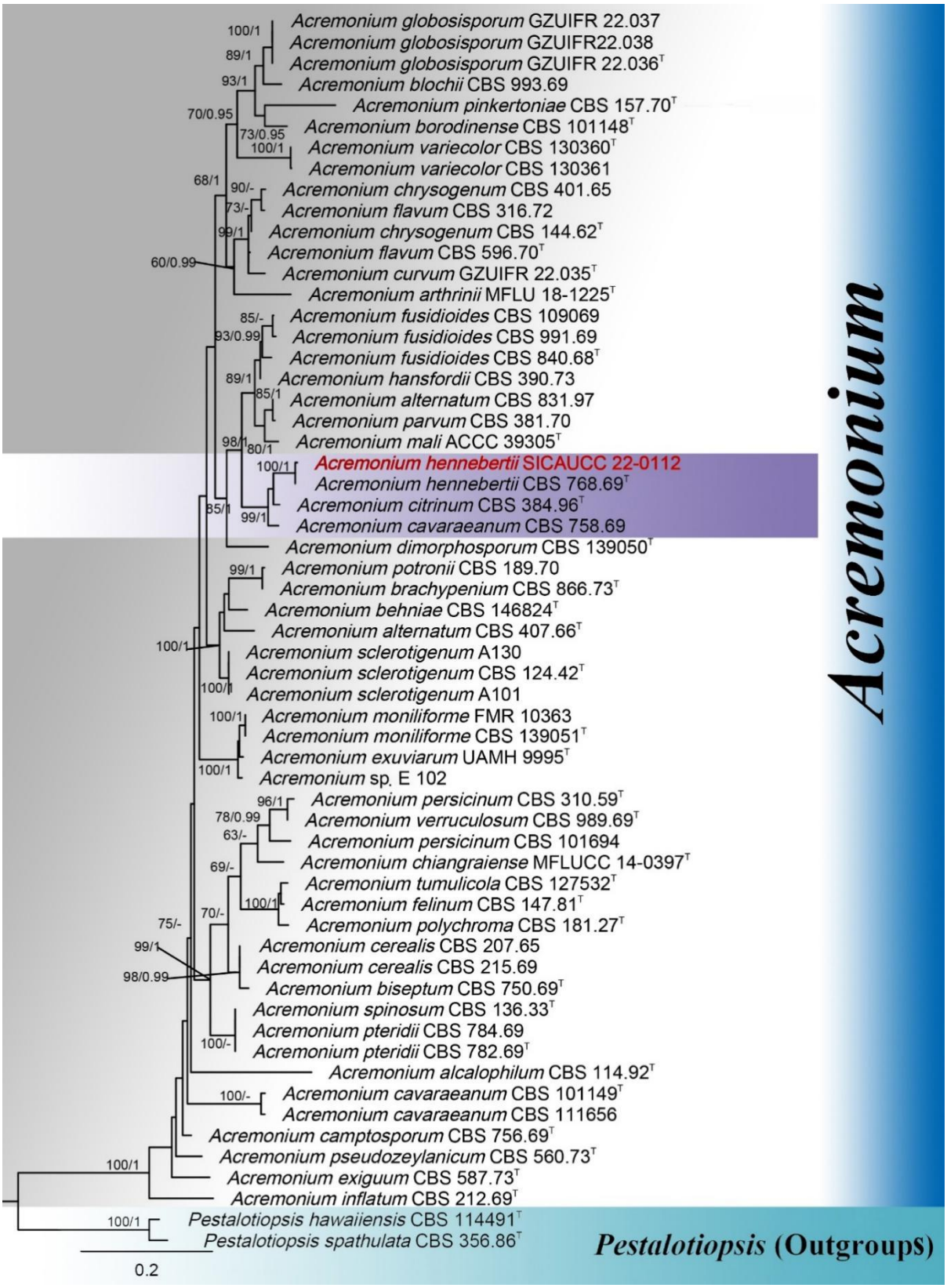


Figure 113 – Best scoring RAxML tree with a final likelihood value of -29,709.191494 based on combined LSU, ITS, *rpb*2, SSU and *tef*1-α sequence data of related species. The tree is rooted with

Pestalotiopsis hawaiiensis (CBS 114491) and *P. spathulata* (CBS 356.86) in *Pestalotiopsis*. Fifty-nine strains were included in the combined analyses which comprised 8,520 characters (2,373 characters for LSU, 2,326 characters for ITS, 1,084 characters for *rpb*2, 1,780 characters for SSU and 953 characters for *tef*1-α, including gap regions). The matrix had 1,660 distinct alignment patterns, with 77.40% undetermined characters and gaps. Estimated base frequencies were as follows; A = 0.246906, C = 0.248396, G = 0.276395, T = 0.228302; substitution rates AC = 1.321100, AG = 2.107287, AT = 1.502543, CG = 1.182781, CT = 6.083609, GT = 1.000000; gamma distribution shape parameter α = 0.310916. The Bayesian inference analyses was implemented by MrBayes v.3.2.2 with the best-fit model (GTR+I+G for LSU, SSU; GTR+G for ITS, *tef*1-α; GTR+I for *rpb*2) of evolution estimated with MrModeltest 2.2. The species determined in this study is indicated in red and bold. Bootstrap support values for maximum likelihood (MLBS, left) ⩾ 60% and Bayesian posterior probabilities (BYPP, right) ⩾ 0.90 are indicated at the nodes, respectively. Hyphens (-) represent support values less than 60% MLBS/0.90 BYPP. The ex-type superscript "T".

72. ***Clonostachys rosea*** (Link) Schroers, Samuels, Seifert & W. Gams, Mycologia 91(2): 369 (1999) Fig. 114

Index Fungorum number: IF461064; Facesoffungi number: FoF06012

Saprobic on branch of *Juglans regia*. Sexual morph: *Ascomata* 150–221 × 140–210 μm ($\bar{x}$ = 200 × 190 μm, n=20), superficial, solitary to gregarious, globose to subglobose, not collapsing or sometimes slightly laterally pinched when dry, yellowish orange, slightly papillate, surface warted. *Peridium* 23–50 μm ($\bar{x}$ = 39μm, n = 20) wide, composed of two regions: outer region 15–30 μm, 4–8 cells thick, cells angular to globose, with uniformly thickened walls, merging with the cells of the warts; inner region 8–20 μm thick, composed of fat hyaline cells. *Paraphyses* not obvious, mix in the gel. *Asci* 42–58 × 5.5–8 μm ($\bar{x}$ = 48 × 6.5 μm, n = 20), 8-spored, unitunicate, cylindrical to narrowly clavate, apex fat with somewhat rounded edges, short pedicellate. *Ascospores* 9–11 × 3–4.5 μm ($\bar{x}$ = 10 × 4 μm, n=30), single or double seriate, hyaline, median or submedian, 1-septate, equilateral or inequilateral, slightly constricted at the septum, ellipsoidal to occasionally subglobose, multi-guttulate, smooth-walled. Asexual morph: Not observed.

Culture characteristics – Ascospores germinating on sterile water within 24 h and germ tubes produced from both ends. Colonies on PDA reaching 40 mm diam., after 12 days at 25 ℃. The mycelium grows on the surface of the medium, surface white or pale yellowish, zonate, aerial mycelium abundant in the center. Reverse, brownish yellow becoming white at the margins. Red pigmentation develops within the culture medium.

Material examined – China, Sichuan Province, Chengdu City, Chongzhou City (30°33′9.37″N 103°39′29.50″E, alt. 512 m), on branch of *Juglans regia*, 28 July 2021, F.-H. Wang, WFH202107017 (SICAU 23-0091), living culture SICAUCC 23-0070.

GenBank numbers – SICAUCC 23-0070: PP060686 (ITS), PP057970 (LSU), PP061179 (*tub*2).

Note – SICAUCC 23-0070 is morphologically and phylogenetically closely related to *Clonostachys rosea* (CML2310) with strong statistical support (81% MLBS/0.99 BYPP) (Fig. 115). Nucleotide comparisons of ITS, LSU, and *tub*2 (SICAUCC 23-0070) also showed a high homology with the sequences of *C. rosea* (CBS 710.86 ex-type), with a similarity of 98.9% (476/481, 0 gap), 99.7% (792/794, 0 gap), 100% (940/940, 0 gap), and 98.8% (254/257, 0 gap), respectively. Moreover, our strain is also similar to the description of *C. rosea* provided by Schroers et al. (1999) except in having slightly larger ascospores (9–11 × 3–4.5 vs. 8–10 × 2.4–3.5 μm). We therefore, identify our taxon as *C. rosea* from Sichuan, China.

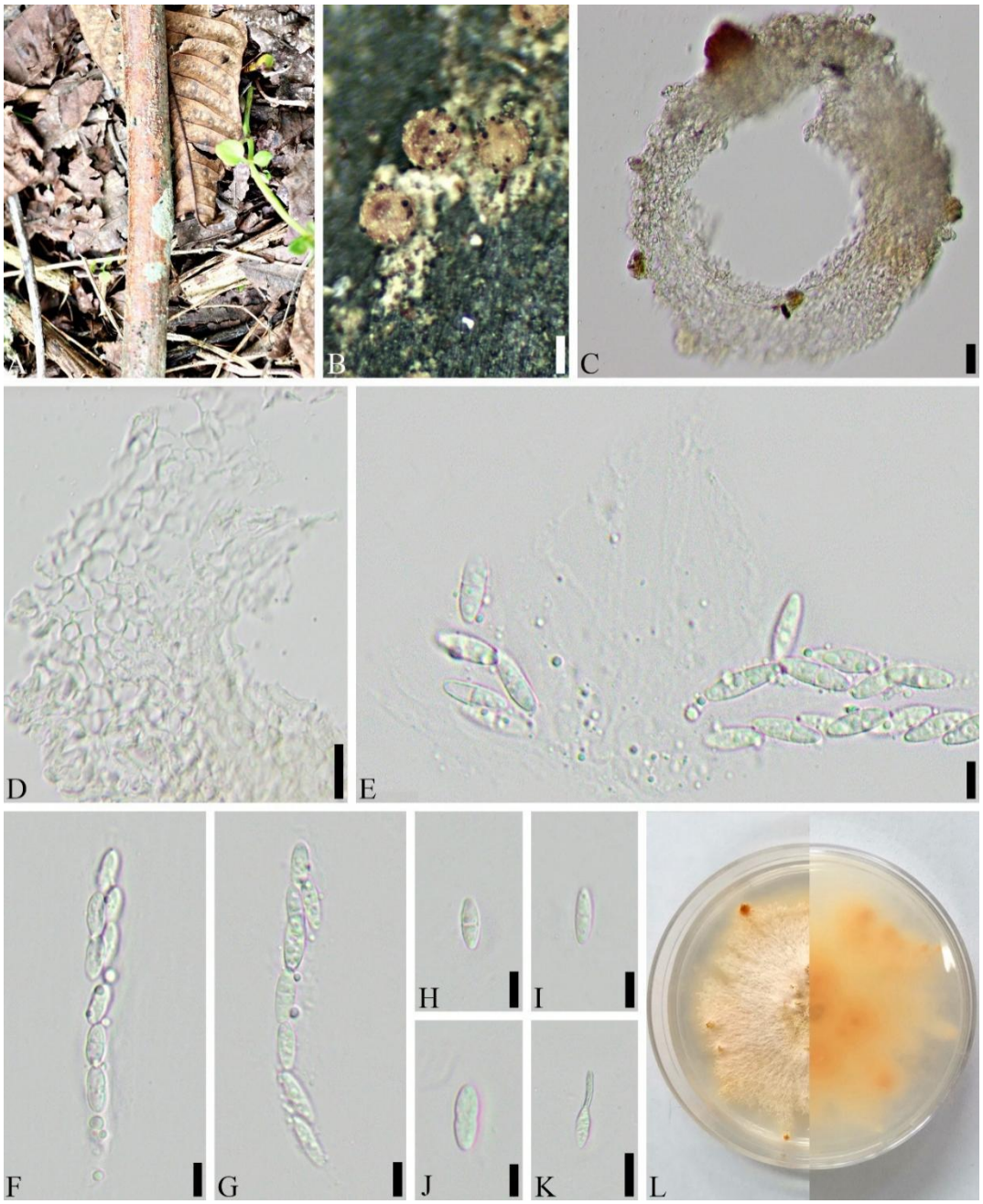


Figure 114 – *Clonostachys rosea* (SICAU 23-0091). A, B Appearance of ascostroma in host substrate. C Vertical section of ascoma. D Peridium. E Pseudoparaphyses and asci. F, G Asci. H–J Ascospores. K Germinating ascospore. L Colonies on PDA. Scale bars: B = 200 μm, C = 20 μm, K = 15 μm, D = 10 μm. F–I = 8 μm, E, J = 5 μm.

Cordycipitaceae Kreisel ex G.H. Sung, J.M. Sung, Hywel-Jones & Spatafora, in Sung, Hywel-Jones, Sung, Luangsa-ard, Shrestha & Spatafora, Stud. Mycol. 57: 48 (2007).

Cordycipitaceae was validated by Sung et al. (2007) to accommodate species of Cordyceps forming brightly coloured, fleshy *Stromata*. Species of *Cordycipitaceae* are known as obligate saprotrophs, parasites and symbionts with insects and fungi or grasses, rushes or sedges (Phookamsak et al. 2019). Species of *Cordycipitaceae* have been reported as obligate saprotrophs, parasites and symbionts with insects and fungi or grasses, rushes or sedges. (Sung et al. 2007, Schardl et al. 2013, Kepler et al. 2013, 2017, Li et al. 2016b, Tibpromma et al. 2017, Huang et al. 2018). Eighteen genera are listed in this family (Wijayawardene et al. 2018). We follow the latest treatment and updated accounts of *Cordycipitaceae* in Wang et al. (2020).

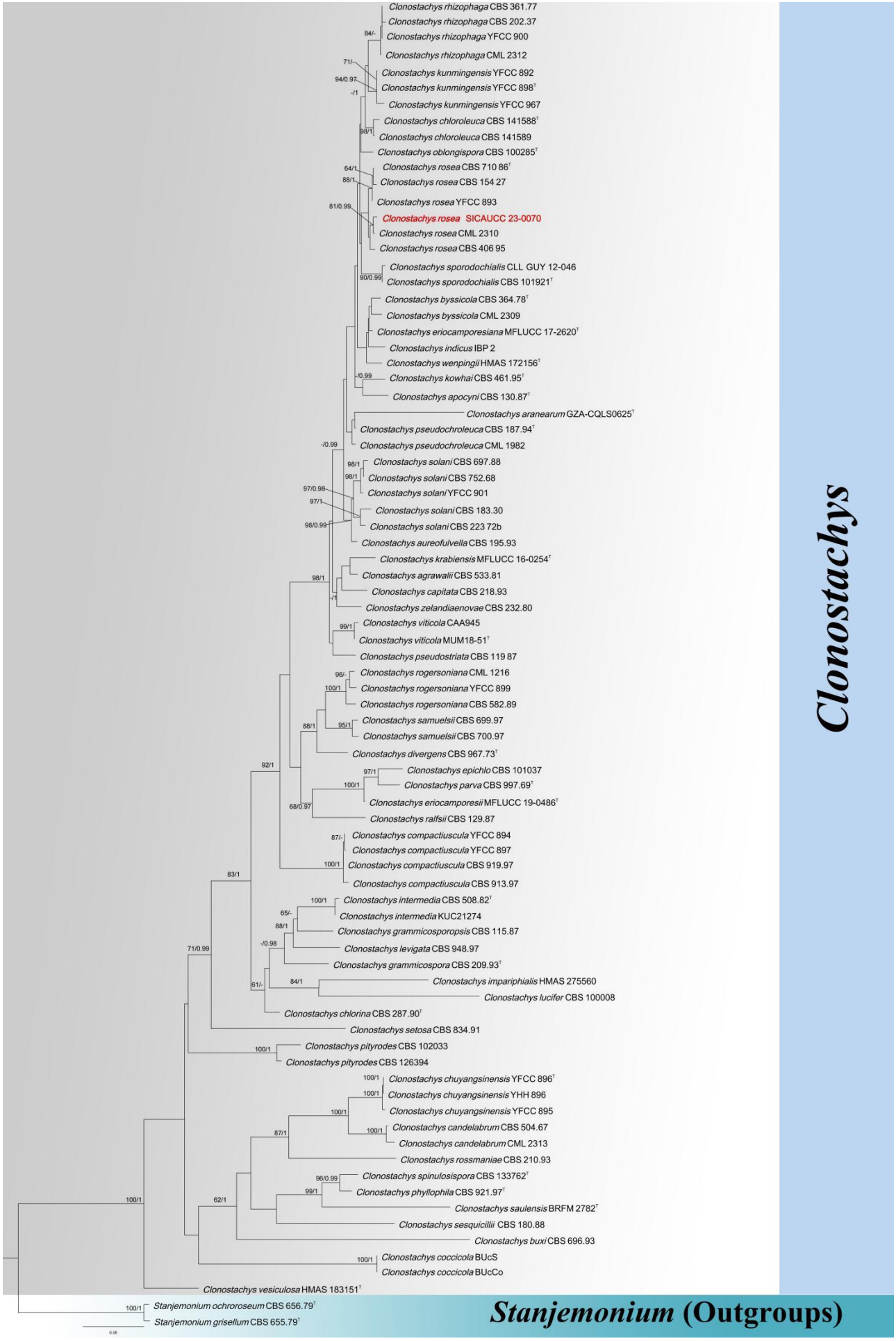

Clonostachys rhizophaga CBS 361.77
Clonostachys rhizophaga CBS 202.37
Clonostachys rhizophaga YFCC 900
Clonostachys rhizophaga CML 2312
Clonostachys kunmingensis YFCC 892
Clonostachys kunmingensis YFCC 898T
Clonostachys kunmingensis YFCC 967
Clonostachys chloroleuca CBS 141588T
Clonostachys chloroleuca CBS 141589
Clonostachys oblongispora CBS 100285T
Clonostachys rosea CBS 710 86T
Clonostachys rosea CBS 154 27
Clonostachys rosea YFCC 893
Clonostachys rosea SICAUCC 23-0070
Clonostachys rosea CML 2310
Clonostachys rosea CBS 406 95
Clonostachys sporodochialis CLL GUY 12-046
Clonostachys sporodochialis CBS 101921T
Clonostachys byssicola CBS 364.78T
Clonostachys byssicola CML 2309
Clonostachys eriocamporesiana MFLUCC 17-2620T
Clonostachys indicus IBP 2
Clonostachys wenpingii HMAS 172156T
Clonostachys kowhai CBS 461.95T
Clonostachys apocyni CBS 130.87T
Clonostachys aranearum GZA-CQLS0625T
Clonostachys pseudochroleuca CBS 187.94T
Clonostachys pseudochroleuca CML 1982
Clonostachys solani CBS 697.88
Clonostachys solani CBS 752.68
Clonostachys solani YFCC 901
Clonostachys solani CBS 183.30
Clonostachys solani CBS 223 72b
Clonostachys aureofulvella CBS 195.93
Clonostachys krabiensis MFLUCC 16-0254T
Clonostachys agrawalii CBS 533.81
Clonostachys capitata CBS 218.93
Clonostachys zelandiaenovae CBS 232.80
Clonostachys viticola CAA945
Clonostachys viticola MUM18-51T
Clonostachys pseudostriata CBS 119 87
Clonostachys rogersoniana CML 1216
Clonostachys rogersoniana YFCC 899
Clonostachys rogersoniana CBS 582.89
Clonostachys samuelsii CBS 699.97
Clonostachys samuelsii CBS 700.97
Clonostachys divergens CBS 967.73T
Clonostachys epichlo CBS 101037
Clonostachys parva CBS 997.69T
Clonostachys eriocamporesii MFLUCC 19-0486T
Clonostachys ralfsii CBS 129.87
Clonostachys compactiuscula YFCC 894
Clonostachys compactiuscula YFCC 897
Clonostachys compactiuscula CBS 919.97
Clonostachys compactiuscula CBS 913.97
Clonostachys intermedia CBS 508.82T
Clonostachys intermedia KUC21274
Clonostachys grammicosporopsis CBS 115.87
Clonostachys levigata CBS 948.97
Clonostachys grammicospora CBS 209.93T
Clonostachys impariphialis HMAS 275560
Clonostachys lucifer CBS 100008
Clonostachys chlorina CBS 287.90T
Clonostachys setosa CBS 834.91
Clonostachys pityrodes CBS 102033
Clonostachys pityrodes CBS 126394
Clonostachys chuyangsinensis YFCC 896T
Clonostachys chuyangsinensis YHH 896
Clonostachys chuyangsinensis YFCC 895
Clonostachys candelabrum CBS 504.67
Clonostachys candelabrum CML 2313
Clonostachys rossmaniae CBS 210.93
Clonostachys spinulosispora CBS 133762T
Clonostachys phyllophila CBS 921.97T
Clonostachys saulensis BRFM 2782T
Clonostachys sesquicillii CBS 180.88
Clonostachys buxi CBS 696.93
Clonostachys coccicola BUcS
Clonostachys coccicola BUcCo
Clonostachys vesiculosa HMAS 183151T
Stanjemonium ochroroseum CBS 656.79T
Stanjemonium grisellum CBS 655.79T
Clonostachys
Stanjemonium (Outgroups)

Figure 115 – Best scoring RAxML tree with a final likelihood value of -24,463.081055 based on combined ITS, LSU, *tef*1-α and *tub*2 sequence data of related species. The tree is rooted with *Stanjemonium ochroroseum* (CBS 656.79) and *S. grisellum* (CBS 655.79) in *Stanjemonium*. Eighty-two strains were included in the combined analyses which comprised 3,969 characters (1,201 characters for ITS, 1,455 characters for LSU, 596 characters for *tef*1-α and 714 characters for *tub*2, including gap regions). The matrix had 1,563 distinct alignment patterns, with 51.59% of undetermined characters and gaps. Estimated base frequencies were as follows; A = 0.232822, C = 0.258423, G = 0.266168, T = 0.242587; substitution rates AC = 1.351204, AG = 3.116007, AT = 1.428280, CG = 0.853304, CT = 4.974735, GT = 1.000000; gamma distribution shape parameter α = 0.189327. The Bayesian inference analyses was implemented by MrBayes v.3.2.2 with the best-fit model (SYM+I+G for ITS; GTR+I+G for LSU; HKY+I+G for *tef*1-α, *tub*2) of evolution estimated with MrModeltest 2.2. The species determined in this study is indicated in red and bold. Bootstrap support values for maximum likelihood (MLBS, left) ⩾ 60% and Bayesian posterior probabilities (BYPP, right) ⩾ 0.90 are indicated at the nodes, respectively. Hyphens (-) represent support values less than 60% MLBS/0.90 BYPP. The ex-type superscript "T".

Lecanicillium W. Gams & Zare, Nova Hedwigia 72(3-4): 332 (2001).

Lecanicillium was introduced by Gams & Zare (2001) to accommodate the taxa with aculeate phialides that cannot be classified in the genera such as *Beauveria*, *Isaria* and *Microhilum* H.Y. Yip & A.C. Rath, with *L. lecanii* (Zimm.) Zare & W. Gams as the generic type (Sung et al. 2007, Park et al. 2015, Huang et al. 2018). While, previous studies of *Cordycipitaceae* based on multi-locus phylogeny showed that *Lecanicillium* is polyphyletic (Sung et al. 2007, Sanjuan et al. 2014, Chiriví-Salomón et al. 2015, Kepler et al. 2017), and several species of *Lecanicillium*, including the type *L. lecanii*, were transferred to the genus *Akanthomyces* Lebert (Kepler et al. 2017).

73. ***Lecanicillium dimorphum*** (J.D. Chen) Zare & W. Gams, Nova Hedwigia 73(1-2): 24 (2001) Fig. 116

Index Fungorum number: 484540; Facesoffungi number: FoF09618

Saprobic on branch of *Juglans regia*. Sexual morph: Not observed. Asexual morph: *Conidiophores* 19–32 × 1.5–3.5 μm ($\bar{x}$ = 24 × 2.5 μm, n = 20), hyaline, tapering towards apex, discrete. *Conidiogenous cells* 10–15 × 2–4 μm ($\bar{x}$ = 12 × 3 μm, n = 30), wide at base, smooth, hyaline. *Conidia* 12–17 × 3–6.5 μm ($\bar{x}$ = 14 × 5 μm, n = 40), hyaline, ovoid to ellipsoidal, kidney-shaped, slightly curved, aseptate, smooth.

Culture characteristics – Ascospores germinating on sterile water within 24 h and germ tubes produced from both ends. Colonies on PDA reaching 50 mm diam., after 15 days at 25 ℃. The mycelium grows on the surface of the medium, fat, felty, margin fimbriate, central hyphae are white, slightly convex and dense. Reverse, plicate, light yellow to yellow. Not produced pigmentation on PDA media.

Material examined – China, Sichuan Province, Chengdu City, Chongzhou City (30°33′9.39″N 103°39′29.10″E, alt. 510 m), on branch of *Juglans regia*, 16 October 2021, F.-H. Wang, WFH202110001 (SICAU 23-0092), living culture SICAUCC 23-0071.

GenBank numbers – SICAUCC 23-0071: PP060687 (ITS), PP057971 (LSU), PP003829 (SSU), PP061123 (*rpb*2), PP061152 (*tef*1-α).

Note – A new collection of *Lecanicillium dimorphum* (SICAUCC 23-0071) was collected from a walnut garden in southwest China. Our collection shares identical morphology to the type species *L. dimorphum* (CBS363.86). Further, phylogenetic analysis based on a combined ITS, LSU, SSU, *tef*1-α and *rpb*2 sequences places our isolate *L. dimorphum* (SICAUCC 23-0070) with a strain of *L. dimorphum* (CBS363.86 and CBS345.37) with strong statistical support (100% MLBS/1.00 BYPP) (Fig. 117). Nucleotide comparisons of ITS, LSU, SSU, and *tef*1-α (SICAUCC 23-0071) also showed a high homology with the sequences of *L. dimorphum* (CBS 363.86 ex-type), with a similarity of 100% (539/539, 0 gap), 99.7% (749/751, 2 gaps), 98.8% (980/992, 0 gap), and 100% (889/889, 0 gap), respectively. Based on morphological characters and phylogenetic analyses, we determine our

specimens as *L. dimorphum*. Therefore, a new host record of *L. dimorphum* is reported from southwest China.

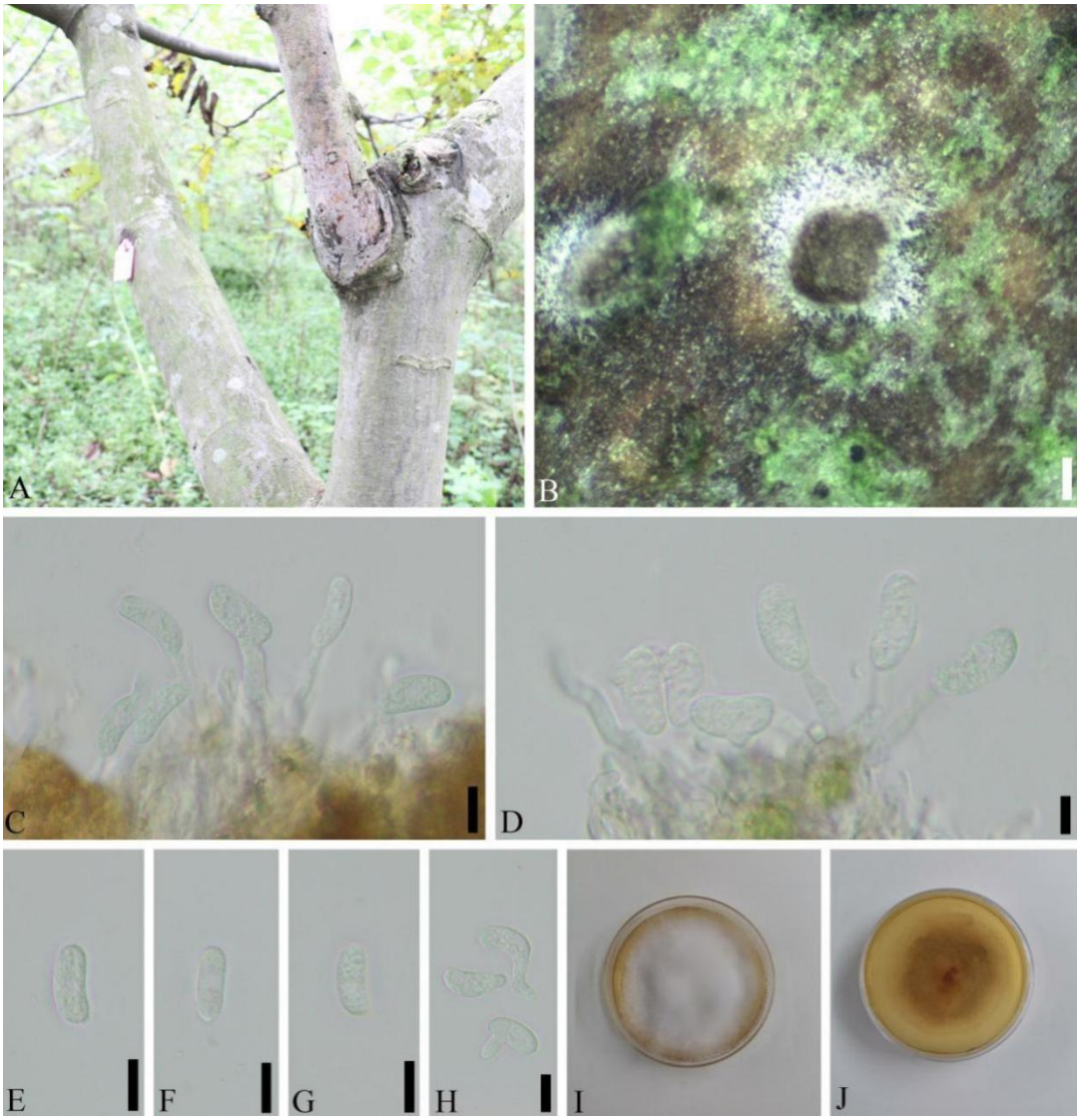


Figure 116 – *Lecanicillium dimorphum* (SICAU 23-0092). A, B Appearance of conidiomata in host substrate. C, D Conidiogenous cells attached with conidia. E–G Conidia. H Germinating conidia. I, J Colonies on PDA (I from above, J from below). Scale bars: B = 200 μm, C, E–H = 10 μm, D = 5 μm.

Nectriaceae Tul. & C. Tul.

The name *Nectria* was initially introduced by Fries (1825) as one of the four sections of Hypocrea, suborder Sphaerini, order Sphaeriacei. *Nectriaceae* was afterwards reported as 'Nectriei', and first spelt correctly at family rank by Nitschke (1869). Rossman et al. (1999) accepted *Nectriceae* as a distinct family, which was defined on the basis of stromatal, ascomatal and ascospore characters. Members of this family are normally characterized by uni-loculate ascomata that are brightly pigmented with fusiform to allantoid ascospores and globose to fusiform phialidic conidia, and occur worldwide (Chaverri et al. 2011, Rossman et al. 2013, Lombard et al. 2015). *Nectriaceae* a highly diverse group with a worldwide distribution and it has higher diversity in warm temperate and tropical regions (Rossman 2000, Schroers et al. 2011, Hyde et al. 2014). The species were reported as saprobes, plant pathogens, fungicolous, insecticolous, and even human pathogens (Chang et al. 2006, De Hoog et al. 2011, Gräfenhan et al. 2011, Guarro 2013). Recently, Perera et al. (2023) provided a profile for *Nectraiceae* and related families, and assigned 77 genera under this family.

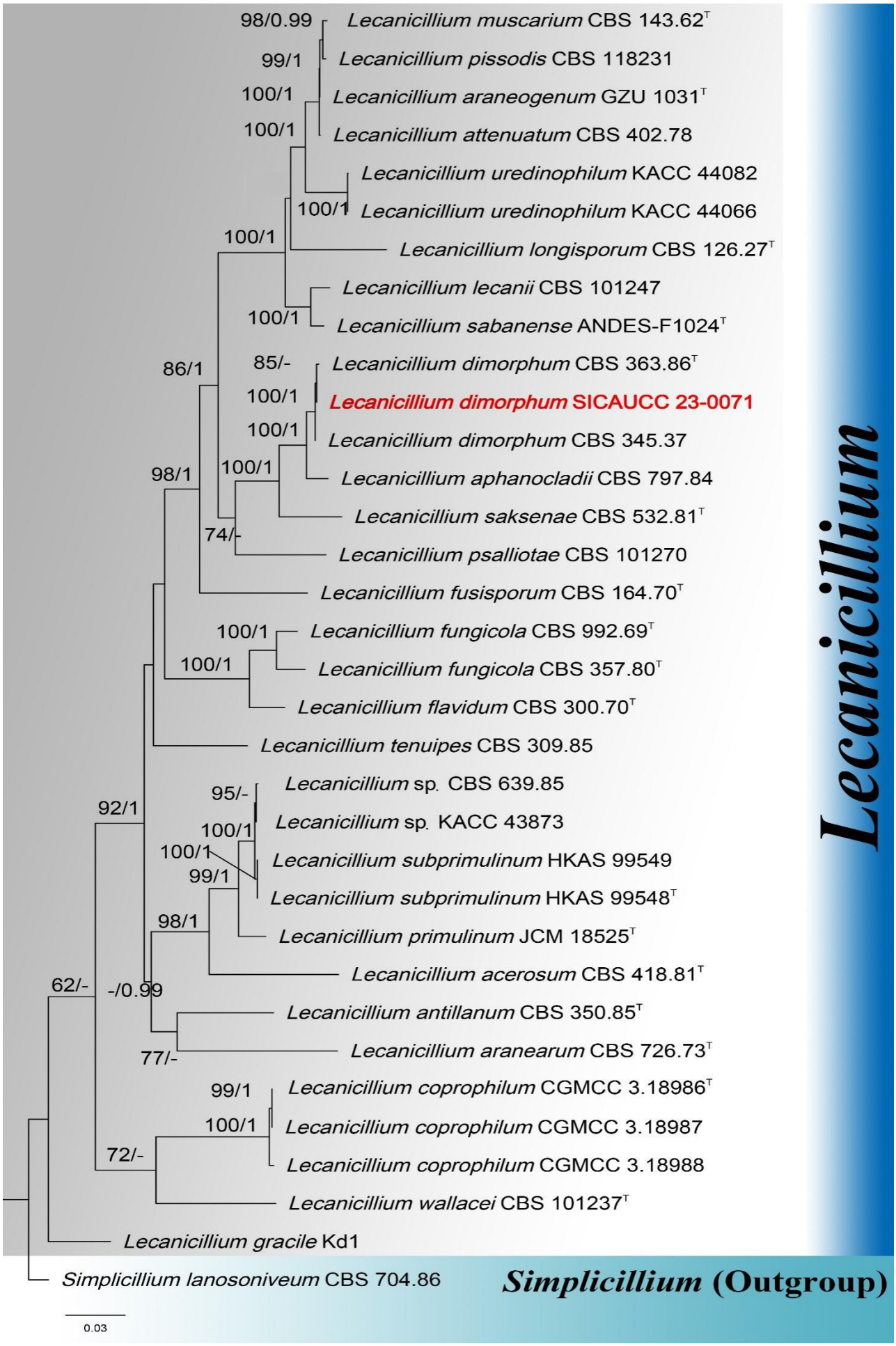

98/0.99
Lecanicillium muscarium CBS 143.62T
99/1
Lecanicillium pissodis CBS 118231
100/1
Lecanicillium araneogenum GZU 1031T
100/1
Lecanicillium attenuatum CBS 402.78
Lecanicillium uredinophilum KACC 44082
100/1
Lecanicillium uredinophilum KACC 44066
100/1
Lecanicillium longisporum CBS 126.27T
Lecanicillium lecanii CBS 101247
100/1
Lecanicillium sabanense ANDES-F1024T
86/1
85/-
Lecanicillium dimorphum CBS 363.86T
100/1
Lecanicillium dimorphum SICAUCC 23-0071
100/1
Lecanicillium dimorphum CBS 345.37
98/1
100/1
Lecanicillium aphanocladii CBS 797.84
Lecanicillium saksenae CBS 532.81T
74/-
Lecanicillium psalliotae CBS 101270
Lecanicillium fusisporum CBS 164.70T
100/1
Lecanicillium fungicola CBS 992.69T
100/1
Lecanicillium fungicola CBS 357.80T
Lecanicillium flavidum CBS 300.70T
Lecanicillium tenuipes CBS 309.85
95/-
Lecanicillium sp. CBS 639.85
92/1
100/1
Lecanicillium sp. KACC 43873
100/1
Lecanicillium subprimulinum HKAS 99549
99/1
Lecanicillium subprimulinum HKAS 99548T
98/1
Lecanicillium primulinum JCM 18525T
Lecanicillium acerosum CBS 418.81T
62/-
-/0.99
Lecanicillium antillanum CBS 350.85T
77/-
Lecanicillium aranearum CBS 726.73T
99/1
Lecanicillium coprophilum CGMCC 3.18986T
100/1
Lecanicillium coprophilum CGMCC 3.18987
72/-
Lecanicillium coprophilum CGMCC 3.18988
Lecanicillium wallacei CBS 101237T
Lecanicillium gracile Kd1
Simplicillium lanosoniveum CBS 704.86
0.03
Lecanicillium
Simplicillium (Outgroup)

Figure 117 – Best scoring RAxML tree with a final likelihood value of -21,132.737731 based on combined ITS, LSU, *rpb*2 and *tef*1-α sequence data of related species. The tree is rooted with *Simplicillium lanosoniveum* (CBS 704.86) in *Simplicillium*. Thirty-four strains were included in the combined analyses which comprised 5,155 characters (1,001 characters for *tef*1-α, 647 characters for ITS, 1,350 characters for LSU, 1,119 characters for *rpb*2 and 1,034 characters for SSU, including gap regions). The matrix had 1,396 distinct alignment patterns, with 25.57% undetermined characters and gaps. Estimated base frequencies were as follows; A = 0.246473, C = 0.259616, G = 0.264515, T = 0.229396; substitution rates AC = 1.557901, AG = 3.104862, AT = 1.170550, CG = 1.052009, CT = 8.722959, GT = 1.000000; gamma distribution shape parameter α = 0.133781. In our analysis, GTR+I+G model was used for each partition in Bayesian posterior analysis. The species determined in this study is indicated in red and bold. Bootstrap support values for maximum likelihood (MLBS, left) ⩾ 60% and Bayesian posterior probabilities (BYPP, right) ⩾ 0.90 are indicated at the nodes, respectively. Hyphens (-) represent support values less than 60% MLBS/0.90 BYPP. The ex-type superscript "T".

Albonectria Rossman & Samuels, in Rossman, Samuels, Rogerson & Lowen, Stud. Mycol. 42: 105 (1999)

Albonectria was established by Rossman et al. (1999) to distinguish species within the *Fusarium* genus that exhibit fusarioid morphological characteristics. *Albonectria rigidiuscula* (Berk. & Broome) Rossman & Samuels serves as the type species of this genus, and currently, only five species have been described within this genus (Perera et al. 2023, Zhang et al. 2024c).

74. ***Albonectria rigidiuscula*** (Berk. & Broome) Rossman & Samuels, Stud. Mycol. 42: 105 (1999). Fig. 118.

Index Fungorum number: IF198322; Facesoffungi number: FoF16308

Associated with leaf spots on the living leaves of *Juglans regia*. Symptoms initially manifest as small brown spots, which later develop into black, circular or irregular patches. In the later stages, these patches lead to leaf wilting and eventual shedding. Sexual morph: Not observed. Asexual morph: *Conidiophores* 10–21 × 2–4 μm ($\bar{x}$ = 15 × 3 μm, n = 20), mononematous, septate, irregularly branched, bearing terminal phialides. *Conidiogenous cells* 19–31 × 2–4.5 μm ($\bar{x}$ = 19.9 × 3.0 μm, n = 35), monophialidic, cylindrical to subcylindrical, periclinal thickening inconspicuous to absent, smooth- and thin-walled. *Macroconidia* 14–33 × 1.5–3.5 μm ($\bar{x}$ = 25 × 2 μm, n = 35), fusoid, 2–4-septate, curved, with a wide, blunt apical cell and a poorly- to well-developed, foot-shaped basal cell, hyaline. *Chlamydospores* not observed.

Culture characteristics – Conidia germinating on sterile water within 12 h and germ tubes produced from both ends. Colonies on PDA reaching 30 mm diam., after 5 days at 25 ℃. The mycelium grows on the surface of the medium, purple or white radiating outwardly to the edge, undulate margin, medium dense, fat, dull, fimbriate, and slightly covered with white aerial mycelium. Reverse, yellow with radiating cream mycelium. There is purple pigmentation within the PDA.

Material examined – China, Sichuan Province, Chengdu City, Chongzhou City (30°33′8.74″N 103°39′29.46″E, alt. 512 m), on living leaf of *Juglans regia*, 21 April 2022, F.-H. Wang, WFH202204022 (SICAU 23-0093), living culture SICAUCC 23-0072.

GenBank numbers – SICAUCC 23-0072: PP060688 (ITS), PP061124 (*rpb*2), PP061153 (*tef*1-α), PP061180 (*tub*2).

Note – *Albonectria rigidiuscula* (SICAUCC 23-0072) formed a well-supported sister clade to *A. rigidiuscula* (CBS 315.73) with strong statistical support (100% MLBS/1.00 BYPP) (Fig. 119). We recognized our collection as *A. rigidiuscula*, because phylogenetically it clustered with other *A. rigidiuscula* strains, and was nearly identical to others in the ITS, *tef*1-α, *tub*2, and *rpb*2 gene sequences. Nucleotide comparisons of ITS, *tub*2, and *tef*1-α *A. rigidiuscula* (SICAUCC 22-0136) also showed a high homology with the sequences of *A. rigidiuscula* (CBS 315.73), with a similarity of 90% (407/757, 0 gap), 100% (591/591, 0 gap), and 100% (510/719, 0 gap), respectively. The morphology of our collection is similar to that of *A. rigidiuscula*, particularly resembling the characteristics found in sample *A. rigidiuscula* (CBS 315.73). *Albonectria rigidiuscula* was reported as a causal agent in more

than 85 host plants (Farr & Rossman 2024). This is the first record of *A. rigidiuscula* recorded on *Juglans regia* from China (new host record).

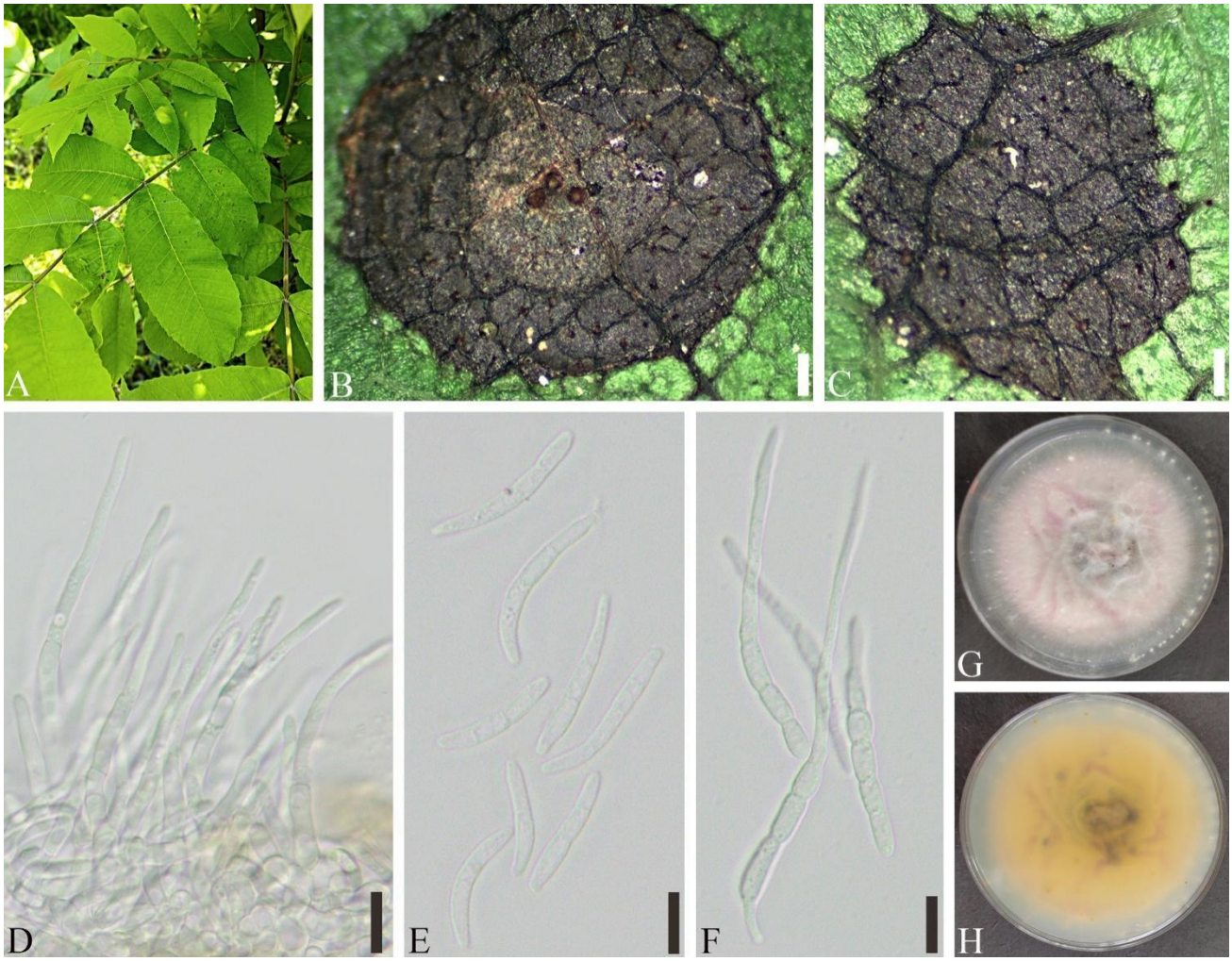


Figure 118 *Albonectria rigidiuscula* (SICAU 23-0093). A–C Sporodochium on the host. D Conidia attached to conidiophores. E Conidia. F. Germinating conidia. G, H Colonies on PDA (G from above, H from below). Scale bars: B, C = 500 μm, D–F = 10 μm.

Fusarium Link, Mag. Gesell. naturf. Freunde, Berlin 3(1–2): 10 (1809).

Fusarium is a large genus in *Nectriaceae*, with more than 1037 epithets in Species Fungorum (http://www.speciesfungorum.org/Index.htm, September 2024). The genus was introduced with *Fusarium roseum* as the type species (Wijayawardene et al. 2018). *Fusarium* species are economically important fungi including, many well-known plant pathogens, which cause blights, cankers, root and stalk rots and wilts of broadacre, horticultural, ornamental and forest plants, and cause human infections worldwide (Jayawardena et al. 2019, Summerell 2019). *Fusarium* is famous for its difficulty in identification and pathogenicity. It has been extensively discussed in recent decades as one of the most taxonomically confusing genera within *Nectriaceae* (Gräfenhan et al. 2011, O'Donnell et al. 2013, Crous et al. 2021, Geiser et al. 2021, Boonmee et al. 2021, Jayawardena et al. 2022, Sandoval-Denis et al. 2025). We describe species of *Fusarium* isolated from walnut (*Juglans regia*) in Sichuan, China, and introduce new records of *F. coffeatum, F. graminearum, F. incarnatum, F. lateritium, F. solani* and *F. decemcellulare* on *Juglans regia* based on morphological characters and multi-locus phylogenetic analyses.

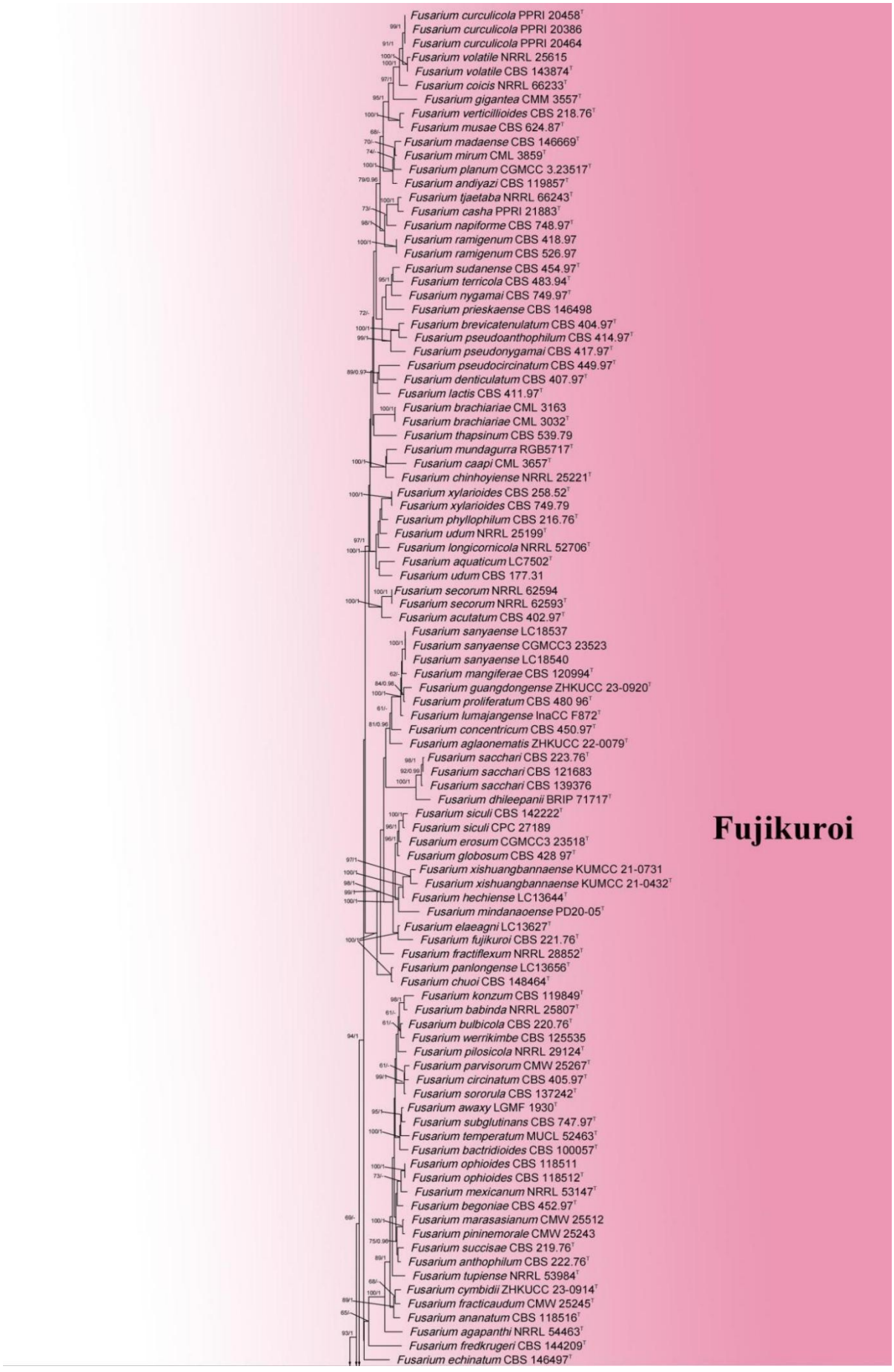


Figure 119 – Continued.

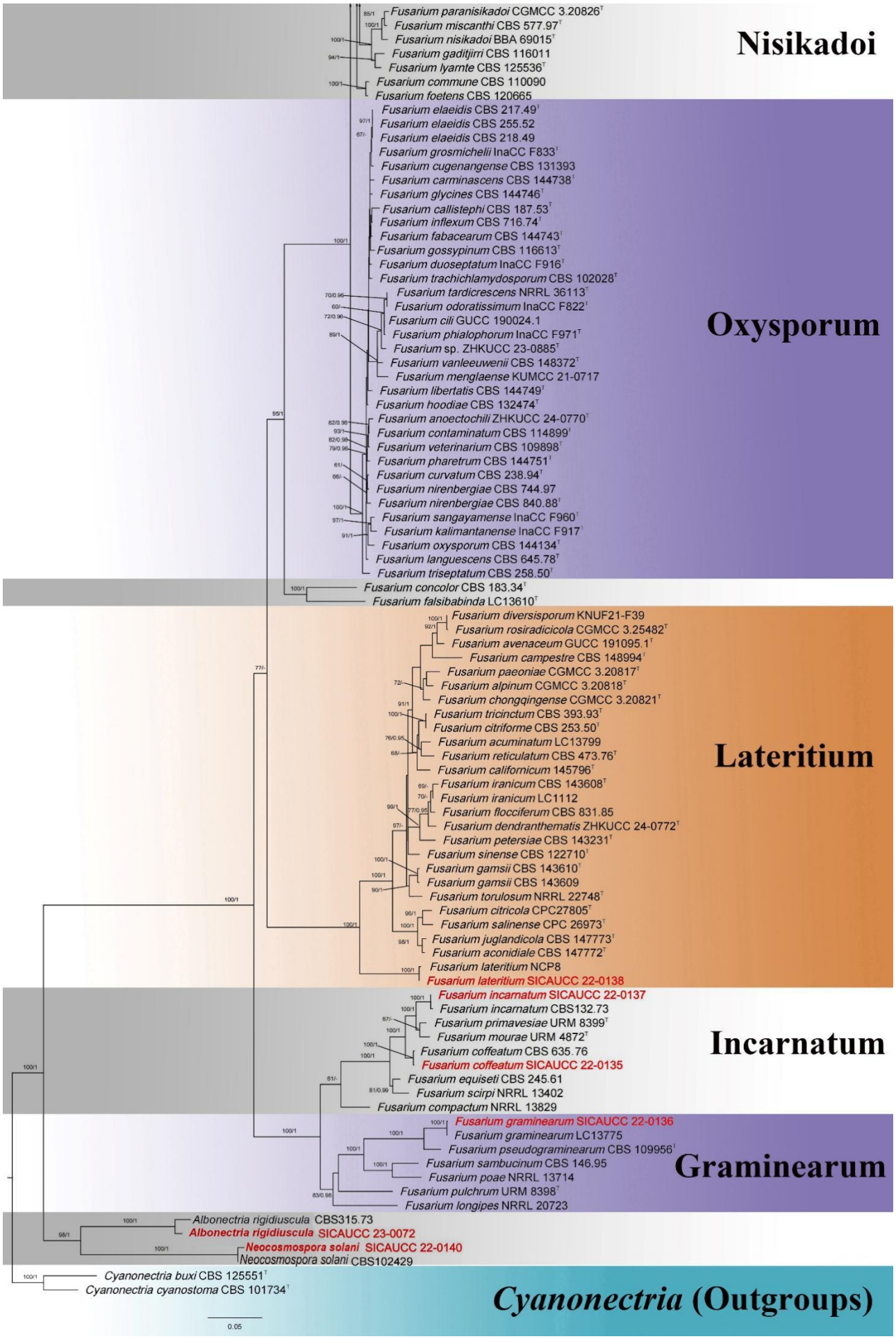

Nisikadoi
Fusarium paranisikadoi CGMCC 3.20826T
Fusarium miscanthi CBS 577.97T
Fusarium nisikadoi BBA 69015T
Fusarium gaditjirri CBS 116011
Fusarium lyarnte CBS 125536T
Fusarium commune CBS 110090
Fusarium foetens CBS 120665
Oxysporum
Fusarium elaeidis CBS 217.49T
Fusarium elaeidis CBS 255.52
Fusarium elaeidis CBS 218.49
Fusarium grosmichelii InaCC F833T
Fusarium cugenangense CBS 131393
Fusarium carminascens CBS 144738T
Fusarium glycines CBS 144746T
Fusarium callistephi CBS 187.53T
Fusarium inflexum CBS 716.74T
Fusarium fabacearum CBS 144743T
Fusarium gossypinum CBS 116613T
Fusarium duoseptatum InaCC F916T
Fusarium trachichlamydosporum CBS 102028T
Fusarium tardicrescens NRRL 36113T
Fusarium odoratissimum InaCC F822T
Fusarium cili GUCC 190024.1
Fusarium phialophorum InaCC F971T
Fusarium sp. ZHKUCC 23-0885T
Fusarium vanleeuwenii CBS 148372T
Fusarium menglaense KUMCC 21-0717
Fusarium libertatis CBS 144749T
Fusarium hoodiae CBS 132474T
Fusarium anoectochili ZHKUCC 24-0770T
Fusarium contaminatum CBS 114899T
Fusarium veterinarium CBS 109898T
Fusarium pharetrum CBS 144751T
Fusarium curvatum CBS 238.94T
Fusarium nirenbergiae CBS 744.97
Fusarium nirenbergiae CBS 840.88T
Fusarium sangayamense InaCC F960T
Fusarium kalimantanense InaCC F917T
Fusarium oxysporum CBS 144134T
Fusarium languescens CBS 645.78T
Fusarium triseptatum CBS 258.50T
Fusarium concolor CBS 183.34T
Fusarium falsibabinda LC13610T
Lateritium
Fusarium diversisporum KNUF21-F39
Fusarium rosiradicicola CGMCC 3.25482T
Fusarium avenaceum GUCC 191095.1T
Fusarium campestre CBS 148994T
Fusarium paeoniae CGMCC 3.20817T
Fusarium alpinum CGMCC 3.20818T
Fusarium chongqingense CGMCC 3.20821T
Fusarium tricinctum CBS 393.93T
Fusarium citriforme CBS 253.50T
Fusarium acuminatum LC13799
Fusarium reticulatum CBS 473.76T
Fusarium californicum 145796T
Fusarium iranicum CBS 143608T
Fusarium iranicum LC1112
Fusarium flocciferum CBS 831.85
Fusarium dendranthematis ZHKUCC 24-0772T
Fusarium petersiae CBS 143231T
Fusarium sinense CBS 122710T
Fusarium gamsii CBS 143610T
Fusarium gamsii CBS 143609
Fusarium torulosum NRRL 22748T
Fusarium citricola CPC27805T
Fusarium salinense CPC 26973T
Fusarium juglandicola CBS 147773T
Fusarium aconidiale CBS 147772T
Fusarium lateritium NCP8
Fusarium lateritium SICAUCC 22-0138
Incarnatum
Fusarium incarnatum SICAUCC 22-0137
Fusarium incarnatum CBS132.73
Fusarium primavesiae URM 8399T
Fusarium mourae URM 4872T
Fusarium coffeatum CBS 635.76
Fusarium coffeatum SICAUCC 22-0135
Fusarium equiseti CBS 245.61
Fusarium scirpi NRRL 13402
Fusarium compactum NRRL 13829
Graminearum
Fusarium graminearum SICAUCC 22-0136
Fusarium graminearum LC13775
Fusarium pseudograminearum CBS 109956T
Fusarium sambucinum CBS 146.95
Fusarium poae NRRL 13714
Fusarium pulchrum URM 8398T
Fusarium longipes NRRL 20723
Albonectria rigidiuscula CBS315.73
Albonectria rigidiuscula SICAUCC 23-0072
Neocosmospora solani SICAUCC 22-0140
Neocosmospora solani CBS102429
Cyanonectria buxi CBS 125551T
Cyanonectria cyanostoma CBS 101734T
Cyanonectria (Outgroups)
0.05

Figure 119 – Best scoring RAxML tree with a final likelihood value of -44,672.054233 based on combined *tef*1-α, *rpb*2 and *tub*2 sequence data of related species. The tree is rooted with *Cyanonectria buxi* (CBS 125551) and *C. cyanostoma* (CBS 101734). One hundred and eighty-nine strains were included in the combined analyses, which comprised 5,807 characters (1,868 characters for *tef*1-α, 2,503 characters for *rpb*2 and 1,433 characters for *tub*2, including gap regions). The matrix had 2,425 distinct alignment patterns, with 59.29% undetermined characters and gaps. Estimated base frequencies were as follows; A = 0.249613, C = 0.267267, G = 0.240906, T = 0.242214; substitution rates AC = 1.215244, AG = 4.047635, AT = 1.280351, CG = 0.790197, CT = 7.336963, GT = 1.000000; gamma distribution shape parameter α = 0.330327. The Bayesian inference analysis was implemented by MrBayes v.3.2.2 with the best-fit model (GTR+I+G for *tef*1-α, *rpb*2; GTR+G for *tub*2) of evolution estimated with MrModeltest 2.2. The species determined in this study is indicated in red and bold. Bootstrap support values for maximum likelihood (MLBS, left) ⩾ 60% and Bayesian posterior probabilities (BYPP, right) ⩾ 0.90 are indicated at the nodes, respectively. Hyphens (-) represent support values less than 60% MLBS/0.90 BYPP. The ex-type superscript "T".

75. ***Fusarium coffeatum*** L. Lombard & Crous, Fungal Systematics and Evolution 4: 191 (2019) Fig.120

Index Fungorum number: IF831560; Facesoffungi number: FoF16307

Associated with leaf spots on the living leaves of *Juglans regia*. Symptoms manifest initially with yellowing leaves, which gradually develop into a brown to tawny color, causing the leaves to dry, curl, and eventually fall off. Sexual morph: Not observed. Asexual morph: *Hyphae* 0.8–3.5 μm diam, hyaline, smooth-walled, septate, branched. *Conidiophores* 19–31 × 2–4.5 μm ($\bar{x}$ = 19.9 × 3.0 μm, n = 30), arises on aerial mycelium, unbranched or irregularly branched. *Conidiogenous cells* 11–20 × 2–4 μm ($\bar{x}$ = 14 × 3 μm, n = 30), polyphialide, subulate to subcylindical, smooth. *Conidia* 16–27 × 3–5 μm ($\bar{x}$ = 22 × 4 μm, n = 40), hyaline, smoothand thin-walled, two types, clavate with truncate base 1–3-septate. *Sporodochia* not observed. *Chlamydospores* not observed.

Culture characteristics – Conidia germinating on sterile water within 12 h and germ tubes produced from both ends. Colonies on PDA reaching 50 mm diam., after 5 days at 25 ℃. The mycelium grows on the surface of the medium, appeared white to pink with abundant aerial mycelium. The reverse side of the colonies is white. Not produced pigmentation on PDA media.

Material examined – China, Sichuan Province, Neijiang City, Dongxing District, Paifang Village (29°48′30.19″N 105°6′36.42″E, alt. 387 m), on living leaves of *Juglans regia*, 27 April 2022, F.-H. Wang, WFH202204063 (SICAU 22-0133), living culture SICAUCC 22-0135.

GenBank numbers – SICAUCC 22-0135: OP963835 (ITS), OP964574 (LSU), OQ281345 (*rpb*2), OQ281373 (*tef*1-α), OQ281414 (*tub*2).

Note – *Fusarium coffeatum* named after refers to the characteristic coffee-brown pigmentation produced in cultures of this fungus (Lombard et al. 2019). In the phylogenetic analyses, our strain clustered with the type strain of *F. coffeatum* (CBS 635.76) with strong statistical support (100% MLBS/1.00 BYPP) (Fig. 118). Nucleotide comparisons of ITS, LSU, *tef*1-α, and *rpb*2 *F. coffeatum* (SICAUCC 22-0135) also showed a high homology with the sequences of *F. coffeatum* (CBS 635.76), with a similarity of 99.3% (544/545, 1 gap), 100% (896/896, 0 gap), 95.5% (636/676, 0 gap), and 100% (879/880, 0 gap), respectively. Morphology, as well as the ITS, LSU, *rpb*2, and *tef*1-α sequence data of our collections and *F. coffeatum* are almost identical (Lombard et al. 2019). Therefore, the specimens collected in this study have been identified as *F. coffeatum*, whereas previous reports have mentioned this fungus being found on corn kernels in India (Navale et al. 2023). This is the first record of *F. coffeatum* recorded on *Juglans regia* from China (new host record).

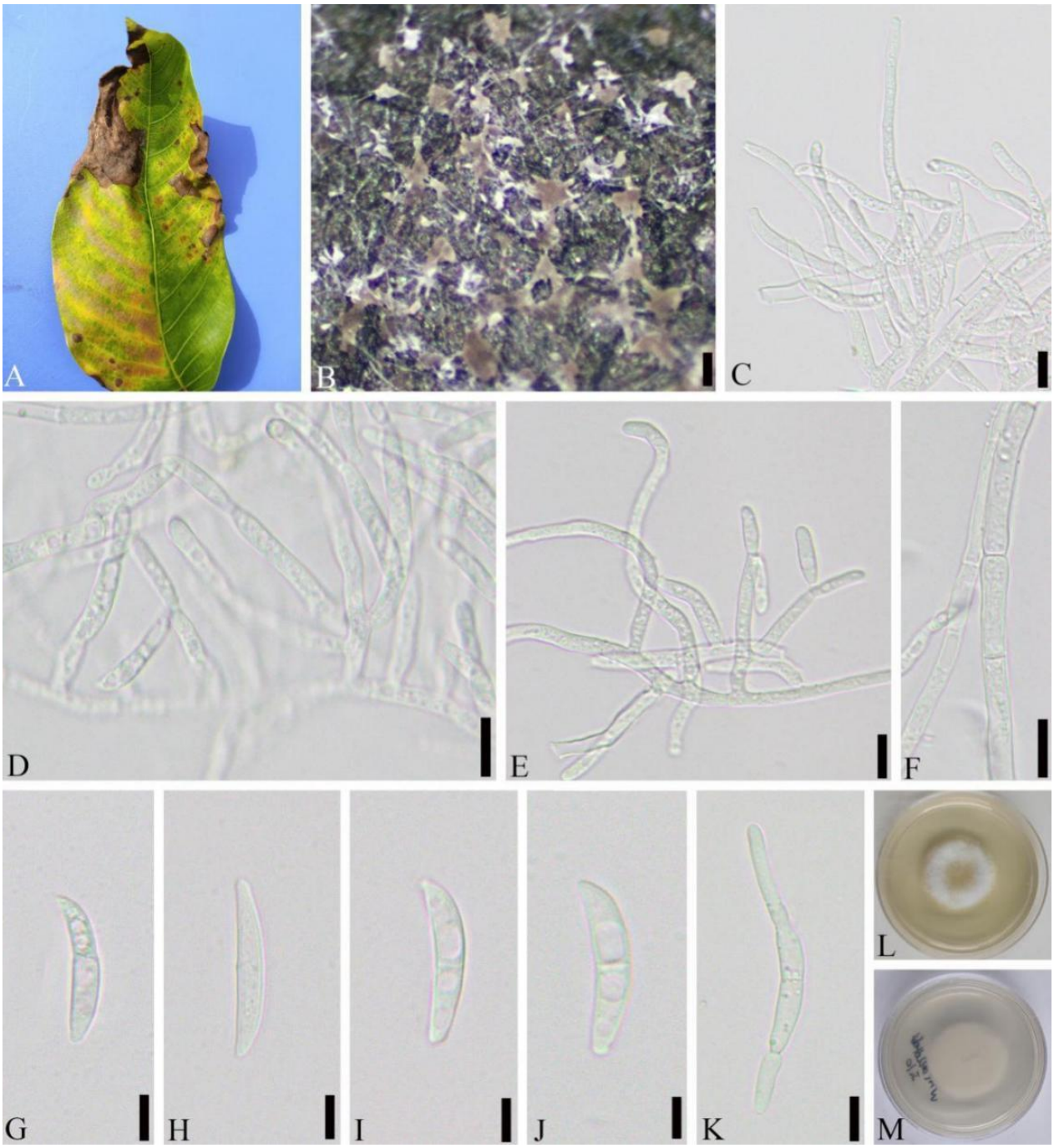


Figure 120 – *Fusarium coffeatum* (SICAU 22-0133). A, B Appearance of conidium in host substrate. C–E Conidia attached to conidiophores. F Hypha. G–J. Conidia. K Germinating conidium. L, M Colonies on PDA (L from above, M from below). Scale bars: B = 500 μm, C–E = 20 μm, F = 10 μm, G–K = 5 μm.

76. *Fusarium graminearum* Schwabe, Flora Anhalt 2: 285 (1839) Fig. 121

Index Fungorum number: IF200256; Facesoffungi number: FoF16309

Saprobic on branch of *Juglans regia*. Sexual morph: *Stromata* aggregation on the host surface, forming clusters, black and carbonaceous. *Ascomata* 200–270 × 170–230 μm ($\bar{x}$ = 240 × 200 μm, n = 10), superficial on host substrate, single or gregarious, sometimes confluent, globose, black, ostiolate, papillate. *Peridium* 28–80 μm ($\bar{x}$ = 58μm, n = 20) wide, comprising an outer indigo blue layer, composed of 4–9 layers of thin-walled cells of *textura angularis*, inner layers, hyaline, thick-walled, several cell layers of *textura angularis*. *Asci* 60–74 × 8–12 μm ($\bar{x}$ = 66 × 10 μm, n = 20), unitunicate, simple pedicel, broad fusiform to oblong. *Ascospores* 18–24 × 3–6 μm ($\bar{x}$ = 20 × 4.5 μm,

n = 50), biseriate, partially overlapping, hyaline, oval, 1–3-septate, constricted at the median septum, slightly constricted at the septa, straight or slightly curved towards the apex, thin-walled, with a minute guttule in each cell, smooth-walled. Asexual morph: Not observed.

Culture characteristics – Ascospores germinating on sterile water within 12 h and germ tubes produced from both ends. Colonies on PDA reaching 60 mm diam., after 7 days at 25 ℃. The mycelium grows on the surface of the medium, colony fat, medium, filamentous, felted to velvety, rhizoid, colony from above; raised, dull, surface orchid bronzing in the center, with abundant aerial mycelium, margin entire. Reverse, be similar. Red pigmentation develops within the culture medium.

Material examined – China, Sichuan Province, Panzhihua City, Renhe District, Ala Township (26°16′22.57″N 101°38′51.39″E, alt. 1686 m), on branch of *Juglans regia*, 24 August 2021, F.-H. Wang, WFH202108008 (SICAU 22-0134), living culture SICAUCC 22-0136.

GenBank numbers – SICAUCC 22-0136: OP963836 (ITS), OP964575 (LSU), OQ281346 (*rpb*2), OQ281374 (*tef*1-α), OQ281415 (*tub*2).

Note – Based on the phylogenetic analysis our strain *Fusarium graminearum* (SICAUCC 22-0136) clustered with the strain of *F. graminearum* (LC13775), which was recorded from USA on *Celtis australis*. Nucleotide comparisons of ITS, LSU, *tub*2, *tef*1-α, and *rpb*2 *F. graminearum* (SICAUCC 22-0136) also showed a high homology with the sequences of *F. graminearum* (LC13775), with a similarity of 99.8% (543/544, 0 gap), 100% (806/806, 0 gap), 99.7% (303/304, 0 gap), 100% (644/644, 0 gap), and 100% (903/903, 0 gap), respectively. Our collection is morphologically identical to *F. graminearum* (Crous et al. 2021). Based on morphological characters and phylogenetic analyses, we determine our specimens as *F. graminearum*.

77. *Fusarium incarnatum* (Desm.) Sacc., Syll. fung. (Abellini) 4: 712 (1886) Fig. 122

Index Fungorum number: IF231142; Facesoffungi number: FoF16310

Saprobic on branch of *Juglans regia*. Sexual morph: Not observed. Asexual morph: *Conidiophores* 13–40 × 3–5 μm ($\bar{x}$ = 27 × 3.5 μm, n = 20), initially occurring as lateral phialides on somatic hyphae, branch, become monochasial to verticillate, hyaline. *Conidiogenous cells* 9–22 × 2–4 μm ($\bar{x}$ = 14 × 3 μm, n = 20), monophialidic, cylindrical to subulate, hyaline. *Microconidia* absent or sparse, when present, ellipsoidal to allantoid, hyaline. *Macroconidia* 18–37 × 3–6 μm ($\bar{x}$ = 28 × 4.5 μm, n = 40), subcylindrical to curved, 1–4-septate, apical cell conical or hooked, basal cell poorly to well-developed, foot-shaped, hyaline. *Chlamydospores* not observed.

Culture characteristics – Conidia germinating on sterile water within 8 h and germ tubes produced from both ends. Colonies on PDA reaching 60 mm diam., after 14 days at 25 ℃. The mycelium grows on the surface of the medium, circular, with effuse surface, edge entire, aerial mycelium dense. Reverse, initially yellowish white, becoming brown to sepia with age. Not produced pigmentation on PDA media.

Material examined – China, Sichuan Province, Suining City, Shehong City, Guangxing Town (30°57′22.67″N 105°18′54.85″E, alt. 403 m), on branch of *Juglans regia*, 17 May 2021, F.-H. Wang, WFH202105013 (SICAU 22-0135), living culture SICAUCC 22-0137.

GenBank numbers – SICAUCC 22-0137: PP563701 (ITS), OQ281347 (*rpb*2), OQ281375 (*tef*1-α).

Note – Multi-gene phylogenetic analysis incorporating sequence data from the ITS, *rpb*2, and *tef*1-α genes (Fig. 119), revealed that our collection clustered with reference specimens of *Fusarium incarnatum* (CBS 132.73) with strong statistical support (100% MLBS/1.00 BYPP) (Vu et al. 2018), Furthermore, our collection exhibited nearly identical sequences in the ITS, *tef*1-α and *rpb*2 genes compared to other specimens. Nucleotide comparisons of ITS, *tef*1-α, and *rpb*2 (SICAUCC 22-0136) also showed a high homology with the sequences of *F. incarnatum* (CBS 132.73), with a similarity of 98.9% (574/1146, 0 gap), 100% (262/262, 0 gap), and 99.8% (839/1110, 0 gap), respectively. Characters of the ex-type strain such as conidiophores, microconidia and macroconidia were reported in Xia et al. (2019) and were similar to our collection. Based on morphological characters and phylogenetic analyses, we determine our specimens as *F. incarnatum*.

78. ***Fusarium lateritium*** Nees, Syst. Pilze (Würzburg): 31 (1816) Fig. 123

Index Fungorum number: IF225937; Facesoffungi number: FoF02453

Associated with rot disease on the green husks of the fruits of *Juglans regia*. Symptom on fruits is water-soaked areas which develop into velvety, green to olive-brown lesions. Sexual morph: Not observed. Asexual morph: Hyphomycetous. *Colonies* white, scattered. Mycelium superficial, comprising hyaline, septate, smooth hyphae. *Conidiophores* 17–36 × 2.5–5.5 μm ($\bar{x}$ = 26 × 3 μm, n = 20), hyaline, branched, sometimes verticillate, septate. *Conidiogenous cells* 10–23 × 2–5 μm ($\bar{x}$ = 18 × 3 μm, n = 20), at the apex, integrated, lateral or terminal, occurring singly, cylindrical or subcylindrical, tapering towards the apex, straight or slightly curved, hyaline, smooth-walled. *Microconidia* not observed. *Macroconidia* 14–49 × 3–7 μm ($\bar{x}$ = 36 × 5 μm, n = 40), falcate, straight to curved, 2–5-septate, apical cell blunt to hooked; basal cell poorly to well-developed, foot-shaped. *Chlamydospores* not observed.

Culture characteristics – Conidia germinating on sterile water within 12 h and germ tubes produced from both ends. Colonies on PDA reaching 60 mm diam., after 13 days at 25 ℃. The mycelium grows on the surface of the medium, circular, edge entire, flat or effuse, aerial, medium sparse, light gray from above. light yellow from below. Not produced pigmentation on PDA media.

Material examined – China, Sichuan Province, Bazhong City, Nanjiang County, Gongshan Town (32°18′36.89″N 106°52′22.73″E, alt. 1013 m), on green husks of *Juglans regia*, 29 June 2021, F.-H. Wang, WFH202206014 (SICAU 22-0136), living culture SICAUCC 22-0138.

GenBank numbers – SICAUCC 22-0138: OP963837 (ITS), OP964576 (LSU), OQ281348 (*rpb*2), OQ281376 (*tef*1-α), OQ281416 (*tub*2).

Note – Our isolate *Fusarium lateritium* (SICAUCC 22-0138), clusters within *F. lateritium* with strong statistical support (99% MLBS/1.00 BYPP) (Fig. 119). The nucleotide sequence was nearly identical to others in the LSU region (with only 1–2 nucleotide differences), as well as in the ITS, *tef*1-α, *tub*2, and *rpb*2 gene sequences. Nucleotide comparisons of ITS, *tef*1-α, *tub*2, and *rpb*2 (SICAUCC 22-0136) also showed a high homology with the sequences of *F. graminearum* (LC13775), with a similarity of 100% (540/541, 0 gap), 99.9% (643/651, 0 gap), 100% (582/585, 0 gap), and 100% (859/945, 0 gap), respectively. Our strains are similar to *F. lateritium* in having hyaline, branched, sometimes verticillate, septate conidiophores, falcate, straight to curved. Macroconidia and the macroconidia size of our isolates is slight differences to *F. lateritium* (Pfenning et al. 2019). Based on morphological characters and phylogenetic analyses, we determine our specimens as *F. lateritium*.

Microcera Desm., Annls Sci. Nat., Bot., sér. 3 10: 359 (1848).

Wollenweber & Reinking (1935) transferred *Microcera* species to *Fusarium* and, this classification was followed by subsequent authors (Booth 1971, Gerlach & Nirenberg 1982, Nelson et al. 1983, Snyder & Hansen 1945, Leslie et al. 2006). Gräfenhan et al. (2011) revived the genus based on phylogenetic analysis which confirmed the generic concept of *Microcera*.

79. ***Microcera chrysomphali*** Feng Liu & C.L. Yang [as '*chrysomphaludis*'], MycoKeys 98: 27 (2023)

Fig. 124

Index Fungorum number: IF663022; Facesoffungi number: FoF16311

Associated with trunk rot on the trunk of *Juglans regia*. A large number of red fruiting bodies grow on the branches and stems of the plant, affecting its growth. Sexual morph: *Ascomata* 210–420 × 170–370 μm ($\bar{x}$ = 315 × 270 μm, n = 20), scattered, gregarious, formed directly on margin of host scales, bright red to dark red, subglobose, ellipsoidal in section, a central, rounded, papillate ostiole, lined internally with periphyses. *Peridium* 50–86 μm ($\bar{x}$ = 60μm, n = 20) wide, comprising two layers, outer stratum 27–46 μm thick, composed of small, hyaline to light brown cells of *textura angularis*; inner stratum 30–45 μm thick, composed of thinner, orange cells of *textura angularis*; thicker at the sides towards apex, thinner at the base. paraphyses 92–145 × 3–8 μm ($\bar{x}$ = 128 × 6 μm, n = 20), numerous, septate, unbranched. *Asci* 80–130 × 9–18 μm ($\bar{x}$ = 112 × 14 μm, n = 20), 8-spored,

bitunicate, cylindrical, straight, or curved, rounded at apex. *Ascospores* 15–22 × 6–10 µm ($\bar{x}$ = 17 × 8 µm, n = 40), uni-seriate, elliptical, with rounded ends, one-septate, slightly constricted at septum, hyaline, smooth-walled, with many guttules. Asexual morph: Not observed.

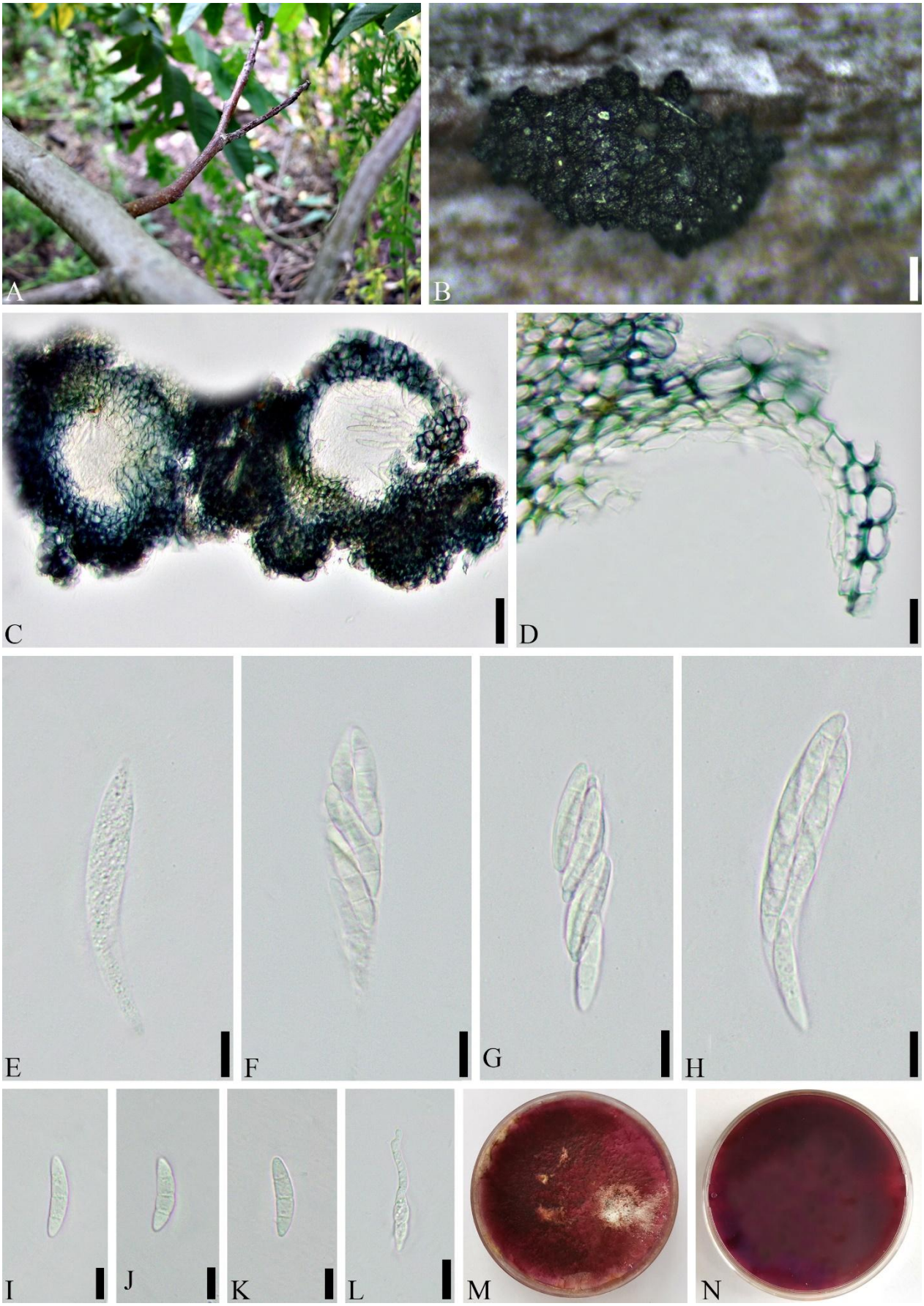


Figure 121 – *Fusarium graminearum* (SICAU 22-0134). A, B Appearance of ascostroma in host substrate. C Vertical section of ascoma. D Peridium. E–H Asci. I–K Ascospores. L Germinating ascospore. M, N Colonies on PDA (M from above, N from below). Scale bars: B = 500 μm, C = 50 μm, D, L = 20 μm, E–K = 10 μm.

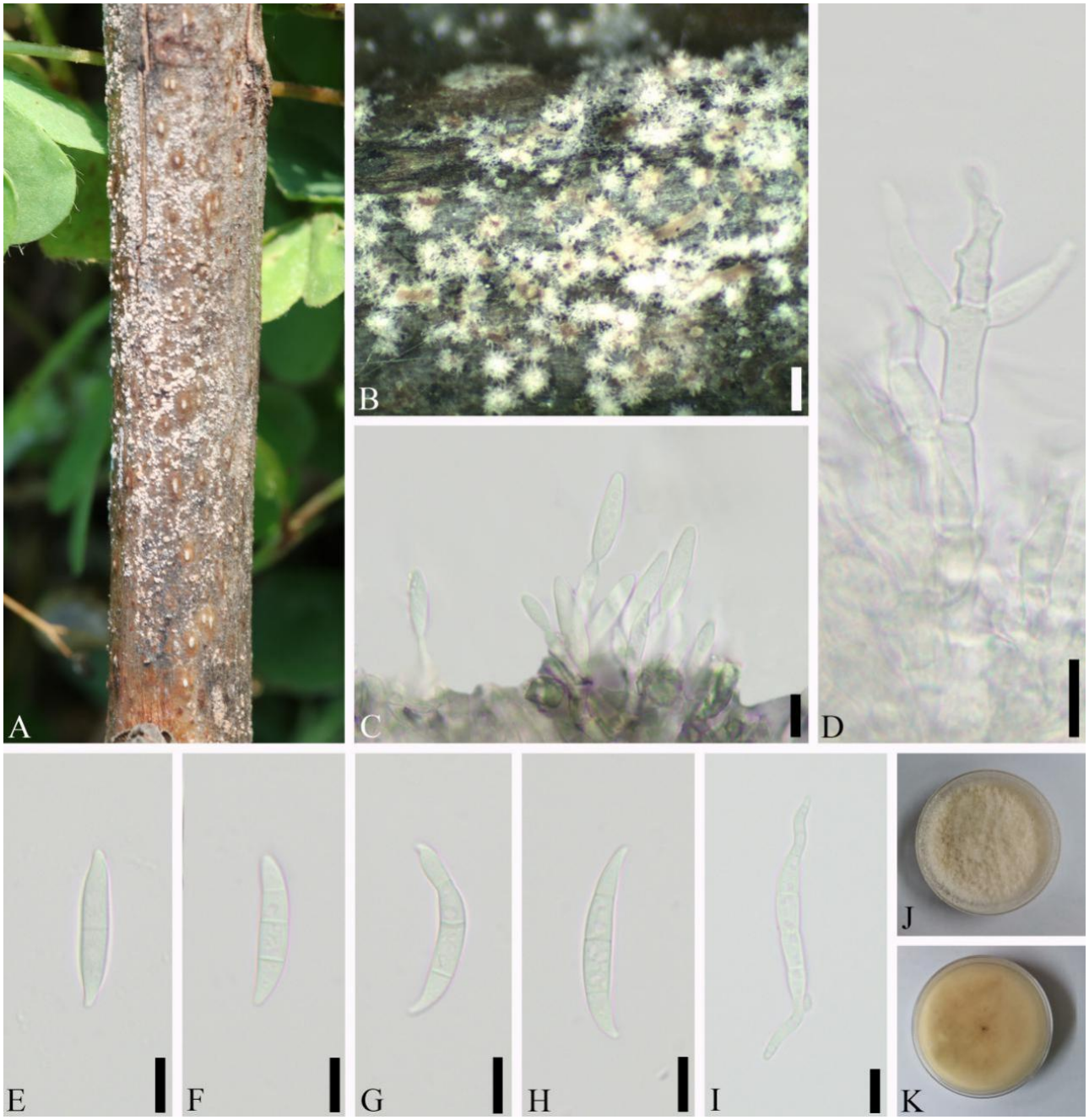


Figure 122 – *Fusarium incarnatum* (SICAU 22-0135). A, B Appearance of conidium in host substrate. C–D Conidia attached to conidiophores. E-H Conidia. I Germinating macroconidium. J, K Colonies on PDA (J from above, K from below). Scale bars: B = 1000 μm, C = 20 μm, D–I = 10 μm.

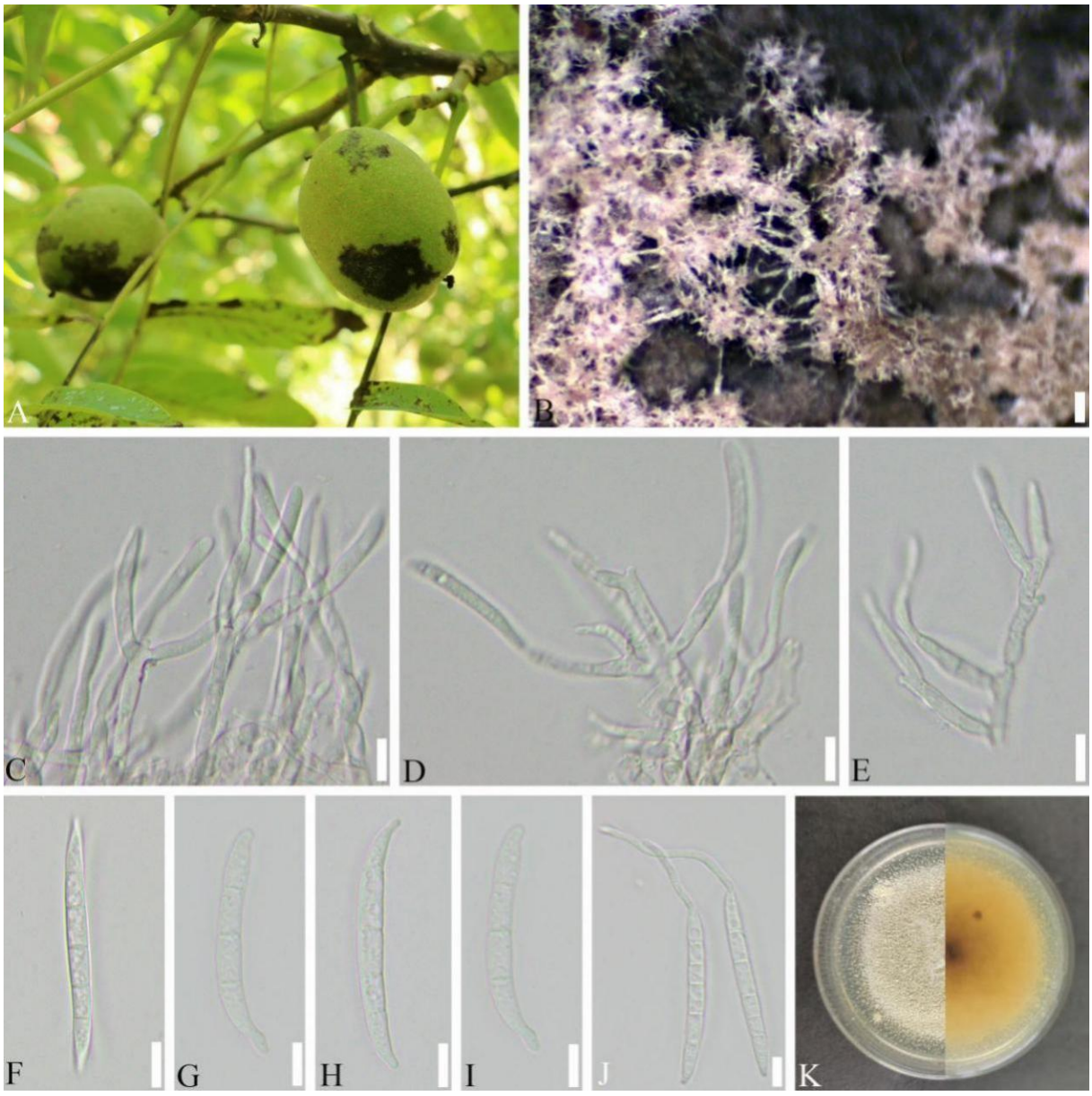


Figure 123 – *Fusarium lateritium* (SICAU 22-0136). A, B Appearance of conidium in host substrate. C–E Conidia attached to conidiophores. F–I Conidia. J Germinating macroconidia. K Colonies on PDA. Scale bars: B = 200 μm, C–E = 20 μm, F–J = 5 μm.

Culture characteristics – Conidia germinating on sterile water within 24 h and germ tubes produced from both ends. Colonies on PDA reaching 20 mm diam., after 28 days at 25 ℃. The mycelium grows on the surface of the medium, cottony and hard, with regular margin, the mycelium is creamy white to pale pink, with concentric rings; and the back of colonies is pale yellow. Not produced pigmentation on PDA media.

Material examined – China, Sichuan Province, Liangshan Yi Autonomous Prefecture Huili City (26°56′43.49″N 102°16′26.76″E, alt. 2008 m), on trunk of *Juglans regia*, 30 September 2022, F.-H. Wang, WFH202209018 (SICAU 23-0094), living culture SICAUCC 23-0073.

GenBank numbers – SICAUCC 23-0073: PP060689 (ITS), PP057972 (LSU).

Note – Our new isolate *Microcera chrysomphaludis* (SICAUCC 23-0073) clustered with isolates *M. chrysomphaludis* (SICAUCC 22-0164 and SICAUCC 22-0165) with strong statistical support (100% MLBS/1.00 BYPP) (Fig. 125). The new specimen is similar to *M. chrysomphaludis* in having 8-spored, bitunicate, cylindrical, straight, or curved, rounded at apex asci, and elliptical, with rounded ends, one-septate, slightly constricted at septum, hyaline, smooth-walled, with many

guttules ascospores (Liu et al. 2023b). However, the size of ascospores between these two specimens are different, perhaps because the asci of *M. chrysomphaludis* by Liu et al. (2023a) are immature and deformed. In addition, each gene region between our new collection and *M. chrysomphaludis* was compared based on the recommendations from Jeewon & Hyde (2016), and the results showed that there is no difference in LSU and ITS. Therefore, this new specimen is identified as *M. chrysomphaludis*.

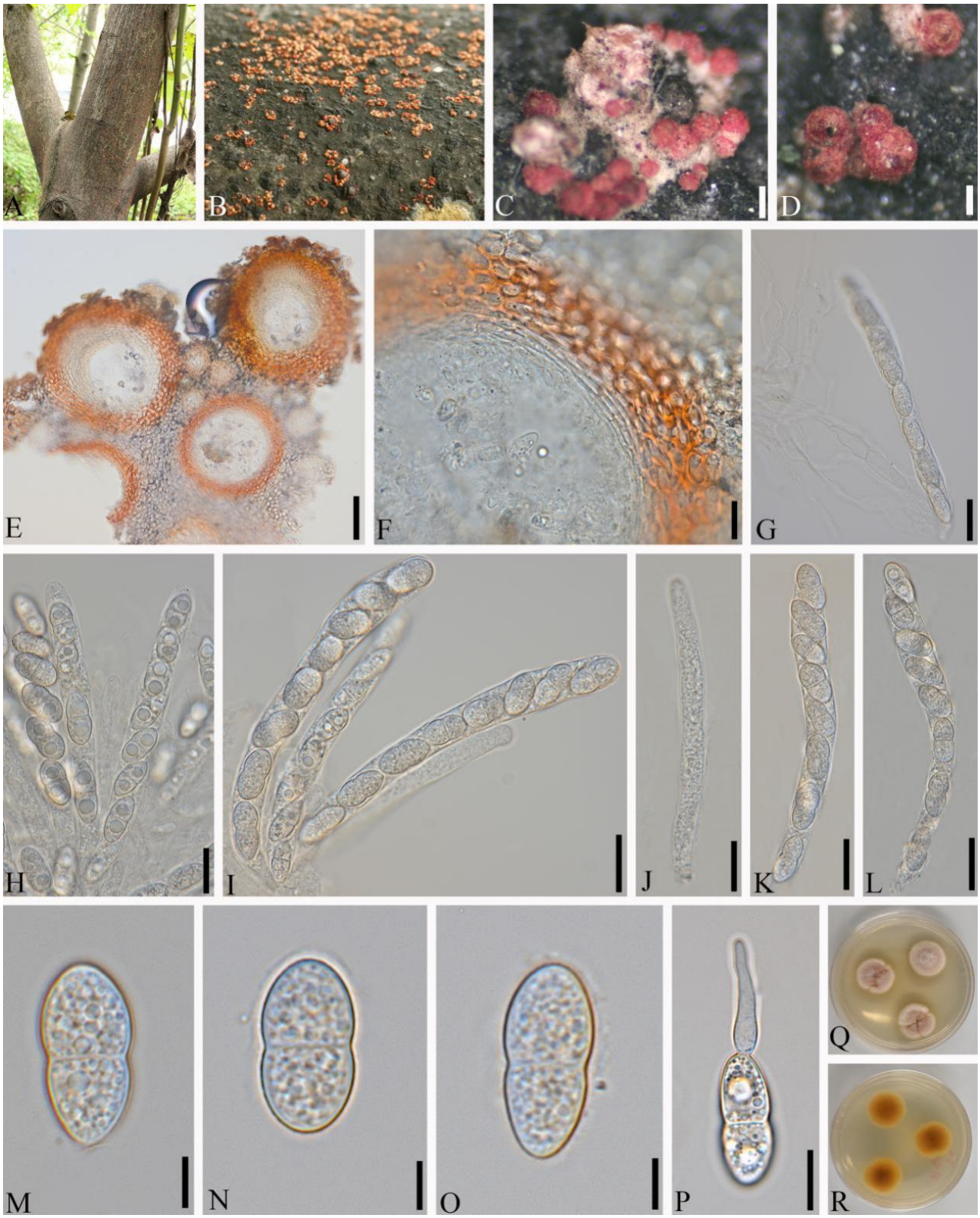


Figure 124 – *Microcera chrysomphali* (SICAU 23-0094). A habitat. B-D Ascomata on host substrate. E Vertical section through ascostromata. F Peridium. G Paraphyses and asci. H–L Asci. M–O Ascospores. P Germinating ascospore. Q, R Colonies on PDA (Q from above, R from below). Scale bars: C = 500 µm, D = 200 µm, E = 100 µm, F–L = 20 µm, P = 10 µm, M–O = 5 µm.

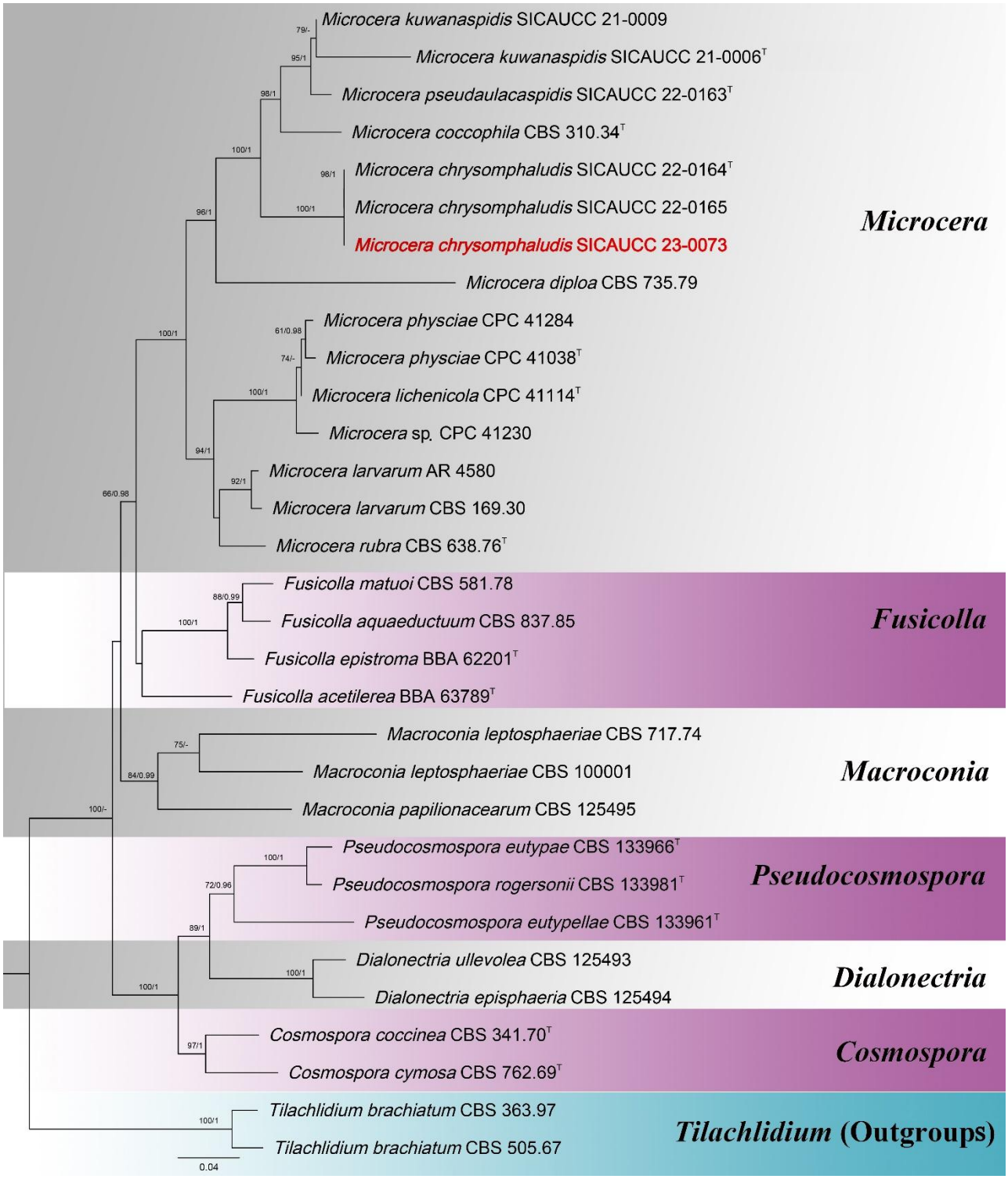


Figure 125 – The best scoring RAxML tree with a final likelihood value of -14,149.212917 of ITS, LSU and *tef*1-α sequence data. The topology and clade stability of the combined gene analyses was compared to the single gene analyses. Thirty-one strains were included in the combined genes sequence analyses which comprised 2,636 characters (690 characters for ITS, 886 characters for LSU and 1,059 characters for *tub*2, including gap regions). Thistree includes selected taxa of *Hypocreales* and rooted with *Tilachlidium brachiatum* (CBS 363.97 and CBS 505.67) in *Tilachlidiaceae*. The

matrix had 985 distinct alignment patterns, with 33.90% of undetermined characters and gaps. Estimated base frequencies were as follows; A = 0.235151, C = 0.260546, G = 0.268634, T = 0.235669; substitution rates AC = 1.117799, AG = 1.947174, AT = 1.494688, CG = 0.918677, CT = 5.122880, GT = 1.000000; gamma distribution shape parameter α = 0.251959. In our analyses, GTR+I+G model was used for each partition in Bayesian posterior analyses. The species determined in this study is indicated in red and bold. Bootstrap support values for maximum likelihood (MLBS, left) ⩾ 60% and Bayesian posterior probabilities (BYPP, right) ⩾ 0.90 are indicated at the nodes, respectively. Hyphens (-) represent support values less than 60% MLBS/0.90 BYPP. The ex-type superscript "T".

Nectria (Fr.) Fr., Summa veg. Scand., Sectio Post. (Stock holm): 387 (1849).

Members of the *Nectria* (Fr.) Fr. (*Hypocreales*, *Nectriaceae*) are typically weak parasites of woody plants and occur on hardwood trees and shrubs throughout the temperate zone of the northern hemisphere (Samuels et al. 2009, Hirooka et al. 2011). Historically, the genus *Nectria* was a repository for all uniloculate, bright-colored, perithecial fungi. For many years, the taxonomic concept of *Nectria* was extremely broad, there are about 814 *Nectria* epithets listed in Species Fungorum (http://www.speciesfungorum.org/Index.htm, September 2024), but only a few species have available sequence data in Gen Bank.

80. ***Nectria fusiformispora*** F.H. Wang & C.L. Yang, sp. nov. Figs 126, 127

Index Fungorum number: IF901578; Facesoffungi number: FoF15595

Etymology – In reference to the fusiform ascospores

Holotype – SICAU 23-0095

Saprobic on dead branch of *Juglans regia*. Sexual morph: *Ascomata* and synnemata occurring on same or distinct stroma. *Mycelium* not observed. *Stromata* up to 500 mm high, well-developed, erumpent through epidermis, orange to bay, composed of pseudoparenchymatous, cells of *textura angularis* to *textura prismatica*. *Ascomata* 190–394 × 211–420 μm ($\bar{x}$ = 270 × 294 μm; n = 20), superficial on *stromata*, caespitose or solitary, globose, papillate, cupulate upon drying, red, with darker apical region. *Peridium* cells forming *textura globulosa* or *textura angularis* in face view; 40–72 μm ($\bar{x}$ = 54μm, n = 20) wide in vertical section, of two strata: outer stratum 25–52 μm ($\bar{x}$ = 34μm, n = 20) wide, comprising pigmented cells forming *textura globulosa* or *textura angularis*, intergrading with stroma; inner stratum 10–20 μm thick, of elongated, thin-walled, hyaline cells, forming *textura prismatica*, intergrading with stroma. *Paraphyses* ellipsoid and cellular, or cylindrical and filamentous, unbranched, septate, guttulate. *Asci* 70–114 × 11–20 μm ($\bar{x}$ = 88 × 16 μm, n = 30), 6–8-spored, unitunicate, clavate, with inconspicuous ring at apex. *Ascospores* 17–33 × 8.3–17.4 μm, ($\bar{x}$ = 23–8 μm, n = 40), muriform, with 4–7 transverse septa and 0–1 longitudinal septum, constricted at each septum, ellipsoidal to fusiform, straight, occasionally slightly curved, hyaline, smooth-walled. Asexual morph: *Conidiomata* 400–700 × 40–75 μm ($\bar{x}$ = 560 × 60 μm, n = 20), sporodochial, white to whitish yellow. *Conidiophores* verticillately branched, septate, hyaline, smooth-walled. *Conidiogenous cells* 14–20 × 1–2 μm ($\bar{x}$ = 17 × 1.5 μm, n = 20), monophialidic, cylindrical, slightly tapering toward tip or narrowly flask-shaped with widest point in middle, with a visible periclinal thickening, collarette inconspicuous, hyaline, smooth-walled. *Conidia* 4–7 × 1.5–3 μm ($\bar{x}$ = 5 × 2.2 μm, n = 40) formed abundantly on slimy heads, ellipsoidal, oblong to cylindrical, aseptate, straight, with round at both ends, hyaline, smooth walled, contains granular objects. *Chlamydospores* not produced.

Culture characteristics – Ascospores germinate within 24 h in sterile water, and each cell is capable of producing germ tubes. Colonies on PDA reaching 60 mm diam., after 20 days at 25 ℃. The mycelium grows on the surface of the medium, circular, surface slightly cottony with aerial mycelium, radial or sometimes wavy, white to whitish yellow. Reverse, white to slightly whitish yellow, sporulated after 20 days. Not produced pigmentation on PDA media.

Material examined – China, Sichuan Province, Liangshan Yi Autonomous Prefecture, Huili City (26°56′43.53″N 102°16′26.46″E, alt. 2007 m), on branch of *Juglans regia*, 24 August 2022, F.-

H. Wang, WFH202208004 (SICAU 23-0095, holotype), ex-type living culture SICAUCC 23-0074. *Ibid.*, WFH202208004B (SICAU 23-0096), living culture SICAUCC 23-0075.

GenBank numbers – SICAUCC 23-0074: PP060690 (ITS), PP057973 (LSU), PP061154 (*tef*1-α); SICAUCC 23-0075: PP060691 (ITS), PP057974 (LSU), PP061155 (*tef*1-α).

Note – Our new collection *Nectria fusiformispora* (SICAUCC 23-0074 and SICAUCC 23-0075) clades sister to the ex-type of *N. pseudotrichia* (CBS 551.84) with strong statistical support (99% MLBS/1.00 BYPP) (Fig. 128). However, nucleotide sequence comparisons reveal specific differences between *N. fusiformispora* (SICAUCC 23-0074) and its related species. Specifically, the sequence divergences between *N. fusiformispora* (SICAUCC 23-0074) and *N. pseudotrichia* (CBS 551.84), viz. 2.27% (12/529, 8 gaps), 0.65% (5/764, 0 gap), and 3.03% (9/297, 2 gaps) in the ITS, LSU and *tef*1-α, respectively. The PHI test revealed no significant recombination event between our strain and the closely related taxa (Φw = 0.69) (Fig. 130). Compared to *N. pseudotrichia*, the morphology of ascospore was different (Hirooka et al. 2012). We therefore introduce *N. fusiformispora* as a new species.

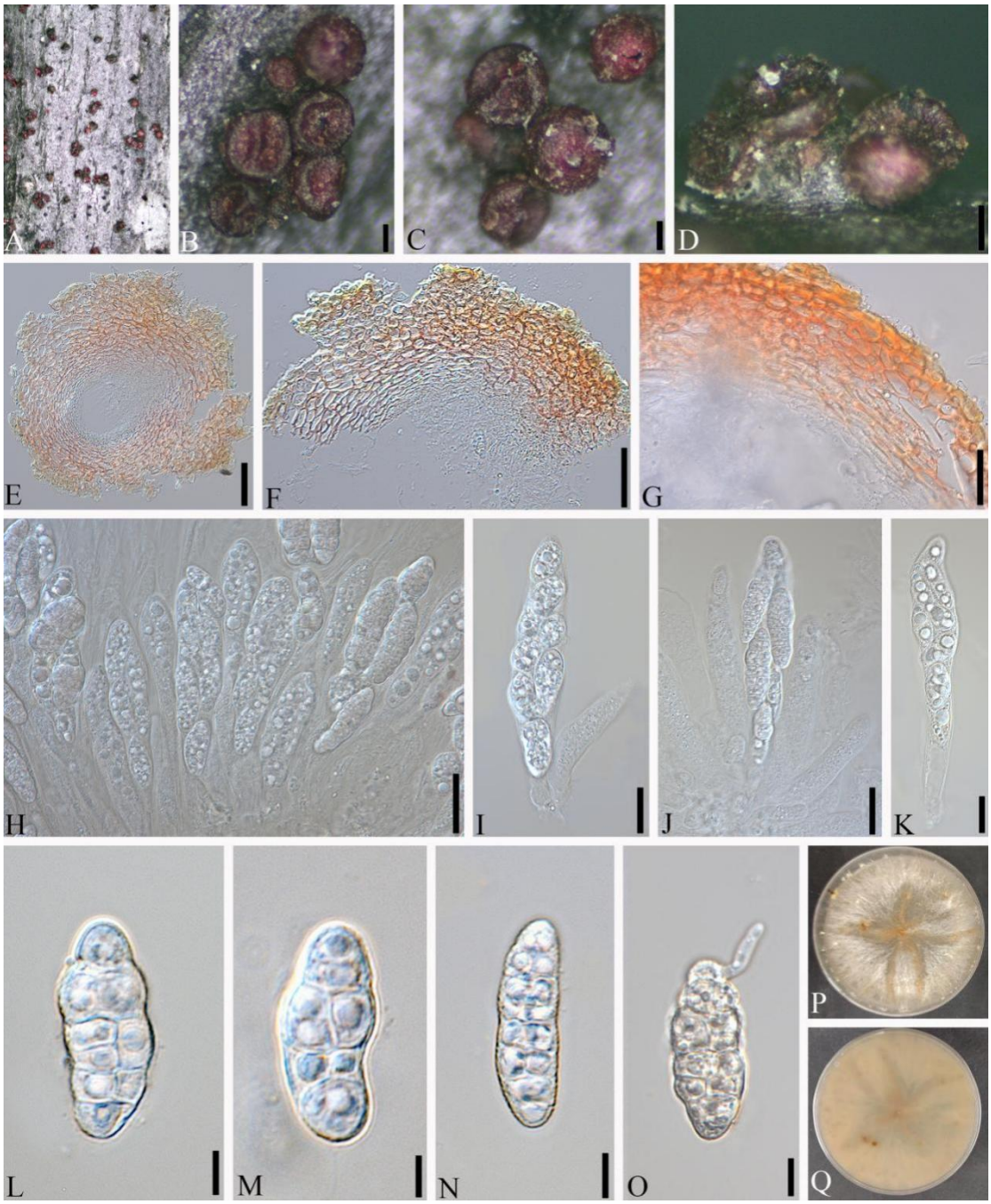


Figure 126 – Sexual morph of *Nectria fusiformispora* (SICAU 23-0095, holotype). A-D Appearance of ascostroma in host substrate. E Vertical sections of ascomata. H Asci and paraphyses. I–K Asci. L–N Ascospores. O Germinating ascospore. P, Q Colonies on PDA (P from above, Q from below). Scale bars: B–D = 200 μm, E = 100 μm, F, G = 50 μm, H–K = 20 μm, L–O = 5 μm.

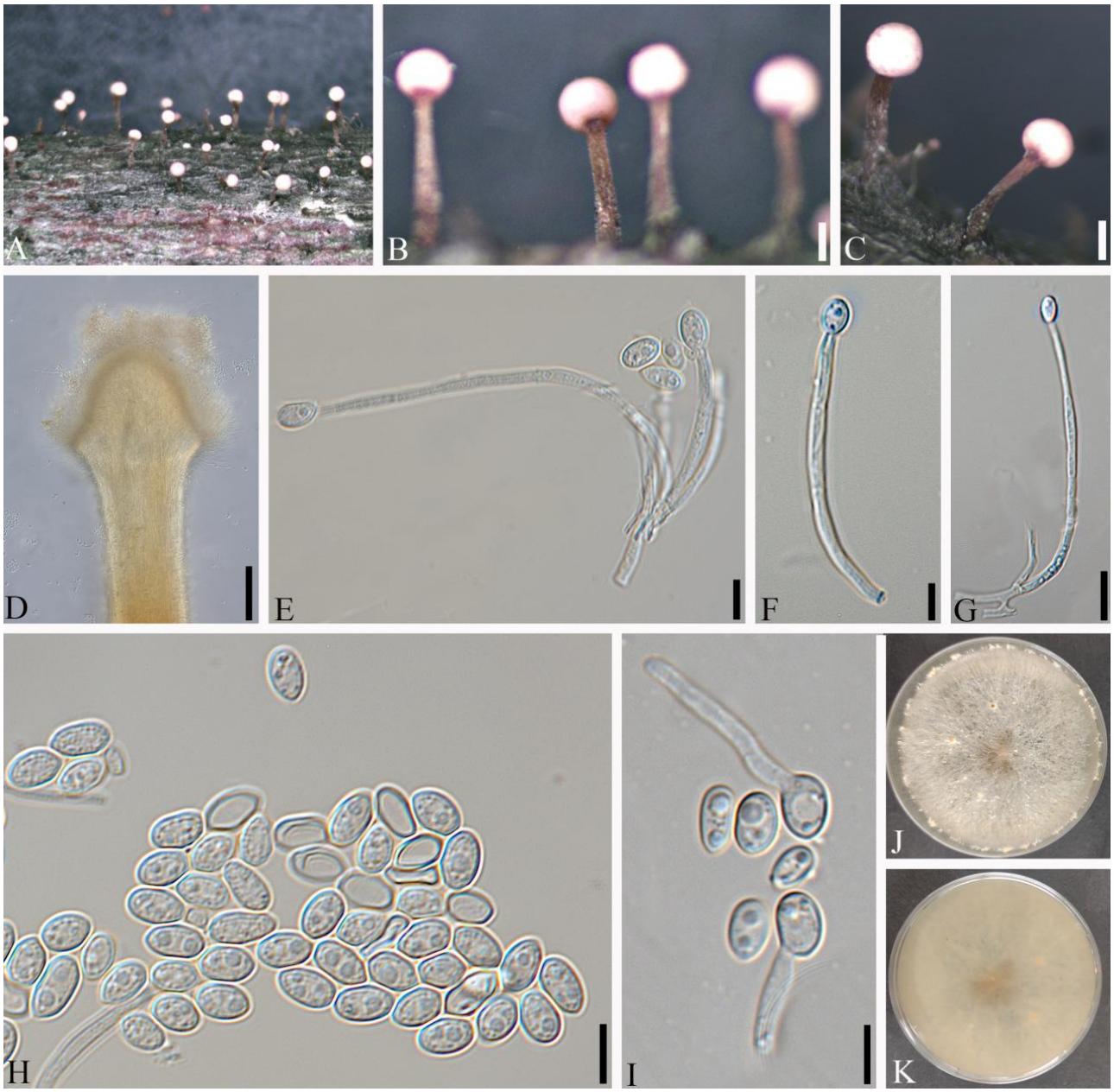


Figure 127 – Asexual morph of *Nectria fusiformispora* (SICAU 23-0096, holotype). A–C Synnemata on host substrate. D Median section of synnema. E–G Conidiophores and conidiogenous cells. H Conidia I Germinating conidia. J, K Colonies on PDA (J from above, K from below). Scale bars: B, C = 100 μm, D = 50 μm, G = 10 μm, E, F = 8 μm, H, I = 5 μm.

81. ***Nectria pseudotrichia*** Berk. & M.A. Curtis, N.S. 2(6): 289 (1854) Fig. 128

Index Fungorum number: IF206961; Facesoffungi number: FoF13447

Saprobic on dead branch of *Juglans regia.* Sexual morph: Not observed. Asexual morph: *Synnemata* 740–1850 × 160–278 μm ($\bar{x}$ = 1250 × 218 μm; n = 20), usually erumpent through epidermis, solitary or gregarious, crowded to caespitose, cylindrical-capitate, subulate-capitate, or claviform, erect or nodding, occasionally branch, medium to slender, soft- textured when fresh, red-brown at base, toward base becoming almost black with age. *Ornamental cells* 5–17 × 1–2.5 μm ($\bar{x}$

= 11 × 1.5 μm; n = 20), cylindrical, straight, curved, sinuous or twisted, arising laterally at more or less right angles, distributed evenly over surface of synnemata or concentrated near base or apex, usually unbranched but occasionally 2-3 branched, aseptate. *Conidiophores* with sterile hyphae, branching monoverticillate or biverticillate. *Conidiogenous cells* 14–34 × 1–2.2 μm ($\bar{x}$ = 26 × 1.6 μm; n = 20), enteroblastic, monophialidic, cylindrical to subulate, straight or curved in terminal whorls with sterile hyphae or lateral and terminal, collarette not conspicuous. Sterile hyphae 14–32 × 1–2 μm ($\bar{x}$ = 24 × 1.4 μm; n = 20), mixed with phialides, acicular, straight, or usually curved, unbranched or dichotomously branched, arising from hyphae, often in groups of 1–4, from *conidiophores* together with phialides. *Conidia* 4.5–7.5 × 2.5–4 μm ($\bar{x}$ = 6 × 3 μm; n = 20), hyaline, ellipsoidal, obovate or oblong, sometimes slightly curved, non-septate, smooth-walled.

Culture characteristics – Conidia germinating on sterile water within 24 h and germ tubes produced from both ends. Colonies on PDA reaching 50 mm diam., after 9 days at 25 ℃. The mycelium grows on the surface of the medium, surface cottony with aerial mycelium white, sometimes faint yellow, with uniform texture, circular. Reverse, white to orange. Conidiomata produced after 30 days. Not produced pigmentation on PDA media.

Material examined – China, Sichuan Province, Garze Tibetan Autonomous Prefecture, Luding County, Kuiwu Village (29°40′32.67″N 102°11′34.53″E, alt. 1315 m), on branch of *Juglans regia*, 18 July 2021, F.-H. Wang, WFH202107012 (SICAU 22-0148), living culture SICAUCC 22-0150. *Ibid.*, WFH202107012-1 (SICAU 22-0149), living culture SICAUCC 22-0151.

GenBank numbers – SICAUCC 22-0150: OP963848 (ITS), OP964587 (LSU), OQ281357 (*rpb*2), OQ281386 (*tef*1-α), OQ190495 (*act*); SICAUCC 22-0150: OP963849 (ITS), OP964588 (LSU), OQ281358 (*rpb*2), OQ281387 (*tef*1-α), OQ190496 (*act*).

Note – The strain SICAUCC 22-0150 clustered with the ex-type strain (CBS 551.84) with 93% MLBS support (Fig. 129). Nucleotide comparisons of ITS, LSU, *rpb*2, *tef*1-α, and *act* (SICAUCC 22-0150) showed a high homology with the sequences of *Nectria pseudotrichia* (CBS 551.84), with a similarity of 99.7% (575/577, 0 gap), 100% (785/785, 0 gap), 100% (887/887, 0 gap), 100% (521/521, 0 gap), and 99.5% (413/415, 0 gap), respectively. *Nectria pseudotrichia* reported as the pathogen on twigs and branches of *Juglans regia*, *Kadsura longipedunculata*, *Ulmus pumila*. (Seifert 1985, Hirooka et al. 2012, Perera et al. 2023). *Nectria pseudotrichia* is a rather common tropical fungus in the genus *Nectria*. The isolates *N. pseudotrichia* (SICAUCC 22-0150) were shown to be *N. pseudotrichia* based on the phylogenetic analysis and their morphological traits. Hence, it is identified as *N. pseudotrichia*.

Neocosmospora E.F. Sm., Bull. U.S. Department of Agriculture 17: 45 (1899).

Species of *Neocosmospora* were previously classified as the Fusarium solani species complex (O'Donnell, 2000). Owing to the distinctive characteristics of its asexual morphs, this group was revised by Nalim et al. (2011). In terms of taxonomic treatment, this study adheres to the research findings of Crous et al. (2021), Wijayawardene et al. (2022), and Zhang et al. (2024b).

82. ***Neocosmospora solani*** (Mart.) L. Lombard & Crous, Stud. Mycol. 80: 228 (2015) Fig. 131

Index Fungorum number: IF190352; Facesoffungi number: FoF01873

Associated with leaf spots on the living leaves of *Juglans regia*. Symptoms manifest as yellowing leaves, with scorched and withered starting from the edges, ultimately leading to the complete withering and death of the leaves in later stages. Sexual morph: Not observed. Asexual morph: Mycelium 1–2.5 μm broad, branched, septate, slightly constricted at the septa, superficial, partly immersed, hyaline, verruculose. *Conidiophores* 70–136 × 2–4 μm ($\bar{x}$ = 93 × 3 μm, n = 20), micronematous, macronematous, densely branched, constricted at the septa, erect to slightly curved, up to 2–10- septate, *conidiogenous cell* 12–17 × 3–5 μm ($\bar{x}$ = 14 × 4 μm, n = 20), polyphialides, long, discrete. *Macroconidia* 37–54 × 4–8 μm ($\bar{x}$ = 45 × 5.5 μm, n = 40), hyaline, slightly curved, 3–6-septate, apical cells papillate, basal cells foot-shaped. *Microconidia* 5–12 × 2–5 μm ($\bar{x}$ = 7 × 4 μm, n = 40), subglobose, oval to truncate, aseptate, hyaline. *Chlamydospores* not observed.

Culture characteristics – Conidia germinating on sterile water within 12 h and germ tubes produced from both ends. Colonies on PDA reaching 60 mm diam., after 14 days at 25 ℃. The mycelium grows on the surface of the medium, white, radiating, to the edge, faintly zonate, margin undulate, dense, fat or umbonate, dark gray in the center of the reverse side, white radiating outwardly. Not produced pigmentation on PDA media.

Material examined – China, Sichuan Province, Neijiang City, Dongxing District, Paifang Village (29°48′30.13″N 105°6′36.48″E, alt. 387 m), on living leaf of *Juglans regia*, 27 April 2022, F.-H. Wang, WFH202204056 (SICAU 22-0138), living culture SICAUCC 22-0140.

GenBank numbers – SICAUCC 22-0140: OP963839 (ITS), OP964578 (LSU), OQ281350 (*rpb*2), OQ281378 (*tef*1-α), OQ281418 (*tub*2).



Figure 128 – *Nectria pseudotrichia* (SICAU 22-0148). A–C Synnemata on host substrate. D Median section of synnema. E Conidiophores and conidiogenous cells. F Conidia. G Germinating conidium. H Colonies on PDA. Scale bars: C = 1000 μm, D = 500 μm, G, E = 10 μm, F = 5 μm.

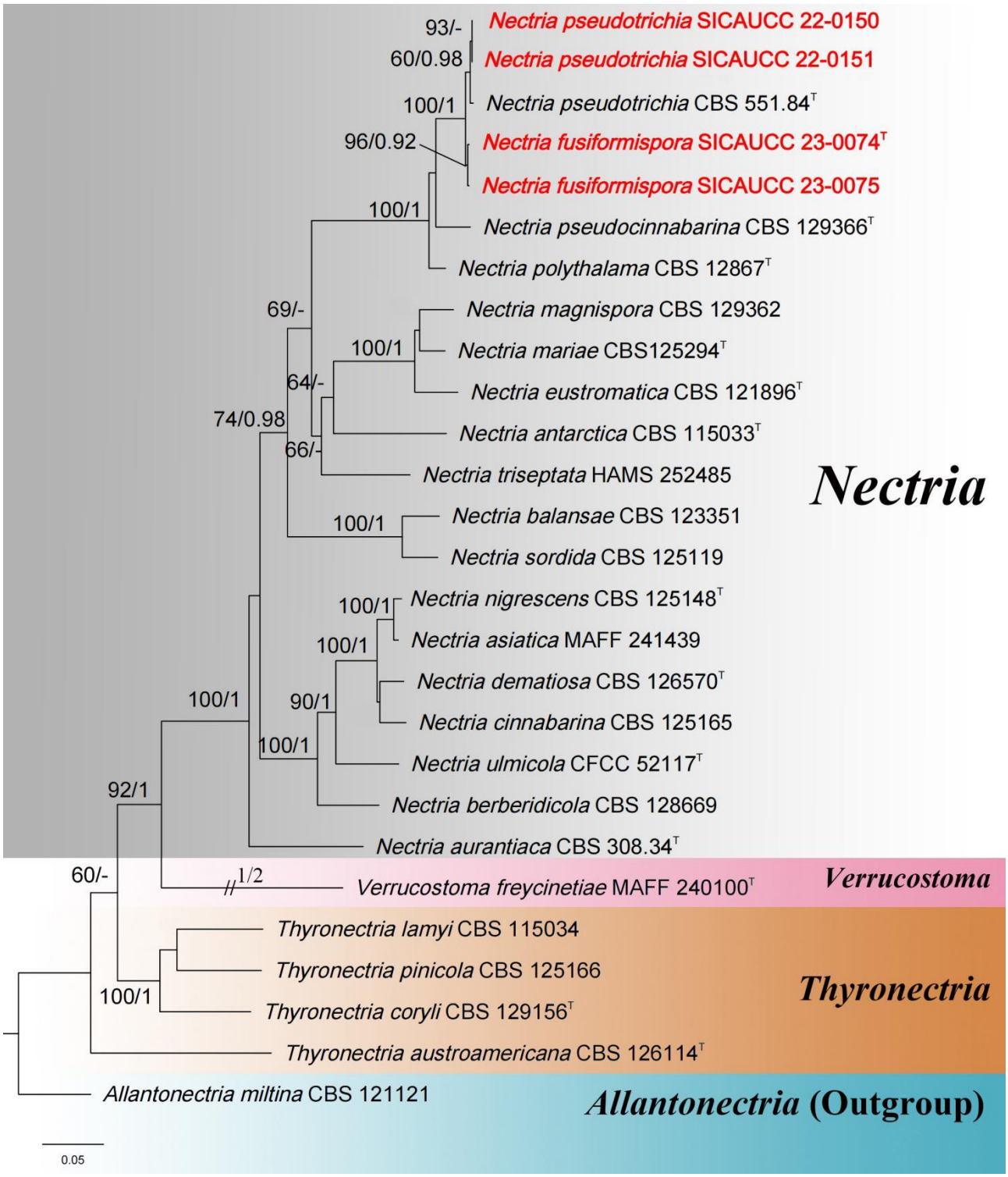


Figure 129 – Best scoring RAxML tree with a final likelihood value of -24,184.870737 based on combined ITS, *act*, LSU, *rpb*2 and *tef*1-α sequence data of related species. The tree is rooted with *Allantonectria miltina* (CBS 121121) in *Allantonectria*. Twenty-seven strains were included in the combined analyses, which comprised 4,554 characters (713 characters for ITS, 685 characters for *act*, 878 characters for LSU, 1,204 characters for *rpb*2 and 1,070 characters for *tef*1-α, including gap regions). The matrix had 1,665 distinct alignment patterns, with 29.30% of undetermined characters and gaps. Estimated base frequencies were as follows; A = 0.231221, C = 0.276176, G = 0.260054, T = 0.232550; substitution rates AC = 0.739243, AG = 2.063080, AT = 1.268091, CG = 0.797656, CT = 4.714115, GT = 1.000000; gamma distribution shape parameter α = 0.195244. In our analysis, GTR+I+G model was used for each partition in the Bayesian posterior analysis. The species

determined in this study is indicated in red and bold. Bootstrap support values for maximum likelihood (MLBS, left) ⩾ 60% and Bayesian posterior probabilities (BYPP, right) ⩾ 0.90 are indicated at the nodes, respectively. Hyphens (-) represent support values less than 60% MLBS/0.90 BYPP. The ex-type superscript "T".

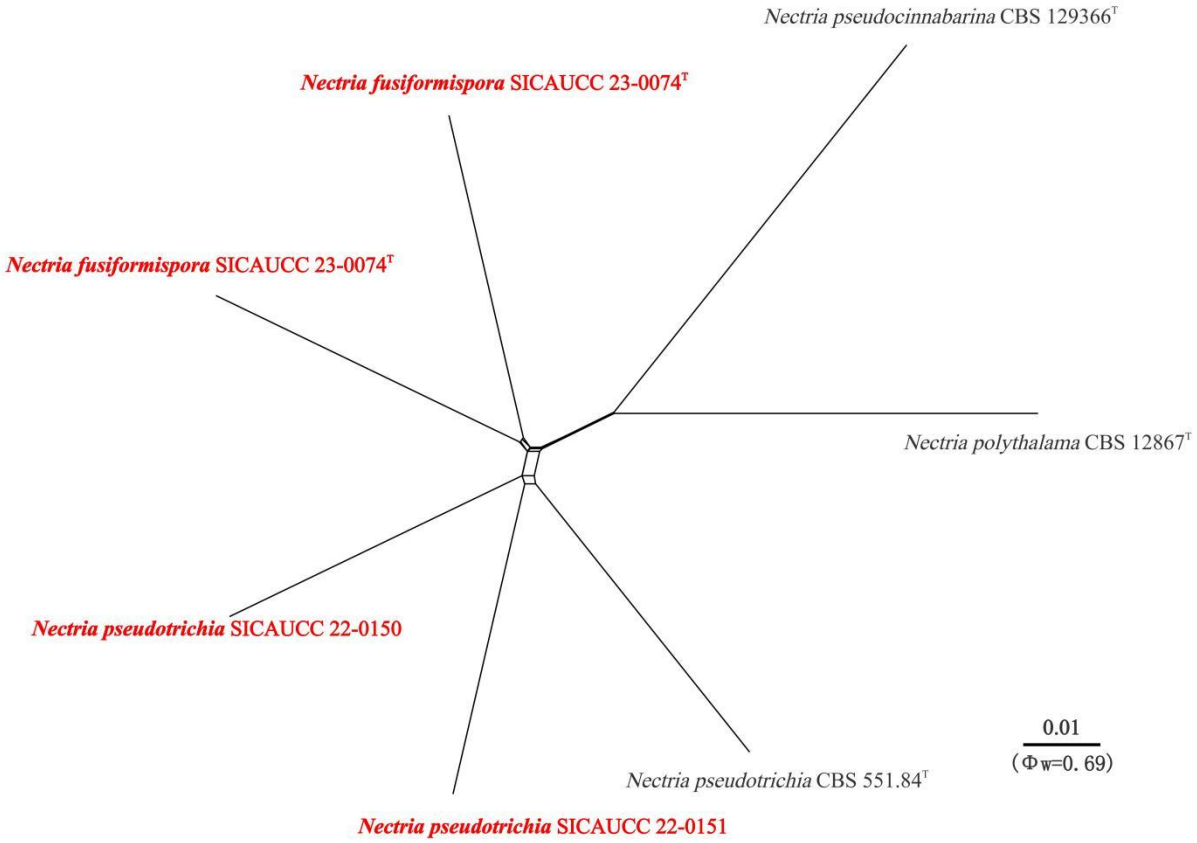


Figure 130 – Results of the PHI test of *Nectria fusiformispora* and closely related species using both LogDet transformation and splits decomposition. The PHI test did not find any statistically significant recombination (Φw = 0.69) in the dataset. The new strains are represented in red and bold. "T" represents the type strain.

Note – In our phylogenetic analyses, our strain *Neocosmospora solani* (SICAUCC 22-0140) clusters with *N. solani* (CBS 102429) with strong statistical support (100% MLBS/1.00 BYPP) (Fig. 119). The nucleotide comparisons showed that our strain (SICAUCC 22-0140) is not significantly different from the type strain o f *N. solani* (CBS 102429) in ITS, LSU, *rpb*2 *tub*2 and *tef*1-α, which indicated that they are the same species. Nucleotide comparisons of ITS, LSU, *tef*1-α, *tub*2, and *rpb*2 *N. solani* (SICAUCC 22-0140) also showed a high homology with the sequences of *N. solani* (CBS 102429), with a similarity of 100% (537/563, 0 gap), 100% (831/842, 0 gap), 99.9% (503/714, 0 gap), 100% (309/376, 0 gap), and 100% (859/945, 0 gap), respectively. Their morphology is similar to *N. solani* (Mart.) Saccardo. (1881). The collections in this study were associated with leaf blight symptoms. *Neocosmospora solani* has previously been reported on walnut in Xingjiang (Tuerdi et al. 2023) and is illustrated here as it is the first report on *Juglans regia* in Sichuan China, and to facilitate identification of this species on walnut in future.

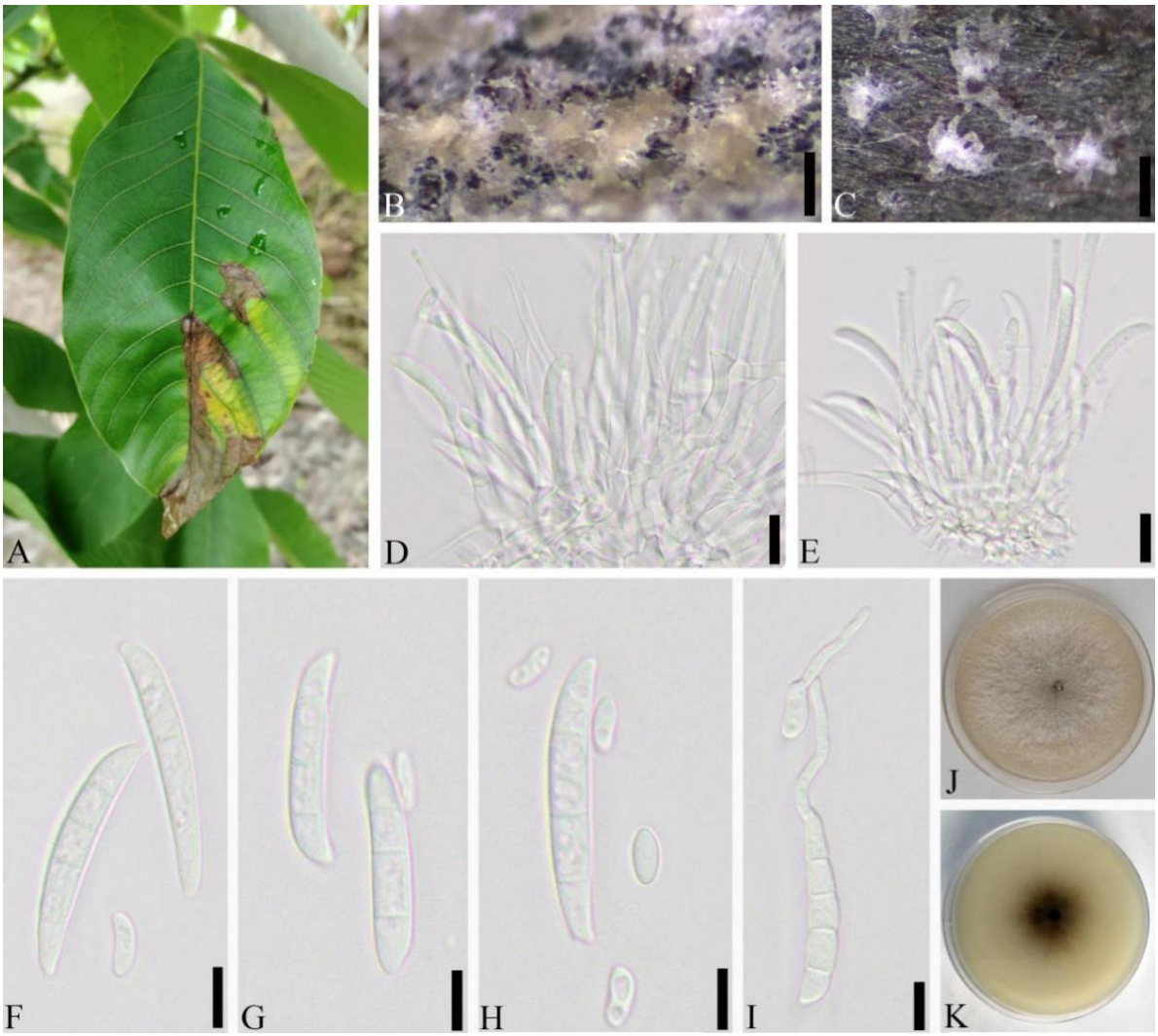


Figure 131 – *Neocosmospora solani* (SICAU 22-0138). A–C Appearance of conidium in host substrate. D, E Conidia attached to conidiophores. F–H Conidia. I Germinating macroconidium and microconidium. K Colonies on PDA (J from above, K from below). Scale bars: B, C = 500 μm, D, E = 20 μm, F–I = 10 μm.

Trichothecium Link, Mag. Gesell. naturf. Freunde, Berlin 3(1-2): 18 (1809).

This genus is a widespread pathogen and saprophyte in nature. Summerbell et al. (2011), the genus *Trichothecium* is revised following the principles of unitary nomenclature based on the, oldest valid anamorph or teleomorph name, and new combinations are made in *Trichothecium* for the tightly interrelated *Acremonium crotocinigenum*, *Spicellum roseum*, and teleomorph *Leucosphaerina* indica. We follow the latest treatments and updated accounts of *Trichothecium* in Hou et al. (2023).

83. *Trichothecium downum* F.H. Wang & C.L. Yang, sp. nov. Fig. 132

Index Fungorum number: IF901579; Facesoffungi number: FoF15596

Etymology – It refers to the color of the colony resembling light yellow duck down

Holotype – SICAU 23–0097.

Associated with leaf spots on the living leaves of *Juglans regia*. Symptoms manifest as yellowing leaves, with scorched and withered starting from the edges, ultimately leading to the complete withering and death of the leaves in later stages. Sexual morph: Not observed. Asexual morph: Conidiogenous apparatus varying by species, featuring one or more of. *Conidiophores* 120–460 × 3–5 μm ($\bar{x}$ = 290 × 4 μm; n = 20), septate, unbranched, with terminal, phialides, producing unicellular, hyaline, smooth, walled. *Conidia* 17–26 × 6–11 μm ($\bar{x}$ = 21 × 9 μm; n = 40), obovate,

oblong or cylindrical, unbranched or uncommonly with, retrogressive, shortening with production, of each conidium, with each conidial base subsuming a portion of, 0–1-septate, ellipsoidal or ovate, with a, decurved, abruptly narrowed basal hilum terminating in a distinct, truncate end.

Culture characteristics – Conidia germinating on sterile water within 24 h and germ tubes produced from both ends. Colonies on PDA reaching 60 mm diam., after 6 days at 25 ℃. The mycelium grows on the surface of the medium, circular, sur, face cottony with aerial mycelium orange, becoming yellowish brown. Reverse, orange to yellowish brown. Not produced pigmentation on PDA media.

Material examined – China, Sichuan Province, Chengdu City, Chongzhou City (30°33′9.64″N 103°39′29.33″E, alt. 512 m), on living leaves of *Juglans regia*, 28 July 2021, F.-H. Wang, WFH202107019 (SICAU 23-0097 holotype), ex-type living culture SICAUCC 23-0076. *Ibid*., WFH202107019B (SICAU 24-0041), living culture SICAUCC 23-0155.

GenBank numbers – SICAUCC 23-0076: PP060692 (ITS), PP057975 (LSU), PP003830 (SSU); SICAUCC 23-0155: PP844883 (ITS), PP826169 (LSU), PP853380 (SSU).

Note – Phylogenetic analysis shows that *Trichothecium downum* (SICAUCC 23-0076) is placed within *Trichothecium*, and close related to *T. roseum* (DAOM 208997) with lower bootstrap support (Fig. 133). *Trichothecium downum* (SICAUCC 23-0076) is typical of *Trichothecium*, by having septate, unbranched, phialides, hyaline, smooth conidiophores, 0–1-septate, ellipsoidal or ovate conidia (Summerbell et al. 2011). Morphologically, these two species are similar, but, the new collection is distinguished from, *T. roseum* and by its comparatively larger conidia (17–26 × 6–11 μm vs. 5–12 × 3–6.5 μm). Therefore, each gene region between these two taxa was compared based on the recommendations of delimitation of species from Jeewon & Hyde (2016). Nucleotide comparisons revealed notable genetic dissimilarities between *T. roseum* (DAOM 208997) and *T. downum* (SICAUCC 23-0076), viz. 8.4% (47/560, 4 gaps), and 6.61% (66/999, 60 gaps) in the LSU, and SSU, respectively. Hence, *T. downum* is introduced as a new species in this study.

Microascales Luttr. et al., Mycotaxon 12(1): 40 (1980).

The order *Microascales* was introduced by Benny & Kimbrough (1980) to accommodate *Chadefaudiellaceae*, *Microascaceae* and *Pithoascaceae*, and later expanded to include *Ceratocystidaceae*, *Gondwanamycetaceae*, *Halosphaeriaceae* and *Graphiaceae*. (Maharachchikumbura et al. 2016b, Hyde et al. 2020a, b, c, Wijayawardene et al. 2022). A total of 109 genera were accepted under Microascales which were distributed in seven families (Jayawardena et al. 2022, Wijayawardene et al. 2022).

Microascaceae Luttr. ex Malloch, Mycologia 62(4): 734 (1970).

The family *Microascaceae* and order *Microascales* were proposed by Luttrell (1951) and validly published with Latin descriptions by Malloch (1970) and Benny and Kimbrough (1980). The description by Luttrell (1951) was confirmed by Corlett (1963, 1966) who showed that asci of *Microascus* and *Petriella* develop directly from the cells of the ascogenous hyphae, and not from croziers. Malloch (1970) reviewed the family *Microascaceae* and included both ostiolate and non-ostiolate taxa. Benny and Kimbrough (1980) suggested that members of the family *Microascaceae* had evolved away from a hymenial configuration. It includes saprobic, plant and opportunistic human pathogenic fungal genera (De Hoog et al. 2000, Sandoval-Denis et al. 2016b, Maharachchikumbura et al. 2016b). The last treatment of *Microascaceae* was provided by Bao et al. (2023), and 23 genera were accepted.

Scopulariopsis Bainier, Bull. Soc. Mycol. Fr. 23: 98 (1907).

Scopulariopsis Sco. was erected by Bainier (1907) with *S. brevicaulis* Bainier as the type. This genus is characterized by its globose or subglobose, annellidic conidia with a truncate base arranged in a chain and frequently branched conidiophores mostly restricted to the apical region Pan et al. (2014). The species of *Scopulariopsis* are mostly saprogenous, widely distributed in soil, fibrous matters, air, bats, and are important for cellulose degradation and humus formation (Morton & Smith

1963, Vanderwolf et al. 2013, Pan et al. 2014, Woudenberg et al. 2017, Ogórek et al. 2020). However, some species of *Scopulariopsis* are conditional pathogens of animals and humans, which can cause tinea unguium Pan et al. (2014)

84. ***Scopulariopsis pseudobrevicaulis*** F.H. Wang & C.L. Yang, sp. nov. Fig. 134

Index Fungorum number: IF901580; Facesoffungi number: FoF15597

Etymology – In reference to its similarity with *Scopulariopsis brevicaulis*.

Holotype – SICAU 23–0098

Associated with leaf spots on the living leaves of *Juglans regia*. Symptoms manifest as yellowing leaves, with scorching starting from the edges, ultimately leading to the complete withering and death of the leaves in later stages. Sexual morph: Not observed. Asexual morph: *Colonies* effuse, white. *Mycelium* mostly immersed, composed of septate, branched, smooth, pale brown to hyaline hyphae. *Synnemata* 190–480 × 160–420 μm ($\bar{x}$ = 340 × 290 μm; n = 20), solitary to gregarious, white, massive. *Conidiophores* 48–130 × 3–5 μm ($\bar{x}$ = 70 × 4.5 μm; n = 20), hyaline, branched, cylindrical stipe, erect. *Conidiogenous cells* 15–21 × 2.5–4 μm ($\bar{x}$ = 18 × 3 μm, n = 20) lateral or terminal formation on solitary conidiophores, hyaline, cylindrical. *Conidia* 5–8 × 4.5–7 μm ($\bar{x}$ = 7 × 6.5 μm, n = 40), globose to subglobose, with truncate base, rounded at top, hyaline, spinulose on surface, thick-walled, arranged in chains, with a disjuncture between adjacent conidia.

Culture characteristics – Conidia germinating on sterile water within 12 h and germ tubes produced from ends. Colonies on PDA reaching 20 mm diam., after 30 days at 25 ℃. The mycelium grows on the surface of the medium, nearly circular, fat, dense, radial sulcate, edge entire, the edge is white and the center is yellow-brown. Reverse, similarity. Not produced pigmentation on PDA media.

Material examined – China, Sichuan Province, Neijiang City, Dongxing District, Paifang Village (29°48′30.68″N 105°6′36.29″E, alt. 389 m), on living leaves of *Juglans sigillata*, 27 April 2022, F.-H. Wang, WFH202204073 (SICAU 23-0098, holotype), ex-type living culture SICAUCC 23-0077. *Ibid*., WFH202204073B (SICAU 24-0042), living culture SICAUCC 23-0156.

GenBank numbers – SICAUCC 23-0077: PP060693 (ITS), PP057976 (LSU), PP061156 (*tef*1-α), PP061181 (*tub*2); SICAUCC 23-0156: PP844884 (ITS), PP826170 (LSU), PP850057 (*tef*1-α), PP850064 (*tub*2).

Note – *Scopulariopsis pseudobrevicaulis* (SICAUCC 23-0077) is phylogenetically close to *S. brevicaulis* (MUCL 40726) with 83% MLBS bootstrap support (Fig. 135). *Scopulariopsis pseudobrevicaulis* is typical of *Scopulariopsis* in having hyaline, branched, cylindrical stipe, erect conidiophores, hyaline, cylindrical conidiogenous cells and globose to subglobose, with truncate base, rounded at top, hyaline, spinulose on surface, thick-walled, arranged in chains conidia (Bainier 1907, Liu et al. 2023a). *Scopulariopsis pseudobrevicaulis* (SICAUCC 23-0077) differed from *S. brevicaulis* (MUCL 40726) by the latter having spinulose on surface conidia, also by shorter conidiogenous cells (15–21 × 2.5–4 μm vs 9–30 × 1–6 μm μm) and slightly small conidia (5–8 × 4.5–7 μm vs 3–9 × 3–8 μm μm). (Liu et al. 2023a). However, nucleotide sequence comparisons reveal specific differences between *S. pseudobrevicaulis* (SICAUCC 23-0077) and its related species. Specifically, the sequence divergences between *S. pseudobrevicaulis* (SICAUCC 23-0077) and *S. brevicaulis* (MUCL 40726) in the LSU, *tef*1-α and *tub*2 regions are 0% (0/500, 0 gap), 2.1% (19/906, 0 gap), and 4.84% (23/475, 2 gaps), respectively. The PHI test revealed no significant recombination event between our strain and the closely related taxa (Φw = 1) (Fig. 136). Based on phylogeny and morphology, the new isolates are identified as new species.

Xylariales Nannf., Nova Acta R. Soc. Scient. upsal., Ser. 4 8(no. 2): 66 (1932).

Xylariales is a large order of subclass *Sordariomycetes*, established by Nannfeldt (1932). The continuous taxonomic studies expand the number of families and genera in *Xylariales*. Recently, Maharachchikumbura et al. (2016a) assigned 22 families to *Xylariales*. We follow the treatments by (Wijayawardene et al. 2022, Jayawardena et al. 2022, Zhang et al. 2023a).

Diatrypaceae Nitschke [as '*Diatrypeae*'], Verh. naturh. Ver. preuss. Rheinl. 26: 73 (1869).

Diatrypaceae was introduced by Nitschke (1869) and is typified by *Diatrype disciformis*. Based on the latest treatment and updated accounts of *Diatrypaceae*, the family contains 28 genera (Maharachchikumbura et al. 2015, 2016a, Hyde et al. 2020a, b, c, Wijayawardene et al. 2022, Jayawardena et al. 2022, Zhang et al. 2023a), respectively are: *Allescherina*, *Allocryptovalsa*, *Allodiatrype*, *Anthostoma*, *Bitrimonospora*, *Cryptosphaeria*, *Cryptosphaerina*, *Cryptovalsa*, *Diatrypasimilis*, *Diatrype*, *Diatrypella*, *Dothideovalsa*, *Echinomyces*, *Endoxylina*, *Eutypa*, *Eutypella*, *Halocryptosphaeria*, *Halocryptovalsa*, *Halodiatrype*, *Leptoperidia*, *Libertella*, *Monosporascus*, *Neoeutypella*, *Paraeutypella*, *Pedumispora*, *Peroneutypa*, *Quaternaria* and *Rostronitschkia*. Numerous saprobic, endopytic and pathogenic diatrypaceous taxa are available in both terrestrial and aquatic habitats worldwide (Wijayawardene et al. 2020a, Dissanayake et al. 2021a, b, Zhu et al. 2021, Li et al. 2023c, Ma et al. 2023).

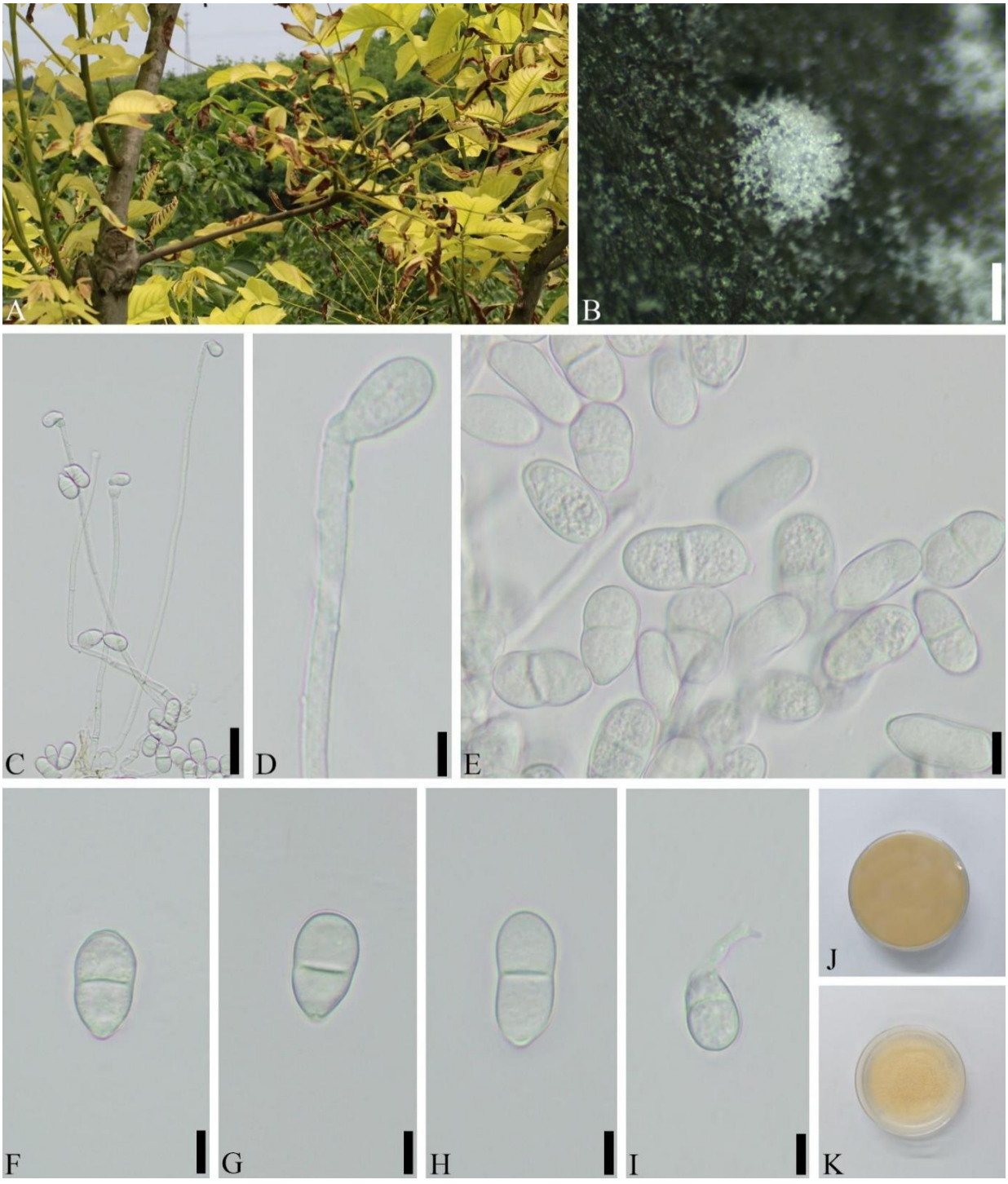


Figure 132 – *Trichothecium downum* (SICAU 23-0097, holotype). A Symptoms of the disease. B Colony on host. C–D Conidiophores with conidiogenous cells and conidia. E–H Conidia. I Germinating conidium. J, K Colonies on PDA (J from above, K from below). Scale bars: B = 1000 µm, C = 40 µm, D–I = 10 µm.

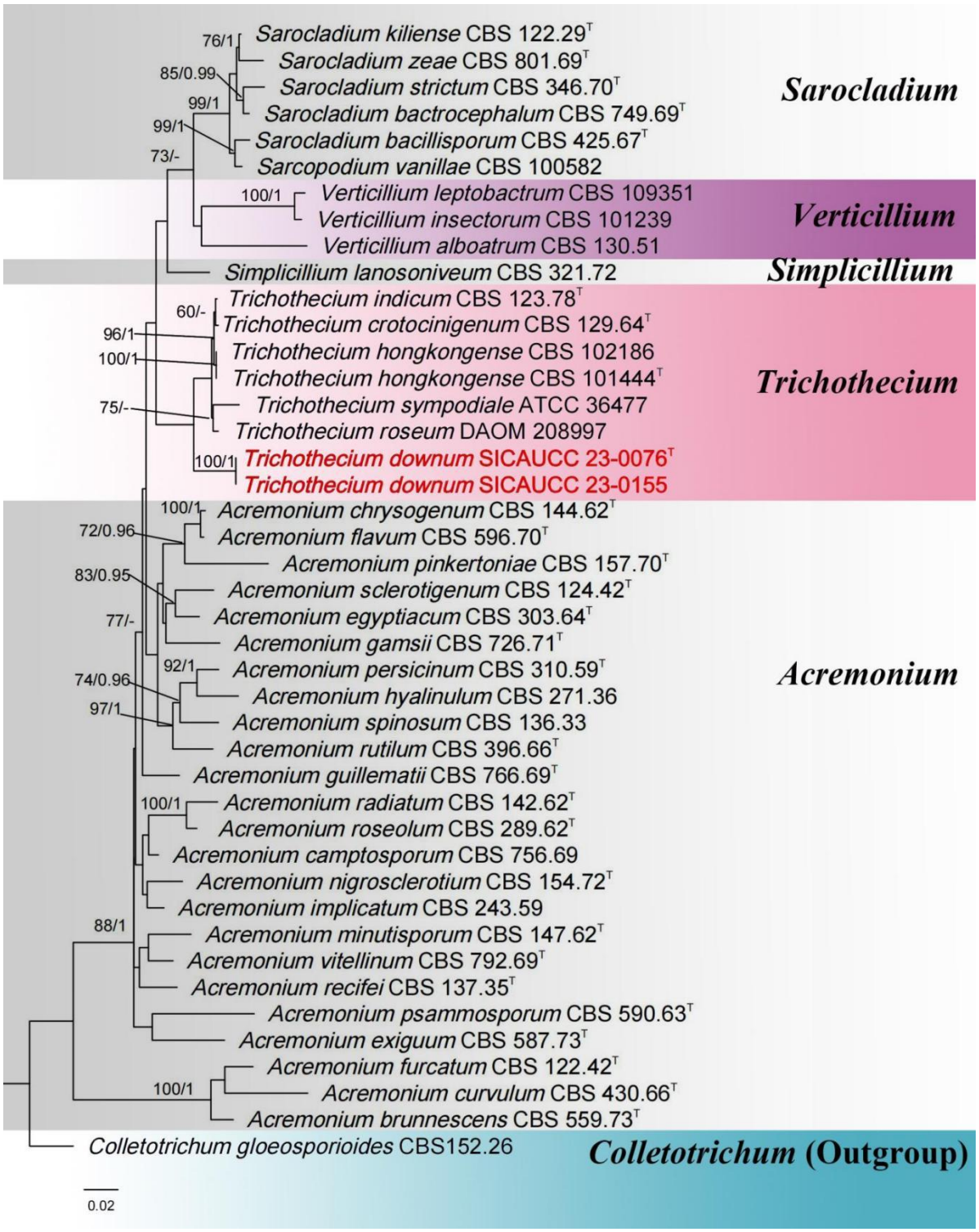


Figure 133 – Best scoring RAxML tree with a final likelihood value of -13,616.453854 based on combined LSU and SSU sequence data of related species. The tree is rooted with *Colletotrichum sphaerospermum* (CBS 152.26) in *Colletotrichum*. Forty-three strains were included in the combined

analyses which comprised 3,205 characters (957 characters for LSU and 2,246 characters for SSU, including gap regions). The matrix had 916 distinct alignment patterns, with 32.75% of undetermined characters and gaps. Estimated base frequencies were as follows; A = 0.255830, C = 0.221455, G = 0.282394, T = 0.240321; substitution rates AC = 1.162519, AG = 2.248154, AT = 1.213335, CG = 0.734229, CT = 6.561276, GT = 1.000000; gamma distribution shape parameter α = 0.184271. In our analysis, GTR+I+G model was used for each partition in Bayesian posterior analysis. The species determined in this study is indicated in red and bold. Bootstrap support values for maximum likelihood (MLBS, left) ⩾ 60% and Bayesian posterior probabilities (BYPP, right) ⩾ 0.90 are indicated at the nodes, respectively. Hyphens (-) represent support values less than 60% MLBS/0.90 BYPP. The ex-type superscript "T".

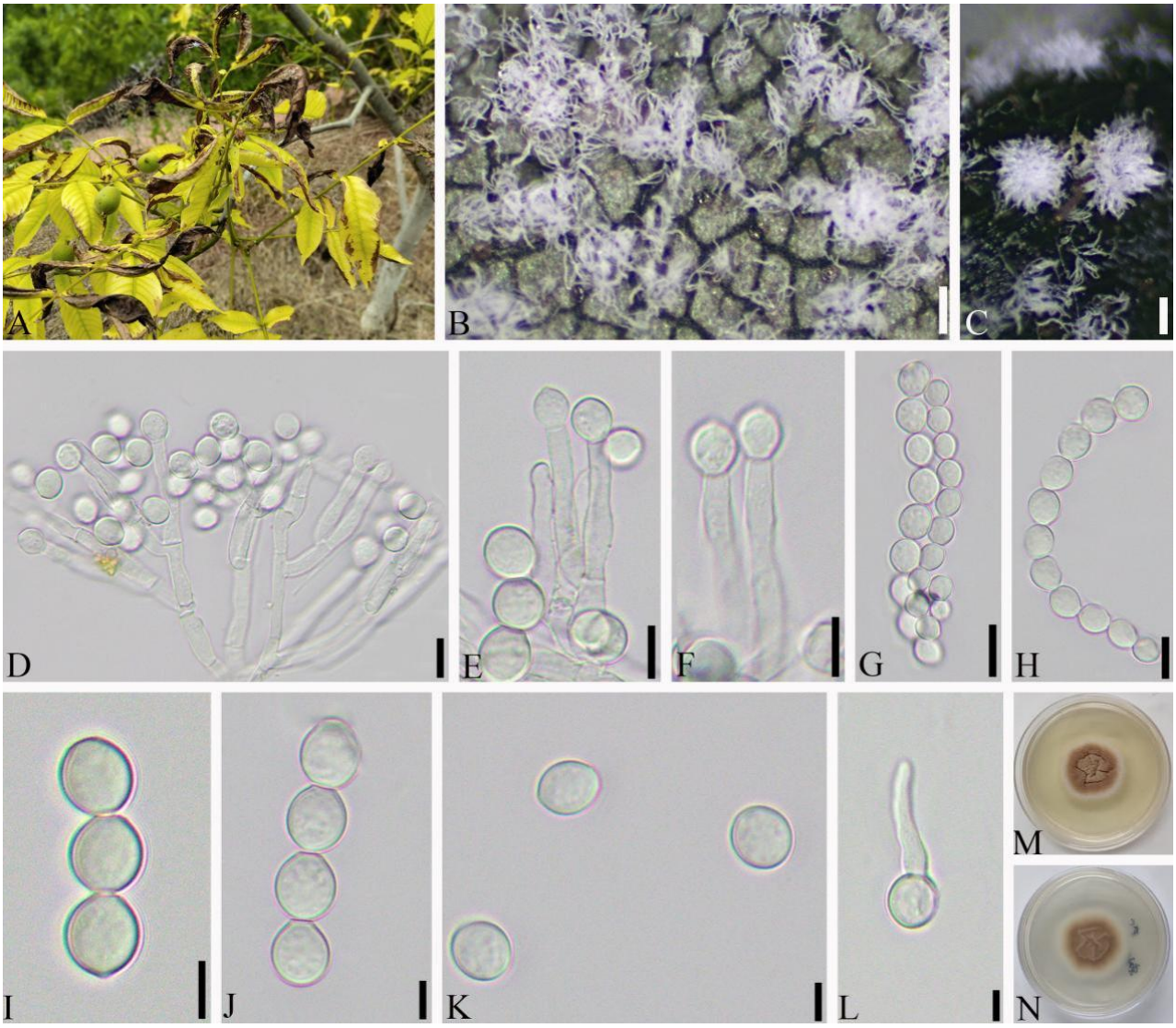


Figure 134 – *Scopulariopsis pseudobrevicaulis* (SICAU 23-0098, holotype). A Symptoms of the disease. B, C Sporodochia on host substrate D–F Conidiophores and conidiogenous cells. G–J arranged in chains conidia. K Conidia L Germinating conidium. M, N Colonies on PDA (M from above, N from below). Scale bars: B, C = 500 µm, D = 20 µm, G, H = 15 µm, E, F = 10 µm, I–L = 5 µm.

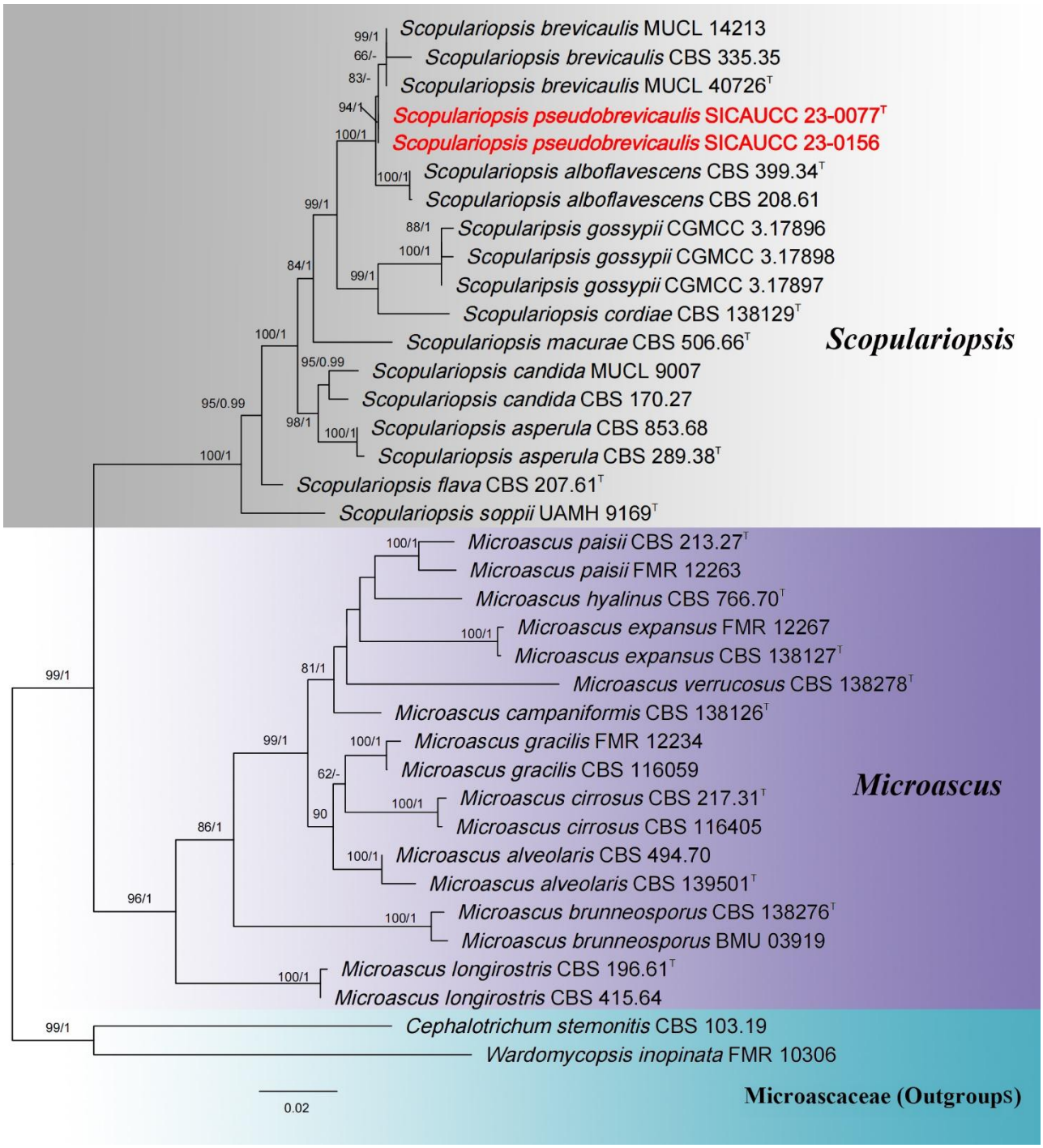


Figure 135 – Best scoring RAxML tree with a final likelihood value of -11,167.597666 based on combined LSU, *tef*1-α and *tub*2 sequence data of related species. The tree is rooted with *Cephalotrichum stemonitis* (CBS 103.19) and *Wardomycopsis inopinata* (FMR 10306) in Microascaceae. Thirty-seven strains were included in the combined analyses which comprised 2,592 characters (955 characters for LSU, 1,032 characters for *tef*1-α and 603 characters for *tub*2, including gap regions). The matrix had 833 distinct alignment patterns, with 20.08% of undetermined characters and gaps. Estimated base frequencies were as follows; A = 0.219388, C = 0.300883, G = 0.277422, T = 0.202308; substitution rates AC = 0.753666, AG = 2.390972, AT = 1.272167, CG = 1.011655, CT = 5.617949, GT = 1.000000; gamma distribution shape parameter α = 0.173864. The Bayesian inference analyses was implemented by MrBayes v.3.2.2 with the best-fit model (GTR+I+G for LSU, *tef*1-α; HKY+I+G for *tub*2) of evolution estimated with MrModeltest 2.2. The species determined in this study is indicated in red and bold. Bootstrap support values for maximum likelihood (MLBS, left) ⩾ 50% and Bayesian posterior probabilities (BYPP, right) ⩾ 0.90 are

indicated at the nodes, respectively. Hyphens (-) represent support values less than 50% MLBS/0.90 BYPP. The ex-type superscript "T".

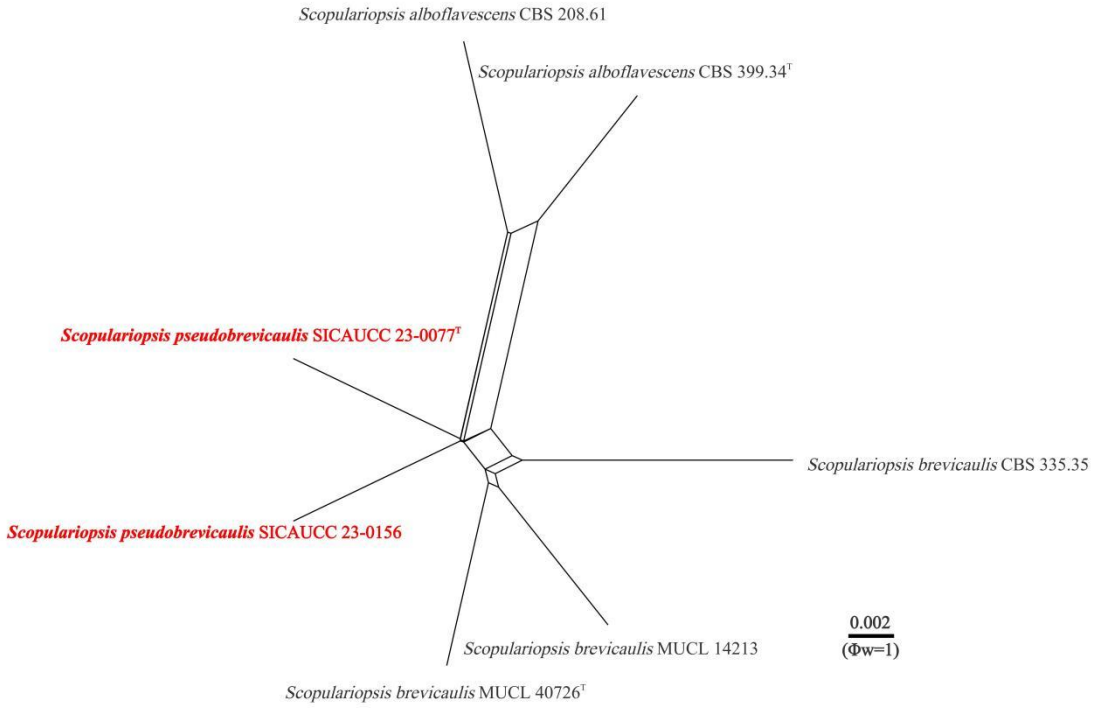


Figure 136 – Results of the PHI test of *Scopulariopsis pseudobrevicaulis* and closely related species using both LogDet transformation and splits decomposition. The PHI test did not find any statistically significant recombination (Φw = 1) in the data set. The new strains are represented in red and bold. "T" represents the type strain.

Diatrypella (Ces. & De Not.) De Not., Sfer. Ital.: 29 (1863).

Diatrypella was introduced by Cesati and Notaris (1863) and typified *D. verruciformis*. The genus is characterized by a libertella-like coelomycetous asexual morph. In the sexual morph, conical to truncate and discoid, cushion-like stromata are delimited by black zones on the substrates, umbilicate or sulcate ostiolar necks, long-stalked, cylindrical and polysporous asci with allantoid, hyaline or yellowish ascospores (Kirk et al. 2008, Dissanayake et al. 2020; Jayawardena et al. 2022, Zhang et al. 2023a). There are over 101 epithets listed in Species Fungorum (http://www.speciesfungorum.org/Index.htm, September 2024), but most of them lack sequence data.

85. ***Diatrypella vulgaris*** Trouillas, W.M. Pitt & Gubler (2011) Fig. 137

Index Fungorum number: IF519404; Facesoffungi number: FoF03591

Saprobic on dead branch of *Juglans regia*. Sexual morph: *Stromata* well developed, in pustules, solitary or gregarious on the substrate, semi-immersed, erumpent through host epidermis, with 5–12 *ascomata* immersed in a single stroma. *Ascomata* 230–373 × 214–345 µm ($\bar{x}$ = 279 × 245 µm, n = 20), perithecial, immersed in stromatic tissues, aggregated, globose to subglobose, coriaceous, pale to dark brown, ostioles sulcate, slightly prominent, periphysate, carbonaceous or fragile at the apex. *Peridium* 18–30 µm ($\bar{x}$ = 26µm, n = 20) wide, composed of two strata, with inner stratum of hyaline, thin-walled, elongated cells of textura prismatica, outer stratum of brown, thick-walled cells of *textura angularis*. *Hamathecium* comprising abundant asci. *Paraphyses* not observed. *Asci* 108–143 × 14–23 µm ($\bar{x}$ = 121 × 19 µm, n = 20), polysporous, unitunicate, clavate, pedicellate, with swollen

upper portion, apex rounded, without an apical apparatus. *Ascospores* 5.5–9.8 × 1–2.3 μm ($\bar{x}$ = 7.8 × 1.8 μm, n = 20), overlapping, allantoid, one-celled, yellowish in mass. Asexual morph: Not observed.

Culture characteristics – Ascospores germinating on sterile water within 12 h and germ tubes produced from both ends. Colonies on PDA reaching 60 mm diam., after 18 days at 25 ℃. The mycelium grows on the surface of the medium, circular, flat, with diffuse margin, white become light brown with age. Reverse similar in colour, conidia were produced after 27 days of culture. Not produced pigmentation on PDA media.

Material examined – China, Sichuan Province, Chengdu City, Chongzhou City (30°33′9.74″N 103°39′29.66″E, alt. 512 m), on dead branch of *Juglans regia*, 6 September 2021, F.-H. Wang, WFH202109002 (SICAU 23-0099), living culture SICAUCC 23-0078.

GenBank numbers – SICAUCC 23-0078: PP060694 (ITS), PP061182 (*tub*2).

Note – In the phylogenetic analysis, the strain *Diatrypella vulgaris* (SICAUCC 23-0078) is closely related to other strains of *D. vulgaris* and clusters together with *D. vulgaris strains* (HVFRA 02 and HVGRF 03) with strong statistical support (99% MLBS/1.00 BYPP) (Fig. 138). The morphology of the new isolate is similar to the description of *D. vulgaris* provided by Trouillas et al. 2011. The comparisons of ITS and *tub*2 sequence data from both strains show 100% similarity for each gene. Based on morphological characters and phylogenetic analyses, we determine our specimens as *D. vulgaris*. *Diatrypella vulgaris*, has been reported from *Citrus paradise* and *Fraxinus angustifolia* in Austria (Trouillas et al. 2011), This is the first report of this species on *Juglans regia*.

Eutypella (Nitschke) Sacc., Atti Soc. Veneto-Trent. Sci. Nat., Padova, Sér. 4 4: 80 (1875).

The genus *Eutypella* (Nitschke) Saccardo, a perithecial ascomycete belonging to the *Diatrypaceae*, was established by Saccardo (1875), based on *E. cerviculata* (Fr.) Sacc. *Eutypella* species are found on a wide range of hosts (Vasilyeva & Stephenson 2006, Trouillas et al. 2011, Luque et al. 2012, Mehrabi et al. 2016). Both Senanayake et al. (2015) and Maharachchikumbura et al. (2016a) included *Eutypella* in *Diatrypaceae*. Currently 149 species epithets are listed in Species Fungorum (http://www.speciesfungorum.org/Index.htm, September 2024), but only a few *Eutypella* species have sequence data. Until more species are collected, epitypified and sequenced, understanding of the genus *Eutypella* will remain incomplete.

86. ***Eutypella microtheca*** Trouillas, W.M. Pitt & Gubler, Fungal Divers. 49: 217 (2011) Fig. 139

Index Fungorum number: IF519407; Facesoffungi number: FoF16312

Saprobic on dead branch of *Juglans regia*. Sexual morph: *Stromata* well developed, elevating the periderm surface (swollen appearance), which become ripped off by the emerging, non-prominent ostioles. *Ascomata* 180–310 × 190–278 μm ($\bar{x}$ = 245 × 230 μm, n = 20), more or less in contact, round to ovoid, surrounded by white, powdery entostromatic tissue, perithecial, immersed in stromatic tissues, aggregated, globose to subglobose, coriaceous, pale to dark brown. *Paraphyses* not observed. *Asci* 80–114 × 6–10 μm ($\bar{x}$ = 98 × 8.5 μm, n = 20), 8-spored, clavate, long stick-shaped, stipitate. *Ascospores* 7–10 × 1.5–2.5 μm ($\bar{x}$ = 9 × 2.2 μm, n = 40), allantoid, subhyaline to light brown, oil drop-like inclusion at each end. Asexual morph: Not observed.

Culture characteristics – Ascospores germinating on sterile water within 12 h and germ tubes produced from both ends. Colonies on PDA reaching 60 mm diam., after 14 days at 25 ℃. The mycelium grows on the surface of the medium, circular to slightly irregular, margin entire, slightly raised, cottony, fluffy appearance, white. Reverse, similar in color. Not produced pigmentation on PDA media.

Material examined – China, Sichuan Province, Mianyang City, Pingwu County (32°12′59.46″N 104°50′15.38″E, alt. 726 m), on dead branch of *Juglans regia*, 9 July 2022, F.-H. Wang, WFH202207073 (SICAU 23-0100), living culture SICAUCC 23-0079.

GenBank numbers – SICAUCC 23-0079: PP060695 (ITS), PP061183 (*tub*2)

Note – Phylogenetically, our new collection (SICAUCC 23-0079) also clustered with *Eutypella microtheca* (BCMX 01) with statistical support (71% MLBS/0.93 BYPP) (Fig. 138). Our strains is similar to *E. microtheca* in having clavate, 8-spored, long stick-shaped, stipitate asci, allantoid,

subhyaline to light brown, oil drop-like inclusion at each end of ascospores. The comparisons of ITS and *tub*2 sequence data from both strains show 100% similarity for each gene. Hence, it is identified as *E. microtheca*, which has been previously reported from *Vitis vinifera* in Australia (Trouillas et al. 2011).

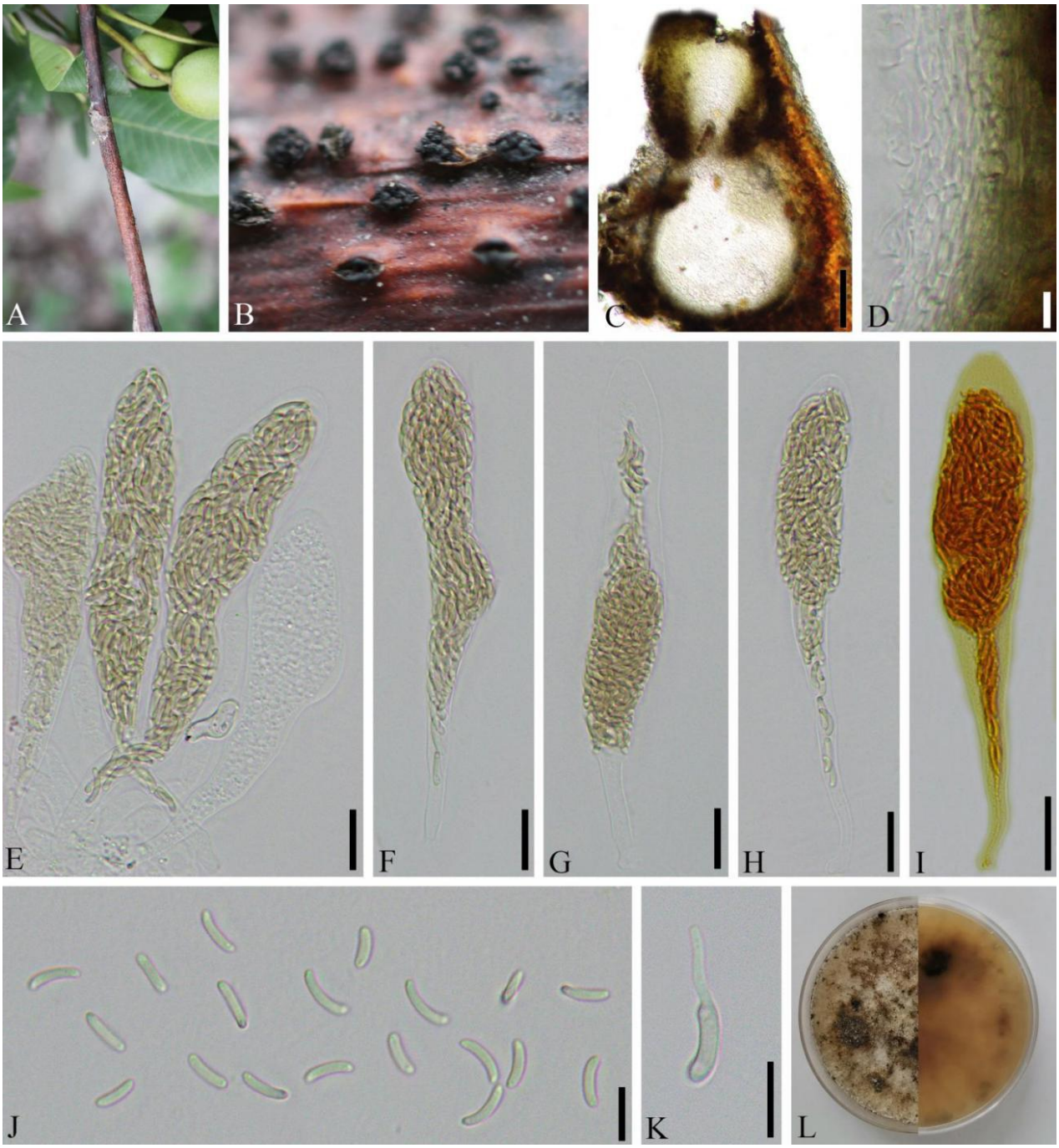


Figure 137 – *Diatrypella vulgaris* (SICAU 23-0099). A, B Appearance of ascostroma in host substrate. C Vertical section of ascoma. D Peridium. E–H Asci. I Asci in Melzer's reagent J Ascospores. K Germinating ascospore. L Colonies on PDA. Scale bars: C = 200 μm, D–I = 15 μm, J, K = 10 μm.

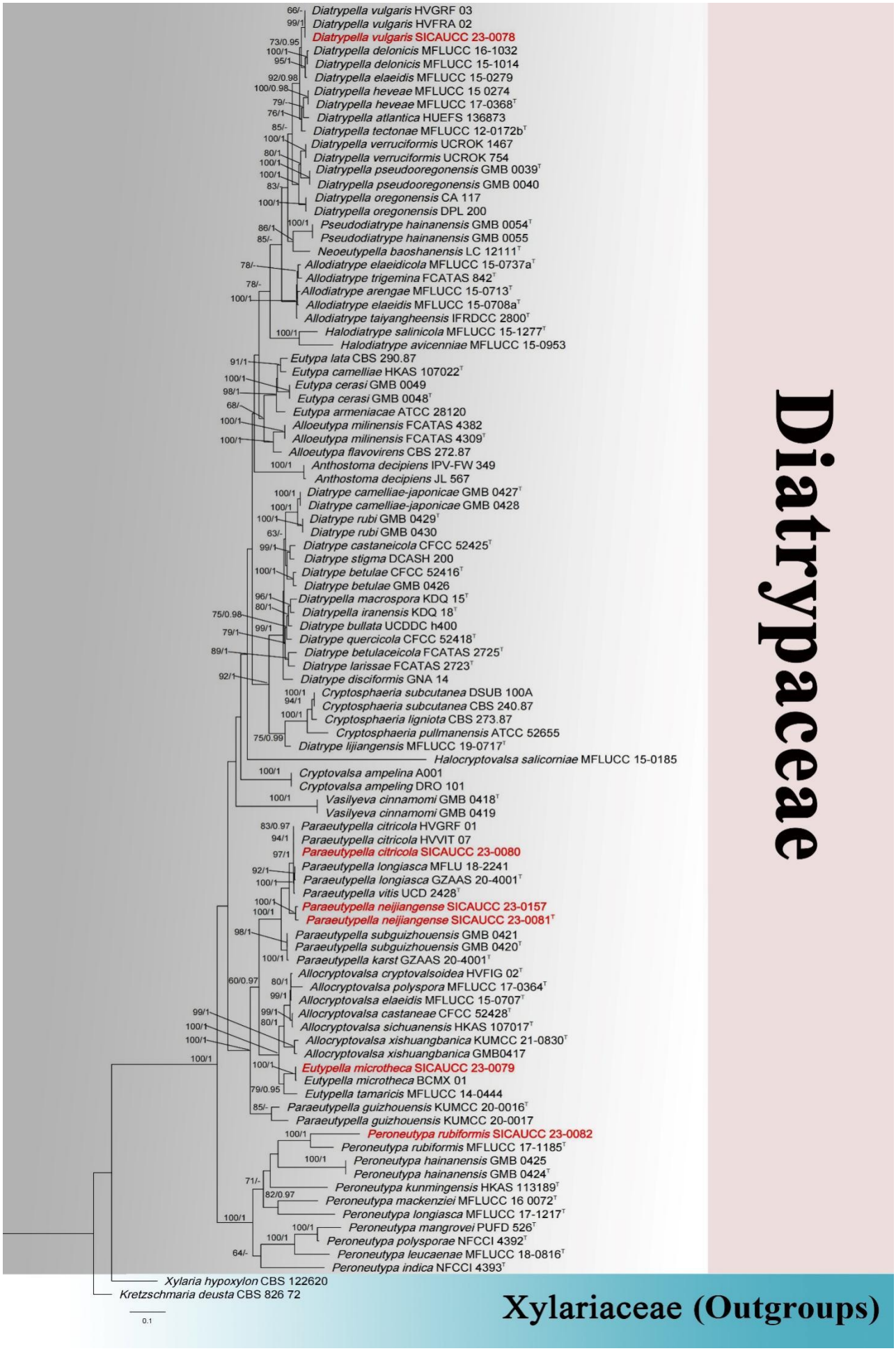

Diatrypaceae
Xylariaceae (Outgroups)
Diatrypella vulgaris HVGRF 03
Diatrypella vulgaris HVFRA 02
Diatrypella vulgaris SICAUCC 23-0078
Diatrypella delonicis MFLUCC 16-1032
Diatrypella delonicis MFLUCC 15-1014
Diatrypella elaeidis MFLUCC 15-0279
Diatrypella heveae MFLUCC 15 0274
Diatrypella heveae MFLUCC 17-0368T
Diatrypella atlantica HUEFS 136873
Diatrypella tectonae MFLUCC 12-0172bT
Diatrypella verruciformis UCROK 1467
Diatrypella verruciformis UCROK 754
Diatrypella pseudooregonensis GMB 0039T
Diatrypella pseudooregonensis GMB 0040
Diatrypella oregonensis CA 117
Diatrypella oregonensis DPL 200
Pseudodiatrype hainanensis GMB 0054T
Pseudodiatrype hainanensis GMB 0055
Neoeutypella baoshanensis LC 12111T
Allodiatrype elaeidicola MFLUCC 15-0737aT
Allodiatrype trigemina FCATAS 842T
Allodiatrype arengae MFLUCC 15-0713T
Allodiatrype elaeidis MFLUCC 15-0708aT
Allodiatrype taiyangheensis IFRDCC 2800T
Halodiatrype salinicola MFLUCC 15-1277T
Halodiatrype avicenniae MFLUCC 15-0953
Eutypa lata CBS 290.87
Eutypa camelliae HKAS 107022T
Eutypa cerasi GMB 0049
Eutypa cerasi GMB 0048T
Eutypa armeniacae ATCC 28120
Alloeutypa milinensis FCATAS 4382
Alloeutypa milinensis FCATAS 4309T
Alloeutypa flavovirens CBS 272.87
Anthostoma decipiens IPV-FW 349
Anthostoma decipiens JL 567
Diatrype camelliae-japonicae GMB 0427T
Diatrype camelliae-japonicae GMB 0428
Diatrype rubi GMB 0429T
Diatrype rubi GMB 0430
Diatrype castaneicola CFCC 52425T
Diatrype stigma DCASH 200
Diatrype betulae CFCC 52416T
Diatrype betulae GMB 0426
Diatrypella macrospora KDQ 15T
Diatrypella iranensis KDQ 18T
Diatrype bullata UCDDC h400
Diatrype quercicola CFCC 52418T
Diatrype betulaceicola FCATAS 2725T
Diatrype larissae FCATAS 2723T
Diatrype disciformis GNA 14
Cryptosphaeria subcutanea DSUB 100A
Cryptosphaeria subcutanea CBS 240.87
Cryptosphaeria ligniota CBS 273.87
Cryptosphaeria pullmanensis ATCC 52655
Diatrype lijiangensis MFLUCC 19-0717T
Halocryptovalsa salicorniae MFLUCC 15-0185
Cryptovalsa ampelina A001
Cryptovalsa ampeling DRO 101
Vasilyeva cinnamomi GMB 0418T
Vasilyeva cinnamomi GMB 0419
Paraeutypella citricola HVGRF 01
Paraeutypella citricola HVVIT 07
Paraeutypella citricola SICAUCC 23-0080
Paraeutypella longiasca MFLU 18-2241
Paraeutypella longiasca GZAAS 20-4001T
Paraeutypella vitis UCD 2428T
Paraeutypella neijiangense SICAUCC 23-0157
Paraeutypella neijiangense SICAUCC 23-0081T
Paraeutypella subguizhouensis GMB 0421
Paraeutypella subguizhouensis GMB 0420T
Paraeutypella karst GZAAS 20-4001T
Allocryptovalsa cryptovalsoidea HVFIG 02T
Allocryptovalsa polyspora MFLUCC 17-0364T
Allocryptovalsa elaeidis MFLUCC 15-0707T
Allocryptovalsa castaneae CFCC 52428T
Allocryptovalsa sichuanensis HKAS 107017T
Allocryptovalsa xishuangbanica KUMCC 21-0830T
Allocryptovalsa xishuangbanica GMB0417
Eutypella microtheca SICAUCC 23-0079
Eutypella microtheca BCMX 01
Eutypella tamaricis MFLUCC 14-0444
Paraeutypella guizhouensis KUMCC 20-0016T
Paraeutypella guizhouensis KUMCC 20-0017
Peroneutypa rubiformis SICAUCC 23-0082
Peroneutypa rubiformis MFLUCC 17-1185T
Peroneutypa hainanensis GMB 0425
Peroneutypa hainanensis GMB 0424T
Peroneutypa kunmingensis HKAS 113189T
Peroneutypa mackenziei MFLUCC 16 0072T
Peroneutypa longiasca MFLUCC 17-1217T
Peroneutypa mangrovei PUFD 526T
Peroneutypa polysporae NFCCI 4392T
Peroneutypa leucaenae MFLUCC 18-0816T
Peroneutypa indica NFCCI 4393T
Xylaria hypoxylon CBS 122620
Kretzschmaria deusta CBS 826 72
0.1

Figure 138 – Best scoring RAxML tree with a final likelihood value of -28,190.803568 based on combined ITS and *tub*2 sequence data of related species. The tree is rooted with *Kretzschmaria deusta* (CBS 826.72) and *Xylaria hypoxylon* (CBS 122620) in *Xylariaceae*. Ninety-eight strains were included in the combined analyses which comprised 2,985 characters (813 characters for LSU and 2,169 characters for *tub*2, including gap regions). The matrix had 1,824 distinct alignment patterns, with 58.63% of undetermined characters and gaps. Estimated base frequencies were as follows; A = 0.218294, C = 0.283843, G = 0.233824, T = 0.264039; substitution rates AC = 0.925989, AG = 3.038833, AT = 1.323971, CG = 0.841396, CT = 3.759087, GT = 1.000000; gamma distribution shape parameter α = 0.393105. The Bayesian inference analyses was implemented by MrBayes v.3.2.2 with the best-fit model (SYM+I+G for ITS; HKY+I+G for *tub*2) of evolution estimated with MrModeltest 2.2. The species determined in this study is indicated in red and bold. Bootstrap support values for maximum likelihood (MLBS, left) ⩾ 60% and Bayesian posterior probabilities (BYPP, right) ⩾ 0.90 are indicated at the nodes, respectively. Hyphens (-) represent support values less than 60% MLBS/0.90 BYPP. The ex-type superscript "T".

Paraeutypella L.S. Dissan., J.C. Kang, Wijayaw. & K.D. Hyde, Biodiversity Data Journal 9: e63864, 11 (2021).

Paraeutypella was established by Dissanayake et al. (2021a) to accommodate the type species *P. guizhouensis* and two new combinations *P. citricola* and *P. vitis*. *Paraeutypella* morphologically resembles *Eutypella*, but they have different numbers of perithecia in the *Stromata*, and they are phylogenetically distant from *Eutypella* in molecular analysis (Dissanayake et al. 2021a). Recently, another species *P. subguizhouensis* was added to this genus by Li et al. (2023c). Moreover, the phylogenetic placement of *Allocryptovalsa* in Li et al. (2023c) was also confused. Therefore, the phylogenetic relationship between these related genera is expected to be fully determined by a further study. Zhang et al. (2023a) revised two kinds of *Allocryptovalsa*, are placed within the genus *Paraeutypella*.

87. ***Paraeutypella citricola*** (Speg.) L.S. Dissan., Wijayaw., J.C. Kang & K.D. Hyde, Biodiver Data J 9: e63864, 14 (2021) Fig. 140

Index Fungorum number: IF558003; Facesoffungi number: FoF15551

Saprobic on dead branch of *Juglans regia*. Sexual morph: *Stromata* 680–970 × 790–1078 μm ($\bar{x}$ = 790 × 810 μm, n = 20), well-developed, solitary to gregarious, erumpent, black, immersed, globose to subglobose. *Ascomata* 380–460 × 490–578 μm ($\bar{x}$ = 420 × 530 μm, n = 20), perithecial, surrounded by white entostroma, immersed in stromata, 2–5 ascomata arranged in a valsoid configuration, subglobose, individual ostiole with a long neck. Neck, cylindrical. *Peridium* 36–45 μm ($\bar{x}$ = 40.5μm, n = 20) wide, composed of two layers: outer layer of black, thick-walled cells; inner layer, hyaline, thick-walled cells forming *textura angularis*. *Hamathecium* 180–310 × 190–278 μm ($\bar{x}$ = 245 × 230 μm, n = 20), paraphyses arising from base of perithecia, hyaline, long, narrow, unbranched, septate, guttulate, narrowing and tapering towards apex. *Asci* 110–130 × 6–9 μm ($\bar{x}$ = 124 × 8 μm, n = 30), 8-spored, polysporous, unitunicate, clavate, apically pointed, long pedicellate. *Ascospores* 4–9(13) × 1–2.5 μm ($\bar{x}$ = 7 × 1.5 μm, n = 40), overlapping, hyaline, yellowish in mass, allantoid, aseptate, guttulate, smooth-walled. Asexual morph: Not observed.

Culture characteristics – Ascospores germinating on sterile water within 12 h and germ tubes produced from both ends. Colonies on PDA reaching 60 mm diam., after 21 days at 25 ℃. The mycelium grows on the surface of the medium, medium dense, circular to slightly irregular, slightly raised, cottony surface, colony from above, white. Reverse, yellowish-white. Conidia were produced after 28 days. Not produced pigmentation on PDA media.



Figure 139 – *Eutypella microtheca* (SICAU 23-0100). A Appearance of ascostroma in host substrate. B Section through ascoma. C Vertical section of ascoma. D–F Asci. G Asci in Melzer's reagent. H Ascospores. I, J Colonies on PDA (I from above, J from below). Scale bars: C = 200 μm, B = 100 μm, D–H = 10 μm.

Material examined – China, Sichuan Province, Suining City, Shehong City, Guangxing Town (30°57′22.57″N 105°18′54.55″E, alt. 408 m), on dead branch of *Juglans regia*, 27 April 2022, F.-H. Wang, WFH202204096-1 (SICAU 23-0101), living culture SICAUCC 23-0080.

GenBank numbers – SICAUCC 23-0080: PP060696 (ITS), PP061184 (*tub*2).

Note – Phylogenetic analyses show that the strain *Paraeutypella citricola* (SICAUCC 23-0080) grouped within the *P. citricola* clade (Fig. 138). Our collection is similar to Paraeutypella citricola (HVGRF01) in having arranged in a valsoid configuration, subglobose, individual ostiole with a long neck ascomata, 8-spored, polysporous, unitunicate, clavate, apically pointed, long pedicellate asci, and overlapping, hyaline, yellowish in mass, allantoid, aseptate, guttulate ascospores (Dissanayake et al. 2021a). In addition, each gene region between *P. citricola* (HVVIT07, HVGRF01) and our new collection was compared, there is no difference between ITS and *tub*2. We, therefore, identified our collection as *P. citricola* which is a new host record for *Juglans regia* in China.

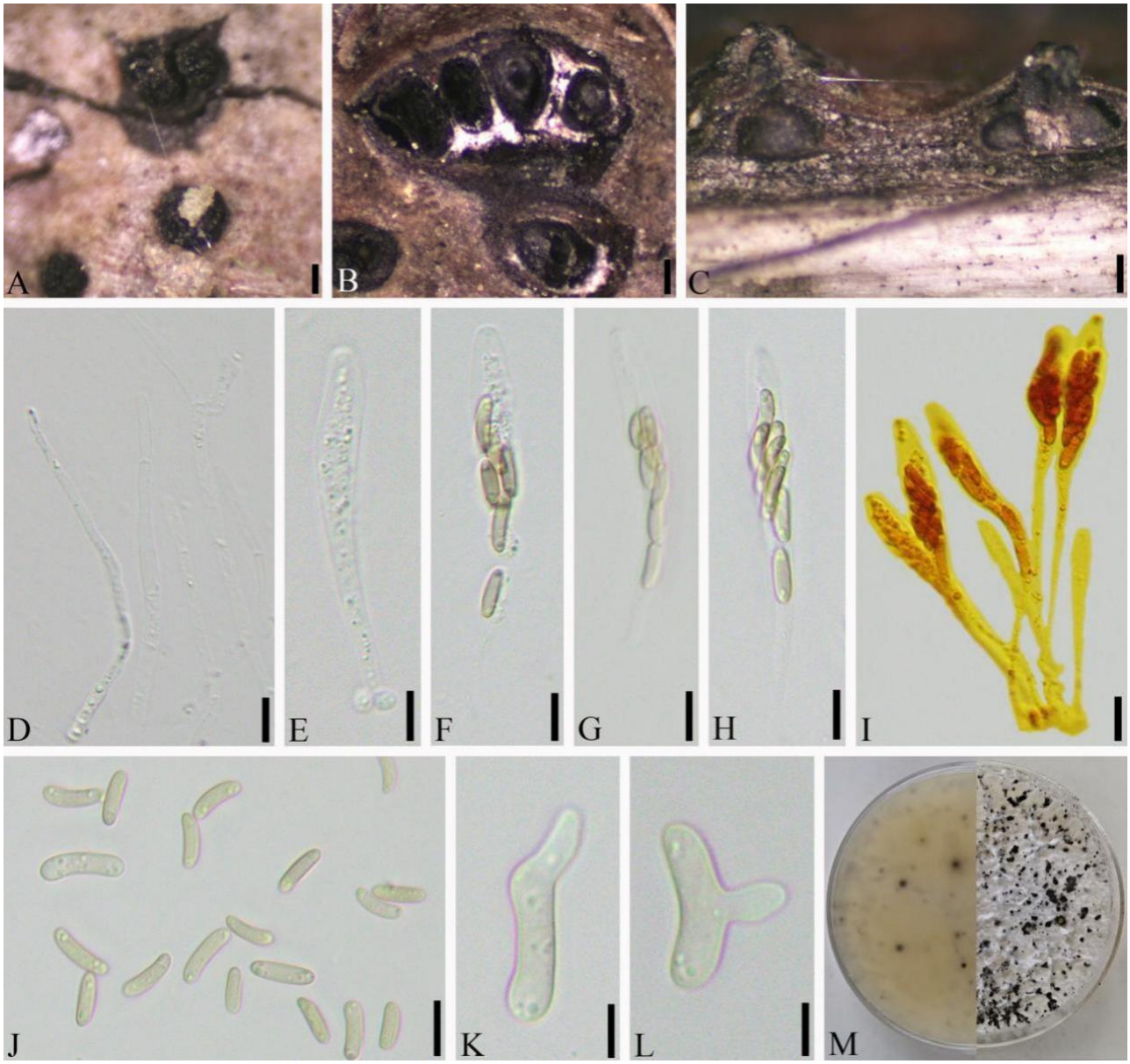


Figure 140 – *Paraeutypella citricola* (SICAU 23-0101). A Appearance of ascostroma in host substrate. B Section through ascoma. D Vertical section of ascomata. F paraphyses. E–H Asci. I Asci in Melzer's reagent. J Ascospores. K, L Germinating ascospores. M Colonies on PDA. Scale bars: B, C = 200 μm, D–I = 15 μm, J = 10 μm, K, L = 5 μm.

88. ***Paraeutypella neijiangense*** F.H. Wang & C.L. Yang, sp. nov. Fig. 141

Index Fungorum number: IF901581; Facesoffungi number: FoF15598

Etymology – Named after locality where the fungus was isolated for the first time.

Holotype – SICAU 23–0102

Saprobic on dead branch of *Juglans regia*. *Stromata* immersed in bark of dead branches, erumpent, aggregated, circular to irregular, superficial, carbonaceous. Sexual morph: *Ascomata* 590–600 × 470–480 μm ($\bar{x}$ = 595 × 475 μm, n = 10), perithecial, with groups of 4–11 perithecia arranged in a valsoid configuration, subglobose, clustered, immersed in stromata, ostiolate. *Peridium* 18–32 μm wide, composed of two layers of *textura angularis*; inner layer cells light brown to hyaline, outer layers cells dark brown to black. *Paraphyses* not observed. *Asci* 68–108 × 5–7 μm ($\bar{x}$ = 89 × 6.5 μm, n = 20), 8-spored, unitunicate, thin-walled, clavate to cylindric-clavate, long pedicellate. *Ascospores*

4–7 × 1–2 μm ($\bar{x}$ = 5 × 1.5 μm, n = 30), overlapping biseriate, allantoid, hyaline to light brown, smooth, aseptate, usually with 2–3 guttules. Asexual morph: Not observed.

Culture characteristics – Ascospores germinating on sterile water within 12 h and germ tubes produced from both ends. Colonies on PDA reaching 60 mm diam., after 14 days at 25 ℃. The mycelium grows on the surface of the medium, medium dense, irregular, flat or effuse, slightly raised, cottony, white, margin rough. Reverse, yellowish-white. Not produced pigmentation on PDA media.

Material examined – China, Sichuan Province, Neijiang City, Dongxing District, Paifang Village (29°48′30.55″N 105°6′36.37″E, alt. 387 m), on branch of *Juglans regia*, 27 April 2022, F.-H. Wang, WFH202204062 (SICAU 23-0102, holotype), ex-type living culture SICAUCC 23-0081. *Ibid*., WFH202204062B (SICAU 24-0043), living culture SICAUCC 23-0157.

GenBank numbers – SICAUCC 23-0081: PP060697 (ITS), PP061185 (*tub*2); SICAUCC 23-0157: PP844885 (ITS), PP850065 (*tub*2).

Note – Based on the multi-gene phylogenetic analyses (Fig. 138), *Paraeutypella neijiangense* (SICAUCC 23-0081) clusters between *P. citricola* (HVGRF 01) and *P. vitis* (UCD 2428). The three species resemble each other in having stromatic ascomata that are clustered and arranged in a valsoid configuration, and 8-spored, unitunicate, clavate to cylindric-clavate, long pedicellate asci and allantoid ascospores. However, *P. citricola* (HVGRF 01) has longer than asci than *P. neijiangense* (SICAUCC 23-0081) (110–125 × 5–8 μm vs. 68–108 × 5–7 μm), but smaller ascospores (7–10 × 2–3 μm vs. 4–7 × 1–2 μm) (Dissanayake et al. 2021a, Senwanna et al. 2021), *P. vitis* (UCD 2428) has short asci than *P. neijiangense* (SICAUCC 23-0081) (40–46 × 6–8 μm μm vs. 68–108 × 5–7 μm) (Glawe & Jacobs 1987). When compared with *P. citricola* (HVGRF 01) and *P. vitis* (UCD 2428), significant base differences were found. In ITS and *tub*2, the differences between *P. neijiangense* (SICAUCC 23-0081) and *P. citricola* (HVGRF 01) were 2.19% (11/503, 11 gaps) and 1.13% (4/354, 4 gaps) respectively. Similarly, the differences between *P. neijiangense* (SICAUCC 23-0081) and *P. vitis* (UCD 2428) were also 3.44% (18/524, 3 gaps) and 4.79% (18/376, 2 gaps) respectively. The PHI test revealed no significant recombination event between our strain and the closely related taxa (Φw = 1) (Fig. 142). Based on the above evidence, *P. neijiangense* is therefore introduced as a new species.

Peroneutypa Berl., Icon. fung. (Abellini) 3(3-4): 80 (1902).

Peroneutypa was erected by Berlese (1902) to accommodate *P. bellula*, *P. corniculata* and *P. heteracantha* without designating the type species. Rappaz (1987) proposed *P. bellula* as the type species of *Peroneutypa*. Carmarán et al. (2006) resurrected eight species from *Echinomyces* and *Eutypella* and accommodated them under *Peroneutypa*. Shang et al. (2018) revised *Peroneutypa* based on multi-gene analyses with an updated key to *Peroneutypa*. Two new species were also introduced by Dayarathne et al. (2020) and three species were moved to other genera. Members of this genus are characterized by valsoid ascostromata, perithecia with long necks octosporous, clavate, sessile to subsessile asci, allantoid, hyaline or yellowish ascospores. Members of this genus are mainly saprobes and pathogens, and they are widely distributed in terrestrial habitats (Lumbsch & Huhndorf 2010b, Maharachchikumbura et al. 2015, Shang et al. 2017, Hyde et al. 2019b, De Silva et al. 2022 Mao et al. 2025). There are 71 epithets listed in Species Fungorum under *Peroneutypa*. Most of them lack molecular data (http://www.speciesfungorum.org/Index.htm, September 2024).

89. ***Peroneutypa rubiformis*** Q.J. Shang, Phukhamsak & K.D. Hyde, Phytotaxa 356(1): 7 (2018) Fig. 143

Index Fungorum number: IF553975; Facesoffungi number: FoF03872

Saprobic on dead branch of *Juglans regia*. Sexual morph: *Stromata* 530–760 × 450–690 μm ($\bar{x}$ = 695 × 570 μm, n = 10), circular to pear-shaped, inflated at the apex, scattered or gregarious, visible as black spots on the substrate, immersed, becoming raised to erumpent by a prolonged ostiolar canal. *Ascomata* (excluding neck) 275–380 × 235–340 μm ($\bar{x}$ = 335 × 290 μm, n = 10), perithecial, fully immersed in a stroma, solitary, dark brown to black, globose to subglobose, glabrous, individual ostiole with a long neck. *Ostioles* cylindrical, sulcate, straight to bent, periphysate, brown to black.

Peridium 27–58 μm wide, composed of two section layers, outer section comprising 4–6 layers, of relatively small, brown to dark brown, thick-walled cells, arranged in a *textura angularis*, inner part comprising 3–5 layers of flattened, hyaline cells of *textura angularis* to textura prismatica. *Hamathecium* 40–76 × 2–3.5 μm ($\bar{x}$ = 58 × 3 μm, n = 10), rare, cylindrical, septate, hyaline, embedded in a mucilaginous matrix, usually longer than the asci. *Asci* 24–32 × 3–5.5 μm ($\bar{x}$ = 27 × 4.5 μm, n = 20), 8-spored, unitunicate, straight or slight curved, hyaline, with a non-amyloid apical ring. *Ascospores* 3–5.2 × 1–1.8 μm ($\bar{x}$ = 4 × 1.4 μm, n = 10), overlapping 1–2-seriate, oblong to allantoid, hyaline to pale grey, aseptate, smooth-walled, usually with 1–2 oil droplets. Asexual morph: Not observed.

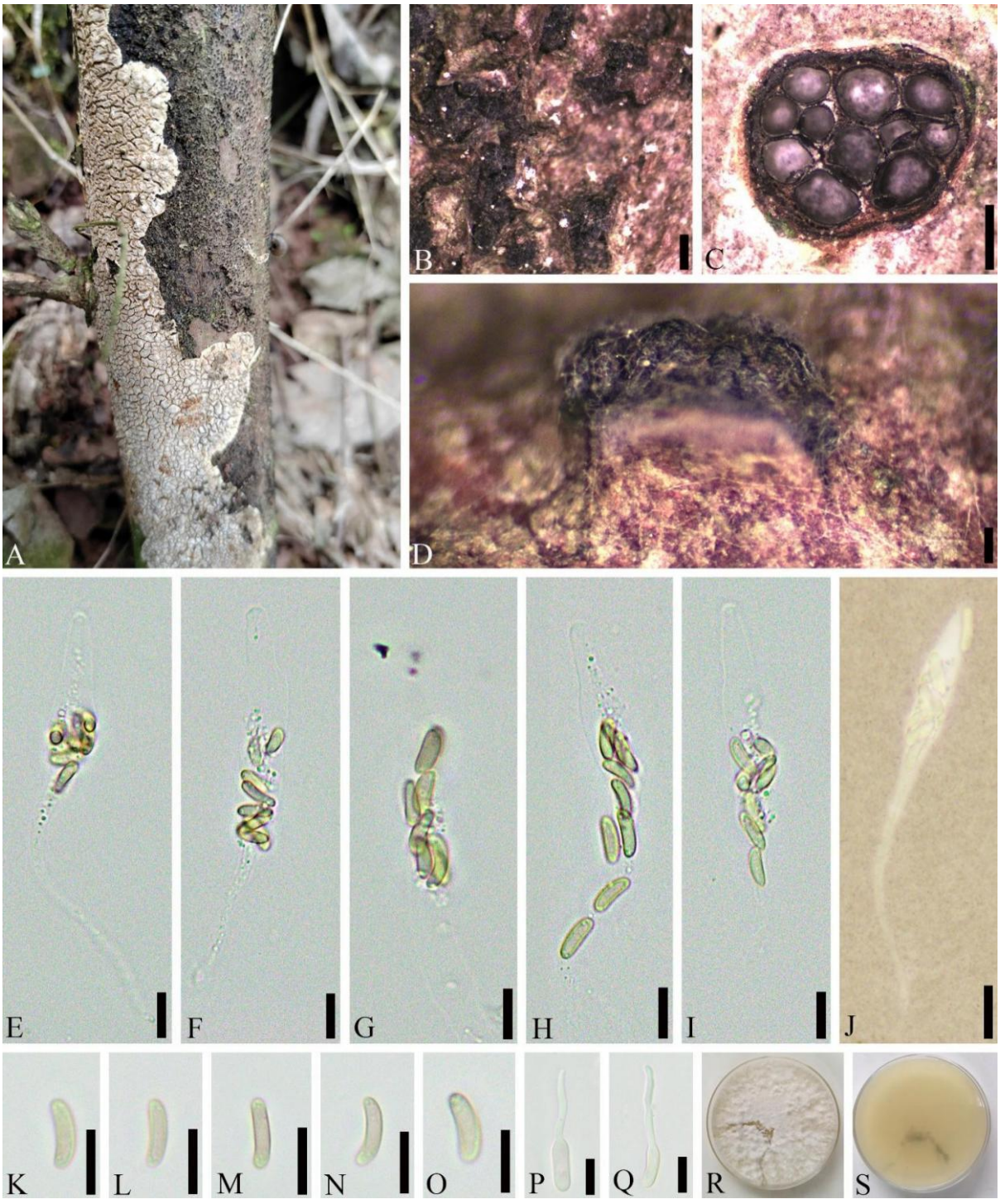


Figure 141 – *Paraeutypella neijiangense* (SICAU 23-0102, holotype). A, B, D Appearance of ascostroma in host substrate. C Section through ascoma. E–I Asci. J Asci in prepared Chinese ink.

K–O Ascospores. P, Q Germinating ascospores. R, S Colonies on PDA (R from above, S from below). Scale bars: B–D = 1000 µm, E–J = 10 µm, K–O = 8 µm, P, Q = 5 µm.

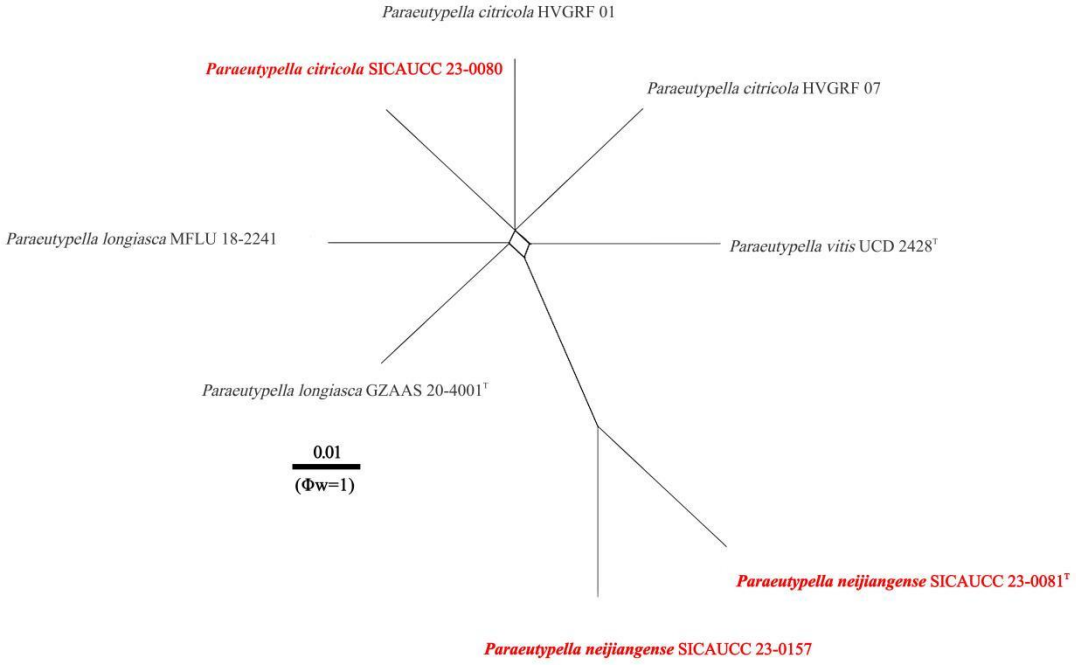


Figure 142 – Results of the PHI test of *Paraeutypella neijiangense* and closely related species using both LogDet transformation and splits decomposition. The PHI test did not find any statistically significant recombination (Φw = 1) in the data set. The new strains are represented in red and bold. "T" represents the type strain.

Culture characteristics – Ascospores germinating on sterile water within 12 h and germ tubes produced from both ends. Colonies on PDA reaching 30 mm diam., after 13 days at 25 ℃. The mycelium grows on the surface of the medium, irregular, fat or effuse, slightly raised, margin fimbriate, with aerial mycelium, and dirty white. Reverse, yellow to pale brown at the center, white at the margin, black conidia were produced after 20 days. Not produced pigmentation on PDA media.

Material examined – China, Sichuan Province, Mianyang City, Pingwu County (32°12′59.44″N 104°50′15.37″E, alt. 722 m), on dead branch of *Juglans regia*, 9 July 2022, F.-H. Wang, WFH202207061 (SICAU 23-0103), living culture SICAUCC 23-0082.

GenBank numbers – SICAUCC 23-0082: PP060698 (ITS), PP061186 (*tub*2).

Note – In our phylogenetic analysis, the new collection *Peroneutypa rubiformis* (SICAUCC 23-0082) clustered with *P. rubiformis* (MLFUCC 17-1185) with strong statistical support (100% MLBS/1.00 BYPP) (Fig. 138). Nucleotide comparisons of ITS, and *tub*2 (SICAUCC 23-0082) also showed a high homology with the sequences of *P. rubiformis* (MLFUCC 17-1185 ex-type), with a similarity of 99.3% (574/578, 3 gap), and 100% (393/393, 0 gap), respectively. Morphologically, our strain shares similar morphology with the type of Peroneutypa rubiformis in having 8-spored, unitunicate, straight or slight curved, hyaline asci (24–32 × 3–5.5 µm vs. 40−55 × 4−6 µm), with overlapping 1–2-seriate, oblong to allantoid, hyaline to pale grey, aseptate, smooth-walled, similar sized ascospores (3–5.2 × 1–1.8 µm vs. 3–5 × 1.4–1.9 µm) (Shang et al. 2018). Although there are some differences in size of asci, the variation may be due to different states of maturity. Based on comprehensive morphological and molecular evidence, this novel collection has been conclusively

identified as *P. rubiformis*, marking its first recorded occurrence in China and thereby constituting a new geographical record, as it was previously solely known to be distributed in Africa (Shang et al. 2018).

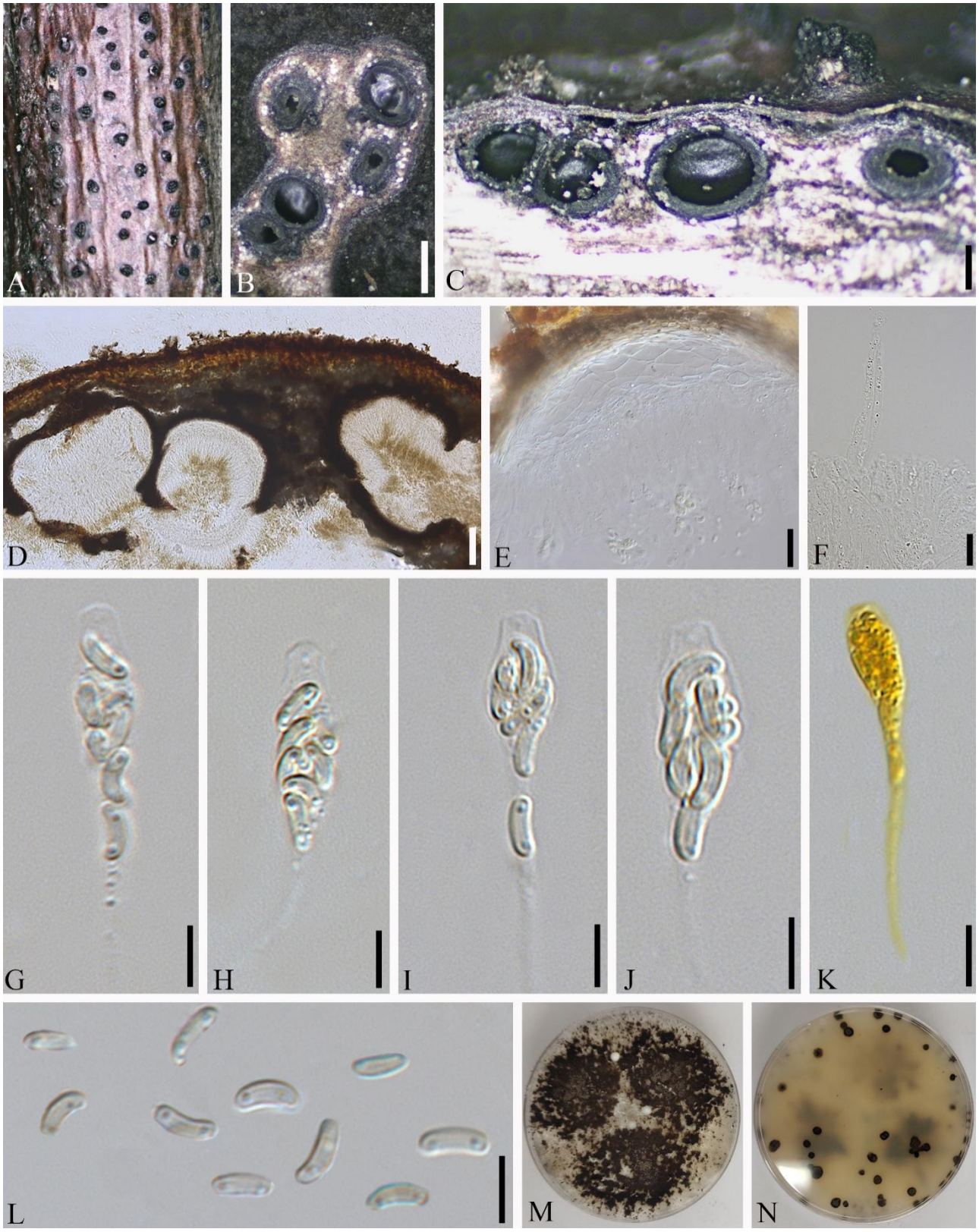


Figure 143 – *Peroneutypa rubiformis* (SICAU 23-0103). A Appearance of ascostroma in host substrate. B Section through ascoma. C, D Vertical section of ascoma. E Peridium. F Hamathecium. G–J Asci. K Asci in Melzer's reagent. L Ascospores. M, N Colonies on PDA (M from above, N from

below). Scale bars: B = 300 μm, C = 200 μm, D = 50 μm, E = 20 μm, F = 10 μm, G–K = 6 μm, L = 5 μm.

Hypoxylaceae DC., in Lamarck & de Candolle, Fl. franç., Edn 3 (Paris) 2: 280 (1805).

The name *Hypoxylaceae* was originally mentioned in Lamarck and Candolle (1805), but generally regarded as a synonym of *Xylariaceae* since they are similar in morphology. Both Daranagama et al. (2018) and Wendt et al. (2018) provided phylogenetic evidence for revising *Hypoxylaceae* and allied families at the familial level, and resurrected *Hypoxylaceae* as a separate family in *Xylariales*. Wibberg et al. (2021) subsequently strengthened the phylogenetic placement of *Hypoxylaceae* based on high quality genome sequences. A different number of genera were accepted within *Hypoxylaceae* in a series of studies (Daranagama et al. 2018, Wendt et al. 2018, Wijayawardene et al. 2018, Lambert et al. 2019, Phookamsak et al. 2019). At present, this family contains 23 genera (Hyde et al. 2020b, Cedeño-Sanchez et al 2023, Zhang et al 2023a). There are more than 1,000 kinds of records in Species Fungorum, and the *Hypoxylaceae* contributes considerably to the *Xylariales* diversity (Helaly et al. 2018). This family usually associated with decaying hardwood (Wendt et al. 2018, Lambert et al. 2019). Members of the *Hypoxylaceae* are also frequently encountered in seed plants, lichens and algae and can even be found in insect nests and sponges (Pažoutová et al. 2013, U'Ren et al. 2016, Medina et al. 2016, Leman-Loubière et al. 2017, Sir et al. 2019).

Hypoxylon Bull., Hist. Champ. Fr. (Paris) 1(1): 168 (1791).

Hypoxylon was introduced by Bulliard (1791) with *H. coccineum* as the type species. *Hypoxylon* species were delimited based mainly on morphological characteristics of stroma and ascospore, as well as the asexual morph and Stromatal pigments (Miller 1961, Ju & Rogers 1996b). Members of this genus are widely distributed and mainly inhabit dead wood as saprobes (Ju & Rogers 1996a, Wendt et al. 2018). Currently, morphological, phylogenetic, and chemotaxonomic evidence, has also been used to infer species limits in inter- and intra-genera in *Hypoxylaceae* (Sir et al. 2016). The type genus *Hypoxylon* is the largest genus in the *Hypoxylaceae* (Pourmoghaddam et al. 2020). *Hypoxylon* is quite common in China, however, the occurrence of the species in China has not been confirmed by molecular phylogenetic analyses, and the species diversity and distribution of the genus in China are unclear (Hyde et al. 2020a, b, c).

90. ***Hypoxylon perforatum*** (Schwein.) Fr., Summa veg. Scand., Sectio Post. (Stockholm): 384 (1849)

Fig. 144

Index Fungorum number: IF187004; Facesoffungi number: FoF16313

Saprobic on dead branch from *Juglans regia*. Sexual morph: *Stromata* 1–3 × 1.5–4 mm ($\bar{x}$ = 2 × 3 mm, n = 10), glomerate, fawn, sessile, gregarious or solitary, with white ostioles. *Ascomata* 243–308 × 269–326 μm ($\bar{x}$ = 270 × 297 μm, n = 10), spherical to obovoid, completely immersed in stromata. *Ostioles* 90–120 μm diam, umbilicate, white. *Asci* not observed. *Ascospores* 8–13 × 4–7 μm ($\bar{x}$ = 10 × 5 μm, n = 40), pale dark brown when immature, becoming dark brown with age, ellipsoid-inequilateral with round ends, unicellular, with germ slit straight that running along. Asexual morph: Not observed.

Culture characteristics – Ascospores germinating on sterile water within 12 h and germ tubes produced from both ends. Colonies on PDA reaching 40 mm diam., after 20 days at 25 ℃. The mycelium grows on the surface of the medium, white, occasionally raised, fluffy, with dense mycelia, umbonate margin. Reverse, chrome yellow, yellow pigment is produced in PDA.

Material examined – China, Sichuan Province, Guangyuan City, Chaotian District (36°32′28.27″N 105°52′26.31″E, alt. 555 m), on dead branch of *Juglans regia*, 19 May 2021, F.-H. Wang, WFH202105049 (SICAU 22-0143), living culture SICAUCC 22-0145.

GenBank numbers – SICAUCC 22-0145: OP963843 (ITS), OP964583 (LSU), OQ281355 (*rpb2*), OQ281419 (*tub2*).

Note – Based on the multi-gene phylogenetic results, our specimen is closely related to *Hypoxylon perforatum* (CBS 115281) (Fig. 145). Nucleotide comparisons of ITS, LSU, *tub*2, and *rpb*2 (SICAUCC 22-0145) also showed a high homology with the sequences of *H. perforatum* (CBS 115281 ex-type), with a similarity of 99.8% (599/600, 1 gap), 98.9% (831/840, 1 gap), 100% (741/741, 0 gap), and 100% (356/356, 0 gap), respectively. Morphologically, the new collections are typical of *Hypoxylon*. Based on morphological and phylogenetic evidence, this one specimen an identified as *H. perforatum.* This is the first report of *H. perforatum* from *Juglans regia*.

.

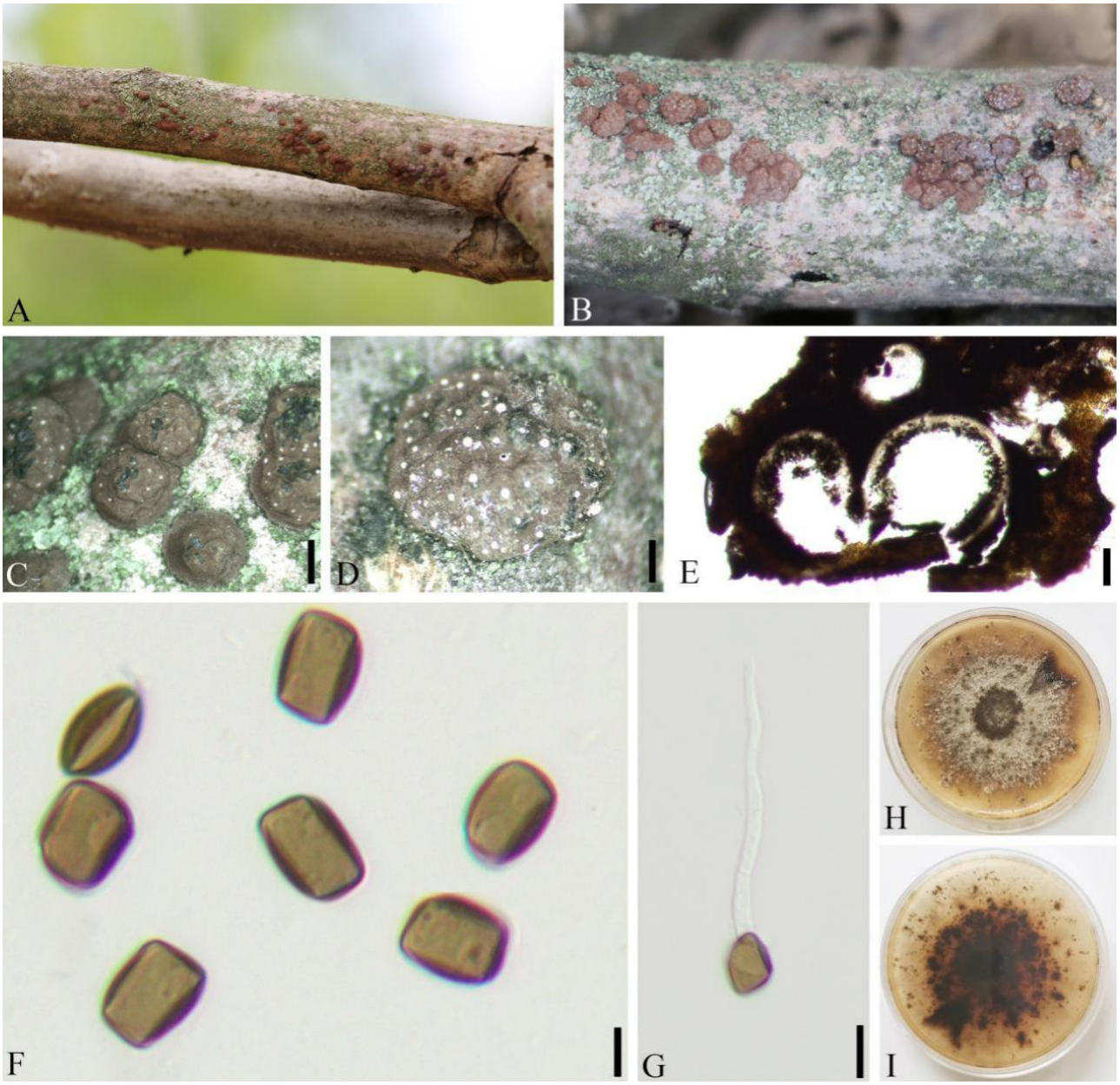


Figure 144 – *Hypoxylon perforatum* (SICAU 22-0143). A–D Appearance of ascostroma in host substrate. E Vertical section of ascoma. F Ascospores. G Germinating ascospore. H, I Colonies on PDA (H from above, I from below). Scale bars: A = 2 mm, D = 1000 μm, E = 200 μm, G = 20 μm, F = 5 μm.

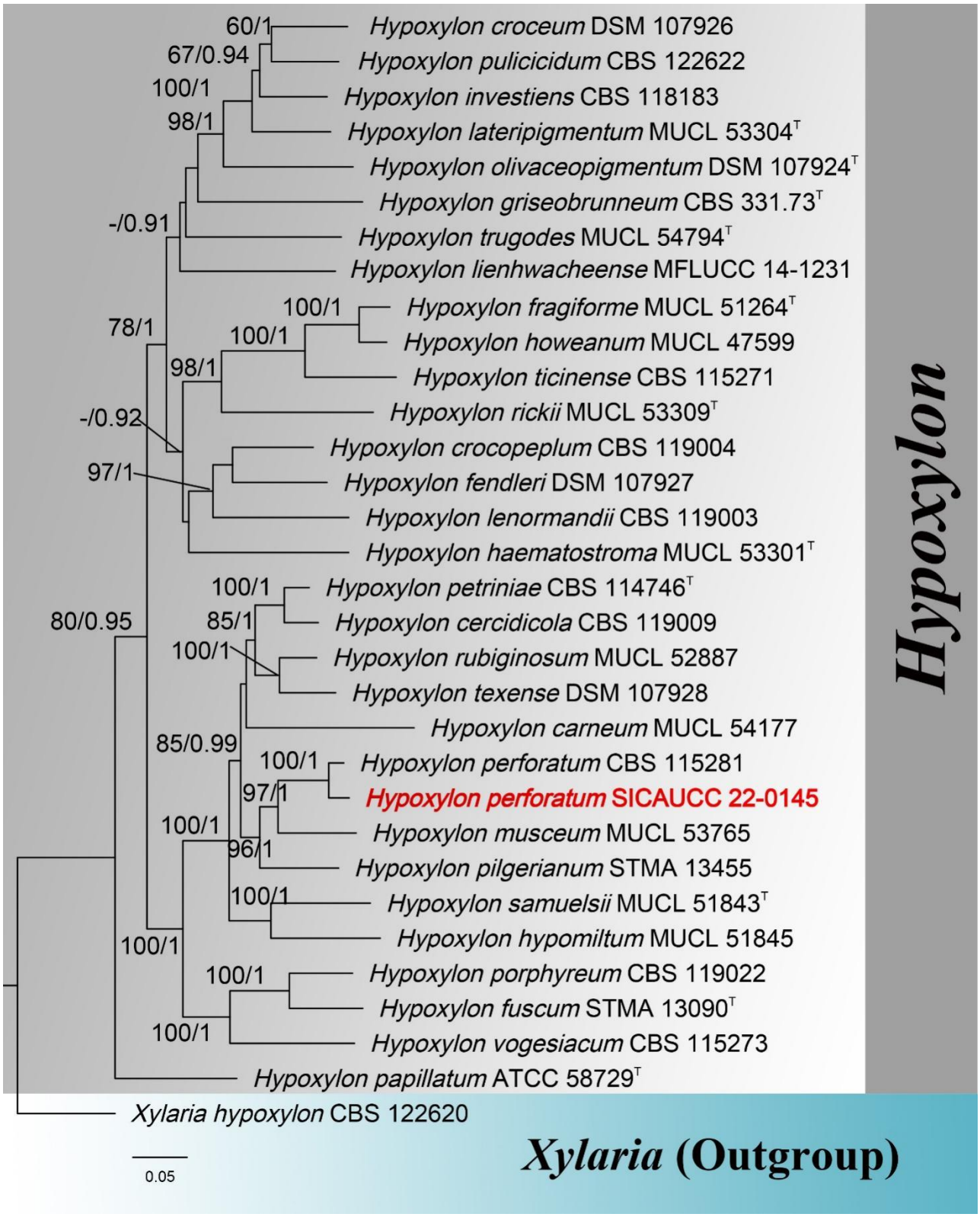


Figure 145 – Best scoring RAxML tree with a final likelihood value of -51,308.961499 based on combined ITS, LSU, *rpb2* and *tub2* sequence data of related species. The tree is rooted with *Xylaria hypoxylon* (CBS122620) in *Xylariaceae*. Thirty-two strains were included in the combined analyses which comprised 6,539 characters (951 characters for ITS, 2,654 characters for LSU, 1,170 characters for *rpb2* and 1,762 characters for *tub2*, including gap regions). The matrix had 2,890 distinct alignment patterns, with 35.40% of undetermined characters and gaps. Estimated base frequencies were as follows; A = 0.243029, C = 0.262008, G = 0.255026, T = 0.239937; substitution rates AC = 1.363003, AG = 3.984253, AT = 1.491738, CG = 1.002975, CT = 5.948331, GT =

1.000000; gamma distribution shape parameter α = 0.233514. The Bayesian inference analysis was implemented by MrBayes v.3.2.2 with the best-fit model (SYM+I+G for ITS; GTR+I+G for LSU, *rpb*2, *tub*2) of evolution estimated with MrModeltest 2.2. The species determined in this study is indicated in red and bold. Bootstrap support values for maximum likelihood (MLBS, left) ⩾ 60% and Bayesian posterior probabilities (BYPP, right) ⩾ 0.90 are indicated at the nodes, respectively. Hyphens (-) represent support values less than 60% MLBS/0.90 BYPP. The ex-type superscript "T".

DISCUSSION

Juglandaceae plants are globally cultivated for their oil, nuts, and ecological value, and studying their symbiotic fungi can enhance our understanding of their role in ecosystem biodiversity (Jahanban-Esfahlan et al. 2019, Jiménez-Luna et al. 2020). Research on walnut-associated fungi has mainly focused on a limited range of fruit and stem pathogens, leaving the broader fungal diversity and distribution largely unexplored (Dissanayake et al. 2017b, Savian et al. 2019, López-Moral et al. 2020, 2022). Through a review of dispersed publications, we looked up 143 *Ascomycota* species associated with walnuts, with the majority of reports originating from China (110 species) and the USA (106 species) (Liu et al. 2014, Dai et al. 2017, Zhang et al. 2023a, Farr and Rossman 2024). However, most studies lack molecular data and primarily focus on pathogenic fungi. In this study, we systematically investigate the diversity of walnut-associated fungi in China's Sichuan Province, using both morphological examination and phylogenetic analysis. A total of 90 species of plant fungi associated with plants in the *Juglandaceae* family have been identified and described, spanning four classes (*Dothideomycetes*, *Sordariomycetes*, *Eurotiomycetes*, and *Leotiomycetes*), 14 orders, 26 families, and 42 genera. Of the species identified, 54 (60%) were from the class *Dothideomycetes* and 34 (37.8%) from *Sordariomycetes*. In contrast, *Eurotiomycetes* and *Leotiomycetes* were represented by only one species each, making up just 2.2% of the total. This exhibits a high degree of similarity to previous research. For instance, Tian et al. (2024) conducted research on the taxonomy of *Ascomycetes* associated with economically important monocotyledonous plants in China and Thailand. Their findings revealed that the fungal species were predominantly concentrated in *Dothideomycetes* (41 species) and *Sordariomycetes* (35 species), with only one species found in *Eurotiomycetes*. While Yang et al. (2024), in their analysis of *Ascomycetes* associated with bamboo, found that the majority of fungi were also concentrated in *Dothideomycetes* and *Sordariomycetes*. The research by Yu et al. (2024) also confirms this point. Numerous other studies have also shown the same situation (Senwanna et al. 2021, Zhou et al. 2023, Konta et al. 2023). This indicates that *Dothideomycetes* and *Sordariomycetes* exhibit high species richness and widespread distribution. In terms of isolation sites, fungi are mainly distributed on the leaves and branches of walnut trees (36 species on branches, accounting for 40%; 25 species on leaves, accounting for 27.78%; 18 species on twigs, accounting for 20%; 5 species on fruits, accounting for 5.56%; 5 species on petiole, accounting for 5.56%; and 1 species on trunks, accounting for 1.1%).

In actual production, it has been found that most walnut varieties are susceptible to various fungal diseases (Chen et al. 2014, Montecchio et al. 2015, Eichmeier et al. 2020, Han et al. 2021). Among them, leaf diseases and stem diseases have the most severe impact and have been frequently reported in recent decades (Yang et al. 2011a, Varjas et al. 2021). These diseases directly affect the yield and quality of walnuts, and even cause large-scale death of walnut plants, resulting in incalculable losses (Antony et al. 2023). The anthracnose disease of walnuts has consistently been one of the most frequently reported diseases affecting walnut trees (Savian et al. 2019, Luongo et al. 2022, Zhang et al. 2023b). The anthracnose disease of walnuts first emerged in the United States in the 1970s. Currently, there is no ideal control method, and some regions primarily rely on chemical control (Fan et al. 2016, 2019). However, chemical agents seriously affect the quality of walnut nuts and even pose a risk for consumption (Zhao et al. 2021). Walnut anthracnose mainly affects the fruits of walnut trees, and can also occur on leaves, buds, and tender shoots, affecting both seedlings and mature trees research shows that the typical damage rate of walnut anthracnose is 20% to 40%, but in severe years, it can reach over 95%, making it a disastrous disease for the walnut industry (Li et

al. 2023b). Numerous studies have revealed that there are multiple pathogens that cause walnut anthracnose, and Concurrent infection by multiple pathogens (Zhang et al. 2023b). This study identified a total of 52 potential pathogenic fungi, among which the leaves were the primary parasitic sites for pathogenic fungi, with 25 species found there. Walnut leaf diseases have always been a focus in disease prevention and control for walnut trees. When leaves become infected, it can weaken the tree, cause premature defoliation, and affect the photosynthesis of the walnut plant. This hinders the synthesis of nutrients in the walnut plant, ultimately making it difficult for the tree to set fruit. Among them, the most severe include fungi belonging to the genera *Alternaria*, *Colletotrichum*, and *Fusarium*. Therefore, conducting systematic surveys and identifications is crucial to understanding the pathogens.

With the advancement of molecular biology, species identification has become more scientific and convenient, and the speed of species discovery has also increased significantly. However, this is still far from sufficient for the vast fungal kingdom (Hyde et al. 2022). Fungi possess not only species diversity but also genetic diversity, ecological diversity, and functional diversity. Some fungi exhibit "obligate parasitism" while others are widely distributed among different plants, with some having as many as 200 or more host species (Udayanga et al. 2014, Dissanayake et al. 2017c, Guo et al. 2020, Chaisiri et al. 2021, Du et al. 2021). Due to the influence of various factors such as the environment and hosts, many fungal species in this study exhibit a broad host range. Fusarioid species cause many notable plant diseases, such as *Fusarium* head blight or scab of cereals by members of the *F. graminearum* species complex (Wang et al. 2022). Initially, classification of *Colletotrichum* fungi primarily relied on morphological characteristics and host range (Liu et al. 2014). However, current research has found that this species is associated with various host plants as both pathogens and endophytes, spanning from the air to stored grains. This suggests that it is not host-specific and exhibits distinctly different lifestyles (Fu et al. 2019). Therefore, further research is needed to investigate the impacts of the environment and hosts on these fungi. Furthermore, the phenomenon of multiple fungal infections occurring in the same location has been observed. These observations indicate that, while specialized pathogenic fungi exhibit a certain degree of host specificity, most fungi can spread among different plants, posing challenges for disease control. Therefore, studying the evolution, community distribution, and interaction mechanisms between fungi and plants will provide assistance in disease prevention and control.

ACKNOWLEDGEMENTS

This study was supported by the Science and Technology Department of Sichuan Province (Grant No. 2022NSFSC1011).

Statements and Declarations

COMPETING INTERESTS

The authors declare no conflicts of interest regarding this article.

REFERENCES

Abdollahzadeh J, Javadi A, Mohammadi-Goltapeh E, Zare R et al. 2010 – Phylogeny and morphology of four new species of *Lasiodiplodia* from Iran. Persoonia 25, 1–10.

Abdollahzadeh J, Zare R, Phillips AJ. 2013 – Phylogeny and taxonomy of *Botryosphaeria* and *Neofusicoccum* species in Iran, with description of *Botryosphaeria scharifi* sp. nov. Mycologia 105, 210–220.

Abdulla ZK. 2023 – Taxonomy and biology of *Cladosporium endophyticum* as the first record in Iraq. Studies in Fungi 8, 1–5.

Abeywickrama PD, Wanasinghe DN, Karunarathna SC, Jayawardena RS et al. 2020 – A new host report of *Diaporthe manihotia* (*Diaporthales*, *Ascomycota*) from *Camellia* sp. in Yunnan Province, China. Asian Journal of Mycology 3, 473–489.

Abou-Mansour E, Débieux J, Ramírez-Suero M, Bénard-Gellon M et al. 2015 – Phytotoxic metabolites from *Neofusicoccum parvum*, a pathogen of Botryosphaeria dieback of grapevine. Phytochemistry 115, 2017–2215.
Adrián R, José EP, Arturo PG, Manuel ÁO. 2018 – Effect of genotype and crop year on the nutritional value of walnut virgin oil and defatted flour. Science of the Total Environment 634, 1092–1099.
Ahmed SA, van de Sande WW, Stevens DA, Fahal A et al. 2014 – Revision of agents of black-grain eumycetoma in the order *Pleosporales*. Persoonia 33, 141–154.
Ahmed SA, Desbois N, Quist D, Miossec C et al. 2015 – Phaeohyphomycosis caused by a novel species, *Pseudochaetosphaeronema martinelli*. Journal of Clinical Microbiology 53, 2927–2934.
Alasadi RMS. 2024 – *Alternaria alternata*: the most common pathogen on date palm. Studies in Fungi 9, e012.
Albu S, Schneider RW, Price PP, Doyle VP. 2016 – *Cercospora cf. fagellaris* and *Cercospora cf. sigesbeckiae* are associated with *Cercospora* leaf blight and purple seed stain on soybean in North America. Phytopathology 106, 1376–1385.
Alizadeh A, Javan-Nikkhah M, Nourmohammadi Nazarian R, Liu F et al. 2022 – New species of *Colletotrichum* from wild *Poaceae* and *Cyperaceae* plants in Iran. Mycologia 114, 89–113.
Alinta F, Nicole B, Xabier VC, Edward CYL et al. 2025 – *Penicillium psychrofluorescens* sp. nov., a naturally autofluorescent Antarctic fungus. Mycology, 1–24.
Almeida ÁMR, Piuga FF, Marin SRR, Binneck E et al. 2005 – Pathogenicity, molecular characterization, and cercosporin content of Brazilian isolates of *Cercospora kikuchii*. Tropical Plant Pathology 30, 594–602.
Alves A, Crous PW, Correia A, Phillips AJL. 2008 – Morphological and molecular data reveal cryptic speciation in *Lasiodiplodia theobromae*. Fungal Diversity 28, 1–13.
Antony S, Billones-Baaijens R, Stodart BJ, Steel CC et al. 2023 – Incidence and distribution of *Botryosphaeriaceae* species associated with dieback in walnut orchards in Australia. Plant Pathology 72, 610–622.
Ariyawansa HA, Hyde KD, Jayasiri SC, Buyck B et al. 2015 – Fungal diversity notes 111–252 taxonomic and phylogenetic contributions to fungal taxa. Fungal Diversity 75, 1–274.
Ariyawansa HA, Hyde KD 2018 – Additions to *Pestalotiopsis* in Taiwan. Mycosphere 9, 999–1013.
Aumentado HD, Balendres MA. 2024 – Novel species and new records of *Diaporthe* causing eggplant leaf and fruit blight in the Philippines. Mycological Progress 23, 1–12.
Bai Q, Wang GP, Hong N, Guo YS et al. 2017 – First report of *Diaporthe tulliensis* and *D. actinidiae* causing kiwifruit stem canker in Hubei and Anhui Provinces, China. Plant Disease 101, 508–509.
Bainier G. 1907 – Mycothèque de lÉcole de Pharmacie, XII-XVI. Bulletin de la Société Mycologique de France 23, 90–110.
Bakhshi M, Arzanlou M, Babay-Ahari A, Groenewald JZ et al. 2015 – Is morphology in *Cercospora* a reliable reflection of generic affinity. Phytotaxa 213, 22–34.
Bakhshi M, Arzanlou M, Babay ahari A, Groenewald JZ et al. 2018 – Novel primers improve species delimitation in *Cercospora*. IMA Fungus 9, 299–332.
Bao DF, Luo ZL, Liu JK, Bhat DJ et al. 2018 – Lignicolous freshwater fungi in China III, New species and record of *Kirschsteiniothelia* from northwestern Yunnan Province. Mycosphere 9, 755–768.
Bao DF, Hyde KD, Maharachchikumbura SSN, Perera RH et al. 2023 – Taxonomy, phylogeny and evolution of freshwater *Hypocreomycetidae* (*Sordariomycetes*). Fungal Diversity 121, 1–94.
Barr ME. 1993 – Notes on the *Pleomassariaceae*. Mycotaxon 49, 129–142.
Barr ME. 2002 – *Teichosporaceae*, another family in the *Pleosporales*. Mycotaxon 82, 373–389.
Belisario A, Scotton M, Santori A, Onofri S. 2008 – Variability in the Italian population of *Gnomonia leptostyla*, homothallism and resistance of *Juglans* species to anthracnose. Forest Pathology 38, 129–145.

Benny GL, Kimbrough JW. 1980 – A synopsis of the orders and families of *Plectomycetes* with keys to genera. Mycotaxon 12, 1–91.
Bensch K, Braun U, Groenewald JZ, Crous PW. 2012 – The genus *Cladosporium*. Studies in Mycology 72, 1–401.
Bensch K, Groenewald JZ, Meijer M, Dijksterhuis J et al. 2018 – *Cladosporium* species in indoor environments. Studies in Mycology 89, 177–301.
Berbee ML, Pirseyedi M, Hubbard S. 1999 – *Cochliobolus* phylogenetics and the origin of known, highly virulent pathogens, inferred from ITS and glyceraldehyde-3-phosphate dehydrogenase gene sequences. Mycologia 91, 964–977.
Berlese AN. 1902 – Icones Fungorum Omnium Hucusque Cognitorum. (1900–1905). 3, pp 80–82.
Bessadat N, Bataillé-Simoneau N, Colou J, Hamon B, et al. 2025 – New members of *Alternaria* (*Pleosporales*, *Pleosporaceae*) collected from *Apiaceae* in Algeria. MycoKeys 113, 169–92.
Bhunjun CS, Phukhamsakda C, Jayawardena RS, Jeewon R et al. 2021 – Investigating species boundaries in *Colletotrichum*. Fungal Diversity 107, 107–127.
Bier JE. 1939 – Septoria canker of introduced and native hybrid poplars. Canadian Journal of Research 17, 195–204.
Boehm EWA, Mugambi GK, Miller AN, Huhndorf SM et al. 2009a – A molecular phylogenetic reappraisal of the *Hysteriaceae*, *Mytilinidiaceae* and *Gloniaceae* (*Pleosporomycetidae*, *Dothideomycetes*) with keys to world species. Studies in Mycology 64, 49–83.
Boehm EWA, Schoch CL, Spatafora JW. 2009b – On the evolution of the *Hysteriaceae* and *Mytilinidiaceae* (*Pleosporomycetidae*, *Dothideomycetes*, *Ascomycota*) using four nuclear genes. Mycological Research 113, 461–479.
Boerema GH, Dorenbosch MMJ. 1979 – Mycologisch-taxonomisch onderzoek in Jaarboek 1978. Verslagen en Mededelingen Plantenziektenkundige Dienst 153, 17–21.
Boerema GH. 1997 – Contributions towards a monograph of *Phoma* (*Coelomycetes*) V. Subdivision of the genus in sections. Mycotaxon 64, 321–333.
Boonmee S, Ko TW, Chukeatirote E, Hyde KD et al. 2012 – Two new *Kirschsteiniotheli* a species with *Dendryphiopsis* anamorphs cluster in *Kirschsteiniotheliaceae* fam. nov. Mycologia 104, 698–714.
Boonmee S, Wanasinghe DN, Calabon MS, Huanraluek N et al. 2021 – Fungal diversity notes 1387-1511, taxonomic and phylogenetic contributions on genera and species of fungal taxa. Fungal Diversity 111, 1–335.
Booth C. 1971 – The genus *Fusarium*. Commonwealth Mycological Institute, Kew, Surrey, England, pp 1–237.
Braun U, Crous PW, Dugan F, Groenewald JE et al. 2003 – Phylogeny and taxonomy of *Cladosporium*-like hyphomycetes, including *Davidiella* gen. nov, the teleomorph of *Cladosporium* sstr. Mycological Progress 2, 3–18.
Bruen TC, Philippe H, Bryant D. 2006 – A simple and robust statistical test for detecting the presence of recombination. Genetics 172, 2665–2681.
Bulliard P. 1791 – Histoire des champignons de la France. BiblioBazaar, Charleston, 1–368.
Cannon PF, Damm U, Johnston PR, Weir B. 2012 – *Colletotrichum* current status and future directions. Studies in Mycology 73, 181–213.
Carbone I, Kohn LM. 1999 – A method for designing primer sets for speciation studies in filamentous ascomycetes. Mycologia 91, 553–556.
Carmarán CC, Romero AI, Giussani LM. 2006 – An approach towards a new phylogenetic classification in *Diatrypaceae*. Fungal Diversity 23, 67–87.
Castlebury LA, Rossman AY, Jaklitsch WJ, Vasilyeva LN. 2002 – A preliminary overview of the Diaporthales based on large subunit nuclear ribosomal DNA sequences. Mycologia 94, 1017–1031.
Cedeño-Sanchez M, Charria-Girón E, Lambert C, Luangsa-ard JJ et al. 2023 – Segregation of the genus *Parahypoxylon* (*Hypoxylaceae*, *Xylariales*) from *Hypoxylon* by a polyphasic taxonomic approach. MycoKeys 95, 131–162.

Cesati V, De Notaris G. 1863 – Schema di classificazione degli sferiacei italici aschigeri piu'o meno appartenenti al genere Sphaeria nell'antico significato attribuitoglide Persoon. Comment Society Crittog Ital 4, 177–240.
Chaisiri C, Liu X, Lin Y, Fu Y et al. 2021 – Phylogenetic and haplotype network analyses of *Diaporthe eres* species in China based on sequences of multiple loci. Biology 10, 179.
Chang DC, Grant GB, O'Donnell K, Wannemuehler K et al. 2006 – Multistate outbreak of *Fusarium* keratitis associated with use of a contact lens solution. JAMA 296, 953–963.
Chang G, Zhang ZB. 2014 – Functional traits determine formation of mutualism and predation interactions in seed-rodent dispersal system of a subtropical forest. Acta Oecologica 55, 43–50.
Chaverri P, Salgado C, Hirooka Y, Rossman A et al. 2011 – Delimitation of *Neonectria* and *Cylindrocarpon* (*Nectriaceae*, *Hypocreales*, *Ascomycota*) and related genera with *Cylindrocarpon*-like anamorphs. Studies in Mycology 68, 35–56.
Chen Q, Bakhshi M, Balci Y, Broders KD et al. 2022a – Genera of phytopathogenic fungi: GOPHY 4. Studies in Mycology 101, 417–564.
Chen SF, Morgan DP, Hasey JK, Anderson K et al. 2014 – Phylogeny, morphology, distribution, and pathogenicity of *Botryosphaeriaceae* and *Diaporthaceae* from English walnut in California. Plant Disease 98, 636–652.
Chen W, Swart WJ. 2000 – First report of stem canker of English walnut caused by *Fusarium solani* in south Africa. Plant Disease 84, 592–592.
Chen Y, Tian W, Guo Y, Madrid H et al. 2022b – *Synhelminthosporium* gen. et sp. nov. and two new species of *Helminthosporium* (*Massarinaceae*, *Pleosporales*) from Sichuan Province, China. Journal of Fungi 8, 712.
Chethana TKW, Jayawardene RS, Zhang W, Zhou YY et al. 2019 – Molecular characterization and pathogenicity of fungal taxa associated with cherry leaf spot disease. Mycosphere 10, 490–530.
Chethana TKW, Jayawardena RS, Chen YJ, Konta S et al. 2021 – Appressorial interactions with host and their evolution. Fungal Diversity 110, 75–107.
Chevallier FF. 1826 – Flore Générale des Environs de Paris. 1, 1–674.
Chiriví-Salomón JS, Danies G, Restrepo S, Sanjuan T. 2015 – *Lecanicillium sabanense* sp. nov. (*Cordycipitaceae*) a new fungal entomopathogen of coccids. Phytotaxa 234, 63–74.
Chomnunti P, Hongsanan S, Hudson BA, Tian Q et al. 2014 – The sooty moulds. Fungal Diversity 66, 1–36.
Chu RT, Dou ZP, He W, Zhang Y. 2021 – Two novel species of *Botryosphaeria* causing stem canker of blueberries from China. Mycosystema 40, 473–486.
Chupp C. 1954 – A monograph of the fungus genus *Cercospora*. AIBS Bulletin 3, 11.
Clements FE. 1909 – The Genera of Fungi. H. W. Wilson Co, Minneapolis, MN.
Clements FE, Shear CL. 1931 – The genera of fungi. HW Wilson Co. Publ, Minneapolis.
Clendenin L. 1896 – *Lasiodiplodia* E. & E, n. gen. Bot Gaz 21, 92
Coates L, Johnson G. 1997 – Postharvest diseases of fruit and vegetables. In, Plant pathogens and Plant Disease (Brown JF, Ogle HJ, eds). Rockvale Publications, Armidale, Australia, 533–548.
Corda ACI. 1831 – Die Pilze Deutschlands. In: Sturm J (ed) Deutschlands flora in abbildungen nach der natur mit Beschreibungen,vol 3, Abt. 12. Sturm, Nürnberg, pp 33–64.
Corda ACJ. 1839 – Pracht—fora. Europaeischer Schimmel-Bildungen.
Corda ACJ. 1842 – Icones fungorum hucusque cognitorum. 5, 1–92.
Corlett M. 1963 – The developmental morphology of two species of *Microascus*. Canadian Journal of Botany 41, 253–266.
Corlett M. 1966 – Developmental studies in the *Microascaceae*. Canadian Journal of Botany 44, 79–88.
Crous, PW, Braun, U. 2003 – *Mycosphaerella* and its anamorphs: 1. Names published in *Cercospora* and *Passalora*. CBS Biodiversity Ser 1, 1–571.
Crous PW, Slippers B, Wingfeld MJ, Rheeder J et al. 2006a – Phylogenetic lineages in the *Botryosphaeriaceae*. Studies in Mycology 55, 235–253

Crous PW, Groenewald JZ, Risède JM, Wingfield BD et al. 2006b – *Calonectria* species and their *Cylindrocladium* anamorphs: species with clavate vesicles. Studies in Mycology 55, 213–226.
Crous PW, Schoch CL, Hyde KD, Wood AR et al. 2009 – Phylogenetic lineages in the *Capnodiales*. Studies in Mycology 64, 17–47.
Crous PW, Tanaka K, Summerell BA, Groenewald JZ. 2011 – Additions to the *Mycosphaerella* complex. IMA Fungus 2, 49–64.
Crous PW, Wingfield MJ, Guarro J, Cheewangkoon R et al. 2013 – Fungal Planet description sheets: 154–213. Persoonia 31, 188–296.
Crous PW, Quaedvlieg W, Hansen K, Hawksworth DL et al. 2014 – *Phacidium* and *Ceuthospora* (*Phacidiaceae*) are congeneric: taxonomic and nomenclatural implications. IMA Fungus 5, 173–193.
Crous PW, Carris LM, Giraldo A, Groenewald JZ et al. 2015a – The genera of fungi–fxing the application of the type species of generic names–G2: *Allantophomopsis*, *Latorua*, *Macrodiplodiopsis*, *Macrohilum*, *Milospium*, *Protostegia*, *Pyricularia*, *Robillarda*, *Rotula*, *Septoriella*, *Torula* and *Wojnowicia*. IMA Fungus 6, 163–198.
Crous PW, Wingfeld MJ, Le Roux JJ, Richardson DM et al. 2015b – Fungal planet description sheets: 371–399. Persoonia 35, 264–327.
Crous PW, Wingfeld MJ, Burgess TI, Carnegie AJ et al. 2017 – Fungal planet description sheets: 625–715. Persoonia 39, 270–467.
Crous PW, Luangsa-Ard JJ, Wingfeld MJ, Carnegie AJ et al. 2018 – Fungal Planet description sheets: 785–867. Persoonia 41, 238–417.
Crous PW, Lombard L, Sandoval-Denis M, Seifert KA et al. 2021 – *Fusarium*: more than a node or a foot-shaped basal cell. Studies in Mycology 98, 100116.
Dai DQ, Bahkali AH, Li WJ, Bhat DJ et al. 2015 – *Bambusicola loculata* sp. nov. (*Bambusicolaceae*) from bamboo. Phytotaxa 213, 122–130.
Dai DQ, Phookamsak R, Wijayawardene NN, Li WJ et al. 2017 – Bambusicolous fungi. Fungal Diversity 82, 1–05.
Damm U, Woudenberg JHC, Cannon PF, Crous PW. 2009 – *Colletotrichum* species with curved conidia from herbaceous hosts. Fungal Diversity 39, 45–87.
Damm U, Cannon PF, Woudenberg JHC, Crous PW. 2012 – The *Colletotrichum acutatum* species complex. Studies in Mycology 73, 37–113.
Dao HT, Beattie GAC, Rossman AY, Burgess LW et al. 2016 – Four putative entomopathogenic fungi of armoured scale insects on *Citrus* in Australia. Mycological Progress 15, 1–14.
Daranagama DA, Hyde KD, Sir EB, Thambugala KM et al. 2018 – Towards a natural classification and backbone tree for *Graphostromataceae*, *Hypoxylaceae*, *Lopadostomataceae* and *Xylariaceae*. Fungal Diversity 88, 1–165.
Dayarathne MC, Jones EBG, Maharachchikumbura SSN, Devadatha B et al. 2020 – Morpho-molecular characterization of microfungi associated with marine based habitats. Mycosphere 11, 1–188.
De Almeida DAC, Gusmão LFP, Miller AN. 2014 – A new genus and three new species of hysteriaceous ascomycetes from the semiarid region of Brazil. Phytotaxa 176, 298–308.
De Gruyter J, Woudenberg JH, Aveskamp MM, Verkley GJ et al. 2010 – Systematic reappraisal of species in *Phoma* section *Paraphoma*, *Pyrenochaeta* and *Pleurophoma*. Mycologia 102, 1066–1081.
De Hoog GS, Gerrits van den Ende AHG. 1998 – Molecular diagnostics of clinical strains of filamentous basidiomycetes. Mycoses 41, 183–189.
De Hoog GS, Guarro J, Gene J, Figueras MJ. 2000 – Atlas of clinical fungi, Centraalbureau voor Schimmelcultures. Utrecht, The Netherlands 276–282.
De Hoog GS, Guarro J, Gené J, Figueras MJ. 2011 – Atlas of clinical fungi (CD-ROM), 3rd edn. CBS-KNAW Fungal Biodiversity Center, Utrecht.

De Silva DD, Groenewald JZ, Crous PW, Ades PK et al. 2019a – Identification, prevalence and pathogenicity of *Colletotrichum* species causing anthracnose of *Capsicum annuum* in Asia. IMA Fungus 10, 1193.
De Silva NI, Phillips AJ, Liu JK, Lumyong S et al. 2019b – Phylogeny and morphology of *Lasiodiplodia* species associated with Magnolia Forest plants. Scientific Reports 9, 1–11
De Silva NI, Hyde KD, Lumyong S, Phillips AJL et al. 2022 – Morphology, phylogeny, host association and geography of fungi associated with plants of *Annonaceae*, *Apocynaceae* and *Magnoliaceae*. Mycosphere 13, 955–1076.
Denman S, Crous PW, Taylor JE, Kang JCet al. 2000 – An overview of the taxonomic history of *Botryosphaeria*, and a re-evaluation of its anamorphs based on morphology and ITS rDNA phylogeny. Studies in Mycology 45, 129–140
Dhillon B, Feau N, Aerts AL, Beauseigle S et al. 2015 – Horizontal gene transfer and gene dosage drives adaptation to wood colonization in a tree pathogen. Proceedings of the National Academy of Sciences 112, 3451–3456.
Dissanayake AJ, Phillips AJL, Hyde KD, Li XH. 2016 – *Botryosphaeriaceae*: current status of genera and species. Mycosphere 7, 1001–1073
Dissanayake AJ, Zhang W, Liu M, Hyde KD et al. 2017a – *Diaporthe* species associated with peach tree dieback in Hubei, China. Mycosphere 8, 533–549.
Dissanayake AJ, Camporesi E, Hyde KD, Zhang W et al. 2017b – Molecular phylogenetic analysis reveals seven new *Diaporthe* species from Italy. Mycosphere 8, 853–877.
Dissanayake AJ, Zhang W, Liu M, Hyde KD et al. 2017c – *Diaporthe* species associated with peach tree dieback in Hubei, China. Mycosphere 8, 533–549.
Dissanayake AJ, Bhunjun CS, Maharachchikumbura SSN, Liu JK et al. 2020 – Applied aspects of methods to infer phylogenetic relationships amongst fungi. Mycosphere 11, 2652–2676.
Dissanayake LS, Wijayawardene NN, Dayarathne MC, Samarakoon MC et al. 2021a – *Paraeutypella guizhouensis* gen. et sp. nov. and *Diatrypella longiasca* sp. nov. *Diatrypaceae* from China. Biodiversity Data Journal 9, e63864.
Dissanayake AJ, Chen YY, Cheewangkoon R, Liu JK et al. 2021b – Occurrence and morpho-molecular identification of *Botryosphaeriales* species from Guizhou Province, China. Journal of Fungi 7, 893.
Drummond AJ, Rambaut A. 2007 – BEAST: Bayesian evolutionary analysis by sampling trees. BMC Evolutionary Biology 7, 214.
Dong W, Wang B, Hyde KD, McKenzie EHC et al. 2020 – Freshwater *Dothideomycetes*. Fungal Diversity 105, 319–575.
Du TY, Dai DQ, Mapook A, Lu L et al. 2023 – Additions to *Rhytidhysteron* (*Hysteriales*, *Dothideomycetes*) in China. Journal of Fungi 9, 148.
Du Y, Wang X, Guo Y, Xiao F et al. 2021 – Biological and molecular characterization of seven *Diaporthe* species associated with kiwifruit shoot blight and leaf spot in China. Phytopathologia Mediterranea 60, 177–198.
Eichmeier A, Pecenka J, Spetik M, Necas T et al. 2020 – Fungal trunk pathogens associated with *Juglans regia* in the Czech Republic. Plant Disease 104, 761–771.
Ellis JB, Everhart BM. 1894 – New species of fungi from various localities. Proc Acad Nat Science Philadelphia 46, 322–386.
Ellis MB. 1961 – Dematiaceous *Hyphomycetes*. III. Commonwealth Mycological Institute, Kew, Surrey, England.
Ellis MB. 1971 – Dematiaceous *Hyphomycetes* X. Commonwealth Mycological Institute, Kew, Surrey, England.
Ellis MB. 1976 – More Dematiaceous *Hyphomycetes*. Commonwealth Mycological Institute, Kew, Surrey, England.
Eriksson OE, Winka W. 1997 – Supraordinal taxa of Ascomycota. Myconet 1, 1–16.
Eriksson OE. 2006 – Outline of Ascomycota. Myconet 12, 1–88.

Fan XL, Yang Q, Bezerra JDP, Alvarez LV et al. 2018a – *Diaporthe* from walnut tree (*Juglans regia*) in China, with insight of the *Diaporthe eres* complex. Mycological Progress 17, 841–853.
Fan XL, Du Z, Bezerra JD, Tian CM. 2018b – Taxonomic circumscription of melanconis-like fungi causing canker disease in China. MycoKeys 42, 89–124.
Fan K, Wang J, Fu L, Li XJ et al. 2016 – Sensitivity of *Botryosphaeria dothidea* from apple to tebuconazole in China. Crop Protection 87, 1–5.
Fan K, Wang J, Fu L, Zhang GF et al. 2019 – Baseline sensitivity and control efficacy of pyraclostrobin against *Botryosphaeria dothidea* isolates in China. Plant Disease 103, 1458–1463.
Fang QL, Li XP, Wang MG, Qiao X et al. 2022 – Walnut green husk ethanol extract improves gut microbiota and their metabolites associated with NLRP3 in non-alcoholic steatohepatitis. Food & function 13, 6387–6403.
Farr DF and Rossman AY. 2024 – Fungal Databases, U.S. National Fungus Collections, ARS, USDA. Retrieved 2 September 2024, from. https: //nt.ars-grin.gov/fungaldatabases/.
Feau N, Mottet MJ, Périnet P, Hamelin RC et al. 2010 – Recent advances related to poplar leaf spot and canker caused by Septoria musiva. Canadian Journal of Plant Pathology 32, 122–134.
Fresenius G 1863 – Beitrage zur Mykologie 3. Heinrich Ludwig Brommer Verlag, Frankfurt.
Fries E. 1825 – Systema orbis vegetabilis. Typographia Academica 1, 1–374.
Fries EM. 1849 – Summa Vegetabilium Scandinaviae 2. Bonnies: Winter Park, FL, USA, 259–572.
Frisvad JC, Smedsgaard J, Larsen TO, Samson RA. 2004 – Mycotoxins, drugs and other extrolites produced by species in *Penicillium* subgenus *Penicillium*. Studies in Mycology 49, 201–241.
Fu M, Crous PW, Bai Q, Zhang PF et al. 2019 – *Colletotrichum* species associated with anthracnose of *Pyrus* spp. in China. Persoonia 42, 1–35.
Gams W. 1971 – *Cephalosporium*-artige *Schimmelpilze* (*Hyphomycetes*). Gustav Fischer Verlag, Stuttgart, Germany.
Gams W, Zare R. 2001 – A revision of *Verticillium* sect. Prostrata. III. Generic classifiation. Nova Hedwigia 72, 329–337.
Gäumann EA. 1949 – Die Pilze, Grundzüge ihrer Entwicklungsgeschichte und Morphologie. Birkhäuser, Basel.
Geiser DM, LoBuglio KF, Gueidan C. 2015 – *Pezizomycotina*: eurotiomycetes. In: Systematics and evolution. Springer, Berlin, pp 121–141.
Geiser DM, Gueidan C, Miadlikowska J, Lutzoni F et al. 2017 – *Eurotiomycetes*: *Eurotiomycetidae* and *Chaetothyriomycetidae*. Mycologia 98, 1053–1064.
Geiser DM, Al-Hatmi AM, Aoki T, Arie T et al. 2021 – Phylogenomic analysis of a 55.1- kb 19-gene dataset resolves a monophyletic *Fusarium* that includes the *Fusarium solani* species complex. Phytopathology 111, 1064–1079.
Gerlach W, Nirenberg HI. 1982 – The genus *Fusarium*–a pictorial. atlas Mitt Biol Bundesanst Land-Forstwirtsch 209, 1–406.
Glass NL and Donaldson GC. 1995 – Development of primer sets designed for use with the PCR to amplify conserved genes from filamentous *Ascomycetes*. Applied and Environmental Microbiology 61, 1323–1330.
Glawe A, Jacobs KA. 1987 – Taxonomic notes on *Eutypella vitis*, *Cryptosphaeria populina*, and *Diatrype stigma*. Mycologia 79, 135-139.
Gomes RR, Glienke C, Videira SIR, Lombard L et al. 2013 – *Diaporthe*, a genus of endophytic, *Saprobic* and plant pathogenic fungi. Persoonia 31, 1–41.
Gong S, Zhang X, Jiang S, Chen C et al. 2017 – A new species of *Ophiognomonia*, from northern china inhabiting the lesions of chestnut leaves infected with *Diaporthe eres*. Mycological Progress 16, 83–91.
Gräfenhan T, Schroers HJ, Nirenberg HI, Seifert KA et al. 2011 – An overview of the taxonomy, phylogeny, and typification of nectriaceous fungi in *Cosmospora*, *Acremonium*, *Fusarium*, Stilbella, and Volutella. Studies in Mycology 68, 79–113.

Griffin WM, Maublanc A. 1909 – Sur une maladie du cacaoyer. Rivista di Patologia Vegetale 25, 51–58
Groenewald JZ, Nakashima C, Nishikawa J, Shin HD et al. 2013 – Species concepts in *Cercospora*: spotting the weeds among the roses. Studies in Mycology 75, 115–170.
Gualberto GF, Catarino ADM, Sousa TF, da CRUZ JC et al. 2021 – *Pseudopestalotiopsis gilvanii* sp. nov. and *Neopestalotiopsis formicarum* leaves spot pathogens from guarana plant: a new threat to global tropical hosts. Phytotaxa 489, 121–139.
Guarro J. 2013 – Fusariosis, a complex infection caused by a high diversity of fungal species refractory to treatment. European Journal of Clinical Microbiology & Infectious Diseases 32, 1491–1500.
Guo YS, Crous PW, Bai Q, Fu M et al. 2020 – High diversity of *Diaporthe* species associated with pear shoot canker in China. Persoonia 45, 132–162.
Hamayun M, Khan SA, Ahmad N, Tang DS et al. 2009 – *Cladosporium sphaerospermum* as a new plant growth-promoting endophyte from the roots of *Glycine max* (L.) Merr. World Journal of Microbiology & Biotechnology 25, 627–632.
Hall TA. 1999 – BioEdit: A user-friendly biological sequence alignment editor and analysis program for Windows 95/98/NT. Nucleic Acids Symposium Series 41, 95–98.
Han S, Li YY, Wang M, Mo YY et al. 2021 – Stem rot disease of *Juglans sigillata* Dode caused by *Fusarium fujikuroi* in China. Plant Disease 105, 2019.
Hassan O, Kim JS, Romain BBND, Chang T. 2022 – An account of *Colletotrichum* species associated with anthracnose of *Atractylodes* ovata in South Korea based on morphology and molecular data. Plos one 17, e0263084.
Hattori Y, Ando Y, Sasaki A, Uechi N et al. 2021 – Taxonomical study of noteworthy species of *Botryosphaeria* in Japan. Mycobiology 49(2), 122–132
Hawksworth DL. 1985 – *Kirschsteiniothelia*, a new genus for the *Microthelia incrustans* group (*Dothideales*). Botanical Journal of the Linnean Society 91, 181–202.
Hawksworth DL, Kirk PM, Sutton BC, Pegler DN. 1995 – Ainsworth and Bisby's Dictionary of the Fungi, 8th edn. CAB International, Wallingford, UK.
He J, Li DW, Cui WL, Huang L. 2024 – Seven new species of *Alternaria* (*Pleosporales*, *Pleosporaceae*) associated with Chinese fir, based on morphological and molecular evidence. MycoKeys 101, 1–44.
Helaly SE, Thongbai B, Stadler M. 2018 – Diversity of biologically active secondary metabolites from endophytic and saprotrophic fungi of the ascomycete order *Xylariales*. Natural Product Reports 35, 992–1014.
Heuchert B, Braun U, Schubert K. 2005 – Morphotaxonomic revision of fungicolous *Cladosporium* species (*Hyphomycetes*). Schlechtendalia 13, 1–78.
Hibbett DS, Binder M, Bischof JF, Blackwell M et al. 2007 – A higher-level phylogenetic classification of the Fungi. Mycological Research 111, 509–547.
Hirooka Y, Rossman AY, Chaverri P. 2011 – A morphological and phylogenetic revision of the *Nectria cinnabarina* species complex. Studies in Mycology 68, 35–56.
Hirooka Y, Rossman AY, Samuels GJ, Lechat C et al. 2012 – A monograph of *Allantonectria*, *Nectria*, and *Pleonectria* (*Nectriaceae*, *Hypocreales*, *Ascomycota*) and their pycnidial, sporodochial, and synnematous anamorphs. Studies in Mycology 71, 1–210.
Hongsanan S, Hyde KD, Phookamsak R, Wanasinghe DN et al. 2020a – Refined families of *Dothideomycetes*: *Dothideomycetidae* and *Pleosporomycetidae*. Mycosphere 11, 1553–2107.
Hongsanan S, Hyde KD, Phookamsak R, Wanasinghe DN et al. 2020b – Refined families of *Dothideomycetes*: Orders and families incertae sedis in *Dothideomycetes*. Fungal Diversity 105, 17–318.
Hou Y, Ma X, Wan W, Long N et al. 2016 – Comparative genomics of pathogens causing brown spot disease of tobacco: *Alternaria longipes* and *Alternaria alternata*. Plos one 11, e0155258.
Hou LJ, Chen SK, Li WT, Ma R. 2022 – One new species and new Chinese record of *Rosa* fruits disease. Journal of Fungal Research 3, 166–172.

Hou WL, Giraldo A, Groenewald ZJ, Raemae T et al. 2023 – Redisposition of acremonium-like fungi in *Hypocreale*. Studies in mycology 105, 23–203.
Houbraken JAMP, Frisvad JC, Samson RA. 2010 – Taxonomy of *Penicillium citrinum* and related species. Fungal Diversity 44, 117–133.
Huang F, Chen GQ, Hou X, Fu YS et al. 2013 – *Colletotrichum* species associated with cultivated Citrus in China. Fungal Diversity 61, 61–74.
Huang CC, Liu HH, Wu PH, Chang HX et al. 2021 – First report of leaf spot caused by *Diaporthe tulliensis* on Boston Ivy (*Parthenocissus tricuspidata*) in Taiwan. Plant Disease 105, 9.
Huang S, Maharachchikumbura SSN, Jeewon R, Bhat DJ et al. 2018 – *Lecanicillium subprimulinum* (*Cordycipitaceae*, *Hypocreales*), a novel species from Baoshan, Yunnan. Phytotaxa 348, 99–108.
Hughes SJ. 1980 – *Helminthosporium velutinum*. Fungi Canadenses 163, 1−2.
Hyde KD, Cai L, McKenzie EHC, Yang YL et al. 2009 – *Colletotrichum*: a catalogue of confusion. Fungal Diversity 39, 1–17.
Hyde KD, Jones EBG, Liu JK, Ariyawansa H et al. 2013 – Families of *Dothideomycetes*. Fungal Diversity 63, 1–313.
Hyde KD, Nilsson RH, Alias SA, Ariyawansa HA et al. 2014 – One stop shop: backbones trees for important phytopathogenic genera: I. Fungal Diversity 67, 21–125.
Hyde KD, Norphanphoun C, Abreu VP, Bazzicalupo A et al. 2017 – Fungal diversity notes 603–708: taxonomic and phylogenetic contributions on genera and species of fungal taxa. Fungal Diversity 87, 1–235.
Hyde KD, Xu JC, Rapior S, Jeewon R et al. 2019a – The amazing potential of fungi: 50 ways we can exploit fungi industrially. Fungal Diversity 97, 1–136.
Hyde KD, Tennakoon DS, Jeewon R, Bhat DJ et al. 2019b – Fungal diversity notes 1036–1150: taxonomic and phylogenetic contributions on genera and species of fungal taxa. Fungal Diversity 96, 1–242.
Hyde KD, Dong Y, Phookamsak R, Jeewon R et al. 2020a – Fungal diversity notes 1151–1276: taxonomic and phylogenetic contributions on genera and species of fungal taxa. Fungal Diversity 100, 5–277.
Hyde KD, Norphanphoun C, Maharachchikumbura SSN, Bhat DJ et al. 2020b – Refined families of Sordariomycetes. Mycosphere 11, 305–1059.
Hyde KD, de Silva NI, Jeewon R, Bhat DJ et al. 2020c – AJOM new records and collections of fungi: 1–100. Asian Journal of Mycology 3, 22–294.
Hyde KD. 2022 – The numbers of fungi. Fungal Diversity 114(1), 1.
Hyde KD, Afshari N, Aumentado HD, Bhunjun CS et al. 2024a – Mycosphere Notes 469–520. Mycosphere 15, 1294–1454.
Hyde KD, Noorabadi MT, Thiyagaraja V, He MQ et al. 2024b – The 2024 Outline of Fungi and fungus-like taxa. Mycosphere 15(1), 5146–6239
Iturritxa E, Slippers B Mesanza N, Wingfield MJ. 2011 – First report of *Neofusicoccum parvum* causing canker and die-back of *Eucalyptus* in Spain. Australasian Plant Disease 6, 57–59.
Jahanban-Esfahlan A, Ostadrahimi A, Tabibiazar M, Amarowicz R. 2019 – A comprehensive review on the chemical constituents and functional uses of walnut (*Juglans* spp.) husk. International Journal of Molecular Sciences 20, 3920.
Jaklitsch WM, Fournier J, Dai DQ, Hyde KD et al. 2015 – *Valsaria* and the *Valsariales*. Fungal Diversity 73, 159–202.
Jaklitsch WM, Baral HO, Lucking R, Lumbsch HT. 2016a – Ascomycota. In: Frey W (ed) Syllabus of plant families-Adolf Engler's Syllabus der Pflanzenfamilien. Borntraeger, Stuttgart.
Jaklitsch WM, Olariaga I, Voglmayr H. 2016b – *Teichospora* and the *Teichosporaceae*. Mycological Progress 15, 1–20.
Jayasiri SC, Hyde KD, Abd-Elsalam KA, Abdel-Wahab MA et al. 2015 – The Faces of fungi database: fungal names linked with morphology, molecular and human attributes. Fungal Diversity 74, 3–18.

Jayasiri SC, Hyde KD, Jones EBG, Persoh D et al. 2018 – Taxonomic novelties of hysteriform *Dothideomycetes*. Mycosphere 9, 803–837.
Jayasiri SC, Hyde KD, Jones EBG, McKenzie E et al. 2019 – Diversity morphology and molecular phylogeny of *Dothideomycetes* on decaying wild seed pods and fruits. Mycosphere 10, 1–186.
Jayawardena RS, Hyde KD, Damm U, Cai L et al. 2016 – Notes on currently accepted species of *Colletotrichum*. Mycosphere 7, 1192–1260.
Jayawardena RS, Hyde KD, Chethana KWT, Daranagama DA et al. 2018 – Mycosphere Notes 102–168: saprotrophic fungi on *Vitis* in China, Italy, Russia and Thailand. Mycosphere 9, 1–114.
Jayawardena RS, Hyde KD, McKenzie EH, Jeewon R et al. 2019 – One stop shop III: taxonomic update with molecular phylogeny for important phytopathogenic genera: 51–75. Fungal Diversity 98, 77–160.
Jayawardena RS, Bhunjun CS, Hyde KD, Gentekaki E et al. 2021 – *Colletotrichum*: lifestyles, biology, morpho-species, species complexes and accepted species. Mycosphere 12, 519–669.
Jayawardena RS, Hyde KD, Wang S, Sun YR et al. 2022 – Fungal diversity notes 1512–1610: Taxonomic and phylogenetic contributions on genera and species of fungal taxa. Fungal Diversity 117, 1–272.
Jeewon R, Hyde KD. 2016 – Establishing species boundaries and new taxa among fungi: recommendations to resolve taxonomic ambiguities. Mycosphere 7, 1669–1677.
Jiménez-Luna I, Cadiz F, Aravena R, Larach A et al. 2020 – First report of *Diaporthe cynaroidis* and *D. australafricana* associated with walnut branch canker in Chile. Plant Disease 104, 2732.
Johnston PR, Park D, Baral HO, Galán R et al. 2014 – The phylogenetic relationships of *Torrendiella* and *Hymenotorrendiella* gen. nov. within the *Leotiomycetes*. Phytotaxa 177, 1–25.
Ju YM, Rogers JD, Huhndorf SM. 1996a – *Valsaria* and notes on *Endoxylina*, *Pseudothyridaria*, *Pseudovalsaria*, and *Roussoella*. Mycotaxon 58, 419–481.
Ju YM, Rogers JD. 1996b – A revision of the genus *Hypoxylon*. APS Press, St. Paul, PP 365.
Juhásová G, Ivanová H, Spisak J. 2006 – Biology of fungus *Gnomonia leptostyla* in agro-ecological environments of Slovakia. Mikologica Fitopatologie. 40, 538– 547.
Katoh K, Rozewicki J, Yamada KD. 2019 – MAFFT online service: multiple sequence alignment, interactive sequence choice and visualization. Briefings in Bioinformatics 20, 1160–1166.
Kepler R, Ban S, Nakagiri A et al. 2013 – The phylogenetic placement of hypocrealean insect pathogens in the genus *Polycephalomyces*: an application of One Fungus One Name. Fungal biology 117, 611–622.
Kepler RM, Luangsa-Ard JJ, Hywel-Jones NL, Quandt CA et al. 2017 – A phylogenetically-based nomenclature for *Cordycipitaceae* (*Hypocreales*). IMA Fungus 8, 335–353.
Kirk PM, Cannon PF, David JC, Stalpers JA. 2001 – Ainsworth and Bisby's Dictionary of the Fungi, 9th edn. CAB International, Wallingford, UK.
Kirk PM, Cannon PF, Minter DW, Stalpers JA. 2008 – Dictionary of the Fungi (10th edn). Wallingford, UK.
Kiyuna T, Hyde KD, Kigawa R, Sano C. 2011 – Molecular assessment of fungi in "black spots" that deface murals in the Takamatsuzuka and Kitora Tumuli in Japan: *Acremonium* sect. Gliomastix including *Acremonium tumulicola* sp. nov. and *Acremonium felinum* comb. nov. Mycoscience 52, 1–17.
Kobayashi T. 1970 – Taxonomic studies of Japanese *Diaporthaceae* with special reference to their life histories. Bull Gov For Exp Station (Japan) 226, 1–242.
Konta S, Tibpromma S, Karunarathna SC, Samarakoon MC et al. 2023 – Morphology and multigene phylogeny reveal ten novel taxa in Ascomycota from terrestrial palm substrates (*Arecaceae*) in Thailand. Mycosphere 14(1), 107–152.
Kumar V, Cheewangkoon R, Thambugala KM Jones GB et al. 2019 – *Rhytidhysteron mangrovei* (*Hysteriaceae*), a new species from mangroves in Phetchaburi Province, Thailand. Phytotaxa 266, 250–260.
Kurup VP, Shen HD, Banerjee B. 2000 – Respiratory fungal allergy. Microbes and Infection 2, 1101–1110.

Kutorga E, Hawksworth DL. 1997 – A re-assessment of the genera referred to the family *Patellariaceae* (*Ascomycota*). Systema Ascomycetum 15, 1–110.
Lamarck JB, De Candolle AP. 1805 – Flore Française 2, 1–600.
Lambert C, Wendt L, Hladki AI, Stadler M et al. 2019 – *Hypomontagnella* (*Hypoxylaceae*): a new genus segregated from *Hypoxylon* by a polyphasic taxonomic approach. Mycological Progress 18, 187–201.
Lantz H, Johnston PR, Park D, Minter DW. 2011 – Molecular phylogeny reveals a core clade of *Rhytismatales*. Mycologia 103, 57–74.
Lechat C, Fournier J. 2018 – *Clonostachys spinulosispora* (*Hypocreales*, *Bionectriaceae*), a new species on palm from French Guiana. Ascomycete.org 10, 127–130.
Lechat C, Fournier J. 2019 – Two new species of *Chaetopsina* (*Nectriaceae*) from Saül (French Guiana). Ascomycete.org 11, 127–134.
Lechat C, Fournier J. 2020 – Two new species of *Clonostachys* (*Bionectriaceae*, *Hypocreales*) from Saül (French Guiana). Ascomycete.org 12, 61–66.
Leslie JF, Summerell BA, Bullock S. 2006 – The *Fusarium* laboratory manual. Blackwell Publishing, Ames, pp 1–388.
Li FX, Chen JW, Chen Q, Liu ZY et al. 2023b – Identification, Pathogenicity, and Sensitivity to Fungicide of *Colletotrichum* Species That Causes Walnut Anthracnose in Beijing. Agronomy 13, 214.
Li G, Liu F, Li J, Liu QL et al. 2016a – Characterization of *Botryosphaeria dothidea* and *Lasiodiplodia pseudotheobromae* from English Walnut in China. Journal of Phytopathology 164, 348–353.
Li GJ, Hyde KD, Zhao RN, Hongsanan S et al. 2016b – Fungal Diversity notes 253–366: taxonomic and phylogenetic contributions to fungal taxa. Fungal Diversity 78, 1–237.
Li GQ, Chen SF, Liu QL, Liu FF. 2018 –. *Botryosphaeriaceae* from *Eucalyptus* plantations and adjacent plants in China. Persoonia 40, 63–95.
Li J, Phookamsak R, Jiang H, Bhat DJ et al. 2022 – Additions to the inventory of the genus *Alternaria* section *Alternaria* (*Pleosporaceae*, *Pleosporales*) in Italy. Journal of Fungi 8(9), 898.
Li JF, Jiang HB, Jeewon R, Hongsanan S et al. 2023d – *Alternaria*: update on species limits, evolution, multi-locus phylogeny, and classification. Studies in Fungi 8, 1.
Li QR, Long SH, Lin Y, Wu YP et al. 2023c – Diversity, morphology, and molecular phylogeny of *Diatrypaceae* from southern China. Frontiers in Microbiology 14, 1140190.
Li WJ, Bhat DJ, Camporesi E, Tian Q et al. 2015 – New asexual morph taxa in *Phaeosphaeriaceae*. Mycosphere 6, 681–708.
Li WL, Liang RR, Dissanayake AJ, Liu JK. 2023a – Mycosphere Notes 413–448: *Dothideomycetes* associated with woody oil plants in China. Mycosphere 14, 1436–1529.
Liao, CF, Hyde, KD, Chethana, KWT, Dong, W et al. 2024 – Three new *Periconia* species isolated from *Wurfbainia villosa* in Guangdong, China: A discussion on the doubtful taxa clustering in this genus. Diversity 16(3), 141.
Liao YCZ, Cao YJ, Wan Y, Li H et al. 2023 – *Alternaria arborescens* and *A. italica* causing leaf blotch on *Celtis julianae* in China. Plants-Basel 12, 3113.
Lindau G. 1897 – Hypocreales. In: Engler HA, Prantl KAE eds Die natiirlichen Pflanzenfamilien, vol 1. Verlag W. Engelman, Leipzig, pp 343–372.
Liu F, Damm U, Cai L, Crous PW. 2014 – Species of the *Colletotrichum gloeosporioides* complex associated with anthracnose diseases of *Proteaceae*. Fungal Diversity 61, 89–105.
Liu F, Hou L, Raza M, Cai L. 2017a – *Pestalotiopsis* and allied genera from Camellia, with description of 11 new species from China. Scientific Reports 7, 866.
Liu F, Bonthond G, Groenewald JZ, Cai L et al. 2019 – *Sporocadaceae*, a family of coelomycetous fungi with appendage-bearing conidia. Studies in Mycology 92, 287–415.
Liu F, Ma ZY, Hou LW, Diao YZ et al. 2022 – Updating species diversity of *Colletotrichum*, with a phylogenomic overview. Studies in Mycology 101, 1–56.

Liu F, Deng Y, Wang FH, Jeewon R et al. 2023b – Morphological and molecular analyses reveal two new species of *Microcera* (*Nectriaceae*, *Hypocreales*) associated with scale insects on walnut in China. MycoKeys 98, 19–35.
Liu JK, Phookamsak R, Doilom M, Wikee S, et al. 2012 – Towards a natural classification of *Botryosphaeriales*. Fungal Diversity 57, 149–210.
Liu JK, Hyde KD, Jones EBG, Ariyawansa HA et al. 2015 – Fungal diversity notes 1–110: taxonomic and phylogenetic contributions to fungal species. Fungal Diversity 72 1, 1–197.
Liu NG, Hongsanan S, Yang J, Bhat DJ et al. 2017b – *Periconia thailandica* (*Periconiaceae*), a new species from Thailand. Phytotaxa 323, 253–263.
Liu XF, Tibpromma S, Hughes AC, Chethana KWT et al. 2023a – Culturable mycota on bats in central and southern Yunnan Province, China. Mycosphere 14, 497–662.
Liu YJ, Whelen S, HallL BD. 1999 – Phylogenetic relationships among ascomycetes: evidence from an RNA polymerse Ⅱ subunit. Molecular Biology and Evolution 16, 1799–1808.
Liu YJ, Huang B. 2018 – *Pestalotiopsis mangiferae* causes leaf spot of Chinese Hickory (*Carya cathayensis*) in China. Plant Disease 102, 674–674.
Link HF. 1809 – Observationes in ordines plantarum naturales. Dissertatio prima, complectens Anandrarum ordines Epiphytas, Mucedines, Gastromycos et Fungos. Magazin der Gesellschaft Naturforschenden Freunde Berlin 3, 3–42.
Link HF. 1816 – Observationes in ordines plantarum naturales. Mag Ges Nat Fr Berl 2, 25–45.
Locquin M. 1984 – Mycologie Ge´ne´rale et Structurale. Masson, Paris. pp 551
Lombard L, Van der Merwe NA, Groenewald JZ, Crous PW. 2015 – Generic concepts in *Nectriaceae*. Studies in Mycology 80, 189–245.
Lombard L, Van Doorn R, Crous PW. 2019 – Neotypification of *Fusarium* chlamydosporum - a reappraisal of a clinically important species complex. Fungal Systematics and Evolution 4, 183–200.
Long Y, Hsiang T, Huang J. 2009 – First report of leaf spot of *Smilax china* caused by *Alternaria longipes* in China. Plant Pathology 58, 800.
López-Moral A, Lovera M, Raya MDC, Cortés-Cosano N et al. 2020 – Etiology of branch dieback and shoot blight of English walnut caused by *Botryosphaeriaceae* and *Diaporthe* species in Southern Spain. Plant Disease 104, 533–550.
López-Moral A, Lovera M, Domínguez BIA, Gámiz AM et al. 2022 – Effects of cultivar susceptibility, branch age, and temperature on the infection by *Botryosphaeriaceae* and *Diaporthe* fungi on English walnut (*Juglans regia* L.). Plant Disease 106, 2920–2926.
Lumbsch HT, Huhndorf SM. 2010a – Myconet volume 14. Part one. Outline of *Ascomycota* 2009 Part two. Notes on *Ascomycete* systematics. Nos. 4751–5113. Fieldiana Life and Earth Sciences 16, 1–65.
Lumbsch HT, Huhndorf SM. 2010b – Myconet volume 14 part one. Outline of *Ascomycota* 2009. Fieldiana Life and Earth Sciences 1, 1–922.
Luo X, Zhou HJ, Cao D, Yan F et al. 2022 – Domestication and selection footprints in Persian walnuts (*Juglans regia*). Plos Genetics 18(12), e1010513
Luo XX, Liao MG, Hu YF, Zhang XG et al. 2025 – Identification of three novel species and one new record of *Kirschsteiniothelia* (*Kirschsteiniotheliaceae*, *Kirschsteiniotheliales*) from Jiangxi, China. MycoKeys 112, 277–306.
Luo ZL, Hyde KD, Liu JK et al. 2019 – Freshwater *Sordariomycetes*. Fungal Diversity 99, 451–660.
Luongo L, Galli M, Garaguso I, Maharachchikumbura SSN et al. 2022 – First Report of *Colletotrichum fioriniae* and *C. nymphaeae* as Causal Agents of Anthracnose on Walnut in Italy. Plant Disease 106, 327.
Luque J, Garcia-Figueres F, Legorburu FJ et al. 2012 – Species of *Diatrypaceae* associated with grapevine trunk diseases in Eastern Spain. Phytopathologia Mediterranea 51, 528–540.
Luttrell ES. 1951 – Taxonomy of the P*yrenomycetes*. University of Missouri Studies 24, 1–3.
Luttrell ES. 1955 – The ascostromatic *Ascomycetes*. Mycologia 47, 511–532.
Luttrell ES. 1957 – *Helminthosporium nodulosum* and related species. Phytopathology 47, 540–548.

Luttrell ES. 1963 – Taxonomic criteria in *Helminthosporium*. Mycologia 55, 643–674.
Luttrell ES. 1964 – Systematics of *Helminthosporium* and related genera. Mycologia 56, 119–132.
Ma HX, Yang ZE, Song ZK, Qu Z et al. 2023 – Taxonomic and phylogenetic contributions to *Diatrypaceae* from southeastern Tibet in China. Frontiers in Microbiology 14, 1073548.
Ma R, Ye SH, Zhao Y, Michailides TJ et al. 2019 – New leaf and fruit disease of *Juglans regia* caused by *Juglanconis juglandina* in Xinjiang China. Forest Pathology 49, e12537.
Maddison WP and Maddison DR 2019 – Mesquite: a modular system for evolutionary analysis, Version 3.61.
Maharachchikumbura SSN, Hyde KD, Groenewald JZ, Xu J et al. 2014 – *Pestalotiopsis* revisited. Studies in Mycology 79, 121–186.
Maharachchikumbura SSN, Hyde KD, Jones EBG, McKenzie, EHC et al. 2015 – Towards a natural classification and backbone tree for *Sordariomycetes*. Fungal Diversity 72, 199–301.
Maharachchikumbura SSN, Larignon P, Hyde KD, Al-Sadi AM et al. 2016a – Characterization of *Neopestalotiopsis*, *Pestalotiopsis* and *Truncatella* species associated with grapevine trunk diseases in France. Phytopathologia Mediterranea 55, 380–390.
Maharachchikumbura SSN, Hyde KD, Jones EBG, McKenzie EHC et al. 2016b – Families of *Sordariomycetes*. Fungal Diversity 79, 1–317.
Malloch D. 1970 – New concepts in the *Microascaceae* illustrated by two new species. Mycologia 62, 727–740.
Maiti CK, Sen S, Acharya A. 2007 – First report of leaf blight of *Medicago sativa* caused by *Alternaria longipes* in India. Journal of Plant Pathology 89, S69.
Manawasinghe IS, Dissanayake A, Liu M, Wanasinghe D et al. 2019 – High genetic diversity and species complexity of *Diaporthe* associated with Grapevine Dieback in China. Frontiers in Microbiology 10, 1936.
Manawasinghe IS, Calabon MS, Jones EBG, Zhang YX et al. 2022 – Mycosphere notes 345–386. Mycosphere 13, 454–557.
Manogaran N, Kayalvizhi AA, Munuswamy K. 2024 – *Hysterium madraspatanum* (*Hysteriaceae*), a new species from Tropical Dry Evergreen Forest of Tamil Nadu, India. Phytotaxa 649(1), 98–110.
Mao X, Habib K, Zulfiqar R, Yang HD et al. 2025 – Three new species of *Peroneutypa* (*Diatrypaceae*, *Xylariales*) and a first record of *Eutypacamelliae* in China with updated description. MycoKeys 114, 213–238.
Markovskaja S, Kačergius A. 2014 – Morphological and molecular characterization of *Periconia pseudobyssoides* sp. nov. and closely related *P. byssoides*. Mycological Progress 13, 291–302.
Martínez ML, Labuckas DO, Lamarque AL, Maestri D et al. 2010 – Walnut (*Juglans regia* L.): Genetic resources, chemistry, by-products. Journal of the Science of Food & Agriculture 90, 1959–1967.
Mathew AJ, Jayachandran K, Mathew J. 2010 – Endophytic *Penicillium citrinum* Thom. From *Scoparia dulcis* Linn. Indian Journal of Microbiology 50, 99–102.
McAlpine D. 1902 – Fungus diseases of stone-fruit trees in Australia and their treatment. pp 1–165.
Medina R, Silva A, Andersen R, Araújo, AR et al. 2016 – Botryane sesquiterpenes and binaphthalene tetrols from endophytic fungi associated to the marine red algae *Asparagopsis taxiformis*. Planta Medica 81, S1–S381.
Meghvansi M, Khan M, Gupta R, Veer V et al. 2013 – Identification of a new species of *Cercospora* causing leaf spot disease in *Capsicum* assamicum in northeastern India. Research in Microbiology 164, 894–902.
Mehrabi M, Hemmati R, Vasilyeva LN, Trouillas FP et al. 2016 – *Diatrypella macrospora* sp. nov. and new records of diatrypaceous fungi from Iran. Phytotaxa 252, 43–55.
Mehrabi M, Hemmati R, Asgari B. 2017 – *Kirschsteiniothelia arasbaranica* sp. nov, and an emendation of the *Kirschsteiniotheliaceae*. Cryptogamie Mycologie 38, 13–25.

Mejía LC, Castlebury LA, Rossman AY, Sogonov MV et al. 2008 – Phylogenetic placement and taxonomic review of the genus *Cryptosporella* and its synonyms *Ophiovalsa* and *Winterella* (*Gnomoniaceae*, *Diaporthales*). Mycological Research 112, 23–35.
Mejía LC, Castlebury LA, Rossman AY, Sogonov MV et al. 2011a – A systematic account of the genus *Plagiostoma Gnomoniaceae*, *Diaporthales* based on morphology, host-associations, and a fourgene phylogeny. Studies in Mycology 68, 211–235.
Mejía LC, Rossman AY, Castlebury LA, White JF. 2011b – New species, phylogeny, host-associations and geographic distribution of genus *Cryptosporella* (*Gnomoniaceae*, *Diaporthales*). Mycologia 103, 379–399.
Mejía LC, Rossman AY, Castlebury LA, Yang ZL et al. 2012 – *Occultocarpon*, a new monotypic genus of *Gnomoniaceae* on *Alnus nepalensis* from China. Fungal Diversity 52, 99–105.
Miller JH. 1961 – A monograph of the world species of *Hypoxylon*. University of Georgia Press, Athens.
Miller MA, Pfeifer W, Schwartz T. 2017 – Creating the CIPRES Science Gateway for inference of large phylogenetic trees. In 2010 – gateway computing environments workshop (GCE), 1–8.
Minnis AM, Kennedy AH, Grenier DB, Palm ME et al. 2012 – Phylogeny and taxonomic revision of the *Planistromellaceae* including its coelomycetous anamorphs: contributions towards a monograph of the genus *Kellermania*. Persoonia 29, 11–28.
Monkai J, Wanasinghe DN, Jeewon R, Promputtha I et al. 2021 – Morphological and phylogenetic characterization of fungi within *Bambusicolaceae*: introducing two new species from the Greater Mekong Subregion. Mycological Progress 20, 721–732.
Monod M. 1983 – Monographie taxonomique des *Gnomoniaceae*. Beihefte zur Sydowia Annales Mycologici Ser 29, 1–315.
Montecchio L, Faccoli M, Short D, Fanchin G et al. 2015 – First report of *Fusarium solani* phylogenetic species 25 associated with early stages of thousand cankers disease on *Juglans nigra* and *Juglans regia* in Italy. Plant Disease 99, 1183.
Montenegro-Calderón JG, Martínez-Álvarez JA, Vieyra-Hernández MT, Rangel Macías LI et al. 2011 – Molecular identification of two strains of *Cercospora rodmanii* isolated from water hyacinth present in Yuriria lagoon, Guanajuato, Mexico and Identification of new hosts for several other strains. Fungal biology 115, 1151–1162.
Moreira GM, Abreu LM, Carvalho VG, Schroers HJ et al. 2016 – Multilocus phylogeny of *Clonostachys* subgenus Bionectria from Brazil and description of *Clonostachys chloroleuca* sp. nov. Mycological Progress 15, 1031–1039.
Morgan-Jones G, White JF. 1983 – Studies on the genus Phoma. III. *Paraphoma*, a new genus to accommodate *Phoma radicina*. Mycotaxon 18, 57–65.
Morton FJ, Smith G 1963 – The genera *Scopulariopsis Bainier*, *Microascus*, Zukal and *Doratomyces* Corda. Mycological Papers 86, 1–96.
Mugambi GK, Huhndorf SM. 2009 – Molecular phylogenetics of *Pleosporales*: *Melanommataceae* and *Lophiostomataceae* recircumscribed (*Plesporomycetidae*, *Dothideomycetes*, *Ascomycota*). Studies in Mycology 64, 103–121.
Müller E, von Arx JA. 1950 – Einige aspekte zur systematik pseudosphärialer ascomycete. Ber Schw Bot Ges 60, 329–397.
Nalim FA, Samuels GJ, Wijesundera RL, Geiser DM. 2011 ‐ New species from the *Fusarium solani* species complex derived from perithecia and soil in the old-world tropics. Mycologia 103(06), 1302 ‐ 1330.
Nannfeldt JA. 1932 – Studien uber die morphologie und systematik der nicht-lichenisierten inoperculaten discomyceten. Nova Acta Regiae Socal Science Upsal Ser IV 8, 1–368.
Nannizzi A. 1934 – Repertorio sistematico dei miceti dell' uomo e degli animali, vol 4. Poligrafa Meimi, Siena, pp 1–557.
Naranjo ‐ Ortiz MA, Gabaldón T. 2019 – Fungal evolution: diversity, taxonomy and phylogeny of the Fungi. Biological Reviews 94, 2101–2137.

Navale VD, Sawant AM, Vamkudoth KR. 2023 – Genetic diversity of toxigenic *Fusarium verticillioides* associated with maize grains, India. Genetics And Molecular Biology 46, 20220073.
Nees von Esenbeck CG. 1816 – Das system der pilze und schwa mme. Wurzburg, Germany.
Nelson PE, Toussoun TA, Marasas WFO 1983 – *Fusarium* species: an illustrated manual for Identification. Pennsylvania State University Press, University Park, Pennsylvania, pp 1–193.
Netto MS, Assunção IP, Lima GS, Marques MW et al. 2014 – Species of *Lasiodiplodia* associated with papaya stem-end rot in Brazil. Fungal Diversity 67, 127–141
Nishikawa J, Nakashima C. 2020 – Japanese species of *Alternaria* and their species boundaries based on host range. Fungal systematics and evolution 5, 197–281.
Nitschke T. 1867 – Pyrenomycetes Germanici: die Kernpilze Deutschlands. Breslau.
Nitschke T. 1869 – Verh Naturhist Vereines Preuss Rheinl 26, 73.
Nwe ZM, Htut KN, Aung SL, Gou YN et al. 2024 – Two novel species and a new host record of *Alternaria* (*Pleosporales*, *Pleosporaceae*) from sunflower (Compositae) in Myanmar. MycoKeys 105, 337–354.
Nylander JAA. 2004 – MrModeltest v2. Program distributed by the author. Evolutionary Biology Centre, Uppsala University, Uppsala.
O'Donnell K and Cigelnik E. 1997 – Two divergent intragenomic rDNA ITS2 types within a monophyletic lineage of the fungus *Fusarium* are nonorthologous. Molecular Phylogenetics and Evolution 7, 103–116.
O'Donnell K, Kistler HC, Cigelnik E, Ploetz, RC. 1998 – Multiple evolutionary origins of the fungus causing *Panama* disease of banana: Concordant evidence from nuclear and mitochondrial gene genealogies. Proceedings of the National Academy of Sciences of the USA 95, 2044–2049.
O'Donnell K, Nirenberg HI, Aoki T, Cigelnik E. 2000 – A multigene phylogeny of the *Gibberella fujikuroi* species complex: detection of additional phylogenetically distinct species. Mycoscience 41, 61–78.
O'Donnell K, Rooney AP, Proctor RH, Brown DW et al. 2013 – Phylogenetic analyses of *rpb*1 and *rpb*2 support a middle Cretaceous origin for a clade comprising all agriculturely and medically important fusaria. Fungal Genetics and Biology 52, 20–31.
Ogórek R, Kurczaba K, Cal M, Apoznański G et al. 2020 – A culture-based ID of micromycetes on the wing membranes of greater mouse-eared bats (Myotis myotis) from the "Nietoperek" site (Poland). Animals 10, 1337.
Ostry ME. 1997 – Butternut canker: history, biology, impact, and resistance. Unknown publisher, pp 1–9.
Orlandi F, Marrapodi S, Proietti C, Ruga LE et al. 2022 – Ecosystem functions of fruit woody species in an urban environment. Environmental Monitoring and Assessment 195(1), 118.
Pan HQ, Wang HF, Jiang YL, Zhang TY. 2014 – *Scopulariopsis*: three new species and a key to species from soils in China. Mycosystema 33, 1–6.
Pangging M, Nguyen TTT, Lee HB 2021 – Seven new records of *Penicillium* species belonging to section Lanata-Divaricata in Korea. Mycobiology 49, 363–375
Pantera A, Burgess PJ, Losada RM, Moreno G et al. 2018 – Agroforestry for high value tree systems in Europe. Agroforestry Systems 92, 945–959.
Park M, Hong S, Shin H. 2015 – *Lecanicillium uredinophilum* sp. nov. associated with rust fungi from Korea. Mycotaxon 130, 997–1005.
Park SH, Choi IY, Lee W, Galea V et al. 2017 – Identification and characterization of *Cercospora malayensis* causing leaf spot on kenaf. Mycobiology 45, 114–118.
Pärtel K, Baral HO, Tamm H, Põldmaa K. 2017 – Evidence for the polyphyly of *Encoelia* and *Encoelioideae* with reconsideration of respective families in *Leotiomycetes*. Fungal Diversity 82, 183–219.
Pažoutová S, Follert S, Bitzer J, Keck M et al. 2013 – A new endophytic insect-associated *Daldinia* species, recognised from a comparison of secondary metabolite profiles and molecular phylogeny. Fungal Diversity 60, 107–123.

Pędzik M, Auriga R, Kristak L, Antov P et al. 2022 – Physical and Mechanical Properties of Particleboard Produced with Addition of Walnut (*Juglans regia* L.) Wood Residues. Materials 15, 1280.

Pem D, Hyde KD, Doilom M, Camporesi E. 2019 – Multigene phylogenetic analyses to establish new *Valsaria* species and taxonomic significance of spore ornamentation. Plos One 14, e0217982.

Peng XJ, Wang QC, Zhang SK, Guo K et al. 2023 – *Colletotrichum* species associated with *Camellia* anthracnose in China. Mycosphere 14, 130–157.

Pennycook SR. 2017 – *Colletotrichum fioriniae* comb. & stat. nov., resolving a nomenclatural muddle. Mycotaxo 132, 149–152.

Perera RH, Hyde KD, Jones EBG, Maharachchikumbura SSN et al. 2023 – Profile of *Bionectriaceae*, *Calcarisporiaceae*, *Hypocreaceae*, *Nectriaceae*, *Tilachlidiaceae*, *Ijuhyaceae* fam. nov, *Stromatonectriaceae* fam. nov. and *Xanthonectriaceae* fam. nov. Fungal Diversity 118, 95–271.

Persoon CH 1801 – Synopsis methodica fungorum. 1–706.

Peterson SW, Vega FE, Posada F, Nagai, C et al. 2005 – *Penicillium coffeae*, a new endophytic species isolated from a coffee plant and its phylogenetic relationship to *P. fellutanum*, *P. thiersii* and *P. brocae* based on parsimony analysis of multilocus DNA sequences. Mycologia 97(3), 659–666.

Pfenning LH, de Melo MP, Costa MM, Reis A et al. 2019 – *Fusarium udum* revisited: a common, but poorly understood member of the *Fusarium fujikuroi* species complex. Mycological Progress 18, 107–117.

Phillips AJL, Alves A, Pennycook SR, Johnston PR et al. 2008 – Resolving the phylogenetic and taxonomic status of dark-spored teleomorph genera in the *Botryosphaeriaceae*. Persoonia 21, 29–55.

Phillips AJL, Alves A, Abdollahzadeh J, Slippers B et al. 2013 – The *Botryosphaeriaceae*: genera and species known from culture. Studies in Mycology 76, 51–167.

Phillips AJL, Hyde KD, Alves A, Liu JK. 2019 – Families in *Botryosphaeriales*: a phylogenetic, morphological and evolutionary perspective. Fungal Diversity 94, 1–22.

Phookamsak R, Liu JK, McKenzie EH, Manamgoda DS et al. 2014 – Revision of *Phaeosphaeriaceae*. Fungal Diversity 68, 159–238.

Phookamsak R, Wanasinghe DN, Hongsanan S, Phukhamsakda C et al. 2017 – Towards a natural classification of *Ophiobolus* and *Ophiobolus*-like taxa; introducing three novel genera *Ophiobolopsis*, *Paraophiobolus* and *Pseudoophiobolus* in *Phaeosphaeriaceae* (*Pleosporales*). Fungal Diversity 87, 299–339.

Phookamsak R, Hyde KD, Jeewon R, Bhat DJ et al. 2019 – Fungal diversity notes 929–1036: taxonomic and phylogenetic contributions on genera and species of fungal taxa. Fungal Diversity 95, 1–273.

Phookamsak R, Hongsanan S, Bhat DJ, Wanasinghe DN et al. 2024 – Exploring ascomycete diversity in Yunnan II: Introducing three novel species in the suborder *Massarineae* (*Dothideomycetes*, *Pleosporales*) from fern and grasses. MycoKeys 104, 9–50.

Phukhamsakda C, Hongsanan S, Ryberg M, Ariyawansa HA et al. 2016 – The evolution of *Massarineae* with *Longipedicellataceae* fam. nov. Mycosphere 7, 1713–1731.

Phukhamsakda C, McKenzie EHC, Phillips AJL, Jones EBG et al. 2020 – Microfungi associated with *Clematis* (*Ranunculaceae*) with an integrated approach to delimiting species boundaries. Fungal Diversity 102, 1–203.

Phukhamsakda C, Nilsson RH, Bhunjun CS, de Farias ARG et al. 2022 – The numbers of fungi: contributions from traditional taxonomic studies and challenges of metabarcoding. Fungal Diversity 114, 327–386.

Pitt JI. 1979 – The genus *Penicillium* and its teleomorphic states *Eupenicillium* and *Talaromyces*. Academic, London, pp 1–634.

Poletto T, Muniz M.F.B, Blume E, Mezzomo R et al. 2017 – First report of *Sirosporium diffusum* causing brown leaf spot on *Carya illinoinensis* in Brazil. Plant Disease 101, 381–381.
Pollack FG. 1987 – An annotated compilation of *Cercospora* names. Mycol Mem 12, 1–212.
Pourmoghaddam MJ, Lambert C, Surup F, Khodaparast SA et al. 2020 – Discovery of a new species of the *Hypoxylon rubiginosum* complex from Iran and antagonistic activities of *Hypoxylon* spp. against the Ash Dieback pathogen, *Hymenoscyphus fraxineus*, in dual culture. MycoKeys 66, 105.
Prasannath K, Shivas RG, Galea VJ, Akinsanmi OA. 2021 – *Neopestalotiopsis* species associated with flower diseases of *Macadamia integrifolia* in Australia. Journal of Fungi 7, 771.
Prasher IB, Chauhan R. 2017 – *Clonostachys indicus* sp. nov. from India. Kavaka 48, 22–26.
Prieto M, Etayo J, Olariaga I. 2021 – A new lineage of mazaediate fungi in the *Eurotiomycetes*: *Cryptocaliciomycetidae subclass*. nov, based on the new species *Cryptocalicium blascoi* and the revision of the ascoma evolution. Mycological Progress 20, 889–904.
Prihastuti H, Cai L, Chen H, McKenzie EHC et al. 2009 – Characterization of *Colletotrichum* species associated with coffee berries in northern Thailand. Fungal Diversity 39, 89–109.
Punithalingam E. 1969 – Studies on Sphaeropsidales in culture. Mycological Papers 119, 1–24.
Punithalingam E. 1979 – *Sphaeropsidales* in culture from humans. Nova Hedwig 31, 119–158.
Quaedvlieg W, Verkley GJM, Shin HD, Barretto RW et al. 2013 – Sizing up Septoria. Studies in Mycology 75, 307–390.
Quaedvlieg W, Binder M, Groenewald JZ, Summerell BA et al. 2014 – Introducing the consolidated species concept to resolve species in the *Teratosphaeriaceae*. Persoonia 33, 1–40.
Ranganathan N and Mahalingam G. 2019 – Secondary metabolite as therapeutic agent from endophytic fungi *Alternaria longipes* strain VITN14G of mangrove plant Avicennia officinalis. Journal of Cellular Biochemistry 120, 4021–4031.
Rappaz F. 1987 – Taxonomie et nomenclature des *Diatrypacées* à asques octosporées. Mycology Helv 2, 285–648.
Rambaut A. 2014 – FigTree v1.4. Institute of Evolutionary Biology, University of Edinburgh, Edinburgh. http://tree.bio.ed.ac.uk/ software/fgtree/.
Rathnayaka AR, Chethana KWT, Phillips AJL, Liu JK et al. 2023 – Re-evaluating Botryosphaeriales: ancestral state reconstructions of selected characters and evolution of nutritional modes. Journal of Fungi 9(2), 184
Razaghi P, Raza M, Han LS, Ma ZY et al. 2024 – *Sporocadaceae* revisited. Studies in mycology 109, 155–272.
Réblová M, Gams W, Seifert KA. 2011 – *Monilochaetes* and allied genera of the *Glomerellales*, and a reconsideration of families in the *Microascales*. Studies in Mycology 68, 163–191.
Réblová M, Untereiner WA, Štěpánek V, Gams W et al. 2017 – Disentangling *Phialophora* section Catenulatae: disposition of taxa with pigmented conidiophores and recognition of a new subclass, *Sclerococcomycetidae* (*Eurotiomycetes*). Mycological Progress 16, 27–46.
Rehner SA and Samuels GJ. 1994 – Taxonomy and phylogeny of *Gliocladium* analysed from nuclear large subunit ribosomal DNA sequences. Mycological Research 98(6), 625–634.
Robyn R. 2018 – Walnut product innovations creating more demand. Western Farm Press Exclusive Insight 0.
Ronquist F, Huelsenbeck JP 2003 – MrBayes 3, Bayesian phylogenetic inference under mixed models. Bioinformatics 19, 1572–1574.
Rossman AY, Samuels GJ, Rogerson CT, Lowen R. 1999 – Genera of *Bionectriaceae*, *Hypocreaceae* and *Nectriaceae* (*Hypocreales*, *Ascomycetes*). Studies in Mycology 42, 1–248.
Rossman AY. 2000 – Towards monophyletic genera in the holomorphic *Hypocreales*. Studies in Mycology 45, 27–34.
Rossman AY, McKemy JM, Pardo-Schultheiss RA, Schroers HJ. 2001 – Molecular studies of the *Bionectriaceae* using large subunit rDNA sequences. Mycologia 93, 100–110.

Rossman AY, Seifert KA, Samuels GJ, Minnis, AM et al. 2013 – Genera in *Bionectriaceae*, *Hypocreaceae*, and *Nectriaceae* (*Hypocreales*) proposed for acceptance or rejection. IMA Fungus 4, 41–51.
Rossman AY, Crous PW, Hyde KD, Hawksworth DL et al. 2015 – Recommended names for pleomorphic genera in *Dothideomycetes*. IMA Fungus 6, 507–523
Rotem J. 1994 – The genus Alternaria. Biology, epidemiology and pathogenicity. APS Press, St. Paul, Minnesota, USA.
Saccardo PA. 1881 – Fungi Veneti novi vel critici vel mycologiae Veneti addendi. Series XII. Michelia 2, 528–563.
Saccardo PA 1875 – Conspectus generum pyrenomycetum italicorum additis speciebus fungorum Venetorum novis vel criticis, systemate carpologico dispositorum. Atti della Società Veneziana-Trentina-Istriana di Scienze Naturali 4, 77–100
Sarkar T, Chakraborty P, Karmakar A, Saha A et al. 2019 – First report of *Periconia macrospinosa* causing leaf necrosis of pointed gourd in India. Journal of Plant Pathology 101, 1281.
Samarakoon BC, Phookamsak R, Wanasinghe DN, Chomnunti P et al. 2020 – Taxonomy and phylogenetic appraisal of *Spegazzinia musae* sp. nov. and *S. deightonii* (*Didymosphaeriaceae*, *Pleosporales*) on *Musaceae* from Thailand. MycoKeys 70, 19.
Samarakoon MC, Hyde KD, Maharachchikumbura SSM, Stadler M et al. 2022 – Taxonomy, phylogeny, molecular dating and ancestral state reconstruction of *Xylariomycetidae* (*Sordariomycetes*). Fungal Diversity 112, 1–88.
Samson RA, Hoekstra ES, Frisvad JC. 2004 – Introduction to food and airborne fungi, 7th edn. Centraalbureau voor Schimmelcultures, Utrecht.
Samson RA, Houbraken J, Thrane U. 2010 – Food and indoor fungi. Utrecht, CBS KNAW Biodiversity Center.
Samuels GJ, Lu BS, Chaverri P, Candoussau F et al. 2009 – *Cyanonectria* a new genus for *Nectria cyanostoma* and its *Fusarium* anamorph. Mycological Progress 8, 49–58.
Sandoval-Denis M, Gené J, Sutton DA, Wiederhold, NP et al. 2016a – New species of *Cladosporium* associated with human and animal infections. Persoonia 36, 281–298.
Sandoval-Denis M, Guarro J, Cano-Lira JF, Sutton DA et al. 2016b – Phylogeny and taxonomic revision of *Microascaceae* with emphasis on synnematous fungi. Studies in Mycology 83, 193–233.
Sandoval-Denis M, Costa MM, Broders K, Becker Y et al. 2025 – An integrative re-evaluation of the *Fusarium sambucinum* species complex. Studies in Mycology 110, 1–110.
Sanjuan T, Tabima J, Restrepo S et al. 2014 – Entomopathogens of Amazonian stick insects and locusts are members of the *Beauveria* species complex (*Cordyceps* sensu stricto). Mycologia 106, 260–275.
Sautua FJ, Searight J, Doyle VP, Læssøe T et al. 2020 – *Cercospora cf. nicotianae* is a causal agent of *Cercospora* leaf blight of soybean. European Journal of Plant Pathology 156, 1227–1231.
Savian LG, Muniz MFB, Poletto T, Maculan LG et al. 2019 – First report of *Colletotrichum nymphaeae* causing anthracnose on *Juglans regia* Fruits in Southern Brazil. Plant Disease 103, 3287–3288.
Schardl CL, Young CA, Hesse U, Amyotte SG et al. 2013 – Plant-symbiotic fungi as chemical engineers: multi-genome analysis of the *Clavicipitaceae* reveals dynamics of alkaloid loci. Plos Genet 9, e1003323.
Schena L, Abdelfattah A, Mosca S, Nicosia MGL et al. 2017 – Quantitative detection of *Colletotrichum godetiae* and *C. acutatum* sensu stricto in the phyllosphere and carposphere of olive during four phenological phases. European Journal of Plant Pathology 149, 337–347.
Schmey T, Small C, Einspanier S, Hoyoz LM et al. 2023 – Small-spored *Alternaria* spp. (section *Alternaria*) are common pathogens on wild tomato species. Environmental Microbiology 25(10), 1830–1846.
Schoch CL, Shoemaker RA, Seifert, KA, Hambleton S et al. 2006 – A multigene phylogeny of the *Dothideomycetes* using four nuclear loci. Mycologia, 98, 1041–52.

Schoch CL, Crous PW, Groenewald JZ, Boehm EWA et al. 2009a – A class–wide phylogenetic assessment of *Dothideomycetes*. Studies in Mycology 64, 1–15.
Schoch CL, Sung GH, Lopez-Giraldez F, Townsend JP et al. 2009b – The *Ascomycota* tree of life: a phylum-wide phylogeny clarifies the origin and evolution of fundamental reproductive and ecological traits. Systematic Biology 58, 224–239.
Schroers HJ, Samuels GJ, Seifert KA, Gams W. 1999 – Classification of the mycoparasite *Gliocladium roseum* in *Clonostachys* as *C. rosea*, its relationship to *Bionectria ochroleuca*, and notes on other gliocladium-like fungi. Mycologia 91, 365–385.
Schroers HJ, Gräfenhan T, Nirenberg HI, Seifert KA. 2011 – A revision of Cyanonectria and Geejayessia gen. nov, and related species with Fusarium-like anamorphs. Studies in Mycology 68, 115–138.
Seifert KA. 1985 – A monograph of *Stilbella* and some allied Hyphomycetes. Studies in Mycology 27, 1–234.
Senanayake IC, Maharachchikumbura SSN, Hyde KD, Bhat JD et al. 2015 – Towards unraveling relationships in *Xylariomycetidae* (*Sordariomycetes*). Fungal Diversity 73, 73–144.
Senanayake IC, Crous PW, Groenewald JZ, Maharachchikumbura SS et al. 2017a – Families of *Diaporthales* based on morphological and phylogenetic evidence. Studies in Mycology 86, 217–296.
Senanayake IC, Maharachchikumbura SSN, Jeewon R, Promputtha I et al. 2017b – Morphophylogenetic study of *Sydowiellaceae* reveals several new genera. Mycosphere 8, 172–217.
Senanayake IC, Jeewon R, Chomnunti P, Wanasinghe DN et al. 2018 – Taxonomic circumscription of *Diaporthales* based on multigene phylogeny and morphology. Fungal Diversity 93, 241–443.
Senanayake IC, Rathnayaka AR, Marasinghe DS, Calabon MS, et al. 2020 – Morphological approaches in studying fungi: collection, examination, isolation, sporulation and preservation. Mycosphere 11, 2678–2754.
Samarakoon BC, Wanasinghe DN, Samarakoon MC, Bundhun D et al. 2024 – Exploring fungi: a taxonomic and phylogenetic study of leaf-inhabiting *Ascomycota* in *Musa* species from northern Thailand, with a global checklist. Mycosphere 15(1), 1901–2174
Senwanna C, Mapook A, Samarakoon MC, Karunarathna A et al. 2021 – Ascomycetes on Para rubber (*Hevea brasiliensis*). Mycosphere 12, 1334–1512.
Senwanna C, Suwannarach N, Phookamsak R, Kumla J et al. 2023 – New host and geographical records of *Rhytidhysteron* in northern Thailand, and species synonymization. Phytotaxa 601(2), 157–173.
Serrato-Diaz LM, Rivera-Vargas LI, French-Monar RD. 2014 – First report of *Diaporthe pseudomangiferae* causing inflorescence rot, rachis canker, and flower abortion of mango. Plant Disease 106, 1004.
Serrato-Diaz LM, Ayala-Silva T, Goenaga R. 2022 – First report of *Diaporthe tulliensis* and *D. pseudomangiferae* causing cacao pod rot in Puerto Rico. Plant Disease 98, 1004–1005.
Shang QJ, Hyde KD, Phookamsak R, Doilom M et al. 2017 – *Diatrypella tectonae* and *Peroneutypa mackenziei* spp. nov. (*Diatrypaceae*) from northern Thailand. Mycological Progress 16, 463–476.
Shang QJ, Hyde KD, Jeewon R, Doilom M et al. 2018 – Morpho-molecular characterization of *Peroneutypa* (*Diatrypaceae*, *Xylariales*) with two novel species from Thailand. Phytotaxa 356, 1–18.
Sharma S, Gautam N, Kaur, H. 2023 – Cytology of *Rhytidhysteron rufulum*: An emerging cause of phaeohyphomycosis. Diagnostic Cytopathology 51, E338–E341.
Shen HW, Luo ZL, Bao DF, Luan S et al. 2024 – Lignicolous freshwater fungi from China Ⅳ: Morphology and phylogeny reveal new species of *Pleosporales* from plateau lakes in Yunnan Province, China. Mycosphere 15(1), 6439–6524.

Shoemaker RA. 1964 – Conidial states of some *Botryosphaeria* species on *Vitis* and *Quercus*. Canadian Journal of Botany 42, 1297–1301.
Si YZ, Sun JW, Wan Y, Chen YN et al. 2023 – *Neofusicoccum cryptomeriae* sp. nov. and *N. parvum* Cause Stem Basal Canker of *Cryptomeria japonica* in China. Journal of Fungi 9, 404.
Sinclair WA, Lyon HH. 2005 – Diseases of trees and shrubs, 2nd edn. Cornell University, Ithaca, NY.
Sir EB, Kuhnert E, Lambert C, Hladki AI et al. 2016 – New species and reports of *Hypoxylon* from Argentina recognized by a polyphasic approach. Mycological Progress 15, 1–42.
Sir EB, Becker K, Lambert C, Bills GF et al. 2019 – Observations on Texas hypoxylons, including two new *Hypoxylon* species and widespread environmental isolates of the *H. croceum* complex identified by a polyphasic approach. Mycologia 111, 832–856.
Sivanesan A. 1984 – The bitunicate *Ascomycetes* and their ananaorphs. J Cramer, Vaduz.
Slippers B, Crous PW, Denman S, Coutinho TA 2004 – Combined multiple gene genealogies and phenotypic characters differentiate several species previously identified as *Botryosphaeria dothidea*. Mycologia 96, 83–101
Slippers B, Boissin E, Phillips AJL, Groenewald JZ et al. 2013 – Phylogenetic lineages in the Botryosphaeriales: a systematic and evolutionary framework. Studies in Mycology 76, 31–49.
Snyder WC, Hansen HN. 1945 – The species concept in *Fusarium* with reference to Discolor and other sections. American Journal of Botany 32, 657–666.
Sogonov MV, Castlebury LA, Rossman AY, Mejía LC et al. 2008 – Leaf-inhabiting genera of the *Gnomoniaceae*, *Diaporthales*. Studies in Mycology 62, 1–77.
Spegazzini C. 1881 – Fungi argentini additis nonnullis brasiliensibus montevide ensibusque. Pugillus quartus (Continuacion). Anales de la Sociedad Científica Argentina 12, 174–189.
Su HY, Hyde KD, Maharachchikumbura SSN, Ariyawansa HA et al. 2016 – The families *Distoseptisporaceae* fam. nov, *Kirschsteiniotheliaceae*, *Sporormiaceae* and *Torulaceae*, with new species from freshwater in Yunnan Province, China. Fungal Diversity 80, 375–409.
Su P, Lu Z, Tian W, Chen Y et al. 2023 – Six additions to the genus *Periconia* (*Dothideomycetes*: *Periconiaceae*) from graminaceous plants in China. Journal of Fungi 9(3), 300.
Suetrong S, Schoch CL, Spatafora JW et al. 2009 – Molecular systematics of the marine *Dothideomycetes*. Studies in Mycology 64, 155–173.
Sui XN, Guo MJ, Wang QT, Wang HQ et al. 2024 – Taxonomy and phylogeny of *Colletotrichum* on important forest plants in China. Mycosphere 15(1), 4569–4743.
Summerbell RC, Gueidan C, Schroers HJ, de Hoog GS et al. 2011 – *Acremonium* phylogenetic overview and revision of *Gliomastix*, *Trichothecium* and *Sarocladium*. Studies in Mycology 68, 139–162.
Summerell BA. 2019 – Resolving *Fusarium*: Current status of the genus. Annual review of phytopathology 57, 323–339.
Sun Q, Harishchandra D, Jia J, Zuo Q et al. 2021a – Role of *Neopestalotiopsis rosae* in causing root rot of strawberry in Beijing, China. Crop Protection 147, 105710.
Sun YR, Jayawardena RS, Hyde KD, Wang Y. 2021b – *Kirschsteiniothelia thailandica* sp. nov. (*Kirschsteiniotheliaceae*) from Thailand. Phytotaxa 490, 172–182.
Sung GH, Hywel-Jones NL, Sung JM, Luangsa-ard JJ et al. 2007 – Phylogenetic classification of *Cordyceps* and the clavicipitaceous fungi. Studies in Mycology 57, 5–59.
Sutton BC. 1980 – The Coelomycetes: fungi imperfecti with pycnidia, acervuli and Stromata. Commonwealth Mycological Institute, Kew, p 496.
Suwannarach N, Kumla J, Lumyong S. 2015 – First report of *Alternaria* leaf blight disease on oil palm caused by *Alternaria longipes* in Thailand. Phytoparasitica 43, 57–59.
Staats M, van Baarlen P, van Kan JAL. 2005 – Molecular phylogeny of the plant pathogenic genus Botrytis and the evolution of host specificity. Molecular Biology & Evolution 22, 333–346.
Stamatakis A. 2014 – RAxML version 8: A tool for phylogenetic analysis and post-analysis of large phylogenies. Bioinformatics 30, 1312–1313.

Steyaert RL. 1949 – Contributions al'etude monographique de (*Pestalotia* de Not. et *Monochaetia* Sacc. (*Truncatella* gen. nov. et *Pestalotiopsis* gen. nov.). Bulletin Jardin Botanique Etat Bruxelles 19, 285–354.

Stukenbrock EH, Quaedvlieg W, Javan-Nikhah M, Zala M. 2012 – *Zymoseptoria ardabilia* and *Z. pseudotritici*, two progenitor species of the septoria tritici leaf blotch fungus *Z. tritici* (synonym: *Mycosphaerella* graminicola). Mycologia 104, 1397–1407.

Tabima JF, Søndreli KL, Keriö S, Feau N et al. 2020 – Population genomic analyses reveal connectivity via human-mediated transport across Populus plantations in North America and an undescribed subpopulation of *Sphaerulina musiva*. Molecular Plant-Microbe Interactions 33, 189–199.

Taylor JW, Jacobson DJ, Kroken S, Kasuga T et al. 2000 – Phylogenetic species recognition and species concepts in fungi. Fungal Genetics and Biology 31, 21–32.

Talhinhas P, Baroncelli R. 2021 – *Colletotrichum* species and complexes: geographic distribution, host range and conservation status. Fungal Diversity 110, 109–198.

Tanaka K, Hirayama K, Yonezawa H, Sato G et al. 2015 – Revision of the *Massarineae* (*Pleosporales*, *Dothideomycetes*). Studies in Mycology 82, 75–136.

Tennakoon DS, Phillips AJL, Phookamsak R, Ariyawansa HA et al. 2016 – Sexual morph of *Lasiodiplodia pseudotheobromae (Botryosphaeriaceae, Botryosphaeriales*, *Dothideomycetes*) from China. Mycosphere 7, 990–1000.

Tennakoon DS, Jeewon R, Thambugala KM, Gentekaki E et al. 2021a – Biphasic taxonomic approaches for generic relatedness and phylogenetic relationships of *Teichosporaceae*. Fungal Diversity 110, 199–241.

Tennakoon DS, Kuo CH, Maharachchikumbura SSN, Thambugala KM et al. 2021b – Taxonomic and phylogenetic contributions to *Celtis formosana*, *Ficus ampelas*, *F. septica*, *Macaranga tanarius* and *Morus australis* leaf litter inhabiting microfungi. Fungal Diversity 108, 1–215.

Thambugala KM, Hyde KD, Tanaka K, Tian Q et al. 2015 – Towards a natural classification and backbone tree for *Lophiostomataceae*, *Floricolaceae*, and *Amorosiaceae* fam. nov. Fungal Diversity 74, 199–266.

Thambugala KM, Hyde KD, Eungwanichayapant PD, Romero AI et al. 2016 – Additions to the genus *Rhytidhysteron* in *Hysteriaceae*. Cryptogam Mycology 37, 99–116.

Thambugala KM, Wanasinghe DN, Phillips AJL, Camporesi E et al. 2017a – Mycosphere notes 1-50: grass (*Poaceae*) inhabiting *Dothideomycetes*. Mycosphere 8, 697–796.

Thambugala KM, Daranagama DA, Phillips AJL, Bulgakov TS et al. 2017b – Microfungi on Tamarix. Fungal Diversity 82, 239–306.

Theissen F, Sydow H. 1918 – Vorentwürfe Zu Den Pseudosphaeriales. Ann Mycology 16, 1–34

Thompson JD, Gibson TJ, Plewniak F, Jeanmougin F et al. 1997 – The ClustalX windows interface: flexible strategies for multiple sequence alignment aided by quality analysis tools. Nucleic Acids Research 24, 4876–4882.

Tian N, Gao M, Liu XH, Liu XM et al. 2022 – Activated carbon derived from walnut green peel as an electrode material for high-performance supercapacitors. Biomass Conversion and Biorefinery 13, 16781–16789.

Tian Q, Liu JK, Hyde KD et al. 2015 – Phylogenetic relationships and morphological reappraisal of *Melanommataceae* (*Pleosporales*). Fungal Diversity 74, 267–324.

Tian Q, Li WJ, Hyde KD, Wanasinghe DN et al. 2017 – Molecular taxonomy of five species of microfungi on *Alnus* spp. from Italy. Mycological Progress 17, 255–274.

Tian XG, Bao DF, Karunarathna SC, Jayawardena RS et al. 2024 – Taxonomy and phylogeny of ascomycetes associated with selected economically important monocotyledons in China and Thailand. Mycosphere 15(1), 1–274.

Tibpromma S, Hyde KD, Jeewon R, Maharachchikumbura SSN et al. 2017 – Fungal diversity notes 491–602: taxonomic and phylogenetic contributions to fungal taxa. Fungal Diversity 83, 1–261.

Tibpromma S, Hyde KD, McKenzie EHC, Bhat DJ et al. 2018a – Fungal Diversity notes 840–928: microfungi associated with *Pandanaceae*. Fungal Diversity 93, 1–160.
Tibpromma S, Hyde K, Bhat J, Mortimer P et al. 2018b – Identification of endophytic fungi from leaves of *Pandanaceae* based on their morphotypes and DNA sequence data from southern Thailand. MycoKeys 33, 25–67.
Tibpromma S, Mortimer PE, Karunarathna SC, Zhan F et al. 2019 – Morphology and multi-gene phylogeny reveal *Pestalotiopsis pinicola* sp. nov. and a new host record of *Cladosporium anthropophilum* from edible Pine (*Pinus armandii*) seeds in Yunnan province, China. Pathogens 8, 1–18.
Tisserat N, Cranshaw W, Leatherman D, Utley C et al. 2009 – Black walnut mortality in Colorado caused by the walnut twig beetle and thousand cankers disease. Phytopathology 99, S128.
To-anun C, Hidayat I, Meeboon J. 2011 – Genus *Cercospora* in Thailand: (taxonomy and phylogeny (with a dichotomous key to species). Plant Pathology Q1, 11–87.
Tode HJ 1791 – Fungi Mecklenburgenses selecti. Fasc. II, Generum novorum appendicem, Lüneburg.
Toledo AV, Virla E, Humber RA, Paradell SL et al. 2006 – First record of *Clonostachys rosea* (Ascomycota: Hypocreales) as an entomopathogenic fungus of *Oncometopia tucumana* and *Sonesimia grossa* (Hemiptera: *Cicadellidae*) in Argentina. Journal of invertebrate pathology 92, 7–10.
Trouillas FP, Pitt WM, Sosnowski MR, Huang RJ et al. 2011 – Taxonomy and DNA phylogeny of *Diatrypaceae* associated with *Vitis vinifera* and other woody plants in Australia. Fungal Diversity 49, 203–223.
Tuerdi M, Lv CH, Dan HX, Shan LL et al. 2023 – First Report of *Fusarium solani* Associated with Twig Canker of English Walnut (*Juglans regia)* in Xinjiang, China. Plant Disease 107, 2858–2858.
Udayanga D, Liu X, Crous PW, McKenzie EH et al. 2012 – A multi-locus phylogenetic evaluation of *Diaporthe* (*Phomopsis*). Fungal Diversity 56, 157–171.
Udayanga D, Manamgoda DS, Liu X, Chukeatirote E et al. 2013 – What are the common anthracnose pathogens of tropical fruits? Fungal Diversity 61, 165–179.
Udayanga D, Castlebury LA, Rossman AY, Chukeatirote E et al. 2014 – Insights into the genus *Diaporthe*: phylogenetic species delimitation in the *D. eres* species complex. Fungal Diversity 67, 203–229.
Udayanga D, Liu X, McKenzie EHC, Chukeatirote E et al. 2011 – The genus *Phomopsis*: Biology, applications, species concepts and names of common phytopathogens. Fungal Diversity 50, 189–225.
Uecker FA. 1994 – Ontogeny of the ascoma of *Glomerella cingulata*. Mycologia 86, 82–88.
Ujat AH, Nakashima C. 2024 – Piecing together the taxonomic puzzle of *Sphaerulina*. Fungal Systematics and Evolution 14, 171–190.
U'Ren JM, Miadlikowska J, Zimmerman NB, Lutzoni F et al. 2016 – Contributions of North American endophytes to the phylogeny, ecology, and taxonomy of *Xylariaceae* (*Sordariomycetes*, *Ascomycota*). Molecular Phylogenetics and Evolution 98, 210–232.
Vakalounakis DJ, Ntougias S, Kavroulakis N, Protopapadakis E 2019 – *Neofusicoccum parvum* and *Diaporthe foeniculina* Associated with Twig and Shoot Blight and Branch Canker of Citrus in Greece. Journal of Phytopathol. 167, 527–537.
Van Kan JA, Van den Ackerveken GFJM, De Wit PJGM. 1991 – Cloning and characterization of cDNA of avirulence gene avr9 of the fungal pathogen *Cladosporium fulvum*, causal agent of tomato leaf mold. Molecular Plant-Microbe Interact 4, 52–59.
Vanderwolf KJ, McAlpine DF, Malloch D, Forbes GJ. 2013 – Ectomycota associated with hibernating bats in eastern Canadian caves prior to the emergence of white-nose syndrome. Northeastern Naturalist 20, 115–130.

Varjas V, Kovács Cs, Lakatos T, Tóth T et al. 2019 – First report of walnut anthracnose caused by *Colletotrichum fioriniae* on English persian walnut fruits in Hungary. Plant Disease 103, 2964–2964.
Varjas V, Lakatos T, Tóth T, Kovács C. 2021 – First Report of *Colletotrichum godetiae* Causing Anthracnose and Twig Blight on (Persian) Walnut in Hungary. Plant Disease 105, 702.
Vasilyeva LN, Stephenson SL. 2006 – Pyrenomycetes of the Great Smoky Mountains National Park. III. *Cryptosphaeria*, *Eutypa* and *Eutypella* (*Diatrypaceae*). Fungal Diversity 22, 243–254.
Vande R, Wall SB. 2010 – How plants manipulate the scatter-hoarding behavior of seed-dispersing animals. Philosophical Transactions of the Royal Society B Biological Sciences 365(1542), 989–997.
Videira SIR, Groenewald JZ, Nakashima C, Braun U et al. 2017 – *Mycosphaerellaceae*–chaos or clarity? Studies in Mycology 87, 257–421.
Vieira WAD, da Costa CA, Veloso JS, Lima WG et al. 2024 – Diversity of *Colletotrichum* species causing anthracnose in chayote in Brazil, with a description of two new species in the *C. magnum* complex. Journal of Fungi 10(12), 847–847.
Vilgalys R, Hester M. 1990 – Rapid genetic identification and mapping of enzymatically amplified ribosomal DNA from several *Cryptococcus* species. Journal of Bacteriology 172, 4238–4246.
Vintal H, Shtienberg D, Shlevin E, Ben-Noon E. 2002 – First report of leaf blight caused by *Alternaria longipes* on carrots in Israel. Plant Disease 86, 186.
Visentin I, Gentile S, Valentino D, Gonthier P et al. 2012 – *Gnomoniopsis castanea* sp. nov. (*Gnomoniaceae*, *Diaporthales*) as the causal agent of nut rot in sweet chestnut. Journal of Plant Pathology 94, 411–419.
Voglmayr H, Jaklitsch, WM. 2017a – *Corynespora*, *Exosporium* and *Helminthosporium* revisited–New species and generic reclassification. Studies in Mycology 87, 43–76.
Voglmayr H, Castlebury LA, Jaklitsch W. 2017b – *Juglanconis* gen. nov. on *Juglandaceae*, and the new family *Juglanconidaceae* (*Diaporthales*). Persoonia 38, 136–155.
Voglmayr H, Jaklitsch WM, Mohammadi H, Chakusary MK et al. 2019 – The genus *Juglanconis* (*Diaporthales*) on *Pterocarya*. Mycological Progress 18, 425–437.
Von Arx JA, Müller E. 1954 – Die Gattungen der amerosporen Pyrenomycetes. Beitr Kryptogamenf Schweiz 11, 1–434.
Von Arx JA, Müller E. 1975 – A re-evaluation of the bitunicate ascomycetes with keys to families and genera. Transactions of the British Mycological Society 9, 1–159.
Von Höhnel F. 1917 – Über die Benennung Stellung und Nebenfrucht formen von Sphaerella Fries. Ber Dtsch Bot Ges 35, 627–631.
Vu D, Groenewald M, De Vries M, Gehrmann T et al. 2018 – Large-scale generation and analysis of flamentous fungal DNA barcodes boosts coverage for kingdom fungi and reveals thresholds for fungal species and higher tax on delimitation. Studies in Mycology 91, 23–36.
Walker DM, Castlebury LA, Rossman AY, Sogonov MV et al. 2010 – Systematics of genus *Gnomoniopsis* (*Gnomoniaceae*, *Diaporthales*) based on a three gene phylogeny, host associations and morphology. Mycologia 102, 1479–1496.
Walker DM, Castlebury LA, Rossman AY, Mejía LC et al. 2012a – Phylogeny and taxonomy of (*Ophiognomonia Gnomoniaceae*, *Diaporthales*), including twenty-five new species in this highly diverse genus. Fungal Diversity 57, 85–147.
Walker DM, Castlebury LA, Rossman AY, White JF. 2012b – New molecular markers for fungal phylogenetics: two genes for species-level systematics in the *Sordariomycetes* (*Ascomycota*). Molecular Phylogenetics and Evolution 64, 500–512.
Wanasinghe DN, Phukhamsakda C, Hyde KD, Jeewon R et al. 2018 – Fungal diversity notes 709–839, taxonomic and phylogenetic contributions to fungal taxa with an emphasis on fungi on *Rosaceae*. Fungal Diversity 89, 1–236.
Wang HK, Hyde KD, Soytong K, Lin FC. 2008 – Fungal diversity on fallen leaves of *Ficus* in northern Thailand. Journal of Zhejiang University Science B9, 835–841.

Wang J, Liu XM. 2007 – Contamination of aflatoxins in different kinds of foods in China. Biomedical and environmental sciences 20(6), 483–7.
Wang QH, Fan K, Li DW, Niu SG et al. 2017 – Walnut anthracnose caused by *Colletotrichum siamense* in China. Australasian Plant Pathology 46, 585–595.
Wang MM, Crous PW, Sandoval-Denis M, Han SL et al. 2022 – *Fusarium* and allied genera from China: species diversity and distribution. Persoonia 48, 1–53.
Wang YB, Wang Y, Fan Q, Duan DE et al. 2020 – Multigene phylogeny of the family *Cordycipitaceae* (*Hypocreales*), new taxa and the new systematic position of the Chinese cordycipitoid fungus *Paecilomyces hepiali*. Fungal Diversity 103(1), 1–46.
Wang Z, Binder M, Schoch CL, Johnston PR et al. 2006 – Evolution of helotialean fungi (*Leotiomycetes*, *Pezizomycotina*): a nuclear rDNA phylogeny. Molecular Phylogenetics and Evolution 41, 295–312.
Weir BS, Johnston PR, Damm U. 2012 – The *Colletotrichum gloeosporioides* species complex. Studies in Mycology 73, 115–180.
Wendt L, Sir EB, Kuhnert E, Heitkämper S et al. 2018 – Resurrection and emendation of the *Hypoxylaceae*, recognised from a multigene phylogeny of the *Xylariales*. Mycological Progress 17, 115–154.
White TJ, Bruns T, Lee S, Taylor J. 1990 – Amplification and direct sequencing of fungal ribosomal RNA genes for phylogenetics, pp 315–322. In: Innis MA, Gelfand DH, Sninsky JJ, White TJ (Eds) PCR protocols: a guide to methods and applications. Acddemic, San Diego 315–322.
Wibberg D, Stadler M, Lambert C, Bunk B et al. 2021 – High quality genome sequences of thirteen *Hypoxylaceae* (*Ascomycota*) strengthen the phylogenetic family backbone and enable the discovery of new taxa. Fungal Diversity 106, 7–28.
Wikee S, Lombard L, Nakashima C, Motohashi K et al. 2013 – A phylogenetic re-evaluation of Phyllosticta (*Botryosphaeriales*). Studies in Mycology 76, 1–29
Wijayawardene NN, Crous PW, Kirk PM, Hawksworth DL et al. 2014 – Naming and outline of *Dothideomycetes* – 2014 including proposals for the protection or suppression of generic names. Fungal Diversity 69, 1–55.
Wijayawardene NN, Hyde KD, Rajeshkumar KC, Hawksworth DL et al. 2017 – Notes for genera: *Ascomycota*. Fungal Diversity 86, 1–594.
Wijayawardene NN, Hyde KD, Lumbsch HT, Liu JK et al. 2018 – Outline of *Ascomycota*: 2017. Fungal Diversity 88, 167–263.
Wijayawardene NN, Hyde KD, Al-Ani LKT, Tedersoo L et al. 2020a – Outline of Fungi and fungus-like taxa. Mycosphere 11, 1060–1456.
Wijayawardene NN, Hyde KD, Dai DQ, Sánchez-García M et al. 2022 – Outline of Fungi and fungus-like taxa - 2021. Mycosphere 13, 53–453.
Wijayawardene NN, Hyde KD, Mikhailov KV, Péter G et al. 2024 – Classes and phyla of the kingdom Fungi. Fungal Diversity 128, 1–165.
Wijesinghe SN, Wang Y, Camporesi E, Wanasinghe DN et al. 2020 – A new genus of *Bambusicolaceae* (*Pleosporales*) on *Corylus avellana* (*Fagales*) from Italy. Biodiversity Data Journal 8, e55957.
Willie ASV, Waléria GL, Eduardo SN, Sami JM et al. 2018 – The impact of phenotypic and molecular data on the inference of *Colleotrichum* diversity associated with Musa. Mycologia 109, 912–934.
Wollenweber HW, Reinking OA. 1935 – Die Fusarien, ihre Beschreibung. Schadwirkung und Bekiimpfung, Paul Parey, Berlin.
Wood AR, Damm U, van Der Linde EJ, Groenewald JZ et al. 2016 – Finding the missing link: resolving the Coryneliomycetidae within Eurotiomycetes. Persoonia 37, 37–56.
Woronichin NN. 1926 – Zur Kenntnis der Morphologie und Systematik der Russtaupilze Transkaukasiens. Annales Mycologici 24, 231–264.
Woudenberg JH, Groenewald JZ, Binder M, Crous PW. 2013 – *Alternaria* redefined. Studies in Mycology 75, 171–212.

Woudenberg JHC, Seidl MF, Groenewald JZ, De Vries M et al. 2015 – *Alternaria* section *Alternaria*: Species, formae speciales or pathotypes? Studies in Mycology 82, 1–21.
Woudenberg JHC, Meijer M, Houbraken J, Samson RA. 2017 – *Scopulariopsis* and *Scopulariopsis*-like species from indoor environments. Studies in Mycology 88, 1–35.
Wu PH, Chang HX. 2021 – First report of leaf spot caused by *Diaporthe tulliensis* on Boston Ivy (*Parthenocissus tricuspidata*) in Taiwan. Plant Disease 105(9).
Wu WP, D YZ. 2023 – The chalara-like anamorphs of *Leotiomycetes.* Fungal Diversity 119, 213–490.
Wu WW, Chen Y, Xiong DW. 2018 – Status quo and utilization considerations of *Juglans* germplasm resources in Sichuan. Journal of Sichuan Forestry Science and Technology 39(6), 79–91.
Wyka SA, Broders KD. 2016 – The new family *Septorioideaceae*, within the *Botryosphaeriales* and Septorioides strobi as a new species associated with needle defoliation of Pinus strobus in the United States. Fungal Biology 120(8), 1030–1040.
Xia JW, Sandoval-Denis M, Crous PW, Zhang XG et al. 2019 – Numbers to names–reappraisal of the *Fusarium incarnatum*-equiseti species complex. Persoonia 43, 186–221.
Xiao XJ, Liu NG, Ma J, Zhang, LJ et al. 2025 – Three new asexual *Kirschsteiniothelia* species from Guizhou Province, China. MycoKeys 113, 147–168.
Xiao YP, Wang YB, Hyde KD, Eleni G et al. 2023 – *Polycephalomycetaceae*, a new family of clavicipitoid fungi segregates from *Ophiocordycipitaceae*. Fungal Diversity 120, 1–76.
Xu RF, Karunarathna SC, Phukhamsakda C, Dai DQ, et al. 2024 – Four new species of *Dothideomycetes* (*Ascomycota*) from Pará Rubber (*Hevea brasiliensis*) in Yunnan Province, China. MycoKeys 103, 71–95.
Xu XL, Wang FH, Liu C, Yang HB et al. 2022a – Morphology and phylogeny of ascomycetes associated with walnut trees (*Juglans regia*) in Sichuan province, China. Frontiers in Microbiology 13, 1016548.
Xu XL, Xiao QG, Yang CL, Jeewon R et al. 2022b – Multigene phylogenetic support for novel *Rhytidhysteron* Speg. species (*Hysteriaceae*) from Sichuan Province, China. Cryptogamie, Mycologie 43, 63–79.
Yang BB, Tao PJ, Zhang YC. 2015 – Analysis on the effect of poverty alleviation based on walnut industry. Advance Journal of Food Science and Technology 7, 499–504.
Yang CL, Deng Y, Wang FH, Yang HB et al. 2021a – Brown leaf spot on *Juglans sigillata* caused by *Ophiognomonia leptostyla* in Sichuan, China. Plant Disease 105, 4160.
Yang CL, Liu F, Zeng Q, Xu XL et al. 2021b – Brown leaf spot of *Juglans hybrid* caused by *Ophiognomonia leptostyla* in China. Plant Disease 105, 3740.
Yang CL, Xu XL, Zeng Q, Liu LJ et al. 2024 – Bambusicolous mycopathogens in China with an update on taxonomic diversity, novel species, pathogenicity, and new insights. Mycosphere 15(1), 4788–4918.
Yang EF, Phookamsak R, Jiang HB, Tibpromma S. 2022 – Taxonomic Reappraisal of *Periconiaceae* with the *Description* of Three New *Periconia* Species from China. Journal of Fungi 8(3), 243.
Yang J, Liu LL, Jones EBG, Hyde KD et al. 2023 – Freshwater fungi from karst landscapes in China and Thailand. Fungal Diversity 119, 1–212.
Yang KQ, Qu WW, Liu X, Liu HX et al. 2011a – First report of *Pantoea agglomerans* causing brown apical necrosis of walnut in China. Plant Disease 95, 773–773.
Yang T, Groenewald JZ, Cheewangkoon R, Jami F et al. 2017 – Families, genera, and species of *Botryosphaeriales*. Biology 121, 322–346.
Yang YL, Cai L, Yu ZN, Liu ZY et al. 2011b – *Colletotrichum* species on *Orchidaceae* in southwest China. Cryptogam. Mycologie. 32, 229–253.
Yu XD, Zhang SN, Liang XD, Zhu JT et al. 2024 – Bambusicolous fungi from Southwestern China. Mycosphere 15(1), 5038–5145.
Yu Z, Tang G, Peng S, Chen H et al. 2015 – *Neofusicoccum parvum* causing canker of seedlings of *Juglans regia* in China. Journal of Forestry Research 26, 1019–1024.

Zeng ZQ, Zhuang WY. 2022 – Three new species of *Clonostachys* (*Hypocreales*), *Ascomycota* from China. Journal of Fungi 8, 1027.
Zhao N, Luo ZL, Hyde KD, Su HY et al. 2018 – *Helminthosporium submersum* sp. nov. (*Massarinaceae*) from submerged wood in north-western Yunnan Province, China. Phytotaxa 348, 269–278.
Zhao Q, Chen X, Liu DY, Xia CJ et al. 2020 – First report of *Cercospora nicotianae* causing frog eye spot in cigar tobacco in Hainan, China. Plant Disease 104, 3257.
Zhao BJ, Liu F, Gong YH, Zhang JP et al. 2021 – Walnut blight investigation, spray materials screening, and bactericide application timing for walnut blight control in Northeast China. European Journal of Plant Pathology 161, 161–170.
Zhang JF, Liu JK, Hyde KD, Chen YY et al. 2023a – *Ascomycetes* from karst landscapes of Guizhou Province, China. Fungal Diversity 122, 1–160.
Zhang L, Yang J, Niu Q, Zhao X et al. 2008 – Investigation on the infection mechanism of the fungus *Clonostachys rosea* against nematodes using the green fluorescent protein. Applied Microbiology & Biotechnology 78, 983–990.
Zhang L, Yin YQ, Zhao LL, Xie YQ et al. 2023b – Two new species of *Colletotrichum* (*Glomerellaceae*, *Glomerellales*) causing walnut anthracnose in Beijing. Mycokeys 99, 131–152.
Zhang N, Castlebury LA, Miller AN, Huhndorf SM et al. 2006 – An overview of the systematics of the *Sordariomycetes* based on four-gene phylogeny. Mycologia 98, 1076–1087.
Zhang SN, Hyde KD, Jones EBJ, Yu XD et al. 2024a – Current insights into palm fungi with emphasis on taxonomy and phylogeny. Fungal Diversity 127, 55–301.
Zhang X, Tibpromma S, Karunarathna SC, Du TY et al. 2025 – Additions to the saprobic fungi (*Ascomycota*) associated with macadamia trees from the Greater Mekong Subregion. MycoKeys 113, 1–29.
Zhang YQ, Hao YB, Chen YH, Qi YY et al. 2024b – Huayi 7: A new cultivar of collectible walnut (Wenwan Walnut) with profound Chinese cultural background. HortScience 59, 371–372.
Zhang YX, Chen C, Nie LT, Maharachchikumbura SSN, Crous PW, Hyde KD, Xiang MM, Al-Otibi F, Manawasinghe IS 2024c – Identification and characterization of *Albonectria*, *Fusarium*, and *Neocosmospora* species associated with ornamental plants in Southern China. Mycosphere 15(1), 6641–6717.
Zhou YY, Zhang W, Wu LN, Zhang J et al. 2023 – Diversity of fungal communities associated with grapevine trunk diseases in China. Mycosphere 14(1), 1340–1435.
Zhou YP, Dou ZP, He W, Zhang XD, Zhang Y. 2016 – *Botryosphaeria sinensia* sp nov., a new species from China. Phytotaxa 245, 043–050.
Zhou S, Stanosz GR. 2001 – Relationships among *Botryosphaeria* species and associated anamorphic fungi inferred from the analysis of ITS and 5.8S rDNA sequences. Mycologia 93, 516–527.